# DESIGN, DEPLOYMENT, AND INITIAL CALIBRATION OF A TOWER FOR GREENHOUSE GAS MEASUREMENTS

by

Lindsay K. Minck

A thesis submitted to the faculty of
The University of Utah
in partial fulfillment of the requirements for the degree of

Master of Science

Department of Civil and Environmental Engineering

The University of Utah

May 2015

**The University of Utah Graduate School**

# STATEMENT OF THESIS APPROVAL

The thesis of **Lindsay K. Minck**

has been approved by the following supervisory committee members:

| | | |
|---|---|---|
| **Brian McPherson** | , Chair | **10/15/2014** Date Approved |
| **Christine Pomeroy** | , Member | **09/23/2014** Date Approved |
| **Steven Burian** | , Member | **09/05/2014** Date Approved |
| **Thomas Rahn** | , Member | **08/25/2014** Date Approved |

and by **Michael Barber** , Chair of

the Department of **Civil and Environmental Engineering**

and by David B. Kieda, Dean of The Graduate School.

# ABSTRACT

Greenhouse gases (GHGs) within the atmosphere are increasing as a result of human activities, per the Intergovernmental Panel on Climate Change (IPCC), and this being a factor in rising temperatures associated with global warming. The general objective of this thesis is detection of $CO_2$ and $CH_4$ by design, deployment and initial calibration of an eddy covariance flux tower (ECFT). While flux measurements are possible, the highly variable atmospheric conditions and the urbanized environment modified the effort of the project from a flux analysis of the data to a concentration analysis. This project began with the design of an ECFT that included a tower structure, 3D sonic anemometer and cavity ring-down spectrometer, constructed and then deployed in three separate locations for surveys conducted on campus, where each location was focused for detection upon the concomitant designated point source (sewer access point).

Three specific objectives of the study with the tower data were 1) determination of the tower abilities to detect $CO_2$ and $CH_4$ above ambient levels, 2) assessment of correlation of the highest ($99^{th}$ percentile) concentrations detected with associated wind directions and establishment of a constant source of emissions, and 3) conclusion of clear detection of the designated point source by the tower. Collection of data began in September 2013 and was completed in March 2014. Because of the small emissions of the designated source, a controlled release of $CO_2$ was executed for tower footprint and threshold investigation.

TABLE OF CONTENTS

LIST OF TABLES

# ABBREVIATIONS

| | |
|---|---|
| C | Celsius temperature measurement |
| $CO_2$ | Carbon Dioxide |
| $CH_4$ | Methane |
| CME | Civil and Materials Engineering |
| CRDS | Cavity Ring-Down Spectroscopy/Spectrometer |
| DTU | Data Transfer Unit |
| E | East |
| ECFT | Eddy Covariance Flux Tower |
| F | Fahrenheit temperature measurement |
| FASB | Frederick Albert Sutton Building |
| FASB1 | Second tower location |
| FASB2 | Third tower location |
| g | grams |
| GHG | Greenhouse Gas |
| hr | Hour |
| Hz | Hertz |
| $H_2O$ | Water |
| IPCC | Intergovernmental Panel on Climate Change |
| km | Kilometer |
| LI-COR | LI-8100 soil flux chamber instrument |
| lpm | Liters per minute |
| m | Meter |
| m/s | Meters per second |
| MH3 | Point source, sanitary sewer access point (manhole 3) |
| MH4 | Point source, sanitary sewer access point (manhole 4) |
| mpg | Miles per gallon |
| mph | Miles per hour |
| $MtCO_2e$ | Metric tonne of $CO_2$ equivalent |
| MWBB | MesoWest Browning Building |
| N | North |
| $N_2$ | Nitrogen |
| PBL | Planetary Boundary Layer |
| Picarro | Picarro cavity ring-down spectrometer instrument |
| ppb | parts per billion |
| ppmv | parts per million volume |
| R | Percentage of footprint |
| S | South |

| | |
|---|---|
| SA | Subsidiary Anemometer |
| SATI/3Sx | Sonic Anemometer/Thermometer Instrumentation |
| SGF | Savitsky Golay Filter |
| SLC | Salt Lake City, Utah |
| TL1 | First tower location |
| W | West |
| WBB | William Browning Building |
| WMO | World Meteorological Organization |
| 2D | Two Dimensional |
| 3D | Three Dimensional |

# SYMBOLS

| | |
|---|---|
| $\eta$ | Quantity being measured (concentration or flux) |
| $\sigma_w$ | Standard deviation of vertical velocity fluctuation |
| $\phi$ | Footprint function |
| atan2 | Arctangent function using 2 variables |
| F* | Non-dimensional footprint function |
| $F_{Hsfc}$ | Kinematic surface heat flux |
| $f^y$ | Dimensional footprint function |
| h | Planetary Boundary Layer height |
| L | Monin-Obukhov Length |
| n | Number of data points |
| P | Percentile |
| $R_C$ | Computed Rank |
| $Q(\hat{x})$ | Source emission strength in the surface-vegetation volume |
| u* | Surface friction velocity |
| UX | Wind speed in the X direction |
| UY | Wind speed in the Y direction |
| X* | Non-dimensional master footprint value |
| x | Dimensional footprint length |
| $z_0$ | Roughness length |
| $z_m$ | Measurement height of tower |

# ACKNOWLEDGEMENTS

The work performed would not have been possible without the guidance and confidence of my advisor, Dr. Brian McPherson. I am grateful for his patience, support, direction and mostly his enthusiasm for science.

I would like to extend my gratitude to Dr. Thom Rahn at the Los Alamos National Laboratory (LANL) in New Mexico, who was brought on as a professional in the field. He provided great insight and was invaluable with respect to his knowledge of tower work. The time he took to mentor and assist with this project was his own and is deeply appreciated.

My advisors Dr. Burian and Dr. Pomeroy deserve to be recognized for their scholastic guidance and overall support. I appreciate their openness and directness.

The undergraduates who worked with this project were priceless, their countless hours with the data collection at the tower and with the Matlab scripting. I wish them the best with their future endeavors and am forever indebted. I would specifically like to thank my colleagues Rich Esser, Amanda Varland, Nate Moodie and Kevin McCormack. The assistance they provided was critical for this project and invaluable.

I would also like to thank my friends and family for their never ending sureness in me, their continued encouragement and love.

Funding for this project was provided by a grant from the U.S. Department of Energy, Project # FC26-05NT42591, and for that I am extremely appreciative.

# CHAPTER 1

# INTRODUCTION AND STATEMENT OF PURPOSE

## 1.1 Introduction

Greenhouse gases (GHGs) are those gases that influence the amount of long wave radiation retained or emitted from the earth's atmosphere. The amount of these gases has been connected to human activities and the United States Environmental Protection Agency (USEPA) reports that levels have been increasing since the Industrial Revolution, which began around 1760. The retention of the radiation within the atmosphere by these gas molecules is believed to be a primary mechanism responsible for observed global average temperature increases. The four gases of most concern are water vapor ($H_2O$), carbon dioxide ($CO_2$), methane ($CH_4$) and nitrous oxide ($N_2O$). The principal focus of this thesis was measurement of atmospheric concentrations of gaseous $CO_2$ and $CH_4$.

According to the USEPA, the United States 2012 total emissions were 6,526 million metric tonnes of $CO_2$ equivalent, where $CO_2$ accounted for 82% and $CH_4$ accounted for 9%. The largest source of carbon dioxide emissions is electricity generation. Methane is primarily released by combustion of natural gas and other petroleum products (followed closely by agricultural digestive process release by farm animals). As the human population continues to increase, the amount of greenhouse gas emissions is anticipated to increase, leading to accelerated global temperature increases.

Another important aspect of greenhouse gases is that they remain in the atmosphere for extended periods of time. Methane is estimated to remain in the atmosphere for 12 years, whereas carbon dioxide has an unknown lifetime because it is absorbed and not destroyed. This long-term detainment likely magnifies rates of warming effects.

The concentrations of these gases are monitored continuously because they are key indicators of how the climate is changing. The Intergovernmental Panel on Climate Change (IPCC) uses an averaged annual global concentration for demonstration and modeling purposes. The IPCC $CO_2$ value in 1950 was 311.2 ppm, compared to the 2011 value of 390.5 ppm, a 25% increase over a 61-year period. Methane was at 1162 ppb in 1950 and the 2011 average value was 1803 ppb, corresponding to a 55% increase over the same period of time. It is clear from this research and monitoring of the atmosphere that these gases are increasing. Increased greenhouse gases are only one contributor to climate change. However if human activities responsible for inputs can be reduced by locating and monitoring for understanding and then elimination, it is possible that atmospheric concentration increases will be impeded.

Generation of these gases by combustion can be quantified, but for some phenomena such as leakage from natural reservoirs or from anthropogenic systems such as sewers, emissions are typically not measured. Such "fugitive" emissions are not included in GHG inventories, unless as estimates with high uncertainty. One approach to detecting sources of fugitive emissions and measuring the quantity of such emissions is with eddy covariance flux tower (ECFT) technology. The eddy covariance or eddy flux method entails the measurement and calculation of vertical turbulent fluxes (or swirling of a fluid around an obstacle and the reverse current) in the atmosphere. The covariance

exists between the wind velocity and gas concentration variation.

The first interest in measuring gas fluxes by use of eddy flux towers began because of the complexity of the earth's surface carbon cycle and its extensive system of sources and sinks. The tower idea became a tangible scientific venture with monitoring and measuring attempts beginning in the 1950s. Initial projects were focused on $CO_2$ and water vapor exchanges between crops and the atmosphere. According to Baldocchi et al. (2001) the concept of a flux gradient over an agricultural piece of land was first documented in the 1960s by several researchers, including Inoue (1958), Lemon (1960), Monteith and Sziec (1960) and Denmead (1969). This work then led to research by others who investigated fluxes associated with different types of natural areas, such as forests and marshes. There were multiple deficiencies within the methods used in the early studies and incomplete understanding mostly due to limitations with equipment. Advances in instrumentation development, especially computers, sonic anemometers and infrared spectrometry, rapidly increased in the 1980s and 1990s and revitalized the flux undertaking (Baldocchi, 2001).

Encouragement and growth was procured when a group of scientists collaborated to create Euroflux in 1996. This group was quickly followed by Ameriflux in 1997. The success of associated data sharing and information gathering attracted the attention of NASA and led to funding of combined efforts in a project called Fluxnet in 1998, which continues and thrives today.

There are several advantages to ECFT technology for GHG monitoring and measurement, including minimal maintenance, ease of operation and ability for long-term surveys. A typical tower consists of a sonic anemometer, fast response instrumentation

(data available instantaneously with multiple measurements per second) and tower structure. The height of the tower is a primary factor in the maximum possible effective size of area of study, also called the footprint. However, atmospheric inconsistency and surface roughness are significantly influential on the footprint. The primary function and ultimate definition of the footprint function is the integral equation of diffusion (Pasquill & Smith, 1983; Vesala, 2008; Wilson & Swaters, 1991), or

$$\eta = \int_x \phi\,(x;\hat{x})Q(\hat{x})d\hat{x}\ ,$$

where $\eta$ is the quantity being measured (either concentration or flux) at distance vector $x$ and $Q(\hat{x})$ is the source emission strength in the surface-vegetation volume. The footprint function is represented by $\phi$ and is correspondingly either concentration or flux. Because of the high irregularity of the sources of GHGs, the dense building infrastructure and associated variability of atmospheric conditions on the University of Utah campus, the tower developed and deployed for this project was used to measure GHG concentrations only (not fluxes). Thus, for this study, $\phi$ and $\eta$ are gas concentration, specifically.

Many studies have focused on quantitative estimation of tower footprints, and four primary types of evaluation are detailed in the literature. These include analytical models, Lagrangian stochastic particle dispersion models, large-eddy simulations and closure models (Vesala, 2008). Several variations of these four main types also exist, reflecting efforts to reduce computational requirements. The tower footprint can often be estimated with such models, but actual field conditions usually require extensive adjustments and refinements, particularly if a very specific area must be included in the footprint. If the emissions source is unknown and a general area is the focus, then the area of interest may be roughly estimated or chosen based upon other priorities. Key

assumptions for developing these models (or aspects of models) include homogeneous terrain with little to no elevation changes and consistent vegetation. Numerous studies have been conducted and literature published with in-depth analysis and discussion of flux theory and associated mathematical approaches to the four differing models, but for sake of brevity these are not discussed in this thesis.

With the increasing global population and associated exploitation of undeveloped land, interest in greenhouse gas fluxes now includes those associated with urban settings. Efforts to model urban areas are highly challenging, especially considering that every urban situation is unique. Despite numerous obstacles, urban flux measurements have been conducted, but resulting data reflected unexpected and inconclusive values, including negative fluxes (Finnigan, 2004). The urban environment presents challenges that are not often seen or quantifiable by mathematical expression. The surface roughness, surface cover and land usage within an urban area usually include a wider ranging of variables than those found within an undeveloped area. Activity, movement and point source mobility associated with greenhouse gas emissions exist and fluctuate highly in an urban area. To increase difficulties, the height of data collection is highly influenced by the urban environment and associated changing atmospheric conditions or wind movement with height. It is recommended by Grimmond et al. (2002) that instrumentation be situated at least two times the average height of the roughness elements (buildings and trees) and that terrain be as homogeneous as possible to assist with meaningful measurements. This recommendation alone provides tower height difficulties.

The original and initial objective of this thesis project was to design, develop and

deploy an eddy covariance flux tower for quantification of fugitive greenhouse gas fluxes from the University of Utah sewer system, and to quantify tower footprint sizes for different emission rates. However, determination of robust values of gas fluxes was extremely difficult because of the complexity of the campus setting, including the relatively dense number of buildings, the highly variable terrain, atmospheric inconsistency, and vegetation dissimilarity. Therefore, the flux calculation goal was abandoned and instead focus shifted to tower footprint analysis and application of the flux tower was limited to measurements of concentration over time. The tower was designed and erected in three separate locations on campus intended to detect and measure emissions from specific emission source points, sewer access covers ("manholes"). The tower locations were chosen based on rough initial estimates of footprint size and anticipated atmospheric conditions specific to each site. This thesis describes the design and erection of the project tower, the three selected site locations, and evaluation of the point source fugitive gas releases data. Surveys of the three locations resulted in 36 days of data collection and associated analysis. To gain additional insight about footprint size (dimensions), a set of controlled $CO_2$ release tests was conducted.

## 1.2 Statement of Purpose

The purpose of this research is to design, deploy and calibrate an ECFT for detection and measurement of $CO_2$ and $CH_4$ emissions within the urban environment of the University of Utah campus, with specific focus on an existing and available point source of fugitive greenhouse gas emissions, the campus sewer system. It will also

provide information pertaining to tower concentration footprint in the urban environment, an area with minimal study.

Fluxes of $CO_2$ and $CH_4$ from specific sewer access points (manholes) on campus were previously measured by placing a modified soil flux chamber directly on the access points (Varland, 2014), and found to exhibit elevated emissions of $CO_2$ and $CH_4$. An initial hypothesis of this thesis was that these elevated emissions could be detected and measured with an ECFT flux tower located tens or even hundreds of feet away from the source. However, over the course of testing, the concentration values were chosen over flux values. This detection and monitoring technique may be applicable to leakage observation in future endeavors, such as oil and gas production fields. The campus urban setting is not typical for detection studies and this case study is intended to provide a basis for future research, specifically for threshold estimation and tower concentration footprint approximation. The detection limits of the tower were investigated with a controlled release of $CO_2$ and threshold limit established for one particular tower setting at the campus study area.

# CHAPTER 2

# INSTRUMENTATION AND TOWER DESIGN

The primary objectives of this project focused on surveys of atmospheric carbon dioxide and methane gas concentrations, but for these goals original equipment needed to be designed and calibrated. This instrumentation is described in this chapter. The design included a custom-built tower, which elevates detection from ground level to a height above ground, increasing the area of detection.

## 2.1 Instrumentation

The main components for collection of data for analysis of this project include a three-dimensional (3D) sonic anemometer and a cavity ring-down spectrometer (CRDS). A soil flux gas analyzer (SFGA) facilitated point source quantification. An explanation of the basic operations and requirements of the three instruments for this project are included in this section. Additional and more in-depth information may be obtained from the manufacturer operation manuals for each instrument (LI-COR, 2007; Picarro, 2012).

### 2.1.1 Anemometer

Typical anemometers provide wind information in two dimensions (2D) and operate by mechanical means. These are inexpensive and readily available for everyday use. The primary anemometer on the tower is described in this section; two additional and separate anemometers for gathering additional wind data are described in Section 2.4.1.

Modern sonic anemometers are electronic, as opposed to mechanical. Specifically, a sonic anemometer emits ultrasonic pulses from probe assemblies, at specific time intervals. Three probe assemblies measure wind along three perpendicular axes for a three-dimensional (3D) interpretation of the wind. The advantages of nonmechanical parts include increased measurement accuracy and decreased maintenance. The availability of a 3D wind field provides more options with respect to wind interpretation and associated calculations.

The sonic anemometer used for this project is the Applied Technologies, Inc. Sonic Anemometer/Thermometer 3Sx, fabricated at the company headquarters in Longmont, Colorado. It will be referred to as the SATI/3Sx. It was built specifically for the University of Utah and this project, but follows the regular design standards of the company. It is an orthogonal design and is shown in Figure 2.1. The three axes contain ultrasonic transducers made of piezoelectric crystals housed in stainless steel with tolerances between all pieces at a maximum of 0.1 degrees, ensuring orthogonality. Each probe is mounted to the end of a square bar made of weather resistant metallic material, attached to a mounting bar that is 30 inches long and constructed with the same material and shape (Figure 2.1). This configuration enables removal of the anemometer without

disassembly of the entire tower. The cable for power and data transport connects at the end of the instrumentation bar and runs inside the mounting bar.

The orientation and explanation of information collection assumes the U axis corresponds to the "X" direction, V to the "Y" direction and W to the vertical direction, "Z." An advantage of orienting the probes 90 degrees to each other is simplified interpretation algorithms compared to nonorthogonal probes. For this model, it is important to note that the vertical velocity is not calculation dependent but rather is a direct measurement with alignment accuracy of greater than ±0.1 degree. The accuracy of the measured wind velocity is ±0.01 m/s with ±0.1 degree accuracy for direction (orthogonality). Resolution of 0.01 m/s wind speed and 0.1 degrees for wind direction. The absolute temperature measurements have ±2 degrees C accuracy and 0.01 degrees C resolution per the operator's manual specifications by Applied Technologies, Inc. Revision J2.

Calibration of the anemometer is simple and was performed in the lab before deployment in the field. The calibration consists of a "zero-air chamber" provided by the manufacturer and is compatible for all three probes. The system prompts the operator for information as the "zero-air chamber" is placed over each probe. Special maintenance is not required for this particular anemometer; however it should be handled with care because the transducers are crystalline and easily break if dropped. The alignment of the probe arms is also a critical factor and care is necessary when placing the SATI/3Sx on (or removing off) the tower and during storage. Once the instrument is mounted on the tower it is rugged enough to withstand typical weather events. It is also important to inspect the probes for interferences such as bird droppings or snow accumulation, as

these will provide skewed readings.

The anemometer has a low-enough power requirement to be powered by battery. For most applications in this research, the uninterrupted power source used with the project computer and other instrumentation was utilized.

The SATI/3Sx connects directly to the CRDS and output data are collected time-sequentially with the CRDS output data. The data rate used was 10 Hz to match the CRDS. The two instruments were synchronized upon installation and the additional output information of the anemometer is comprised of the wind velocities in the UX, UY and UZ orientations, temperature and the speed of sound (not utilized in this project).

### 2.1.2 Cavity Ring-Down Spectrometer

The main equipment used was the cavity ring-down spectrometer (CRDS) gas analyzer G2311-f by Picarro© with a required external vacuum pump. Picarro is a company specializing in gas measurements and instrumentation, headquartered in Santa Clara, California. The cavity ring-down spectroscopy (CRDS) technology is patented by Picarro and is the basis of measurement for the G2311-f evaluation of greenhouse gases, specifically carbon dioxide, methane and water vapor. The CRDS is an optical absorption technology where the instrument recirculates laser light multiple times through the gas sample, creating a long path length for interaction of the light with the gas sample. The increased interaction time allows a high sensitivity of gas concentration measurement, which is achieved by determining the extent to which the laser wavelength spectra are altered by increasing concentration of $CO_2$, $CH_4$ and/or water vapor. Concentration readings are provided in parts-per-billion with $CO_2$ precision of 200 ppb,

$CH_4$ of 3 ppb and $H_20$ of 6 ppb + 0.3% of reading as per the Picarro© G2311-f User's Guide. It is an open system and the effluent air is released into the atmosphere after measurement.

The flow of the instrument can be switched between "Flux" and "Flux (Low Flow)" with gas flow rates corresponding to 5 and 0.25 lpm, respectively, and both flow settings were used in this project. Calibration of the instrument (beyond factory calibration) was not required as per instruction by the manufacturer.

The analyzer requires constant power and is sensitive to water. Therefore it was operated and monitored by a student researcher at all times and an interrupter was installed between the CRDS and the power source. The operation of the instrument requires a warm-up period of approximately 15-25 minutes, with external pump turned on and the sampling tubing and anemometer connected. Containing the CRDS in a simple garden wagon and using extension cords for power requirements accomplished portability required for this particular research application. The sampling tube and anemometer remained on the tower even between surveys, for convenience. After each survey, the CRDS was turned off and stored indoors; the tower typically stayed on site except during prolonged breaks between surveys.

The analyzer is connected to a monitor for easy operator interaction and readouts are presented real time for the gases in concentration versus time. Measurements of carbon dioxide and methane were reported at 10 Hz for this project. Data were output into files corresponding to sampling times and included 31 variables, stored on the instrument computer for retrieval when necessary.

The CRDS was used for tower measurements and it was utilized with flux

chamber measurements pertaining to point source quantification, conducted in a separate study (detailed in the following section).

### 2.1.3 Soil Flux Gas Analyzer

Readers are referred to Varland (2014) for details regarding the design of a flux chamber and associated gas flux and emissions data. The soil flux gas analyzer (SFGA) was utilized in a secondary role for this is project, as it was not used for tower measurements, but rather only for point source quantification. The instrument employed for the secondary role in this study is the LI-8100A, manufactured by LI-COR®, Corporate. LI-COR® is an instrumentation company headquartered in Lincoln, Nebraska that creates environmental testing equipment. The LI-8100A is designed as an automated soil $CO_2$ flux system with a chamber for gas measurements. The system is a closed system that is designed to measure the soil flux of carbon dioxide with an infrared gas analyzer that detects and records the changes over time in the concentration of carbon dioxide (or water vapor) within the chamber. The sampling air is collected by inlet tubing, analyzed and then returned to the chamber by outlet tubing. The LI-COR® system from the manufacturer is provided with a chamber created by LI-COR® for soil measurements. Multiple settings within the LI-COR® software system are designed to be tailored by the researcher to reflect the specific test. The time of data collection can also be changed by the researcher depending on location and other site-specific requirements. This flexibility was conducive to expansion of the soil parameters to non-soil situations.

For this project, the LI-COR® instrumentation was used in conjunction with a new chamber designed and developed specifically to measure fluxes from sewer access covers

(a.k.a. “manholes”). The need for a project-specific chamber was based on the size of the sewer access covers on the University of Utah campus. Each of the sewer access covers is approximately 26.5 inches in diameter; for complete coverage, a chamber of 26.5 inches in diameter was necessary. This was accomplished with a common 55-gallon plastic garbage receptacle (can). The garbage receptacle was modified with inlet and outlet air ports for connection of the tubes from the LI-8100A. For a full description of the chamber design, readers are referred to Varland (2014).

The raw output data of the LI-8100A include carbon dioxide and water vapor concentration with respect to time. Therefore, it was also utilized at the sewer access point MH4 to gather continuous $CO_2$ concentration measurements. For this specific application, a chamber was not used, but rather a sample inlet tube was simply inserted into one of the venting holes in the cover. Concentrations were measured at a depth of approximately 6-8 inches below the cover. The air outlet tube was also inserted into a vent hole and the gas was returned to the sewer system to mimic the closed system design.

For the remainder of this project this instrumentation will be referred to as the SFGA. These three components will be referenced for the remainder of the research. The tower configuration and design are important with regard to the SATI/3Sx and the CRDS, and these are described in the following section.

## 2.2 Design and Construction of Tower

The tower for this project was expected to be a temporary structure with periods of implementation ranging from weeks to months. It was deployed in the northern section of the University of Utah campus and the intent was to be as nonintrusive as

possible. Three locations for monitoring and detection of fugitive greenhouse gases were occupied over the course of the project, each with a point source specific to tower location.

The project tower is composed of six major components; 1) 3D sonic anemometer with mounting bar, 2) mast, 3) prefabricated mast mount base, 4) stabilizing system, 5) sampling instrumentation and 6) power source. Each of the components is discussed in this section with relationship to the tower design.

The anemometer is a 3D Sonic Anemometer manufactured by Applied Technologies, Inc. A detailed description is provided in the Instrumentation Section 2.1.1. It is composed of a probe with extension arm and a separable mounting arm 30 inches in length. It is located at the top of the tower and connects to the mast at a 90 degree angle. The mounting arm connection to the mast was not provided and therefore was fabricated at the University of Utah. The connection involves a steel plate and two U-bolts that fit around the mast. Four screws connect the plate to the mounting bar at a transferable location. The hardware is tightened to secure the mounting arm to the mast. After initial deployment, it became clear that a means of leveling was required. Thus, a bubble level was also installed on the mounting arm to enable visual inspection of horizontal alignment of the bar after the tower was deployed. It is critical that the anemometer be removed from the mounting arm when relocating the tower because inaccurate readings may result if the anemometer probe arms are bent or damaged to any extent. The anemometer seems rugged enough to withstand continuous mounting on the tower for extended periods. Figure 2.2 is a photo of the configuration of the top of the tower.

The mast consists of a 10-foot-long aluminum pole with a 2" outer diameter and 1.5" inner diameter. The anemometer arm is mounted at the top (Figure 2.2), and the bottom of the mast is attached to the prefabricated base by a manufactured MC-200 Mast Clamp. A separate mast clamp was used for guy wire connection (Figure 2.3).

The base of the tower is the Tipper$^{TM}$ TP-24 manufactured by Penninger Radio. This base is designed for portable (nonpermanent) deployment and facilitates minimal relocation efforts. As depicted in Figure 2.3, it expands for use and folds up for transportation. The base system is used by assembling the 10-foot mast on the ground, aligning the mast horizontally with the base pole and securing with a MC-200 Mast Clamp. A pivoting system then allows the mast to be moved into the vertical position and locked into place. Four stabilizing legs may be adjusted to terrain and may be staked for added stability. The system is comprised of stainless steel components and is more than sufficient for this specific application, inasmuch as the manufacturer designed it for a maximum 36-foot mast.

The stabilizing system is comprised of three separate parts: stakes, guy wires and prefabricated mast clamps. The stakes are 18-inch-long steel from a local hardware store and seven were used for this project. Four were used with the prefabricated base and three were used for the guy wires. The guy wires are 1/8-inch stainless steel and include turnbuckle and shackle adjustment components. The mast clamp to which guy wires were attached was approximately 10 feet above ground level for the surveys on the University of Utah campus. The guy wires were hand-tightened and staked into the ground between 11 and 13 feet radially out from the base of the tower. The adjustment system was then used to additionally stabilize and assist with horizontal alignment of the anemometer.

Figures 2.5 and 2.6 are photos showing the full tower assembly.

The instrumentation associated with the tower is the CRDS, Picarro© G2311-f. Details regarding the sampling process and abilities of the CRDS are explained in Section 2.1.2. The sampling tube is attached to the center of the anemometer vertical measurement probe arm and runs along the mounting arm and down the mast to the CRDS. It is secured with electrical tape and plastic zip-ties. The tubing is NYCOIL, nylon-tubing (1/8-inch outer diameter and 3/32-inch inner diameter). The anemometer cable was attached to the mast and secured along with the sampling tubing. The anemometer data were collected by the CRDS, using a RS-232C connection. The CRDS is not waterproof, and thus surveys were somewhat weather-dependent. A wagon carried the CRDS, for portability (Figure 2.6).

Power was required for operation of the instrumentation of the tower, including 12 VDC for the anemometer and 110 VAC for the CRDS requires. A generator was employed for initial measurements, but to eliminate measurement of $CO_2$ emissions from the generator, an extension cord from buildings within the vicinity of the tower proved to be an effective power source. A surge protector with battery backup capabilities was necessary and retained.

Students and faculty/staff were walking on campus during the majority of tower measurements and thus, for safety purposes, the tower guy wires and stakes were outlined with orange caution tape and orange construction cones were placed at areas where pedestrian traffic would encounter the extension cords. Maintenance employees were also aware of the tower for lawn care.

## 2.3 Tower Footprint

The tower was deployed at three locations. The design of the tower was intended to maximize the area monitored. Specifically, the actual area that the tower can detect and measure gas concentrations effectively is referred to as the footprint. Footprint estimates for flux towers are typically calculated using complex modeling approaches.

The determination and calculation of flux tower footprints has been an issue of investigation with significant documentation since the 1990s (Baldocchi, 2001). Footprint estimation is particularly difficult for urban environments (Finnigan, 2004). Assumptions associated with calculating a tower footprint typically included a homogeneous and level terrain and ideally, a flux tower area would be similar to an agricultural field. This would provide measurements of an average for the amount of gas emitted over the monitored area over time (the flux). The height of the measurement, atmospheric conditions and surface roughness are three keys factors influential to data collection.

Multiple approaches are used to establish a footprint function and four model types have emerged as the most successful and accepted. These include analytical models, Lagrangian stochastic particle dispersion models, large-eddy simulations and closure models. These models are often very complex and tedious, requiring large efforts by researchers to establish a highly probable footprint dimension prediction (Vesala, 2008). In response, several approaches to simplify the models have emerged and specifically for this study the parameterisation by Kljun et al. (2004) will be employed, along with a corresponding online calculator published in conjunction with the Kljun et al. (2004) research. The Kljun et al. (2004) parameterisation is based on footprint values that utilize the Lagrangian method and the online calculator was developed and created

with previously evaluated footprint model results by Kljun et al. (2004).

Multiple variables describing the area of observation are implemented to establish the tower footprint. Greater description and knowledge of the study area for inclusion to the model is believed to result in greater precision and accuracy of footprint determination. The main parameters employed for this study are basic and fundamental variables, and include the height of the receptor, atmospheric stability and surface roughness. These main parameters are key in the process of footprint estimation and will be used for an evaluation that will enable the initial design of the project tower and location determination.

The initial tower design employs the use of the parameterisation by simplifying the area of interest to a homogeneous, nonurbanized area. This assumption is necessary in order to utilize the Kljun et al. (2004) online calculator, described below in subsequent sections, for predicting flux footprints for passive scalar emissions. (http://footprint.kljun.net/varinput.php).

The following section will discuss the Kljun et al. (2004) online calculator in more detail and show how it was utilized for the project specific flux tower. The required input variables and associated restrictions are examined along with the inputs used for the project tower. The output of the calculator is provided and explained to estimate an appropriate but preliminary tower design.

### 2.3.1 Project Specific Tower

The Kljun et al. (2004) online calculator was used to develop an initial tower design. The values chosen for the tower will be discussed and then the results from the

calculator presented and restrictions checked. Table 2.2 shows a breakdown of the input parameterisation variables.

The standard deviation of the vertical velocity fluctuations (σw) was used as 0.54 because it was the value given in the example and the actual fluctuations are difficult to estimate in an urban area without extensive wind flow modeling efforts.

The surface friction velocity (u*) has a minimum value of 0.2 m/s for use in the calculator. The influence it has on the footprint size is positive; specifically, footprint size increases as the velocity increases, a value of 0.3 m/s was used because it was just above the minimum value and 0.3 m/s is the value used to calculate L, the Monin-Obukhov length, (which is related to buoyancy forces on turbulent air flow in the lower atmosphere) with the online calculator developed by SHODOR (a national resource for computational science, http://www.shodor.org/os411/courses/_master/tools/calculators/moninobukhov/).

The measurement height (zm) restriction is a minimum of 1 meter but less than the planetary boundary layer. This keeps measurements within reasonable tower heights. A substantial consideration when determining the tower height is the cost and feasibility of construction and the ease with which the tower can be relocated. The height of 3.66 meters would not require an elaborate tower construction or base structure and it is an even height that does not necessitate special construction. The security of the instrumentation at 3.66 meters above ground is also better, because the anemometer and other tower-top components are not within easy reach of students (humans) and animals. The urban setting of the campus project area also restricts the height of the tower because the footprint cannot be too large or it will detect too many gas sources for effective

interpretation. The wind patterns associated with an urban environment are also difficult to assess and with a shorter height leading to a smaller footprint, the wind interpretation can hypothetically be decreased in complexity. The mast used is 10 feet and the base sits 2 feet above ground, leading to a total of 12 feet or 3.66 meters.

The planetary boundary layer (PBL) height (h) value input did not impact the calculated footprint size. The restriction associated with the planetary boundary states that it must be higher than the tower height. Normal values of the PBL are 1000-2000 meters and so an average of 1500 was used (much higher than the project tower), even though it does not appear to impact estimates by the Kljun et al. (2004) online calculator.

Values of roughness length (z0) are readily available for most vegetation and field type applications. These range from 0.0001 meters for a flat snowfield, 0.065 meters for a matured crop, and 0.8 to 1.6 meters for a matured pine forest (Wiernga, 1992). However, since this tower was deployed in an urban setting with buildings, trees, multiple materials and human activity, the value of 2 was chosen (Table 2.2). This number is associated with "center of large towns and cities, irregular forests with scattered clearings" and basically chaotic environments (Stull, 2000).

The R value is a ratio reflecting the percentage of the footprint included in detection, and it must be 90% or lower. This input is a statistical evaluation. Including values above 90% result in large variations with low correlation numbers and values for lower percentages result in better statistics, but are not realistic. The value of 80% was used, as shown in Table 2.2.

The final restriction to verify is that $-200 \leq z_m/L \leq 1$, where L represents the Monin-Obukhov length. Utilization of the online calculator developed by SHODOR

resulted in an L = 40.13 meters. This corresponds to $z_m/L$ equal to 0.091, which falls within the required range.

Using the online footprint calculator with the input variables previously described and presented in Table 2.1, provided the following results for tower footprint, shown in Table 2.2. The results are shown graphically in Figure 2.7, with distance on the x-axis and estimated flux on the y-axis. The value of 16.2 meters (for xmax) represents the location for peak detection and the value of 35.3 meters (for xR) is the extent or threshold of the footprint with regards to the R value percentage (80%), shown as the orange line. The estimated flux values shown on the y-axis are disregarded due to the actual location of the tower within an urban environment and the calculator being designed for a homogeneous terrain.

The final value of estimated flux measurement footprint via the Kljun et al. (2004) online calculator was 35.3 meters (116 feet) for a 3.66 meters (12 feet) tall tower. While this footprint estimate is for measurement of flux specifically, this thesis project was limited to concentration detection and interpretation, for simplicity. And, more specifically, the goals of this project did not include making advances in flux calculations, but rather for design and deployment of an effective method for detecting $CO_2$ and $CH_4$ leaks. According to Vesala (2008), estimated concentration footprints exceed those for flux footprints, and thus the 35.3 meter footprint is conservative. However, the urban characteristics of the project area are only accounted for by the roughness variable for the parameterization (Table 2.1), which may not be sufficient. In general, the wind is highly influenced by buildings, trees, sidewalks and human interactions, and therefore the actual footprint may actually be less than the calculated

value; hopefully, this limitation is offset by the conservative approach of using a flux footprint for a concentration survey. Regardless, the footprint was estimated just to serve as a general guideline for tower placement and location determination.

## 2.4 Tower Surveys

There are multiple factors to consider when siting a tower and taking measurements. The major components related to this study include height of the tower, predominant wind direction, terrain and point source. Because this tower was situated on campus, the effects of construction, a need for easy and/or rapid relocation, low impact and safety concerns were addressed when locations were chosen.

First, the point source was established as the sewer line running east and west between the Student Union Building parking lot and the Civil and Materials Engineering (CME) Building. The assessment of the area surrounding this sewer line limited the possible locations of the tower. Figure 2.8 shows the sewer line and highlights the two sewer access points (MH3 and MH4) that were determined to be favorable options for tower placement with respect to power requirements, safety and effective detection.

During the 8-month period of tower surveys on campus, the tower was deployed in three different locations. The first was targeted to detect emissions from MH3 and the other two were aimed towards MH4 releases. These are shown on Figure 2.8 (star symbols). The tower hardware configuration, including the height of instrumentation, was identical for all three locations. At each location the anemometer was positioned to face towards the point source and directed into the predominant wind direction. The coordination of these two factors was intended to maximize gas concentration detection

sensitivity. A mean streamline coordinate system is one way to orient the anemometer with the x-axis parallel to the dominant wind direction, the y-axis averaging the nonlevel terrain slope and the vertical axis at the 90 degree orientation (Wilczak, 2001). The deflection of the anemometer from north was recorded for resultant calculations.

The estimated footprint of the tower was preliminarily calculated from the parameterisation calculator described previously and was used for guidance in measurement distance from the point source. The height of the tower remained constant at 3.66 meters (12 feet). This height enabled a tower that could be transported and erected by one or two people.

The details of each tower location are provided in Table 2.3, including the latitude and longitude, dates of deployment at each location, distance to designated sewer access point source and the angle of the anemometer, offset from north. Measurements were conducted at TL1 for 19 days within the period of deployment at that location. Surveys at FASB1 took place for 15 days and FASB2 for 3 days, within the respected time frames of each location deployment. The maximum $CO_2$ level measured was 500 ppmv at FASB1, whereas the maximum $CH_4$ level measured was 2.87 ppmv at TL1. Details of data analysis are provided in Chapter 4.

The information from Table 2.3 is shown schematically in Figures 2.9, 2.10 and 2.11 for each tower survey location. Each location differs in distance from point source and anemometer angle, which was estimated from dominant wind direction and source location. The tower was relocated from TL1 to FASB1 because wind direction was not dominant from the south, as previously researched and results of detection could not be anticipated. The distance from the point source to the tower at TL1 was also an issue

because it resided at the fringe of the calculated flux footprint. The FASB1 location ensured that the point source MH4 was within the calculated footprint. This location was occupied until winter weather disrupted measurements and it was taken down. A negative aspect of the FASB1 location and the point source MH4 was that the Frederick Albert Sutton Building (FASB) and the William Browning Building (WBB) block wind from the west and may have create eddies. The sidewalks may induce a bit of "wind tunnel" effects, and a major campus road is nearby. In order to address the wind variability and assess wind direction, two subsidiary anemometers were purchased and assembled in January 2014. The two anemometers were sited specifically to interpret wind variations in the vicinity of location FASB2, at which the tower was deployed in March 2014 and remained for the remainder of the project.

### 2.4.1 Subsidiary Anemometers

The area of campus around the point source MH4 is an urban site with trees, sidewalks, signs, buildings and undulating terrain. Initial data for atmospheric conditions were gathered from two existing weather stations located on the northern side of campus. One weather station is located on the roof of the William Browning Building (WBB; seven stories tall) and the second is situated on the roof of the Civil and Materials Engineering (CME) Building (four stories tall). Positioning the weather stations above obstructions is a common practice when general weather data are required. Given their height, the wind data collected by these two weather stations are more useful for a whole-campus-scale wind assessment. Two additional or subsidiary anemometers (SAs) were set up close to MH4 for continuous wind direction data collection. These ground-level

anemometers were intended to provide a better assessment of how wind is affected by obstructions in the area of interest. Figure 2.12 shows the locations of the weather stations and SAs.

Two subsidiary anemometers (SA#1 and SA#2) were acquired for localized wind analysis. SA#1 was positioned directly above MH4 and SA#2 was located at the FASB1 tower location. These SAs were manufactured by Davis Instruments, each consisting of a wind vane (for direction) and wind cups (for speed) for two-dimensional data collection. Each anemometer was installed on a 6-foot tall fence post with SA#1 at 60 inches off the ground and SA#2 at 64 inches from the ground, (Figure 2.13).

North was calibrated separately for each anemometer as 360 degrees. Each installation used a solar panel to power a transmitter that sent data to a Davis Instruments Envoy8x receiver physically connected to a dedicated computer located in an office of the CME Building. Only one receiver was needed to collect data from both setups. The MySQL database was used for data analysis. The streaming data can be viewed in real-time, as it is transmitted, using the "Weather Data Transfer Utility (DTU)" software by Davis Instruments. Output data included wind speed (average value over 10 second period), high wind speed (maximum value over 10 second period), high wind direction (wind direction associated with high wind speed), dominant wind direction, inside/indoor (location of receiver) temperature, inside/indoor humidity and barometric pressure for each ten second interval. These data were analyzed in February/March and then, during March, the tower was relocated to FASB2 based on analysis of wind data from the two subsidiary anemometers.

### 2.4.2 Subsidiary Anemometer Wind Analysis

Data analysis began with wind information collected by the SAs. All data were transferred from the MySQL database into Excel for manipulation and evaluation. Data were extracted for each entire day (24 hours) and appropriate conversions completed (for example, from hectometers per day to miles per hour wind speeds). The "wind speed" and "high wind speed" were both graphed with respect to time for visual inspection. Then the wind direction was evaluated. The instrumentation recorded the wind direction in numeric intervals, where a number was given corresponding to a direction; the interpretation of the numbers is given in Table 2.4.

Resulting data were graphed as the values 0 thru 15 versus time for visual interpretation. The average wind direction and wind speed were also calculated for each SA. However, the wind direction data were better expressed as percentages in the form of a pie chart serving as a histogram to exhibit dominant wind direction.

This analysis was performed daily for each SA individually, and then repeated for a truncated time frame of 10am to 7pm and 10am to 5pm. The more specified time frames corresponded to the intervals of actual tower data collection and more closely represented wind direction associated with the data collection sessions. The data from the established MesoWest weather station MWBB was included in the analysis in an attempt to illustrate impacts of ground-level interference (buildings, trees, etc.) on wind direction.

The weather station MWBB is located approximately 100 feet above ground level and is operated by the MesoWest cooperative project. MesoWest is a project run by a group of researchers at the University of Utah, weather forecasters at the Salt Lake City

National Weather Service Office, the National Weather Service Western Region Headquarters and other persons associated with agencies or universities and firms. This group began in 1996 and provides weather observations across the United States. Archived weather data are also provided via the group website, www.mesowest.utah.edu/. All data used for the MWBB weather station were downloaded from this site for comparison with the two subsidiary anemometers specific to this project. The data underwent the same analysis as the data from SA#1 and SA#2.

The complete weather analysis was conducted for most days from January 22 through March 3, 2014. A comparison table with dominant wind direction for each station and each time frame is shown in Table 2.5.

Further investigation suggested that the daily average wind direction for SA#1 fluctuates evenly between the north-northwest and northwest. The truncated daytime intervals are both predominantly north and north-northwest. SA#2 has daily averages almost exclusively from the northeast. The truncated daytime intervals are both dominant for the north-northeast direction. MWBB measured wind primarily from the west.

A direct comparison of SA#1 and SA#2 indicate that the two anemometers are not reading wind from the same direction, but the data nevertheless appear to be consistent. The urban setting of the measurements influences the slight directional difference. Additionally, the building appears to inhibit wind from the west (indicated by the MWBB weather station) that would reach the other two stations. The MWBB readings were steadier than the two SA readings. This is most likely due to the location within the atmosphere. The MWBB station is apparently above localized disturbances, as it is

attached to a tower that is approximately 20 feet in the air above the roof of the building where it is mounted. At this location, the amount of turbulence is less, compared to the two subsidiary anemometers that are 5 feet off the ground and surrounded by trees, buildings and other features. The MWBB station is located within the planetary boundary layer and the SAs are within the roughness layer. The difference is in the atmospheric levels or the height within the atmosphere (or above the ground) of measurement and how it is impacted by the Earth's surface. The MWBB weather station has been established above major surface impacts and even though influences do exist, they are minimal compared with the roughness sublayer. The vertical velocities influencing the wind direction within the roughness sublayer are significant because of shear stresses related to inconsistent densities, frictional surfaces, wind tunnels and blockages and movements associated with human activities, which are at ground level.

Another factor with respect to comparison between the three anemometers is the scale to which they collect data. The two subsidiary secondary anemometers apply to the "microscale" (less than 1 $km^2$ in area), whereas the MWBB station operates at the "mesoscale" (less than 1000 $km^2$ in area). Based upon all of the different factors for the weather stations, the MWBB site was not used to assist with relocation of the tower at the FASB2 site, but was used to gain insight to wind behavior within the tower area.

The tower was moved approximately 14 feet west from the previous location, FASB1. The orientation of the anemometer remained towards the point source MH4 and was measured at 6 degrees from north. The tower height remained at 12 feet. The final factor in influence of detection from the point source to the tower is the emission of the gases $CO_2$ and $CH_4$ from the point source, which will be discussed in Chapter 3.

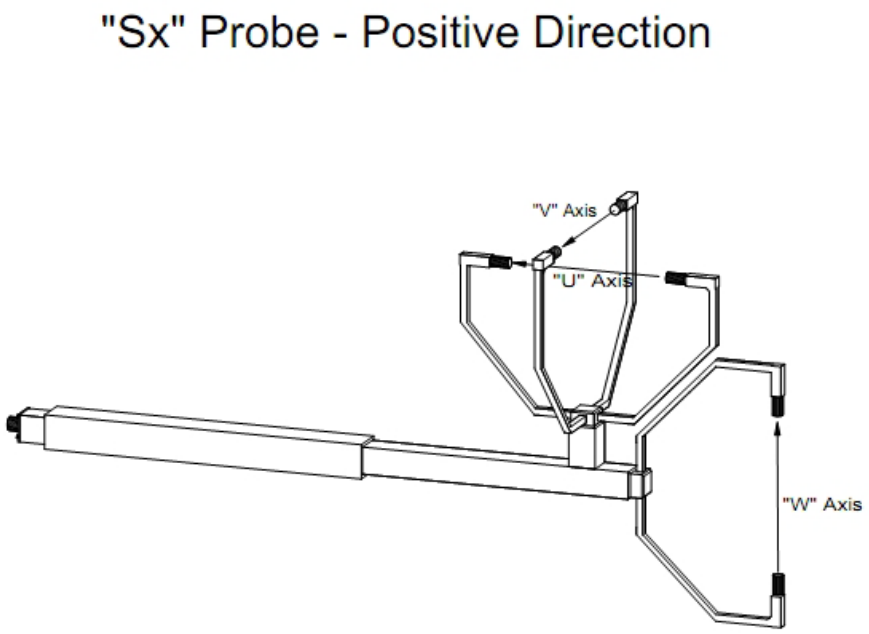


Figure 2.1: Sketch of Sx Probe on instrument arm, by Applied Technologies, Inc.

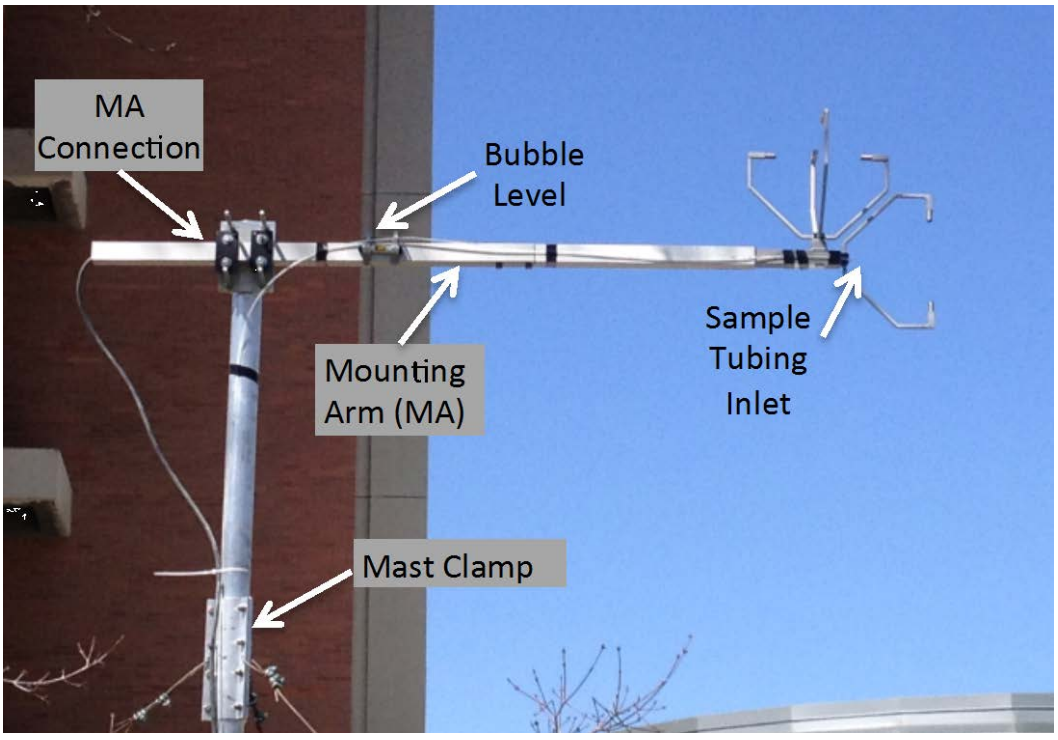


Figure 2.2: Schematic of the tower top configuration, illustrating specific components.

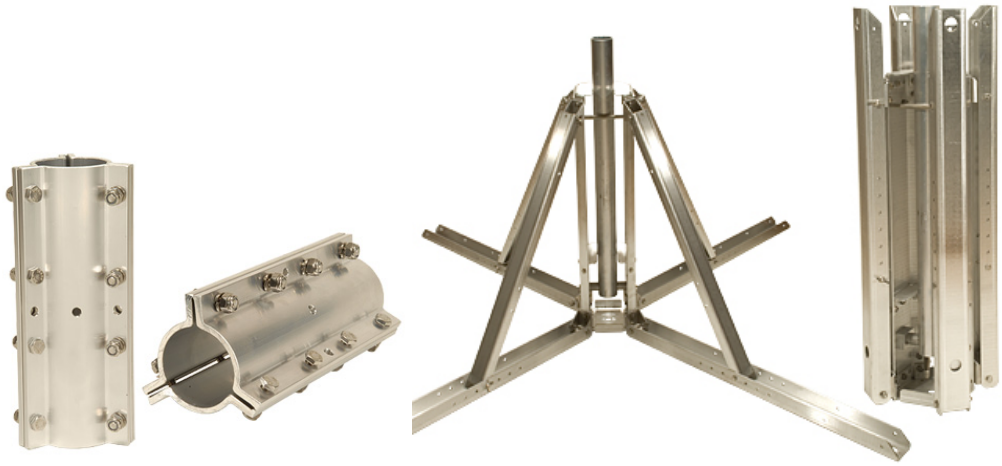

Figure 2.3: Tower components include the MC-200 Mast Clamp (left), and Tipper TP-24 Base (right), photos courtesy of Penninger Radio.

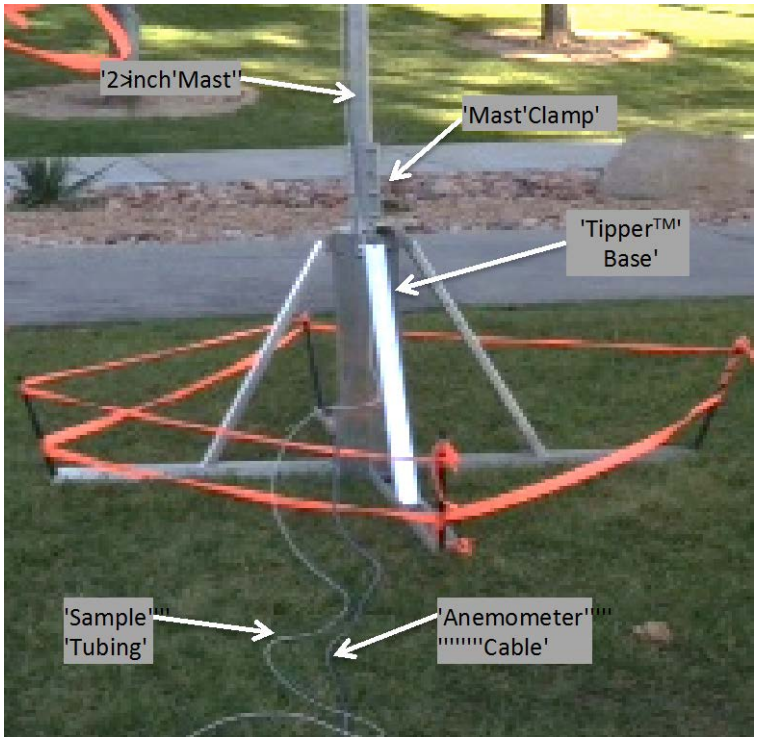


Figure 2.4: Photograph of tower base.

Figure 2.5:  Photograph of the tower deployed at location 1.

Figure 2.6:  Photograph of the tower at location FASB2; note the CRDS in the wagon.

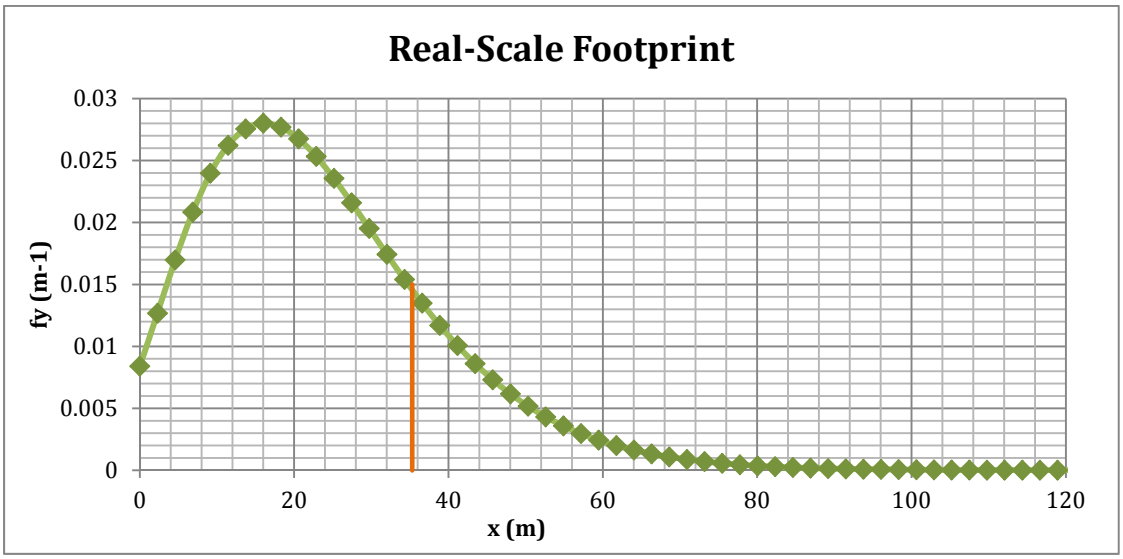


Figure 2.7: Footprint estimation for the flux tower calculated using the Kljun et al. (2004) online calculator with line representing R=80%.

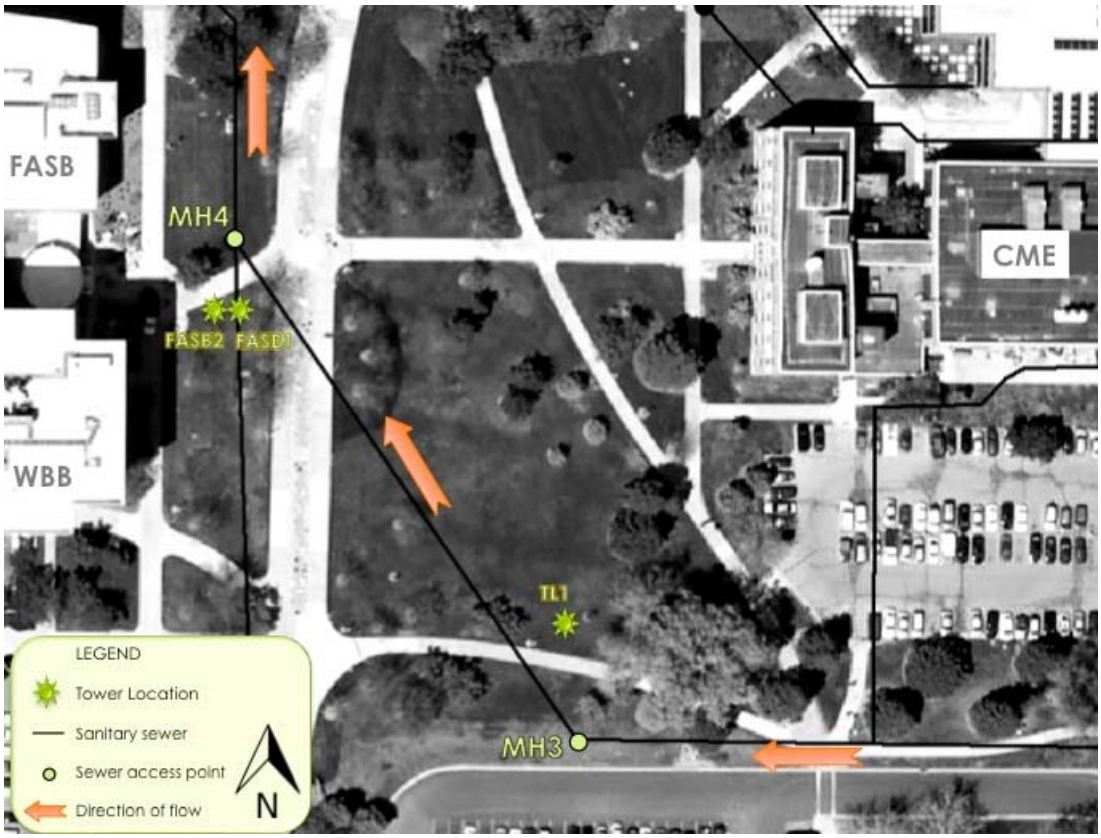


Figure 2.8: Project area with sewer flow and point sources highlighted.

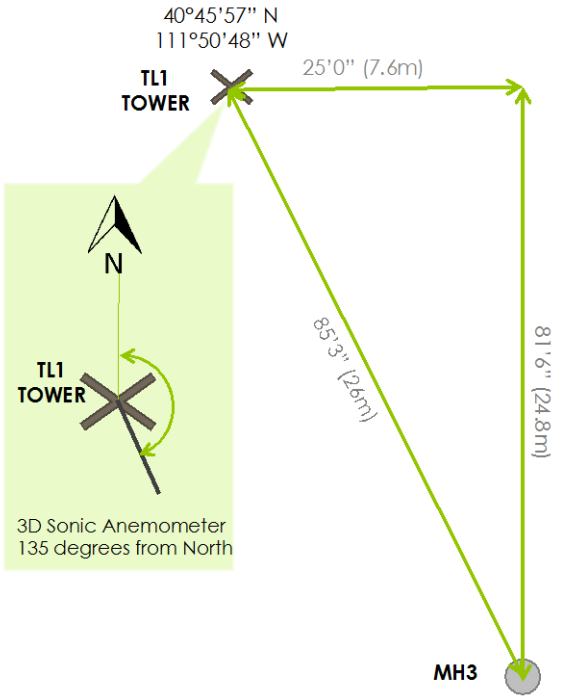


Figure 2.9: Schematic of tower location 1 (TL1).

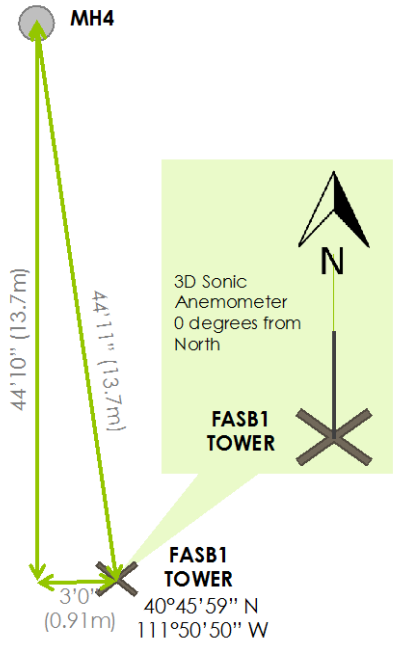


Figure 2.10: Schematic of FASB1 tower location.

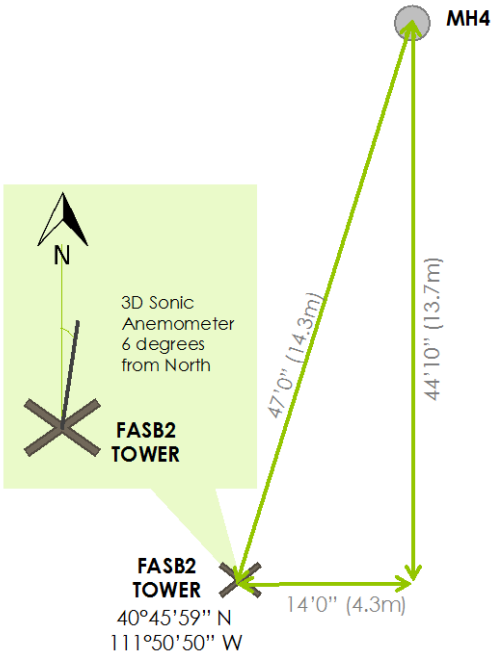


Figure 2.11: Schematic of FASB2 tower location.


Figure 2.12: Locations of existing weather stations and project subsidiary anemometers.

Figure 2.13:  Photo of SA#2.

Table 2.1: Project specific tower input data.

| Input Data: | | |
|---|---|---|
| σw (m/s) = | 0.54 | Standard deviation of vertical velocity fluctuations |
| u* (m/s) = | 0.3 | Surface friction velocity |
| zm (m) = | 3.66 | Measurement height |
| h (m) = | 1500 | Planetary Boundary-layer height |
| z0 (m) = | 2 | Roughness length |
| R (0-90%) = | 80 | Percentage of footprint included |
| L = | 40.13 | Monin-Obukhov Length |

Table 2.2: Results from online calculator for project tower.

| **Real-scale Footprint** | |
|---|---|
| **Peak location of footprint xmax:** | **16.2 m** |
| **Longitudinal dimension of footprint xR (R=80%):** | **35.3 m** |

Table 2.3: Tower location descriptions.

| **Location** | **Latitude** | | **Longitude** | | **Start Date** | **End Date** | **Distance to MH** | **Anemometer Angle** |
|---|---|---|---|---|---|---|---|---|
| TL1 | 40.7660256 | N | 111.8466266 | W | 7-Sep-13 | 18-Oct-13 | 26 meters | 135 deg |
| FASB1 | 40.7665762 | N | 111.8473174 | W | 18-Oct-13 | 2-Dec-13 | 13.7 meters | 0 deg |
| FASB2 | 40.766443 | N | 111.847378 | W | 5-Mar-14 | 24-Apr-14 | 14.3 meters | 6 deg |

Table 2.4: Database wind direction legend.

| Recorded Data Number | Corresponding Wind Direction | Recorded Data Number | Corresponding Wind Direction |
|---|---|---|---|
| 0 | N | 8 | S |
| 1 | NNE | 9 | SSW |
| 2 | NE | 10 | SW |
| 3 | ENE | 11 | WSW |
| 4 | E | 12 | W |
| 5 | ESE | 13 | WNW |
| 6 | SE | 14 | NW |
| 7 | SSE | 15 | NNW |

Table 2.5: Summary table of wind direction analysis for SAs.

| SA#1 | Average Wind Direction | | |
|---|---|---|---|
| Date | Daily | 10am-7pm | 10am-5pm |
| 1/22/14 | NW | NW | NW |
| 1/23/14 | NW | NE | NE |
| 1/24/14 | NW | N | N |
| 1/25/14 | NW | NNW | N/A |
| 1/26/14 | NNW | NNW | NNW |
| 1/27/14 | NW | NNW | NNW |
| 1/28/14 | NW | NW | NW |
| 1/29/14 | NW | NW | NW |
| 1/31/14 | NW | NW | NW |
| 2/5/14 | N | N | N |
| 2/6/14 | NNW | NNW | NNW |
| 2/7/14 | S | S | S |
| 2/8/14 | NNW | NNE | NNW |
| 2/9/14 | N | N | N |
| 2/13/14 | N | N | N |
| 2/14/14 | N | N | NNW |
| 2/15/14 | NE | NNE | N |
| 2/16/14 | NNW | NNW | N |
| 2/17/14 | NNE | SSW | SSW |
| 2/18/14 | N | N | N |
| 2/19/14 | NNW | NNW | NNW |
| 2/20/14 | N | S | S |
| 2/21/14 | NNW | N | N |
| 2/22/14 | NNE | N | N |
| 3/1/14 | SSW | S | SSW |
| 3/2/14 | NNW | S | S |
| 3/3/14 | NNW | S | S |

| SA#2 | Average Wind Direction | | |
|---|---|---|---|
| Date | Daily | 10am-7pm | 10am-5pm |
| 1/22/14 | NE | NE | NE |
| 1/23/14 | E | E | E |
| 1/24/14 | NNE | E | E |
| 1/25/14 | N | N | N |
| 1/26/14 | N | NNE | E |
| 1/27/14 | NNE | NNE | NNE |
| 1/28/14 | NE | NNE | NNE |
| 1/29/14 | NNE | NNE | NNE |
| 1/31/14 | NE | NNE | NNE |
| 2/5/14 | NE | NNE | NE |
| 2/6/14 | NE | NNE | NNE |
| 2/7/14 | WSW | WSW | WSW |
| 2/8/14 | NE | ENE | ENE |
| 2/9/14 | NE | NNE | NNE |
| 2/13/14 | NE | NE | NE |
| 2/14/14 | NE | NNE | NNE |
| 2/15/14 | ENE | ENE | NNE |
| 2/16/14 | NE | NNE | NNE |
| 2/17/14 | NE | WSW | WSW |
| 2/18/14 | NNE | NNE | NE |
| 2/19/14 | NE | NE | NNE |
| 2/20/14 | NE | WSW | WSW |
| 2/21/14 | NE | NE | NE |
| 2/22/14 | NE | NNE | NNE |
| 3/1/14 | WSW | WSW | WSW |
| 3/2/14 | NE | WSW | WSW |
| 3/3/14 | NE | WSW | WSW |

| MWBB | Average Wind Direction | | |
|---|---|---|---|
| Date | Daily | 10am-7pm | 10am-5pm |
| 1/22/14 | WSW | WSW | 0 |
| 1/23/14 | W | W | 0 |
| 1/24/14 | W | W | 0 |
| 1/25/14 | W | W | 0 |
| 1/26/14 | W | W | 0 |
| 1/27/14 | WSW | WSW | 0 |
| 1/28/14 | W | W | 0 |
| 1/29/14 | N | NE | 0 |
| 1/31/14 | W | WNW | 0 |
| 2/5/14 | W | W | 0 |
| 2/6/14 | W | W | 0 |
| 2/7/14 | S | S | 0 |
| 2/8/14 | SSW | E | 0 |
| 2/9/14 | NNE | E | 0 |
| 2/13/14 | E | E | 0 |
| 2/14/14 | NE | NNE | 0 |
| 2/15/14 | E | E | 0 |
| 2/16/14 | WNW | WNW | 0 |
| 2/17/14 | S | S | 0 |
| 2/18/14 | W | W | 0 |
| 2/19/14 | NW | NW | 0 |
| 2/20/14 | WNW | SW | 0 |
| 2/21/14 | NE | W | 0 |
| 2/22/14 | NE | WNW | 0 |
| 3/1/14 | S | S | 0 |
| 3/2/14 | SW | SW | 0 |
| 3/3/14 | SSW | SSW | 0 |

# CHAPTER 3

## POINT SOURCE DISCUSSION

The sanitary sewer lines on the University of Utah campus and used for this project are gravity fed, and were constructed in the 1950s (University of Utah Plumbing Shop, personal communication, 2013). Concentration measurements conducted with the CRDS instrumentation during the past 2 years recorded concentrations far above ambient atmospheric concentrations, with maximum $CO_2$ at 18,000 ppmv and $CH_4$ at 130 ppmv, compared to atmospheric values of 390.5 ppmv $CO_2$ and 1.803 ppmv $CH_4$. These values were found from work conducted in association with the thesis work of Varland (2014). The tower was designed with the specific intention of detecting a designated point source of $CO_2$ and $CH_4$, where this source was a sewer access point previously monitored. The specific sewer line targeted for this study is located just south of the CME Building and runs west until diagonally running northwest towards 100 South (Figure 3.1). The two sewer access points that enable the most feasible tower deployments are MH3 and MH4 (Figure 3.1), and these will be the focus of the following point source discussion.

Measurements of $CO_2$ and $CH_4$ gases emitted by the sewer (via the vent holes in the sewer access cover) were conducted in collaboration with the thesis work of Varland (2014), where the measurements exhibited inconsistency throughout a given day. To gain better understanding of how concentrations change over time and to evaluate factors

that affect those emissions, continuous measurements were conducted at several sewer access points along the sewer line.

## 3.1 Sewer Continuous Measurements

Concentration measurements were performed with the CRDS and SFGA at several sewer access points along the sanitary sewer for the duration of several hours per survey. The concentrations were measured approximately 4-8 inches below the sewer access cover by inserting the sampling tube into one of the vent holes on the cover. MH0 and MH1 are "upstream" of MH3 and MH4, and with exception of the vent holes, the sewer is considered a closed system. Based on this information, the sewer transferring the waste will exhibit similar traits throughout the system. This was found to be true based on multiple measurements of concentration and flux (via chamber measurements), where the morning values were found to be relatively steady and the afternoon values increased (even though the magnitude and actual values were found to differ with respect to day). This evaluation will be restricted to the dates when continuous hourly measurements were made, but the results will be used for further understanding of the sewer and anticipated reactions typical of such a system.

Data for MH1 on June 21, 2013 are shown in Figure 3.2 and data for MH0 on June 27, 2013, are plotted in Figure 3.3. Both figures display $CO_2$ and $CH_4$ concentration verses time (recall that the CRDS is capable of measuring both gases).

Additional continuous readings of $CO_2$ were conducted on MH4 with the SFGA on March 6$^{th}$, 7$^{th}$ & 8$^{th}$, 2014 (these 3 days of measurements coincided with tower measurements taken by the CRDS and evaluation of the concurring data will be discussed

in Section 4.3). An additional 2 days of continuous $CO_2$ measurements were also taken with the SFGA on March 12th and 14th, 2014. These five additional continuous measurements were conducted to identify the similarity of $CO_2$ source release at MH4, acting in the same manner as MH1 and MH0. This was evident by all of the continuous measurements exhibiting an increase in concentration readings beginning around 12:00pm (noon), even though scaling and maximum values were different.

As part of Varland's (2014) work, continuous MH4 studies were conducted with the flux chamber, utilizing both the CRDS and SFGA instrumentation. A continuous survey was performed on October 25th and 26th for a 24-hour period. Figure 3.4 shows the continuous flux measurements conducted with the two instruments. The differences between the two measuring techniques are discussed by Varland (2014). The significance of the calculated fluxes for this research pertain to the afternoon values 12:00pm (noon) to 9:00pm, once again being larger than the morning or evening values.

Quantification of the releases from MH3 and MH4 assisted with regard to tower detection. For further analysis, the flux values obtained were broken down into morning and afternoon sessions and averages calculated.

## 3.2 MH3 and MH4 Emissions

Varland (2014) evaluated emissions from MH3 with 52 measurements and MH4 with 65 measurements from September thru October, and the flux values determined were 0.0053 and 0.0097 metric tonnes/year, respectively. Table 3.1 summarizes releases based on morning and afternoon surveys. As previously discussed, it is evident that the afternoon has larger release rates than the morning or evening hours.

The results also indicate that MH4 releases almost twice the amount of $CO_2$ than MH3, and about 5 times the $CH_4$ in carbon equivalents.

During January and February 2014 an additional 62 flux chamber measurements were conducted at MH4. These data were added to previous measurements and new averages calculated. The entire data set was evaluated and then an additional three scenarios were evaluated. These three additional situations include Weekdays, Weekends and School days. Weekdays consist of Monday through Friday measurements, Weekends are Saturday and Sunday and School days are days when the University of Utah was in session (i.e., Fall Break and Winter Break measurements excluded). All four scenarios were also bisected into morning and afternoon sections as previously shown with the first set of measurements. Table 3.2 summarizes results.

Resulting $CO_2$ values measured by the different instruments were compared, but $CH_4$ results were not compared because the SFGA instrumentation does not have $CH_4$ measurement capabilities.

Between the four scenarios described, there are differences noted. The Weekdays are found to be releasing the largest amounts with approximately 0.000044 tonnes/day (4.05%) more than the School days and 0.000113 tonnes/day (10.4%) more than the entire data set, or All days. The Weekend values are an order of magnitude lower than the Weekdays and School days and 5.75 times smaller than All days.

If the afternoon values are evaluated separately, the Weekdays continue to produce the largest $CO_2$ release with School days at 0.0000520 tonnes/day (5.44%) smaller. The largest morning releases are during School days, approximately 5.29% larger than Weekdays but still smaller than all afternoon values.

Further analysis of the releases with each scenario suggest that the sewer access point MH4 releases the largest amounts of carbon dioxide during times when students, professors and other university employees are on campus.

As a result of the concentration and flux measurement analysis, tower detection of $CO_2$ and $CH_4$ from the sanitary sewer line has the highest probability if operation occurs in the afternoon of weekdays at MH4.

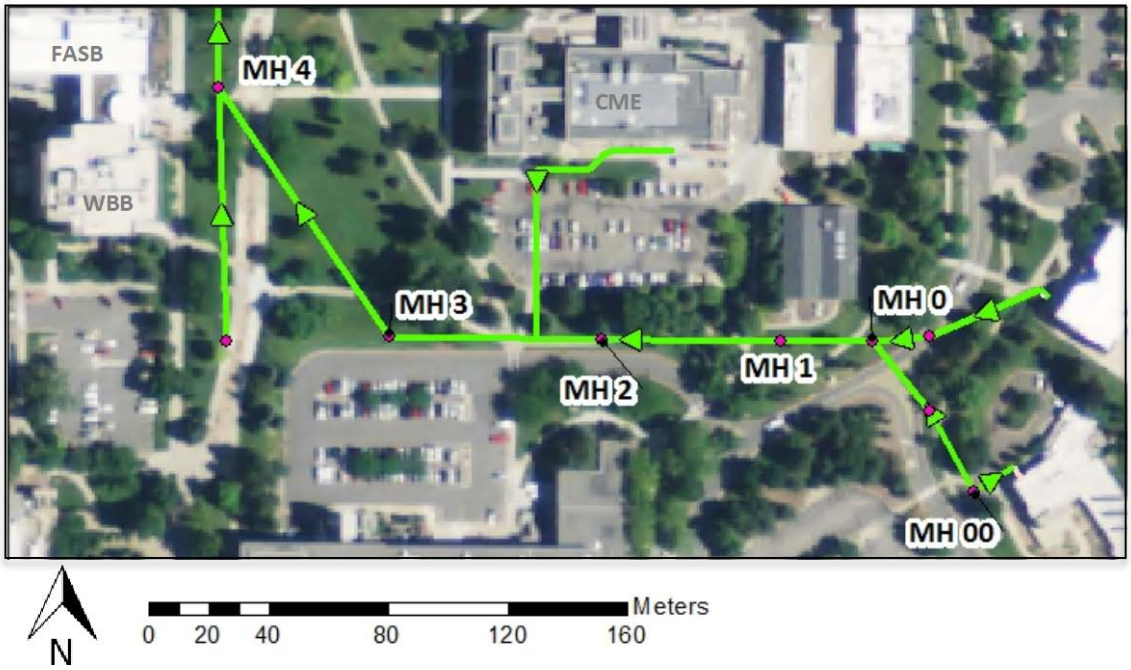


Figure 3.1: Map of selected University of Utah gravity-driven sewer lines.

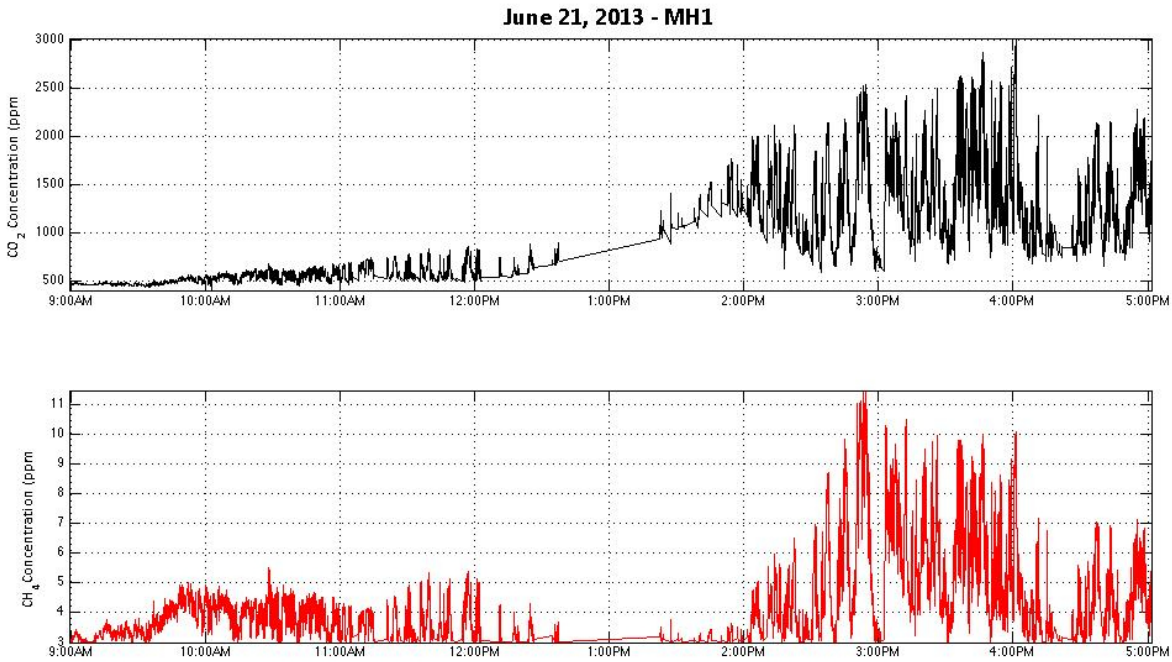


Figure 3.2: Continuous GHG concentration measurements at MH1 (Varland, 2014).

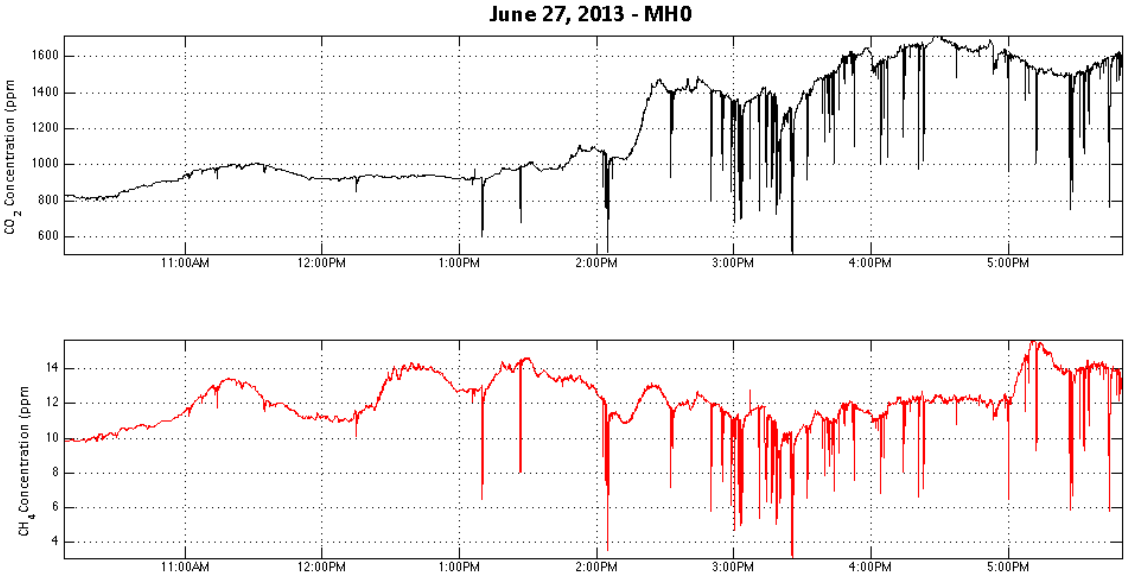


Figure 3.3: Continuous GHG concentration measurements at MH0 (Varland, 2014).

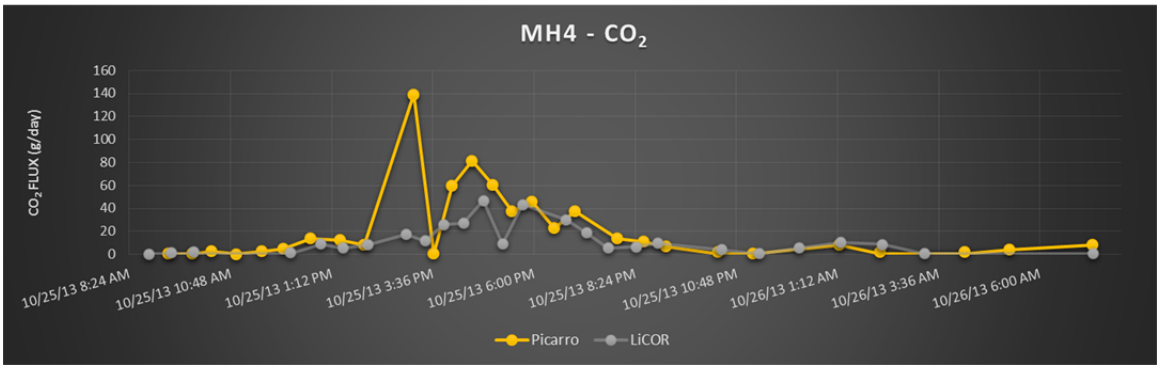


Figure 3.4: CRDS and SFGA continuous $CO_2$ flux measurements at MH4 (Varland, 2014).

Table 3.1: MH3 and MH4 release rates (Varland, 2014).

| | **Morning** | **Afternoon** | **Morning** | **Afternoon** | **Sum** |
|---|---|---|---|---|---|
| | (g/day) | (g/day) | ($MtCO_2e$)/ year | (Mt $CO_2e$)/ year | (Mt $CO_2e$)/ year |
| **MH3** | | | | | |
| Average of $CO_2$ Flux | 2.484 | 11.93 | 0.0009 | 0.0044 | 0.0053 |
| Average of $CH_4$ Flux | 0.003 | 0.0254 | 0.00002 | 0.0002 | 0.0002 |
| **MH4** | | | | | |
| Average of $CO_2$ Flux | 3.630 | 22.99 | 0.0013 | 0.0084 | 0.0097 |
| Average of $CH_4$ Flux | 0.0356 | 0.0915 | 0.0003 | 0.0007 | 0.0010 |

Table 3.2: MH4 release rates (from Table 3.1) with additional measurements.

| | | | **Average $CO_2$ Release** | | |
|---|---|---|---|---|---|
| **MH4** | **g/day** | | **g/day** | **tonnes/day ($MtCO_2e$/day)** | **tonnes/year ($MtCO_2e$/year)** |
| **All days** | SUM | DAYS | | | |
| Morning | 2282 | 28 | 81.51 | 0.0000815 | 0.030 |
| Afternoon | 79379 | 89 | 891.9 | 0.0008919 | 0.326 |
| TOTAL | | 117 | 973 | 0.000973 | 0.355 |
| **Weekdays** | | | | | |
| Morning | 2222 | 17 | 130.73 | 0.0001307 | 0.048 |
| Afternoon | 77406 | 81 | 955.63 | 0.0009556 | 0.349 |
| TOTAL | | 98 | 1086 | 0.001086 | 0.397 |
| **School days** | | | | | |
| Morning | 1932 | 14 | 138.0 | 0.0001380 | 0.050 |
| Afternoon | 48794 | 54 | 903.6 | 0.0009036 | 0.330 |
| TOTAL | | 68 | 1042 | 0.001042 | 0.380 |
| **Weekends** | | | | | |
| Morning | 60 | 12 | 4.98 | 0.0000050 | 0.002 |
| Afternoon | 1974 | 12 | 164.47 | 0.0001645 | 0.060 |
| TOTAL | | 24 | 169 | 0.000169 | 0.062 |

# CHAPTER 4

# DATA ANALYSIS

This chapter describes the process of data analysis, and reports the results of $CO_2$ and $CH_4$ concentration detection from all three locations of the tower on the University of Utah campus. The data are summarized, but inclusion of all session plots and calculated values are provided in Appendices D thru G.

There were three main objectives of the data analysis:

1. Verification that the tower can detect concentration levels of $CO_2$ and $CH_4$ above ambient values over a measurement session.
2. Utilization of the highest levels of concentration detection with associated wind directions to determine constant source(s) of emissions.
3. Clear and unquestionable depiction by the tower of the known point source emissions released.

These main points will be investigated in this chapter. The anticipated results include the detection of the gases by the tower with emissions of the two gases from the designated point sources being clearly evident. The many sessions of data collection should provide a clear source direction and indicate the sewer access by high concentrations emitted and detected in correlation to the investigated sewer release. In addition, an analysis was performed on the three daily sessions in March of coinciding

point source concentrations and tower measurements to elucidate possible trends between emission source(s) and detection.

## 4.1 Tower Data Analysis Process

Data collection with the tower began September 13, 2013 and ended March 8, 2014. During the span of the project, the tower was deployed in three separate locations, depicted in Figure 2.9 and described individually in Section 2.4. The majority of data were collected during the daytime hours of 9:00am to 5:00pm and during weekdays in conjunction with the greatest possible magnitude of point source emissions, as described in Chapter 3. Two overnight data collections were conducted in October at two different locations.

The operation of the tower involved the connection of a Picarro© cavity ring-down spectrometer, or CRDS, to the sonic anemometer and sampling tube on the tower. Once connection was successfully established, the next step was to maintain the connection and ensure correct operation until the end of the measurement session. The data collected by the CRDS were recorded in files delineated sequentially by time and stored on the CRDS hard drive. Once a measurement session was complete and the CRDS was returned to a secure area, the data files could be transferred to a university server for manipulation and data analysis. Data collection at 10 Hz produced 35 measurements per second and resulted in large datasets. These were reduced in size by eliminating superfluous measurement variables (those that were logged but not required for analysis). The specific components used for analysis are included in Table 4.1.

All measured data were used in the original form collected with exception of the

time variable, which was recorded in Greenwich Mean Time and required conversion to Mountain Standard Time and Mountain Daylight Time (March 10 through November 3, 2013).

The dry concentration of each gas was calculated by the CRDS and obviates the need for sample drying or correction factors. Dry concentration values are required for consistency with standards set forth by the World Meteorological Organization (WMO) to achieve interlaboratory comparability. Utilizing dry measurements eliminates humidity inconsistency which effects mixing ratios of the gases and concentrations (Rella, 2010). Variations between the dry measurements and the nondry measurements recorded by the CRDS instrumentation were not significant (less than 5%) for the majority of datasets due to the subhumid climate of the Salt Lake region; however, the calculated dry concentrations were used, consistent with established best practices.

The primary computational analysis tools selected for these data were Matlab R2012b by MathWorks® and Microsoft® Excel 2013. The primary data analysis consisted of resolving several key variables over time, including the lag time associated with concentration collection, vertical velocity equilibrium, wind direction and concentration spikes (sudden increases in concentration over short time periods). The combination of wind direction and spiking then needed to be evaluated to discern the most probable source location. Probability "rose diagrams" (discussed in subsequent sections) were created for long-term measurement data sets.

### 4.1.1 Lag Time Determination

Lag time is the time interval between the gas intake at the sampling tube inlet, (secured on the arm of the anemometer) and time of actual measurement in the cavity of the instrument. The length of sample tubing and time within the CRDS cavity are the two main factors affecting total lag time. The sampling rate used is also a major factor and for the tower the rate was the Low Flow rate of 0.5 lpm. To establish the lag time, the sampling tube was removed from the tower and tested using a manual procedure. Specifically, one researcher exhaled or blew into the sampling tube and another researcher started a stopwatch. When the real-time graph on the CRDS screen began to increase in response to the exhale, the time duration was recorded. Thirteen cycles were recorded for time measurements. The highest and lowest values were removed and the remaining 11 measurements were averaged to give a lag time of 27.7 seconds with a standard deviation of 0.21 seconds. All measured values are provided in Appendix B.

All measured gas concentrations recorded by the CRDS were adjusted to reflect actual time of detection at the sampling inlet. It is a simple calculation of subtraction of the lag time from the time stamp. This adjustment was important for correlating detection values with the wind direction values associated at the same time.

### 4.1.2 Vertical Velocity Equilibrium

The wind speed in the vertical direction is a direct measurement by the SATI/3Sx anemometer. The physical level of the anemometer can be evaluated by graphing and averaging the vertical velocity readings, where the average should be at zero for a level system. If the equipment is not level then skewness corrections must be applied to

anemometer measurements. The average vertical velocity for all 37 days of measurements ranged from -0.1307 to 0.0499 m/s. This range was deemed acceptable for the terrain associated with the urban area of study. A graph of typical acceptable vertical velocity is shown in Figure 4.1 for November 1, 2013 at the FASB1 location.

This averaging of approximately zero also indicates stability within the atmosphere at the level of measurement.

### 4.1.3 Wind Direction Evaluation

The wind direction is a function of velocity measurements by the two horizontal probes on the SATI/3Sx anemometer. The SATI/3Sx has U, V and W axes, as designated by the manufacturer. The orientation of the anemometer results for the U axis representing the northerly velocity measurements and corresponding to the "X" variable. The V axis represents easterly wind measurements and is represented by "Y." The wind direction was calculated by the following equation:

$$\text{Wind Direction} = \text{atan2}(UY, UX),$$

where atan2 is the arctangent function using two variables, UX and UY are wind speed values output over time from the CRDS and which cancel to provide unitless values for the equation. The output of this equation (using analysis algorithms coded in Matlab command language scripts) was provided in degrees between -180 and 180. The corresponding four-quadrant is shown in Figure 4.2.

Output values were reformatted to provide a compass direction (with north equal to zero) and converted to a 0-359 degree scale. Adjustment of the degrees for the orientation of the anemometer with respect to north was mandatory because the

anemometer was not always situated directly north. The orientation of the SATI/3Sx was positioned towards the known point source (sewer maintenance covers) for each survey, and into the predominant wind direction. Addition of the degree angle of the anemometer (measured in the field) to the calculated wind direction degree (from anemometer data) provided the corrected wind direction or the actual wind direction.

Evaluation of the wind direction started with a plot against time and as a wind rose; for March 6$^{th}$ see Figures 4.3 and 4.4.

As illustrated by Figure 4.4, a wind rose is a histogram with a designated number of bins or intervals. The bins separate the calculated wind data into degrees and number of measurements within each specific interval of degrees (or bin) to exhibit the predominant wind direction. The wind rose of Figure 4.4 has a bin size of 3 degrees, for a total of 120 bins. The numbers emanating radially are the number of measurements in each bin. All directions for this rose have at least 4000 measured values in each 3 degree bin. This wind rose does not express a clearly prevailing wind direction. The wind during this day was apparently highly variable with respect to direction and yielded consistent numbers of measured values for all wind directions, as also shown in the accompanying plot of wind direction verses time (Figure 4.3). However, the time series does indicate dominant directions for time periods throughout the day. As an example, the wind was primarily from the south (at 180 degrees) between the times of 14:30 to 15:00. The next analysis step was to evaluate concentration levels for spiking.

4.1.4 Spike Determination

A spike in concentration of $CO_2$ or $CH_4$ is a sudden increase above ambient readings with a magnitude and duration that are a function of the point source size, distance to that source, and atmospheric conditions. Based on previous point source studies of MH4 and MH3, high readings of $CO_2$ and $CH_4$ released from the point source should produce coincident concentration spikes within the dataset occurring after noon. Plotting the concentration with respect to time provided a useful visual representation of the dataset and enabled an initial examination for spikes.

Percentile was used to determine significant spikes, where percentile is a basic calculation of the entire dataset. Specifically, the 99$^{th}$ percentile is the magnitude of value for which 99% of the data values fall below that specific magnitude of value. To determine the 99$^{th}$ percentile all the values of the dataset were ranked from lowest to highest. The following equation was then used to find the value for the desired percentile for a given dataset:

$$\mathrm{R_C} = \frac{P}{100}(n+1),$$

where $R_C$ is the computed rank, $P$ is the desired percentile and $n$ is the total number of data points. Even though Lane, 2010 states, "there is no universally accepted definition of a percentile" the process above handles rounding errors and results in the median of the dataset being the 50$^{th}$ percentile (Lane 2010).

This type of calculation is dataset-dependent and therefore provided a different value for each measurement session. This was preferred to an arbitrary hard value set as a limit because the percentile calculation accounts for fluctuations associated with ambient conditions. For each dataset (each individual survey), the 99$^{th}$ percentile was

calculated and plotted against time for visual interpretation. The 99$^{th}$ value was chosen because of the extensive amount of data, where the large amount of ambient values dominated the dataset. The high percentile removed ambient fluctuations and only highlighted the dominant spikes. The resultant 99$^{th}$ percentile data corresponding to $CO_2$ and $CH_4$ were plotted separately and as an example the March 6$^{th}$ data are shown in Figures 4.5 and 4.6.

The values of the 99$^{th}$ percentile for the March 6$^{th}$ dataset were 424.96 and 1.78 ppmv for the $CO_2$ and $CH_4$, respectively (see also Figures 4.5 and 4.6). The spikes occurred throughout the data collection period, and the next step in the assessment was to include the wind direction associated with the spikes.

### 4.1.5 Spiking with Wind Direction for Source Evaluation

Combination of the concentration percentile evaluation with the wind direction calculations and identification (elimination) of ambient fluctuations, made it possible to associate a wind direction with increased gas concentration detection. Mathematical scripts were developed for this specific task, including graphical representation of the results for each gas.

The two previous plots (Figures 4.5 and 4.6) show several instances of elevated levels of the two gases. The two plots do not track each other (exhibit correlation), but in an urban environment and with associated wind variability, this was not entirely expected. The wind direction corresponding to the 99$^{th}$ percentile concentration values (corrected for the lag time) was plotted for source evaluation. Such plots may elucidate whether observed spiking was from a predominant direction, indicating a persistent

source. It is believed that as the correlation of wind direction with concentration increases, the likelihood of a significant source (e.g., a leak) increases. Figures 4.7 and 4.8 show the graphical representations of wind directions corresponding to the 99$^{th}$ percentile of gas concentrations for each gas on March 6$^{th}$. Review of the wind direction plots for March 6$^{th}$ (Figures 4.7 and 4.8) suggests that the source of $CO_2$ and $CH_4$ was from the northwest through the north-northeast (310 through 40 degrees) with a secondary source of $CH_4$ observed from the east-southeast through the south (125 to 175 degrees).

These observations were unique to the day and time of data collection, and cannot be called general results. From limited data like these, it is essentially impossible to identify if a source was of a definitively constant nature, such as a pipeline leak, or if it was an ephemeral occurrence only observed during that particular day, such as yard work or delivery vehicle emissions, etc. Additional data collections at this site would show if this source is definitively constant or if it was specific to March 6$^{th}$.

### 4.1.6 Probability Rose Diagram

The data collected were used to create a probability diagram to portray which direction exhibits the highest likelihood location of a source. The diagram accounts for wind speed, wind direction and gas concentration. Wind speed was calculated by the following equation:

$$Wind\ Speed = \sqrt{UX^2 + UY^2 + UZ^2}\ .$$

The resultant wind speed is in m/s and the UX, UY and UZ variables are the three-wind speed measurements attained by the SATI/3Sx and recorded by the CRDS. The wind

direction and concentration percentile were previously described in Sections 4.1.3 and 4.1.4.

The first step was to calculate the wind speed and designate what range to plot. For example the 0-100% range of values would include all wind speeds, whereas the 0-33% range would provide the lower third range of wind speeds. The next step in the process was to create bins for the wind directions. Bins can be described as groupings of data that fall within the limits established for that bin. This program will create bins that are 5 degrees in size, so there are a total of 72 bins for the 360 degree rose diagram.

The 99$^{th}$ percentile was the designated threshold for concentration data. The plot displays concentration probability by bin, or

$$Probability = \frac{\#\ of\ Values\ Above\ 99th\ Percentile\ Concentration\ Value\ in\ Bin}{\#\ \text{of}\ All\ Concentration\ Values\ in\ Wind\ Speed\ Bin}.$$

The final rose diagram represents the probability (shown by the value on the concentric circles) that a given wind direction bin or interval contained a high (99$^{th}$ percentile) concentration of the specific greenhouse gas. Figure 4.9 is a 0-100% wind speed probability rose diagram for the FASB1 location during the October 18-19$^{th}$ overnight data collection, and it is for $CO_2$. Interpretation of the diagram suggests that the highest probability of $CO_2$ concentration above the 99$^{th}$ percentile value was approximately 0.021 and corresponded to the 17 degree (NNE) wind direction for all wind speeds.

The level of detail performed for each tower deployment session includes all of the previous steps with the exception of the probability rose diagram, which was only created for long-term measurements. Collective days at each location can determine a constant source and indicate source direction. Certain wind directions can dispel or

support detection of the sewer access point source since it is a fixed location source. An evaluation of each of the three tower locations in this project is provided and discussed in the next section.

## 4.2 Data Analysis Results by Location

Each tower location was orientated differently in order to attempt to maximize the possible capture of gas emission signatures released from the specific targeted sewer access cover. Each of the locations underwent the data analysis process previously described. This section will highlight the results for each location and provides tables that summarize $CO_2$ and $CH_4$ separately. The information includes the $99^{th}$ percentile values, maximum detected values and wind directions associated with the maximum concentration. The dominant source wind direction will be presented by degrees and compass direction taken from the interpretation of the plots. In some cases a secondary source direction will be provided in degrees, if applicable. An overview of the area with possible sources will then be described. Longer-term data collection occurred for two of the three tower locations and are provided for interpretation along with the hourly measurements.

### 4.2.1 Tower Location 1

Tower location 1 (TL1) was aimed at MH3 (Figure 2.10 in Section 2.4) and was erected with anticipation of winds developing from the south. The anemometer was oriented at 135 degrees from north and the distance to MH3 was approximately 26 meters (85 feet). Measurements were taken September 10, 2013 through October 18, 2013. The

anticipated value for direct alignment of the wind with the anemometer was 162.5 degrees. Table 4.2 summarizes results for $CO_2$ and Table 4.3 summarizes those for $CH_4$.

Results suggest that northwest and south-southeast were the two dominant directions from which elevated levels of greenhouse gases were released. Detections from the northeast, south, southwest and southeast are also evident. An overview of the area is presented in Figure 4.10, with these specific wind directions indicated by arrows; larger arrows represent more dominant directions.

The parking area directly south of MH3 was probably the primary source of emissions detection, probably primarily vehicle exhaust. A similar interpretation may apply to the northeasterly wind and the parking lot in that zone. There is no clear source from the northwest direction, unless the urban wind flow was directing gases from the road north of MH4.

The most deterrent issue for detection of the point source was that MH3 was not found to emit a large enough concentration of gas for detection above the other sources within the area. Another downfall of this location was that MH3 was in the path of airflow from the parking lot to detection. Without isotopes or tracers or another methodology, a definitive source cannot be determined.

*4.2.1.1 Overnight Data Collection at TL1*

An extended time frame study was conducted at this location. It began on Thursday, October 17$^{th}$ at 9:00 and ended Friday, October 18$^{th}$ at 15:00. This longer period of measurements may provide insight to daily readings with respect to vehicle emissions and source trends. However, the measurements were taken during fall break

and therefore deviations from typical trends probably occurred. The concentration of $CO_2$ and $CH_4$ was plotted over the time frame of collection and is presented in Figures 4.11 and 4.12, respectively.

The gas signatures track each other, as anticipated. They also suggest that during the period of collection, spiking occurred for both gases at about 5:00 and another at about 9:00 in the morning. Vehicles might have been entering the parking lots for normal working hours at 9:00. Hardly any variance was observed during the afternoon hours of 12:00 through 18:00, evident for both days. A small increase from 18:00 through the evening occurs until early morning. Association of wind direction with the $99^{th}$ percentile provided some insight as to the source of the spiking. Figures 4.13 and 4.14 show the wind direction associated with the $99^{th}$ percentile for each gas.

The wind direction associated with the high concentration values was clearly from the northwest for both gases. This direction does not coincide with previous source identification of vehicle emissions from the parking lot directly south of the tower. This does however eliminate detection of the point source by the tower, releasing $CO_2$ and $CH_4$ within the $99^{th}$ percentile.

Probability rose diagrams were created for this long-term data collection and are displayed in Figure 4.15 for both $CO_2$ and $CH_4$.

Both of these rose diagrams exhibit a clear dominant direction and similar signatures. The highest probability for both gases is in the 315 degree (NW) direction, at 0.041 and 0.04 respectively. Reducing the wind speed range may provide better insight regarding how concentrations correspond to wind speed, such as the high wind speed range (67-100% wind speed) rose diagrams, which are shown in Figure 4.16.

The rose diagrams for the highest third of wind speeds show that the probabilities were lower in value but that the two gases continue to exhibit the same signature. Focusing upon the high wind speeds eliminated the source from the southeast, indicated in the complete wind speed diagram. The high winds containing the 99$^{th}$ percentile of both detected gases were probably from the same source, but not the designated sewer access cover. All wind speed rose diagrams are presented in Appendix G.

### 4.2.2 FASB1 Tower Location

The second location, FASB1, was aimed at MH4 and was erected with the anticipation of winds developing from the north (Figure 2.11 in Section 2.4). The anemometer was oriented at 0 degrees and the distance to the point source, MH4, was approximately 13.7 meters (45 feet). The distance between the tower and the point source was decreased due to the urban area limitations and to increase probability of detection. Measurements were taken on a frequent (but not continuous) basis from October 19, 2013 through December 2, 2013. The anticipated value for direct alignment of the wind with the anemometer was 0 degrees. Table 4.4 provides the results for $CO_2$ and Table 4.5 for $CH_4$.

The results clearly suggest a source from the northwest and the north directions. An overview of the area is presented in Figure 4.17 with these directions indicated by arrows.

The arrows illustrate the interpretation that wind was traveling from the road towards the tower. This corner is a busy car/bus/pedestrian traffic area, with buses frequently stopping and cars slowing down, speeding up and stopping for pedestrians in

the cross walk, all providing probable sources of $CO_2$ and $CH_4$. The FASB/WBB buildings are situated as to block wind from the west and perhaps create a "tunnel effect" for the wind coming from the north. They also likely create wind eddies and velocity disturbances.

Wind blowing from the north probably passed over the designated point source but distinguishing the sewer emissions from the vehicles and other sources was impossible. Spikes were generally observed during all hours of tower operation with no discernable pattern to time or concentration.

*4.2.2.1 Overnight Data Collection at FASB1*

A continuous 25-hour data collection with the tower was conducted beginning Friday, October 18th at 16:30 and ending Saturday, October 19th at 18:00. This extended period of measurements may provide insight to daily readings with respect to vehicle emissions and source trends. However, it was conducted during fall break and therefore deviations from typical trends are likely. The concentration of $CO_2$ and $CH_4$ was plotted over the time frame of collection and is presented in Figures 4.18 and 4.19, respectively.

As expected the two gas signatures track each other closely. There is a definite increase in both gases at 5:00 and another peak at about 8:00 in the morning, possibly from rush-hour traffic. Wind direction was calculated for the 99th percentile of each gas and associated corresponding plots are provided in Figures 4.20 and 4.21.

Examination of the plots suggest that the wind direction was dominantly from the 300 to 50 degree range, corresponding to northwest through north to northeast. These directions are once again associated with the road and most probably emissions from

vehicles. They also agree with the directions from the hourly datasets. It is still noted that the designated point source is not distinguishable from other greenhouse gas sources. The probability rose diagram plots are shown in Figure 4.22 for $CO_2$ and $CH_4$ at FASB1.

These plots indicate that the highest probability was at 0.02 for $CO_2$ and 0.017 for $CH_4$. The associated wind direction for a high concentration for both gases is expected to be from the 15 degree (NNE) direction. If the highest third of the wind speed is assessed, the revised rose diagrams are shown in Figure 4.23.

The revised rose diagrams show overall probabilities that are greater than those shown for the entire wind speed data. They also indicate that with higher wind speeds separated out, the $CH_4$ concentrations remain from the north-northeast direction whereas the $CO_2$ high concentrations shift towards a northeast direction and have a higher probability. The inclusion of wind speed results in better resolved probability, or so might be contended if only because of more information. All wind speed rose diagrams are presented in Appendix G.

### 4.2.3 FASB2 Tower Location

The third location, FASB2 (Figure 2.12 in Section 2.4) was intended to measure emissions from MH4. It was erected with the anticipation of winds developing from the north and northeast based on data from the subsidiary anemometers, along with possible influences by sidewalks and buildings that may redirect wind across MH4 to the new tower location. The anemometer was oriented at 6 degrees and the distance to MH4 was approximately 14.3 meters (47 feet). Measurements were taken March 6$^{th}$, 7$^{th}$ and 8$^{th}$, 2014. The anticipated value for direct alignment of the wind is 17.5 degrees. Table 4.6

provides the results for $CO_2$ and Table 4.7 for $CH_4$.

The results suggest a source from the north and north-northwest. An overview of the area is presented in Figure 4.24 with an arrow indicating north and north-northwest.

This situation mimics the results from FASB1 and supports the dominant source being detected as the road. Once again the desired point source for detection (MH4) is between the road and tower, where detection cannot be eliminated or proved without further investigation into variables differentiating sources.

## 4.3 Emission and Detection Trending Analysis

The point source MH4 was subjected to continuous measurements of $CO_2$ emissions with the SFGA in conjunction with tower measurements in March 2014. A statistical comparison of the concentration data to the coinciding tower concentration measurements was an important part of the subsequent analysis.

A direct correlation may be evident if the $CO_2$ concentration release from the point source and the $CO_2$ concentration detection by the tower held matching concentration pattern readings with respect to time. A shift would be anticipated and magnitudes not identical due to diffusion, but a clear relationship might supervene. The lag time between release and detection could be established by adjusting times to match spikes or peaks between datasets.

### 4.3.1 Analysis

Removing duplicate time values, utilization of a spline function and a smoothing filter were the steps performed for the analysis of the data from the tower and the SFGA.

Then a visual interpretation was conducted.

The first step of analysis involved evaluation for repeated time values among both SFGA and CRDS measurements. All multiple time values were removed from the dataset before the next step, consisting of a spline function application, could be properly administered.

The basic premise of a spline function application is to identify a data point at a specific time value by interpolation of the collected data (e.g., if the measured data do not fall at the specific time interval or value desired). Matlab's spline function was utilized, which uses a cubic spline interpolation process to find values at the requested time intervals. This spline application approach was necessary because the SFGA data was measured every second, whereas the CRDS data were taken 35 times per second. In order to evaluate the data correctly, the smallest increment of collection is determined to be the limiting factor and the other data must match the segmentation. The spline function accomplishes this task and provides (estimated or exact) values for the SFGA and CRDS data at the same time intervals. This enables appropriate comparisons and data manipulation for trend analysis.

The next step was to smooth the data of each instrument so that it was easier to interpret visually for trending. One option that is commonly used is the moving average calculation. However, a moving average will often eliminate important information inherent to the trend of those data. For this project the Savitzky-Golay Filter (SGF) was used to smooth the dataset of each instrument. The SGF was proposed in 1964 and comprises smoothing and differentiation of data by simplified least squares. The filter enables elimination of noisy data without losing the overall shape of the curves and

associated peaks and troughs. The two requirements for this filter, per Savitsky and Golay, 1964 are 1) points must be at a fixed, uniform interval and 2) the curves formed by plotting the data must be continuous and mostly smooth. These two requirements were met by previous data preparation (spline function application) described above. This filtering method is also included in the Signal Processing Toolbox of Matlab and the input values include the dataset, polynomial order and the frame size. Several combinations of polynomial magnitude and frame size were performed. A fifth order polynomial was selected for smoothing the data (better results were not achieved with higher orders and smaller polynomials did not provide sufficient smoothing for visual analysis). The frame size (incremental number of data points to be smoothed) that worked best with the dataset was found to be 101.

The filtered $CO_2$ data were plotted versus time for both the point source (MH4) concentration release and the detected concentration by the tower. In Figures 4.25, 4.26 and 4.27 the source is shown in green and the tower is shown in blue for visual trending inspection for the dates available (March $6^{th}$, $7^{th}$ and $8^{th}$), also included in each figure is the wind direction data for that day.

### 4.3.2 Results

Unfortunately no direct or obvious trending is evident for any of the three dates of coincident concentration data. One major variable associated with the tower detection is the wind direction. If the point source is not in the path of the wind then there is no anticipated detection. Plots of wind direction are situated next to the concentration graphs in the Figures 4.25, 4.26 and 4.27. The wind direction for direct passage over the

point source was 17.5 degrees from north. However, taking into account the size of the sewer access cover, wind variability after passage over the point source, diffusion and orientation of the anemometer, it is generalized that the wind needs to be from the north-northeast direction for possible detection by the tower of the point source. Detection of the point source would also require that the source of emission be strong enough for detection at the height of sampling.

The wind direction is highly variable with no consistent wind pattern between the three days. The urban setting of the campus area creates wind turbulence that is not easily accounted for. March 6$^{th}$ and 8$^{th}$ data both exhibit southerly winds during the middle of the afternoon. Similarly both days show a steady ambient value of $CO_2$ during the time period of predominantly southern winds, which is compatible with the lack of point source detection. They also show more dominant northwest and northeasterly winds during the evening (at 16:00) along with an increased $CO_2$ reading from the tower, but not unambiguously the point source. March 6$^{th}$ has spiking occurring after 16:00, which visually appears to be coordinated with the point source but is indefinable.

March 7$^{th}$ shows predominantly northwest and north-northeast winds throughout the entire day. If the carbon dioxide detected were from the designated point source then it would be anticipated to increase and mimic MH4 readings. This is not the case as the tower maximum detection of $CO_2$ is 411 ppmv and average for the measurement period is 391 ppm (values from actual data rather than smoothed data). There are small fluctuations but no evident spikes occurring or overall increase in concentration during the afternoon.

In conclusion, trending is seen for the concentration increases in fugitive gases at

the point source MH4 throughout the day. The largest values for each day are measured during the afternoon periods of 12:00 through 19:00. The magnitude of the emissions of these gases is not predictable or constant, but the average can be estimated at 1086 g/day and occurs during the afternoons of weekdays. The urban campus setting does not provide a constant wind pattern to be of assistance when predicting fugitive greenhouse gas emissions from the designated point source. The analysis presented does not provide a clear trend between point source release and concentration tower detection, most likely due to weak emission values in perspective of other source values and highly turbulent and unpredictable wind directions. Generally however, when the wind was from the south there was no observed spiking and when wind was relatively constant then the detection by the tower was relatively constant if not in direction association with source emissions.

## 4.4 Discussions and Deliberations

The data analysis provided great insight into the workings of the tower designed and erected for this project, specifically with a designated point source and the three main objectives. All data sessions in the three different locations proved that the tower could detect $CO_2$ and $CH_4$. It also demonstrated that the ambient levels were evident even through slight fluctuation due to high-resolution data collection and atmospheric conditions. Spiking of the gases was seen in all datasets and concluded that emissions due to incidental episodes (such as vehicles, leaks, etc.) occurred and were revealed by the implementation of the tower. This spiking was visually represented by plots of the data and utilization of the $99^{th}$ percentile calculation.

Combination of the multiple data session acquisitions provided constant source evaluation. The FASB1 and FASB2 locations both clearly indicated that the highest concentrations were from the wind blowing from the northwest. The area in this location is comprised of a high traffic area, which leads to the belief that the vehicular emissions were high enough to reach the tower and exhibit signification detection above ambient values. The wind speed and urban effects were not easily understood and are considered to greatly influence the wind patterns and concentration readings. In contrast to the FASB locations, the sources of emissions in the vicinity of TL1 were found to be less focused with respect to a wind direction association to the high concentration signature values. There were multiple prevailing directions that could be attributed to the multiple parking areas within the vicinity of the tower. In addition, the urban environment was completely different from that of the FASB1 and FASB2 tower.

One of the main issues associated with this project was that multiple sources within the areas of the towers were present. The point source gases were indistinguishable from other sources and the release from the sewer access point was believed to not be large enough to be dominant. The study of the point sources indicated that there was no consistent or predicable concentration to be associated with the sewer release and from the data analysis it was impossible to differentiate if the sewer access source point was detected or not. If the sewer point source released $CO_2$ and $CH_4$, and the detection by the tower resulted in concentrations lower than that of the other more dominant sources in the area, then they were eliminated by the $99^{th}$ percentile calculation. Another major issue related to the fact that the vehicular areas were included in the tower footprint because of high concentrations and strong urban environmental influences,

therefore the result of the third objective of this analysis, “clear and unquestionable depiction by the tower of the known point source emissions released” is determined null.

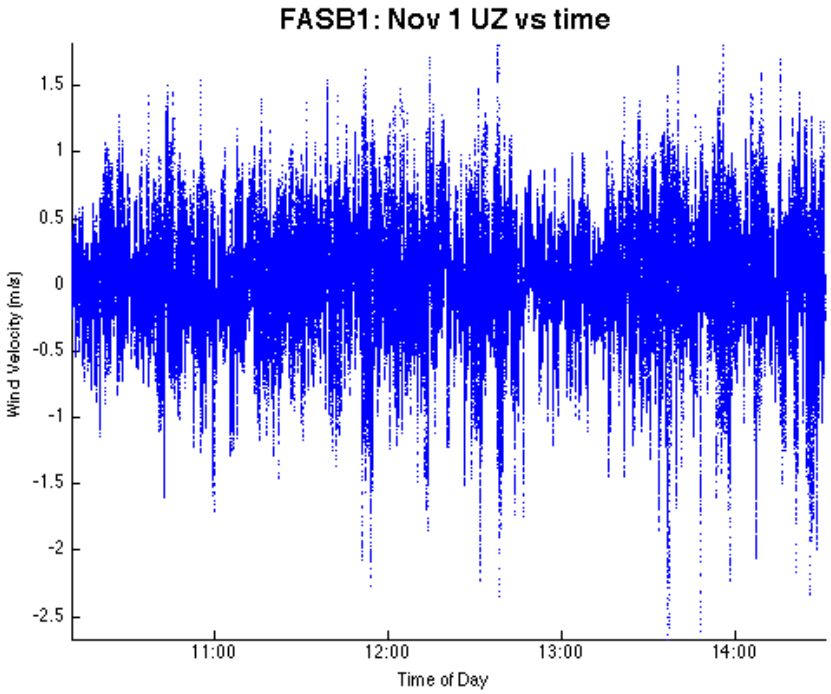


Figure 4.1: Typical vertical wind velocity vs. time plot (average of -0.00033 m/s).

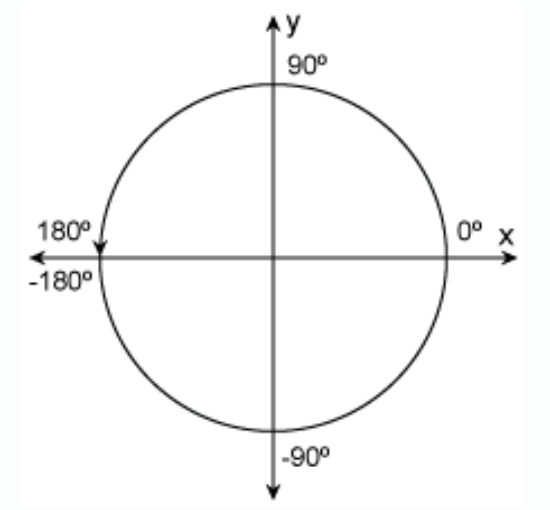


Figure 4.2: Output degree orientation of wind direction calculation (provided by Matlab Documentation).

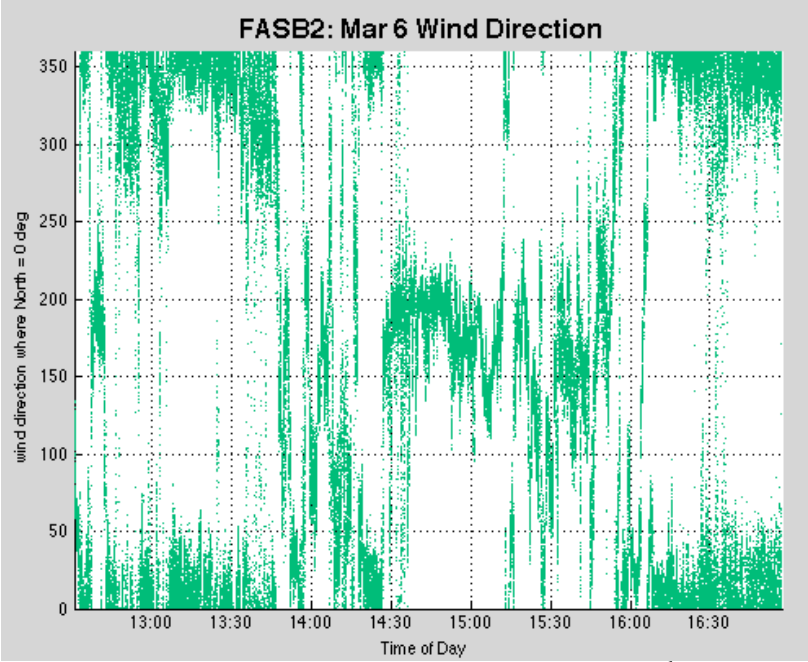


Figure 4.3: Wind direction vs. time for March 6th, 2014.

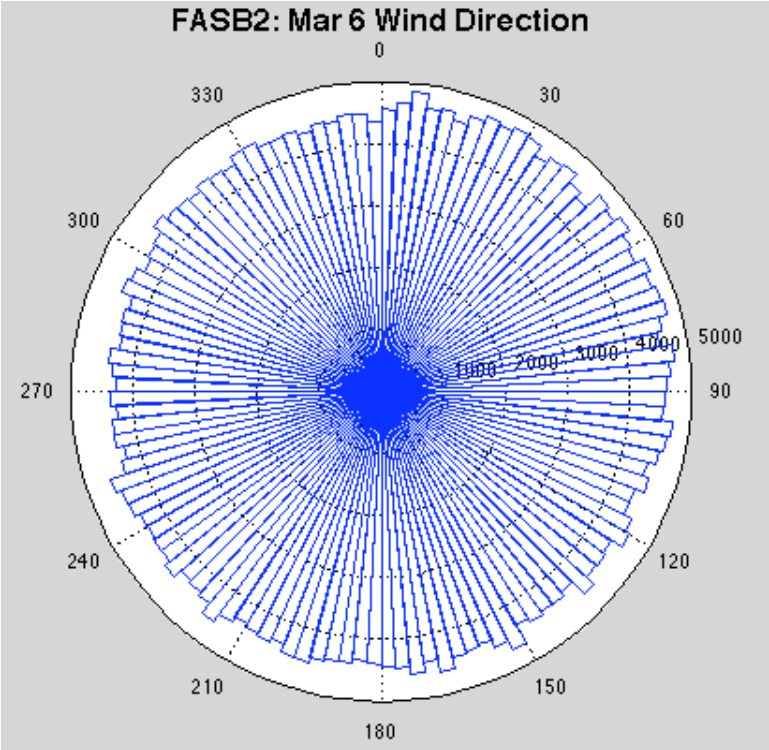


Figure 4.4: Wind rose with 120 bins for March 6th, 2014 (dominant direction is between 30 and 90 degrees).

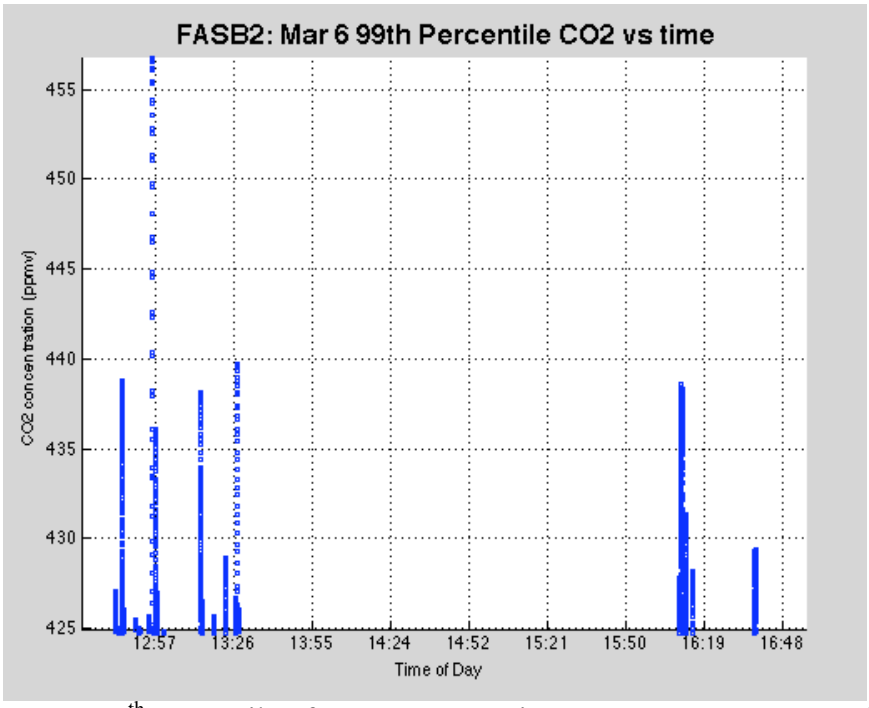


Figure 4.5: 99th percentile of $CO_2$ concentration measurements on March 6th.

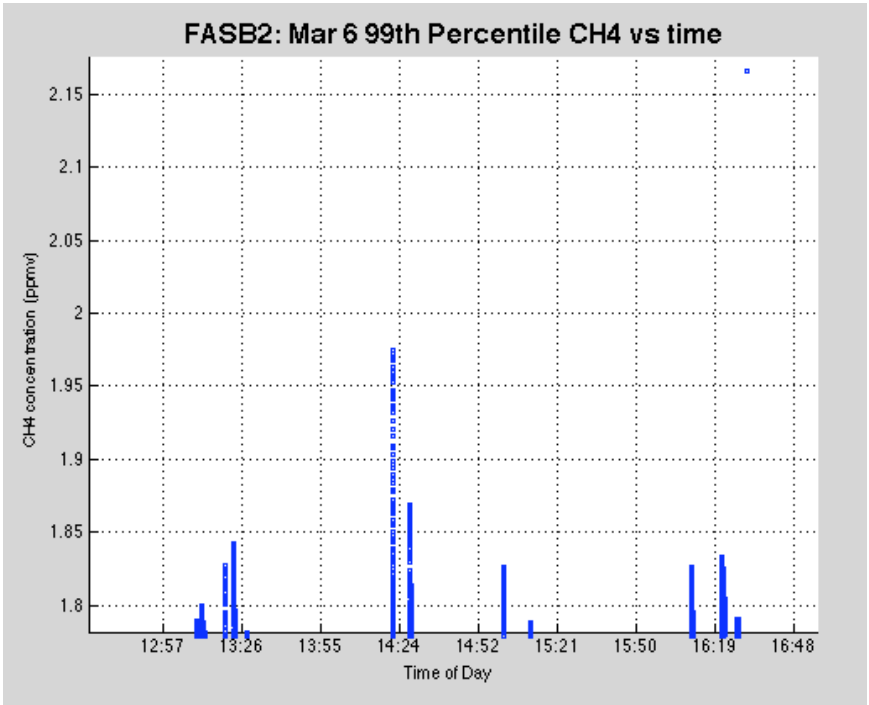


Figure 4.6: 99th percentile of $CH_4$ concentration measurements on March 6th.

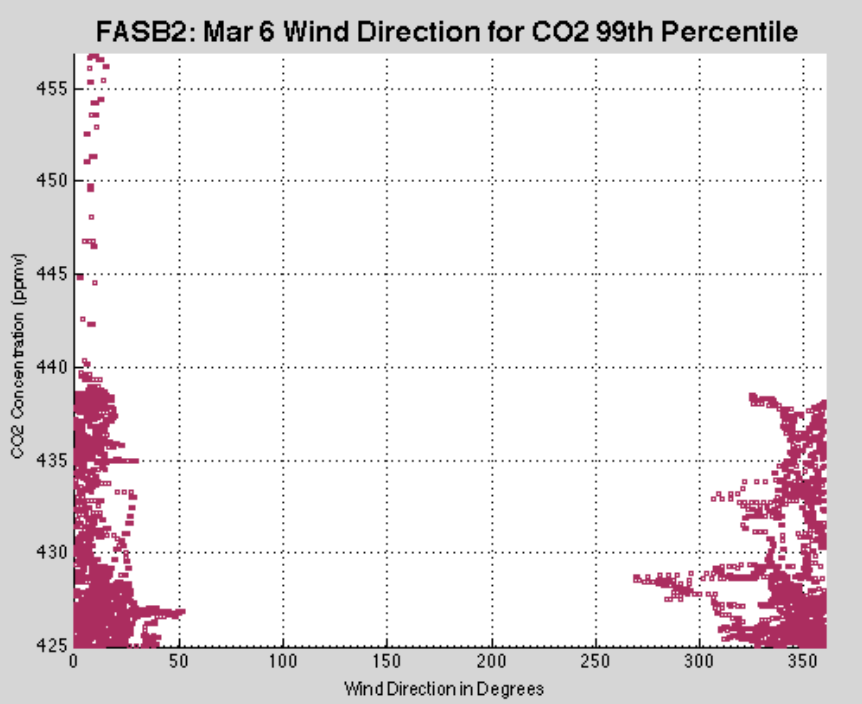


Figure 4.7: 99th percentile of $CO_2$ concentrations vs. wind direction for March 6th at FASB2 location.

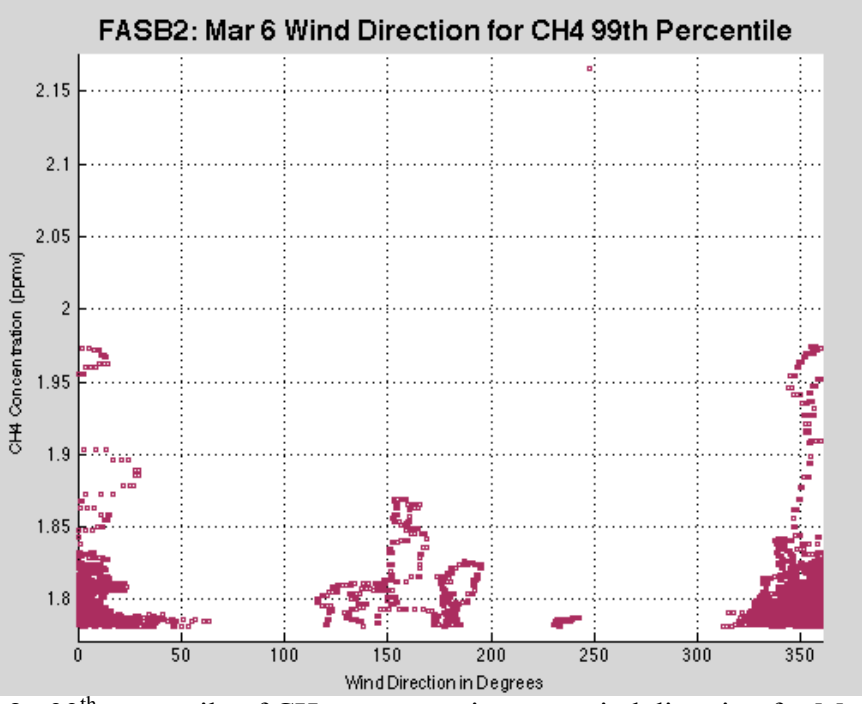


Figure 4.8: 99th percentile of $CH_4$ concentrations vs. wind direction for March 6th at FASB2 location.

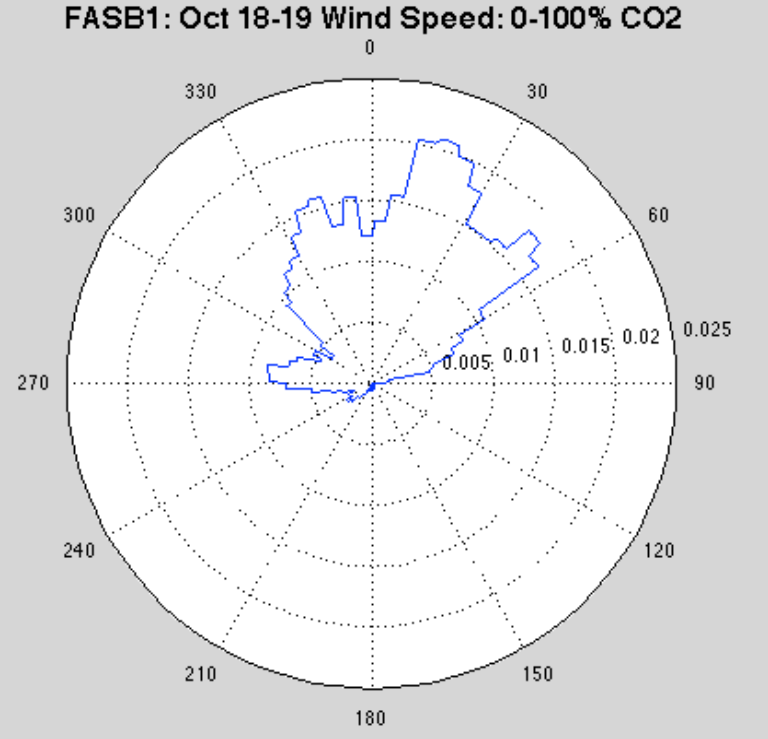


Figure 4.9: Probability rose diagram for all wind speeds (0-100%) at FASB1 overnight session.

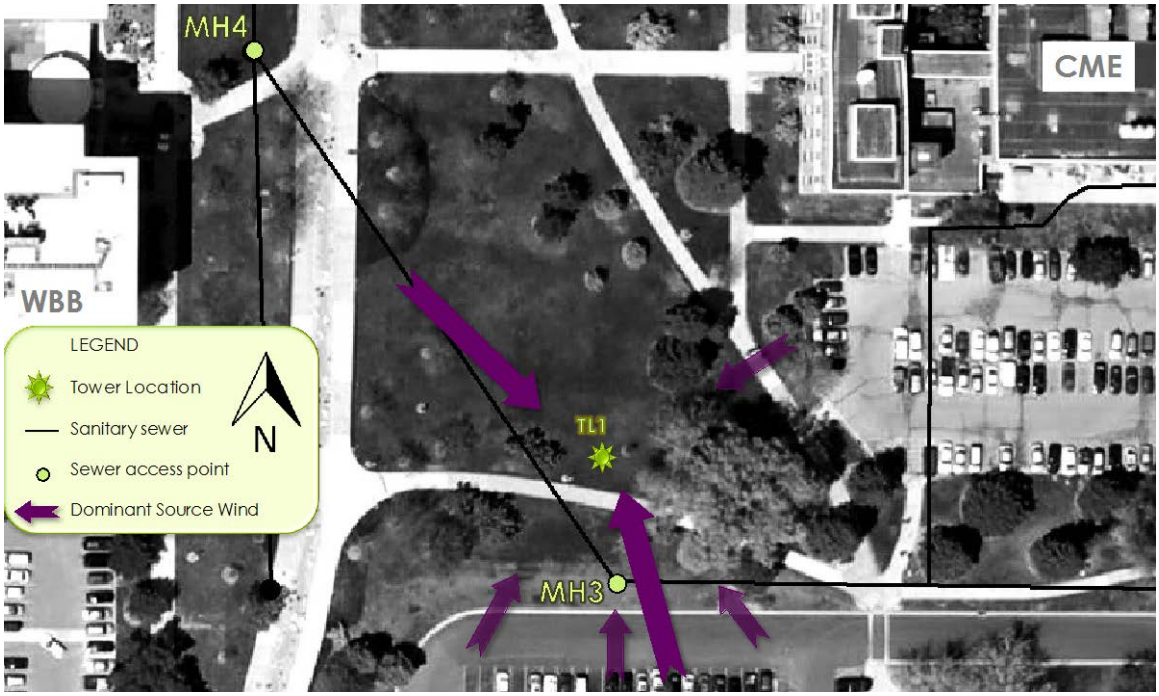


Figure 4.10: Dominant wind directions associated with gas detection for TL1.

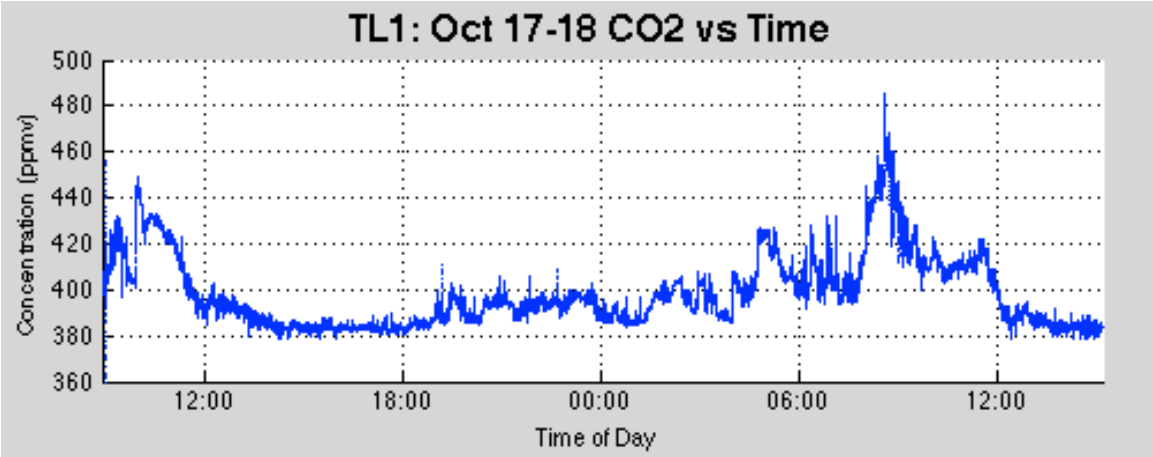


Figure 4.11: $CO_2$ measurements at TL1 for a 30-hour collection period.

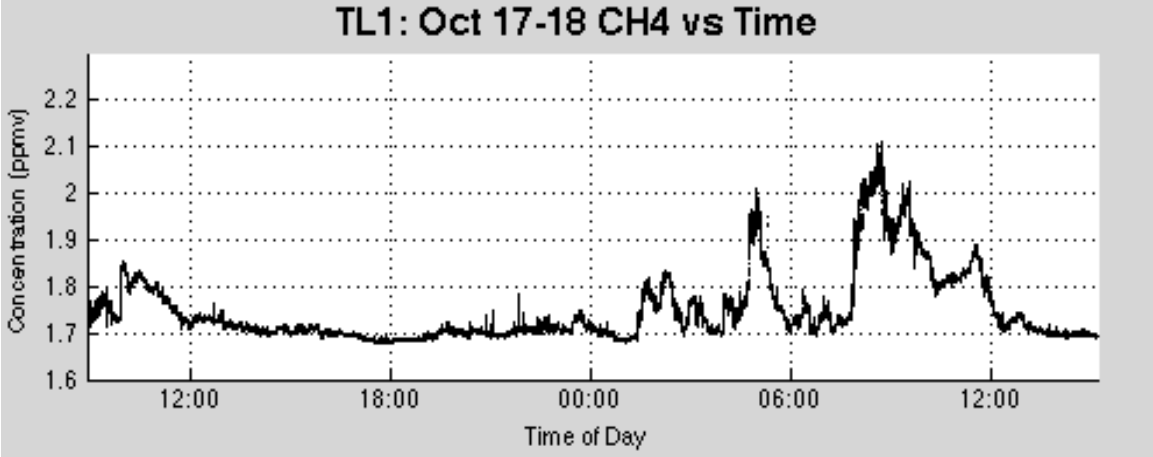


Figure 4.12: $CH_4$ measurements at TL1 for a 30-hour collection period.

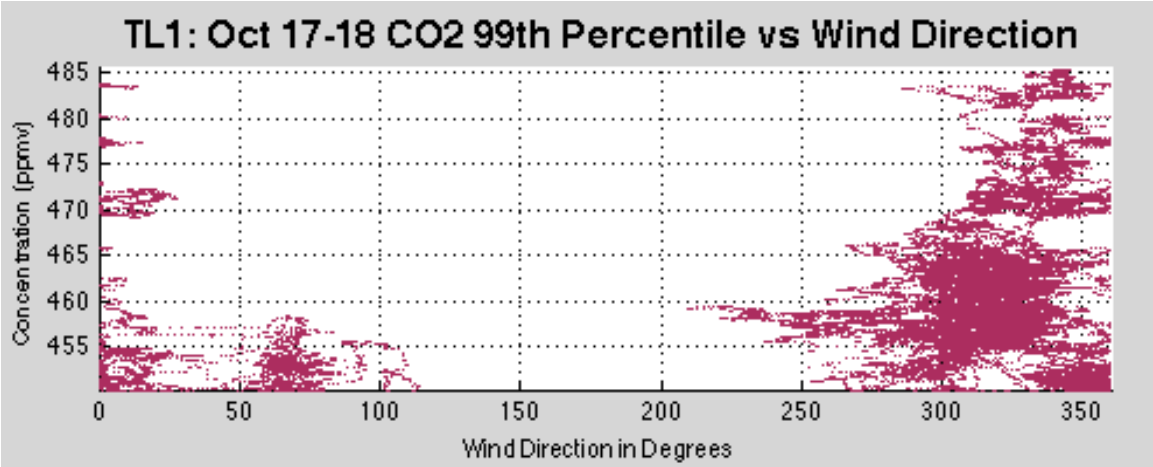


Figure 4.13: Wind directions associated with the $CO_2$ 99$^{th}$ percentile at TL1 for 30-hour collection.

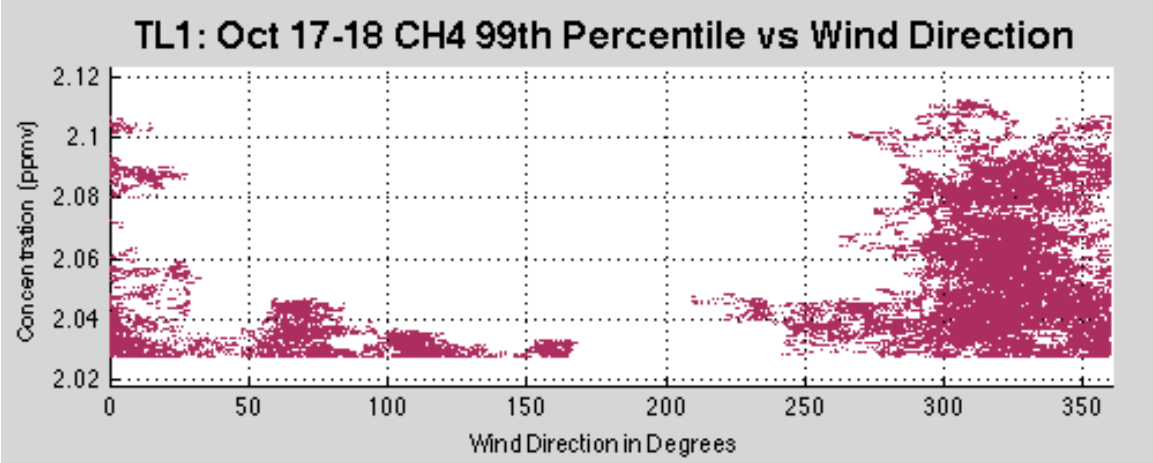


Figure 4.14: Wind directions associated with the $CH_4$ 99$^{th}$ percentile at TL1 for 30-hour collection.

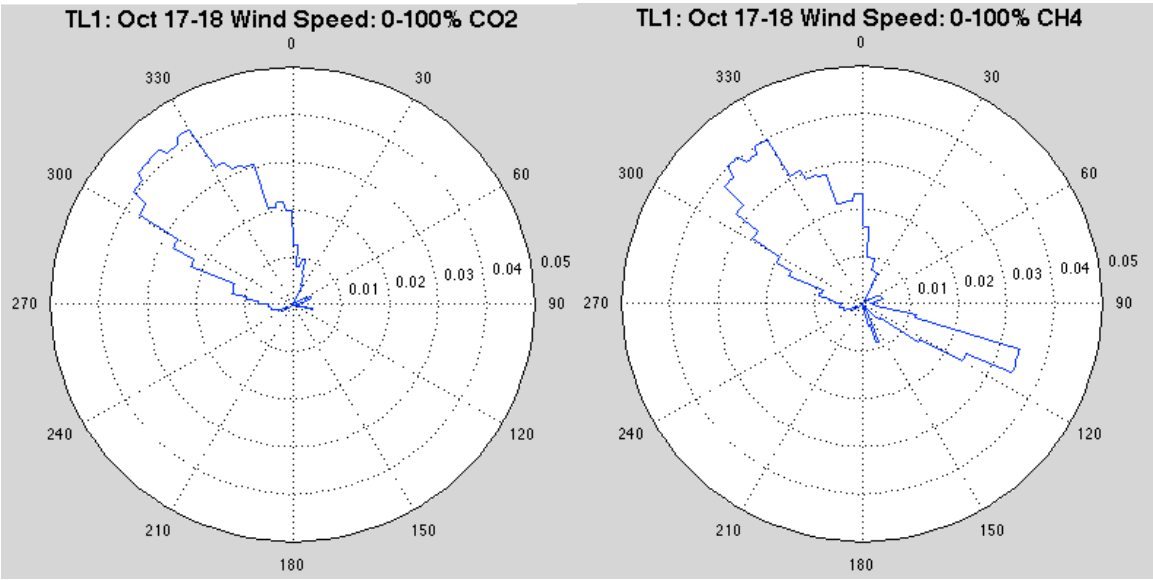


Figure 4.15: Probability rose diagrams for $CO_2$ and $CH_4$ at TL1 for 30-hour collection (0-100% wind speed).

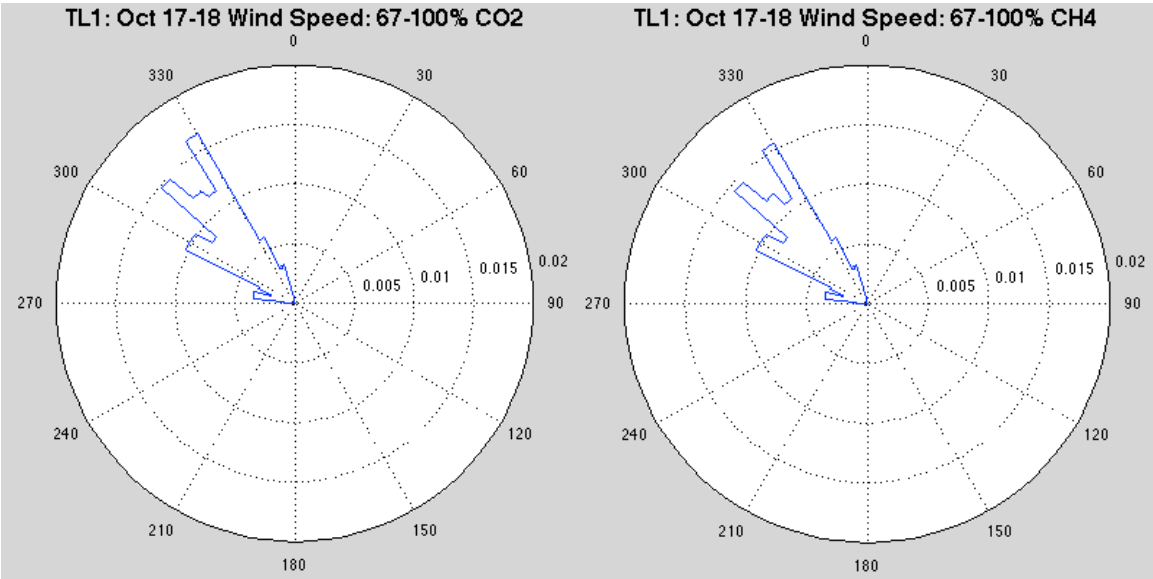


Figure 4.16: Probability rose diagrams for $CO_2$ and $CH_4$ at TL1 for 30-hour collection (67-100% wind speed).


Figure 4.17: Dominant wind directions associated with gas detection for FASB1.

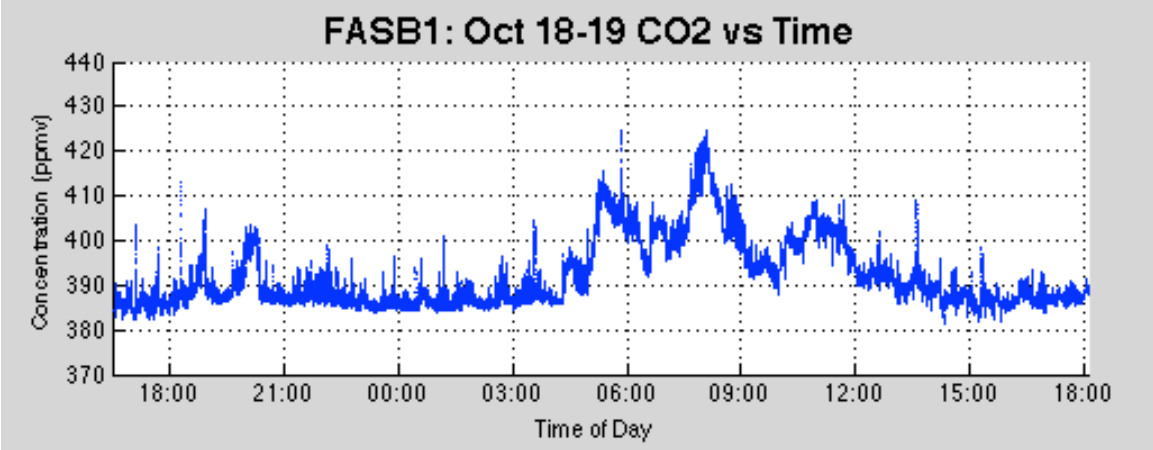


Figure 4.18: $CO_2$ measurements at FASB1 for a 25-hour collection period.

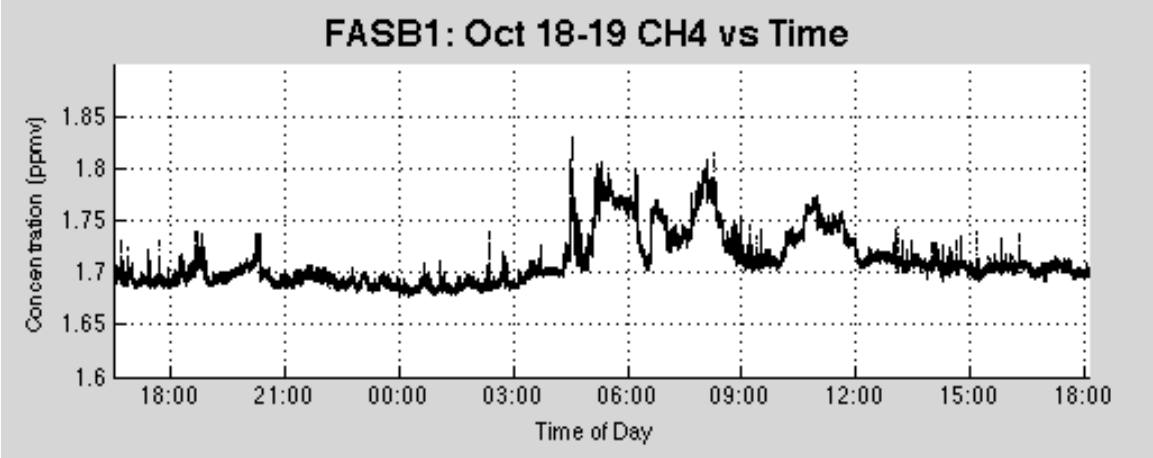


Figure 4.19: $CH_4$ measurements at FASB1 for a 25-hour collection period.

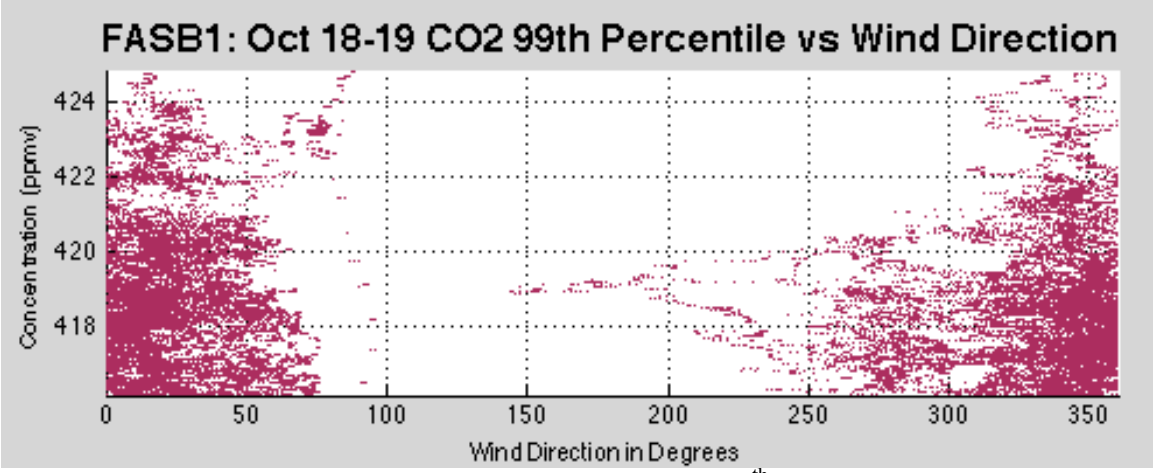


Figure 4.20: Wind directions associated with the $CO_2$ 99$^{th}$ percentile at FASB1 for 25-hour collection.

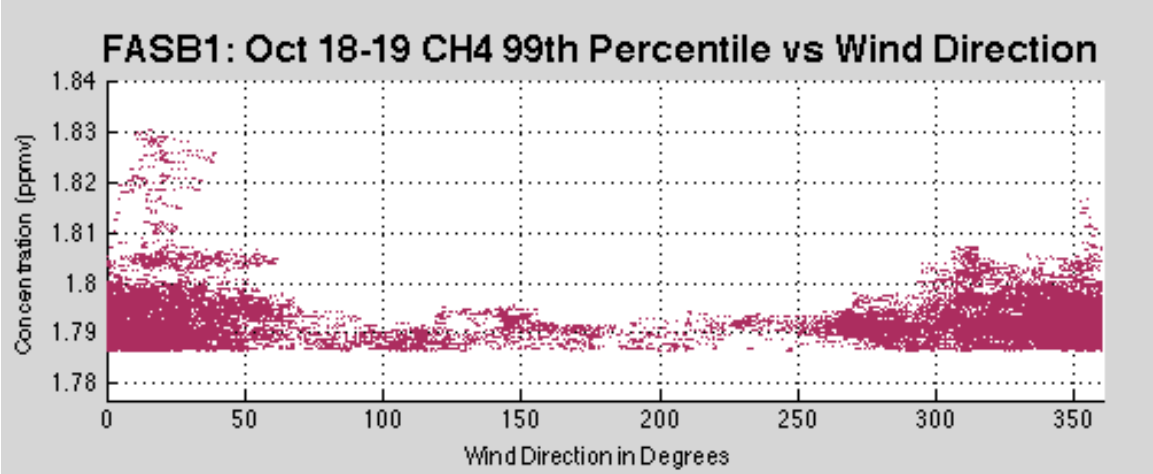


Figure 4.21: Wind directions associated with the $CH_4$ 99$^{th}$ percentile at FASB1 for 25-hour collection.

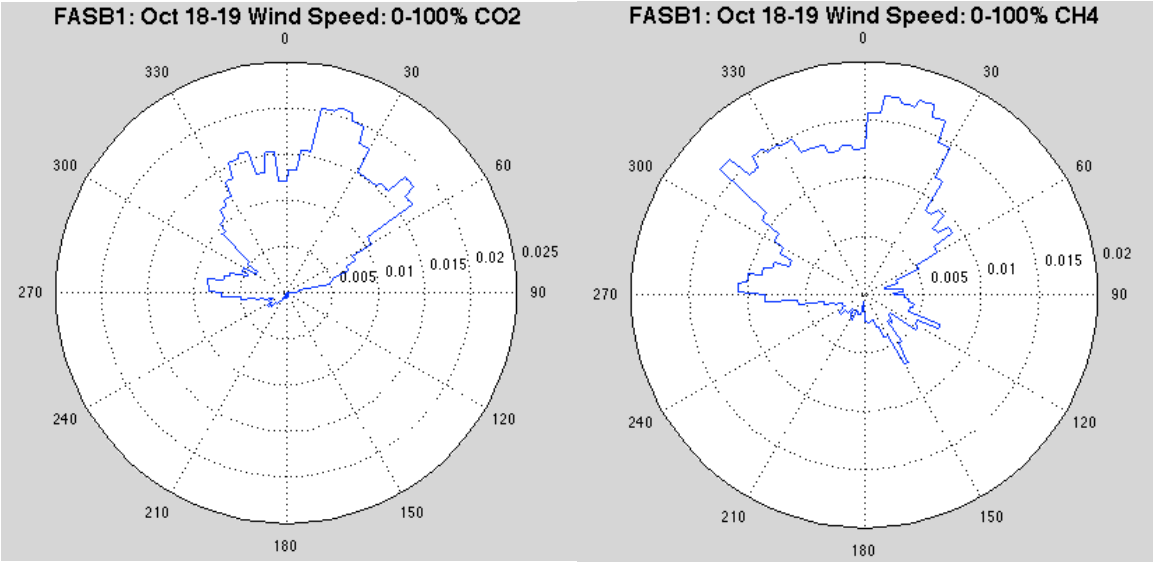


Figure 4.22: Probability rose diagrams for $CO_2$ and $CH_4$ at FASB1 for 25-hour collection (0-100% wind speed).

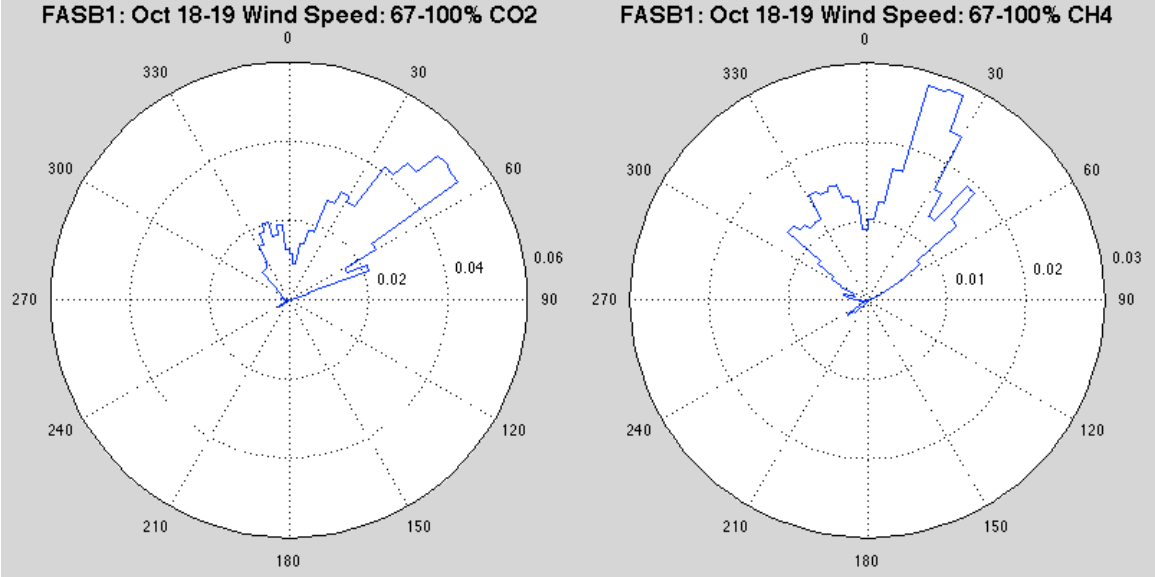


Figure 4.23: Probability rose diagrams for $CO_2$ and $CH_4$ at FASB1 for 25-hour collection (67-100% wind speed).


Figure 4.24: Dominant wind direction associated with gas detection for FASB2.

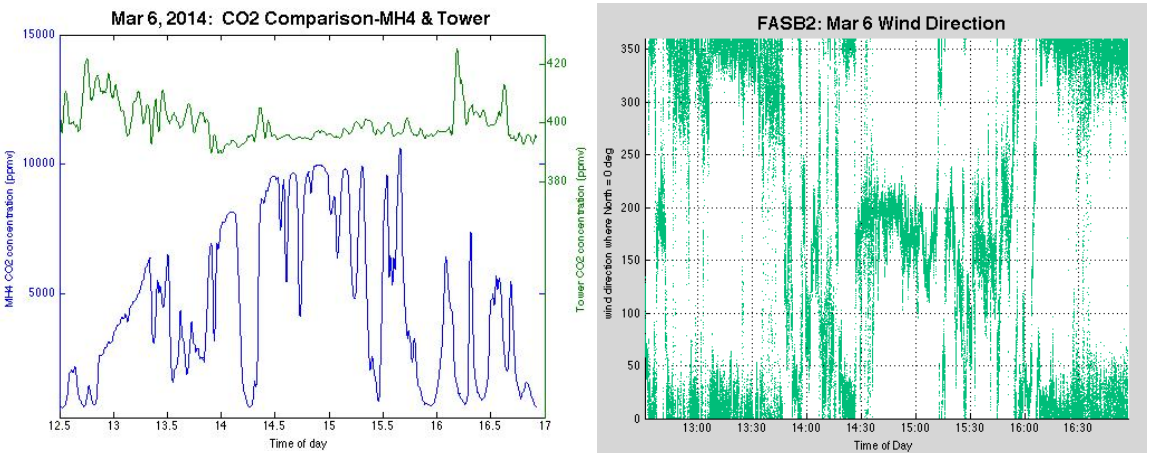


Figure 4.25: $CO_2$ coinciding measurements for point source (MH4-Blue) and tower (FASB2-Green) and daily wind direction for March 6th.

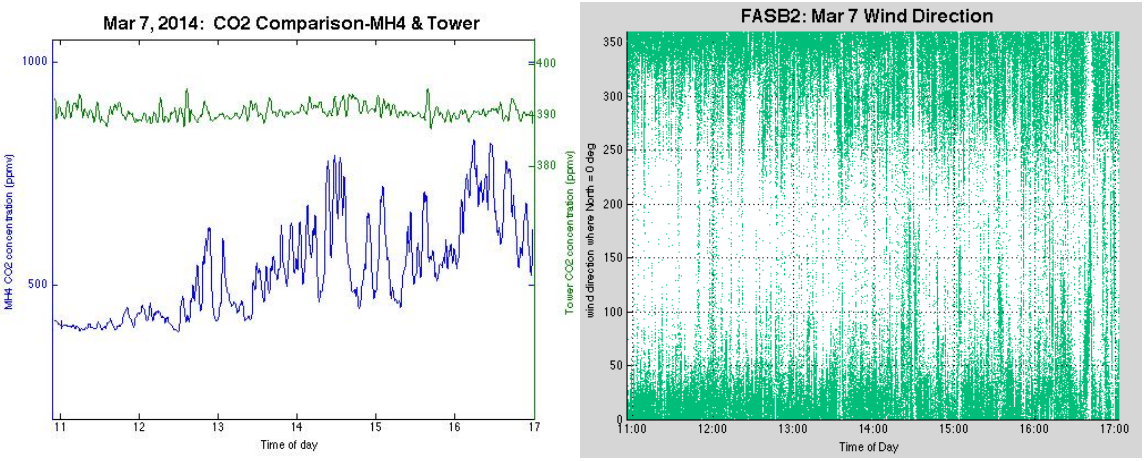


Figure 4.26: $CO_2$ coinciding measurements for point source (MH4-Blue) and tower (FASB2-Green) and daily wind direction for March 7th.

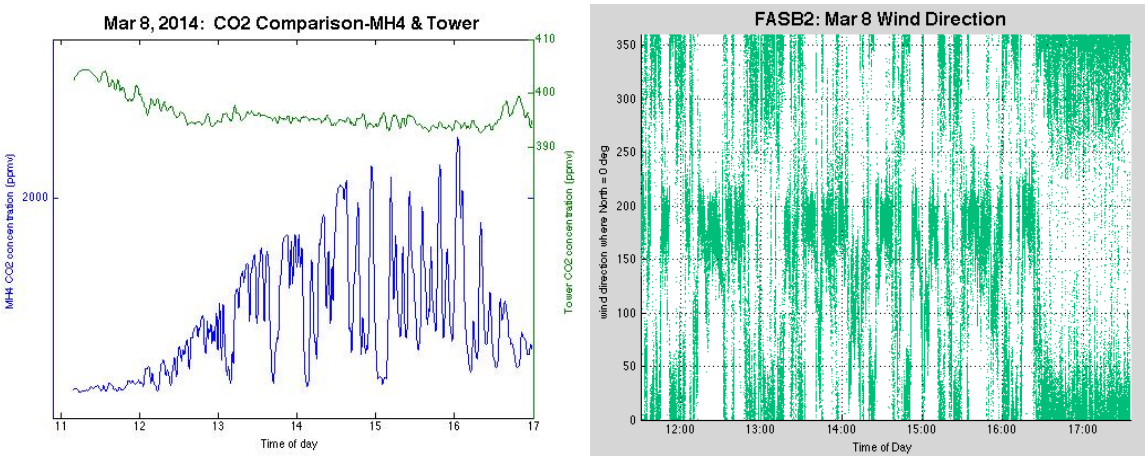


Figure 4.27: $CO_2$ coinciding measurements for point source (MH4-Blue) and tower (FASB2-Green) and daily wind direction for March 8th.

Table 4.1: Data variables used for tower analysis.

| **Variable** | **Description** | **Units** |
|---|---|---|
| Date | Year, month, day | Standard |
| Time | Time of day | Military time |
| CH4_dry | Dry concentration measurement of $CH_4$ | ppmv |
| CO2_dry | Dry concentration measurement of $CO_2$ | ppmv |
| Anemometer_UX | Wind speed in X direction | m/s |
| Anemometer_UY | Wind speed in Y direction | m/s |
| Anemometer_UZ | Wind speed in Z direction | m/s |

Table 4.2: Wind and concentration data analysis results for $CO_2$ at TL1.

| **TOWER LOCATION 1** | | | **$CO_2$ 99th Percentile of Dataset** | | | | | |
|---|---|---|---|---|---|---|---|---|
| Date | Start | End | 99th Percentile (ppmv) | Max Detection (ppmv) | Max Detection Wind Direction | Dominant Source Wind Direction | | Secondary Source Wind Direction |
| Tuesday, September 10, 13 | 11:50 | 12:50 | 401.02 | 416.29 | 65 | 50-100 | NE | 125 |
| Wednesday, September 11, 13 | 13:00 | 16:00 | 392.23 | 445.20 | 180 | 100-200 | SSE | 45 |
| Thursday, September 12, 13 | 10:30 | 12:00 | 399.71 | 446.03 | 135 | 125-150 | SE | 200 |
| Friday, September 13, 13 | 11:00 | 15:00 | 408.63 | 423.36 | 245 | 200-275 | SW | 75-150 |
| Monday, September 16, 13 | 12:00 | 14:30 | 399.11 | 410.30 | 180 | 150-225 | S | n/a |
| Wednesday, September 18, 13 | 10:00 | 13:30 | 390.24 | 409.04 | 335 | 300-350 | WNW | n/a |
| Friday, September 20, 13 | 10:00 | 12:15 | 422.35 | 462.65 | 240 | 175-300 | WSW | n/a |
| Monday, September 23, 13 | 13:30 | 15:00 | 382.90 | 394.07 | 330 | 275-350 | NW | 210 |
| Tuesday, September 24, 13 | 15:20 | 16:10 | 380.01 | 384.48 | 150-175 | 100-180 | SE | n/a |
| Wednesday, September 25, 13 | 10:20 | 11:40 | 408.52 | 414.56 | 270 | 275-350 | NW | 215 |
| Monday, September 30, 13 | 12:30 | 15:00 | 384.66 | 405.89 | 135 | 75-160 | ESE | 275 |
| Tuesday, October 1, 13 | 15:00 | 17:00 | 392.00 | 396.09 | 210 | 200-300 | WSW | 300-45 |
| Wednesday, October 2, 13 | 10:45 | 13:00 | 405.41 | 424.26 | 170 | 160-225 | SSW | 275 |
| Friday, October 4, 13 | 10:00 | 13:00 | 382.89 | 415.21 | 180 | 175-225 | SSW | 125 |
| Monday, October 7, 13 | 13:45 | 14:40 | 405.53 | 496.21 | 100-125 | 75-150 | SE | 300 |
| Wednesday, October 9, 13 | 12:00 | 16:15 | 402.98 | 413.01 | 190 | 160-240 | SSW | n/a |
| Friday, October 11, 13 | 14:15 | 16:30 | 384.60 | 388.15 | 350-15 | 325-15 | N | n/a |
| Thursday, October 17, 13 | 9:00 | 18:30 | 441.33 | 456.35 | 325 | 175-325 | SW | n/a |
| 10/17/2013 (overnight) | 18:30 | 4:30 | 404.27 | 411.34 | 50 | 40-80 | NE | 225-300 |
| Friday, October 18, 13 | 4:30 | 15:00 | 462.16 | 485.39 | 340 | 280-5 | NW | n/a |
| October 17-18 complete | 9:00 | 15:00 | 450.03 | 485.39 | 340 | 280-355 | NW | 60 |

Table 4.3: Wind and concentration data analysis results for $CH_4$ at TL1.

| TOWER LOCATION 1 | | | $CH_4$ 99th Percentile of Dataset | | | | | |
|---|---|---|---|---|---|---|---|---|
| Date | Start | End | 99th Percentile (ppmv) | Max Detection (ppmv) | Max Detection Wind Direction | Dominant Source Wind Direction | | Secondary Source Wind Direction |
| Tuesday, September 10, 13 | 11:50 | 12:50 | 1.93 | 2.23 | 75 | 50-100 | NE | n/a |
| Wednesday, September 11, 13 | 13:00 | 16:00 | 1.70 | 2.09 | 70 | 150-200 | SSE | 50 |
| Thursday, September 12, 13 | 10:30 | 12:00 | 1.83 | 2.87 | 135 | 100-175 | SE | 75 |
| Friday, September 13, 13 | 11:00 | 15:00 | 1.78 | 1.93 | 245 | 200-275 | SW | 75-150 |
| Monday, September 16, 13 | 12:00 | 14:30 | 1.71 | 1.80 | 155 | 125-175 | SSE | n/a |
| Wednesday, September 18, 13 | 10:00 | 13:30 | 1.74 | 1.75 | 300 | 300-350 | WNW | 250 |
| Friday, September 20, 13 | 10:00 | 12:15 | 1.79 | 1.81 | 180 | 150-250 | SSE | n/a |
| Monday, September 23, 13 | 13:30 | 15:00 | 1.69 | 1.72 | 360 | 250-340 | NW | n/a |
| Tuesday, September 24, 13 | 15:20 | 16:10 | 1.70 | 1.71 | 220 | 125-225 | S | n/a |
| Wednesday, September 25, 13 | 10:20 | 11:40 | 1.80 | 1.81 | 225 | 225-340 | WNW | n/a |
| Monday, September 30, 13 | 12:30 | 15:00 | 1.69 | 1.71 | 185 | 100-220 | SSE | n/a |
| Tuesday, October 1, 13 | 15:00 | 17:00 | 1.75 | 1.75 | 340 | 0-25 | NE | 300-350 |
| Wednesday, October 2, 13 | 10:45 | 13:00 | 1.81 | 1.82 | 175 | 300-25 | NW | 175 |
| Friday, October 4, 13 | 10:00 | 13:00 | 1.75 | 1.78 | 340 | 150-200 | S | 340 |
| Monday, October 7, 13 | 13:45 | 14:40 | 1.83 | 1.83 | 200 | 275-325 | WNW | 200 |
| Wednesday, October 9, 13 | 12:00 | 16:15 | 1.75 | 1.79 | 125 | 125-240 | S | n/a |
| Friday, October 11, 13 | 14:15 | 16:30 | 1.69 | 1.70 | 345 | 275-360 | NW | 175 |
| Thursday, October 17, 13 | 9:00 | 18:30 | 1.84 | 1.85 | 265 | 175-325 | SW | n/a |
| 10/17/2013 (overnight) | 18:30 | 4:30 | 1.82 | 1.83 | 25 | 40-100 | ENE | 250-300 |
| Friday, October 18, 13 | 4:30 | 15:00 | 2.06 | 2.11 | 315 | 280-360 | NW | n/a |
| October 17-18 complete | 9:00 | 15:00 | 2.03 | 2.11 | 315 | 280-360 | NW | n/a |

Table 4.4: Wind and concentration data analysis results for $CO_2$ at FASB1.

| FASB1 Tower Location | | | $CO_2$ 99th Percentile of Dataset | | | | | |
|---|---|---|---|---|---|---|---|---|
| Date | Start | End | 99th Percentile (ppmv) | Max Detection (ppmv) | Max Detection Wind Direction | Dominant Source Wind Direction | | Secondary Source Wind Direction |
| October 18-19 complete | 16:30 | 18:00 | 416.17 | 424.81 | 350-25 | 350-75 | NE | n/a |
| Friday, October 18, 13 | 16:30 | 0:30 | 400.57 | 413.35 | 350-5 | 350-150 | N | n/a |
| 10/19/2013 (overnight) | 0:30 | 9:00 | 418.94 | 424.81 | 75 | 300-50 | N | n/a |
| Saturday, October 19, 13 | 9:00 | 18:00 | 406.96 | 409.03 | 280 | 250-25 | W | 50-100 |
| Wednesday, October 23, 13 | 11:00 | 16:30 | 434.88 | 453.90 | 260-275 | 300-10 | NW | n/a |
| Friday, November 1, 13 | 10:00 | 14:30 | 399.80 | 418.39 | 200 & 25 | 275-25 | NW | 150-200 |
| Tuesday, November 5, 13 | 14:45 | 16:15 | 395.61 | 421.89 | 125 | 20 | NE | 350 |
| Wednesday, November 6, 13 | 9:45 | 11:45 | 429.11 | 437.15 | 325 | 250-355 | NW | 100 |
| Thursday, November 7, 13 | 13:30 | 16:00 | 423.38 | 433.56 | 280 | 300-15 | NW | n/a |
| Friday, November 8, 13 | 10:30 | 16:30 | 398.29 | 432.87 | 350 | 300-15 | NW | n/a |
| Monday, November 11, 13 | 10:00 | 15:00 | 424.56 | 449.08 | 280 | 250-350 | NW | 0 |
| Tuesday, November 12, 13 | 14:20 | 16:00 | 431.41 | 436.04 | 310 | 275-350 | NW | 0 |
| Wednesday, November 13, 13 | 10:00 | 16:00 | 482.69 | 500.01 | 320 | 250-325 | NW | 40-50 |
| Thursday, November 14, 13 | 14:30 | 16:30 | 398.99 | 405.78 | 0 | 350-25 | N | 150-200 |
| Monday, November 18, 13 | 9:30 | 15:00 | 451.96 | 485.01 | 255 | 275-5 | NW | n/a |
| Monday, November 25, 13 | 10:00 | 15:00 | 422.54 | 436.86 | 280 | 300-15 | NW | 100 |
| Monday, December 2, 13 | 10:30 | 13:45 | 413.18 | 436.11 | 325 | 320-15 | N | 175-200 |

Table 4.5: Wind and concentration data analysis results for $CH_4$ at FASB1.

| **FASB1 Tower Location** | | | **$CH_4$ 99th Percentile of Dataset** | | | | | |
|---|---|---|---|---|---|---|---|---|
| Date | Start | End | 99th Percentile (ppmv) | Max Detection (ppmv) | Max Detection Wind Direction | Dominant Source Wind Direction | | Secondary Source Wind Direction |
| October 18-19 complete | 16:30 | 18:00 | 1.79 | 1.83 | 25 | 300-50 | NE | n/a |
| Friday, October 18, 13 | 16:30 | 0:30 | 1.73 | 1.74 | 315 | 300-75 | N | n/a |
| 10/19/2013 (overnight) | 0:30 | 9:00 | 1.79 | 1.83 | 15 | 300-50 | NE | 115-150 |
| Saturday, October 19, 13 | 9:00 | 18:00 | 1.76 | 1.77 | 350 | 250-25 | W | 50-100 |
| Wednesday, October 23, 13 | 11:00 | 16:30 | 1.86 | 1.92 | 250-265 | 250-10 | W | 150-250 |
| Friday, November 1, 13 | 10:00 | 14:30 | 1.73 | 1.83 | 325 | 300-25 | NW | 150 |
| Tuesday, November 5, 13 | 14:45 | 16:15 | 1.71 | 1.74 | 110 | 110-160 | SE | 350-0 |
| Wednesday, November 6, 13 | 9:45 | 11:45 | 1.77 | 1.79 | 255 | 340-5 | NW | 250-300 |
| Thursday, November 7, 13 | 13:30 | 16:00 | 1.80 | 1.85 | 315 | 300-350 | NW | 275 |
| Friday, November 8, 13 | 10:30 | 16:30 | 1.71 | 1.83 | 300 | 280-10 | NW | n/a |
| Monday, November 11, 13 | 10:00 | 15:00 | 1.85 | 1.90 | 255 | 250-300 | NW | 175-200 |
| Tuesday, November 12, 13 | 14:20 | 16:00 | 1.88 | 1.92 | 250-300 | 250-300 | NW | 150-200 |
| Wednesday, November 13, 13 | 10:00 | 16:00 | 2.24 | 2.26 | 55 | 175-225 | WSW | 50-100 |
| Thursday, November 14, 13 | 14:30 | 16:30 | 1.75 | 1.89 | 160-200 | 100-215 | S | n/a |
| Monday, November 18, 13 | 9:30 | 15:00 | 1.82 | 2.01 | 260 | 225-350 | W | n/a |
| Monday, November 25, 13 | 10:00 | 15:00 | 1.80 | 2.08 | 350-10 | 300-60 | NE | n/a |
| Monday, December 2, 13 | 10:30 | 13:45 | 1.73 | 1.88 | 350 | 310-25 | NNW | 160-225 |

Table 4.6: Wind and concentration data analysis results for $CO_2$ at FASB2.

| **FASB2 Tower Location** | | | **$CO_2$ 99th Percentile of Dataset** | | | | | |
|---|---|---|---|---|---|---|---|---|
| Date | Start | End | 99th Percentile (ppmv) | Max Detection (ppmv) | Max Detection Wind Direction | Dominant Source Wind Direction | | Secondary Source Wind Direction |
| Thursday, March 6, 14 | 12:30 | 17:00 | 424.96 | 456.78 | 5-15 | 325-30 | N | n/a |
| Friday, March 7, 14 | 11:00 | 17:00 | 397.57 | 410.92 | 225 | 325-40 | N | 225-275 |
| Saturday, March 8, 14 | 11:30 | 17:30 | 403.73 | 407.92 | 325 | 325-25 | NNW | 200 |

Table 4.7: Wind and concentration data analysis results for $CH_4$ at FASB2.

| **FASB2 Tower Location** | | | **$CH_4$ 99th Percentile of Dataset** | | | | | |
|---|---|---|---|---|---|---|---|---|
| Date | Start | End | 99th Percentile (ppmv) | Max Detection (ppmv) | Max Detection Wind Direction | Dominant Source Wind Direction | | Secondary Source Wind Direction |
| Thursday, March 6, 14 | 12:30 | 17:00 | 1.78 | 2.17 | 245 | 315-25 | N | 125-175 |
| Friday, March 7, 14 | 11:00 | 17:00 | 1.71 | 1.79 | 330-5 | 300-40 | NNW | n/a |
| Saturday, March 8, 14 | 11:30 | 17:30 | 1.76 | 1.77 | 130-150 | 175-225 | SSW | n/a |

# CHAPTER 5

# $CO_2$ CONTROLLED RELEASE

## 5.1 Controlled $CO_2$ Release Experiments

During the final stages of the project, it became clear that sensitivity of the CRDS and the variability of atmospheric conditions dictate effectiveness of detection under field conditions. To examine such sensitivity and to gain insight regarding what may be a typical effective "footprint" of survey size, a controlled release of $CO_2$ was executed with two types of experiments. The first was designed as a semicontrolled environment and the second consisted of a field location (on the University of Utah campus). The experiments were performed to evaluate detection for different release rates and different distances between the source and CRDS.

One primary reason for the experiments was that the point source of this project, MH4, has been found to discharge $CO_2$ and $CH_4$ but the release is nonsteady and unpredictable. A controlled release will help to eliminate the erratic source release. The first type of experiment was performed in a semicontrolled environment consisting of a hallway on campus, and the second was performed with the project tower at location FASB2. The hallway location minimized inconsistent weather patterns and the experiment conducted outside with the tower postulated actual tower detection abilities. Both investigations followed similar procedures.

There is minimal literature pertaining to controlled releases and actual tower detection. J. Lewicki et al. at the Zero Emissions Research and Technology (ZERT) site in Montana published one study in 2009 that was influential in this project experiment design. The ZERT study was performed over a flat field 0.12 $km^2$ in size and used eddy covariance towers for detection of the released gas. The main objective of this project was to test the abilities of the technology with respect to detection, location identification and quantification, as there are few documented experiments of this type. Two release rates were established as Release 1 at 0.1 tonnes $CO_2$/day and Release 2 at 0.3 tonnes $CO_2$/day. Release 1 was a rate that would "provide a challenging detection problem" while Release 2 was chosen for "demonstration purposes" per Lewicki et al. (2009). The release was 27 meters from the towers and the height of detection was 3.2 meters over the entire period with additional detection at 3.0 meters for Release 1 and 2.8 meters for Release 2. The results concluded that Release 1 was difficult to discern from background, while Release 2 showed an upward shift in average values. Release 1 was determined to be undetectable in the $95^{th}$ percentile (18.6 $g/m^2/d$) but Release 2 was seen in the $95^{th}$ percentile.

The Lewicki et al. (2009) releases were 92 and 276 times greater than the estimated rate of release from this research project point source (MH4) at 0.0011 tonnes $CO_2$/day, the distance was twice as long and over homogeneous flat ground with a flux tower, but detection was at the same height. From the Lewicki et al. (2009) study at the ZERT facilities, the concept of a challenging release rate and a demonstration release rate were applied to this experiment. The challenging rate was close to MH4 release and the three larger flows provided data for threshold and footprint characterization. The flow

rates established for the controlled release were 0.5, 5, 10 and 20 lpm. Even though the rates were held constant, the amount of $CO_2$ released varied slightly during the allotted experiments because of different atmospheric conditions (temperature and pressure). The atmospheric values were provided by the MesoWest U of U station MWBB and Table 5.1 shows the resulting values for each day.

The largest release rate at 20 lpm was 40 times that of the estimated source release, corresponding to the lowest release rate of 0.5 lpm. This high flow rate was expected to impart a high and definite detection by the instrumentation.

To cast perspective on the relative amount of $CO_2$ released during this experiment, information from the EPA fact sheet "Greenhouse Gas Emissions from a Typical Passenger Vehicle" is examined. This EPA study indicates that combustion of one gallon of gasoline will produce almost 9000 grams of $CO_2$, and the average passenger vehicle emits almost 425 grams $CO_2$ per mile. The annual emissions for the same passenger car will total 5.1 metric tonnes $CO_2$ (at 12,000 miles per year). Conversions of these numbers would result in 0.01397 tonnes/day, or 13,970 g/d. Comparison of these values to those in Table 5.1 illustrate that the range of emissions/releases for this experiment are above and below the average vehicle rate. Another aspect is to compare with vehicle mileage per gallon. The two intermediate releases, 5 and 10 lpm, are calculated to be at approximate vehicle emission rates from an efficient vehicle (25 mpg) to a less efficient vehicle (13 mpg), respectively. Whereas the largest release rate of 20 lpm would be equivalent to a vehicle with an extremely low gas mileage (5-8 mpg).

For this experimentation, however, it is important to note that the duration of gas

release for each test is only 1 minute. Therefore it is perhaps more meaningful to consider that the total carbon dioxide released during this entire experiment (indoor hallway and at the field location) would be equivalent to a typical vehicle driving less than 2 miles or burning less than 0.1 gallons of gas.

### 5.1.1 Equipment

An Omega® FMA5528 Mass Flow Controller (MFC) was used to control the flow of the $CO_2$ from the tank to the atmosphere. The mass flow controller operates by splitting the incoming flow and streaming a smaller portion through a small capillary stainless steel sensor tube. Coils wound around the tube add heat, and a differential is measured from the upstream to the downstream section of the sample tubing by the electronic control circuit. This measurement is used to obtain a flow rate within the small tube. Flow is kept in a laminar state, and by fluid dynamics laws the principle of proportionality between the sampling tube and remainder of gas is held as true for the calculation of the flow rate out of the instrument. Flow control is achieved by a solenoid valve that automatically adjusts to achieve the desired outflow rate based on the incoming value. The operator has the ability to choose a value between 0 and 50 with precision of one tenth and instrument accuracy of ±1.5% (per the instrument's user's guide). The MFC has a range of 0-50 lpm and is calibrated for Nitrogen ($N_2$). Conversion to $CO_2$ was done with a multiplication factor provided by the manufacturer. The corresponding range for $CO_2$ is 0-36.9 lpm. The instrument requires 12 VDC power provided by the building power and a converter.

The gas source used was an industrial, high pressure $CO_2$ tank provided by a gas

supplier. It contained 100% $CO_2$ concentration.

Connections between the MFC and the gas tank were achieved with ¼ inch plastic tubing and fittings. The entire setup was tested for leaks before the controlled release experiment was conducted.

The CRDS was used for gas detection with a flow of 5 lpm.

A box fan with three speeds (low, medium and high) was used for the "semi-controlled environment" to induce airflow at a relatively constant speed and direction through the hallway of the experiment, as described in the next section.

### 5.1.2 Controlled Release Setup and Execution in Semicontrolled Environment

A semicontrolled environment on campus was the location for the first experiment. This was done to remove effects of inconsistent atmospheric conditions and wind variations associated with the outdoor field location. In this setting, the wind variable was controlled (to the greatest extent possible) with a box fan; at minimum, air movement was maintained at a steady rate and direction. The source release was coordinated with the MFC, or flowmeter. The hallway eliminated crosswind influences by closing all doors and windows and sealing the space between the door and floor. The experiment was conducted on Saturday, April 26, 2014 when the building was mostly empty to eradicate human interaction and related increased $CO_2$ levels and turbulences. It was also conducted the evening of May 20, 2014 during evening hours of 19:00 to 21:00.

The CRDS sampling tubing was placed at one end of the hallway at a level of 3 feet above the floor on an easel. This placement allowed air circulation around the

sampling tubing and reduction of influences by walls, ceiling and floor. The detection point remained in the designated location for the duration of the experiment.

The $CO_2$ tank and attached flowmeter were systematically arranged at specified distances of 10, 30 and 50 feet from the detection point (the actual detection point at the FASB2 location was 43 feet from the point source in the field). The release of gas was at floor level and through a ¼ inch OD tube facing up, for sake of maintaining a level surface. The release at ground level was intended to mimic the release from a point source into the atmosphere. Figure 5.1 shows the experimental setup in the hallway.

Three researchers carried out the experiment. One researcher was responsible for maintaining, resetting and controlling the flowmeter. The other two observed the CRDS screen during the test (in real time), and also timed each aspect and wrote associated notes. Coordination among all three personnel was critical.

The first hallway experiment was conducted with three flow rates, where the lowest rate of 0.5 lpm corresponded to the average release rate from the point source MH4 (that was previously determined as 1086 g/d) equivalent to approximately 0.5 lpm of pure $CO_2$. A maximum flow rate of 10 lpm and an intermediate flow of 5 lpm were the other two rates applied, both in $CO_2$ flow rate values. The second experiment on May 20$^{th}$ was conducted only with a 20 lpm release rate.

At each distance and flow rate, $CO_2$ was released for 1 minute, after a 5-minute period of flushing. Flushing of the area involved opening doors and turning the box fan on at its highest rate. Each flow rate release was performed twice at each location.

During the active (nonflushing) period of each test, the fan was used at its lowest speed and placed 6 feet behind the $CO_2$ release point, targeting the gas towards the

detection point. This was done to simulate an ideal condition of a consistent dominant wind direction and speed.

The CRDS was continuously operated for monitoring of the gas concentration within the hallway, and the real-time readout was the basis of detection. It was operated at a flow rate of 5 lpm (this rate increased detection accuracy).

The expected outcome of the experiment was that the CRDS instrumentation would detect the released $CO_2$ by measuring an explicit and significant increase in concentration level for each test. From the concentration readings, values could be recorded and ultimately a threshold graph produced. This experiment was intended to help establish what type of response to expect from different release rates at different distances, especially with regard to spike magnitude. Most importantly, these tests were intended to determine whether the tower is actually capable of registering a point source release for a range of release rates. An ideal outcome would be a threshold release rate criterion for different distances, but many tests would be required to identify a comprehensive or general set of such criteria.

### 5.1.3 Controlled Release Setup and Execution at FASB2 Tower Location

The flowmeter and $CO_2$ tank were set up outside near the FASB2 tower location, and the CRDS was connected to the sampling tubing on the tower. MH4 was covered with a tarp to sequester any release of gases during the experiment. The testing was performed during the evening hours of 18:00 through 20:00 on May 1, 2014, and the wind was calm and unsteady.

The release of the $CO_2$ was stationed at 10, 30 and 43 feet (horizontally) from the

detection point of the tower, and the 43 feet location is located on MH4. All locations were in line with the sewer access cover and the tower.

The release rate was maintained at 20 lpm of $CO_2$ for the duration of the release. Initial measurements were taken with 10 lpm (the highest flow rate from the first experiment), but detection was not prominent on the real time screen. Therefore, the flow rate was doubled. Each release was 1 minute and measurements at each location were performed at least twice. Once again, the gas was emitted directly from the plastic tubing at ground level into the atmosphere and was directed straight up to mimic release from the sewer access cover.

Two researchers conducted the experiment, and the outcome was expected to produce results of lower accuracy than the semicontrolled setup, primarily due to the atmospheric (weather) conditions and the presence of additional sources that the tower would likely detect during the testing. It was anticipated that the larger flow rate of 20 lpm would be detected and exhibit some extent of trending between distances and detection.

### 5.1.4 Controlled Release Data Analysis

Following completion of the experiments, the data were retrieved from the hard drive of the CRDS and the files were reduced in size for the variables required, consisting of time and dry $CO_2$ concentration. The files were analyzed alongside the field notes to verify the time intervals of gas release. This coordination ensured that the observed spikes were definitively resulting from the controlled source. The intervals for anticipated detection were reduced to 5 minutes. The period included the 1 minute prior

to controlled gas release, to establish ambient conditions, and several minutes after the emissions release was turned off, to facilitate detection of emissions following cessation. Detected emissions were plotted as concentration versus time to visualize potential spikes corresponding to controlled releases. This graphical analysis provided confirmation that the tower is capable of detecting released $CO_2$, at least for the conditions (design) of this test. The remainder of this chapter is intended to discuss these results and associated implications. A well-defined spiking interval is shown in Figure 5.2.

An initial comparison of different distances and flow rates was analyzed for maximum spike value. However, this method proved unreliable. A more effective method of comparison was to determine the area under the spiking curve to yield a total amount of $CO_2$ detected over time. This was calculated by a semiqualitative form of integration, in which the estimated ambient value was removed from the concentration values within the 1 to 4 minute range. Then the values of the average concentration over an infinitesimal time segment were multiplied by the corresponding time segment and then summed. The resultant dimensions (or units) are concentration×time or ppmv×minute. This was then multiplied by the total time interval (3 minutes) to yield a ppmv value which was then compared among all tests and represents the amount of $CO_2$ detected above ambient during the release detection (or spiking).

The 1 to 4 minute range was utilized as a window to focus the data down to the time when carbon dioxide was release and detected; this also limits the file sizes and makes utilizing the data more manageable in a practical context. This window (time interval) comprised both the 1-minute of carbon dioxide release and the subsequent lag time between release and detection. The release distances close to the tower did not

require the entire window for gas detection. However the larger source-tower distances exhibited detection within that 1 to 4 minute window in response to dispersion and distance.

The interval concentration values were plotted with respect to distance from the tower. The next step applied a trendline to each flow rate in an effort to discern a relationship between flow rate and distance for the three sets of distances and concentrations detected. A polynomial of second degree was the best fit for all datasets and goodness-of-fit ($R^2$) values were calculated.

### 5.1.5 Results and Discussion

The calculated interval concentration values were plotted for each flow rate with respect to distance. The four flow rates of 0.5, 5, 10 and 20 lpm that were released in the semicontrolled environment resulted in relationships between the distance and interval concentration values with $R^2$ values of 0.638, 0.756, 0.965 and 0.787, respectively. Figure 5.3 shows the datasets with corresponding trendlines. As expected, the higher flow rates provided larger interval concentrations of the $CO_2$, because more gas was released during the experiment. The plot also exhibits that the furthest distance (50 feet) resulted in the smallest interval concentration values for each flow rate. The smaller detection is anticipated because the increased distance allows diffusion and dispersion to decrease the amount of $CO_2$ reaching the detection point. Another important observation is that range of values at differing flow rates at the 50 foot distance are more compact. Specifically, the range of values for different flow rates is from 14 to 62 ppmv (48 ppmv difference), but at the 10 foot distance, the range is from 40 to 250 ppmv (210 ppmv

difference). This can be attributed to the high rate of detection by the CRDS and extremely high sensitivity to the release, especially at a close distance. As illustrated in Figure 5.3, a line was fit to each individual set of flow rate data.

The 10 lpm flow rate data exhibited the best fit ($R^2$ approaching unity), indicating that this release rate may be optimum for effective detection. The shape of the 0.5 lpm release differs from the other three trendlines, perhaps because of additional (unknown, not controlled release) sources detected from the 50 feet distance. The flow rate of 0.5 lpm appears to be so small that it is nearly impossible to distinguish its signal from uncontrolled sources.

The semicontrolled environment (indoor hallway tests) provided larger concentration overall values than those for the field trials; this result was anticipated. The field experiment performed at a release rate of 20 lpm, did not produce integral values higher than the 10 lpm flow rate of the hallway experiment; in fact, the values were closer to the 0.5 lpm flow rate release and the trendline was more similar in shape to the 0.5 lpm values from the indoor experiment. Figure 5.4 shows the field experiment integral values versus distance.

The trendline once again is best fit with a $2^{nd}$ degree polynomial and is similar to that of the hallway experiment, but with a more defined increase at the intermediate distance of 30 feet, most similar to the 0.5 lpm release rate. The $R^2$ value calculated was 0.313, which is lower than the first experiment and which is expected for the uncontrolled environment because of the atmosphere influences and unknown gas sources that were present during experimentation.

The similar shape of data trendlines for the 0.5 lpm semicontrolled experiment

and the 20 lpm release at FASB2 show higher interval concentrations at the intermediate distance (30 feet), similar to the footprint shape presented in Section 2.3. These trendlines for two experiments (0.5 lpm and 20 lpm; Figure 5.5) are most similar in shape because they are impacted more by uncontrolled sources than the other experiments. For the 0.5 lpm experiment, the emissions rate appears to be just too small compared to uncontrolled sources (people, air conditioning, etc.). For the 20 lpm experiment, it was conducted outdoors and was also too small for the outdoor uncontrolled sources. It is possible that these uncontrolled sources affect the footprint shape in a consistent manner, but more analysis is required to confirm such.

Figure 5.5 contains all of the controlled release data values to provide comparison between field data and the indoor data. The plot shows the field data in red, where even though the 20 lpm flow rate is 40 times as large as the 0.5 lpm flow rate used in the hallway, it does not provide integral values as high as the lowest flow rate.

Interpretation would lead to an explanation reliant upon increased amounts of wind variation in regard to direction and speed instabilities to be one cause of the distortion. The other main issue would be the height of detection; where the actual field tower is 3.65 times higher than the hallway detection point, leading to more dispersion and diffusion before detection.

## 5.2 Tower Threshold Determination

The controlled release data will be utilized to estimate the maximum distance where detection by the tower of an emission of pure $CO_2$ could occur. The estimated limit is referred to as the "threshold detection distance," and is a key aspect of the "tower

footprint," or the maximum distance of detection for the tower under specific field conditions. One initial goal of this study was to determine a general protocol for estimating threshold distances and detection footprints, but during the course of the work it became clear that a general protocol is difficult, if not impossible, simply because terrain, vegetation and meteorological conditions are so highly variable within the urban environment on campus.

### 5.2.1 Threshold Discussion

All of the controlled released data were utilized to establish the threshold detection distance of the project tower. The data trendlines (previously displayed and discussed) for all four semicontrolled environment releases and the one field release were extrapolated down to an interval concentration value of 0 ppmv. This 0 ppmv value would be equivalent to no detection (or spiking) of $CO_2$ above ambient $CO_2$ levels. The trendlines were used as an acceptable means to establish a threshold range determination because additional experimentation for could not be performed for this project.

Figure 5.6 shows all five scenarios, where the four semicontrolled environment experiments are shown in grey and the field experiment in red. Dashed lines in Figure 5.6 represent extensions of the actual collected data down to 0 ppmv, where each scenario resulted in a different distance equating to 0 ppmv. These five values created a range that is shown with a horizontal solid black line. The threshold detection distance is indicated by the black star symbol and is an average of the five distances found from extrapolation to 0 ppmv.

The five different scenarios suggested maximum threshold distances between 52.9

and 65.4 feet from the tower detection point, which, for the specific conditions of these tests, is a meaningful estimate of the threshold range. The average threshold detection distance for these tests is 56.9 feet.

### 5.2.2 Footprint Discussion

Estimation of detection footprint was previously discussed in Section 2.3 with project tower modeling via the parameterisation calculator created by Kljun et al. (2004). The typical detection footprint associated with a typical flux tower is portrayed by a bell type curve (or Gaussian distribution) with a peak at the maximum detection location, which is positioned at some distance from the tower. The 0.5 lpm semicontrolled experiment and the 20 lpm tower experiment provided shapes most similar to the footprint described and modeled in Section 2.3.

The modeling efforts in Chapter 2 provided an outcome flux footprint value of 53 feet (16.2 meters) for the distance of the peak location. This peak value corresponded to a distance that was roughly 46% of the entire modeled footprint of 116 feet (35.3 meters). When comparing a flux footprint with a concentration footprint, generally concentration footprints are larger in size. However, when comparing the modeling results (for a flux tower) and the experimental results (for the concentration tower), it was evident that the established footprint of the tower was much smaller than the modeled value. This was most likely attributed to the highly urbanized environment, nonhomogeneous terrain, and highly variable atmospheric conditions that could be not accounted for in the parameterisation modeling calculations. The size of the concentration threshold detection footprint is also supportive of not using the eddy covariance flux evaluations for this area,

based upon the flux footprint being smaller in size than the established concentration footprint, found to be at 56.9 feet.

If the 46% distance is assumed to be a constant proportion for all footprints, then the peak detection distance for the project tower would be approximately 26 feet. The shaping of the controlled release experiment data generally agreed with this estimation, and if smaller increments of distance had been used for the controlled release, the exact value may have been established at 26 feet. However, the distances tested were 10, 30 and 43 feet so this degree of precision was not available. Additional data collection for smaller incremental distances would likely increase the resolution of maximum detection location and the associated estimated footprint. Results of the controlled release experiments at FASB2 also mimicked the bell shaped curvature seen with tower footprints. It is important to note that the detection threshold and estimated footprint distances are all specific to this tower environment and specifications.

The resources utilized for this controlled release were minimal, especially when compared with the ZERT studies conducted. The amount of time and resources needed to actually determine the footprint of a detection tower has proven to be highly variable, especially considering the uncontrollable and undefined sources present. This footprint approach (for this research) created a minimal and general understanding of how this tower might react to a release within the area of detection by the tower. Many larger efforts and resources are required for continuation and reliability of the tower footprint.


Figure 5.1: Controlled release experiment within semicontrolled environment, an indoor hallway.

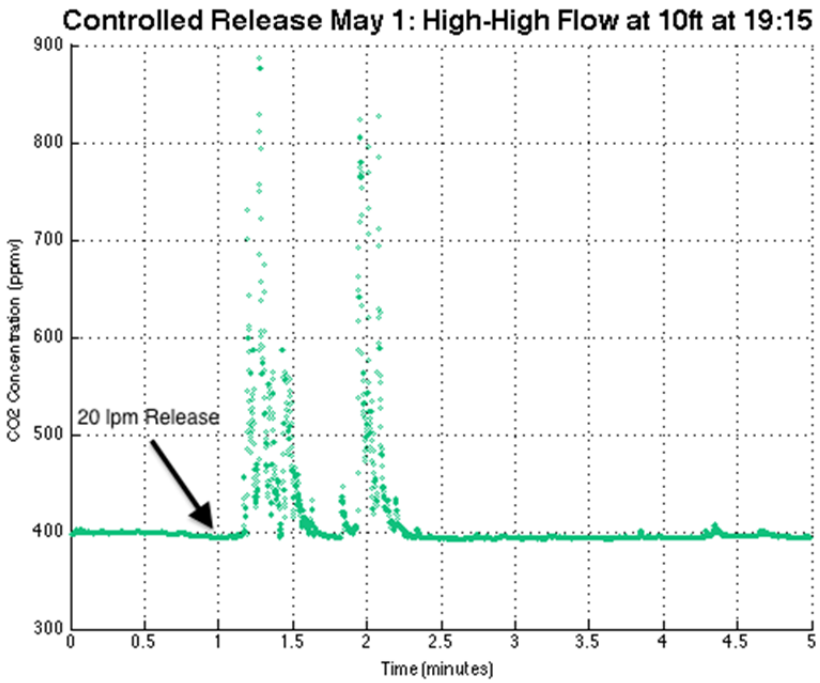


Figure 5.2: Concentration vs. time plot from $CO_2$ controlled release at 10 feet distance from FASB2 tower location and at 20 lpm flow rate, conducted on May 1st, 2014.

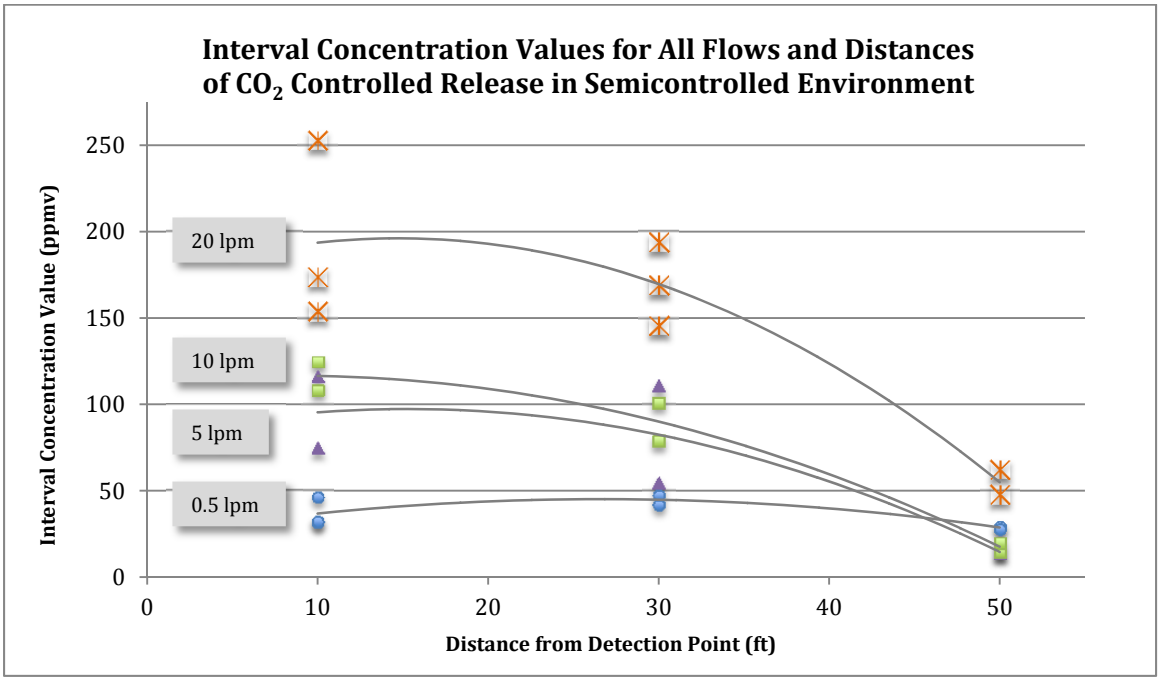


Figure 5.3: Semicontrolled environment (indoor hallway) results for $CO_2$ controlled release, separated by flow rate.

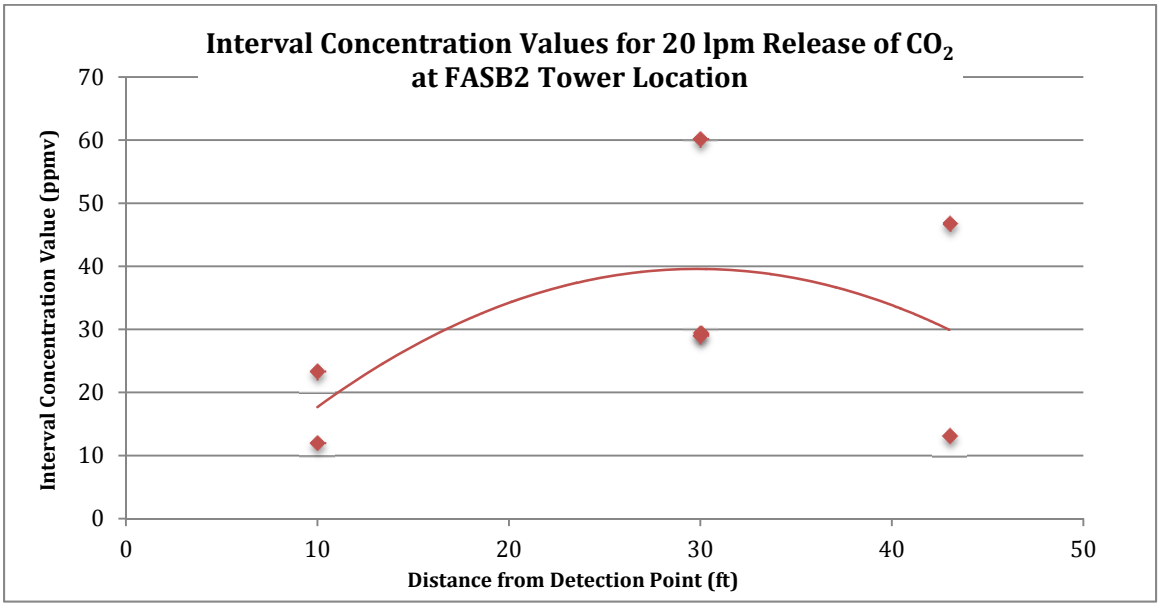


Figure 5.4: FASB2 controlled release results of integral value with respect to distance.

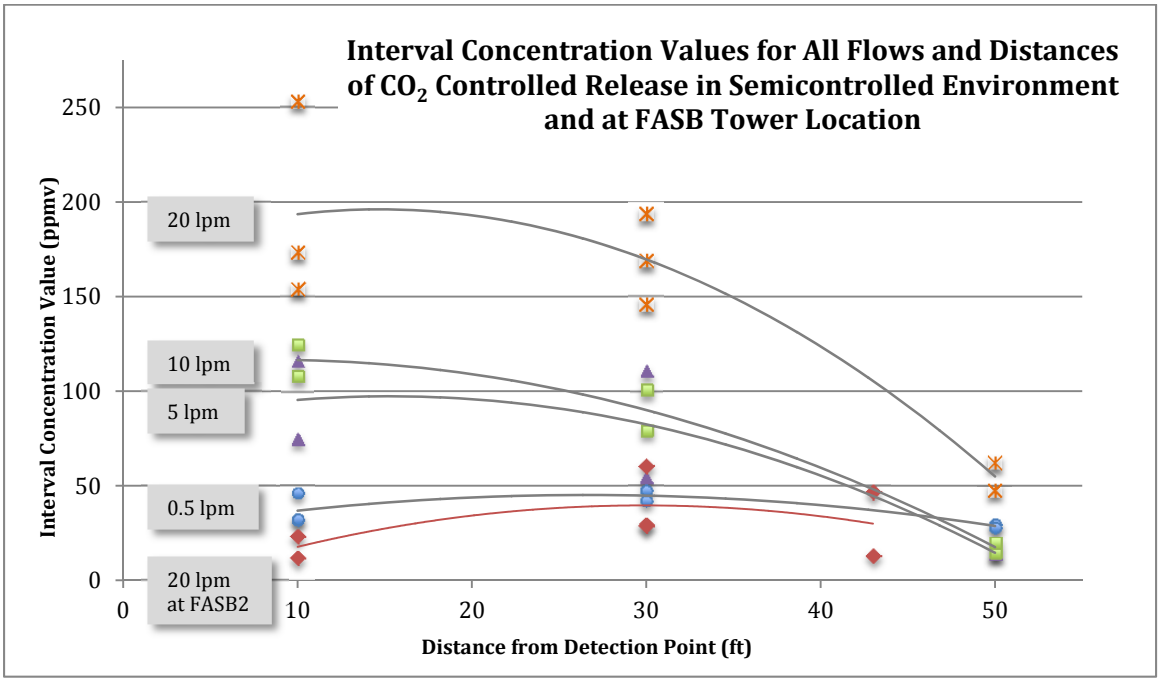


Figure 5.5: All controlled release data points from semicontrolled environment (indoor hallway) and field experimental tests.

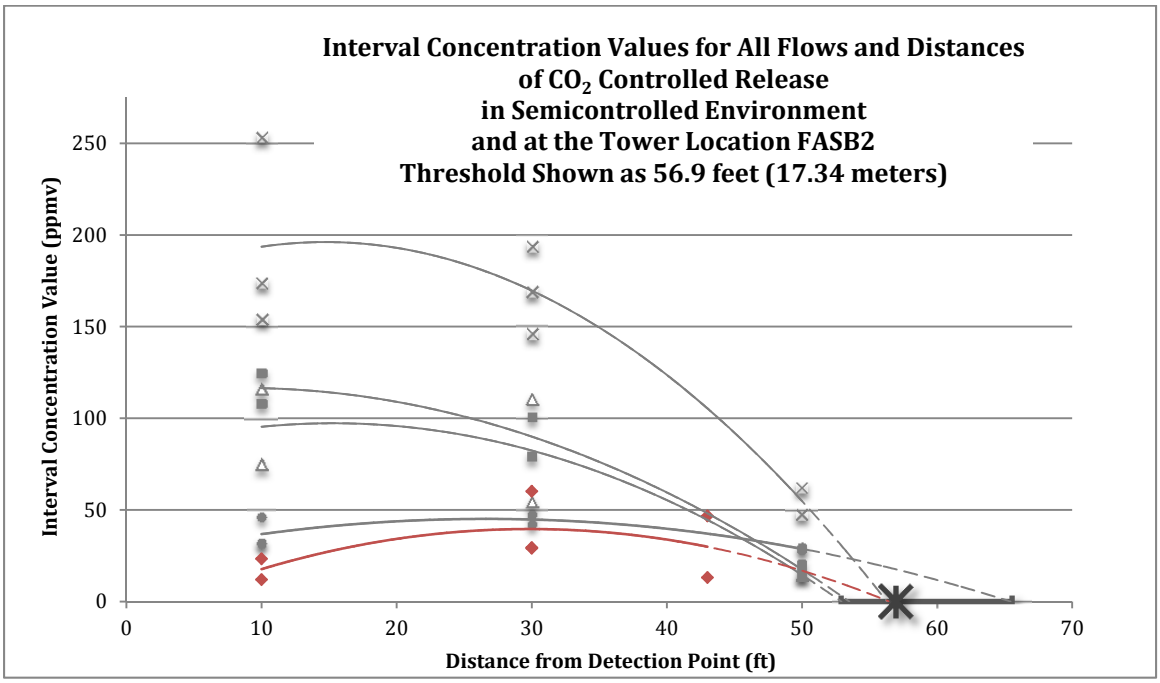


Figure 5.6: Tower threshold estimate (indicated by black star at 56.9 feet) with recognized range (indicated by black line with horizontal distance of 52.9 to 65.4 feet).

Table 5.1: Controlled release experiments, $CO_2$ flow rates pertaining to daily atmospheric conditions.

| Flow rate | 26-Apr | | 1-May | | 20-May | |
|---|---|---|---|---|---|---|
| lpm | g/d | tonnes $CO_2$/d | g/d | tonnes $CO_2$/d | g/d | tonnes $CO_2$/d |
| 0.5 | 1148 | 0.00115 | 1120 | 0.00112 | 1084 | 0.00108 |
| 5 | 11,480 | 0.01148 | 11,200 | 0.01120 | 10,840 | 0.01084 |
| 10 | 22,955 | 0.02296 | 22,400 | 0.02240 | 21,680 | 0.02168 |
| 20 | 45,910 | 0.04591 | 44,800 | 0.04480 | 43,360 | 0.04336 |

# CHAPTER 6

# CONCLUSIONS AND RECOMMENDATIONS

## 6.1 Conclusions

The design and implementation of an eddy flux covariance tower at the University of Utah campus was developed and deployed for this project. The urban setting and the high turbulence associated with a heterogeneous environment precluded using the tower for full flux calculations, but measurement of $CO_2$ and $CH_4$ concentrations were successful, including definitive "spikes" of concentration that suggest specific point sources. A three-dimensional sonic anemometer provided wind information that was utilized with measured concomitant concentration data to establish approximate source locations in the form of compass directions. The project tower was deployed in three locations (TL1, FASB1 and FASB2; see Figure 2.9 in Section 2.4) during the 8-month period of study. These three locations were chosen based on assumed known point sources of access points (sewer line access covers, or manholes) along a campus sewer line. The point sources were analyzed in a previous flux chamber measurement study (Varland, 2014) that determined an average emission rate of 1086 g/day or 0.00109 $MtCO_2e$/day. The flux chamber surveys also evaluated time of day release by continuous concentration data collection. Results of Varland (2014) and of this study indicate that

the sewer line point sources do not release a constant or predictable amount of $CO_2$, but that the release was dominant during the afternoon hours between 12:00 noon and 19:00.

Data from the three tower locations were collected during daylight hours with two overnight sessions, each at a different location. Measured gas sources were persistent for each location over the period of collection and based on the overall set of results. The most significant point sources are probably vehicular emissions, not the sewer access points. The data collected for this study suggest that emissions from the sewer access points were not great enough to produce significant spikes in the measured trends, and could not be distinguished from the other gas sources.

The final activity of this study was a controlled release of known CO2 emissions, to evaluate the qualitative sensitivity of the CRDS under controlled (indoor hallway) conditions and the local conditions of the campus (outdoor) testing. The most important objective of the controlled release of pure $CO_2$ was to provide more information for threshold and footprint estimates. The values established are strictly for the project tower at the specific site within the highly urban environment found on campus and for the atmospheric conditions of the study.

## 6.2 Future Work and Recommendations

There is an increase in interest for use of eddy flux towers for leak detection in urban areas and commercial settings, from oil fields to college campuses. A general protocol for estimating footprints and threshold distances for flux towers has not been developed yet, mostly because these locations are extremely variable. One goal of this thesis project was to gain insight regarding the limitations or constraints of developing

such a general protocol. Understanding wind patterns and how terrain, buildings and other aspects of an urban environment affect wind patterns may facilitate development of a general procedure for threshold distance and footprint estimation. However, a substantial recommendation of this thesis project is to determine unique threshold distances and footprints for each new project area. This could be accomplished with multiple controlled release experiments, and the use of an isotope or tracer gas would provide better understanding by distinguishing the released gas from the other sources within the area. Additional experimental design with respect to gas diffusion during release, steady release intervals and wind analysis may also produce more reliable results.

Regarding the results of this project specifically, the multiple flow rates measured at several distances from the tower to establish the detection threshold would be greatly expanded upon by measuring additional distances further from the tower than MH4 and by testing at smaller increments. These additional tests are anticipated to provide a more robust footprint estimate. Conducting several days of controlled release experiments with differing atmospheric conditions may also be of value to indicate impacts of wind speed, ambient fluctuations and other factors that affect the concentration measurements for this particular location and setup. Another aspect that was not scrutinized for this study was the height of measurement at the tower. Collecting concentrations at different heights would increase knowledge for such tower data collection and point source detection. Threshold levels for each height may be important and could be determined. Another interesting factor would be the insight into seasonal variances and daily emission concentrations. These could be transpired through more constant and long term data collection, specifically with respect to timeframes during the day, including a secure

schedule and detailed note taking for activities possibly producing gases. With this information, systematic releases could be anticipated or seen as background fluctuations, just as seasonal variances could be incorporated and distinguished from leaks.

# APPENDIX A

# MATLAB SCRIPTS FOR DATA ANALYSIS

Included in this appendix are the scripts written and used in Matlab by MathWorks® for data analysis of the project data.

## A.1 towerplot.m

This script uses Picarro© CRDS data to find maximum, minimum, average and standard deviation of the $CO_2$ and $CH_4$. It produces plots of concentration vs. time.

```
function towerplot(DATE, TIME, tcorrection, ydata1, ydata2, heading1, heading2)
%
%  THIS PROGRAM WILL CREATE A PLOT FROM PICARRO TEXT FILES.
%  THE TEXT FILE NEEDS TO IMPORTED TO MATLAB
%  IT IS INTENDED FOR TOWER DATA CONCENTRATIONS OF CO2 AND CH4
%
%  AUTHOR:  LINDSAY MINCK
%  DATE CREATED:  FEBRUARY 26, 2014
%
%  INPUT VARIABLES;
%       NAME:          DESCRIPTION:                        EXAMPLE:
%       DATE           COLUMN OF DATE VALUES              '2013-10-01'
%                      STRING
%                      'YYYY-MM-DD'
%                      PICARRO OUTPUT
%
%       TIME           COLUMN OF TIME VALUES              '13:45:56.002'
%                      STRING
%                      'HH:MM:SS.FFF'
%                      24 HR FORMAT
%                      GREENWICH MEAN TIME
%                      PICARRO OUTPUT
%
%       tcorrection    CORRECTION VALUE FROM GMT TO MST    0.25
%                      DECIMAL NUMBER                      0.2917
%                      6 HOURS = 0.25
%                      DAYLIGHT SAVINGS TIME
%                      NOVEMBER 3, 2013
%                      7 HOURS = 0.2917
%
%       ydata1         DATA TO BE PLOTTED ON Y-AXIS        '398'
```

```
%       heading        TITLE OF GRAPH                       'OCT 10 CO2 DATA'
%                      INCLUDE DATE, DECRIPTION, ETC.
%
%%
%
% COMBINES THE DATE AND TIME AND CONVERTS TO MST
%
timeseries = datenum(strcat(DATE,TIME),'yyyy-mm-ddHH:MM:SS');
timeseries = timeseries - tcorrection;
%
%%
%
%  CH4 Information
%
CH4_max=max(ydata1)
CH4_min=min(ydata1)
CH4_average=mean(ydata1)
CH4_SD=std(ydata1)
%
%  CO2 Information
CO2_max=max(ydata2)
CO2_min=min(ydata2)
CO2_average=mean(ydata2)
CO2_SD=std(ydata2)
%
%%
% PLOT THE DATA
%
figure (1)
%
scatter(timeseries, ydata1)
title(heading1,'FontWeight','bold','FontSize',16)
ylabel('Concentration (ppmv)')
xlabel('Time of Day')
datetick('x','HH:MM')
axis tight
%
%
figure (2)
%
scatter(timeseries, ydata2)
title(heading2,'FontWeight','bold','FontSize',16)
ylabel('Concentration (ppmv)')
xlabel('Time of Day')
datetick('x','HH:MM')
axis tight
%
end
```

## A.2 WDirGas.m

This script uses Picarro© CRDS data to determine wind direction and requires anemometer orientation. It also calculates the desired percentile value.
Four plots are output where;

Figure 1 is Wind Direction vs. Time,
Figure 2 is Concentration above Percentile vs. Time,
Figure 3 is Percentile Concentration vs. Wind Direction and
Figure 4 is a window of wind direction for percentile concentration.

```
function WDirGas(DATE, TIME, TIMECOR, ANEMOMETERUX, ANEMOMETERUY, OFFNDEG,
heading1, heading2, heading3, ydata, P)
%
%   THIS PROGRAM WILL TAKE THE ANEMOMETER UX AND UY DATA AND CREATE PLOTS.
%   IT WILL ALSO CORRECT FOR NORTH BY USING THE DEGREES OF WHICH THE
%   ANEMOMETER IS OFF FROM NORTH.
%   THE DESIRED PERCENTILE IS CALCULATED AND RETURNED.
%
%   CREATED BY: LINDSAY MINCK and Kevin McCormack
%
%   DATE CREATED:  MARCH 18, 2014
%        REVISED:  May 15, 2014
%
%   INPUT VARIABLES;
%       NAME:               DESCRIPTION:                    EXAMPLE:
%       DATE                OUTPUT FROM PICARRO             DATE
%                           'YYYY-MM-DD'                    '2014-03-18'
%
%       TIME                OUTPUT FROM PICARRO             TIME
%                           HH:MM:SS.FFF'                   '15:24:16.123'
%                           24 HOUR FORMAT
%                           GREENWICH STANDARD TIME
%
%       TIMECOR             TIME CORRECTION                 0.25
%                           PICARRO TIME IS GREENWICH       0.2917
%                           MOUNTAIN STANDARD TIME IS
%                           NOV 3, 2013 TO MARCH 9, 2014
%                             (0.2917)
%                           DAYLIGHT SAVINGS
%                           BEFORE NOV 3, 2013 & AFTER
%                           MAR 9, 2014
%                             (0.25)
%
%       ANEMOMETERUX        OUTPUT FROM ANEMOMETER          ANEMOMETERUX
%                           WIND VELOCITY (M/S)             '0.1523'
%                           PARALLEL AXIS TO BAR
%
%       ANEMOMETERUY        OUTPUT FROM ANEMOMETER          ANEMOMETERUY
%                           WIND VELOCITY (M/S)             '-0.1452'
%                           PERPENDICULAR AXIS TO BAR
%
%       OFFNDEG             DEGREES FROM NORTH THAT         6
%                           ANEMOMETER IS OFF
%                           FIELD MEASUREMENT
%                           **POSITIVE NUMBER 0 TO 360**
%
%       heading             TITLE OF PLOTS         'TL1: OCT 10 WIND DIRECTION'
%                           INCLUDE DATE, LOCATION, ETC
%
%       ydata               DATA TO BE COMPARED WITH WIND   CH4dry
```

```
%                           OUTPUT FROM PICARRO             '1.71258'
%
%       P                   PERCENTILE                      99
%
%%
%  COMBINES DATE AND TIME AND CORRECTS FOR GREENWICH TIME TO MOUNTAIN TIME
%
tts = datenum(strcat(DATE, TIME), 'yyyy-mm-ddHH:MM:SS.FFF');
ts = tts - TIMECOR;
%
%%
%  USE the atan2d(Y,X) function to compute the four-quadrant inverse
%  tangent of points specified in the x-y plant, results are in degrees
%
%  **with matlab function,
%  X is 0 degrees or East
%  Y is 90 degrees or North
%  in order to agree with anemometer orientation, the coordinates are
%  renamed so that north is 0 degrees = X
%
N = ANEMOMETERUX;
E = ANEMOMETERUY;
D = atan2d(E,N);
%
%   OUTPUT VALUES ARE BETWEEN -180 AND 180 DEGREES
%   AND THEY MUST BE CONVERTED TO 0 TO 360 DEGREES
%
%   conditional functions
% if D<0 then D1=D*(-1)
% if D>0 then D1=D*(-1)+360
%
for i=1:length(D)

if D(i)<0
    D1(i)=D(i)*(-1);
elseif D(i)>=0
    D1(i)=(D(i)*(-1))+360;
end

end
%
%%
%  USE DIRECTION FROM NORTH FOR ANEMOMETER ORIENTATION CORRECTION
%  This is also taking into account that orientation correction must not
%  output a negative number, therefore adjustments must be made for values
%  less than the offset.
%
for j=1:length(D1)
    if 360-D1(j)<=OFFNDEG
        DEG(j)=D1(j)-360+OFFNDEG;
    elseif 360-D1(j)>OFFNDEG
        DEG(j)=D1(j)+OFFNDEG;
    end
end
%
%%
%   Reduce dataset by keeping every "x" number of measurement
n=0;
for i=1:5:length(DEG)
    n=n+1;
    DEG2(n)=DEG(i);
end
%
```

```
m=0;
for i=1:5:length(ts)
    m=m+1;
    tsred(m)=ts(i);
end
%
%%
%   ADJUST TIME FOR LAG TIME FROM POINT OF MEASUREMENT TO PICARRO
%   DONE FOR GASES BEING ANALYZED
%   LAG TIME MEASURED IN LAB TO BE 27.7 SECONDS
%   CONVERT TO FRACTION OF DAY
LT = 27.7/60/60/24;
%
%   CREATE NEW TIMESERIES
TS1 =   ts - LT;
%
%%
%   RETURN AVERAGE OF GAS DATA
DataAvg = mean(ydata)
Max = max(ydata)
%
%   RETURN VALUE OF DESIGNATED PERCENTILE OF Y DATA
Percentile = prctile(ydata,P)
%
%%
%   ONLY WANT DATA THAT IS ABOVE DESIGNATED PERCENTILE
%   ydata>Percentile
%
for k=1:length(TS1)
    if ydata(k)>=Percentile
        YP(k)=ydata(k);
        WD(k)=DEG(k);
        TS2(k)=TS1(k);
    end
end
%
%%
%   PLOT DEGREE VS TIME
%
%  Figure 1 is the scatter plot from 0 to 360 degrees with reduced dataset
%  timeseries is not adjusted for lag time
%
figure(1)
scatter(tsred, DEG2, 2, [0 0.7 0.4])
title(heading1, 'FontWeight', 'bold', 'FontSize', 16)
xlabel('Time of Day')
ylabel('wind direction where North = 0 deg')
datetick('x','HH:MM')
grid on
axis tight
axis ([min(ts), max(ts), 0, 360])
%
%   Figure 2 is the gas concentration updated for lag time
%
figure(2)
scatter(TS1, ydata, 4)
title(heading2, 'FontWeight', 'bold', 'FontSize', 16)
xlabel('Time of Day')
ylabel('CH4 concentration (ppmv)')
datetick('x','HH:MM', 'keeplimits', 'keepticks')
grid on
axis tight
axis ([min(ts), max(ts-LT), Percentile, max(Max+0.01)])
```

```
%
%   Figure 3 is the wind direction associated with the percentile
%   concentration
%
figure (3)
scatter(WD, YP, 4, [0.6 0.1 0.3])
title(heading3, 'FontWeight', 'bold', 'FontSize', 16)
xlabel('Wind Direction in Degrees')
ylabel('CH4 Concentration (ppmv)')
grid on
axis([0, 360, min(Percentile-0.01), max(Max+0.01)])
%
%   Figure 4 is Figure 3 but for a designated window of degrees
%
figure (4)
scatter(WD, YP, 5, [0.6 0.1 0.7])
title('99th Percentile Concentration for 0-45 degree Wind', 'FontWeight',
'bold', 'FontSize', 16)
xlabel('Wind Direction in Degrees')
ylabel('CH4 Concentration (ppmv)')
grid on
%
%   Change x axis values for degrees of window
axis([0, 45, min(Percentile-0.01), max(Max+0.01)])
%
%
end
```

## A.3 Spline.m

This script uses the spline function and the Savitzky-Golay filter to smooth the Picarro© CRDS and LI-COR® SFGA data. It produces a $CO_2$ concentration graph with both datasets plotted against time.

```
function Spline
%
% This script performs three tasks.
% (1) Converts the Picarro date and time strings into usable hour decimals.
% (2) Uses cubic splines to interpolate within the Picarro and Licor
%     concentration data in order to create datasets with matching time
%     values.
% (3) Graphs the data.
%
% Authors: Kevin McCormack
%          Lindsay Minck
%
% Date Created:  March 27, 2014
%
%% (1) Time Conversion

n=datenum(TIME, 'HH:MM:SS.FFF');
%  Subtract days from 1/1/1990
n2=n-floor(n(1));
%
TC=7/24;
%  Correct for Greenwich time
n3=n2-TC;
%  Make into hours from days and apply tubing correction
n4=(n3*24)-(27.7/3600);

%% (2) Spline the Data

%Locate and eliminate the duplicate Licor time values
[Hour2, iH1, iH2]=unique(Hour,'stable');

Cdry2=Cdry(iH1);

%Locate and eliminate the duplicate Picarro time values
[n5, in1, in2]=unique(n4,'stable');

CO2dry2=CO2dry(in1);


%Cubic spline interpolation

%Create time vector onto which to map the two splines.
xx=max(min(Hour2),min(n5))+.01:.001:min(max(Hour2),max(n5))-.01;

%Splines
yLicor=spline(Hour2,Cdry2,xx);
yPicarro=spline(n5,CO2dry2,xx);


%% (3) Plot the Splined Data

%Plot on a double y axis
figure(1)
plotyy(xx,yLicor,xx,yPicarro)
title('Spline Data - March 6th, 2014')
```

```
%% (4) Smooth the Picarro Data

%Savitzky-Golay Filter to smooth the data
Spicarro=sgolayfilt(yPicarro,5,101);

figure(2)
[AX,H1,H2]=plotyy(xx,yLicor,xx,Spicarro);
title('Mar 6, 2014:  CO2 Comparison-MH4 & Tower ', 'FontWeight', 'bold',
'FontSize', 16)
xlabel('Time of day');
set(get(AX(1),'Ylabel'),'String','MH4 CO2 concentration (ppmv)')
set(get(AX(2),'Ylabel'),'String', 'Tower CO2 concentration (ppmv)')

%code to change axes as needed
%[AX h1 h2] = plotyy(xx,yLicor,xx,Spicarro);
xlim(AX(1),[12.5 17]);
xlim(AX(2),[12.5 17]);
ylim(AX(1),[200 15000]);
ylim(AX(2),[300 430]);
```

## A.4 Integrate.m

This script performs a rough integration for a designated time frame corresponding to a spike from the controlled release experiments. Index values are required for the imported data and correspond to the start and end of the data to be integrated. The output is an integral value of the specified spike.

```
function Integrate
%
%   THE PURPOSE OF THIS SCRIPT IS TO FIND THE AREA UNDER THE SPIKE
%   OF THE CONTROLLED RELEASE OF CO2
%
%   DATE:  MAY 5
%
%   WRITTEN BY: KEVIN MCCORMACK
%   ANNOTATED BY: LINDSAY MINCK
%
%   INPUT FILES ARE TEXT FILES CREATED WITH RFLUX.M FOR CONTROLLED RELEASE
%   OF CO2
%
%%
%   ESTIMATE THE AMBIENT LEVEL OF CO2 FROM THE PLOT AND SUBTRACT FROM ALL
%   MEASURED CONCENTRATION VALUES
Con=Concentration-470;
%
%   DETERMINE THE TIME FRAME OF DESIRED DATASET, AS EXAMPLE 1-4 MINUTES
%   THEN FIND CORRESPONDING INDEX OF TIMES FROM IMPORTED DATA AND USE FOR
%   i RESTRAINTS
%
n=0;
for i=2050:8177
    n=n+1;
    Area(n)= (Con(i)+Con(i+1))*(Time(i+1)-Time(i))/2;

end

%Area=C.*T;

Integral=sum(Area)
```

# APPENDIX B

## LAG TIME DATA

Included are the notes and data from lag time determination for the eddy flux tower sample tubing measurements.

Tower tubing - Lag time

Tube was tested
14-Mar-14
Lindsay Minck
Kevin McCormack
11:30 to 12:00
In "the cave"

Kevin blew into tubing and stopwatch was started
Lindsay stopped stopwatch when CO2 reading increased dramatically

| Trial # | Time (sec) | Notes |
|---|---|---|
| 1 | 27.50 | |
| 2 | 28.44 | Removed as High measurement |
| 3 | 28.00 | |
| 4 | 27.81 | |
| 5 | 27.64 | |
| 6 | 28.10 | |
| 7 | 27.62 | |
| 8 | 27.65 | |
| 9 | 27.44 | |
| 10 | 27.39 | Removed as Low measurement |
| 11 | 27.73 | |
| 12 | 27.60 | |
| 13 | 27.45 | |
| | **27.69** | Average Lag Time |
| | **0.21** | Standard Deviation |

# APPENDIX C

# CONTROLLED RELEASE EXPERIMENTS DATA

The controlled release experiments were conducted on 3 separate days. The field notes are provided and followed by plots of the spiking intervals for each day.

## C.1 Semi-Controlled Environment Experiment

### Field Notes

This experiment was performed April 26, 2014, included are the field measurements and notes.

**Table C.1: Controlled Release Semi-Controlled Environment Experiment Field Notes**

**INDOOR HALLWAY RELEASE OF CO2**
**PICARRO DETECTION**
**WIND CONTROLLED BY FAN**

Conducted April 26, 2014
Lindsay Minck
Kevin McCormack
Monica Morales

| | | **LOW FLOW** | | | | **Y/N ?** | **Level** | | | |
|---|---|---|---|---|---|---|---|---|---|---|
| **ft** | **m** | **Flowmeter** | **Fan level** | **Tube Height** | **TIME START** | **Detection** | **Spike Conc** | **Time of Spike** | **Est. Avg** | **TIME STOP** |
| 10 | 3.048 | 0.7 | LOW | 3 feet | 12:36 | Yes | 525 | n/a | 480 | 12:37 |
| 10 | 3.048 | 0.7 | LOW | 3 feet | 2:53 | Yes | 566 | 45 sec | 480 | 2:54 |
| 30 | 9.144 | 0.7 | LOW | 3 feet | 1:28 | Yes | 565 & 620 | 18 & 40 sec | 500 | 1:29 |
| 30 | 9.144 | 0.7 | LOW | 3 feet | 1:38 | Yes | 612 | 50 sec | 475 | 1:39 |
| 50 | 15.24 | 0.7 | LOW | 3 feet | 2:36 | Maybe | 540 | 24 sec | 450 | 2:37 |
| 50 | 15.24 | 0.7 | LOW | 3 feet | 2:45 | Maybe | n/a | n/a | n/a | 2:46 |

| | | **MEDIUM FLOW** | | | | | | | | |
|---|---|---|---|---|---|---|---|---|---|---|
| **ft** | **m** | **Flowmeter** | **Fan level** | **Tube Height** | **TIME START** | **Detection** | **Spike Conc** | **Time of Spike** | **Est. Avg** | **TIME STOP** |
| 10 | 3.048 | 6.8 | LOW | 3 feet | 12:47 | Yes | 781 | 18 sec | 580 | 12:48 |
| 10 | 3.048 | 6.8 | LOW | 3 feet | 3:00 | Yes | 681 | 34 sec | 550 | 3:01 |
| 30 | 9.144 | 6.8 | LOW | 3 feet | 1:19 | Yes | 621 | 17 sec | 500 | 1:20 |
| 30 | 9.144 | 6.8 | LOW | 3 feet | 1:47 | Yes | 558 | 30 sec | 480 | 1:48 |
| 50 | 15.24 | 6.8 | LOW | 3 feet | 1:55 | Yes | 512 & 513 | 17 & 40 sec | 450 | 1:56 |
| 50 | 15.24 | 6.8 | LOW | 3 feet | 2:26 | Yes | 497 | 31 sec | 440 | 2:27 |

| | | HIGH FLOW | | | | | | | | |
|---|---|---|---|---|---|---|---|---|---|---|
| ft | m | Flowmeter | Fan level | Tube Height | TIME START | Detection | Spike Conc | Time of Spike | Est. Avg | TIME STOP |
| 10 | 3.048 | 13.6 | LOW | 3 feet | 12:59 | Yes | 949 | 13 sec | 650 | 1:00 |
| 10 | 3.048 | 13.6 | LOW | 3 feet | 3:08 | Yes | 850 | 50 sec | 700 | 3:09 |
| 30 | 9.144 | 13.6 | LOW | 3 feet | 1:09 | Yes | 770 | 50 sec | 550 | 1:10 |
| 30 | 9.144 | 13.6 | LOW | 3 feet | 3:16 | Yes | 592 & 716 | 14 & 51 sec | 550 | 3:17 |
| 50 | 15.24 | 13.6 | LOW | 3 feet | 2:04 | Yes | 569 | 31 sec | n/a | 2:05 |
| 50 | 15.24 | 13.6 | LOW | 3 feet | 2:13 | Yes | 506 | 32 sec | 460 | 2:14 |

| | | Other | | | | | | | | |
|---|---|---|---|---|---|---|---|---|---|---|
| ft | m | Flowmeter | Fan level | Tube Height | TIME START | Detection | Spike Conc | Time of Spike | Est. Avg | TIME STOP |
| 10 | 3.048 | 0.7 | LOW | 3 feet | 3:26 | Yes | 682 | 30 sec | n/a | 3:27 |

CO2 tank pressure at 10 psi

Ambient Values at beginning of experiment

| ppmv | 12:30 | 1:30 | 2:00 | 2:30 | 3:15 | 3:30 |
|---|---|---|---|---|---|---|
| CO2 = | 455 | 420 | 420 | 430 | 440 | 440 |
| CH4 = | 1.67 | 1.69 | 1.69 | 1.7 | 1.69 | 1.69 |

K = 0.7382

| lpm | lpm |
|---|---|
| Flowmeter Reading | CO2 Flow |
| 0.6 | 0.44 |
| 0.7 | 0.52 |
| 6.8 | 5.02 |
| 13.6 | 10.04 |
| 20.3 | 14.99 |
| 27.1 | 20.01 |

Lag Time = 4.5 seconds

NOTES

Fan located 6 feet behind source

Fan was on ground level on LOW speed

Release time of 1 minute

Flushing time minimum of 5 mins

Detection height 3 feet off ground on easel

Flowmeter zeroed at 11:50

**Plots of Spiking Intervals**

Included are the spike intervals plotted with respect to time utilizing Matlab for the controlled release experiment conducted April 26, 2014 in the hallway of the CME Building on the University of Utah campus. Plots are segregated by distance and then flowrate.

***Release at 10-feet***

**Low flowrate – 0.5 lpm**

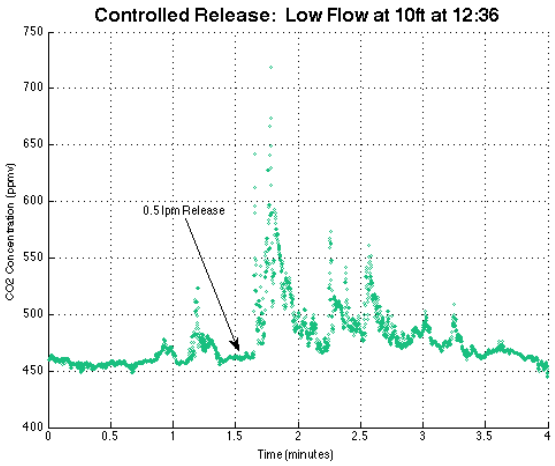


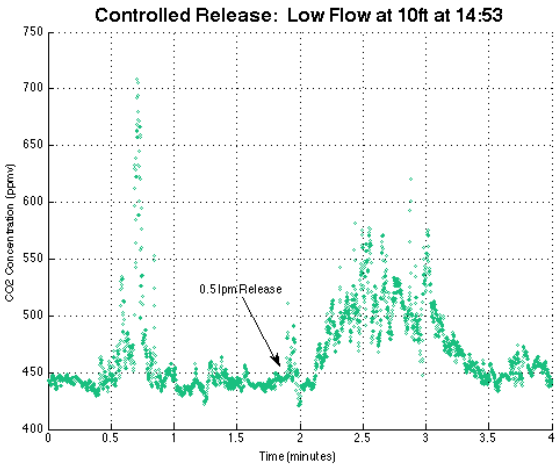


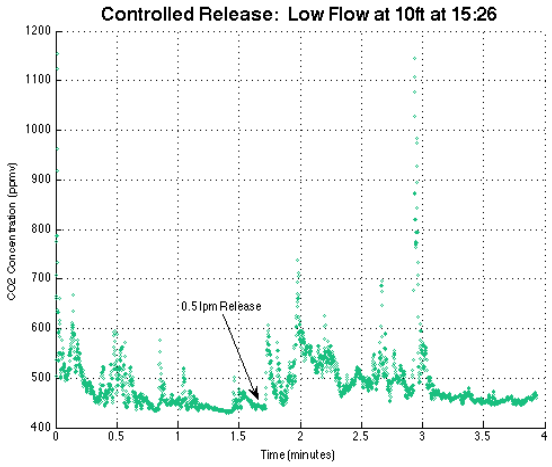

## Medium flowrate – 5 lpm

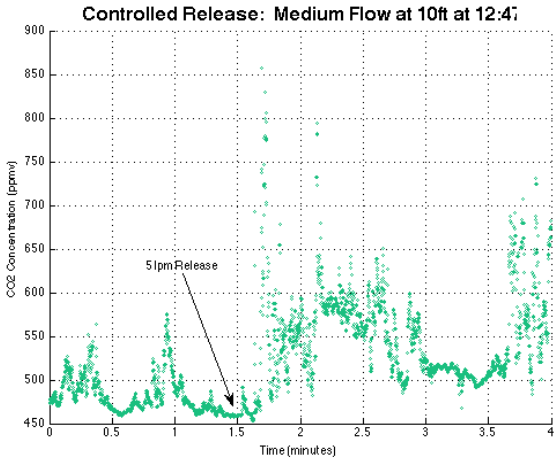


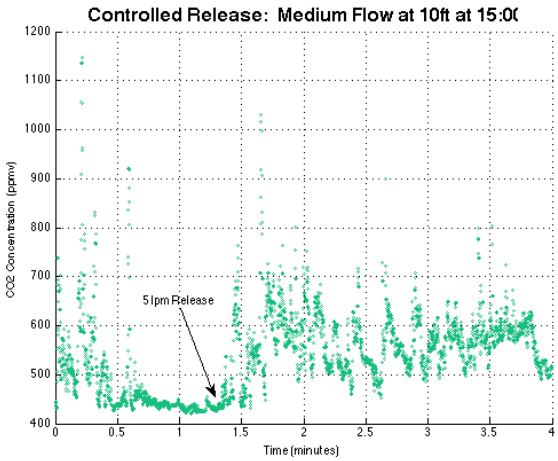


## High flowrate – 10 lpm

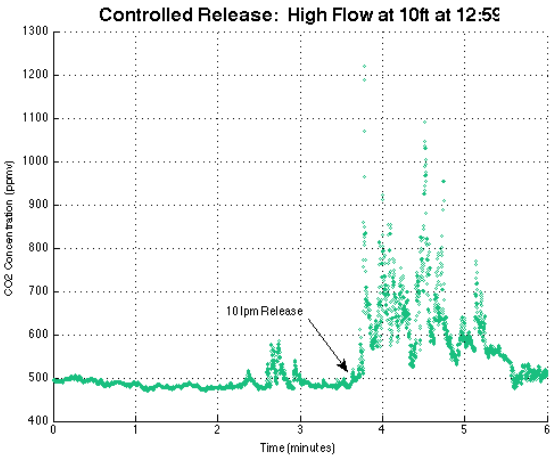


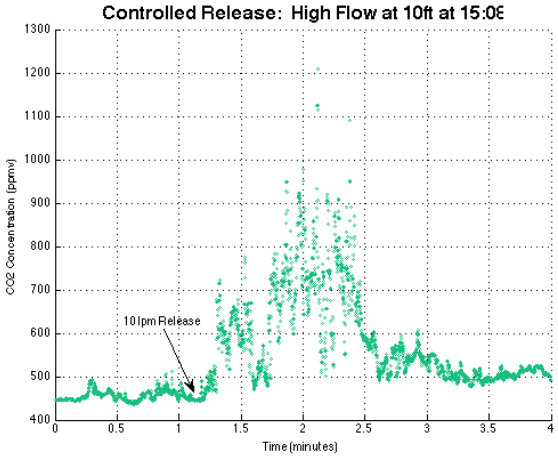

***Release at 30 ft***

## Low flowrate – 0.5 lpm

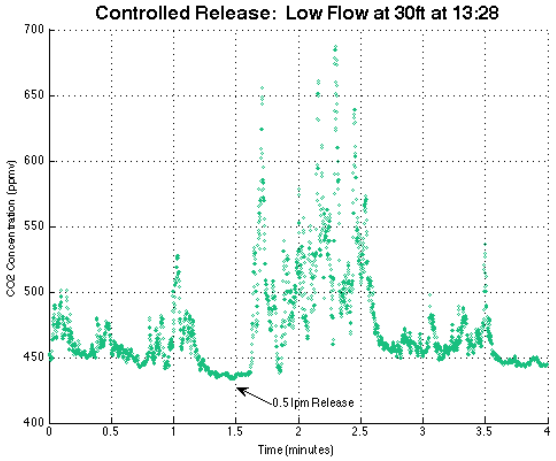


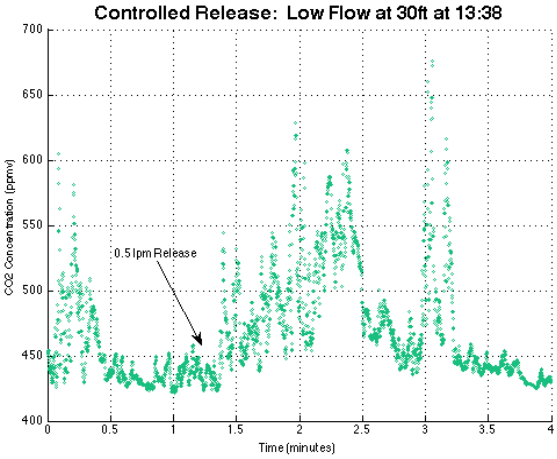


## Medium flowrate – 5 lpm

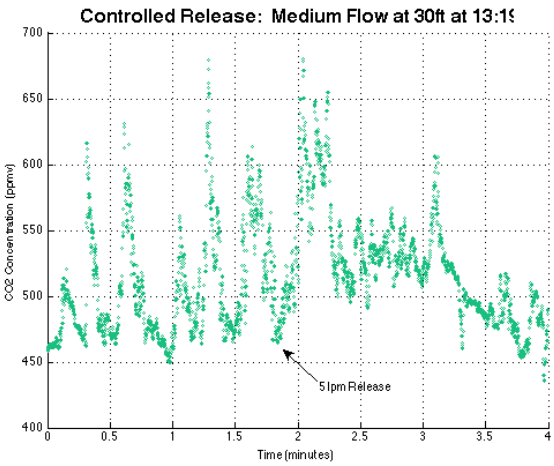


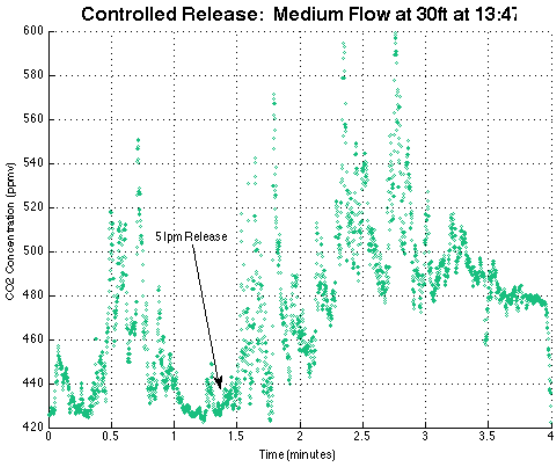

## High flowrate – 10 lpm

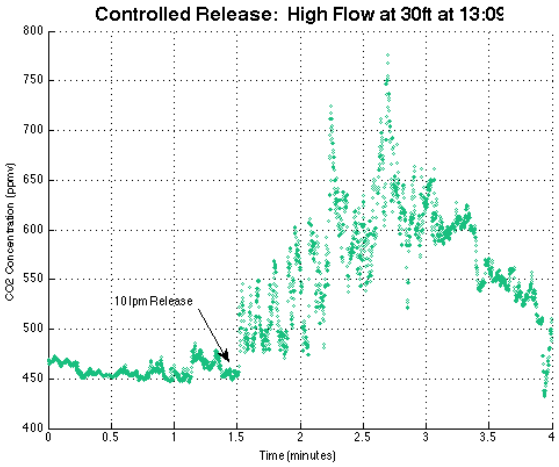


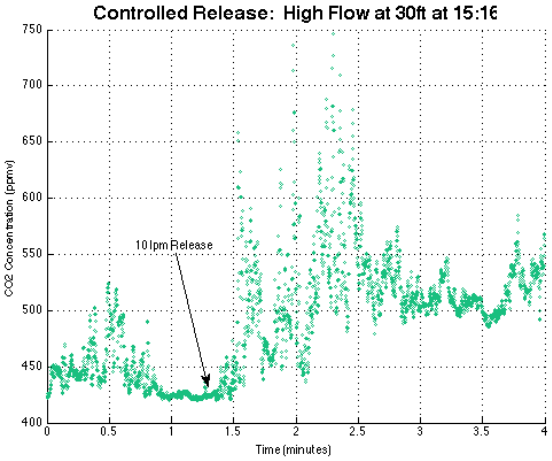


***Release at 50 ft***

## Low flowrate – 0.5 lpm

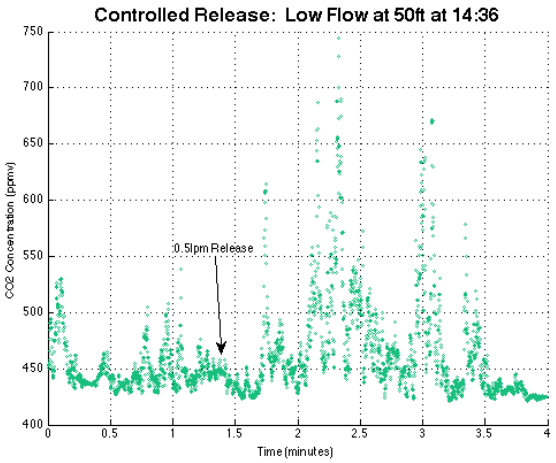


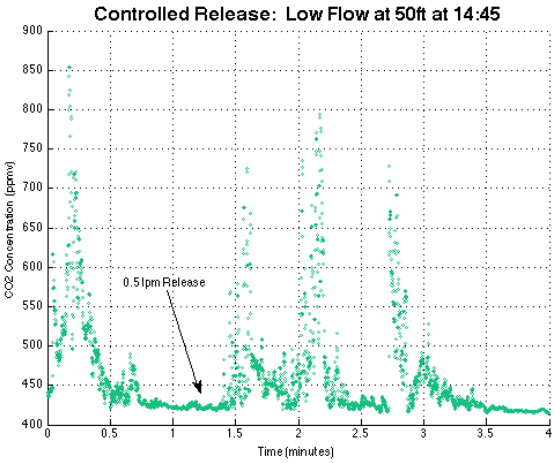

## Medium flowrate – 5 lpm

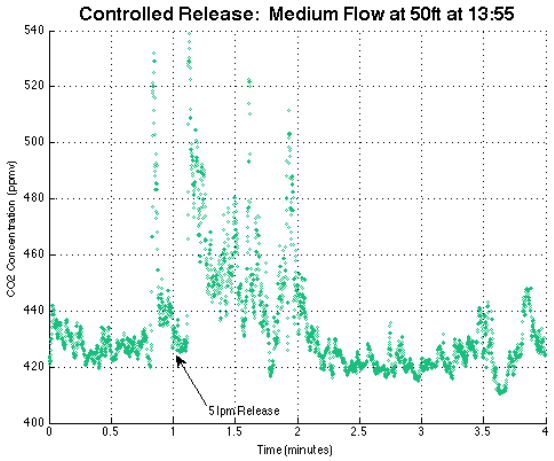


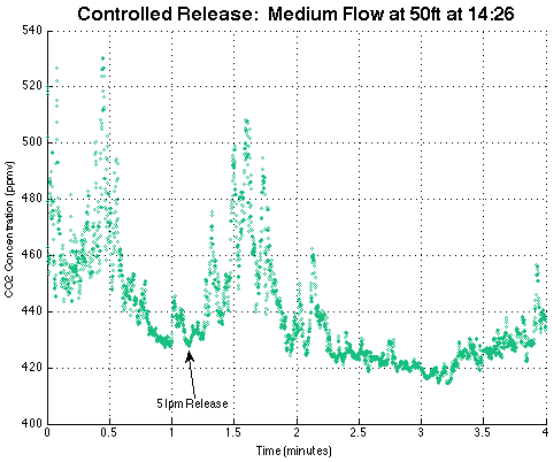


## High flowrate – 10 lpm

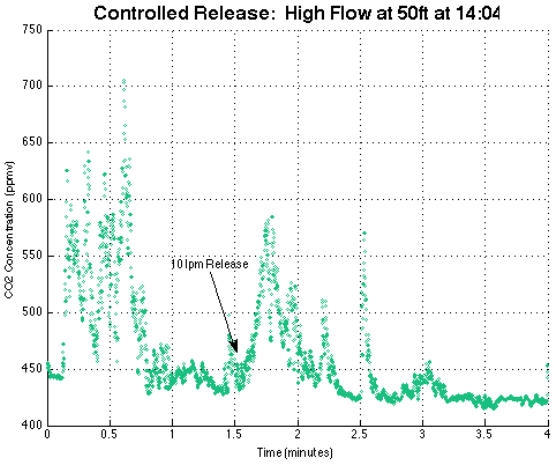


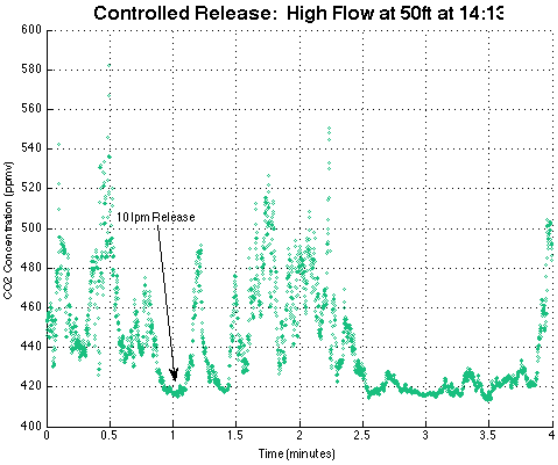

## C.2 FASB2 Field Experiment

**Field Notes**

This experiment was performed May 1, 2014, included are the field measurements and notes.

Table C.2: Controlled Release FASB2 Field Experiment Field Notes

**OUTDOOR RELEASE OF CO2 AT TOWER**

| | | |
|---|---|---|
| **PICARRO DETECTION** | Conducted May 1, 2014 | |
| | Lindsay Minck | 6-8 pm |
| | Kevin McCormack | 6-8 pm |

**Picarro on High Flux Flow**

| ft | m | Flowmeter | TIME START | Y/N ? Detection | Level Spike Conc | Time of Spike | Location | TIME STOP |
|---|---|---|---|---|---|---|---|---|
| 10 | 3.048 | 13.6 | 18:22 | | 440 | | | 18:23 |
| 10 | 3.048 | 13.6 | 18:26 | | | | | 18:27 |
| 10 | 3.048 | 13.6 | 18:30 | | | | | 18:31 |
| 30 | 9.144 | 13.6 | 18:35 | | 750 | | | 18:36 |
| 30 | 9.144 | 13.6 | 18:38 | | | | | 18:39 |
| 50 | 15.24 | | | | | | | |

| ft | m | Flowmeter | TIME START | Detection | Spike Conc | Time of Spike | Location | TIME STOP |
|---|---|---|---|---|---|---|---|---|
| 10 | 3.048 | 27.1 | 18:57 | | | | | 18:58 |
| 10 | 3.048 | 27.1 | 19:03 | | | | | 19:03 |
| 10 | 3.048 | 27.1 | 19:05 | | | | N | 19:06 |
| 10 | 3.048 | 27.1 | 19:15 | yes | 800 | 7:15:45 PM | MH4 line | 19:16 |
| 10 | 3.048 | 27.1 | 19:19 | yes | 800 | 7:19:45 PM | MH4 line | 19:20 |
| 30 | 9.144 | 27.1 | 19:25 | yes | 900 | 7:25:27 PM | MH4 line | 19:26 |
| 30 | 9.144 | 27.1 | 19:30 | No? | | | WD South | 19:31 |
| 30 | 9.144 | 27.1 | 19:39 | yes | 700 | 7:41:15 PM | MH4 line | 19:40 |
| 30 | 9.144 | 27.1 | 18:46 | | | | | 18:47 |
| 30 | 9.144 | 27.1 | 18:50 | | 750 | 6:51:30 PM | N | 18:51 |
| 43 | 13.1064 | 27.1 | 19:46 | yes | 750 | 7:47:45 PM | MH4 | 19:47 |
| 43 | 13.1064 | 27.1 | 19:50 | yes | 900 | 7:50:50 PM | MH4 | 19:51 |

CO2 tank pressure at 10 psi

Ambient Values at beginning of experiment

| ppmv | 18:15 |
|---|---|
| CO2 = | 389 |
| CH4 = | 1.698 |

K = 0.7382

| lpm | lpm |
|---|---|
| Flowmeter Reading | CO2 Flow |
| 0.6 | 0.44 |
| 0.7 | 0.52 |
| 6.8 | 5.02 |
| 13.6 | 10.04 |
| 20.3 | 14.99 |
| 27.1 | 20.01 |

Lag Time = 27.7 seconds

NOTES

Beginning readings were taken due north for wind

Later readings were done in the line to MH4

Calm and sunny

Release was from ground level

Flow at Flux Flow = 5 lpm

Anemometer was not used

**Plots of Spiking Intervals**

Included are the spike intervals plotted with respect to time utilizing Matlab for the controlled release experiment conducted May 1, 2014 at the tower location FASB2 on the University of Utah campus. Plots are segregated by distance and then flowrate.

***Release at 10 ft***

**High-High flowrate – 20 lpm**

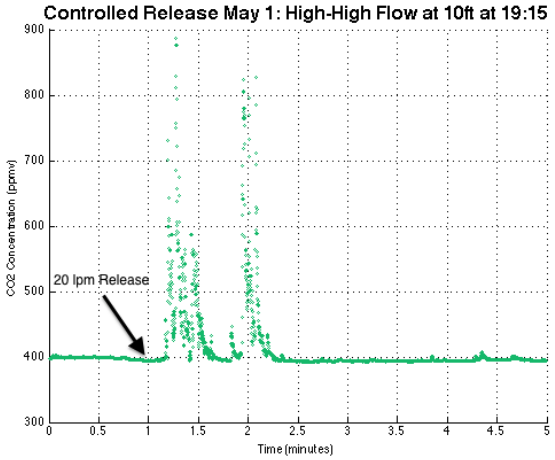


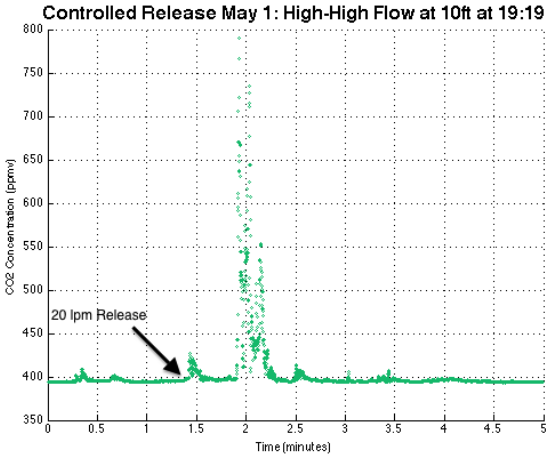


***Release at 30 ft***

**High-High flowrate – 20 lpm**

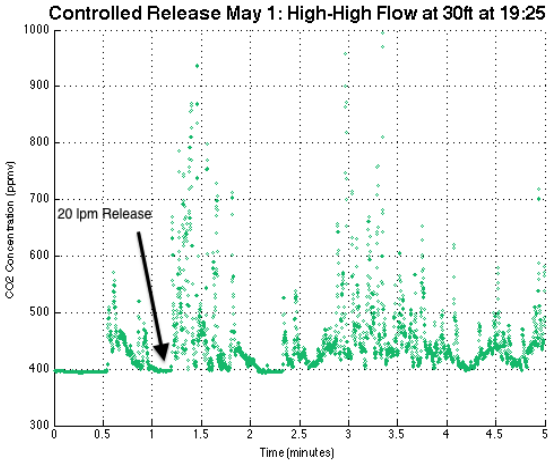


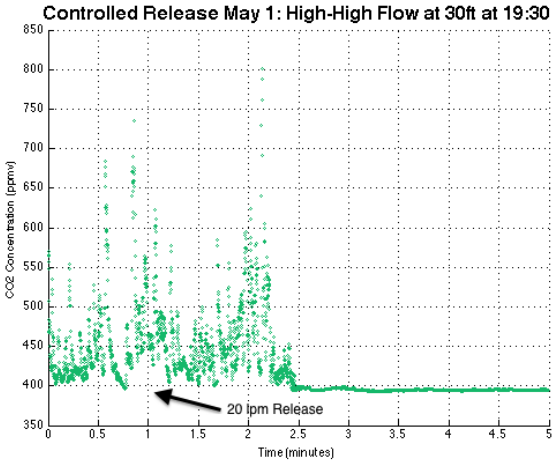

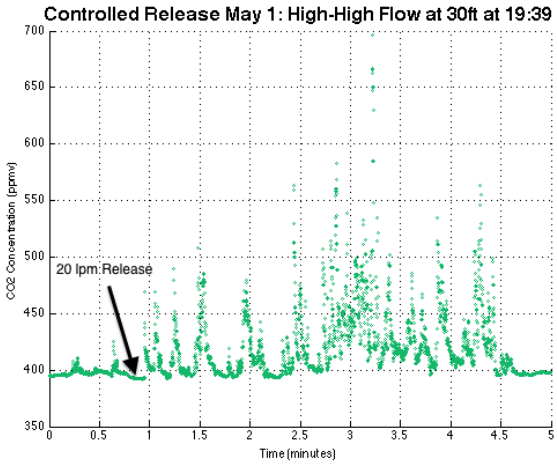


***Release at 43 ft***

**High-High flowrate – 20 lpm**

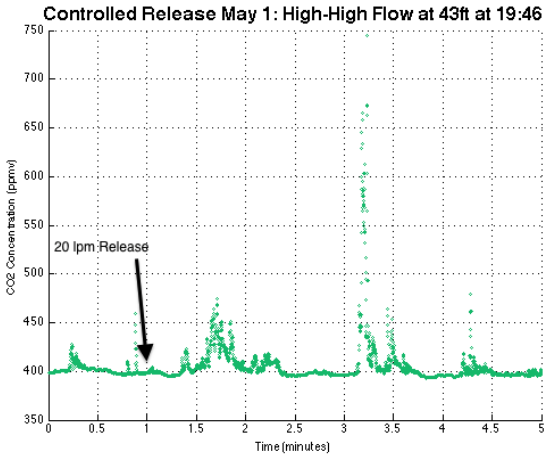


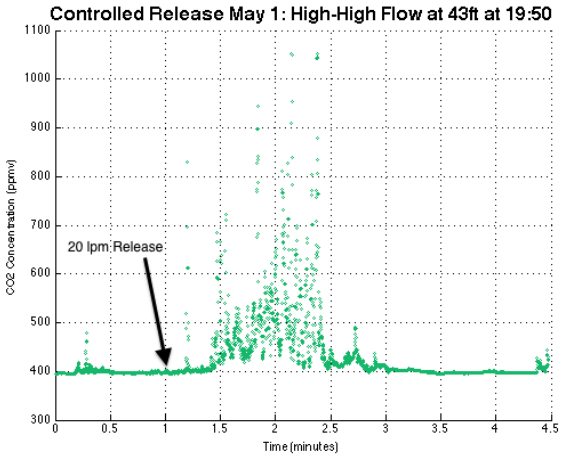


* the measurement data taken at High-High flowrate at 43 feet at 19:50 was not used for analysis

## C.3 Semi-Controlled Environment Experiment

### Field Notes

This experiment was performed May 20, 2014, included are the field measurements and notes.

Table C.2: Controlled Release Semi-Controlled Environment Experiment Field Notes

**INDOOR HALLWAY RELEASE OF CO2**

**PICARRO DETECTION**
**WIND CONTROLLED BY FAN**

Conducted May 20, 2014
Lindsay Minck
Kevin McCormack

7-9 pm

**HIGH-HIGH Flow**

| ft | m | Flowmeter | Fan level | Tube Height | TIME START | Detection | Spike Conc | Time of Spike | Est. Avg | TIME STOP |
|---|---|---|---|---|---|---|---|---|---|---|
| 10 | 3.048 | 27.09 | LOW | 3 feet | 19:17 | yes | 1300 | | | 19:18 |
| 10 | 3.048 | 27.09 | LOW | 3 feet | 19:24 | yes | 1200 | | | 19:25 |
| 30 | 9.144 | 27.09 | LOW | 3 feet | 19:37 | yes | 1200 | | | 19:38 |
| 30 | 9.144 | 27.09 | LOW | 3 feet | 19:45 | yes | 1000 | | | 19:46 |
| 50 | 15.24 | 27.09 | LOW | 3 feet | 20:41 | maybe | ? | | | 20:42 |
| 50 | 15.24 | 27.09 | LOW | 3 feet | 20:48 | maybe | ? | | | 20:49 |

**Other**

| ft | m | Flowmeter | Fan level | Tube Height | TIME START | Detection | Spike Conc | Time of Spike | Est. Avg | TIME STOP |
|---|---|---|---|---|---|---|---|---|---|---|
| 10 | 3.048 | 27.09 | LOW | 3 feet | 19:30 | yes | 1200 | | | 19:31 |
| 30 | 9.144 | 27.09 | LOW | 3 feet | 19:51 | yes | 900 | | | 19:52 |
| 30 | 9.144 | 27.09 | LOW | 3 feet | 19:57 | yes | 1100 | | | 19:58 |
| 50 | 15.24 | 27.09 | LOW | 3 feet | 20:55 | maybe | ? | | | 20:56 |
| | | | | | | | | | | |

CO2 tank pressure at 10 psi
Ambient Values at beginning of experiment

| ppmv | 7:15 | 7:30 | 7:45 | 8:45 | 9:00 |
|---|---|---|---|---|---|
| CO2 = | 515 | 540 | 540 | 540 | 540 |
| CH4 = | 1.88 | 1.8 | 1.75 | 1.8 | 1.8 |

K = 0.7382
lpm lpm

| Flowmeter Reading | CO2 Flow |
|---|---|
| 27.09 | 20.00 |

NOTES
Fan located 6 feet behind source
Fan was on ground level on LOW speed
Release time of 1 minute
Flushing time minimum of 5 mins
Detection height 3 feet off ground on easel

**Plots of Spiking Intervals**

Included are the spike intervals plotted with respect to time utilizing Matlab for the controlled release experiment conducted May 20, 2014 in the hallway of the CME Building on the University of Utah campus. Plots are segregated by distance and then flowrate.

***Release at 10 ft***

**High-High flowrate – 20 lpm**

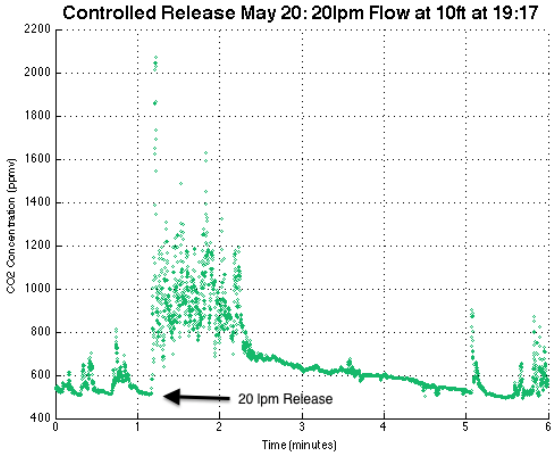


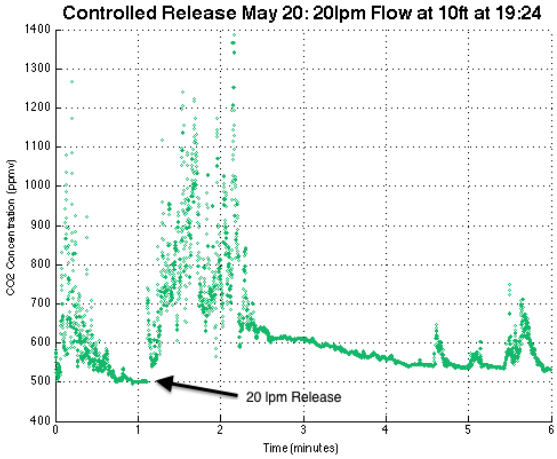


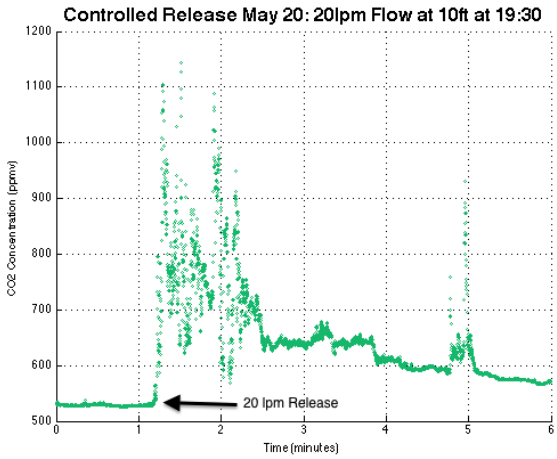

***Release at 30 ft***

**High-High flowrate – 20 lpm**

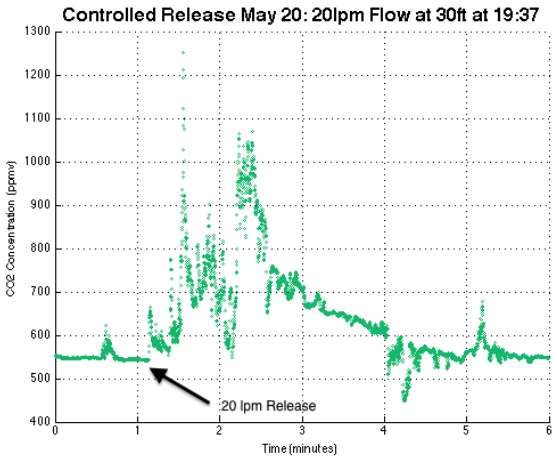


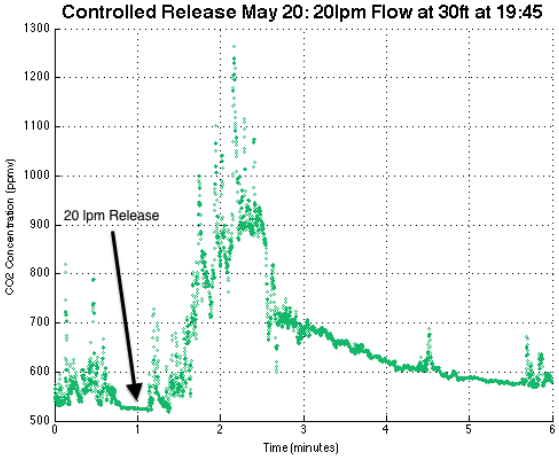


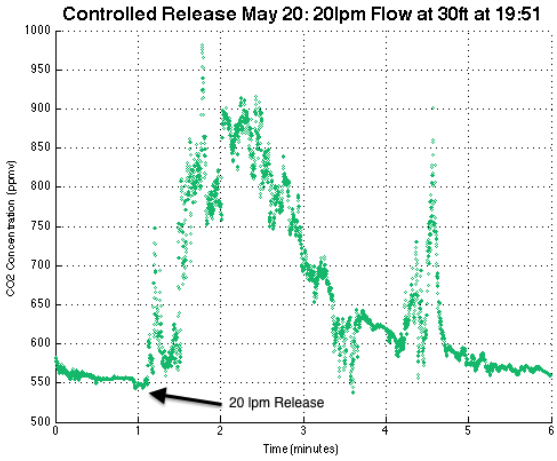


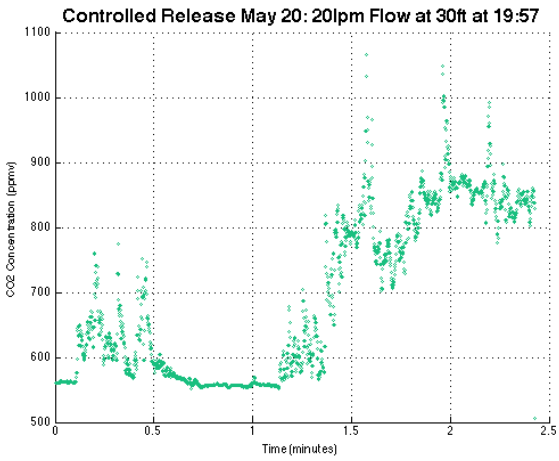


* the measurement data taken at High-High flowrate at 30 ft at 19:57 was not used for analysis

***Release at 50 ft***

**High-High flowrate – 20 lpm**

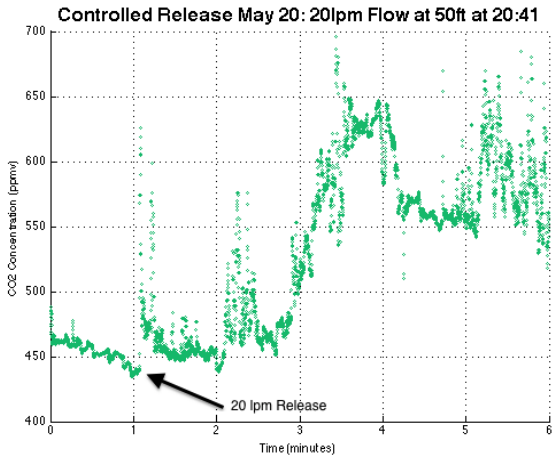


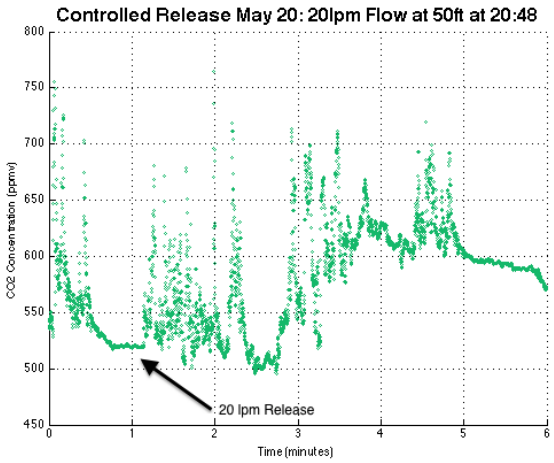


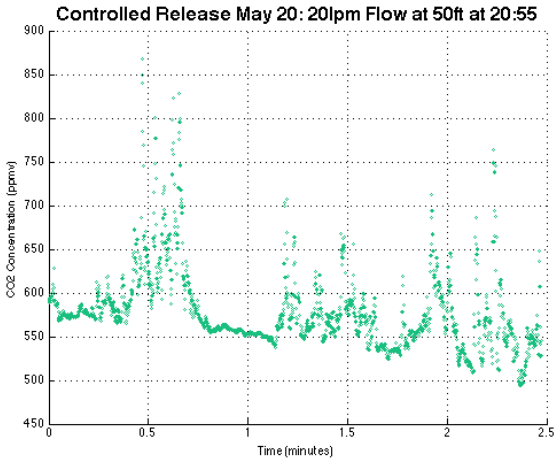


* the measurement data taken at High-High flowrate at 50 feet at 20:55 was not used for analysis

# APPENDIX D

## TOWER LOCATION 1 (TL1) DATA

The tower was located at the first location (TL1) beginning September 10th and ending October 18th, 2013. Included for each day are the values for the maximum, minimum, average and standard deviation of the two gases ($CO_2$ and $CH_4$) and the vertical velocity (UZ). The 99th percentile is provided for the two gases.
Also included are nine plots of the data for each day.

The plots are;

1. $CO_2$ Concentration vs. Time
2. $CH_4$ Concentration vs. Time
3. $CH_4$ Concentration vs. CO2 Concentration
4. Wind Direction vs. Time
5. Vertical Wind Velocity vs. Time
6. 99th Percentile $CO_2$ Concentration vs. Time
7. 99th Percentile $CO_2$ Concentration vs. Wind Direction
8. 99th Percentile $CH_4$ Concentration vs. Time
9. 99th Percentile $CH_4$ Concentration vs. Wind Direction

The final session at TL1 was the overnight session and is presented in Appendix G.

## D.1 Tuesday, September 10th, 2013

| | Maximum | Minimum | Average | Standard Deviation | 99th Percentile |
|---|---|---|---|---|---|
| $CO_2$ (ppmv) | 416.292 | 365.0719 | 386.3569 | 4.184 | 401.0205 |
| $CH_4$ (ppmv) | 2.2274 | 1.6826 | 1.7192 | 0.0486 | 1.9317 |
| UZ (m/s) | 2.3619 | -3.0998 | 0.0499 | 0.3655 | N/A |

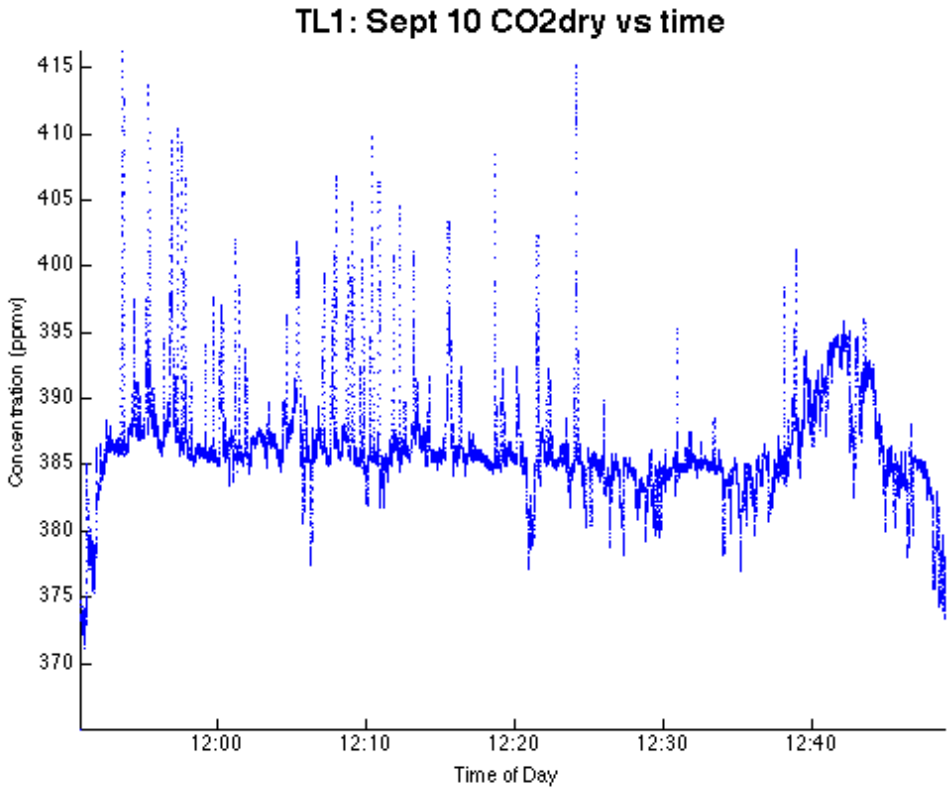

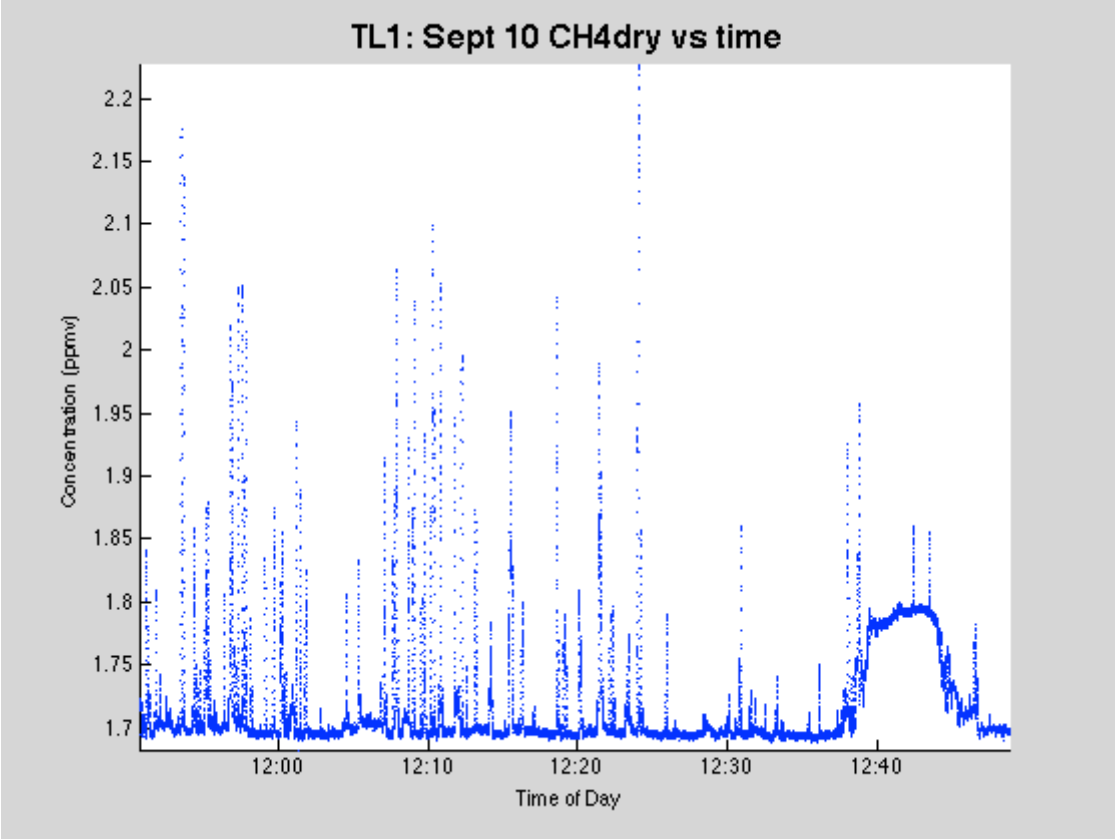
TL1: Sept 10 CH4dry vs time
Concentration (ppmv)
2.2
2.15
2.1
2.05
2
1.95
1.9
1.85
1.8
1.75
1.7
12:00
12:10
12:20
12:30
12:40
Time of Day

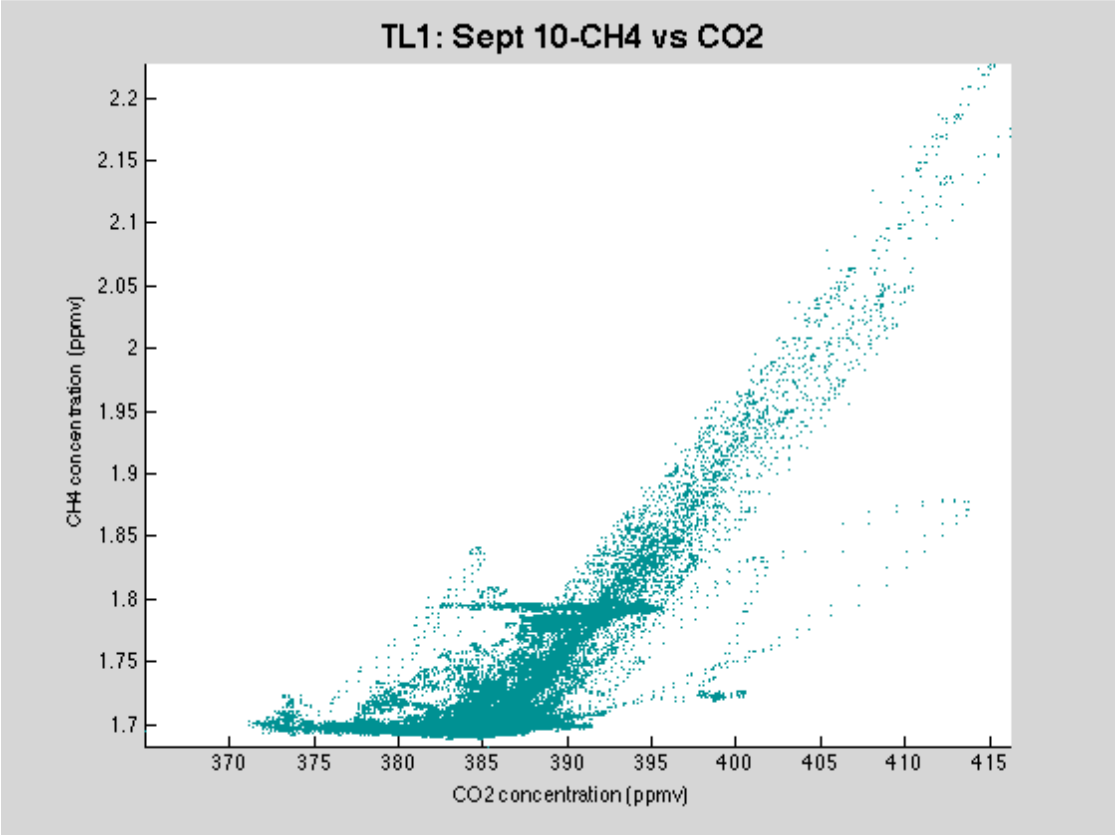
TL1: Sept 10-CH4 vs CO2
CH4 concentration (ppmv)
2.2
2.15
2.1
2.05
2
1.95
1.9
1.85
1.8
1.75
1.7
370
375
380
385
390
395
400
405
410
415
CO2 concentration (ppmv)

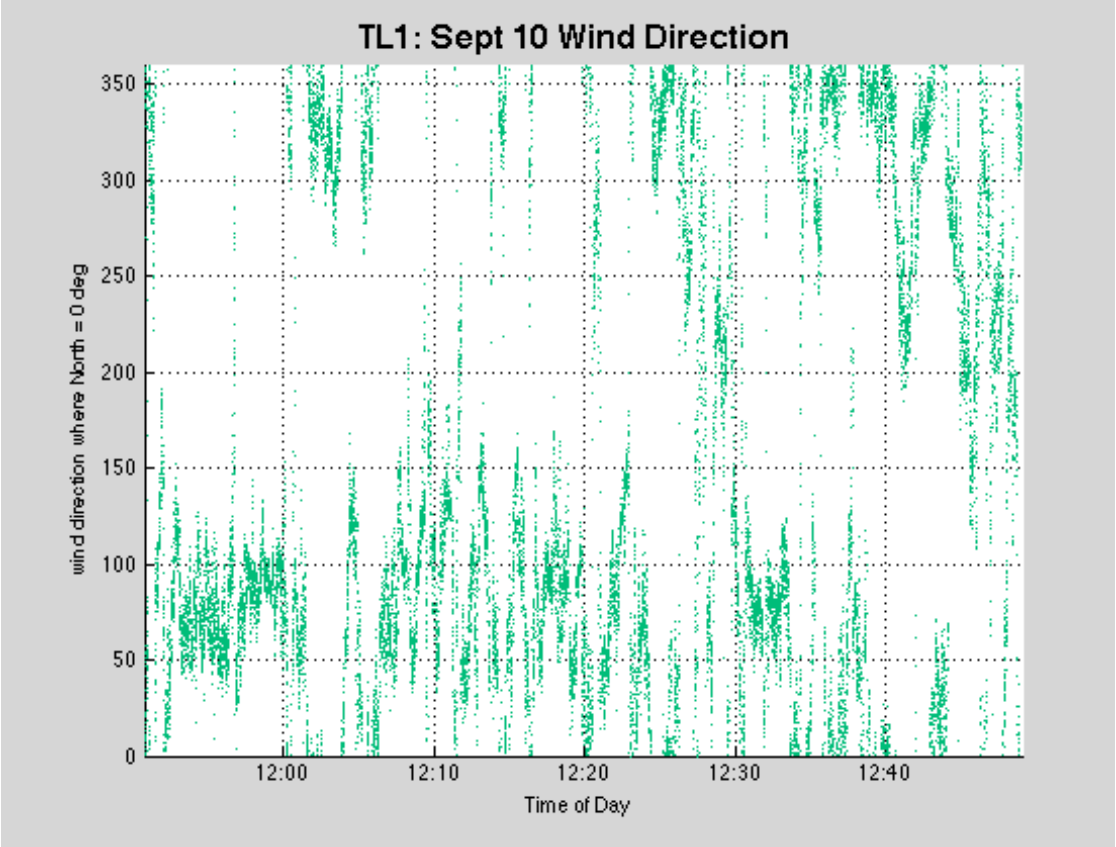
TL1: Sept 10 Wind Direction
wind direction where North = 0 deg
350
300
250
200
150
100
50
0
12:00
12:10
12:20
12:30
12:40
Time of Day

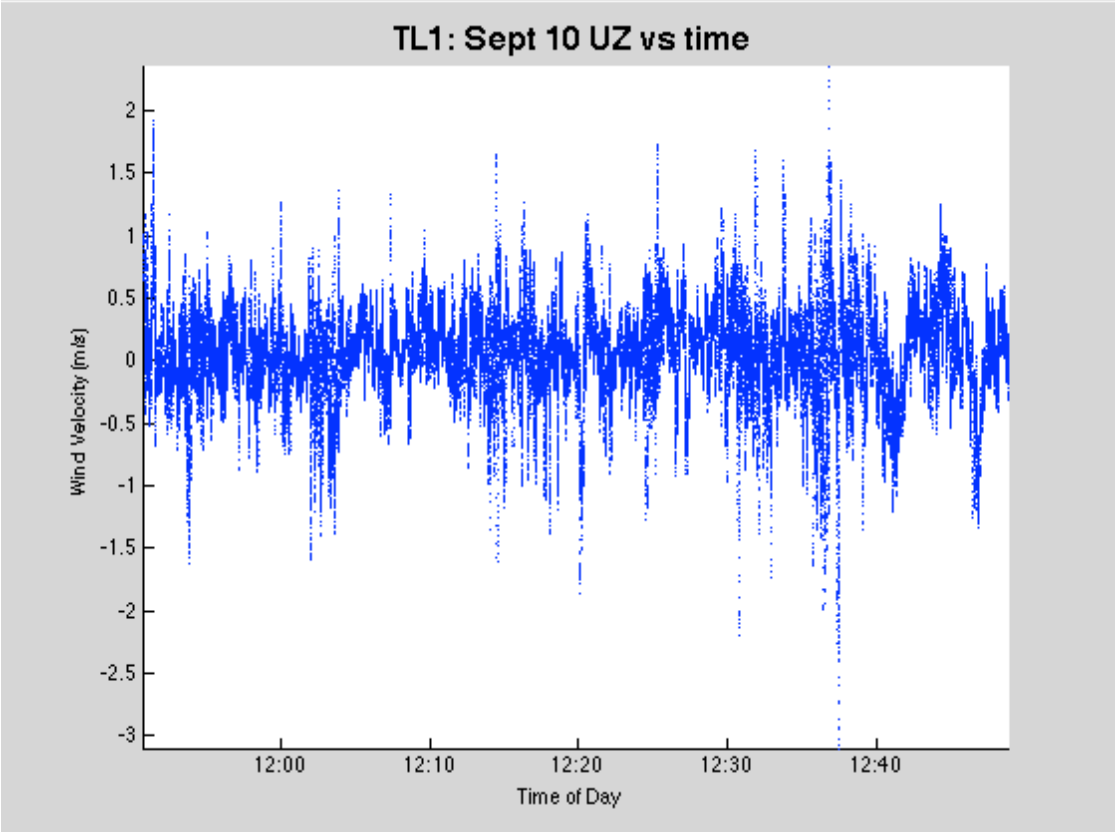
TL1: Sept 10 UZ vs time
Wind Velocity (m/s)
2
1.5
1
0.5
0
-0.5
-1
-1.5
-2
-2.5
-3
12:00
12:10
12:20
12:30
12:40
Time of Day

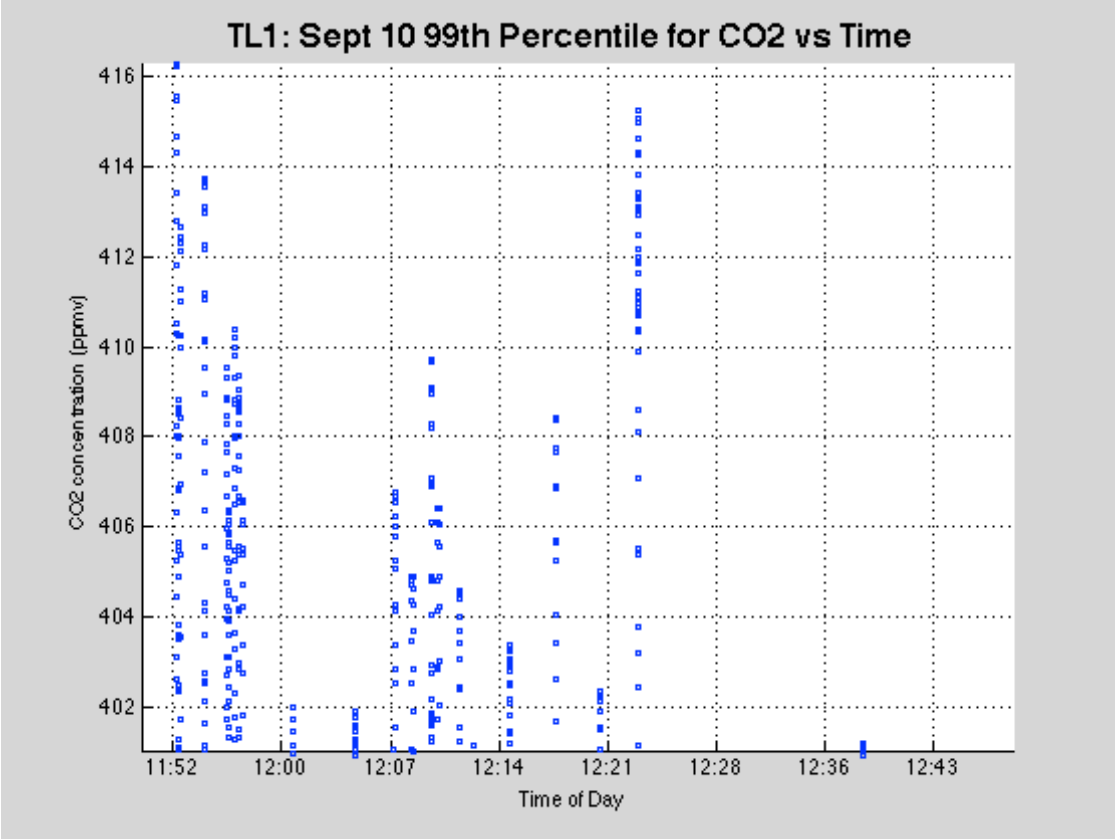
TL1: Sept 10 99th Percentile for CO2 vs Time
CO2 concentration (ppmv)
416
414
412
410
408
406
404
402
11:52
12:00
12:07
12:14
12:21
12:28
12:36
12:43
Time of Day

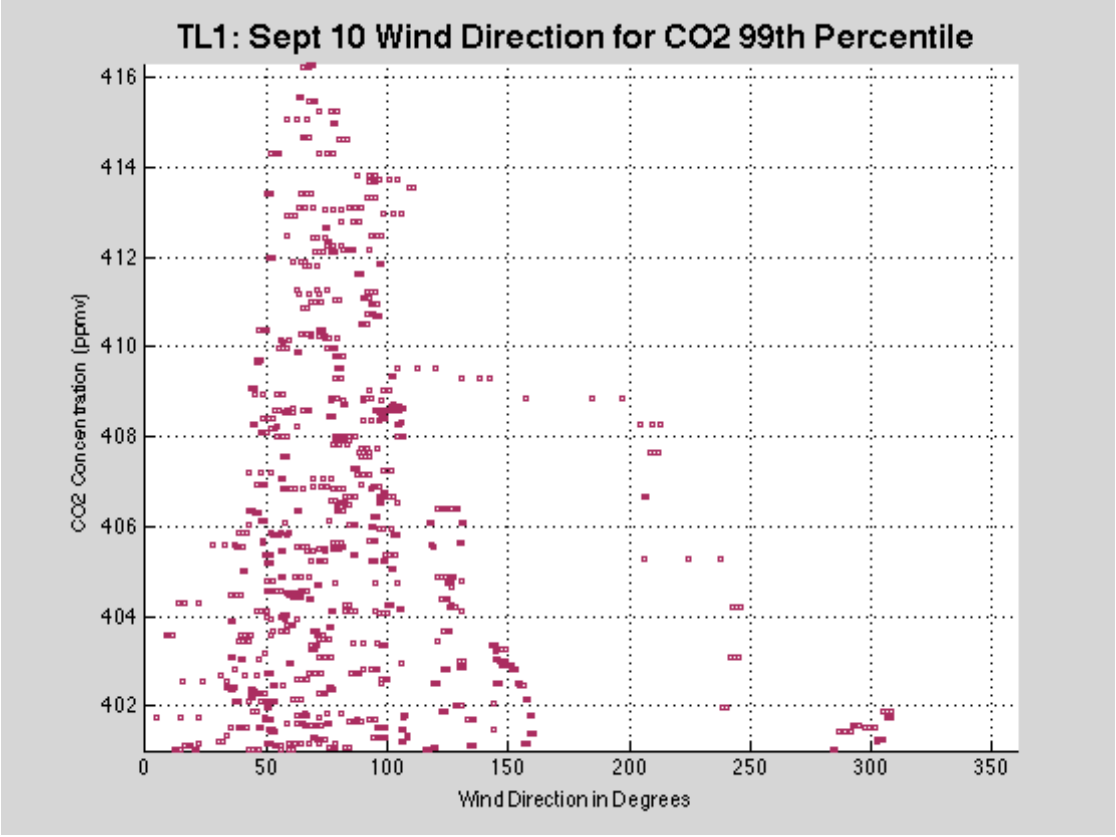
TL1: Sept 10 Wind Direction for CO2 99th Percentile
CO2 Concentration (ppmv)
416
414
412
410
408
406
404
402
0
50
100
150
200
250
300
350
Wind Direction in Degrees

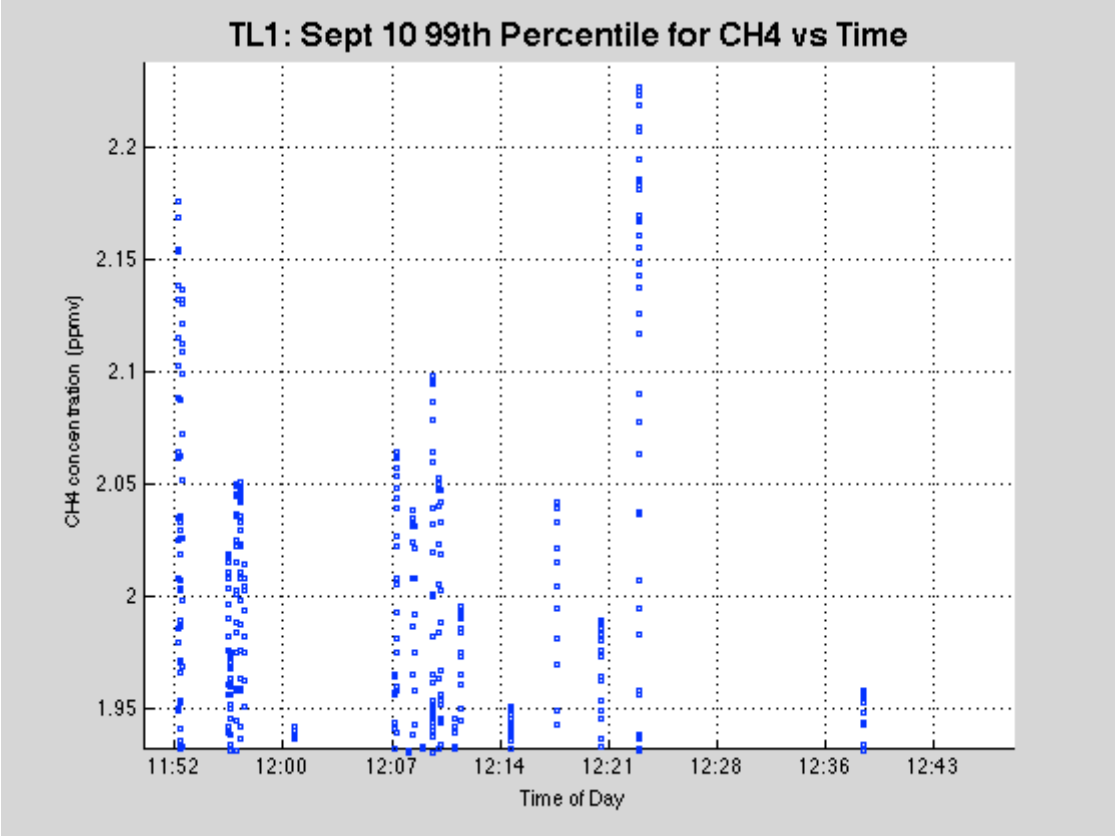
TL1: Sept 10 99th Percentile for CH4 vs Time
CH4 concentration (ppmv)
2.2
2.15
2.1
2.05
2
1.95
11:52
12:00
12:07
12:14
12:21
12:28
12:36
12:43
Time of Day

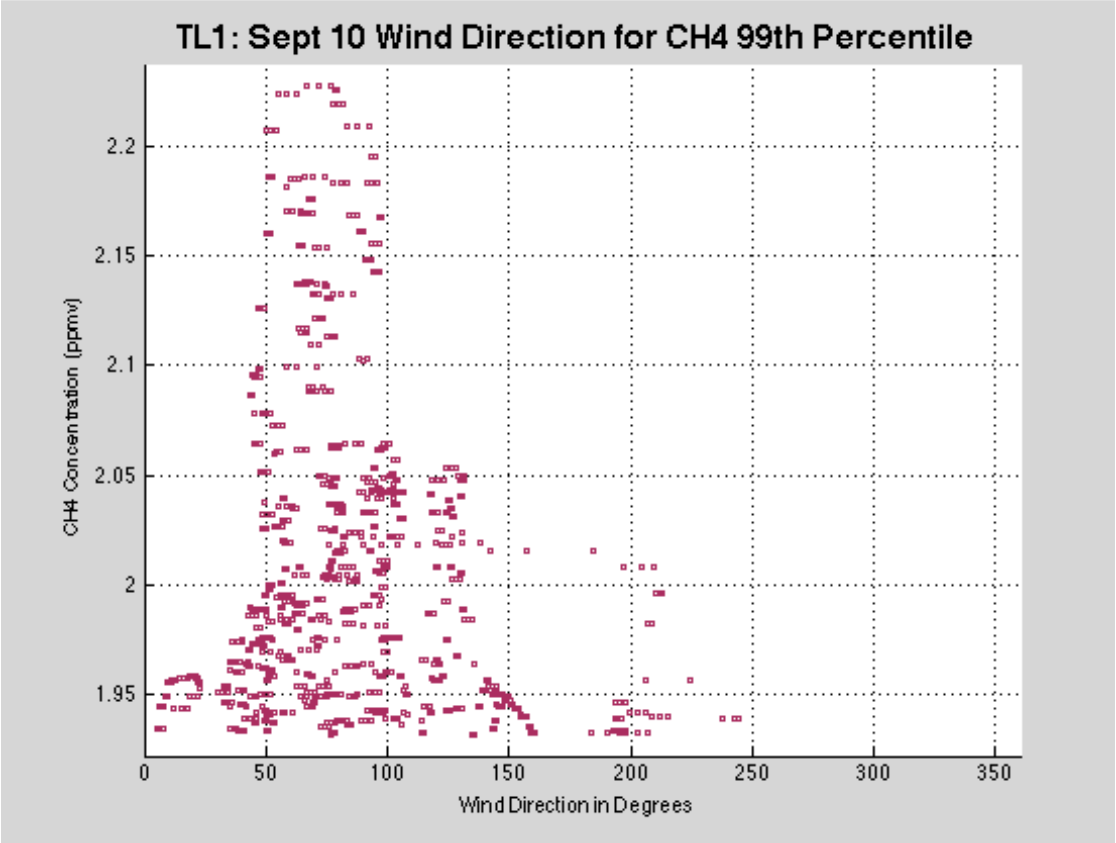
TL1: Sept 10 Wind Direction for CH4 99th Percentile
CH4 Concentration (ppmv)
2.2
2.15
2.1
2.05
2
1.95
0
50
100
150
200
250
300
350
Wind Direction in Degrees

## D.2 Wednesday, September 11th, 2013

| | Maximum | Minimum | Average | Standard Deviation | 99th Percentile |
|---|---|---|---|---|---|
| $CO_2$ (ppmv) | 445.2015 | 376.343 | 386.9351 | 2.5459 | 392.2277 |
| $CH_4$ (ppmv) | 2.0894 | 1.6588 | 1.6747 | 0.0135 | 1.6972 |
| UZ (m/s) | 2.3373 | -2.687 | -0.0475 | 0.4084 | N/A |

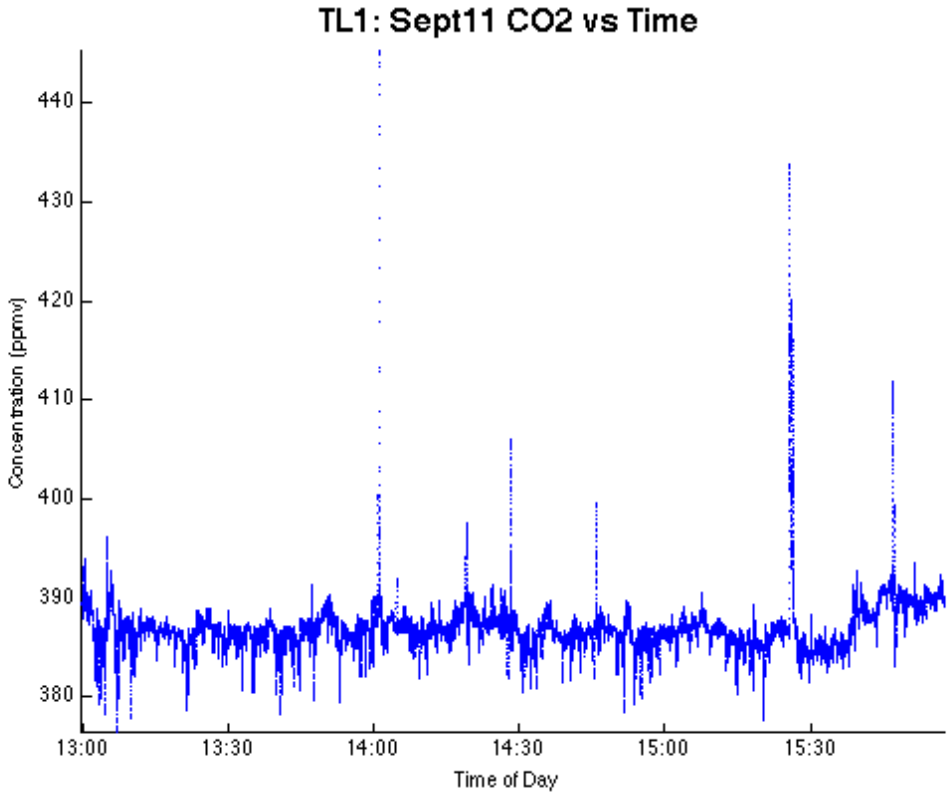

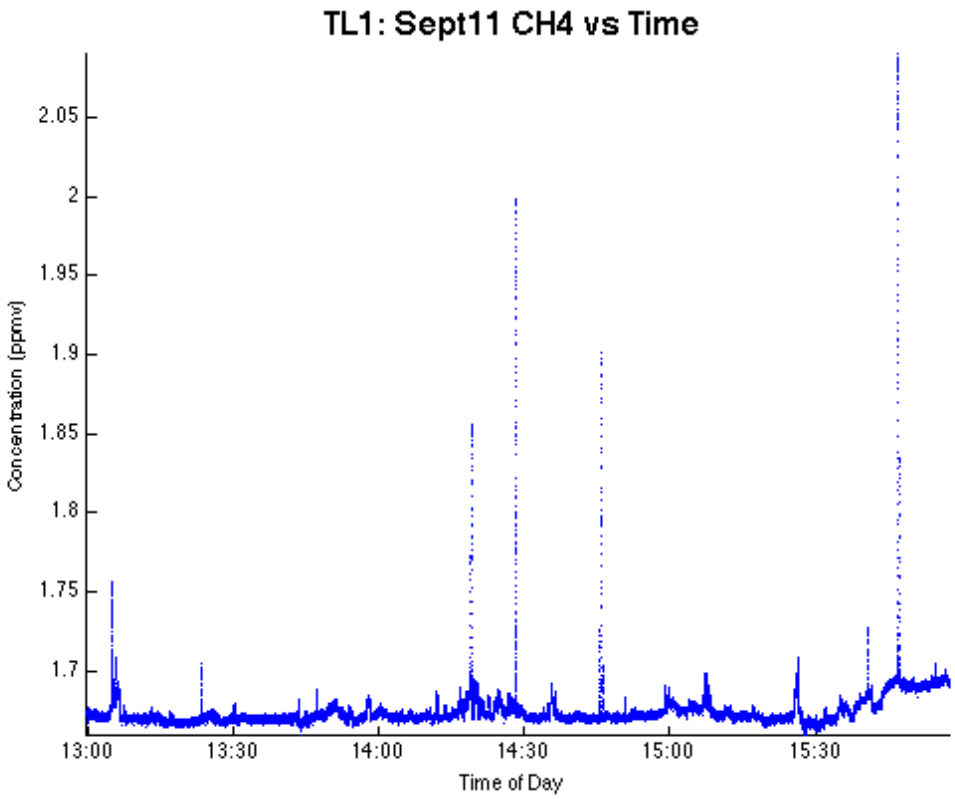
TL1: Sept11 CH4 vs Time
Concentration (ppmv)
2.05
2
1.95
1.9
1.85
1.8
1.75
1.7
13:00
13:30
14:00
14:30
15:00
15:30
Time of Day

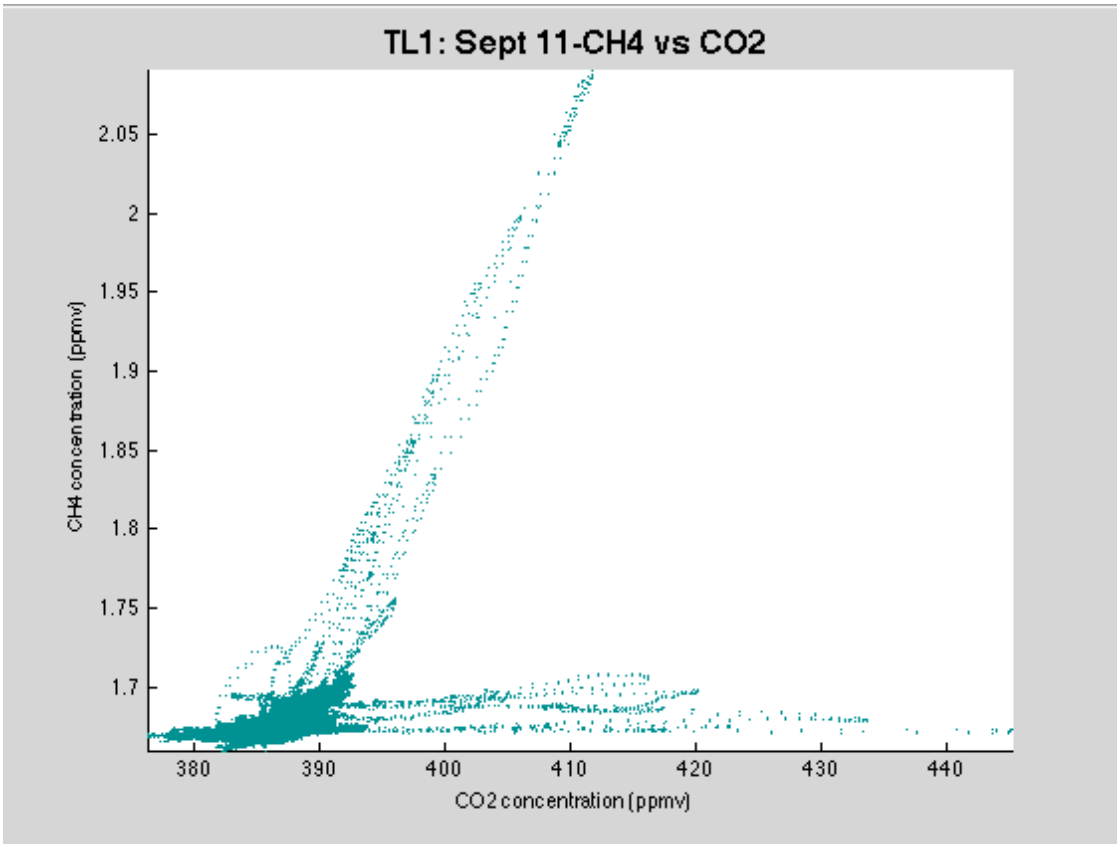
TL1: Sept 11-CH4 vs CO2
CH4 concentration (ppmv)
2.05
2
1.95
1.9
1.85
1.8
1.75
1.7
380
390
400
410
420
430
440
CO2 concentration (ppmv)

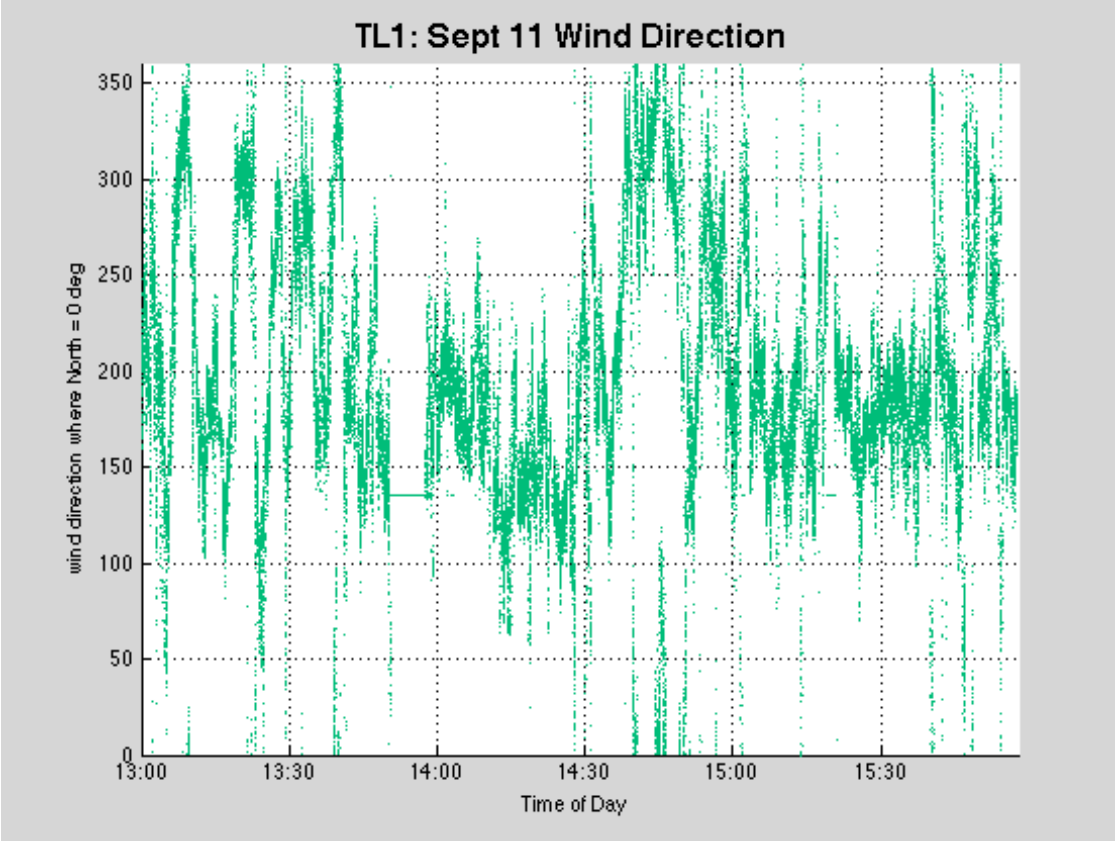
TL1: Sept 11 Wind Direction
wind direction where North = 0 deg
350
300
250
200
150
100
50
0
13:00
13:30
14:00
14:30
15:00
15:30
Time of Day

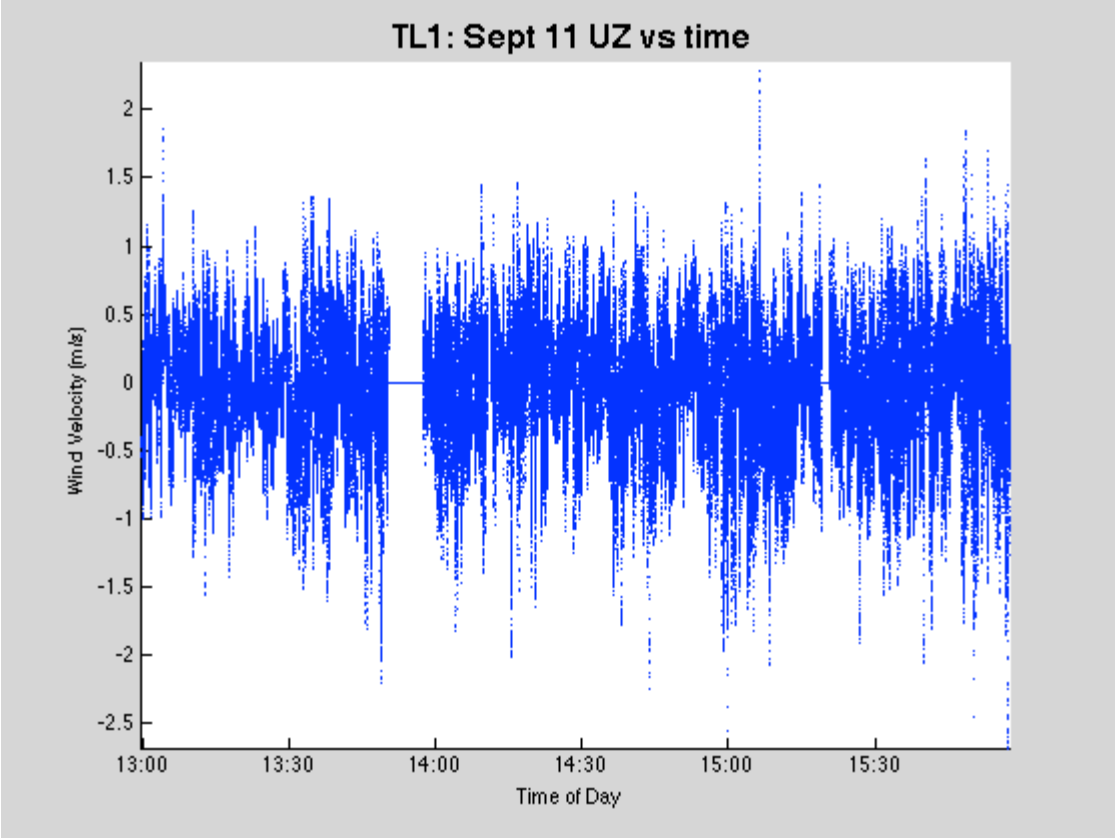
TL1: Sept 11 UZ vs time
Wind Velocity (m/s)
2
1.5
1
0.5
0
-0.5
-1
-1.5
-2
-2.5
13:00
13:30
14:00
14:30
15:00
15:30
Time of Day

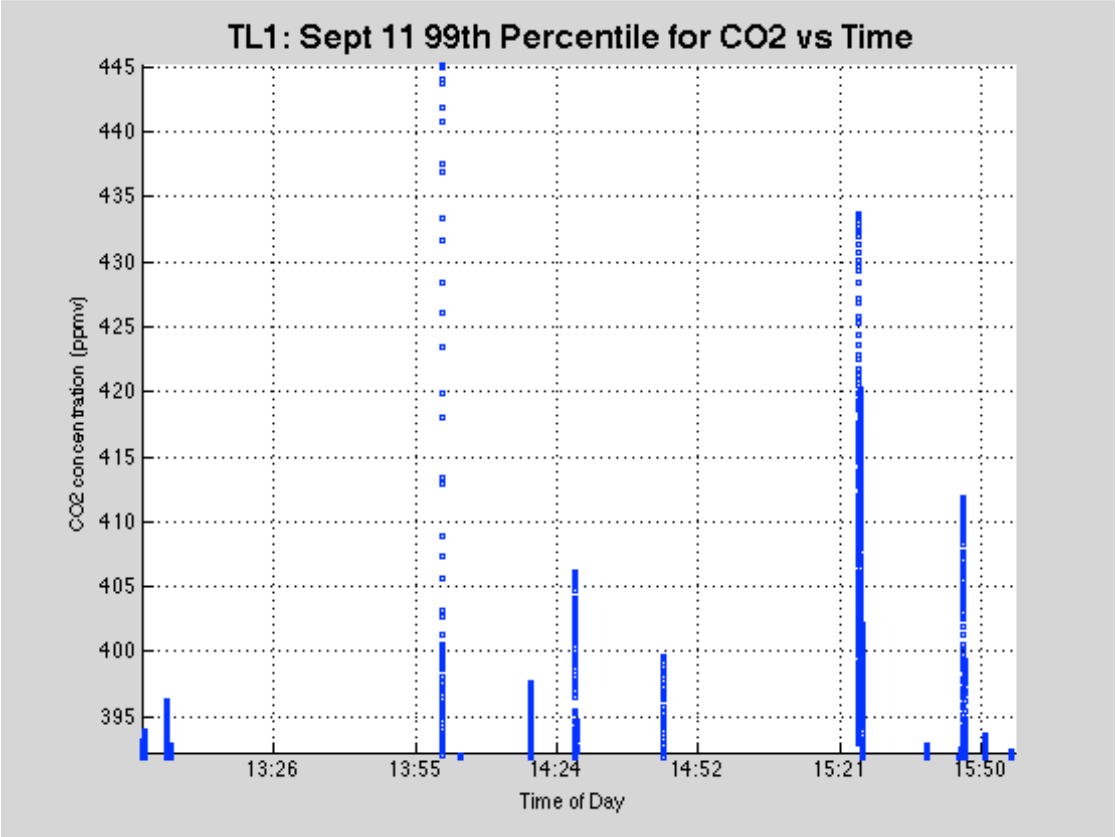
TL1: Sept 11 99th Percentile for CO2 vs Time
CO2 concentration (ppmv)
445
440
435
430
425
420
415
410
405
400
395
13:26
13:55
14:24
14:52
15:21
15:50
Time of Day

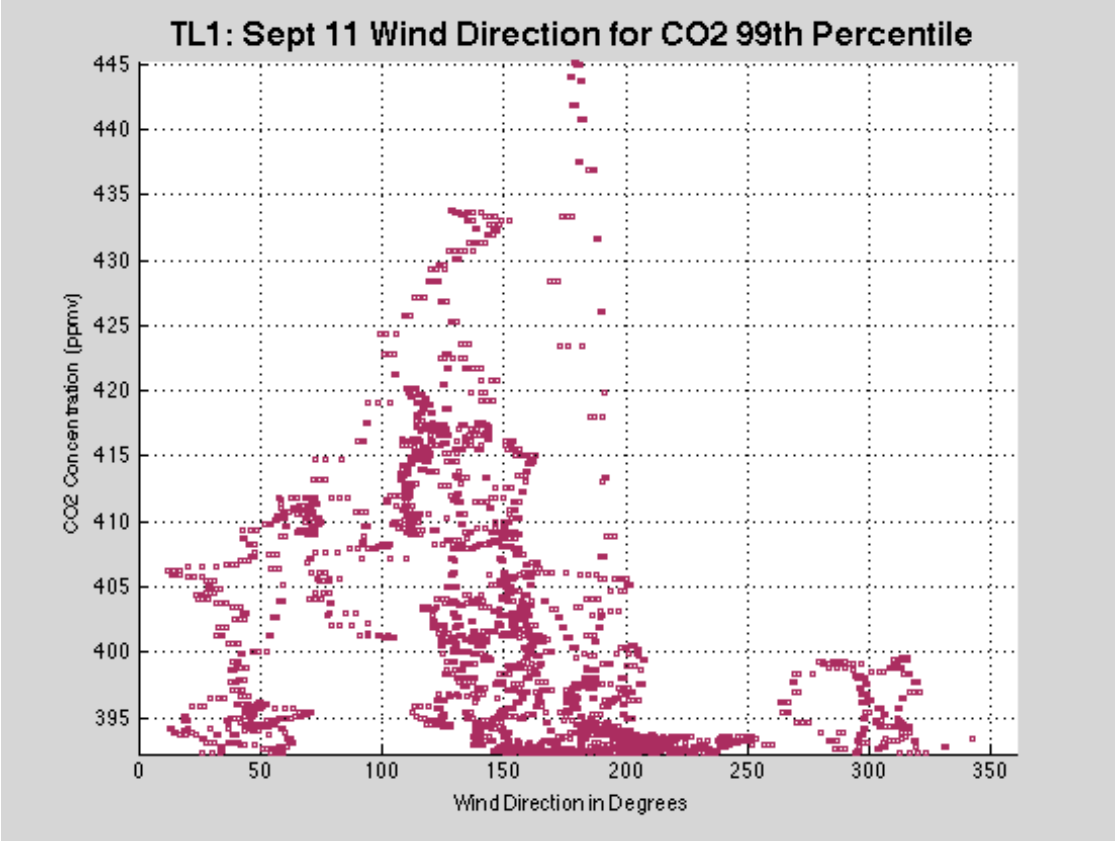
TL1: Sept 11 Wind Direction for CO2 99th Percentile
CO2 Concentration (ppmv)
445
440
435
430
425
420
415
410
405
400
395
0
50
100
150
200
250
300
350
Wind Direction in Degrees

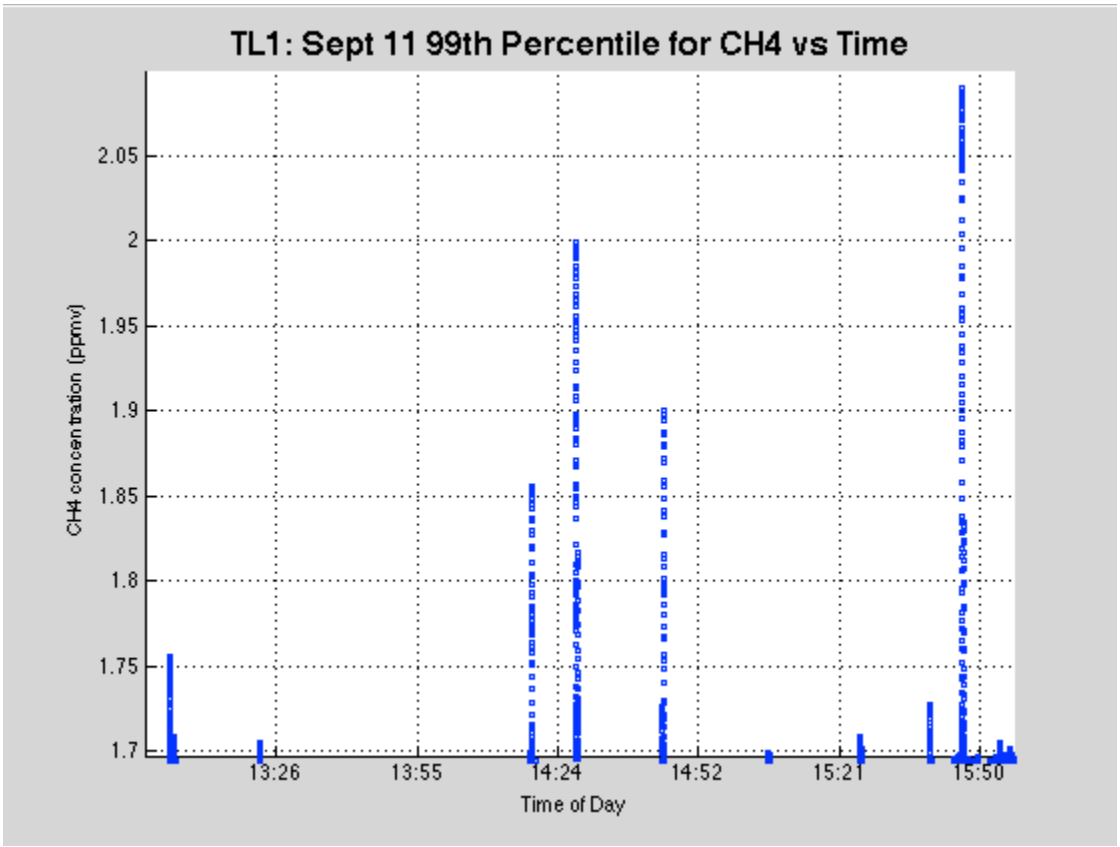
TL1: Sept 11 99th Percentile for CH4 vs Time
CH4 concentration (ppmv)
2.05
2
1.95
1.9
1.85
1.8
1.75
1.7
13:26
13:55
14:24
14:52
15:21
15:50
Time of Day

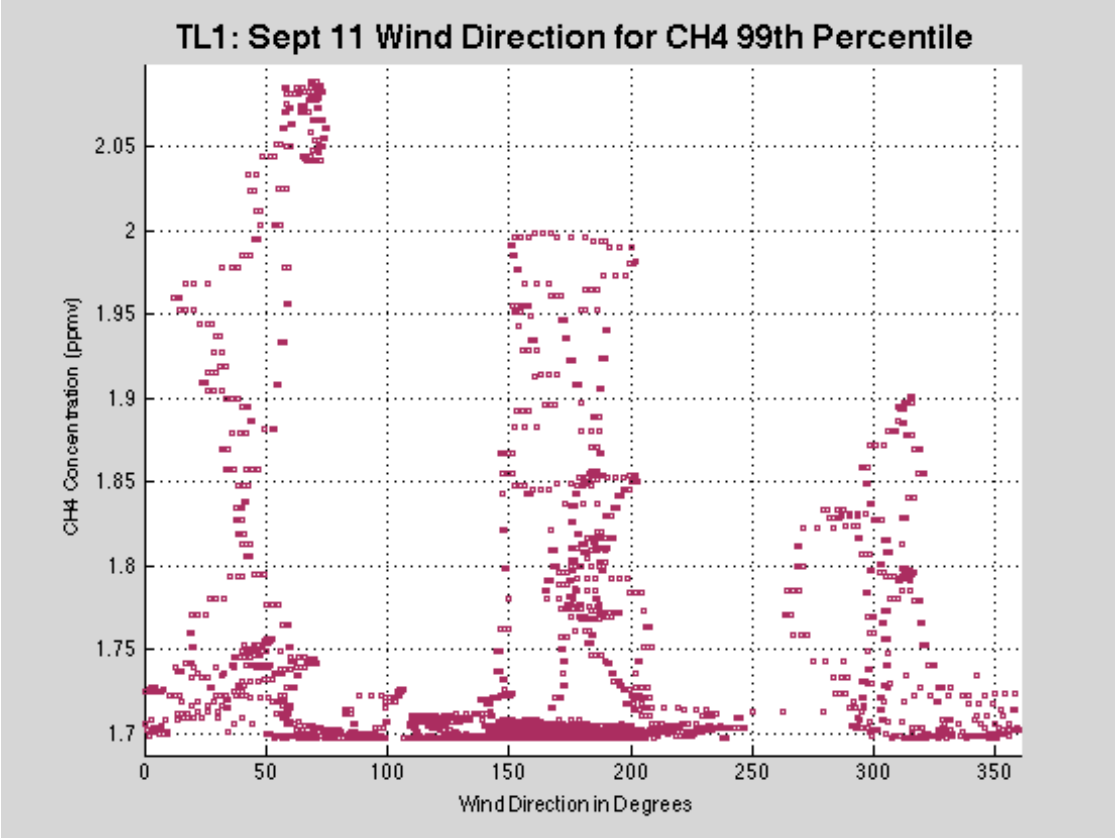
TL1: Sept 11 Wind Direction for CH4 99th Percentile
CH4 Concentration (ppmv)
2.05
2
1.95
1.9
1.85
1.8
1.75
1.7
0
50
100
150
200
250
300
350
Wind Direction in Degrees

D.3 Thursday, September 12th, 2013

| | Maximum | Minimum | Average | Standard Deviation | 99th Percentile |
|---|---|---|---|---|---|
| $CO_2$ (ppmv) | 446.0317 | 375.9432 | 386.7413 | 5.555 | 399.7087 |
| $CH_4$ (ppmv) | 2.8684 | 1.6457 | 1.6783 | 0.0472 | 1.8288 |
| UZ (m/s) | 2.1704 | -3.5599 | -0.0174 | 0.4047 | N/A |

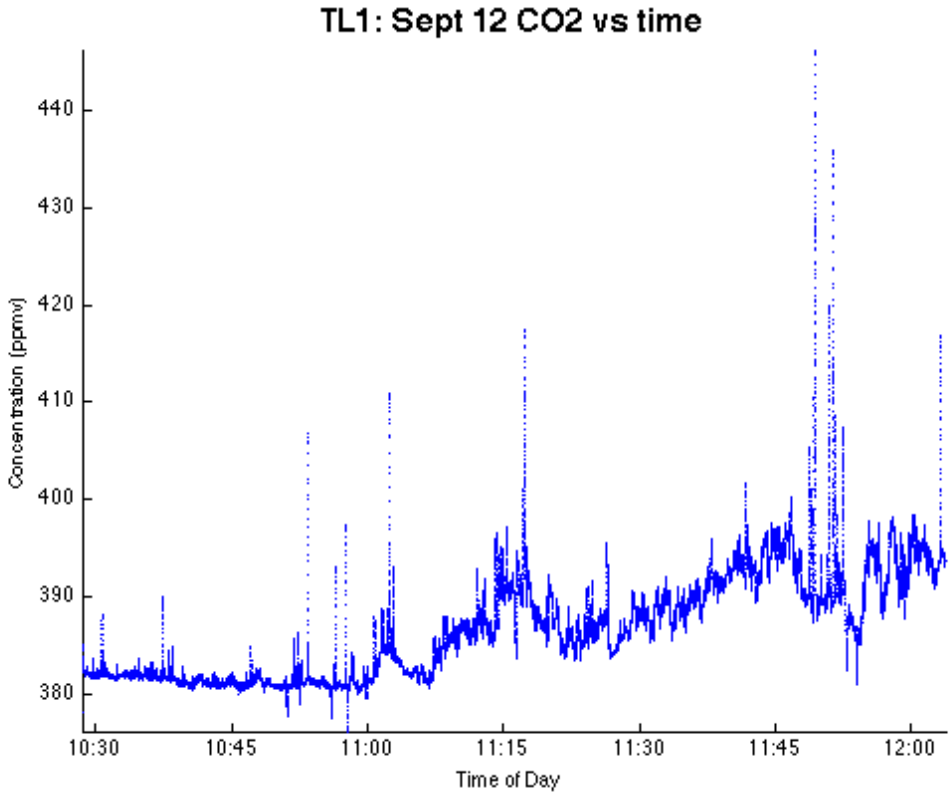

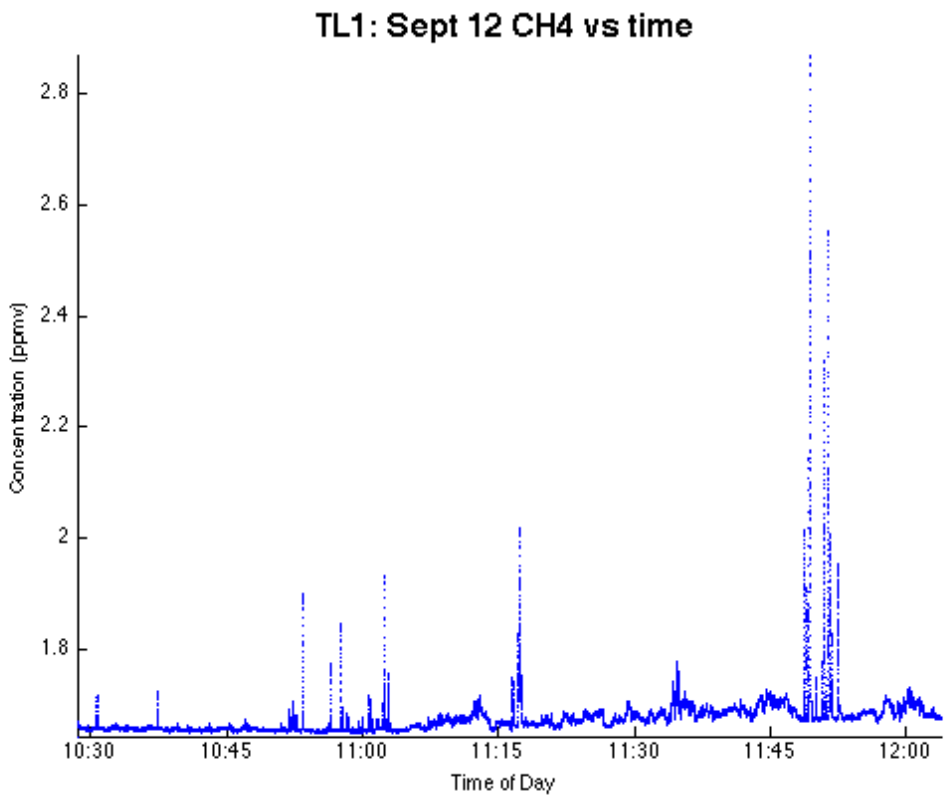
TL1: Sept 12 CH4 vs time
Concentration (ppmv)
2.8
2.6
2.4
2.2
2
1.8
10:30
10:45
11:00
11:15
11:30
11:45
12:00
Time of Day

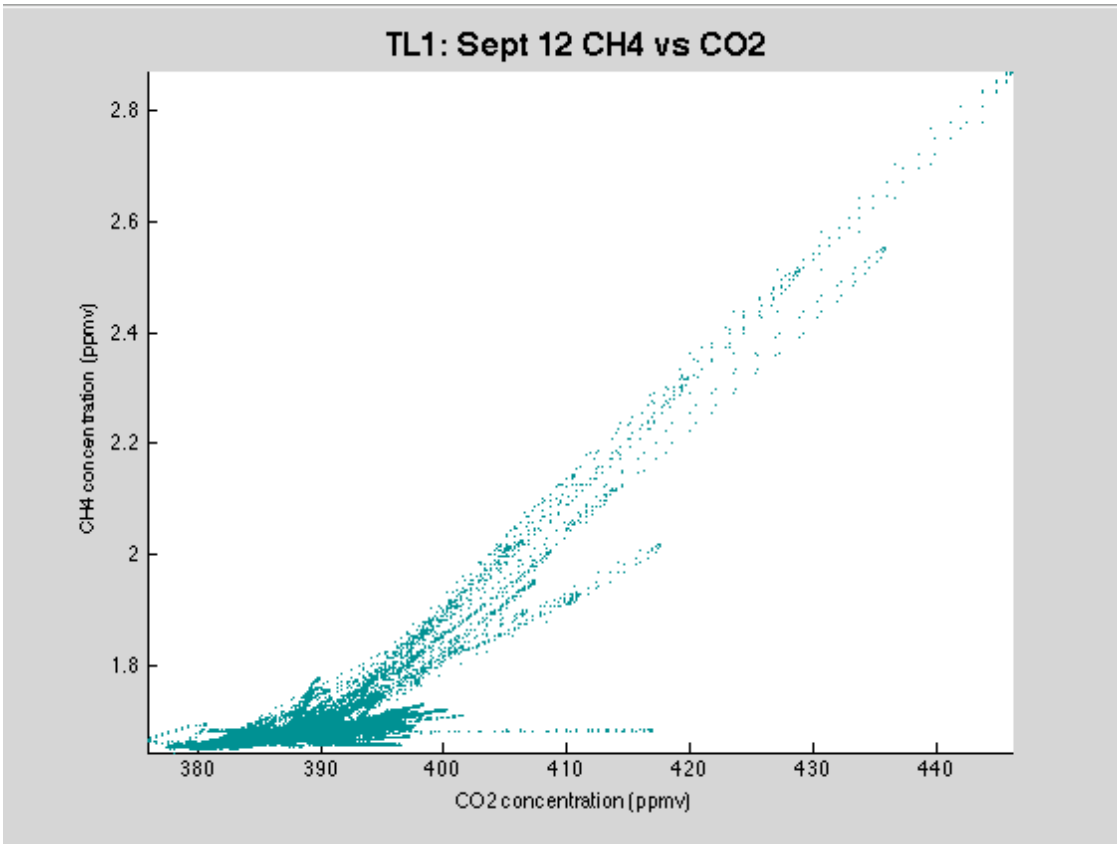
TL1: Sept 12 CH4 vs CO2
CH4 concentration (ppmv)
2.8
2.6
2.4
2.2
2
1.8
380
390
400
410
420
430
440
CO2 concentration (ppmv)

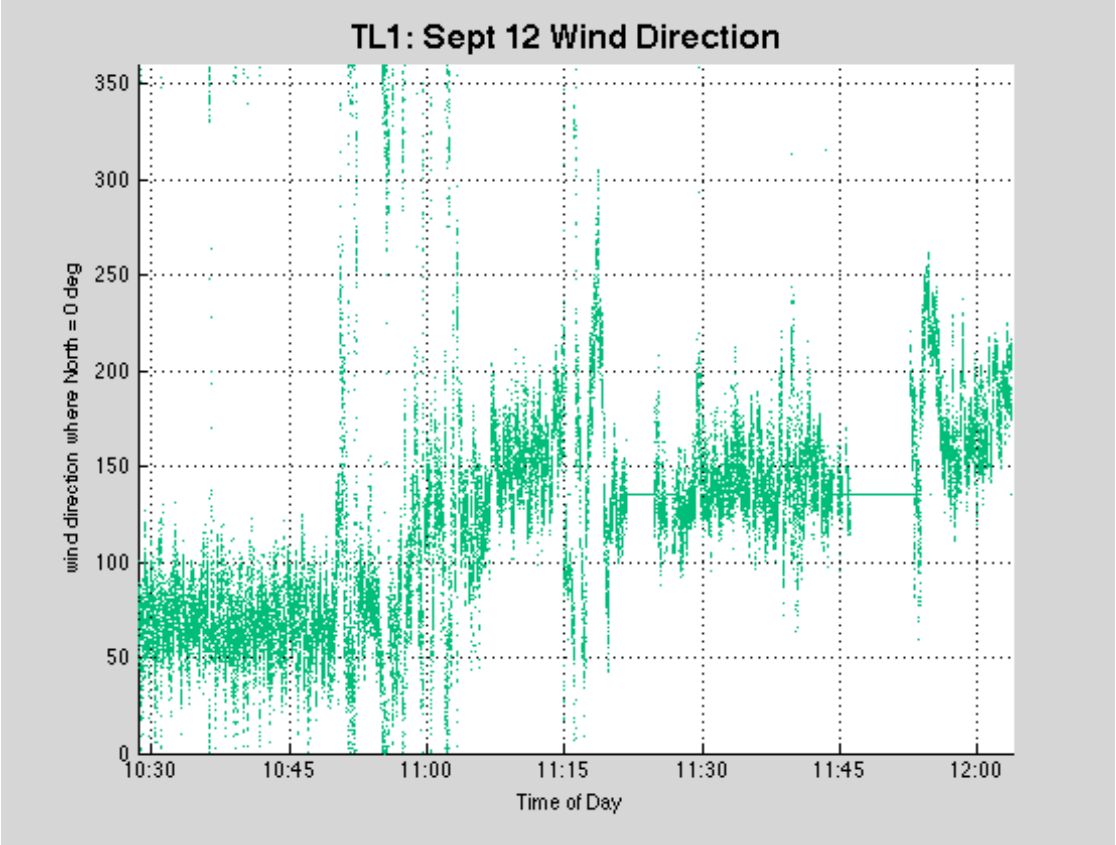
TL1: Sept 12 Wind Direction
wind direction where North = 0 deg
0
50
100
150
200
250
300
350
10:30
10:45
11:00
11:15
11:30
11:45
12:00
Time of Day

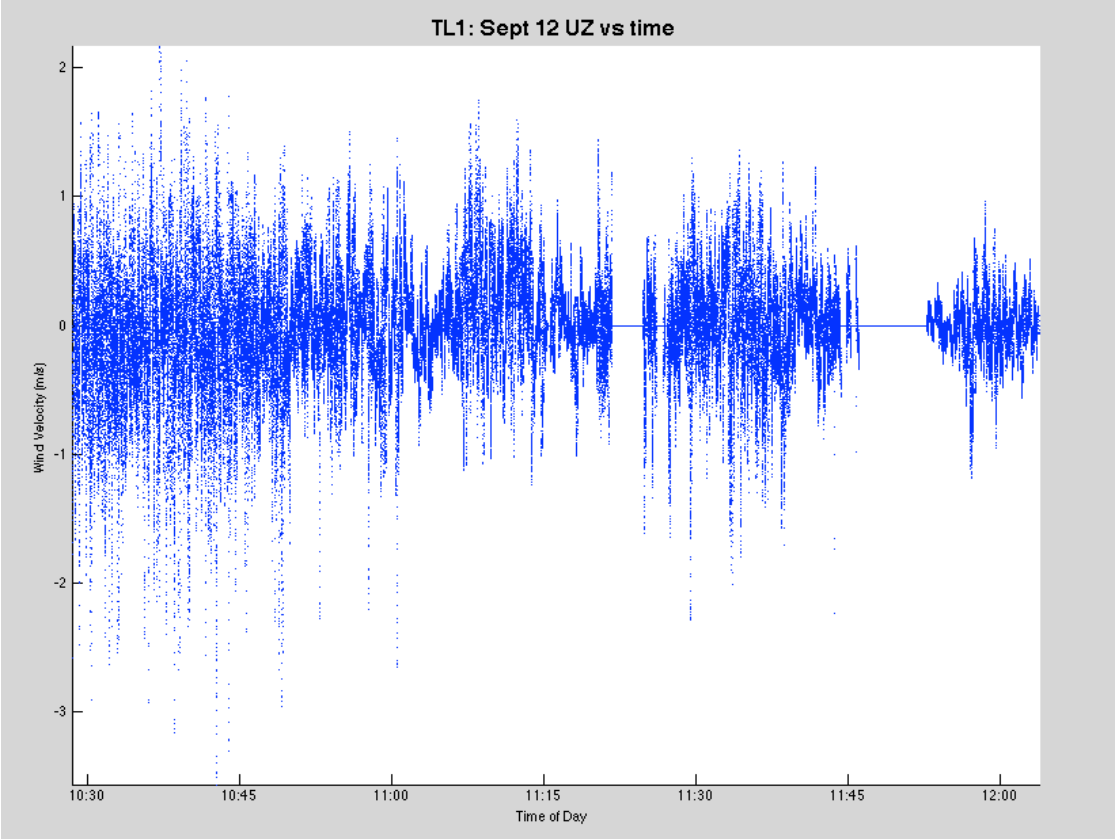
TL1: Sept 12 UZ vs time
Wind Velocity (m/s)
2
1
0
-1
-2
-3
10:30
10:45
11:00
11:15
11:30
11:45
12:00
Time of Day

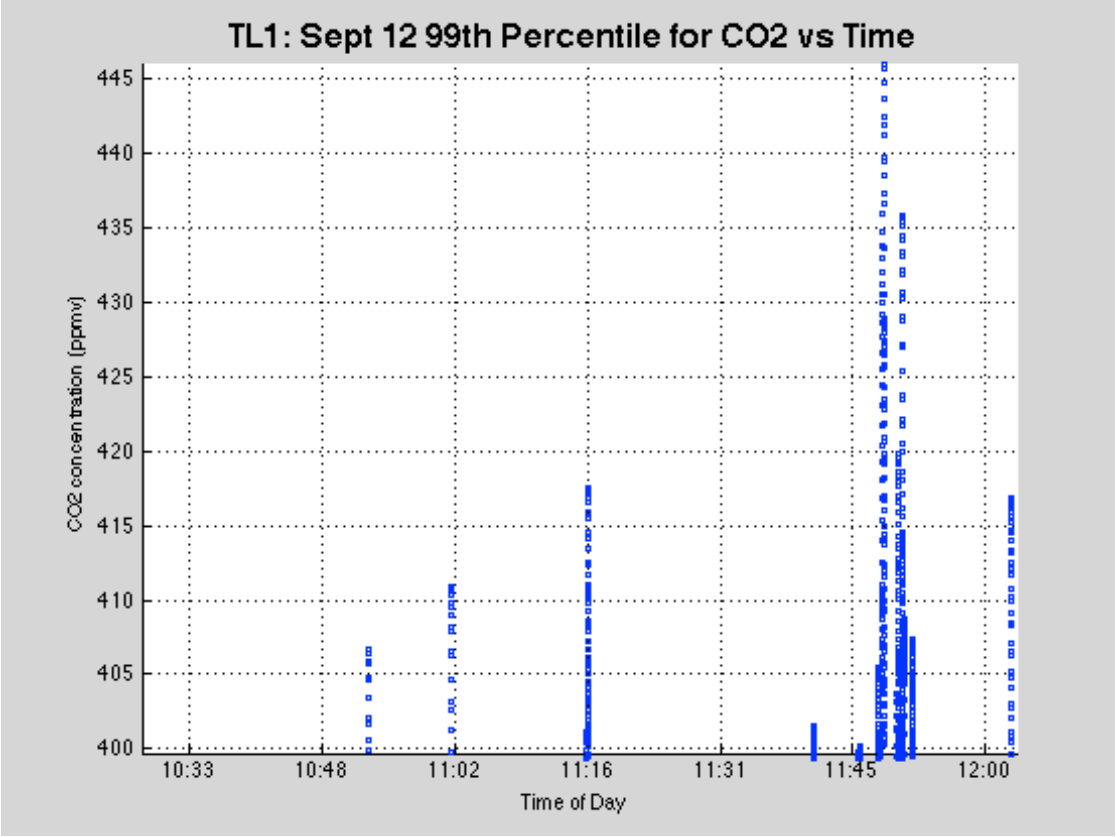
TL1: Sept 12 99th Percentile for CO2 vs Time
CO2 concentration (ppmv)
445
440
435
430
425
420
415
410
405
400
10:33
10:48
11:02
11:16
11:31
11:45
12:00
Time of Day

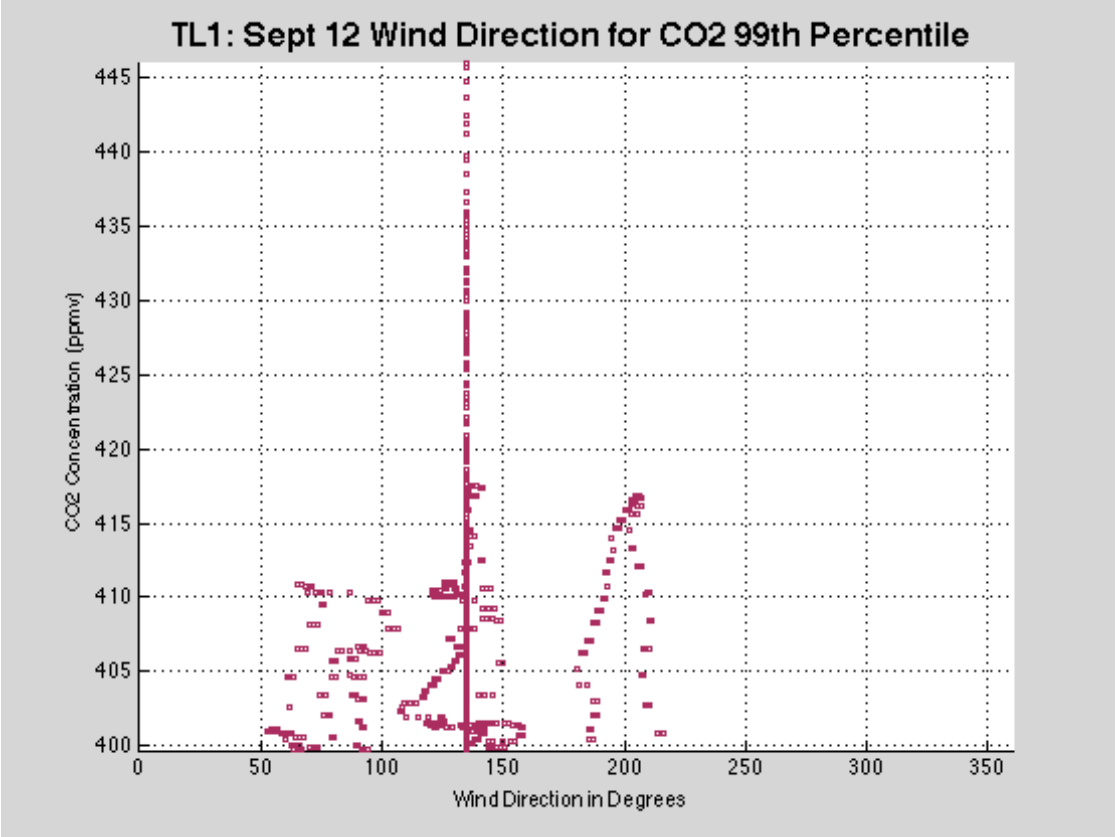
TL1: Sept 12 Wind Direction for CO2 99th Percentile
CO2 Concentration (ppmv)
445
440
435
430
425
420
415
410
405
400
0
50
100
150
200
250
300
350
Wind Direction in Degrees

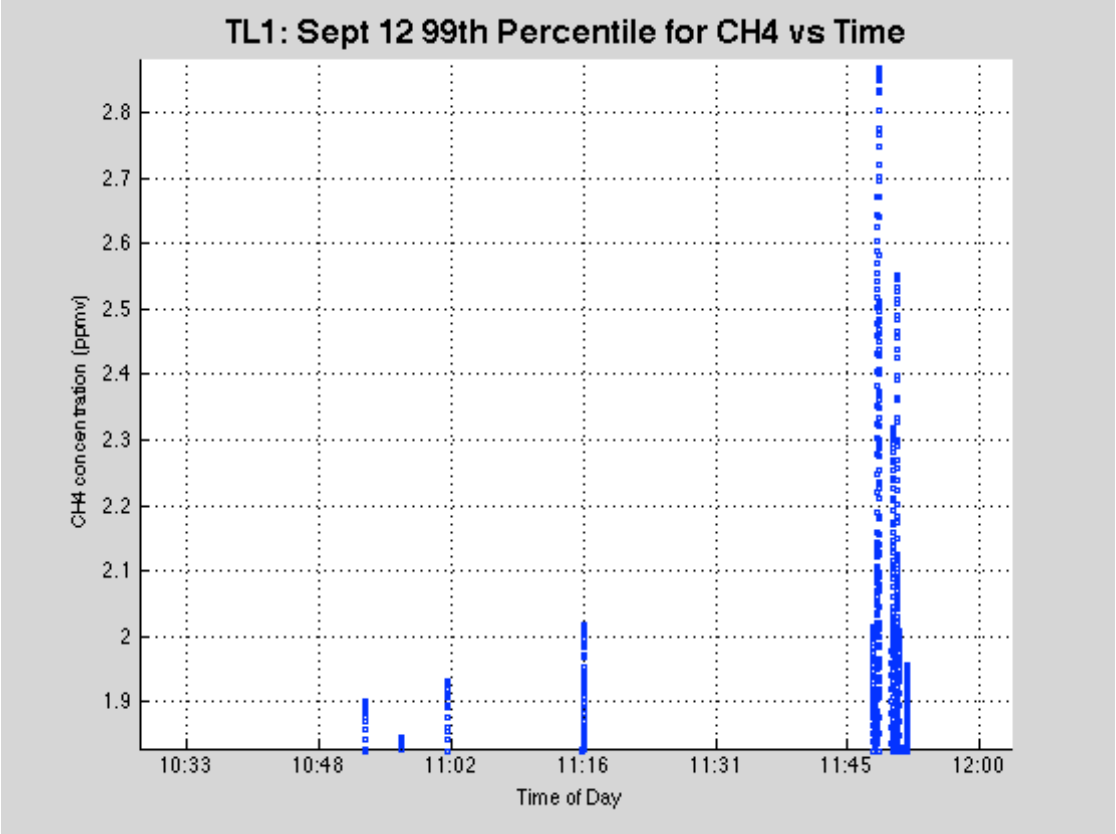
TL1: Sept 12 99th Percentile for CH4 vs Time
CH4 concentration (ppmv)
2.8
2.7
2.6
2.5
2.4
2.3
2.2
2.1
2
1.9
10:33
10:48
11:02
11:16
11:31
11:45
12:00
Time of Day

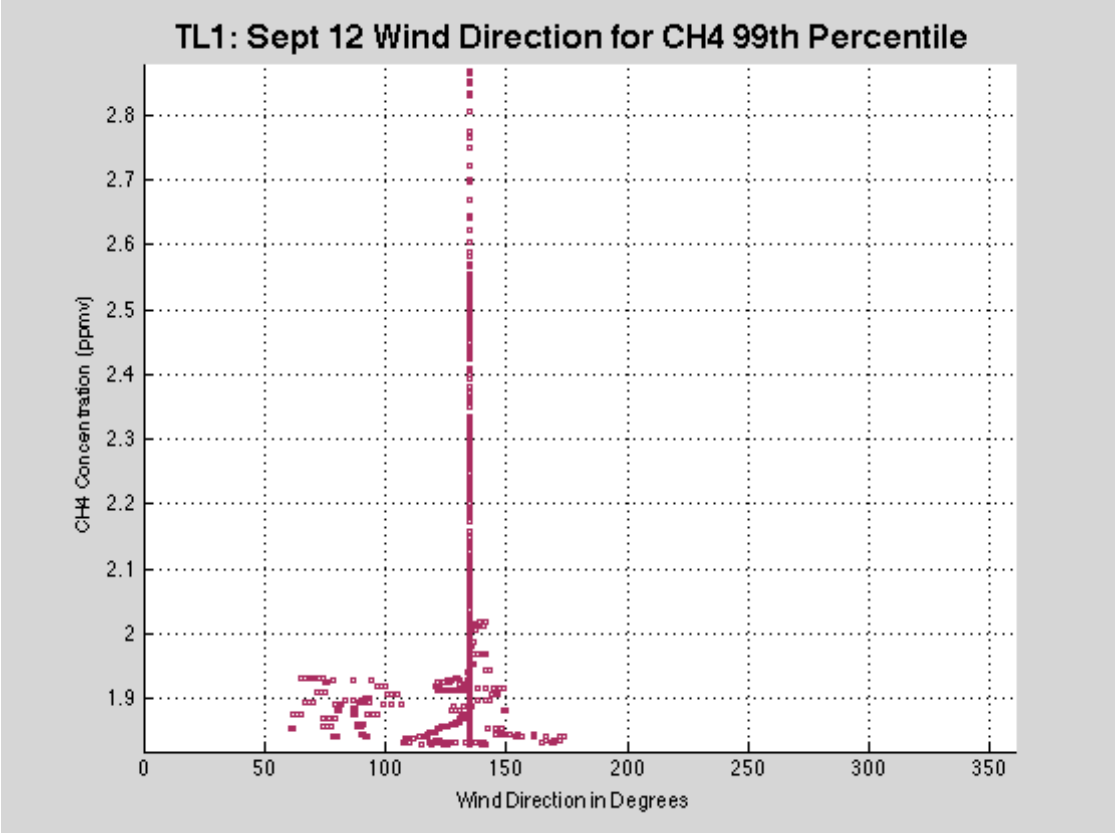
TL1: Sept 12 Wind Direction for CH4 99th Percentile
CH4 Concentration (ppmv)
2.8
2.7
2.6
2.5
2.4
2.3
2.2
2.1
2
1.9
0
50
100
150
200
250
300
350
Wind Direction in Degrees

D.4 Friday, September 13th, 2013

| | Maximum | Minimum | Average | Standard Deviation | 99th Percentile |
|---|---|---|---|---|---|
| $CO_2$ (ppmv) | 423.3595 | 381.235 | 395.01 | 6.3171 | 408.6254 |
| $CH_4$ (ppmv) | 1.9333 | 1.6799 | 1.7176 | 0.0282 | 1.7789 |
| UZ (m/s) | 4.006 | -6.5075 | -0.0431 | 0.547 | N/A |

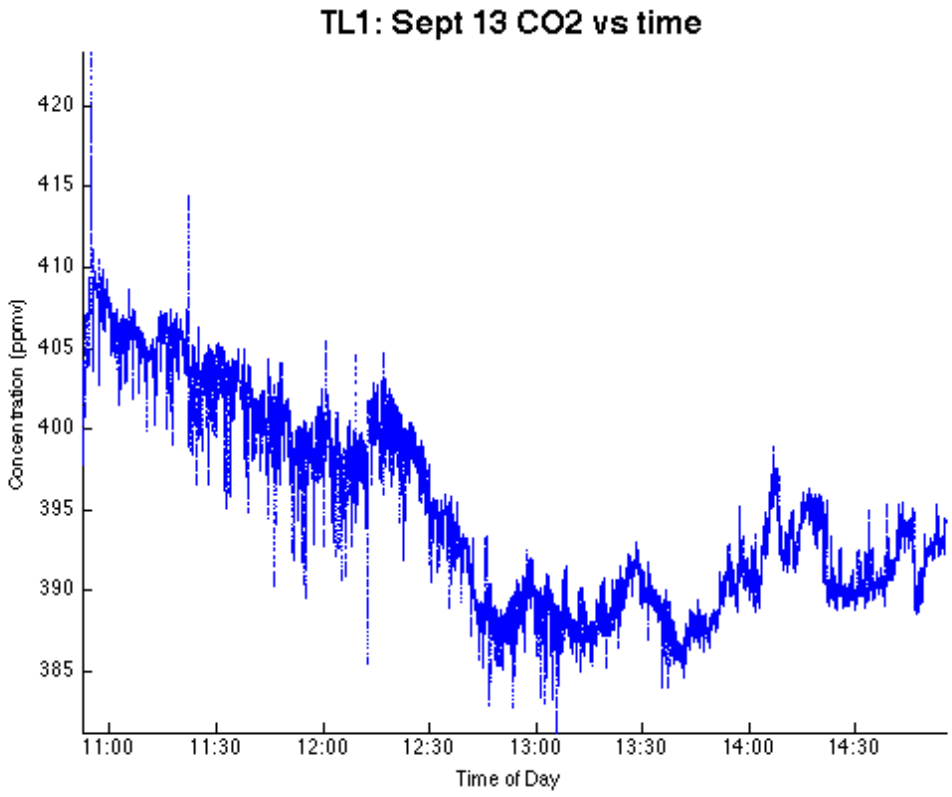

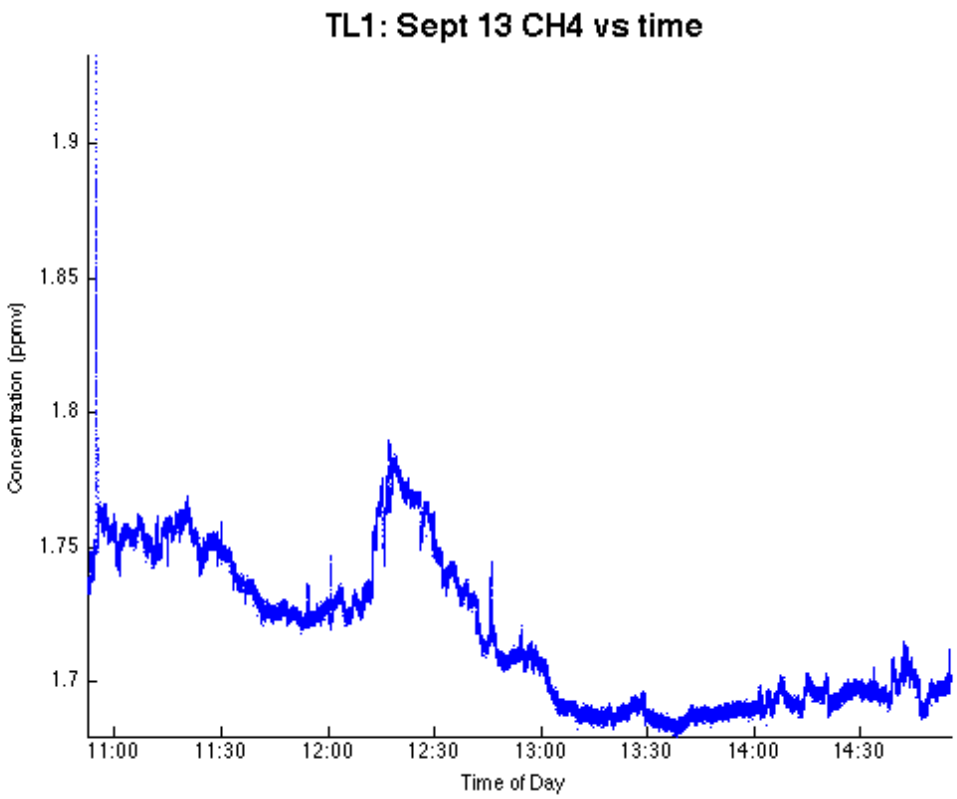
TL1: Sept 13 CH4 vs time
Concentration (ppmv)
1.9
1.85
1.8
1.75
1.7
11:00
11:30
12:00
12:30
13:00
13:30
14:00
14:30
Time of Day

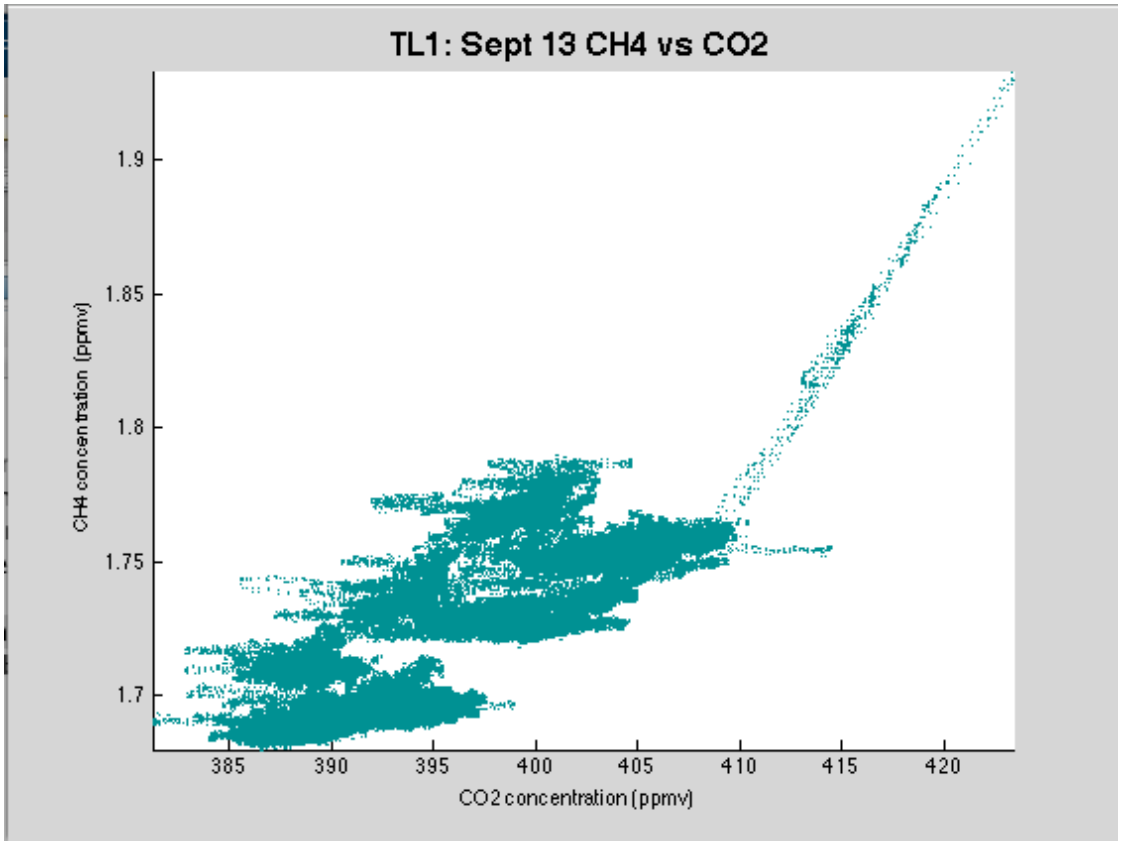
TL1: Sept 13 CH4 vs CO2
CH4 concentration (ppmv)
1.9
1.85
1.8
1.75
1.7
385
390
395
400
405
410
415
420
CO2 concentration (ppmv)

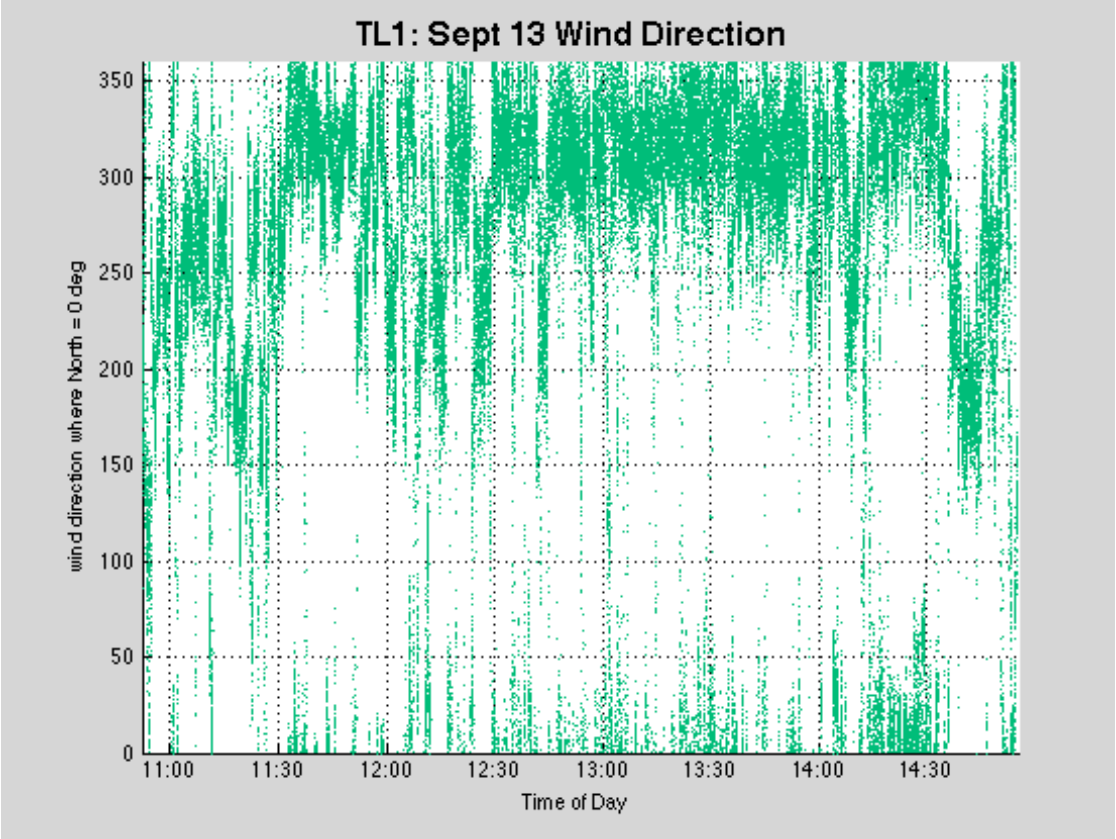
TL1: Sept 13 Wind Direction
wind direction where North = 0 deg
350
300
250
200
150
100
50
0
11:00
11:30
12:00
12:30
13:00
13:30
14:00
14:30
Time of Day

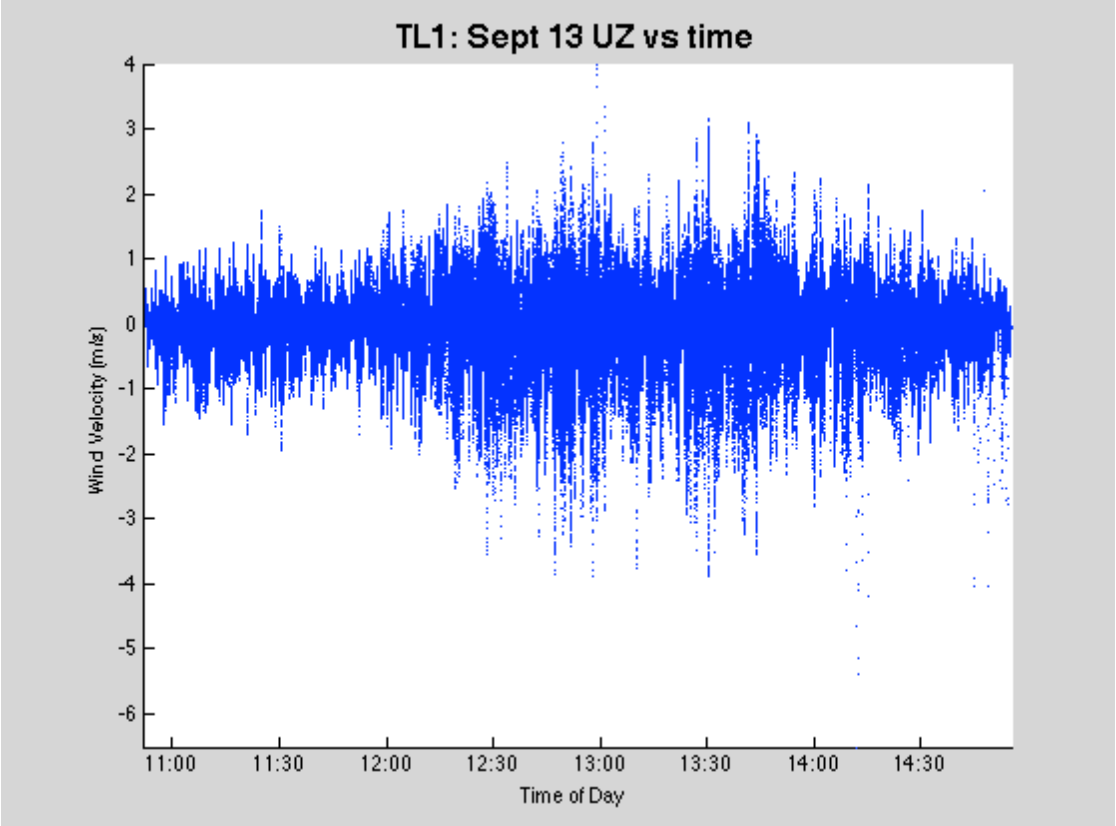
TL1: Sept 13 UZ vs time
Wind Velocity (m/s)
4
3
2
1
0
-1
-2
-3
-4
-5
-6
11:00
11:30
12:00
12:30
13:00
13:30
14:00
14:30
Time of Day

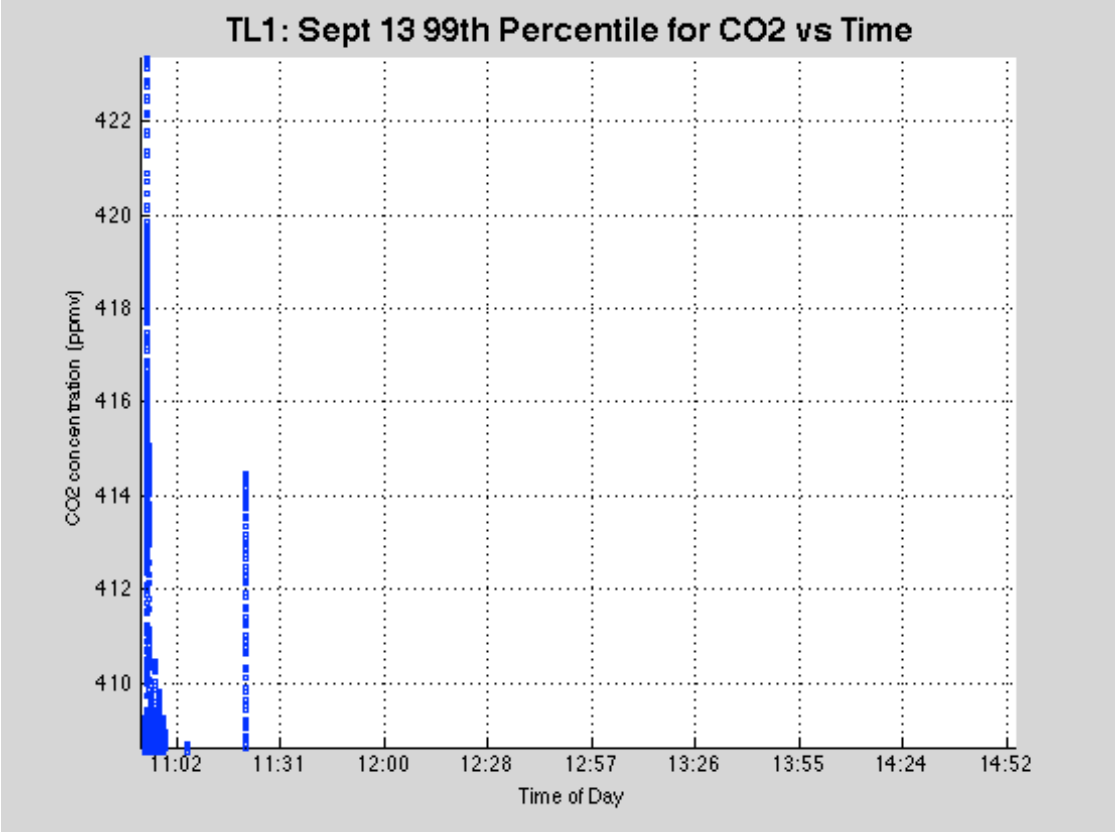
TL1: Sept 13 99th Percentile for CO2 vs Time
CO2 concentration (ppmv)
422
420
418
416
414
412
410
11:02
11:31
12:00
12:28
12:57
13:26
13:55
14:24
14:52
Time of Day

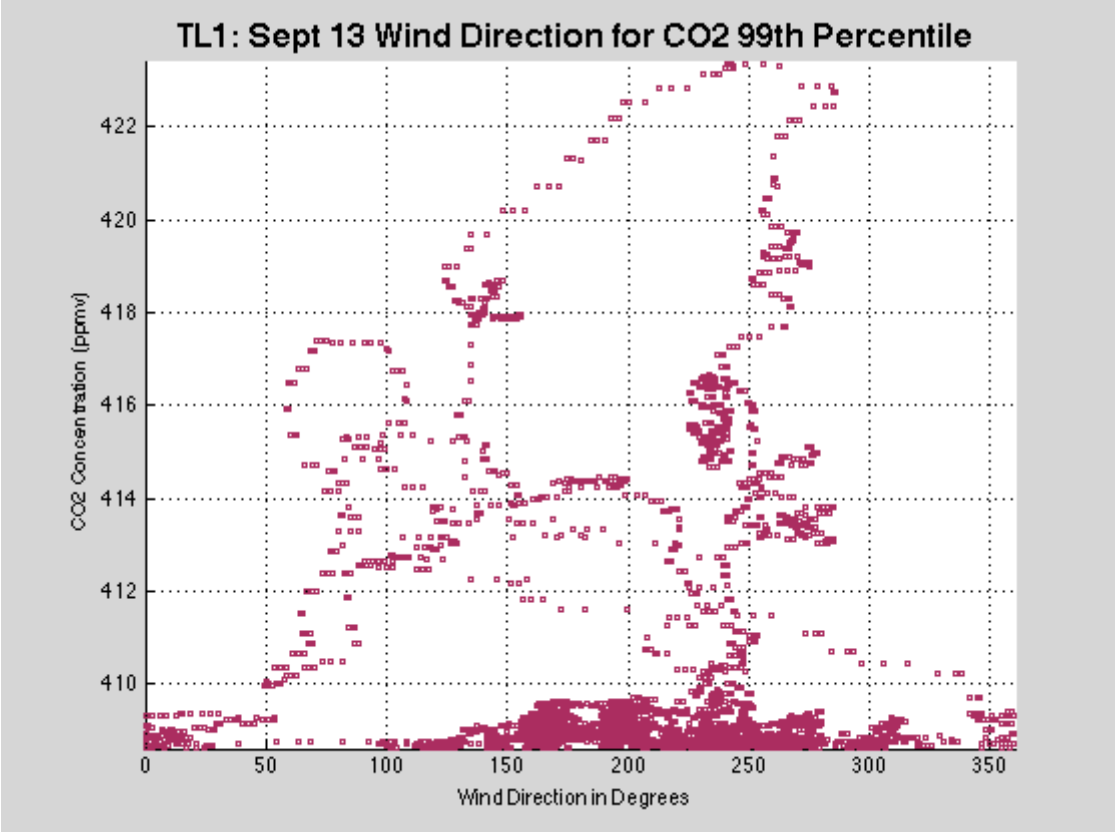
TL1: Sept 13 Wind Direction for CO2 99th Percentile
CO2 Concentration (ppmv)
422
420
418
416
414
412
410
0
50
100
150
200
250
300
350
Wind Direction in Degrees

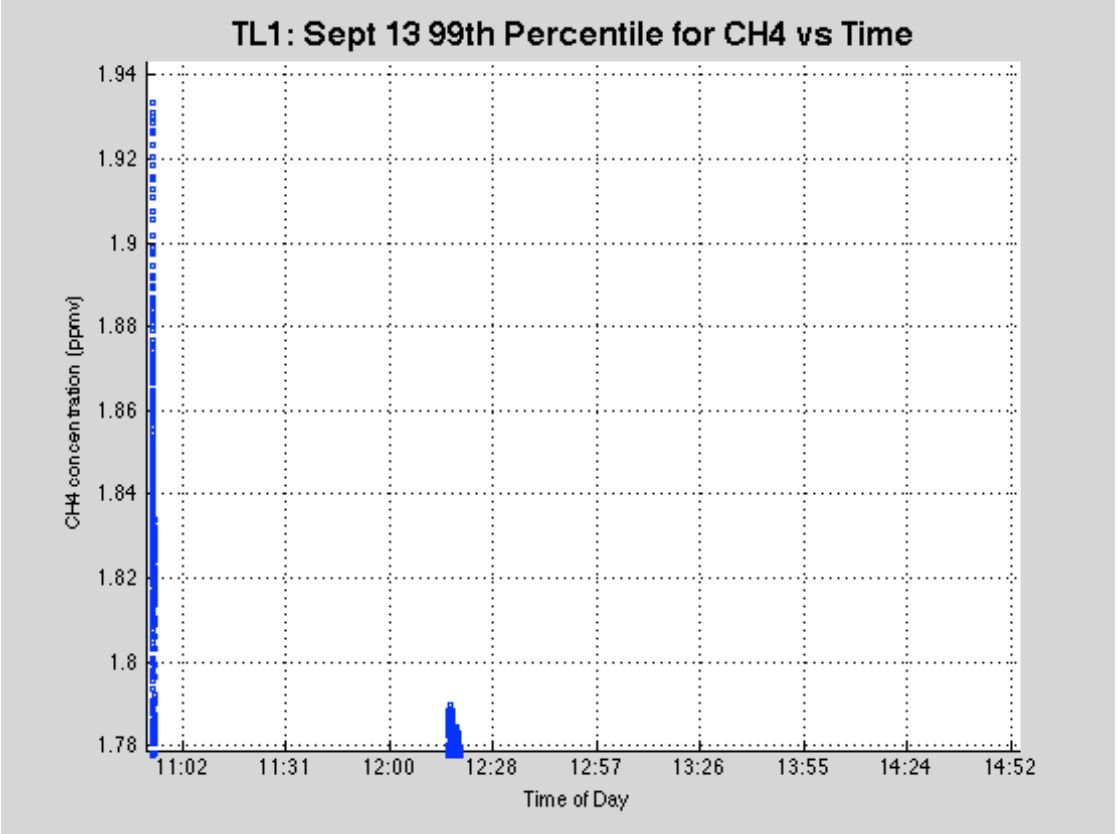
TL1: Sept 13 99th Percentile for CH4 vs Time
CH4 concentration (ppmv)
1.94
1.92
1.9
1.88
1.86
1.84
1.82
1.8
1.78
11:02
11:31
12:00
12:28
12:57
13:26
13:55
14:24
14:52
Time of Day

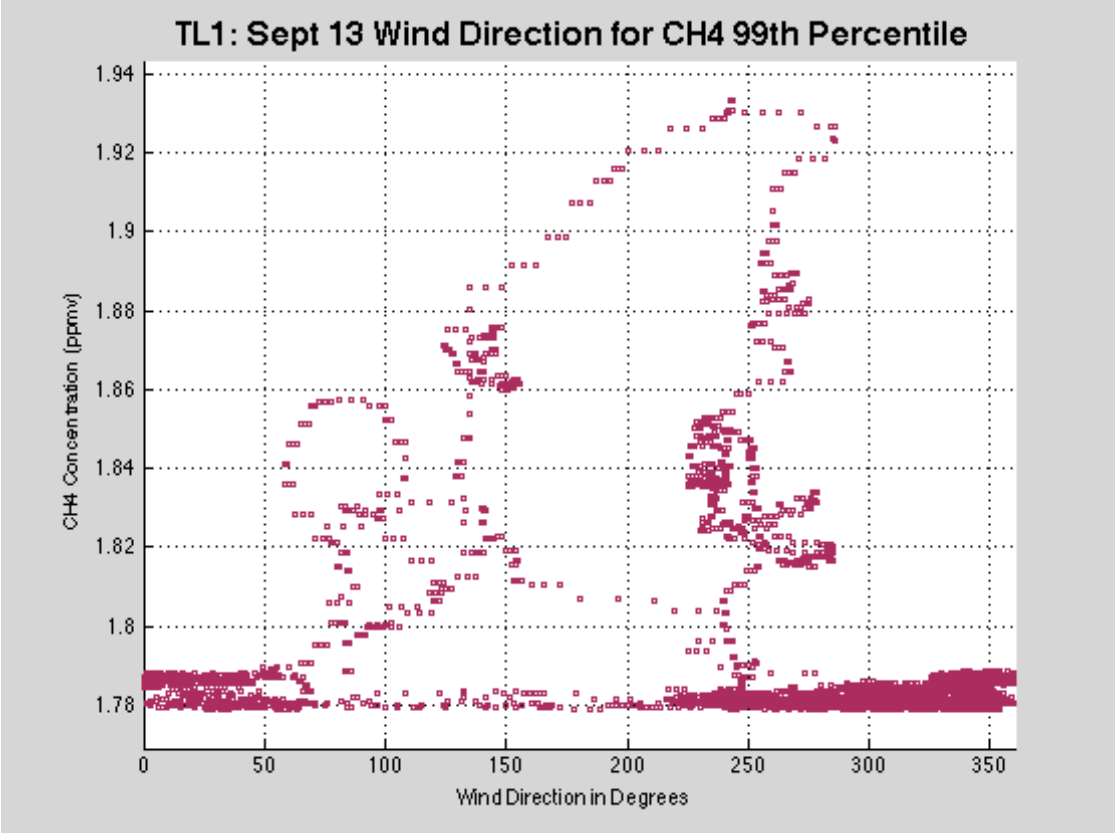
TL1: Sept 13 Wind Direction for CH4 99th Percentile
CH4 Concentration (ppmv)
1.94
1.92
1.9
1.88
1.86
1.84
1.82
1.8
1.78
0
50
100
150
200
250
300
350
Wind Direction in Degrees

## D.5 Monday, September 16th, 2013

| | Maximum | Minimum | Average | Standard Deviation | 99th Percentile |
|---|---|---|---|---|---|
| $CO_2$ (ppmv) | 410.2971 | 357.1815 | 387.5679 | 4.0311 | 399.1058 |
| $CH_4$ (ppmv) | 1.8013 | 1.6345 | 1.6805 | 0.0075 | 1.706 |
| UZ (m/s) | 2.5606 | -3.0436 | -0.0153 | 0.404 | N/A |

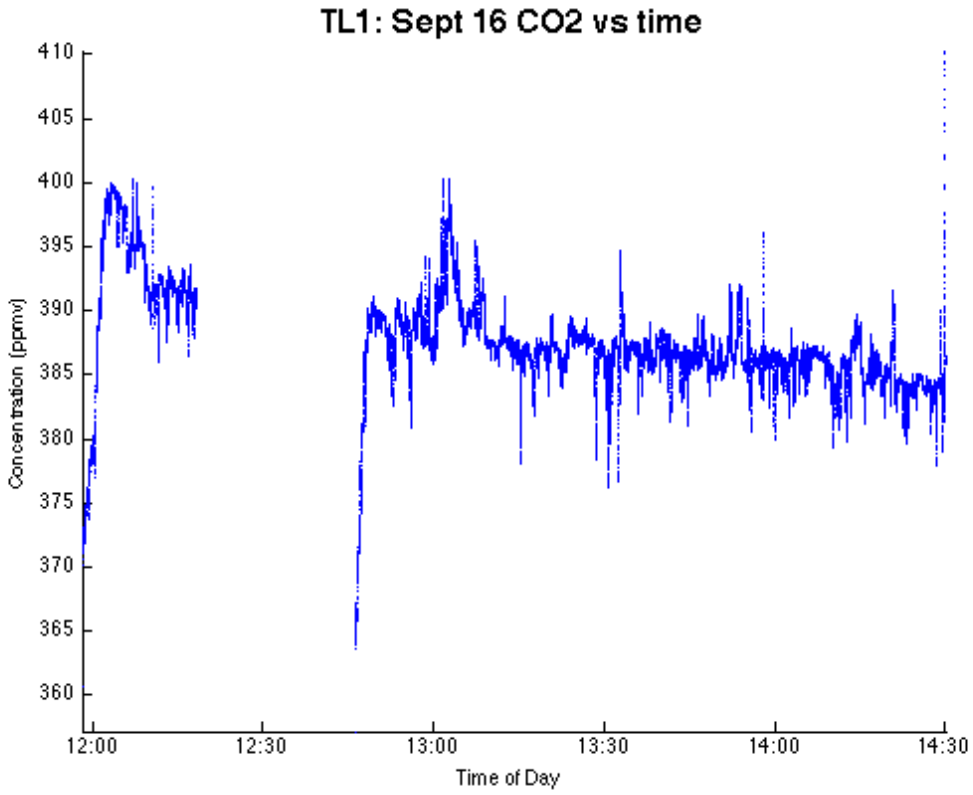

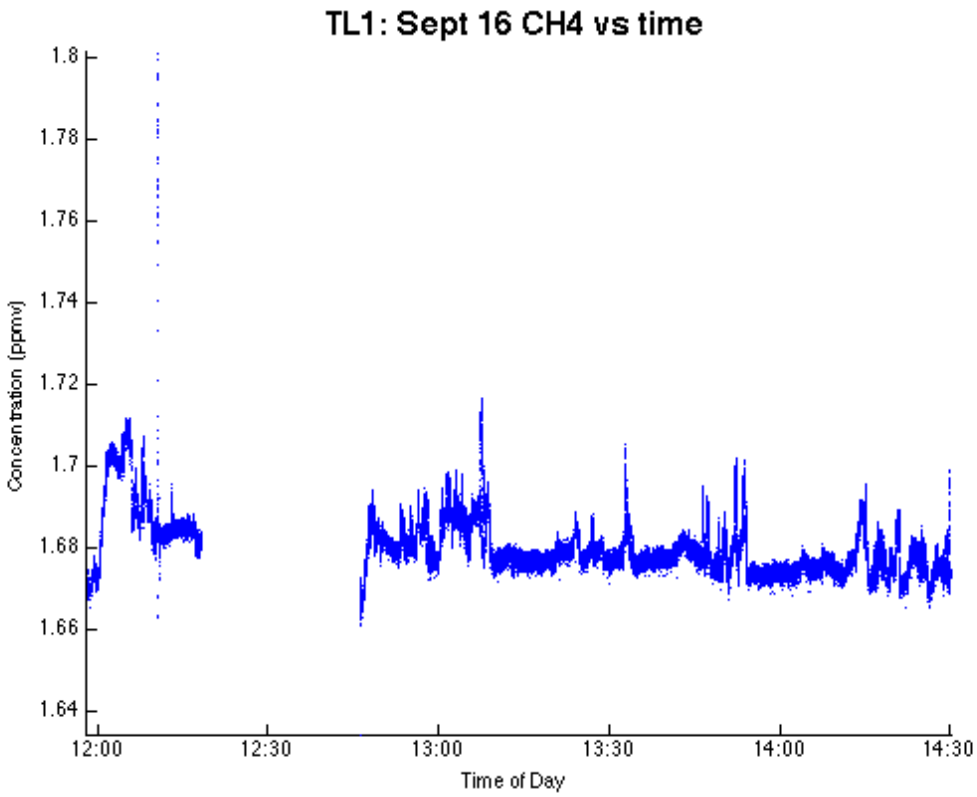
TL1: Sept 16 CH4 vs time
Concentration (ppmv)
1.8
1.78
1.76
1.74
1.72
1.7
1.68
1.66
1.64
12:00
12:30
13:00
13:30
14:00
14:30
Time of Day

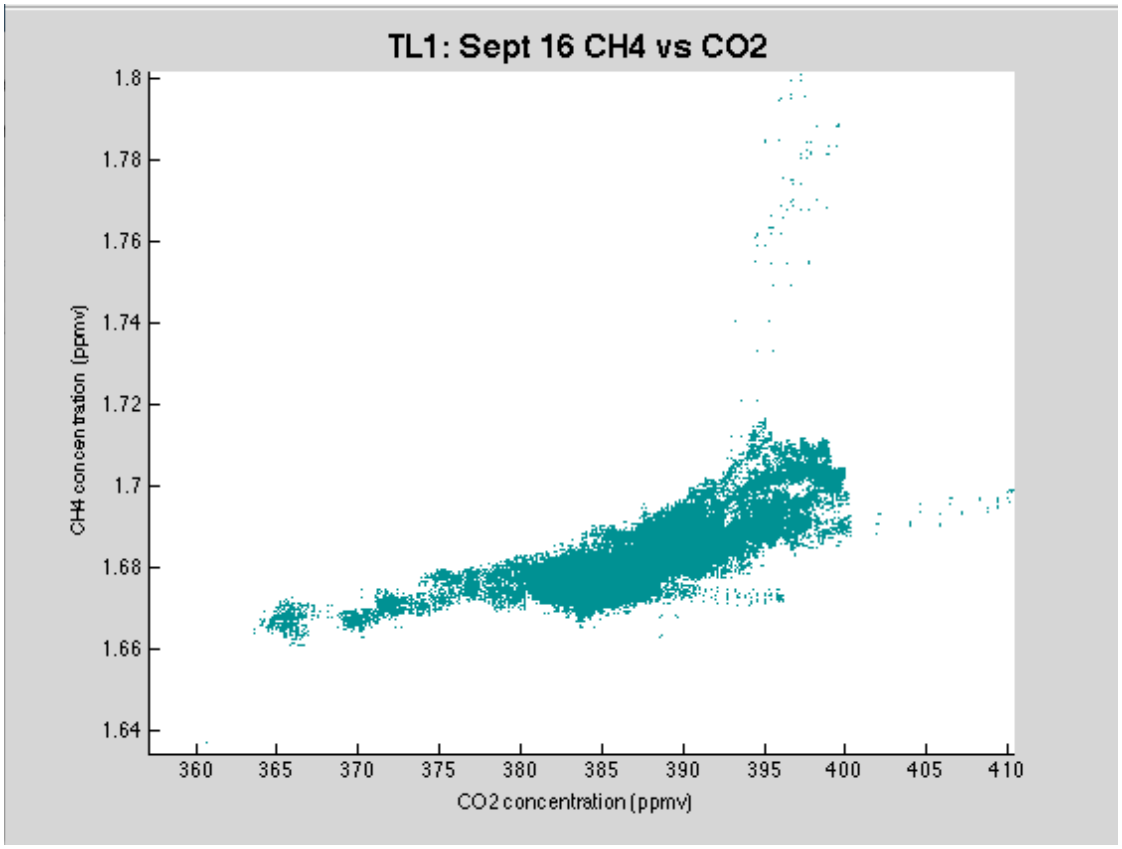
TL1: Sept 16 CH4 vs CO2
CH4 concentration (ppmv)
1.8
1.78
1.76
1.74
1.72
1.7
1.68
1.66
1.64
360
365
370
375
380
385
390
395
400
405
410
CO2 concentration (ppmv)

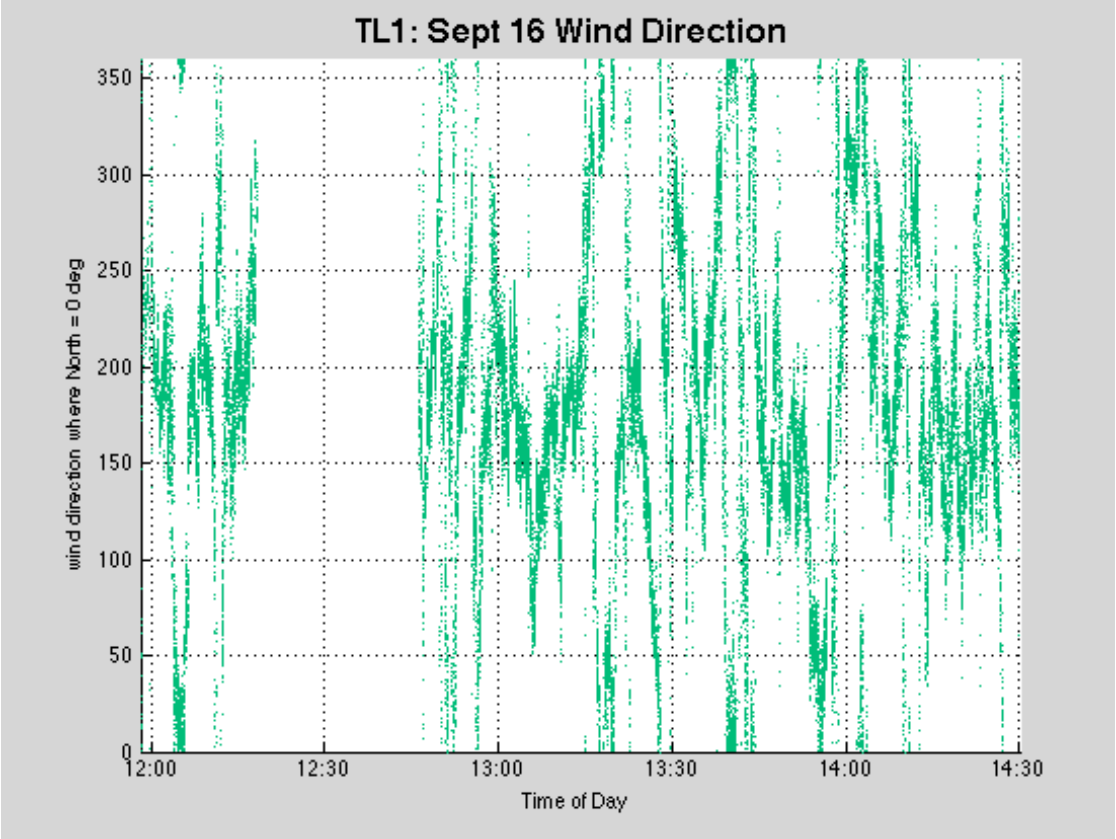
TL1: Sept 16 Wind Direction
wind direction where North = 0 deg
350
300
250
200
150
100
50
0
12:00
12:30
13:00
13:30
14:00
14:30
Time of Day

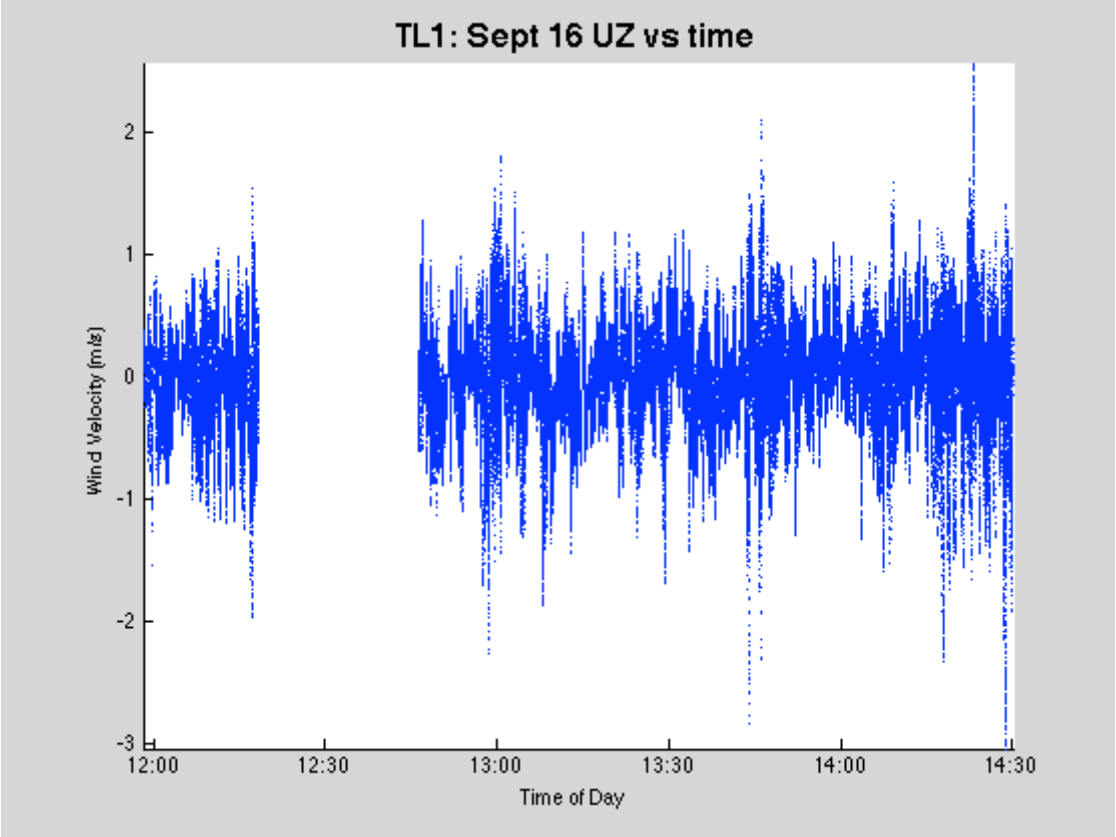
TL1: Sept 16 UZ vs time
Wind Velocity (m/s)
2
1
0
-1
-2
-3
12:00
12:30
13:00
13:30
14:00
14:30
Time of Day

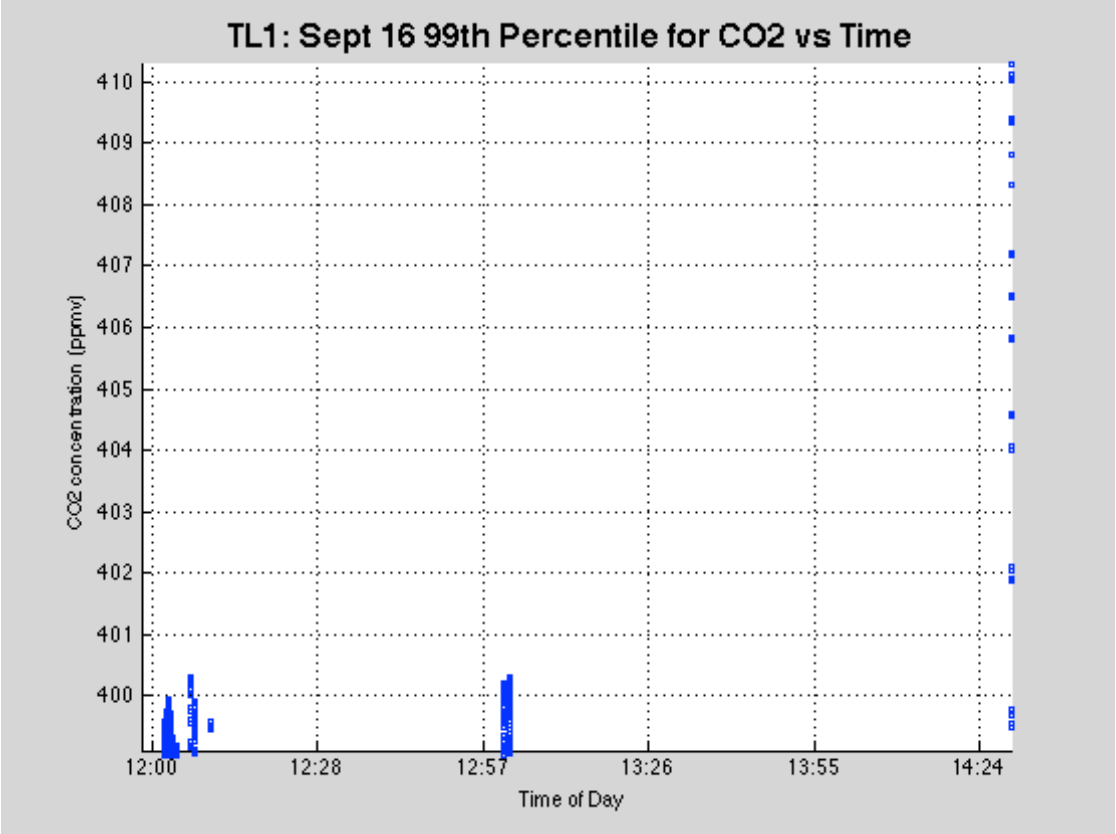
TL1: Sept 16 99th Percentile for CO2 vs Time
CO2 concentration (ppmv)
410
409
408
407
406
405
404
403
402
401
400
12:00
12:28
12:57
13:26
13:55
14:24
Time of Day

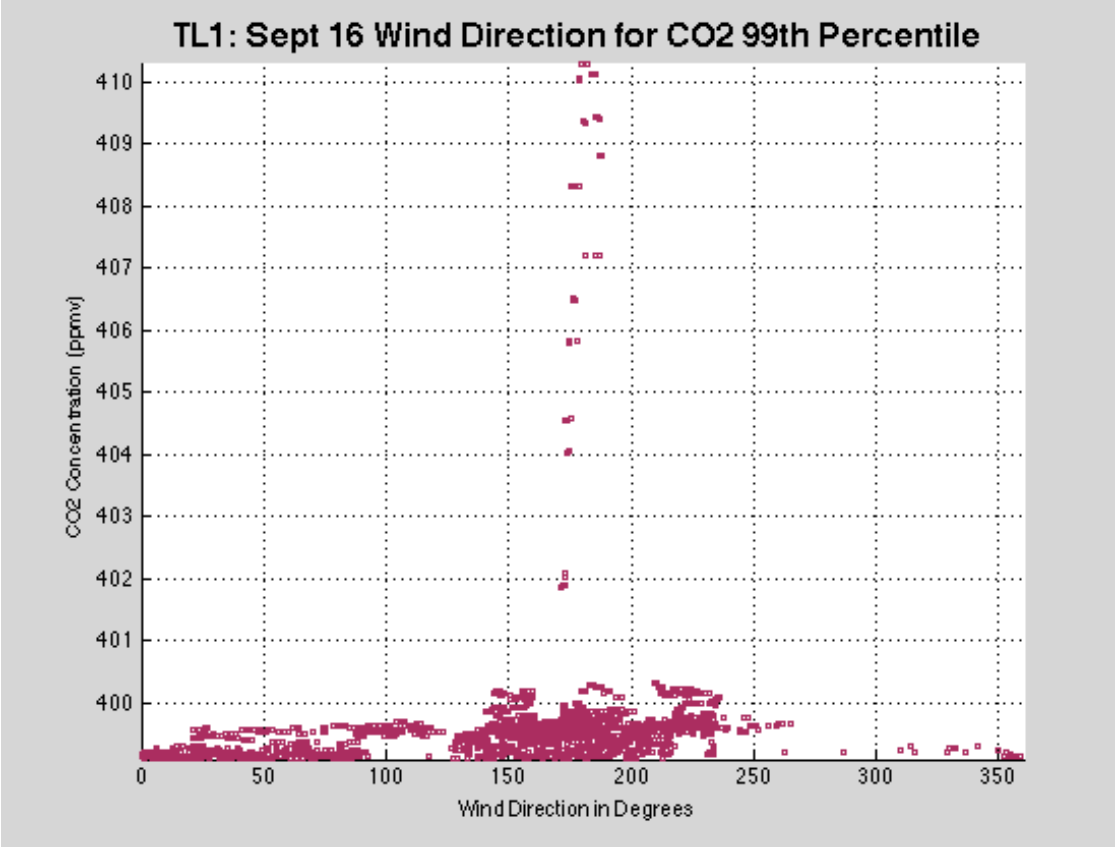
TL1: Sept 16 Wind Direction for CO2 99th Percentile
CO2 Concentration (ppmv)
410
409
408
407
406
405
404
403
402
401
400
0
50
100
150
200
250
300
350
Wind Direction in Degrees

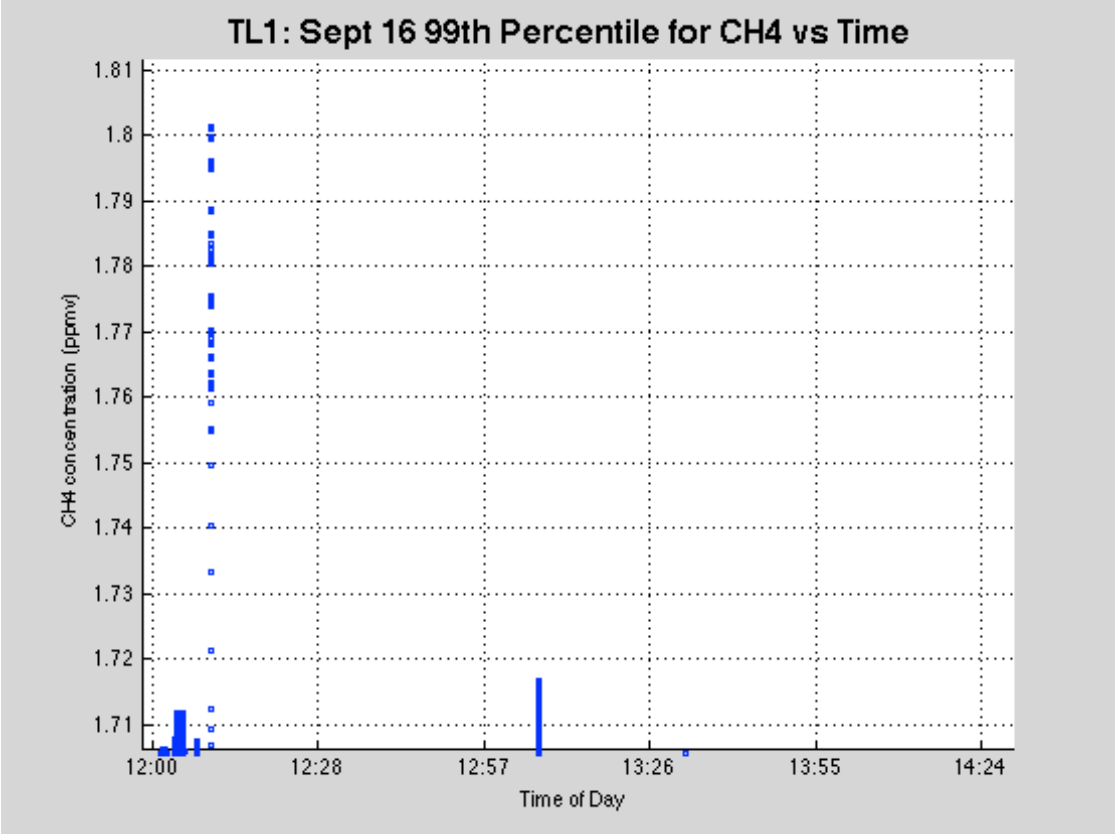
TL1: Sept 16 99th Percentile for CH4 vs Time
CH4 concentration (ppmv)
1.81
1.8
1.79
1.78
1.77
1.76
1.75
1.74
1.73
1.72
1.71
12:00
12:28
12:57
13:26
13:55
14:24
Time of Day

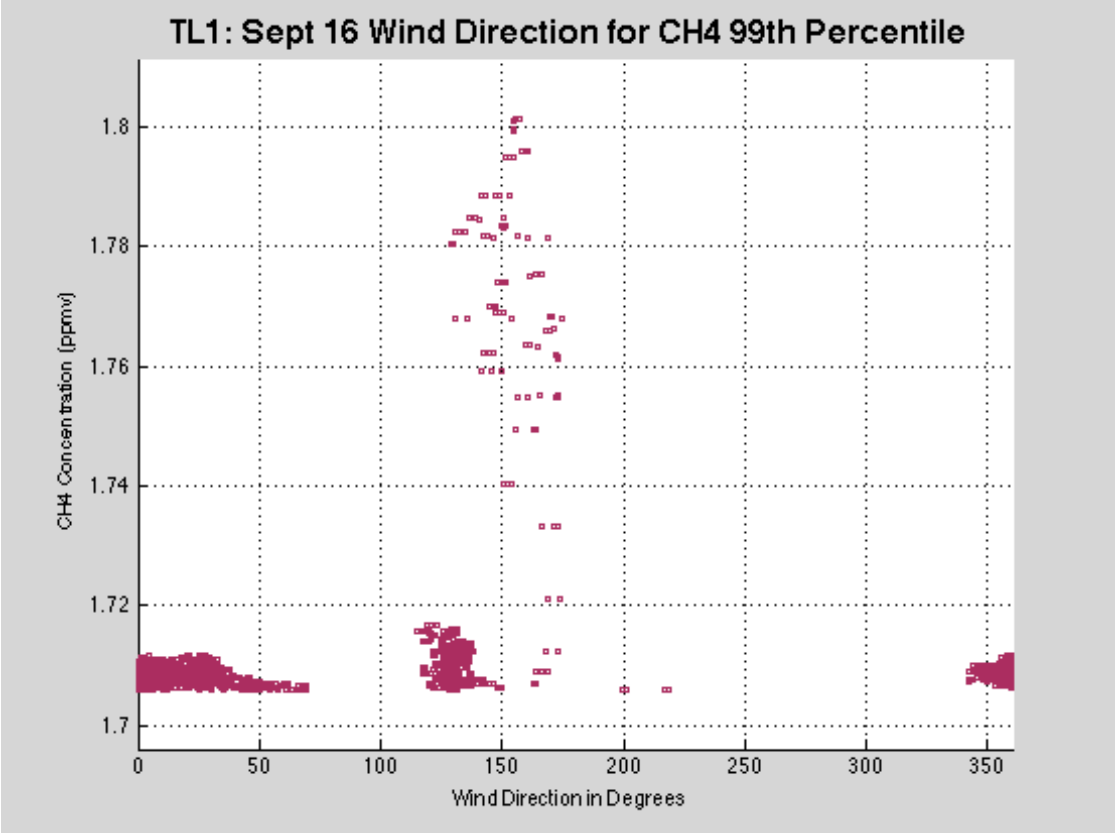
TL1: Sept 16 Wind Direction for CH4 99th Percentile
CH4 Concentration (ppmv)
1.8
1.78
1.76
1.74
1.72
1.7
0
50
100
150
200
250
300
350
Wind Direction in Degrees

D.6 Wednesday, September 18th, 2013

| | Maximum | Minimum | Average | Standard Deviation | 99th Percentile |
|---|---|---|---|---|---|
| $CO_2$ (ppmv) | 409.0391 | 319.8443 | 380.3198 | 3.0106 | 390.2441 |
| $CH_4$ (ppmv) | 1.7519 | 1.6573 | 1.6869 | 0.0139 | 1.7445 |
| UZ (m/s) | 3.9017 | -4.9216 | -0.1188 | 0.6401 | N/A |

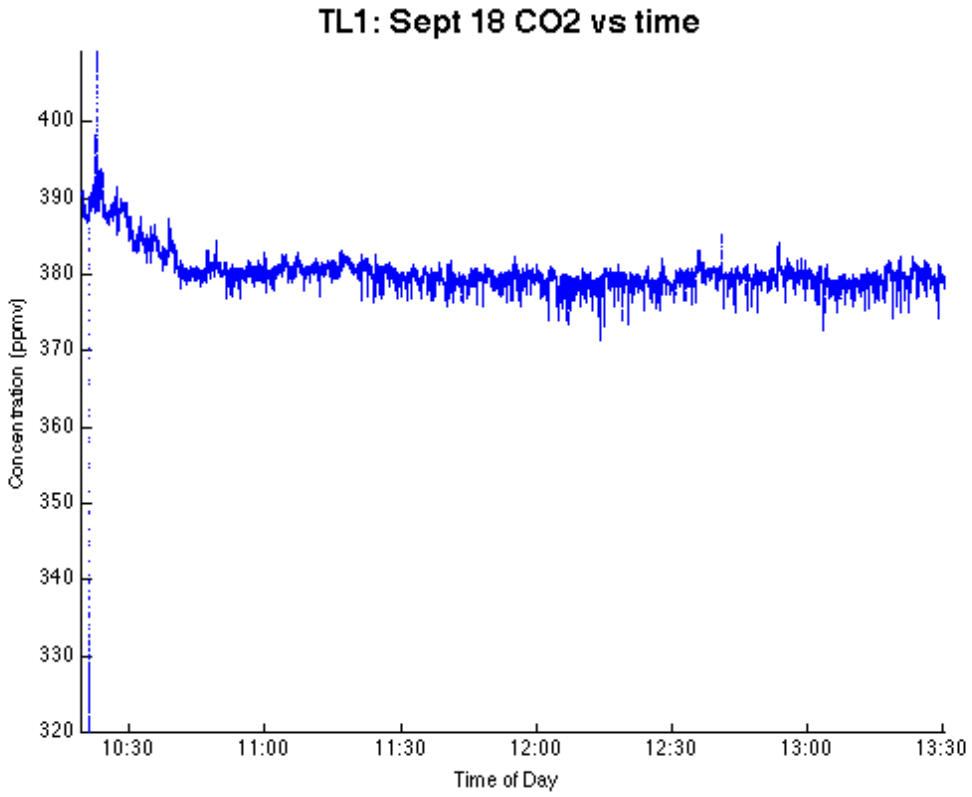

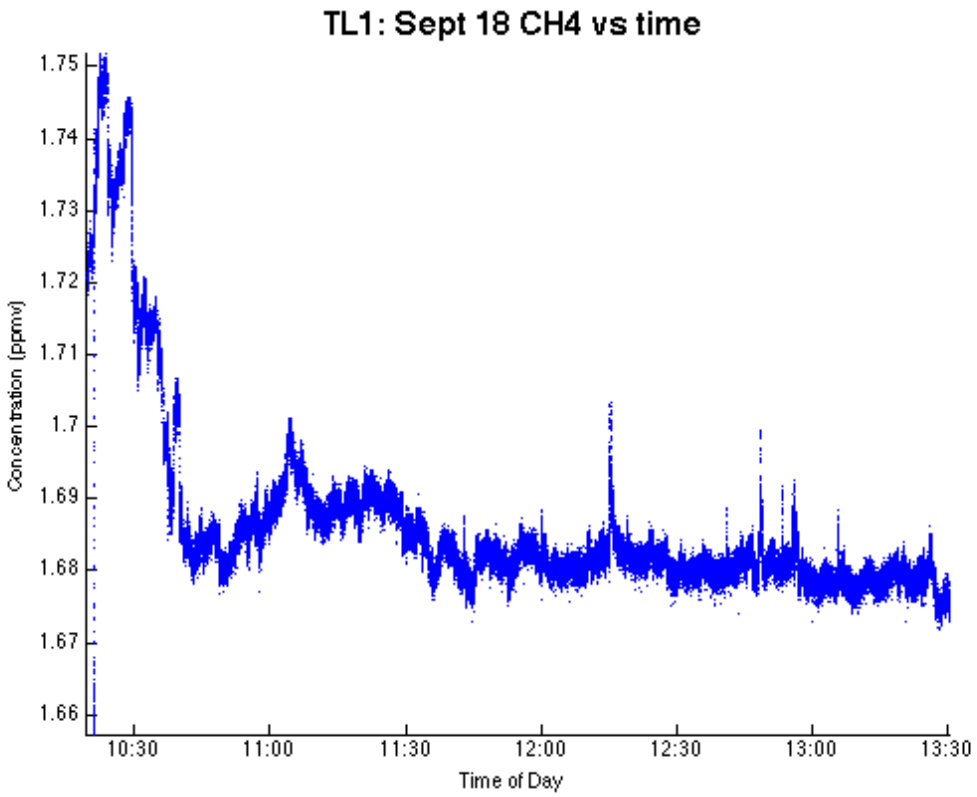
TL1: Sept 18 CH4 vs time
Concentration (ppmv)
1.75
1.74
1.73
1.72
1.71
1.7
1.69
1.68
1.67
1.66
10:30
11:00
11:30
12:00
12:30
13:00
13:30
Time of Day

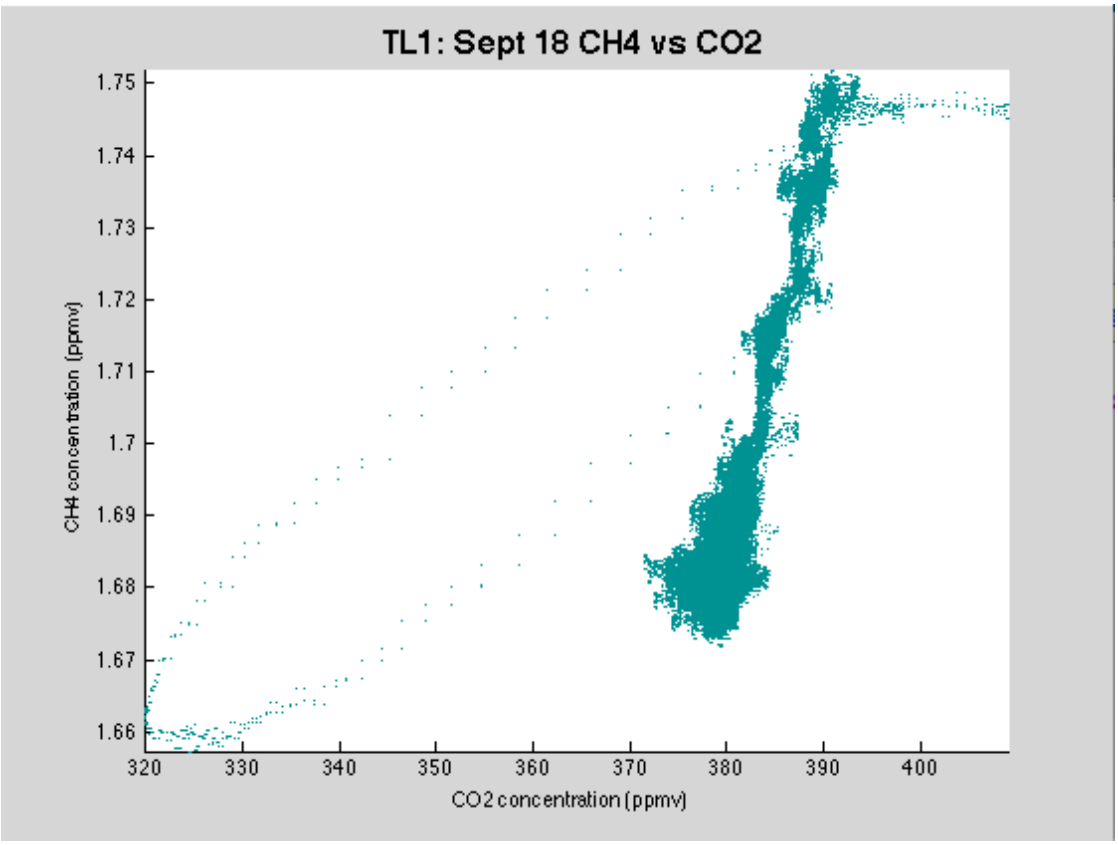
TL1: Sept 18 CH4 vs CO2
CH4 concentration (ppmv)
1.75
1.74
1.73
1.72
1.71
1.7
1.69
1.68
1.67
1.66
320
330
340
350
360
370
380
390
400
CO2 concentration (ppmv)

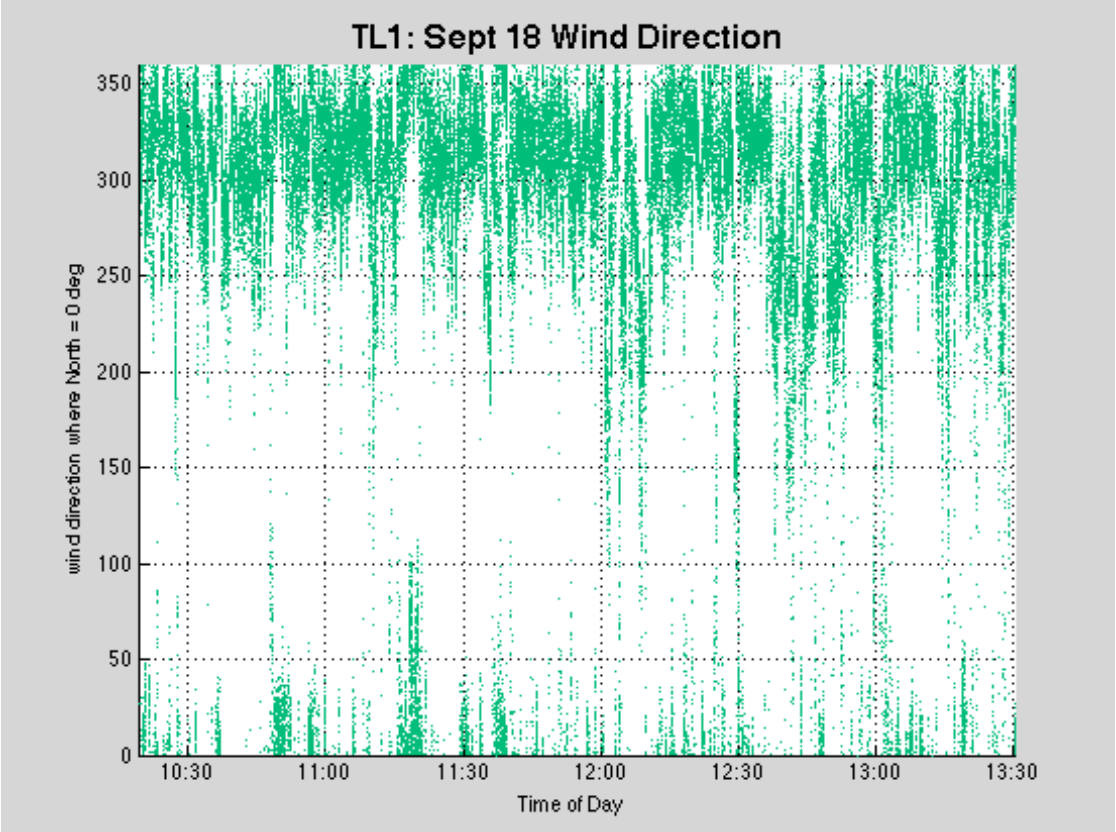
TL1: Sept 18 Wind Direction
wind direction where North = 0 deg
0
50
100
150
200
250
300
350
10:30
11:00
11:30
12:00
12:30
13:00
13:30
Time of Day

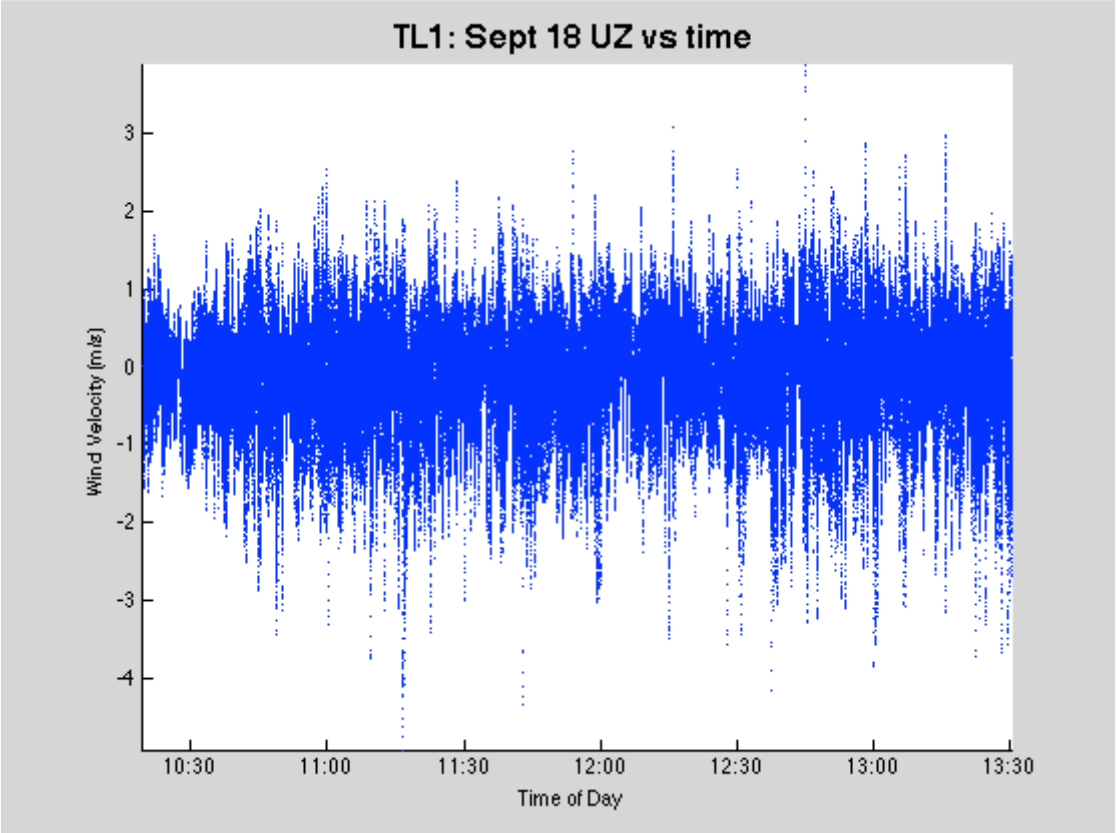
TL1: Sept 18 UZ vs time
Wind Velocity (m/s)
3
2
1
0
-1
-2
-3
-4
10:30
11:00
11:30
12:00
12:30
13:00
13:30
Time of Day

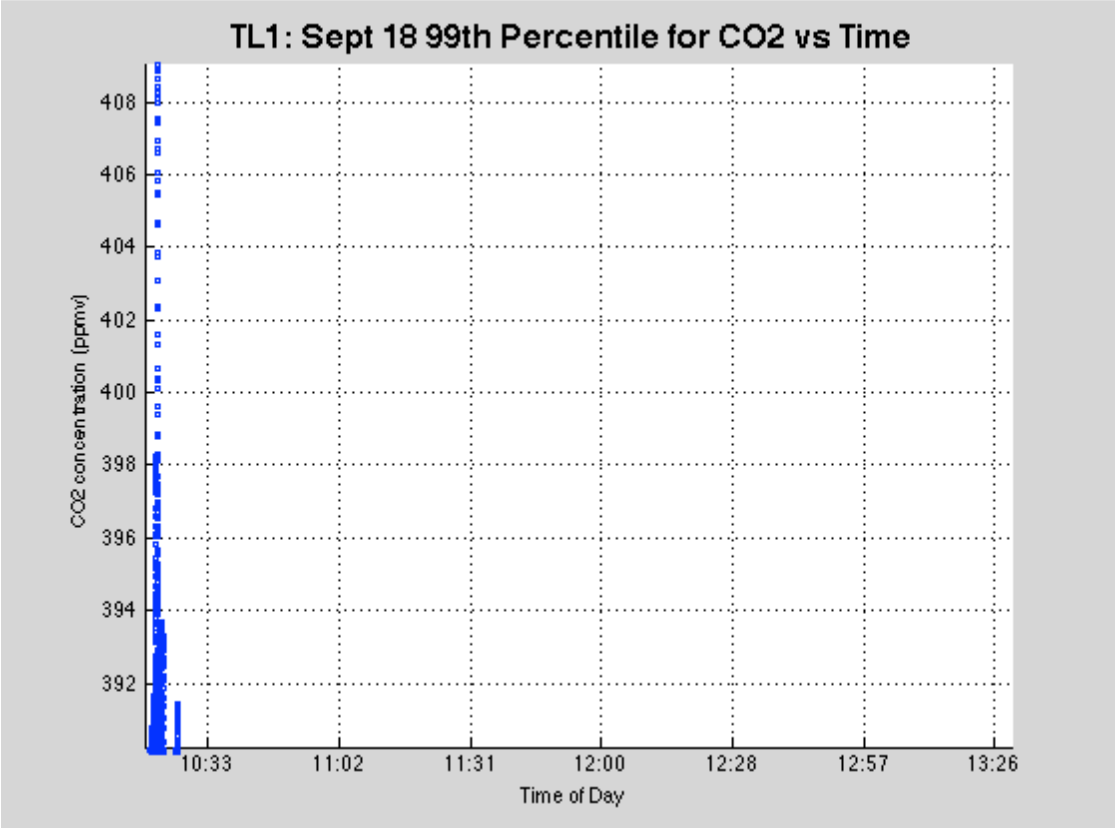
TL1: Sept 18 99th Percentile for CO2 vs Time
CO2 concentration (ppmv)
408
406
404
402
400
398
396
394
392
10:33
11:02
11:31
12:00
12:28
12:57
13:26
Time of Day

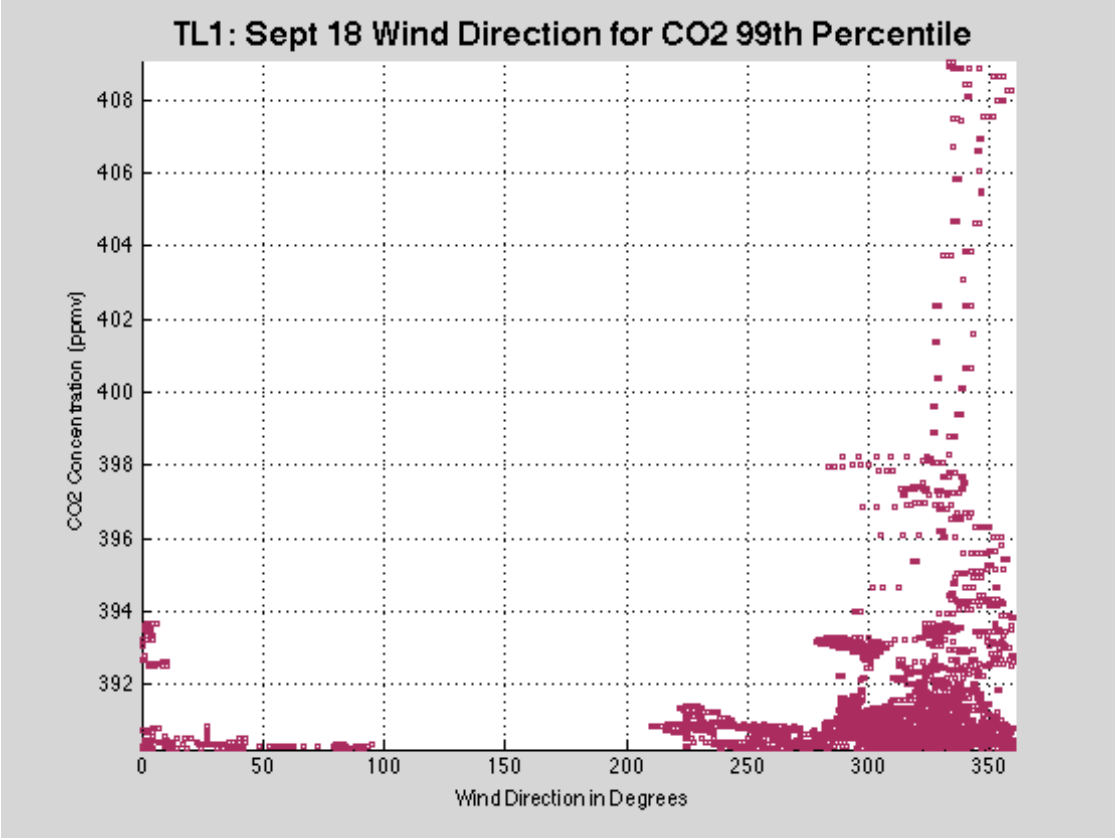
TL1: Sept 18 Wind Direction for CO2 99th Percentile
CO2 Concentration (ppmv)
408
406
404
402
400
398
396
394
392
0
50
100
150
200
250
300
350
Wind Direction in Degrees

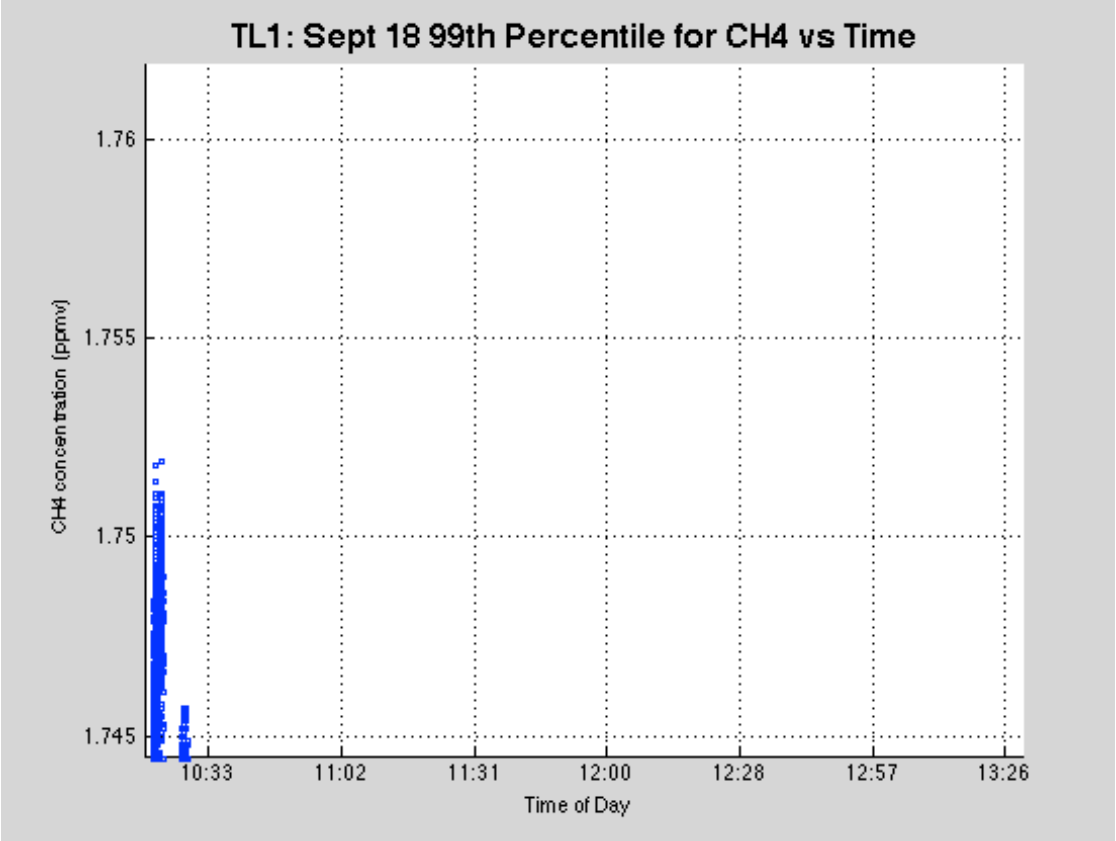
TL1: Sept 18 99th Percentile for CH4 vs Time
CH4 concentration (ppmv)
1.76
1.755
1.75
1.745
10:33
11:02
11:31
12:00
12:28
12:57
13:26
Time of Day

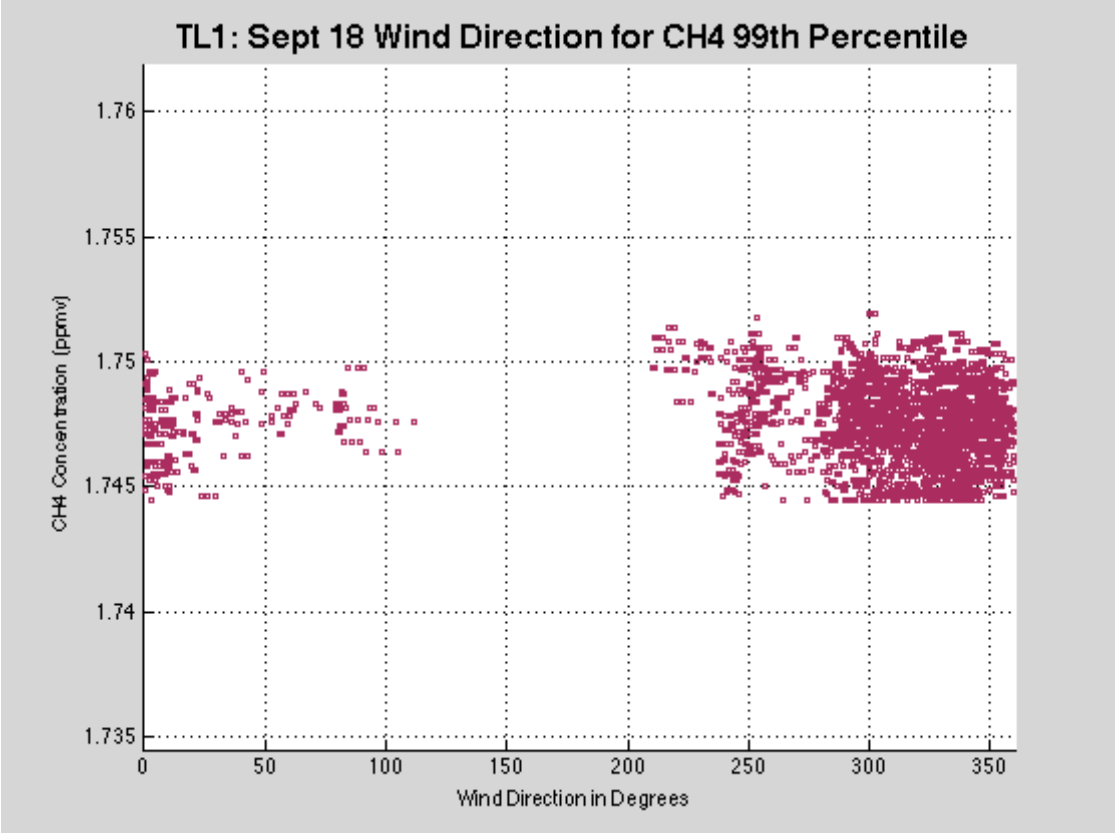
TL1: Sept 18 Wind Direction for CH4 99th Percentile
CH4 Concentration (ppmv)
1.76
1.755
1.75
1.745
1.74
1.735
0
50
100
150
200
250
300
350
Wind Direction in Degrees

## D.7 Friday, September 20th, 2013

| | Maximum | Minimum | Average | Standard Deviation | 99th Percentile |
|---|---|---|---|---|---|
| $CO_2$ (ppmv) | 462.6543 | 391.1521 | 406.8372 | 7.2249 | 422.345 |
| $CH_4$ (ppmv) | 1.8123 | 1.7281 | 1.7539 | 0.0161 | 1.7897 |
| UZ (m/s) | 1.5094 | -1.4168 | -0.0325 | 0.3049 | N/A |

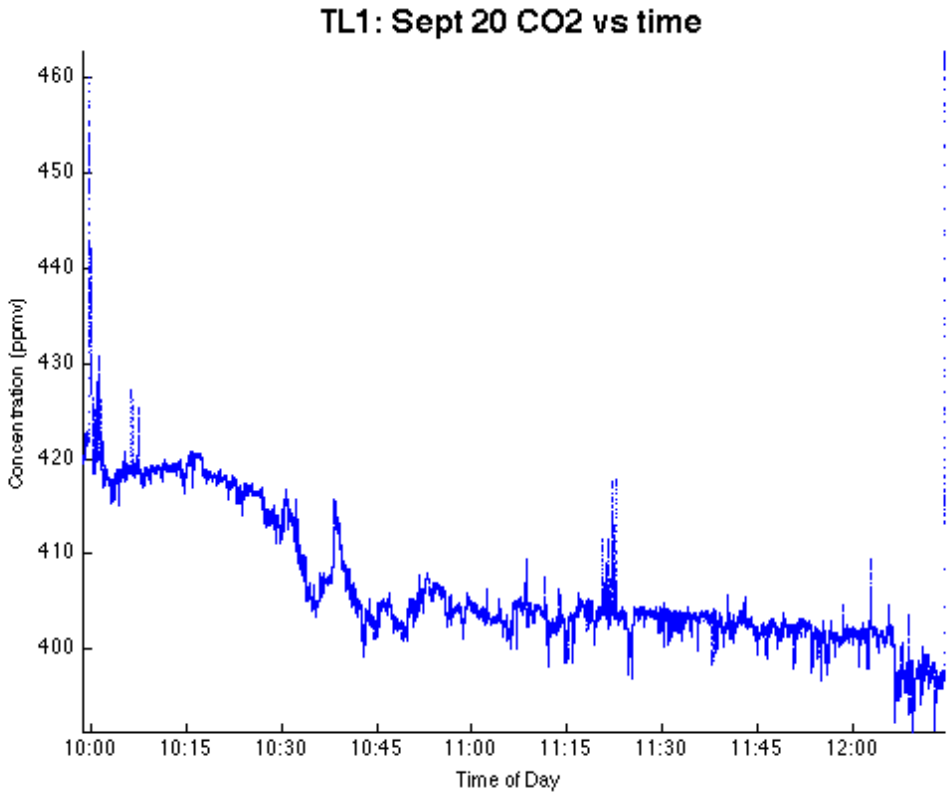

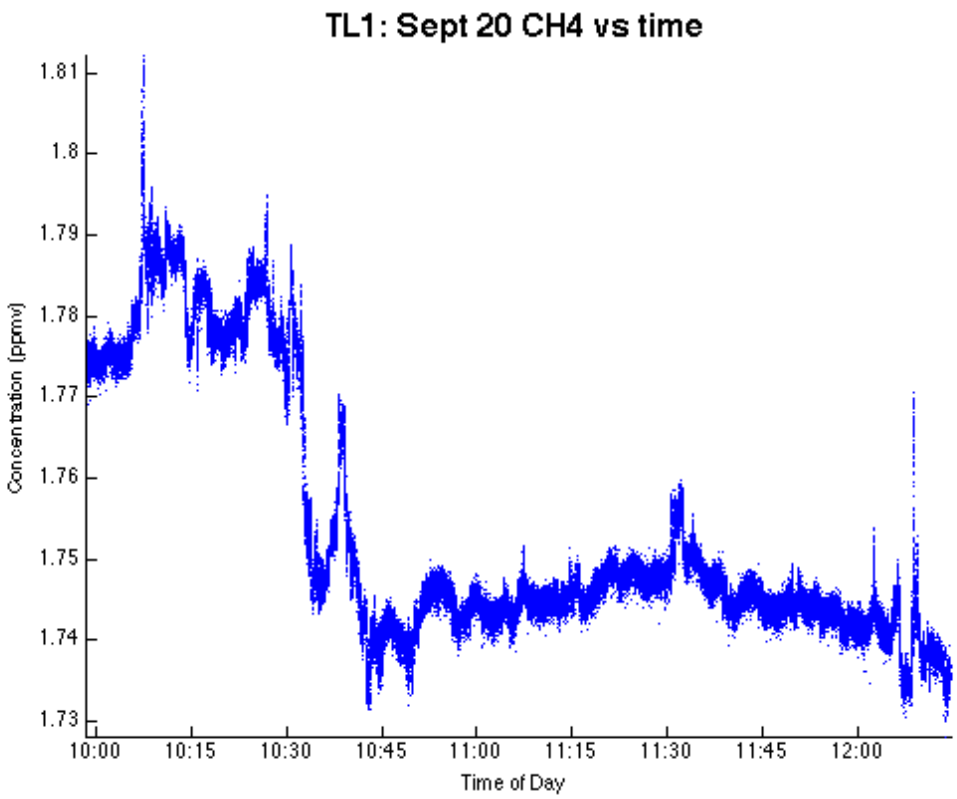
TL1: Sept 20 CH4 vs time
Concentration (ppmv)
1.81
1.8
1.79
1.78
1.77
1.76
1.75
1.74
1.73
10:00
10:15
10:30
10:45
11:00
11:15
11:30
11:45
12:00
Time of Day

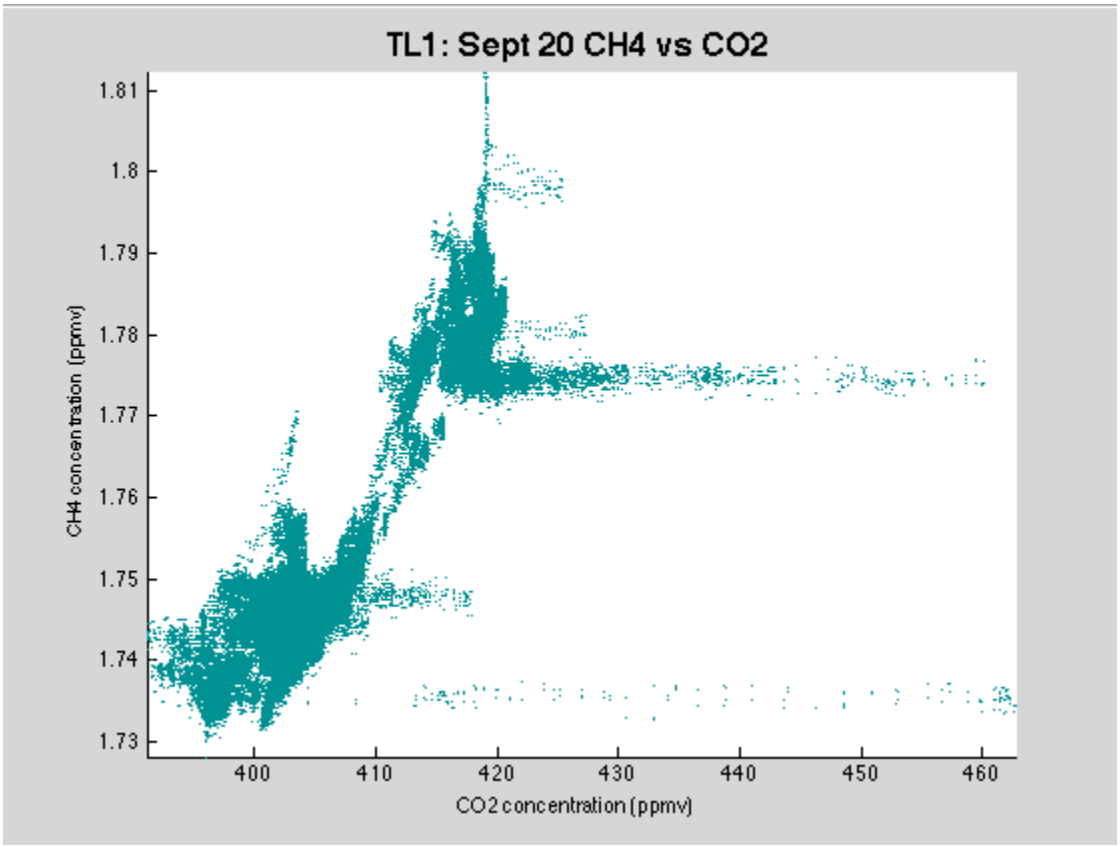
TL1: Sept 20 CH4 vs CO2
CH4 concentration (ppmv)
1.81
1.8
1.79
1.78
1.77
1.76
1.75
1.74
1.73
400
410
420
430
440
450
460
CO2 concentration (ppmv)

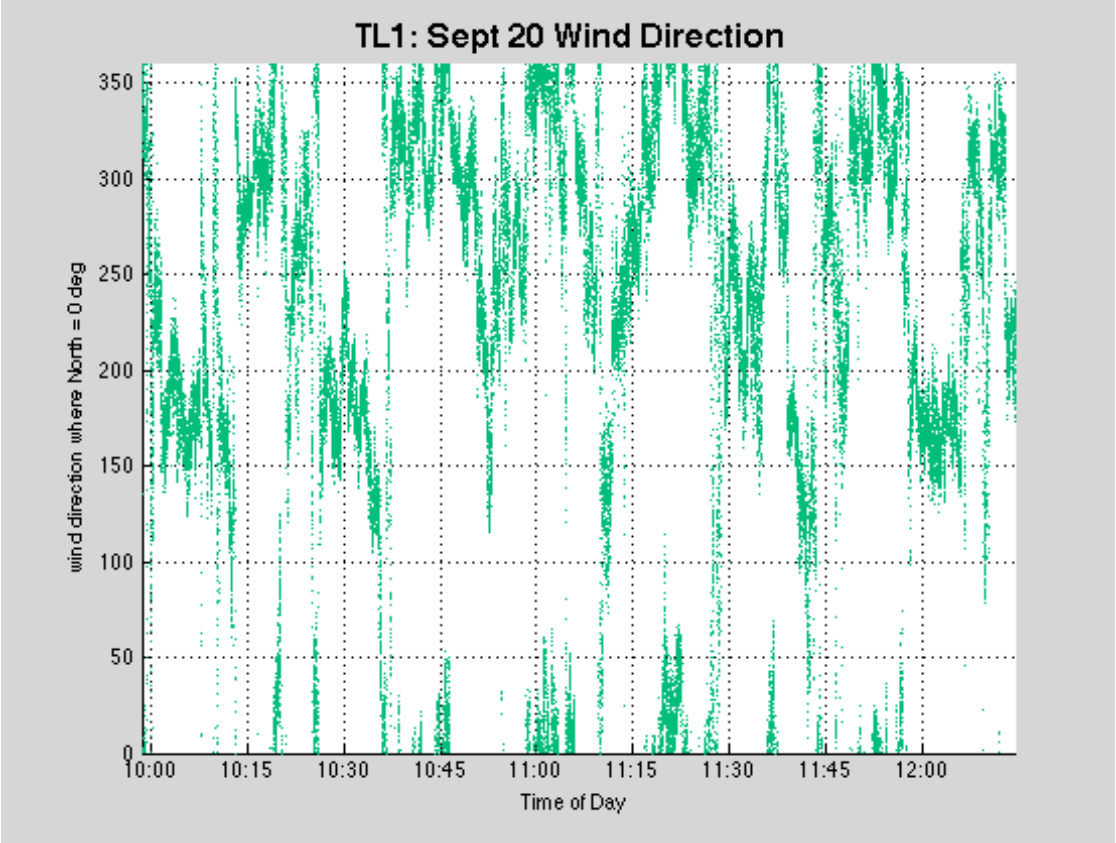
TL1: Sept 20 Wind Direction
wind direction where North = 0 deg
350
300
250
200
150
100
50
0
10:00
10:15
10:30
10:45
11:00
11:15
11:30
11:45
12:00
Time of Day

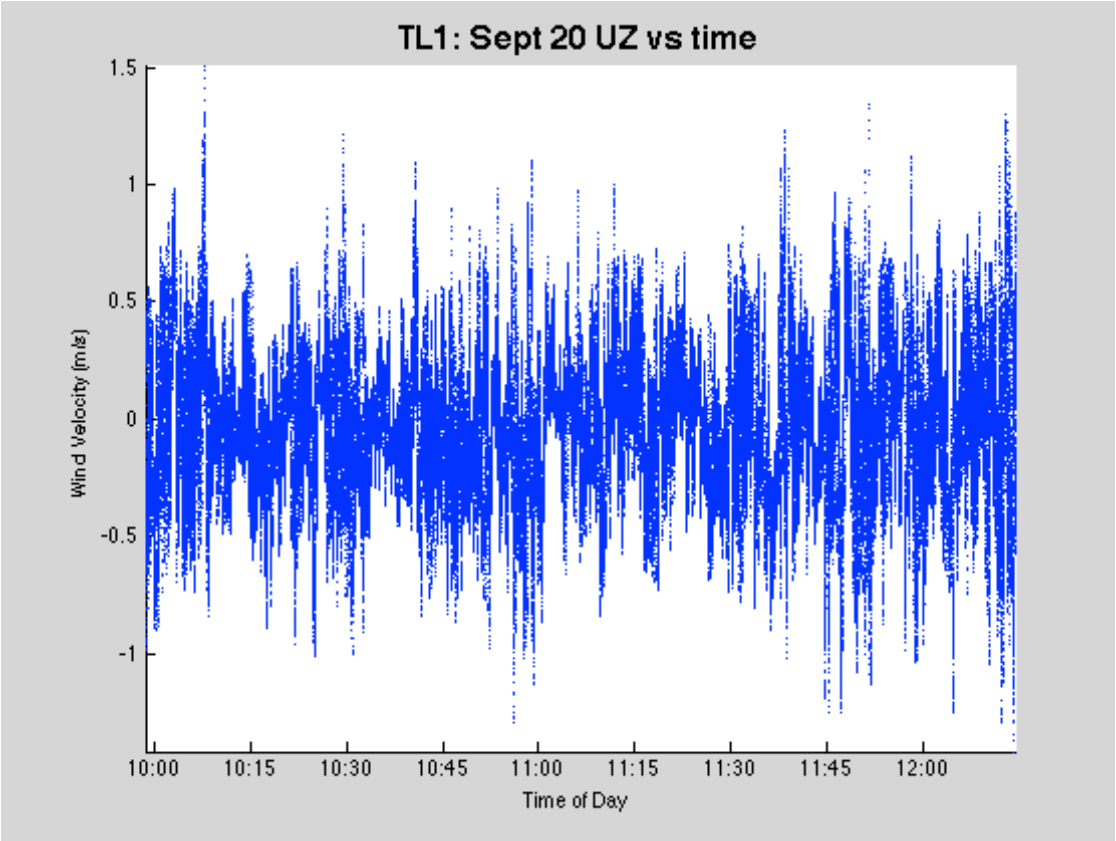
TL1: Sept 20 UZ vs time
Wind Velocity (m/s)
1.5
1
0.5
0
-0.5
-1
10:00
10:15
10:30
10:45
11:00
11:15
11:30
11:45
12:00
Time of Day

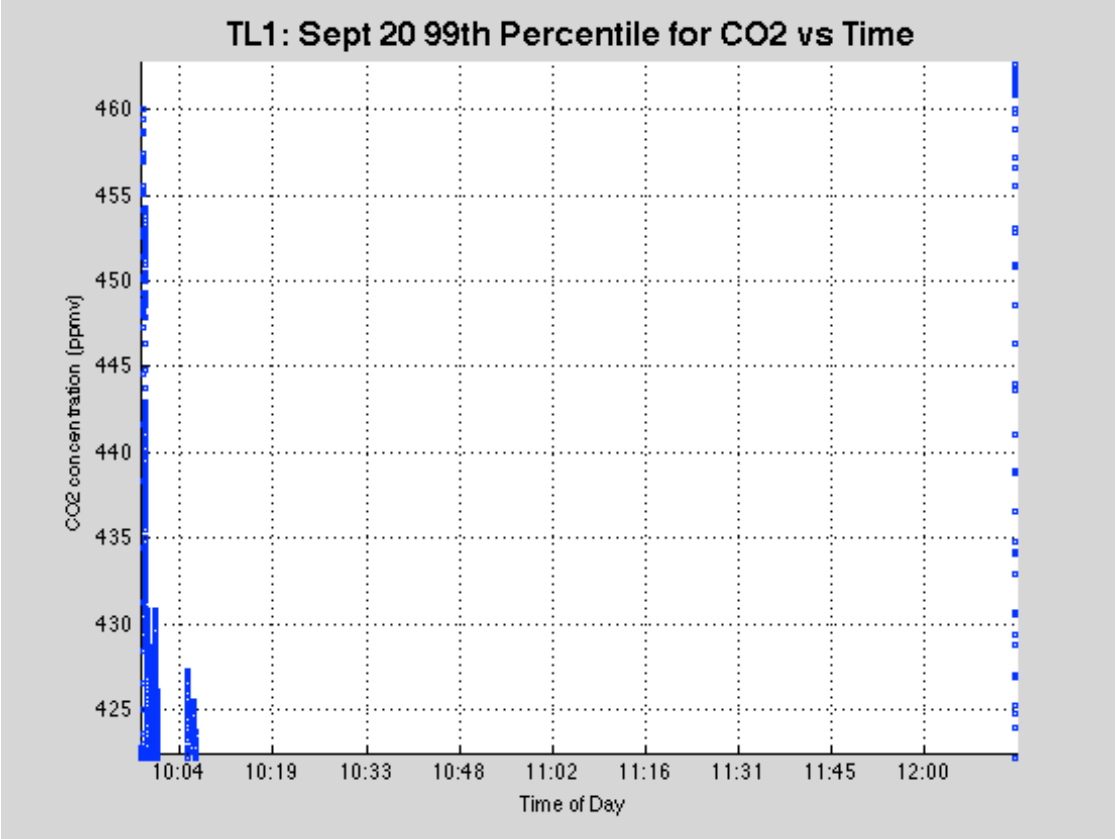
TL1: Sept 20 99th Percentile for CO2 vs Time
CO2 concentration (ppmv)
460
455
450
445
440
435
430
425
10:04
10:19
10:33
10:48
11:02
11:16
11:31
11:45
12:00
Time of Day

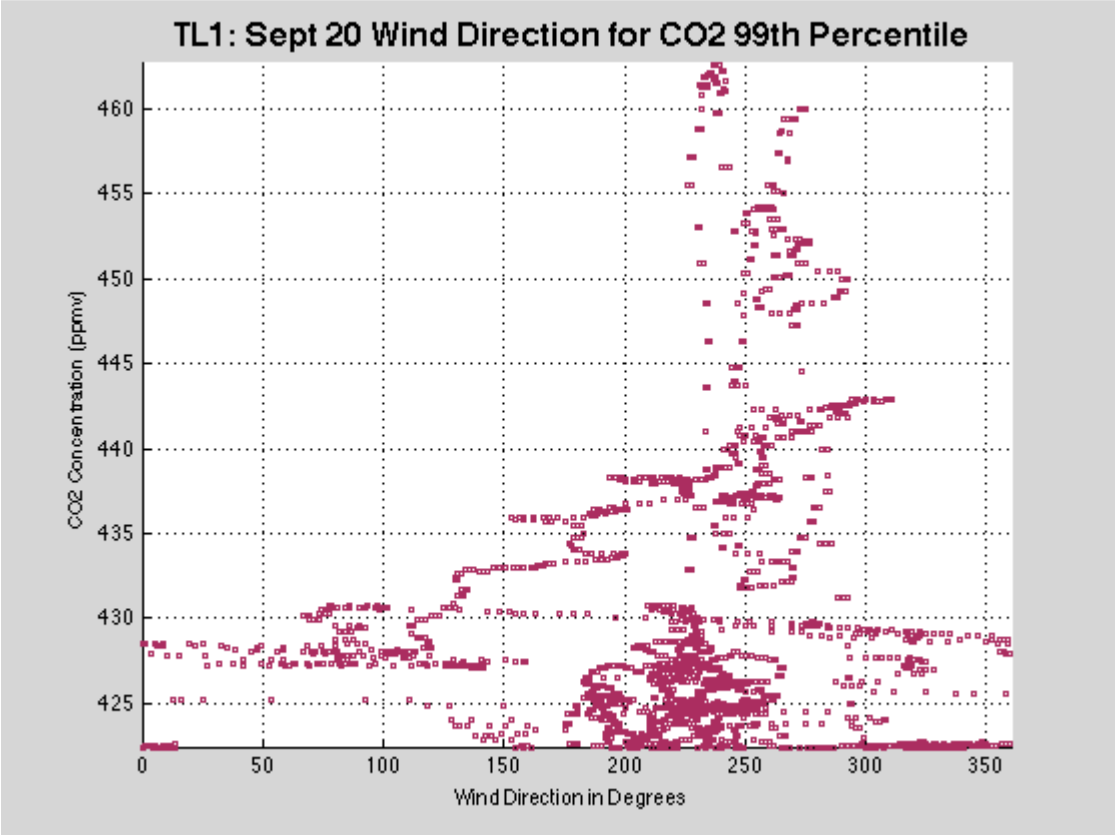
TL1: Sept 20 Wind Direction for CO2 99th Percentile
CO2 Concentration (ppmv)
460
455
450
445
440
435
430
425
0
50
100
150
200
250
300
350
Wind Direction in Degrees

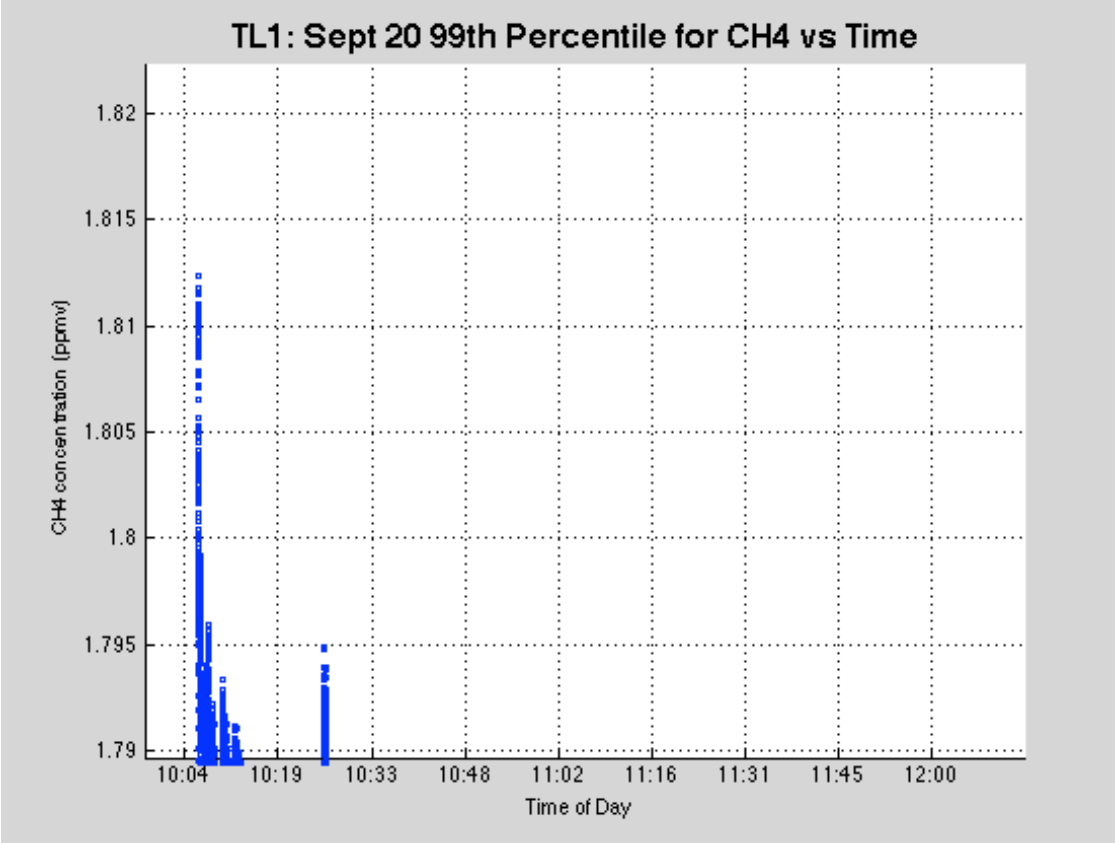
TL1: Sept 20 99th Percentile for CH4 vs Time
CH4 concentration (ppmv)
1.82
1.815
1.81
1.805
1.8
1.795
1.79
10:04
10:19
10:33
10:48
11:02
11:16
11:31
11:45
12:00
Time of Day

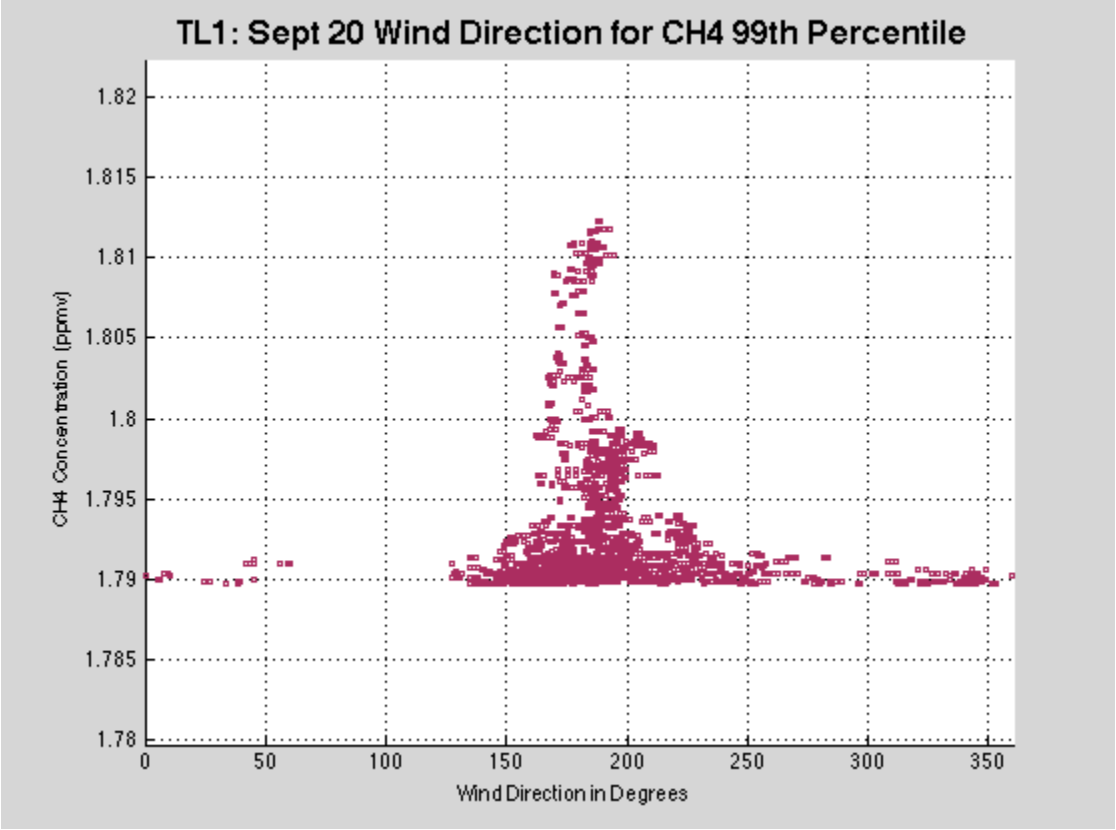
TL1: Sept 20 Wind Direction for CH4 99th Percentile
CH4 Concentration (ppmv)
1.82
1.815
1.81
1.805
1.8
1.795
1.79
1.785
1.78
0
50
100
150
200
250
300
350
Wind Direction in Degrees

D.8 Monday, September 23rd, 2013

| | Maximum | Minimum | Average | Standard Deviation | 99th Percentile |
|---|---|---|---|---|---|
| $CO_2$ (ppmv) | 394.065 | 372.5426 | 379.8805 | 1.3545 | 382.8974 |
| $CH_4$ (ppmv) | 1.7191 | 1.6757 | 1.6839 | 0.0027 | 1.6917 |
| UZ (m/s) | 2.2216 | -3.3303 | -0.0812 | 0.5158 | N/A |

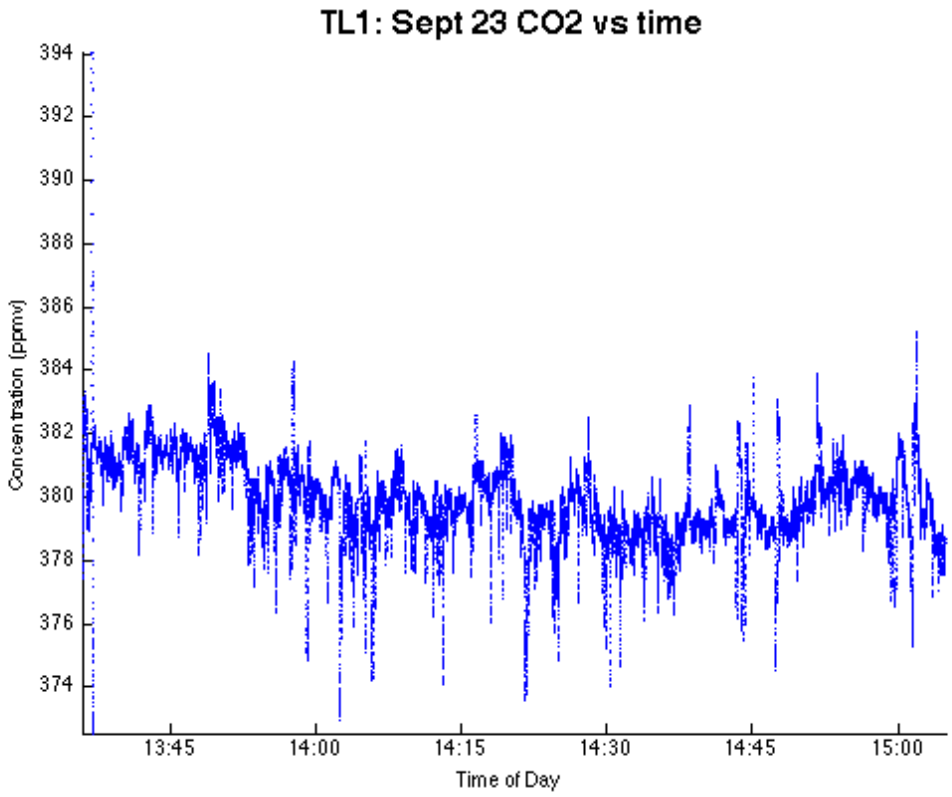

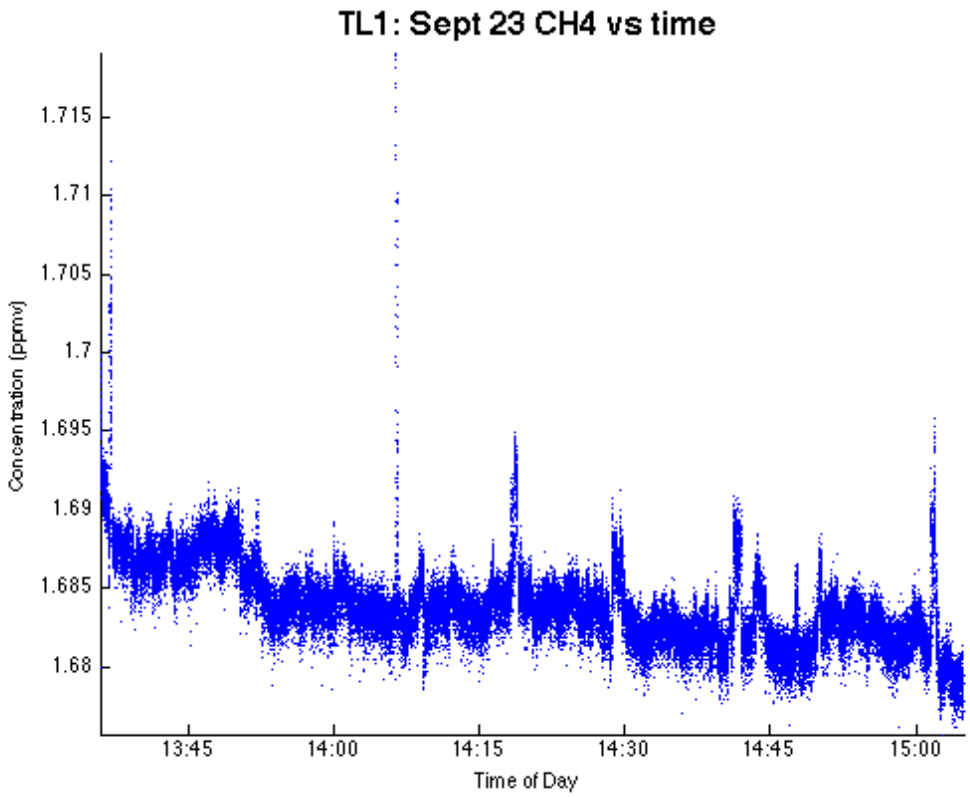
TL1: Sept 23 CH4 vs time
Concentration (ppmv)
1.715
1.71
1.705
1.7
1.695
1.69
1.685
1.68
13:45
14:00
14:15
14:30
14:45
15:00
Time of Day

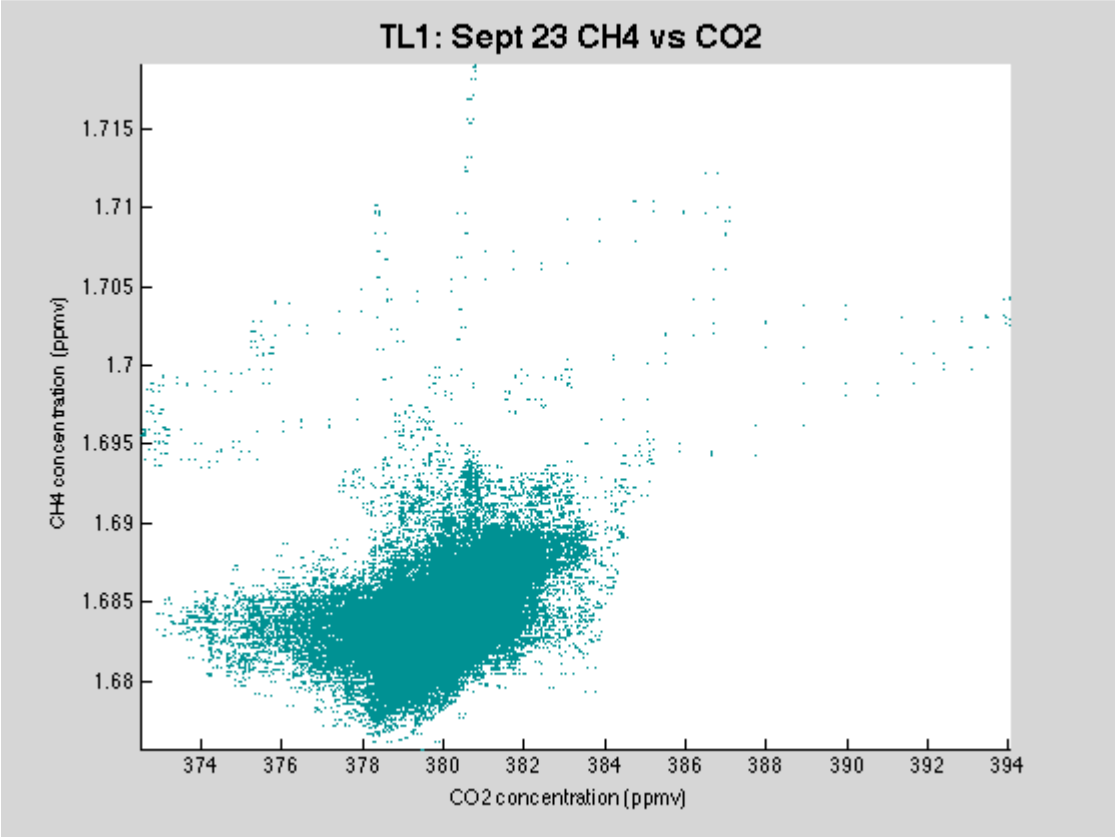
TL1: Sept 23 CH4 vs CO2
CH4 concentration (ppmv)
1.715
1.71
1.705
1.7
1.695
1.69
1.685
1.68
374
376
378
380
382
384
386
388
390
392
394
CO2 concentration (ppmv)

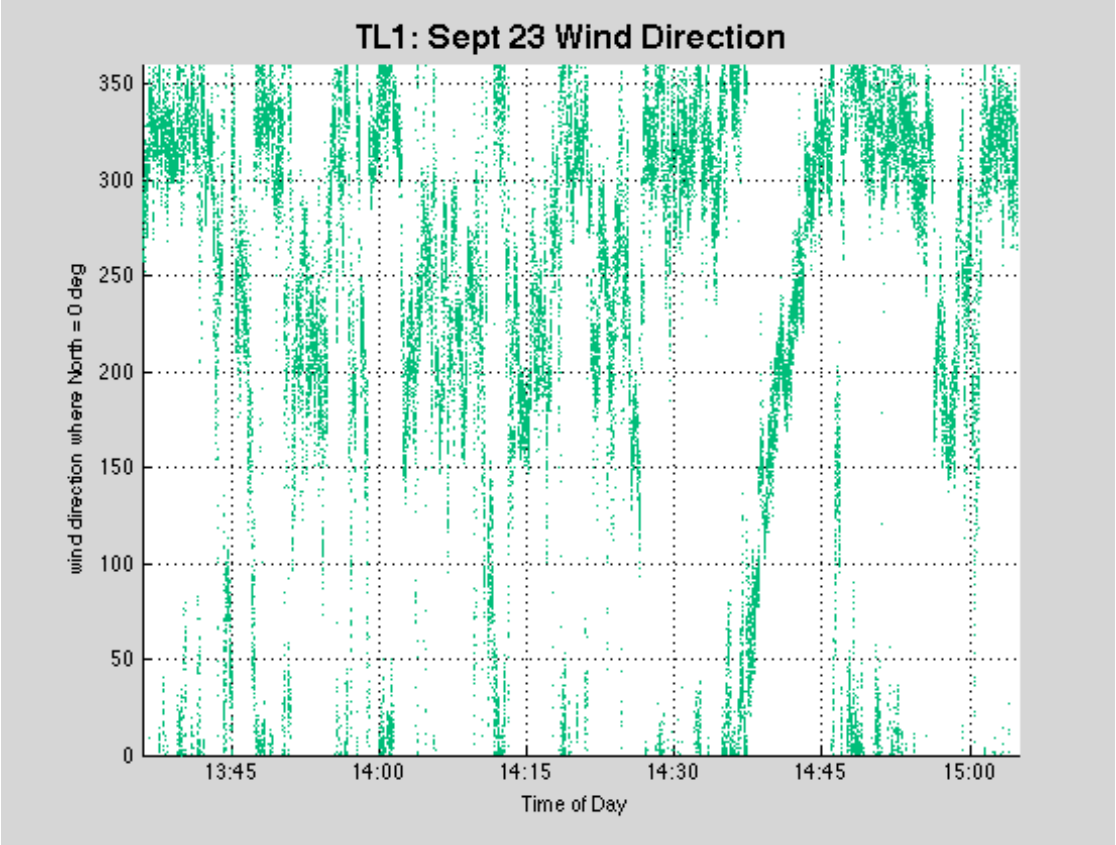
TL1: Sept 23 Wind Direction
wind direction where North = 0 deg
350
300
250
200
150
100
50
0
13:45
14:00
14:15
14:30
14:45
15:00
Time of Day

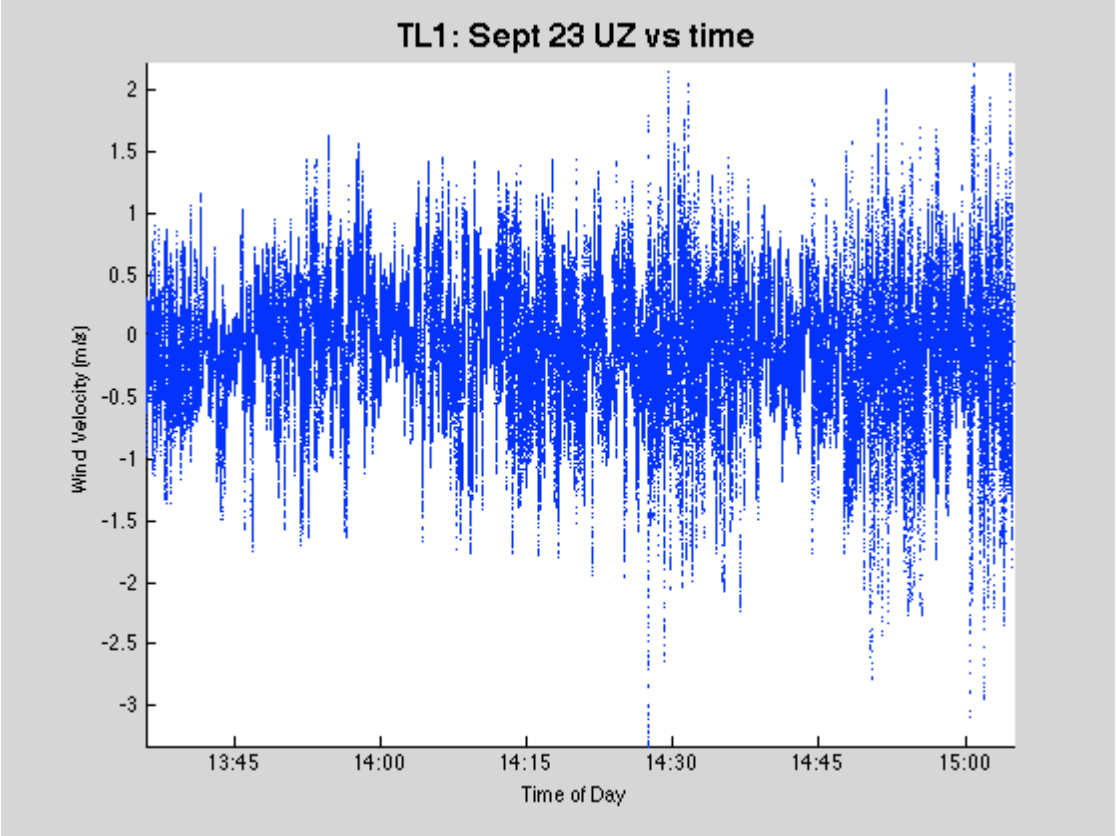
TL1: Sept 23 UZ vs time
Wind Velocity (m/s)
2
1.5
1
0.5
0
-0.5
-1
-1.5
-2
-2.5
-3
13:45
14:00
14:15
14:30
14:45
15:00
Time of Day

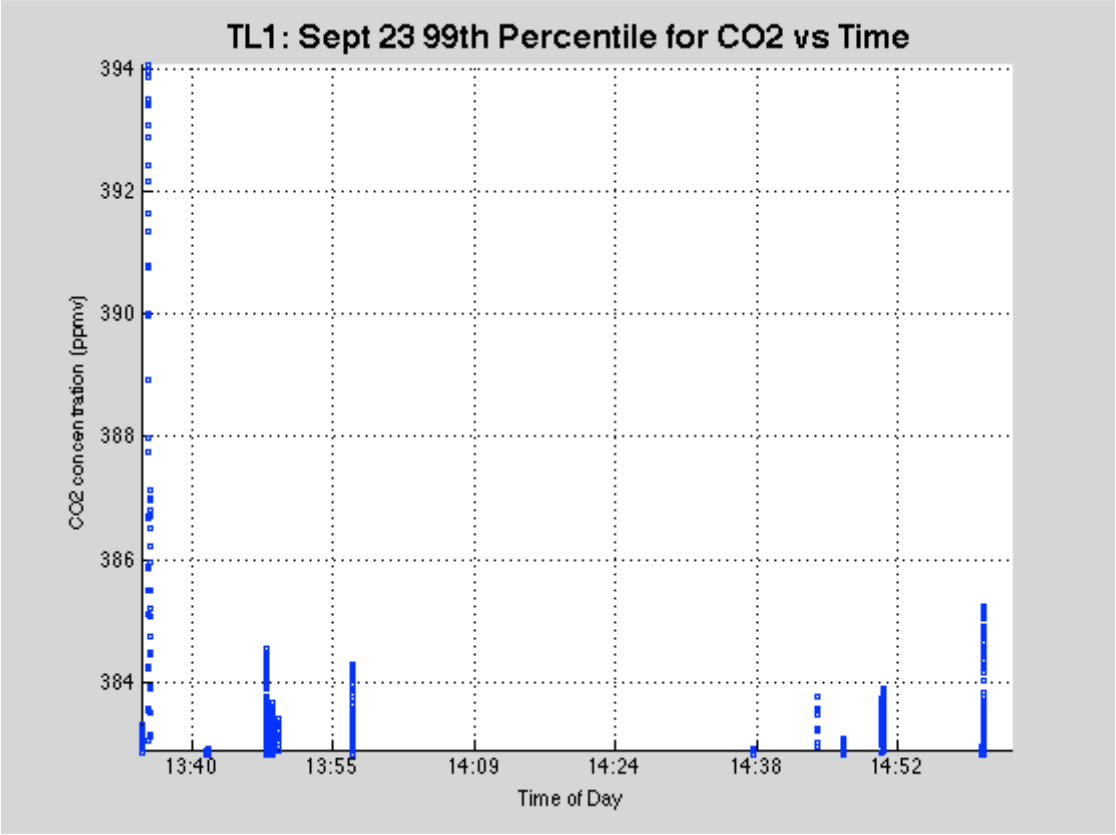
TL1: Sept 23 99th Percentile for CO2 vs Time
CO2 concentration (ppmv)
394
392
390
388
386
384
13:40
13:55
14:09
14:24
14:38
14:52
Time of Day

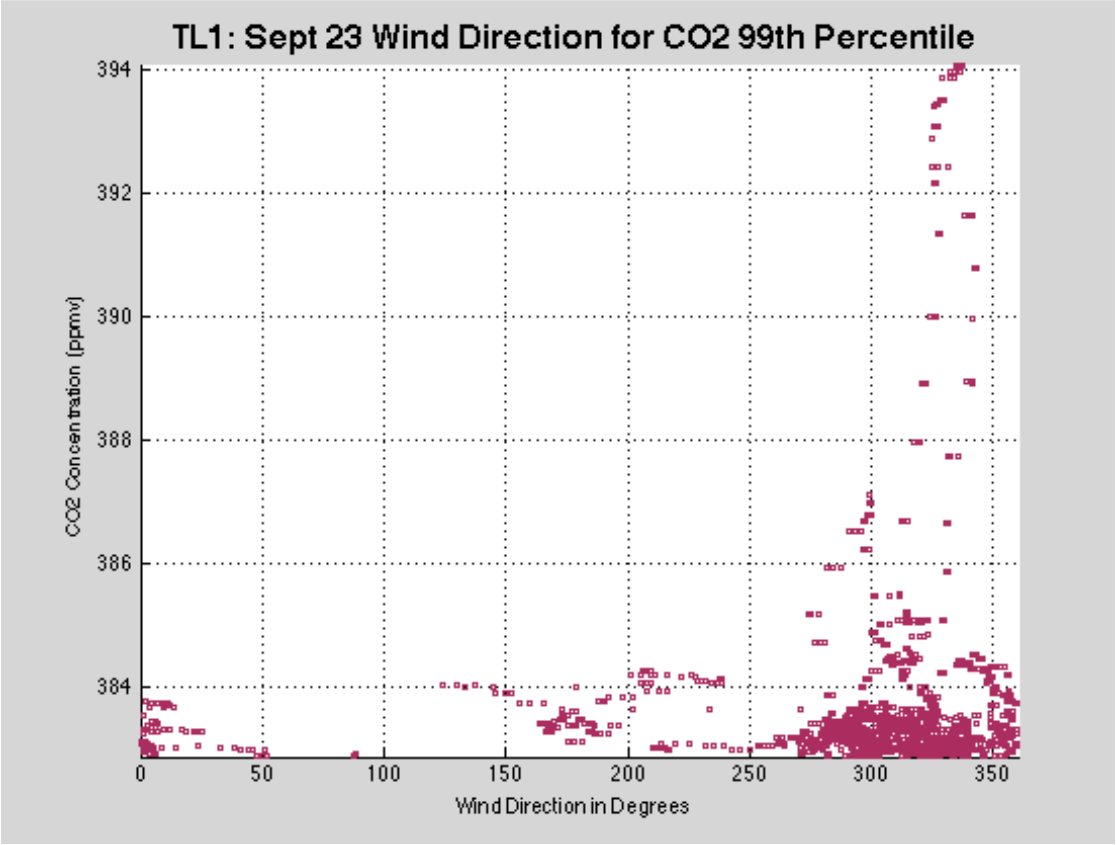
TL1: Sept 23 Wind Direction for CO2 99th Percentile
CO2 Concentration (ppmv)
394
392
390
388
386
384
0
50
100
150
200
250
300
350
Wind Direction in Degrees

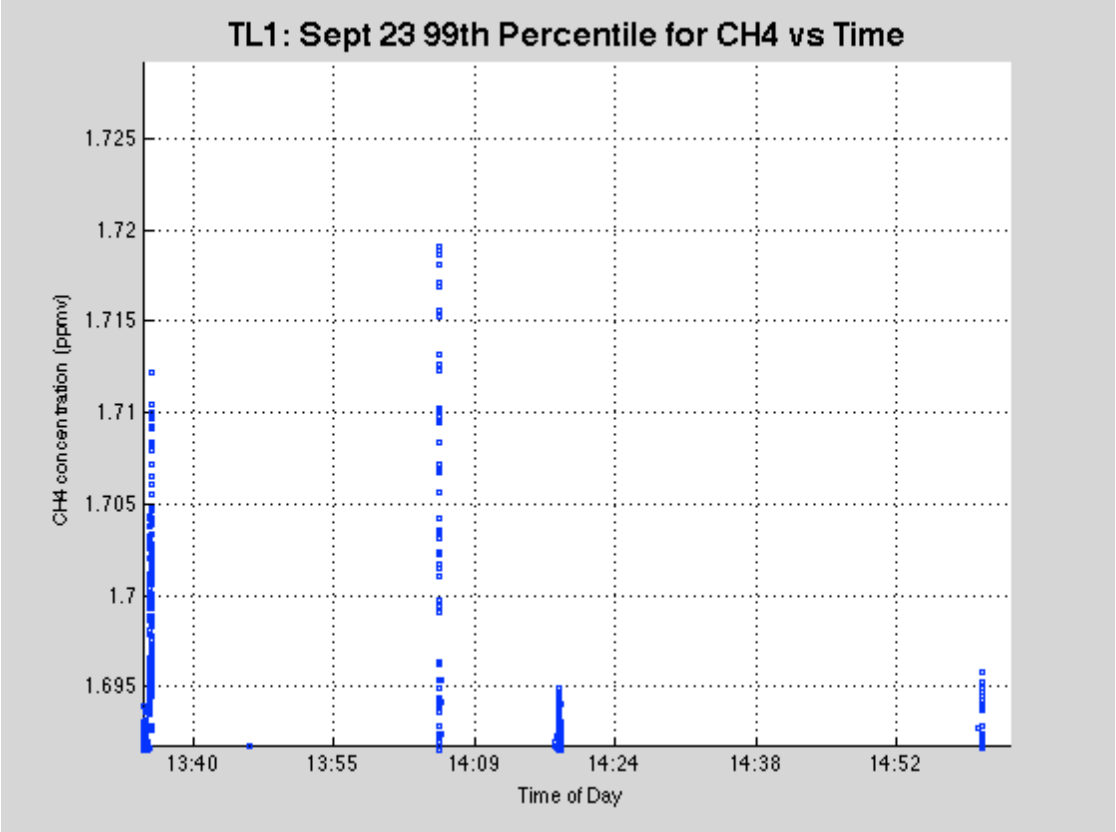
TL1: Sept 23 99th Percentile for CH4 vs Time
CH4 concentration (ppmv)
1.725
1.72
1.715
1.71
1.705
1.7
1.695
13:40
13:55
14:09
14:24
14:38
14:52
Time of Day

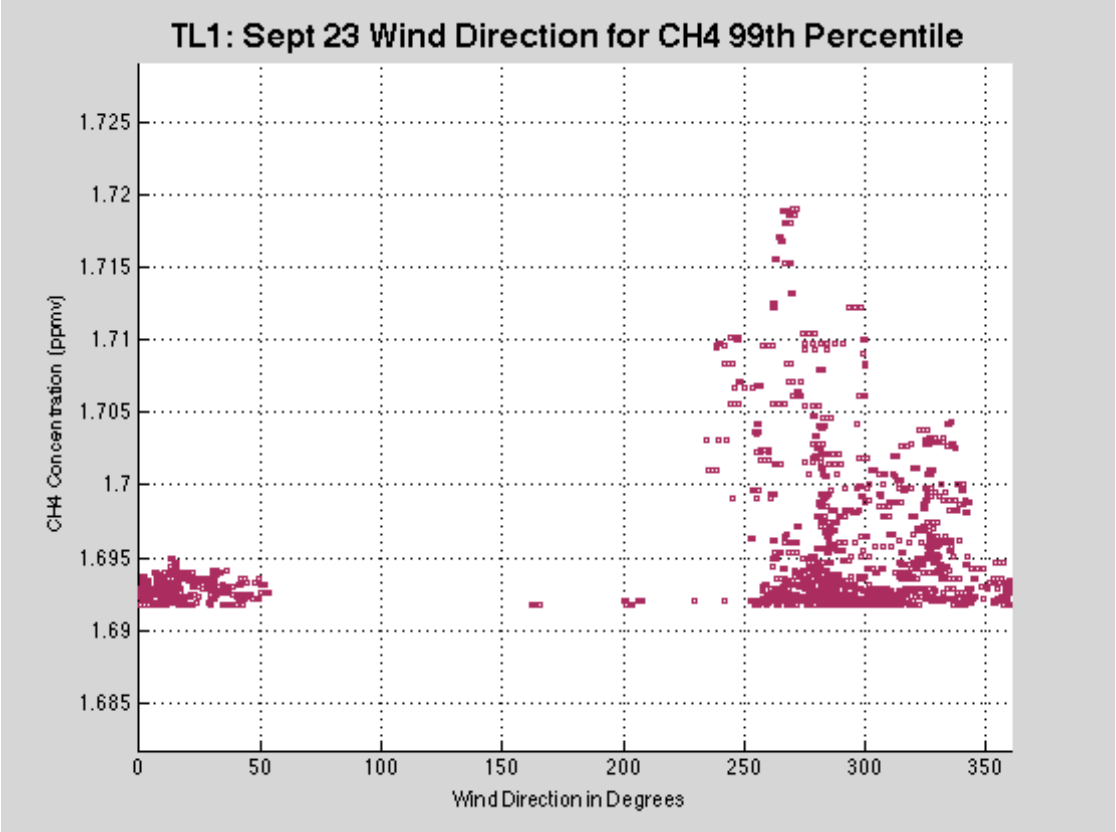
TL1: Sept 23 Wind Direction for CH4 99th Percentile
CH4 Concentration (ppmv)
1.725
1.72
1.715
1.71
1.705
1.7
1.695
1.69
1.685
0
50
100
150
200
250
300
350
Wind Direction in Degrees

## D.9 Tuesday, September 24th, 2013

| | Maximum | Minimum | Average | Standard Deviation | 99th Percentile |
|---|---|---|---|---|---|
| $CO_2$ (ppmv) | 384.4802 | 377.3893 | 380.6744 | 0.8855 | 380.0086 |
| $CH_4$ (ppmv) | 1.7058 | 1.6754 | 1.6867 | 0.0035 | 1.6969 |
| UZ (m/s) | 4.4246 | -5.6547 | -0.0849 | 0.9322 | N/A |

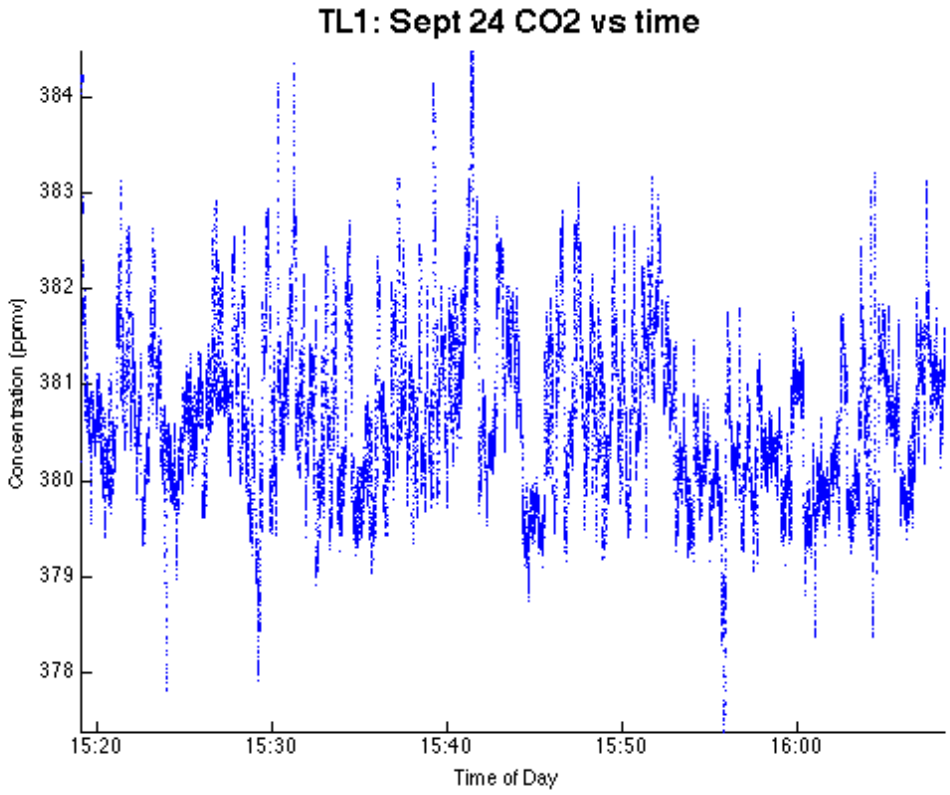

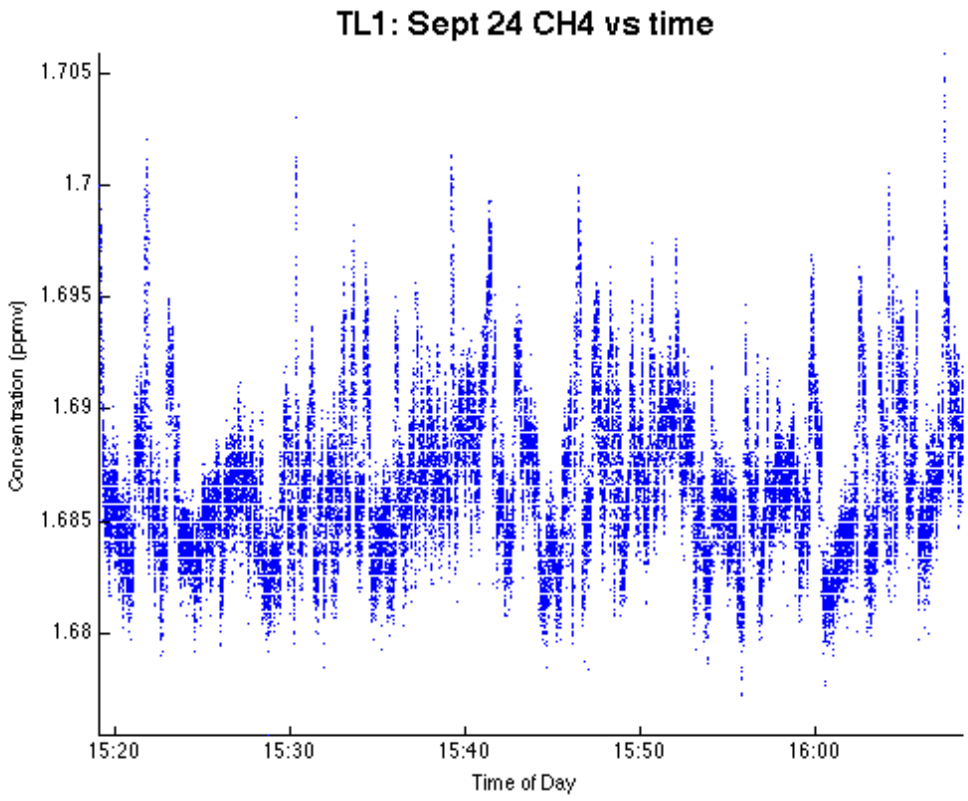
TL1: Sept 24 CH4 vs time
Concentration (ppmv)
1.705
1.7
1.695
1.69
1.685
1.68
15:20
15:30
15:40
15:50
16:00
Time of Day

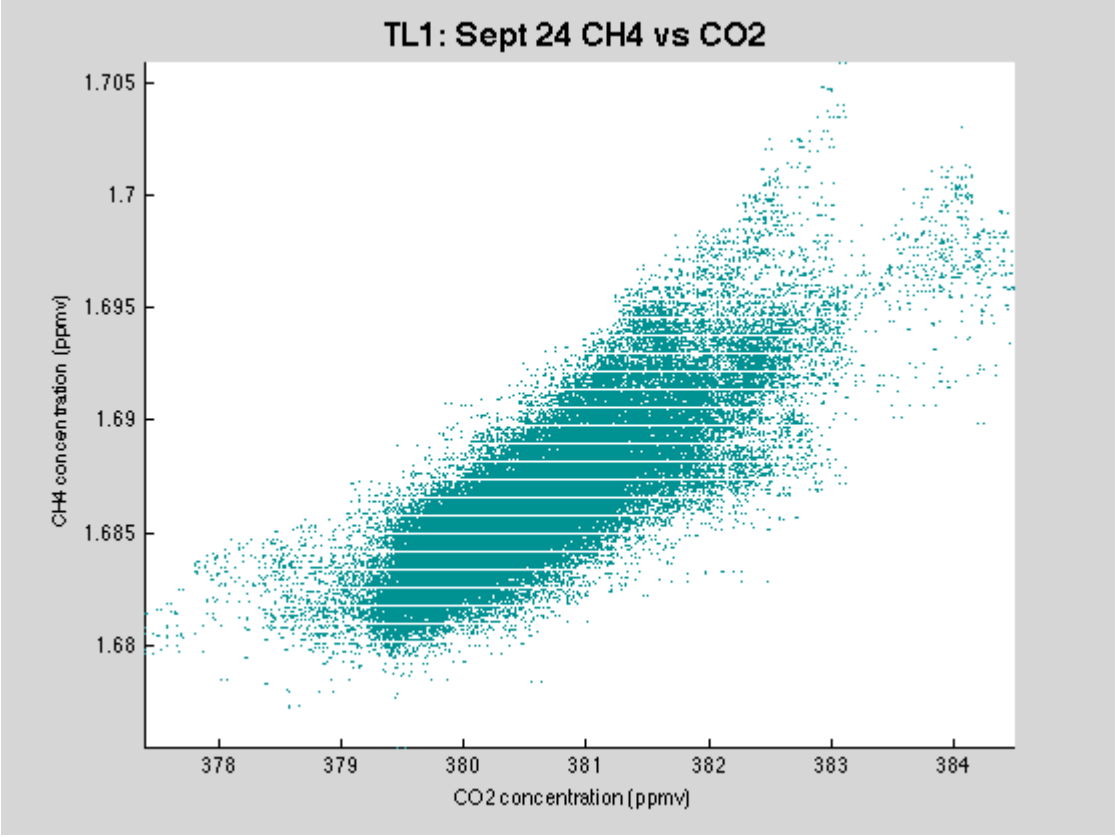
TL1: Sept 24 CH4 vs CO2
CH4 concentration (ppmv)
1.705
1.7
1.695
1.69
1.685
1.68
378
379
380
381
382
383
384
CO2 concentration (ppmv)

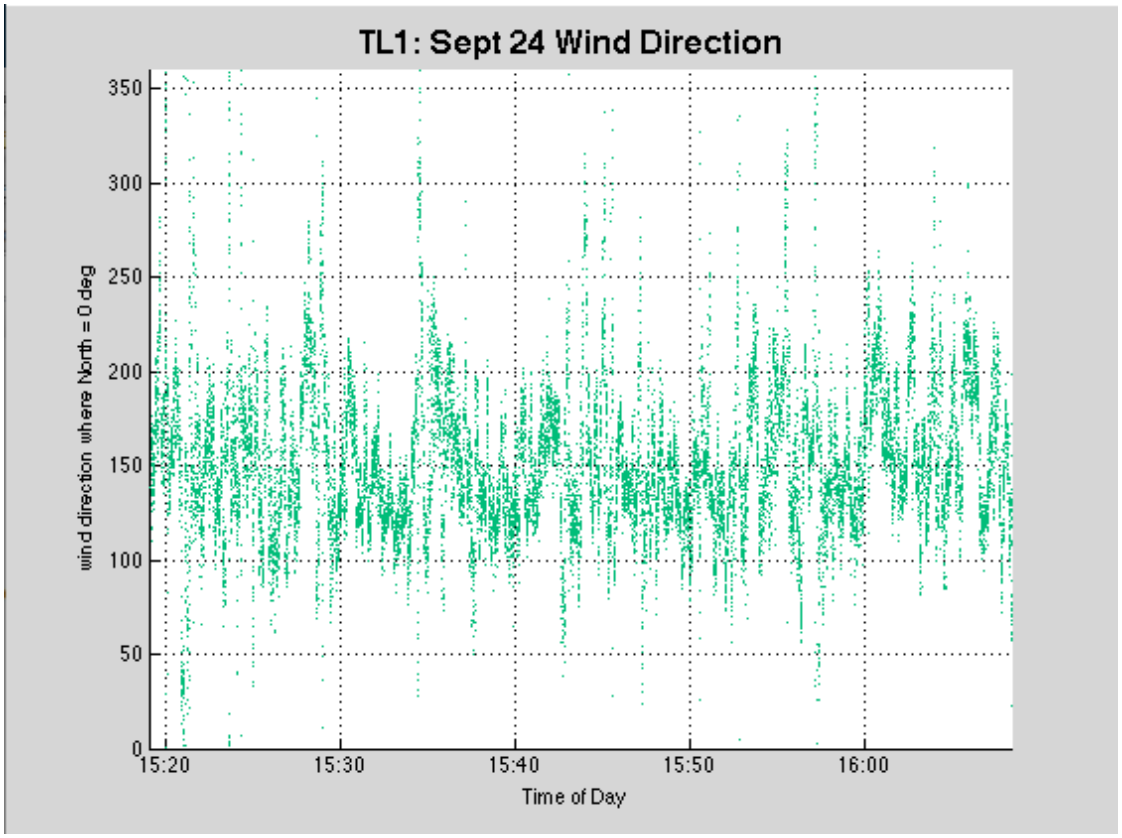
TL1: Sept 24 Wind Direction
wind direction where North = 0 deg
350
300
250
200
150
100
50
0
15:20
15:30
15:40
15:50
16:00
Time of Day

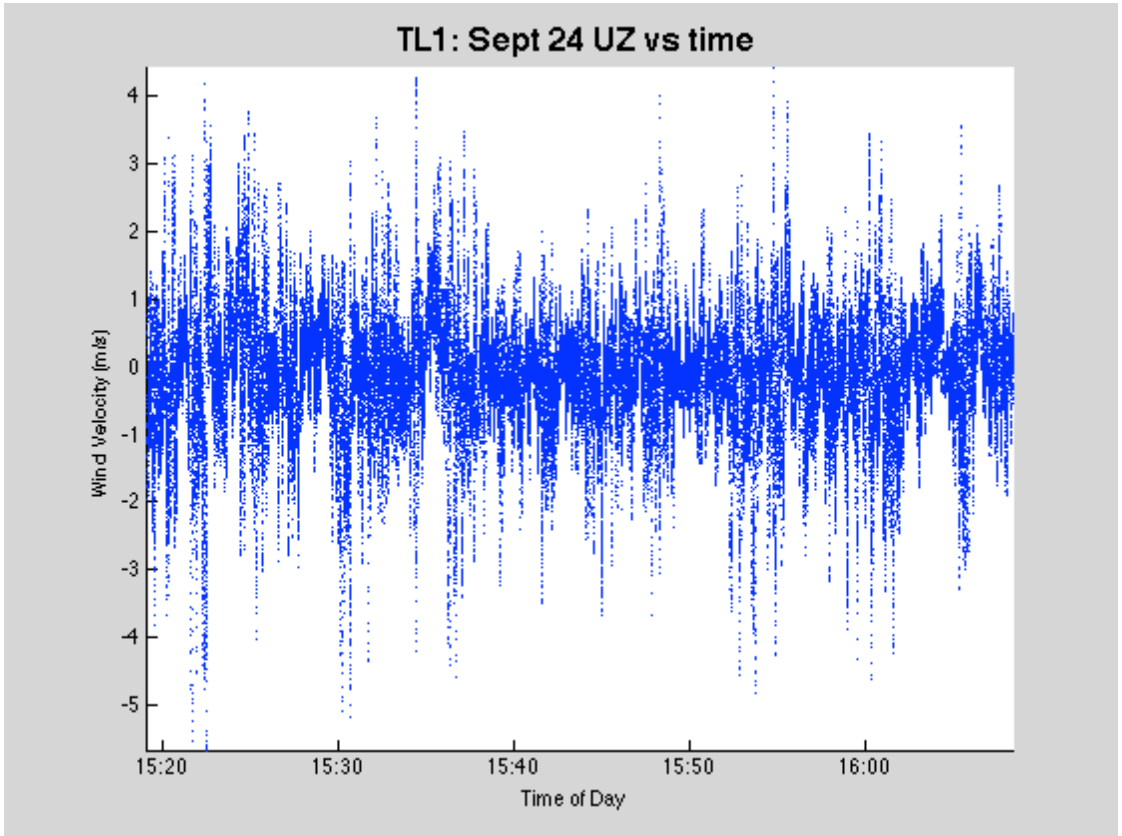
TL1: Sept 24 UZ vs time
Wind Velocity (m/s)
4
3
2
1
0
-1
-2
-3
-4
-5
15:20
15:30
15:40
15:50
16:00
Time of Day

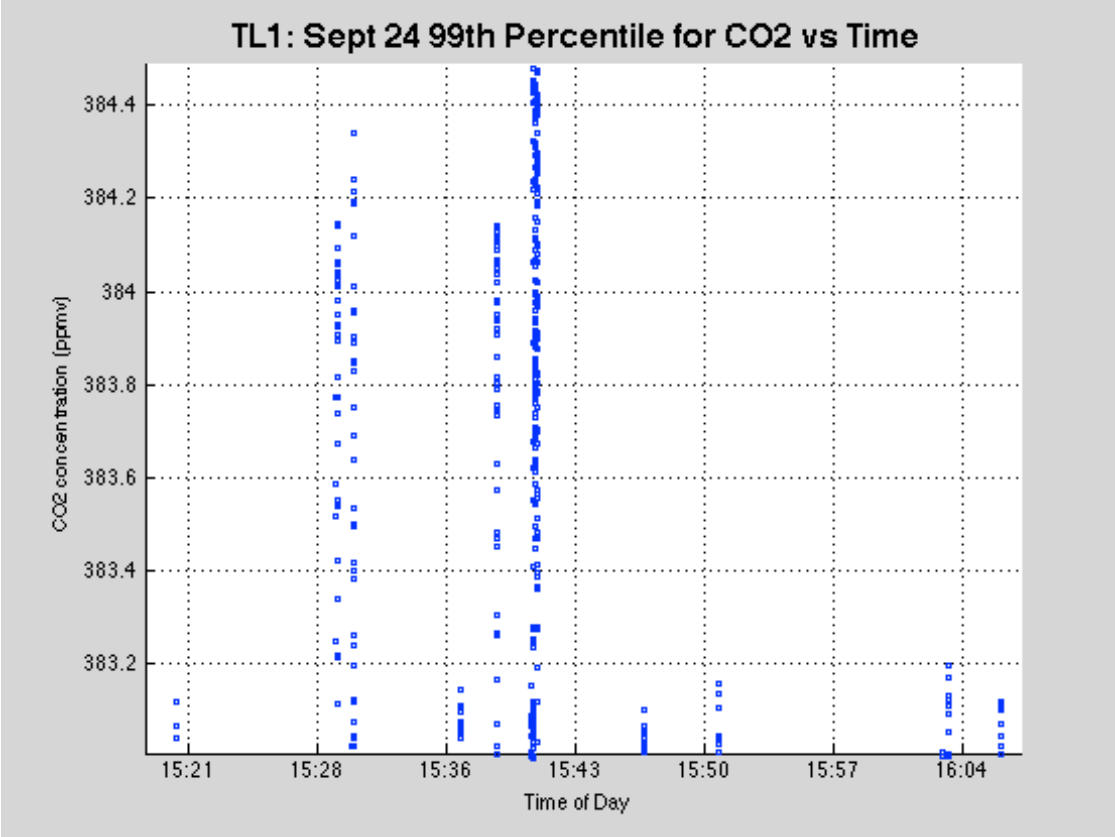
TL1: Sept 24 99th Percentile for CO2 vs Time
CO2 concentration (ppmv)
384.4
384.2
384
383.8
383.6
383.4
383.2
15:21
15:28
15:36
15:43
15:50
15:57
16:04
Time of Day

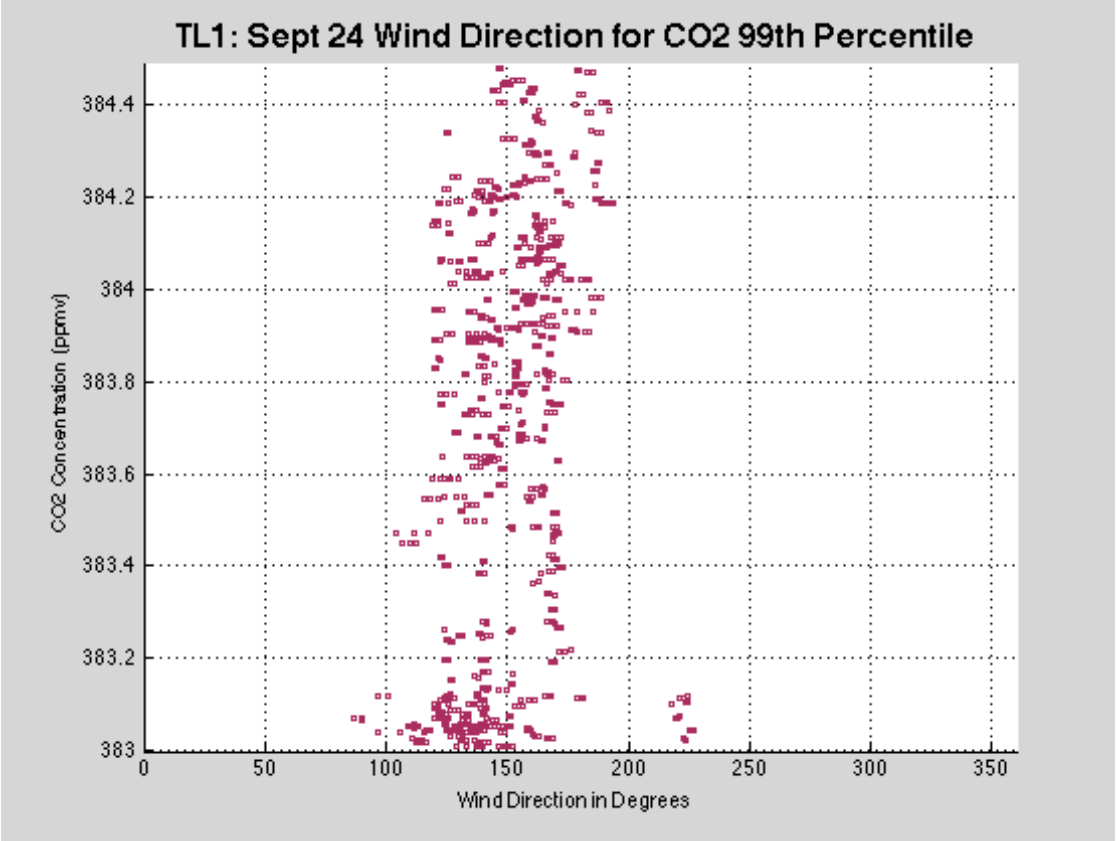
TL1: Sept 24 Wind Direction for CO2 99th Percentile
CO2 Concentration (ppmv)
384.4
384.2
384
383.8
383.6
383.4
383.2
383
0
50
100
150
200
250
300
350
Wind Direction in Degrees

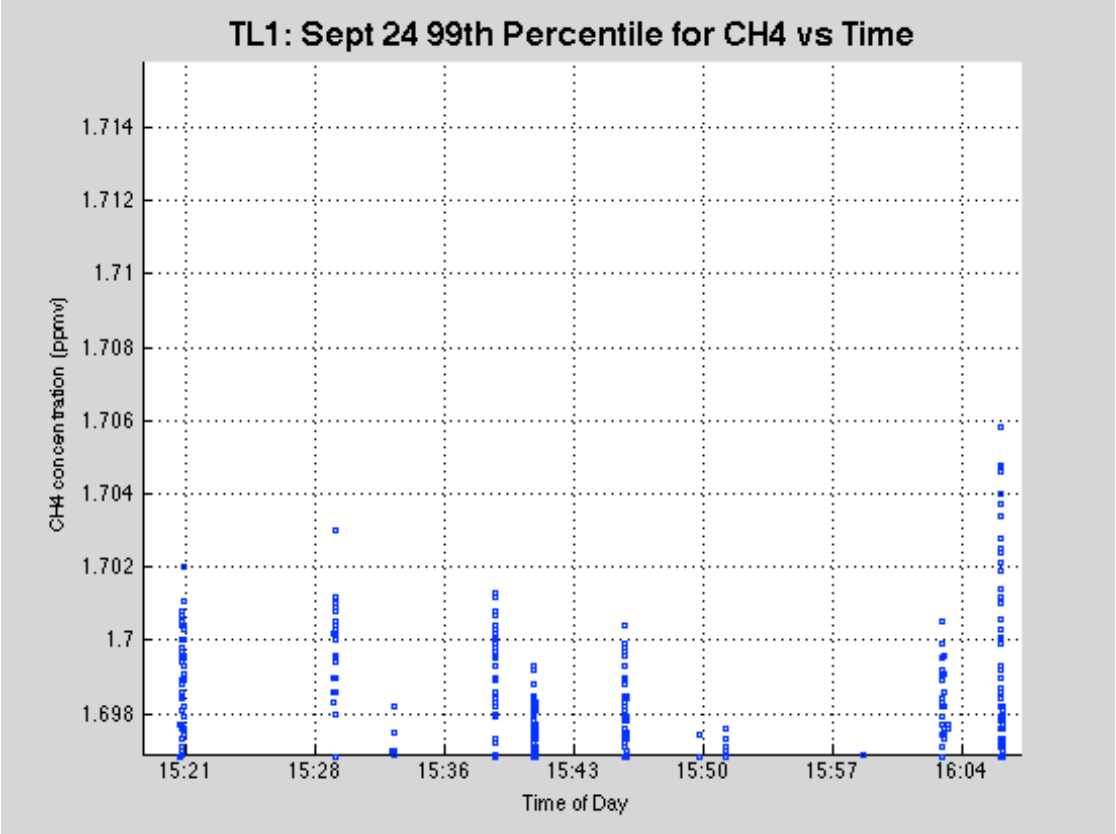
TL1: Sept 24 99th Percentile for CH4 vs Time
CH4 concentration (ppmv)
1.714
1.712
1.71
1.708
1.706
1.704
1.702
1.7
1.698
15:21
15:28
15:36
15:43
15:50
15:57
16:04
Time of Day

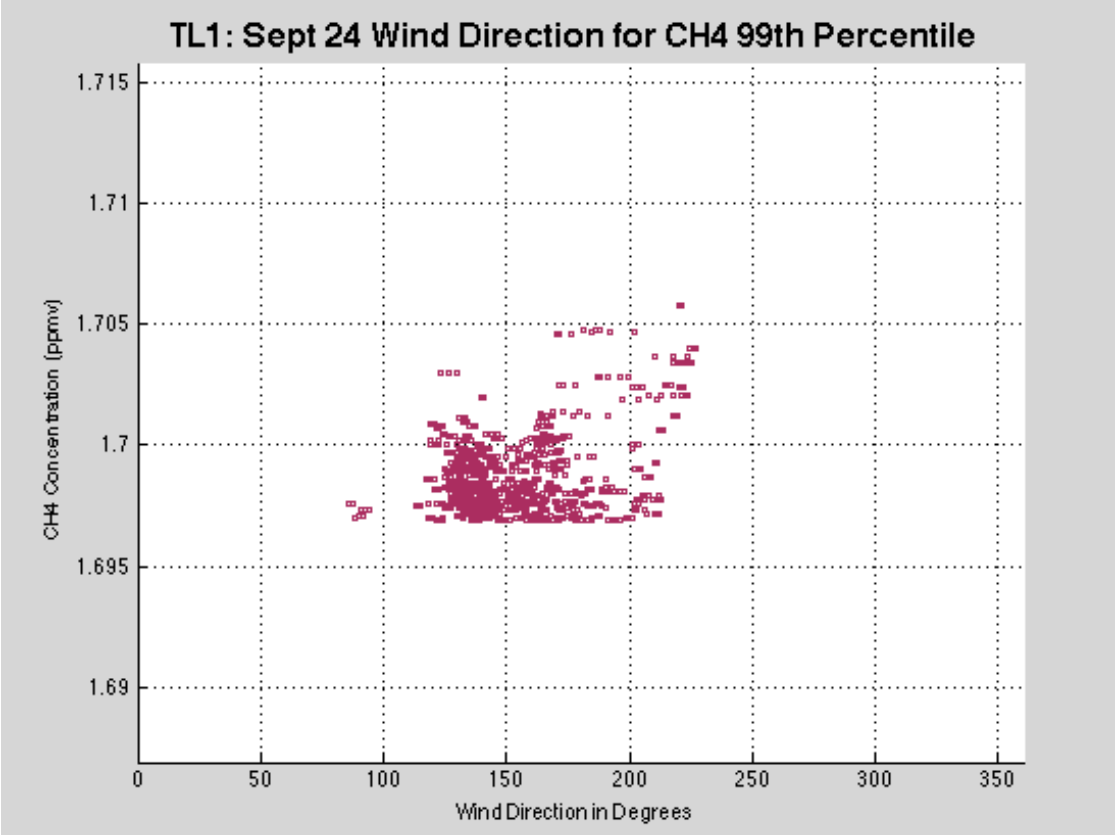
TL1: Sept 24 Wind Direction for CH4 99th Percentile
CH4 Concentration (ppmv)
1.715
1.71
1.705
1.7
1.695
1.69
0
50
100
150
200
250
300
350
Wind Direction in Degrees

D.10 Wednesday, September 25th, 2013

| | Maximum | Minimum | Average | Standard Deviation | 99th Percentile |
|---|---|---|---|---|---|
| $CO_2$ (ppmv) | 414.5609 | 330.4174 | 388.5765 | 7.412 | 408.5249 |
| $CH_4$ (ppmv) | 1.8102 | 1.6823 | 1.7142 | 0.0295 | 1.8026 |
| UZ (m/s) | 5.4294 | -8.0624 | -0.1204 | 0.6938 | N/A |

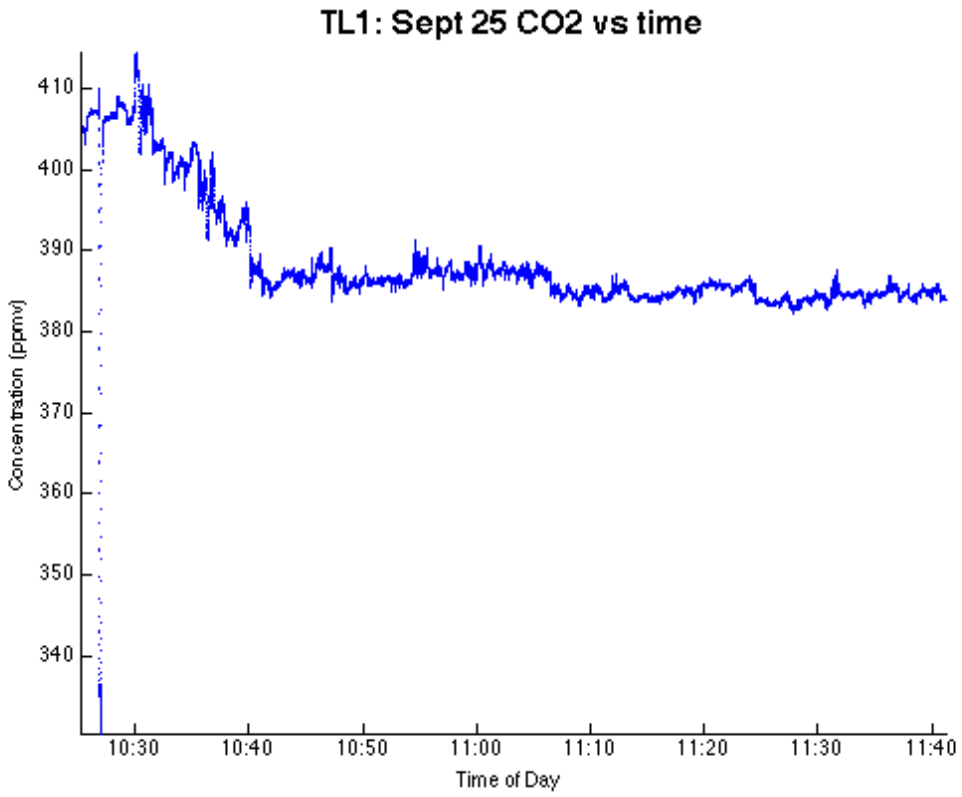

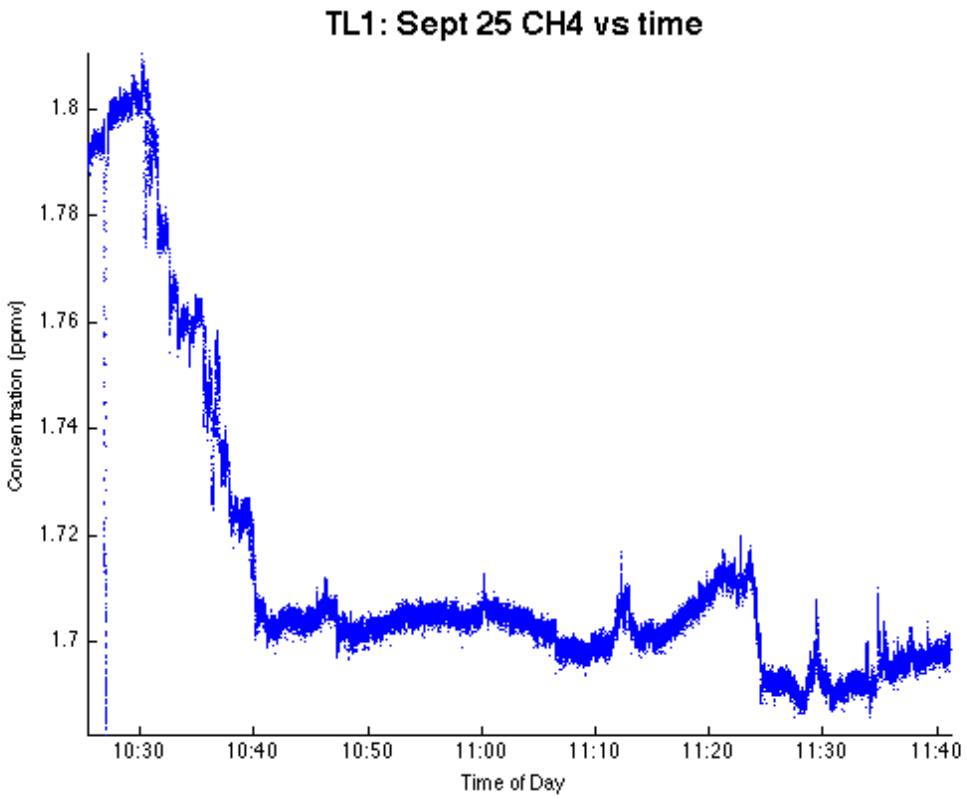
TL1: Sept 25 CH4 vs time
Concentration (ppmv)
1.8
1.78
1.76
1.74
1.72
1.7
10:30
10:40
10:50
11:00
11:10
11:20
11:30
11:40
Time of Day

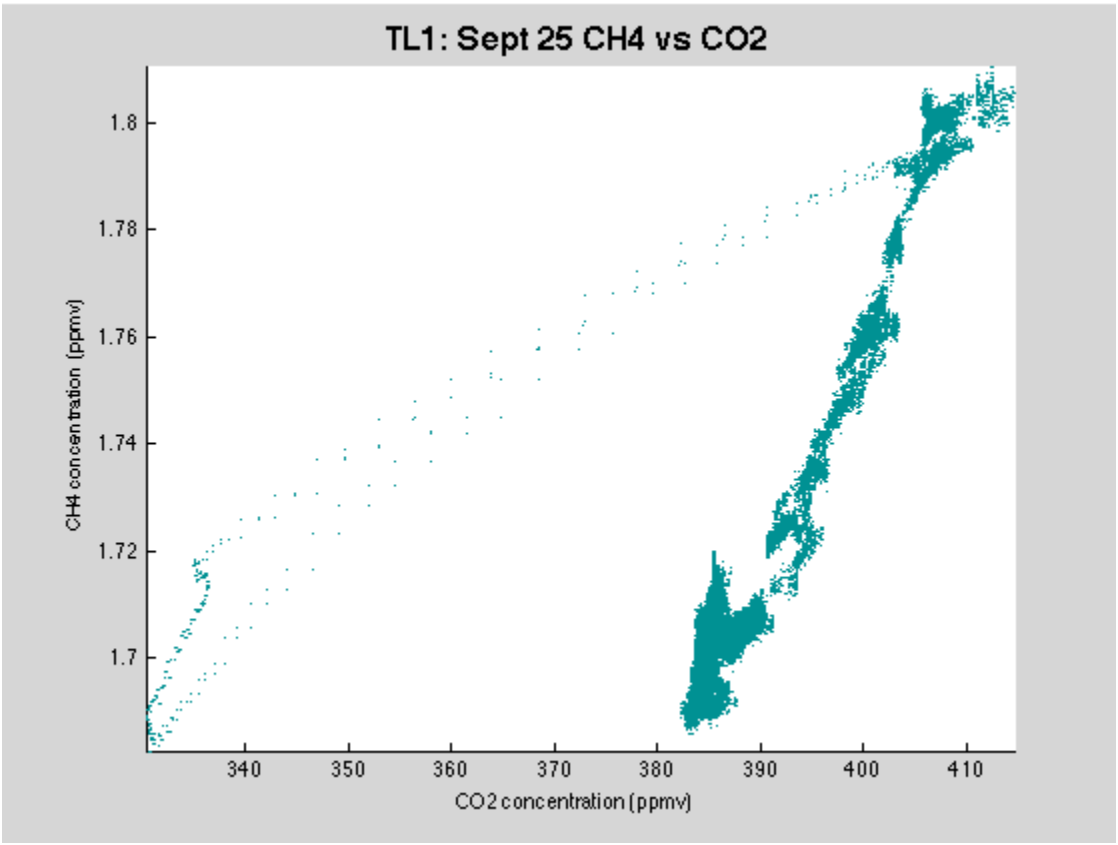
TL1: Sept 25 CH4 vs CO2
CH4 concentration (ppmv)
1.8
1.78
1.76
1.74
1.72
1.7
340
350
360
370
380
390
400
410
CO2 concentration (ppmv)

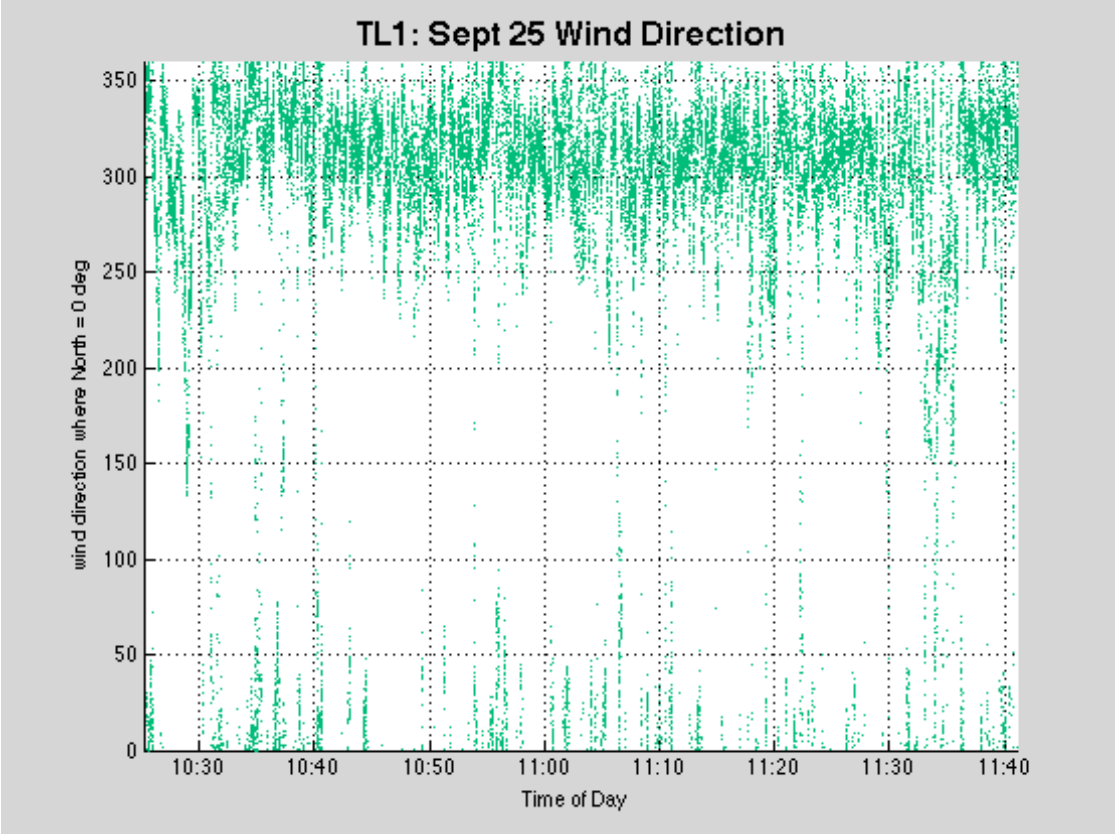
TL1: Sept 25 Wind Direction
wind direction where North = 0 deg
350
300
250
200
150
100
50
0
10:30
10:40
10:50
11:00
11:10
11:20
11:30
11:40
Time of Day

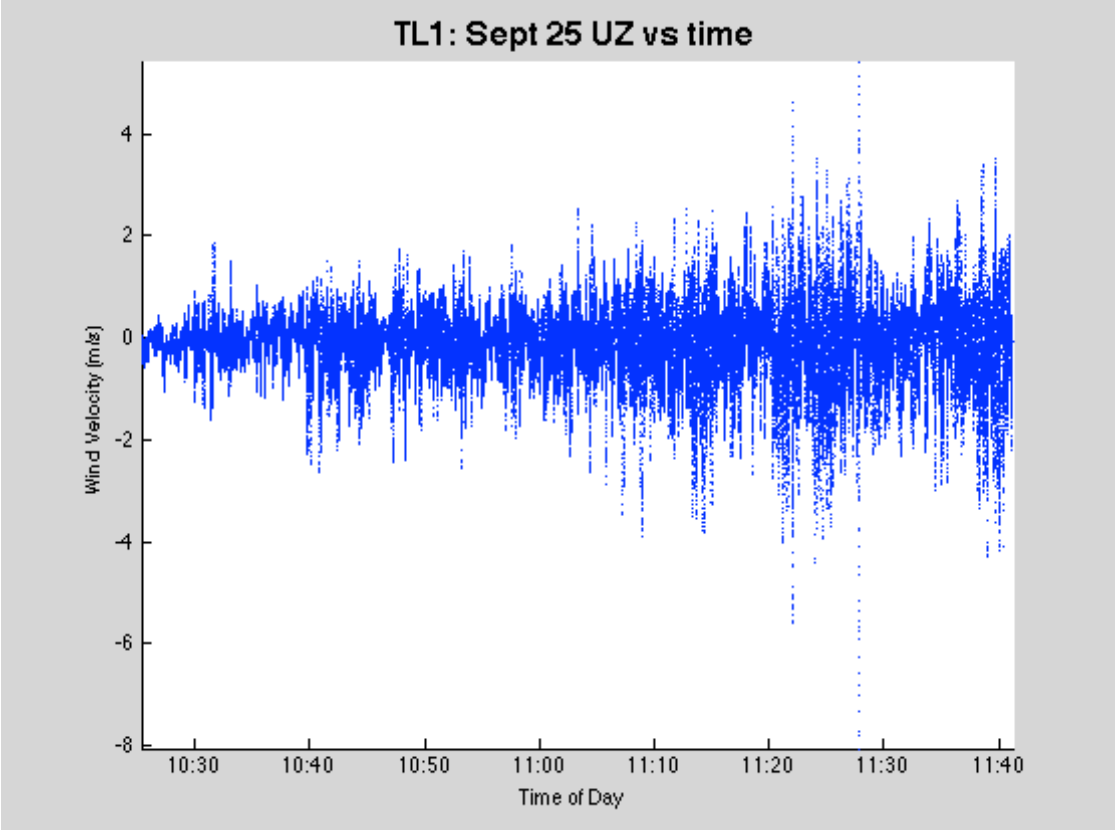
TL1: Sept 25 UZ vs time
Wind Velocity (m/s)
4
2
0
-2
-4
-6
-8
10:30
10:40
10:50
11:00
11:10
11:20
11:30
11:40
Time of Day

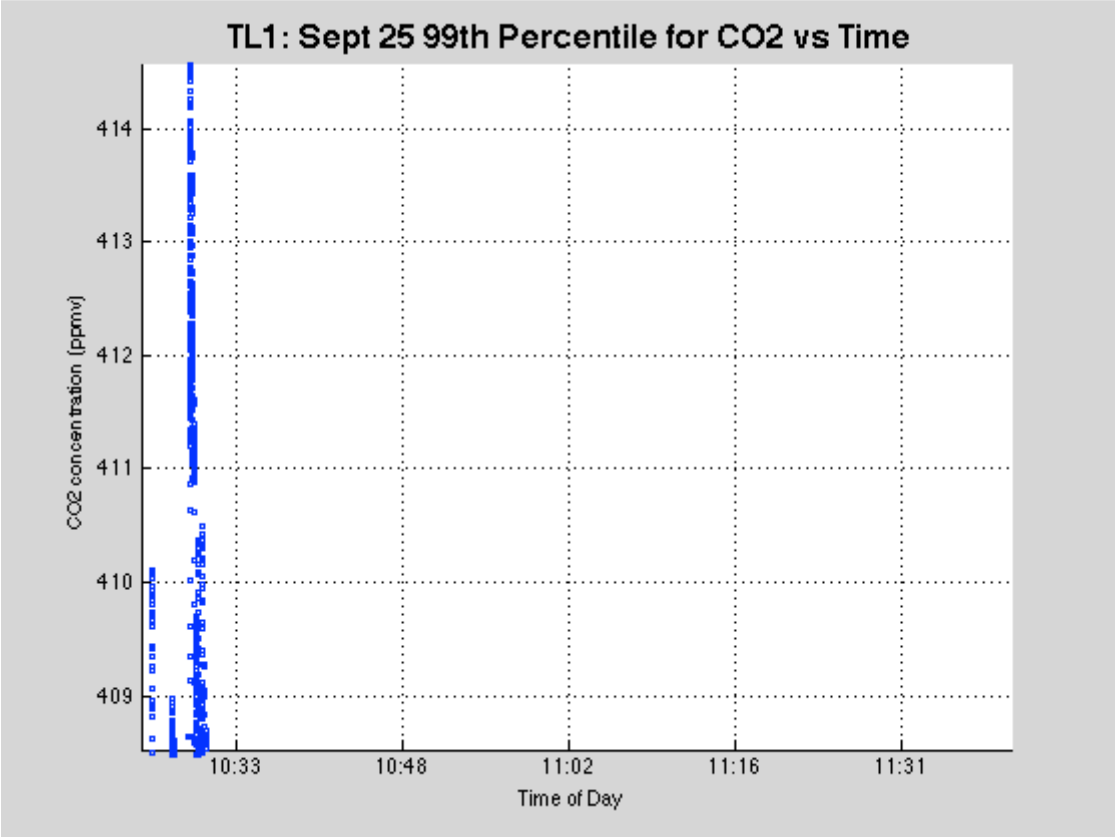
TL1: Sept 25 99th Percentile for CO2 vs Time
CO2 concentration (ppmv)
414
413
412
411
410
409
10:33
10:48
11:02
11:16
11:31
Time of Day

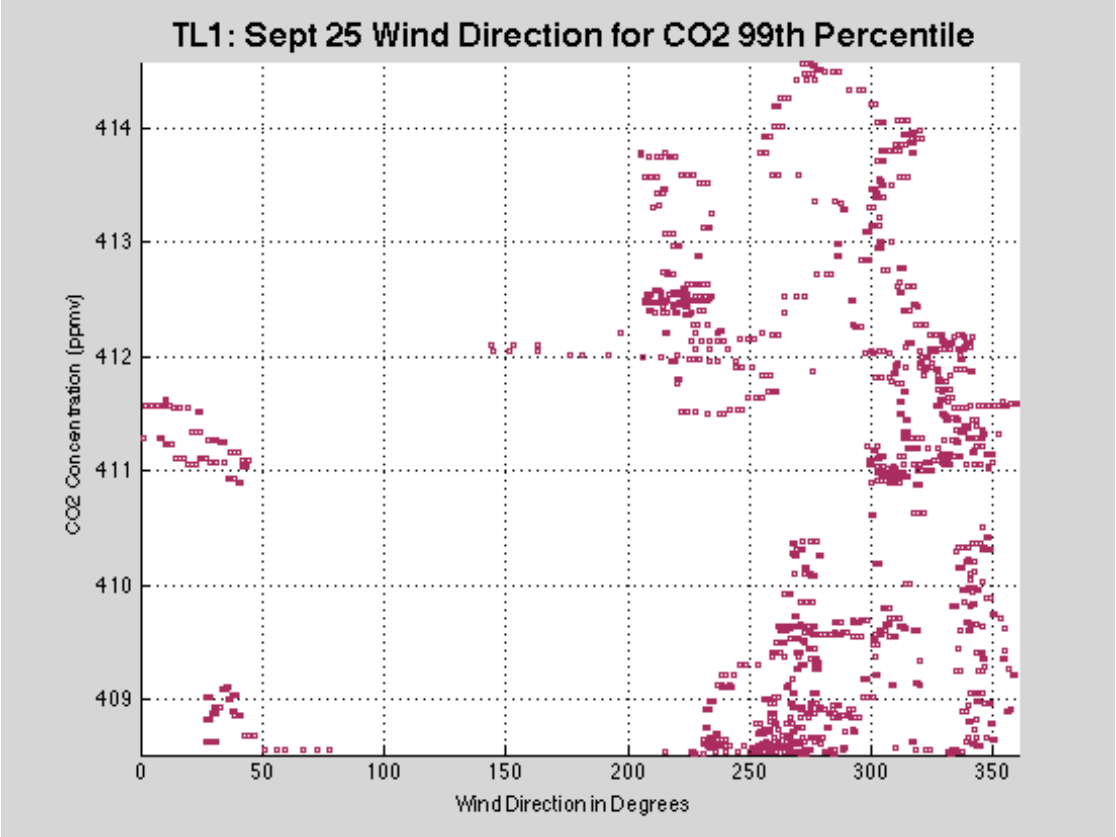
TL1: Sept 25 Wind Direction for CO2 99th Percentile
CO2 Concentration (ppmv)
414
413
412
411
410
409
0
50
100
150
200
250
300
350
Wind Direction in Degrees

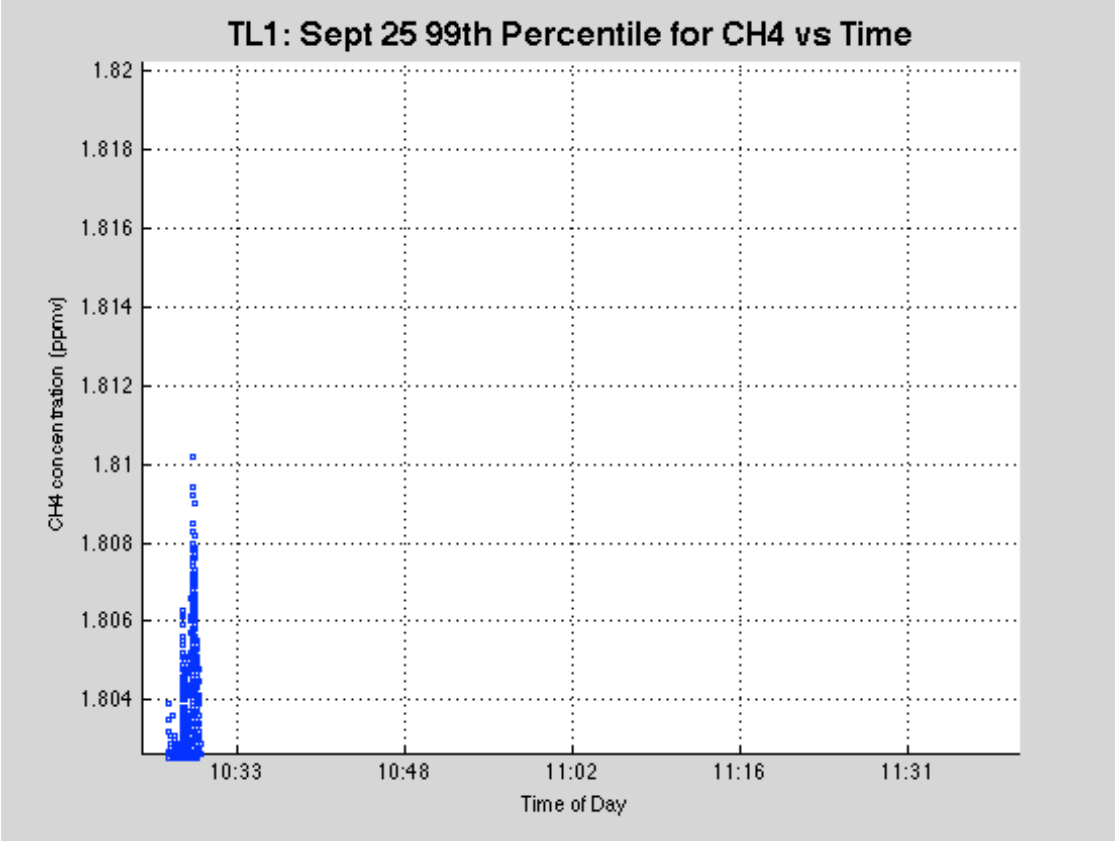
TL1: Sept 25 99th Percentile for CH4 vs Time
CH4 concentration (ppmv)
1.82
1.818
1.816
1.814
1.812
1.81
1.808
1.806
1.804
10:33
10:48
11:02
11:16
11:31
Time of Day

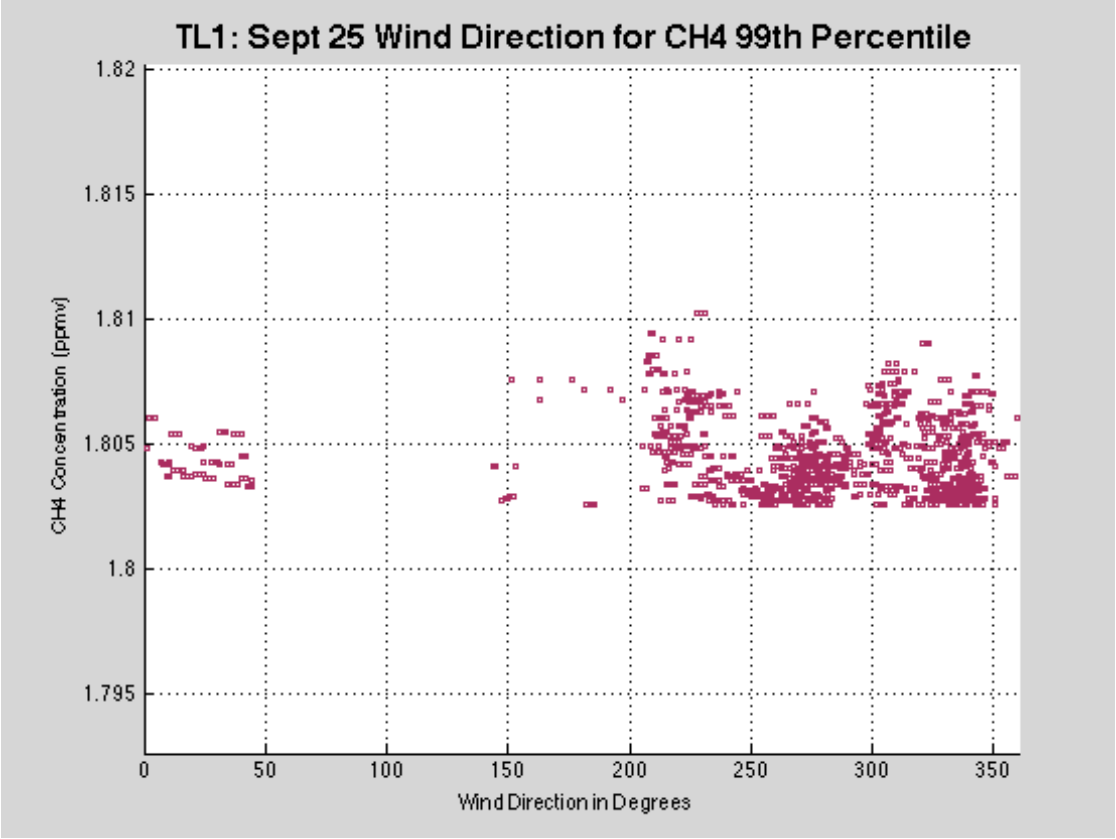
TL1: Sept 25 Wind Direction for CH4 99th Percentile
CH4 Concentration (ppmv)
1.82
1.815
1.81
1.805
1.8
1.795
0
50
100
150
200
250
300
350
Wind Direction in Degrees

D.11 Monday, September 30th, 2013

| | Maximum | Minimum | Average | Standard Deviation | 99th Percentile |
|---|---|---|---|---|---|
| $CO_2$ (ppmv) | 405.8915 | 376.0208 | 381.1733 | 1.2796 | 384.6552 |
| $CH_4$ (ppmv) | 1.7086 | 1.6661 | 1.6777 | 0.0046 | 1.6926 |
| UZ (m/s) | 3.4698 | -4.3583 | -0.0315 | 0.6807 | N/A |

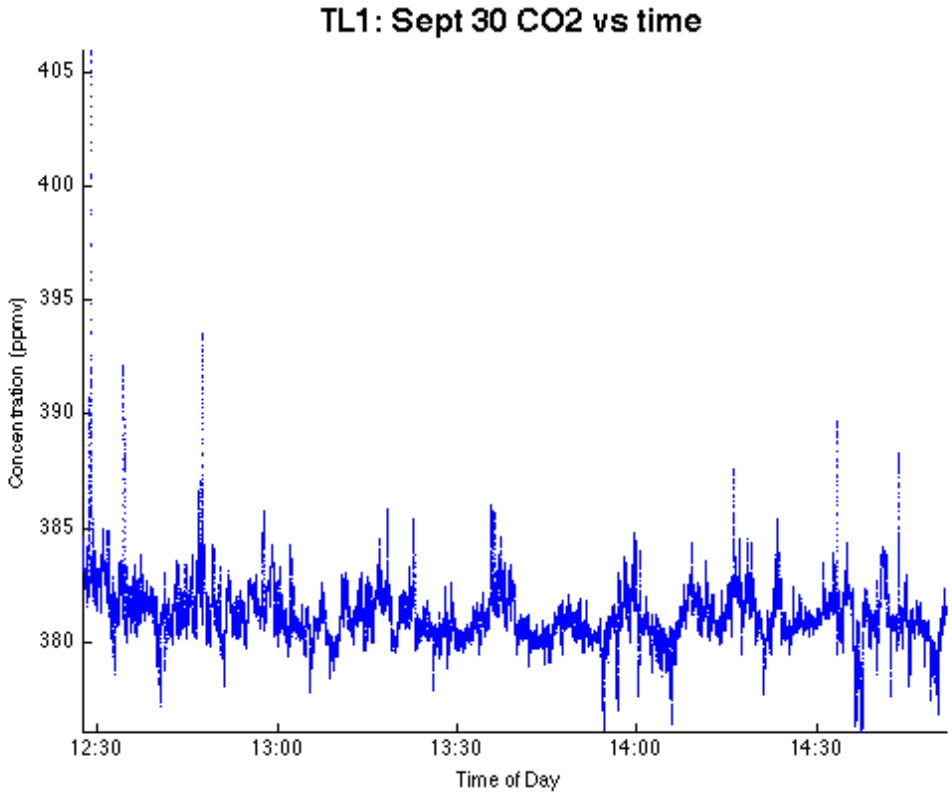

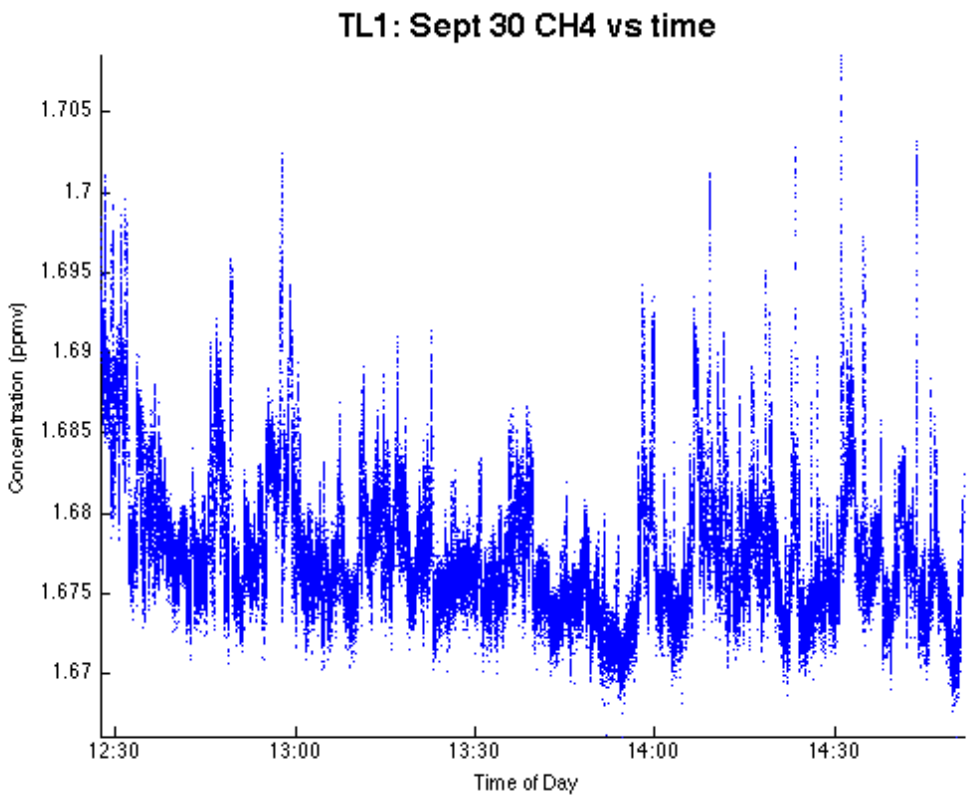
TL1: Sept 30 CH4 vs time
Concentration (ppmv)
1.705
1.7
1.695
1.69
1.685
1.68
1.675
1.67
12:30
13:00
13:30
14:00
14:30
Time of Day

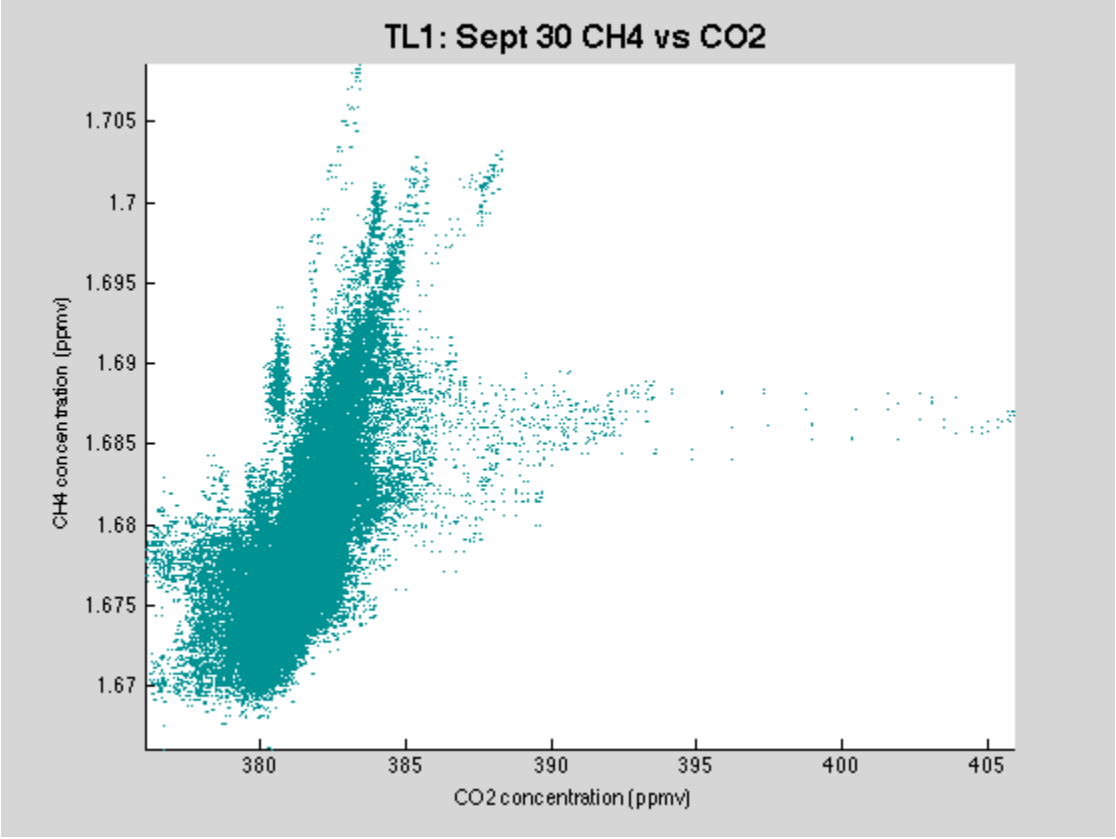
TL1: Sept 30 CH4 vs CO2
CH4 concentration (ppmv)
1.705
1.7
1.695
1.69
1.685
1.68
1.675
1.67
380
385
390
395
400
405
CO2 concentration (ppmv)

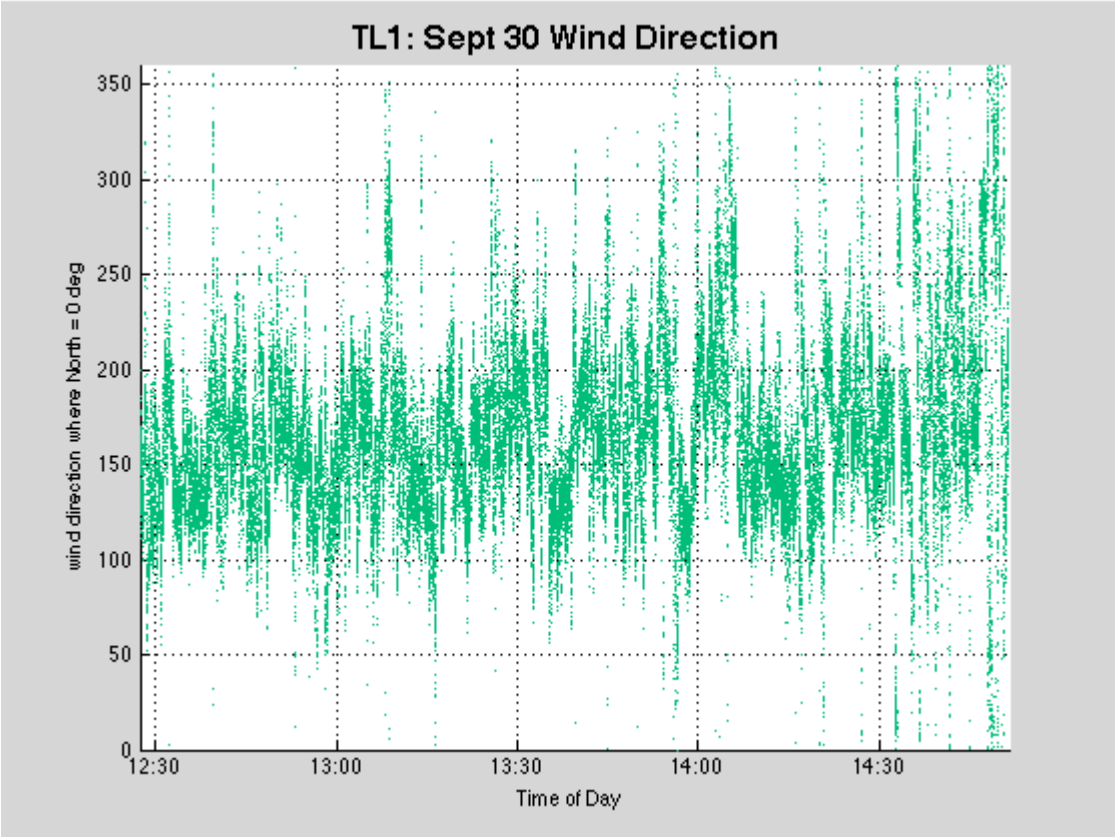
TL1: Sept 30 Wind Direction
wind direction where North = 0 deg
350
300
250
200
150
100
50
0
12:30
13:00
13:30
14:00
14:30
Time of Day

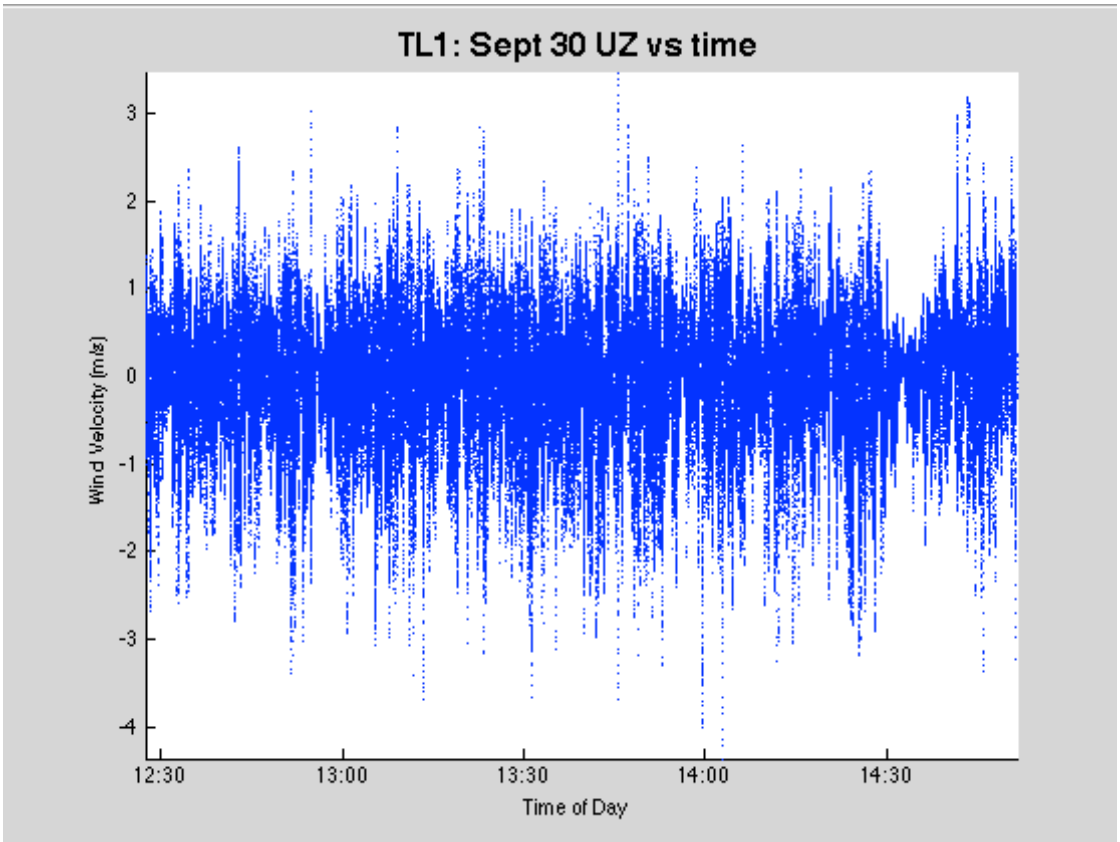
TL1: Sept 30 UZ vs time
Wind Velocity (m/s)
3
2
1
0
-1
-2
-3
-4
12:30
13:00
13:30
14:00
14:30
Time of Day

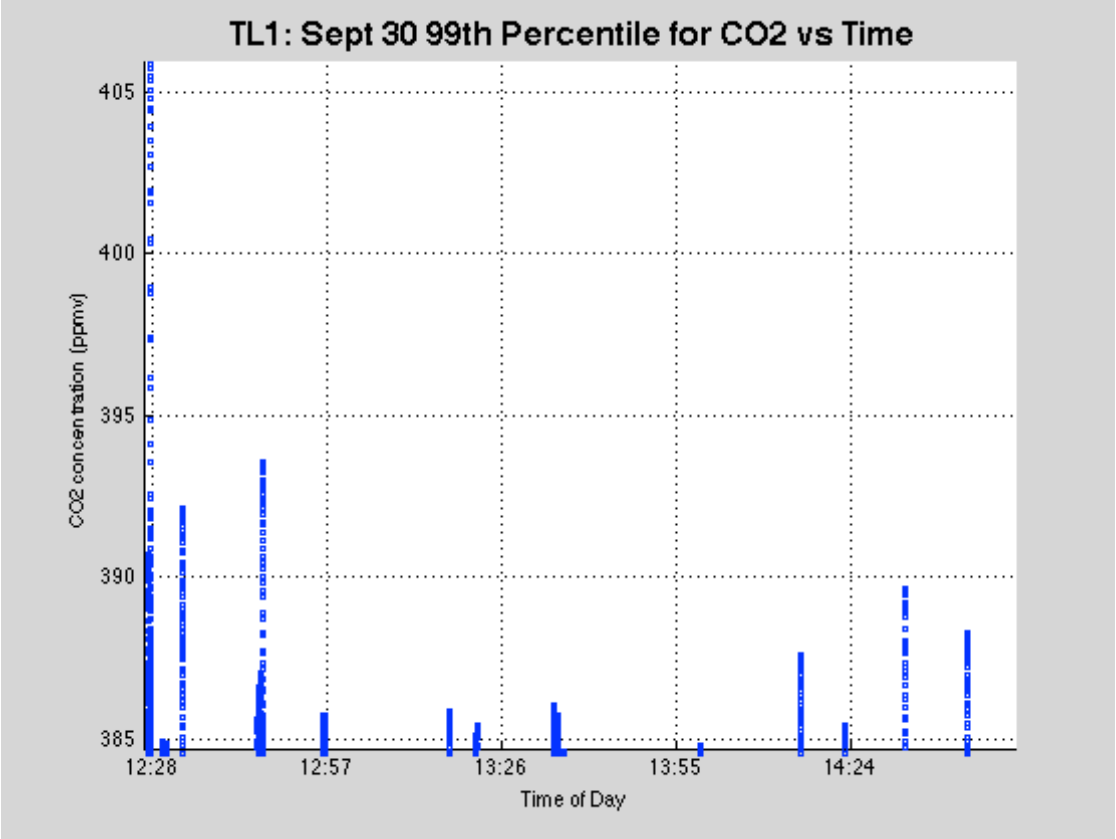
TL1: Sept 30 99th Percentile for CO2 vs Time
CO2 concentration (ppmv)
405
400
395
390
385
12:28
12:57
13:26
13:55
14:24
Time of Day

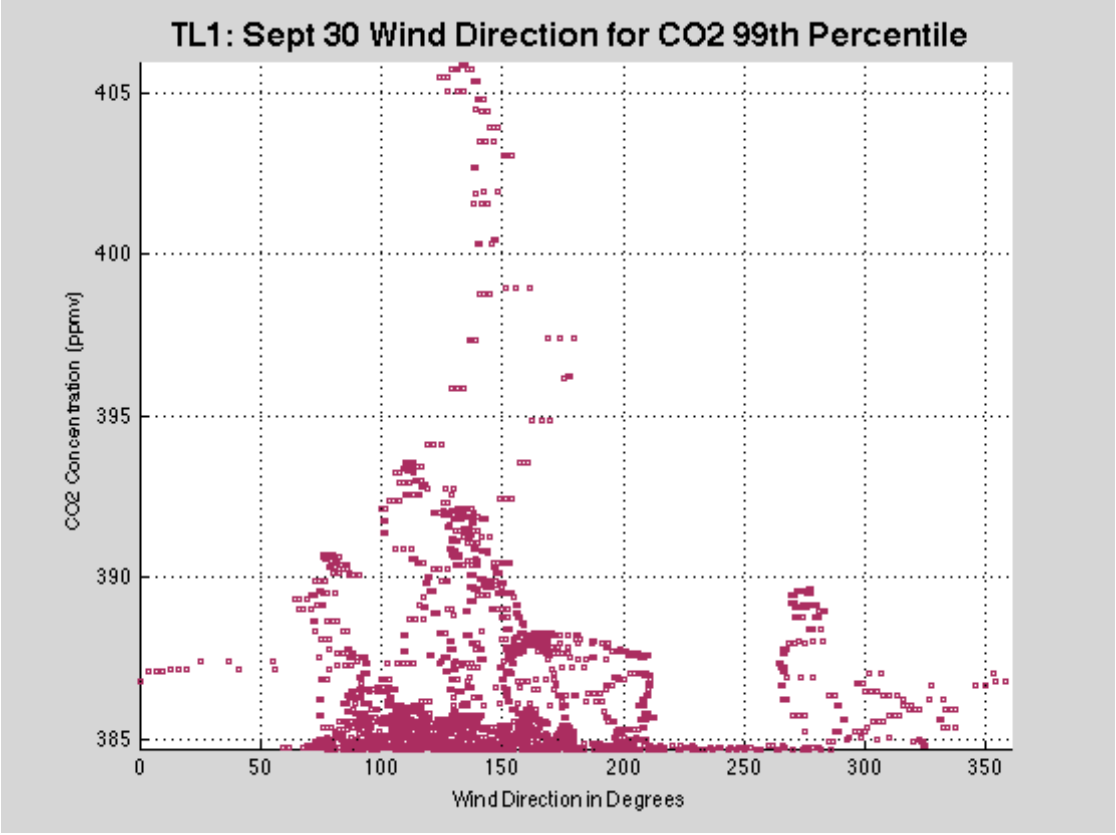
TL1: Sept 30 Wind Direction for CO2 99th Percentile
CO2 Concentration (ppmv)
405
400
395
390
385
0
50
100
150
200
250
300
350
Wind Direction in Degrees

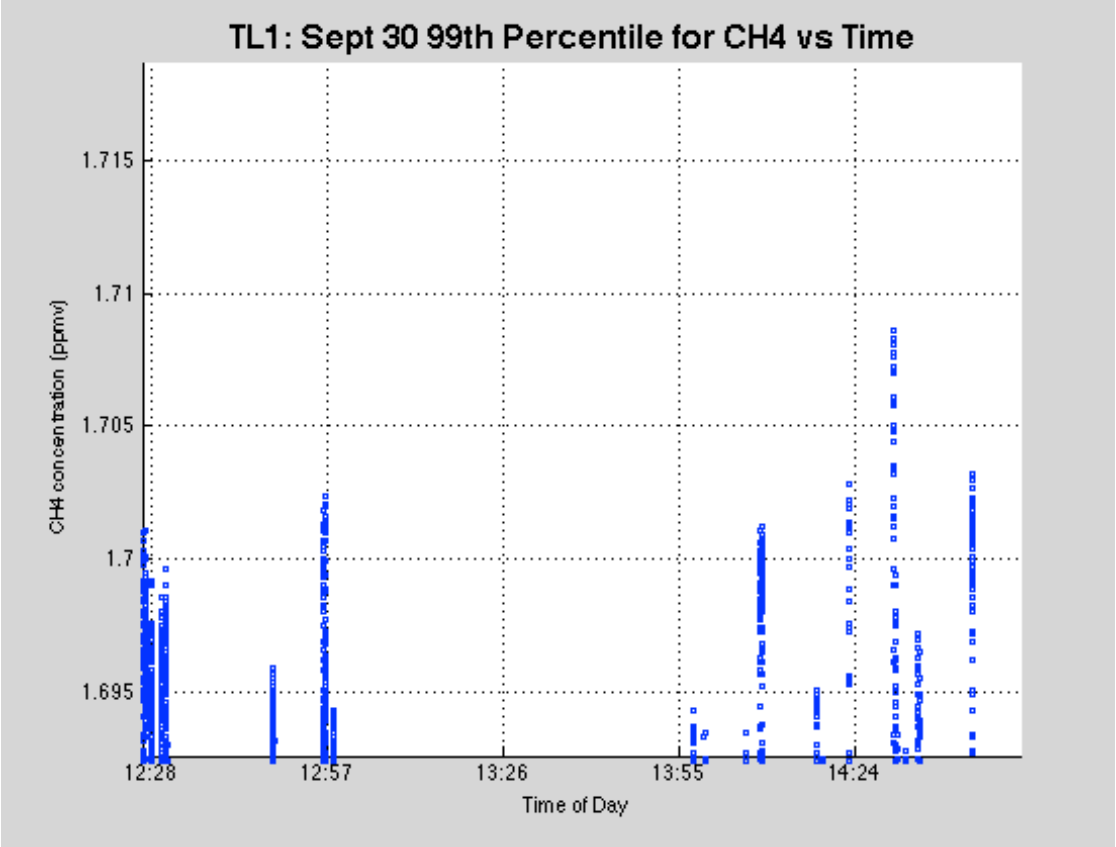
TL1: Sept 30 99th Percentile for CH4 vs Time
CH4 concentration (ppmv)
1.715
1.71
1.705
1.7
1.695
12:28
12:57
13:26
13:55
14:24
Time of Day

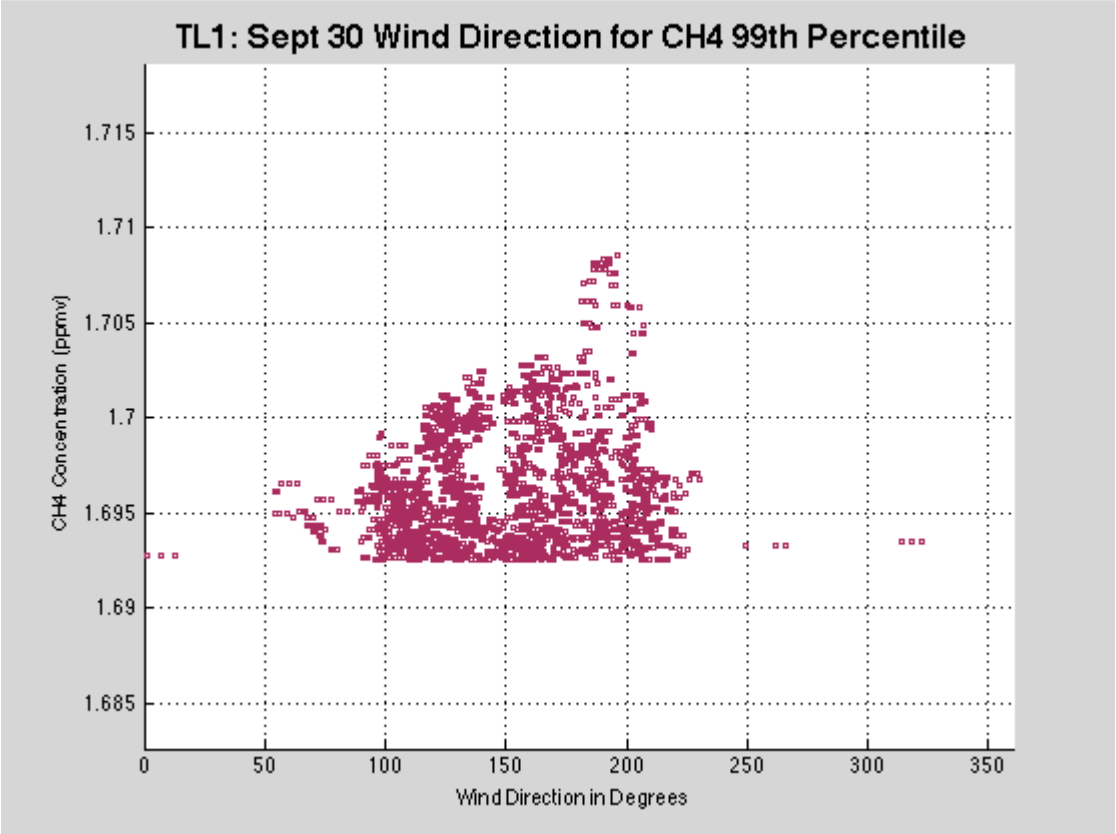
TL1: Sept 30 Wind Direction for CH4 99th Percentile
CH4 Concentration (ppmv)
1.715
1.71
1.705
1.7
1.695
1.69
1.685
0
50
100
150
200
250
300
350
Wind Direction in Degrees

D.12 Tuesday, October 1st, 2013

| | Maximum | Minimum | Average | Standard Deviation | 99th Percentile |
|---|---|---|---|---|---|
| $CO_2$ (ppmv) | 396.0878 | 379.9355 | 387.315 | 2.2062 | 392.0001 |
| $CH_4$ (ppmv) | 1.753 | 1.7008 | 1.7291 | 0.0106 | 1.7496 |
| UZ (m/s) | 2.4 | -3.4485 | -0.073 | 0.4689 | N/A |

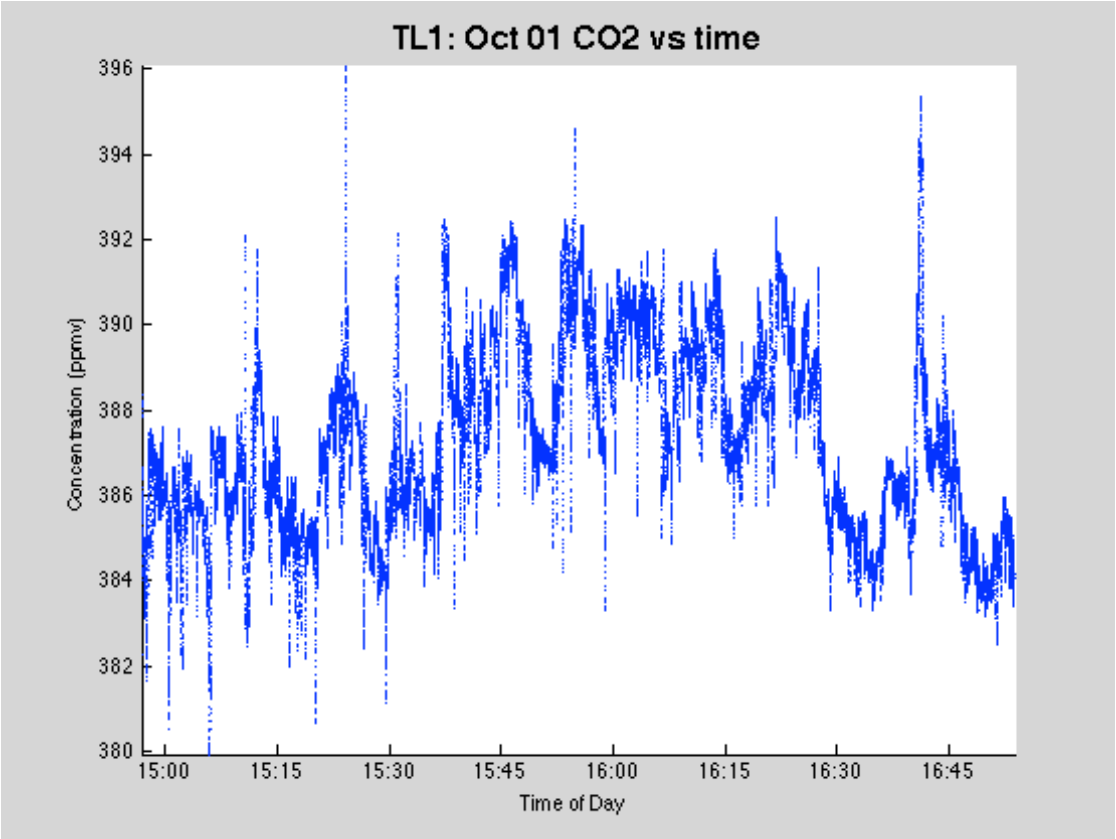

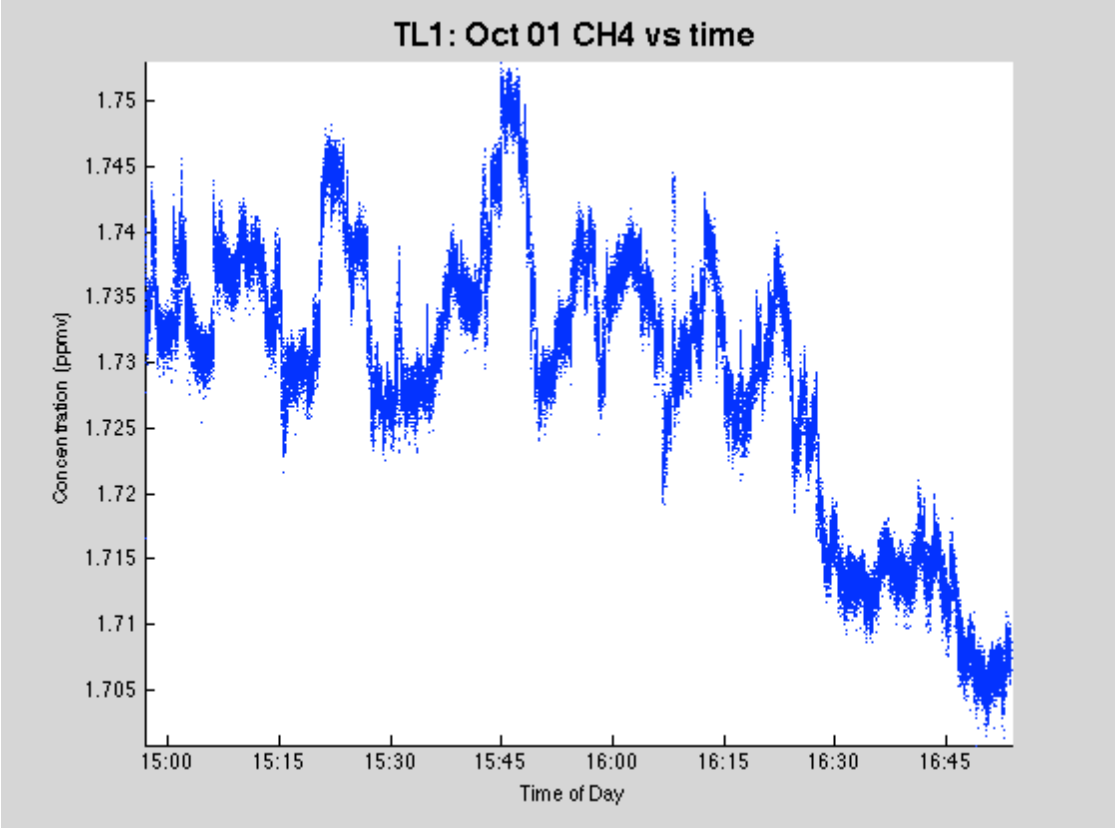
TL1: Oct 01 CH4 vs time
Concentration (ppmv)
1.75
1.745
1.74
1.735
1.73
1.725
1.72
1.715
1.71
1.705
15:00
15:15
15:30
15:45
16:00
16:15
16:30
16:45
Time of Day

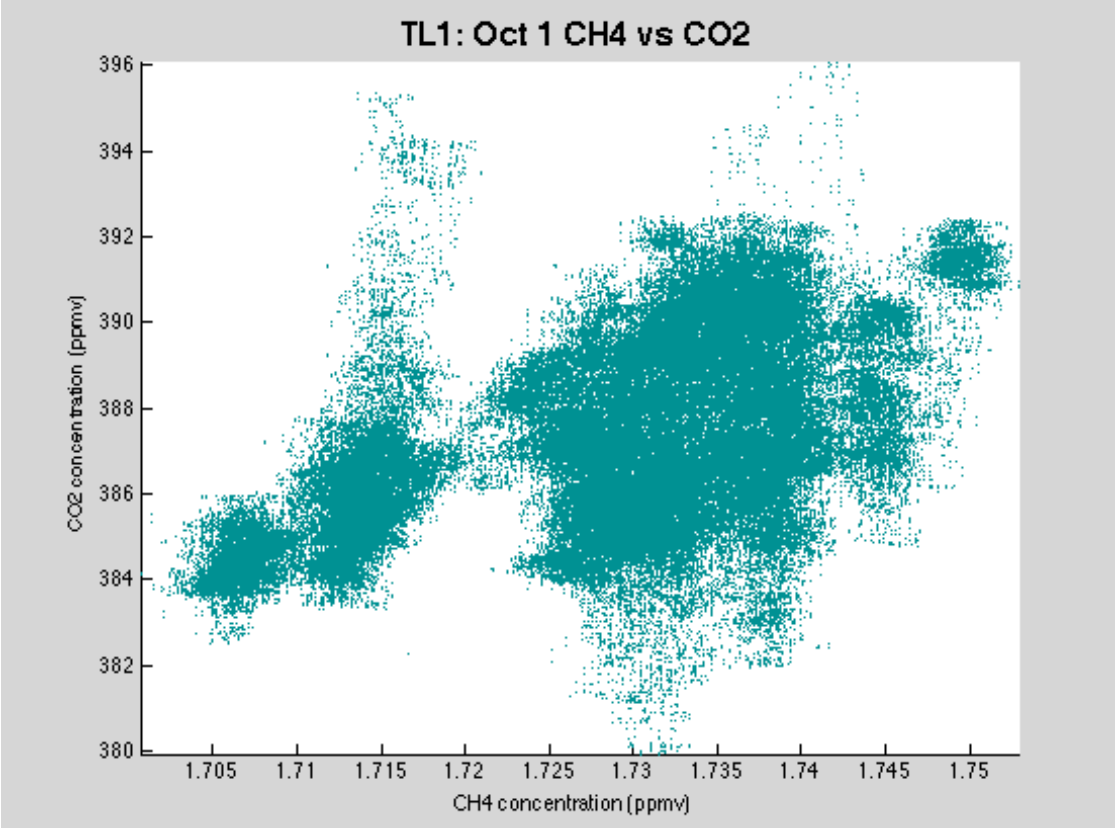
TL1: Oct 1 CH4 vs CO2
CO2 concentration (ppmv)
396
394
392
390
388
386
384
382
380
1.705
1.71
1.715
1.72
1.725
1.73
1.735
1.74
1.745
1.75
CH4 concentration (ppmv)

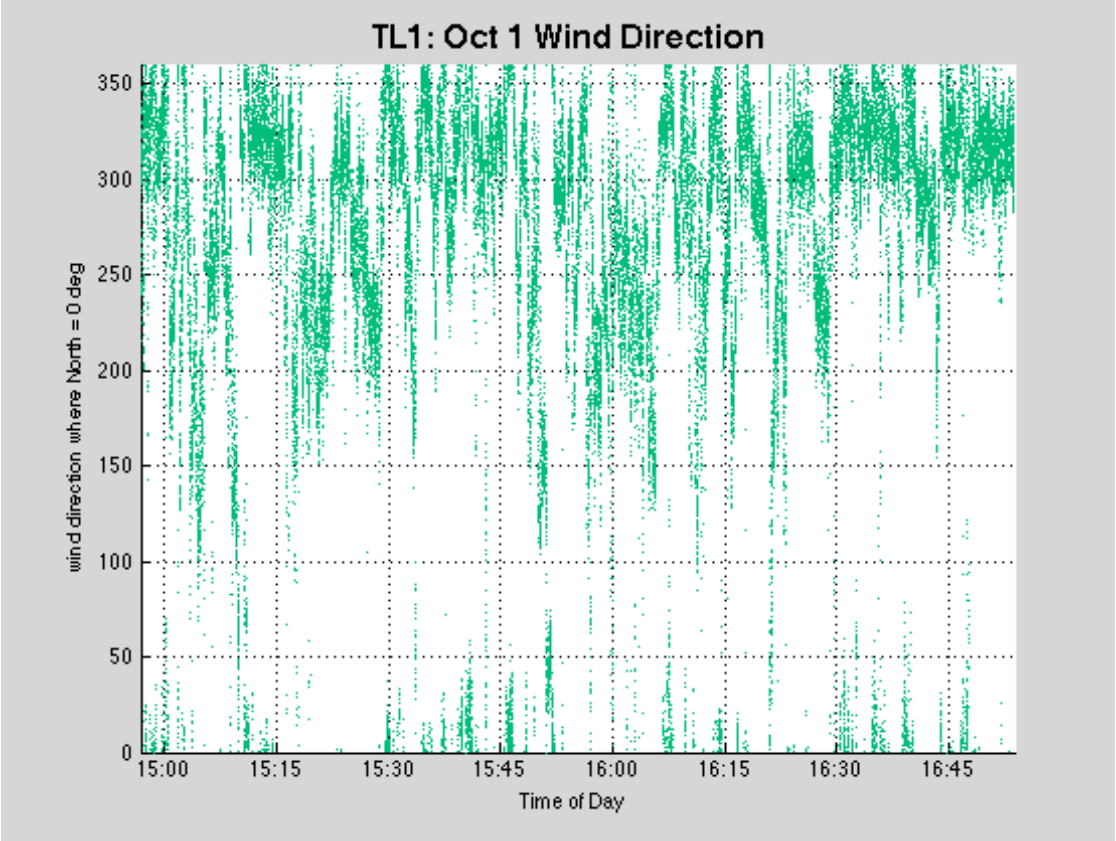
TL1: Oct 1 Wind Direction
wind direction where North = 0 deg
350
300
250
200
150
100
50
0
15:00
15:15
15:30
15:45
16:00
16:15
16:30
16:45
Time of Day

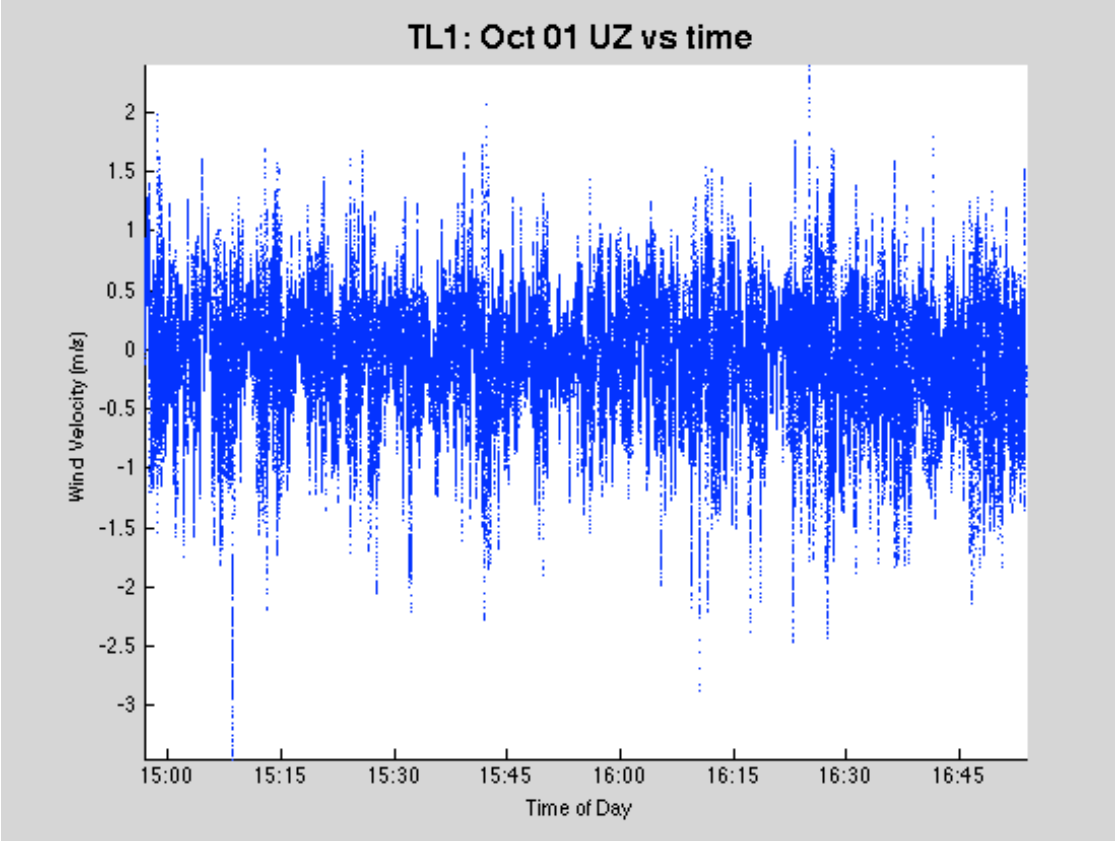
TL1: Oct 01 UZ vs time
Wind Velocity (m/s)
2
1.5
1
0.5
0
-0.5
-1
-1.5
-2
-2.5
-3
15:00
15:15
15:30
15:45
16:00
16:15
16:30
16:45
Time of Day

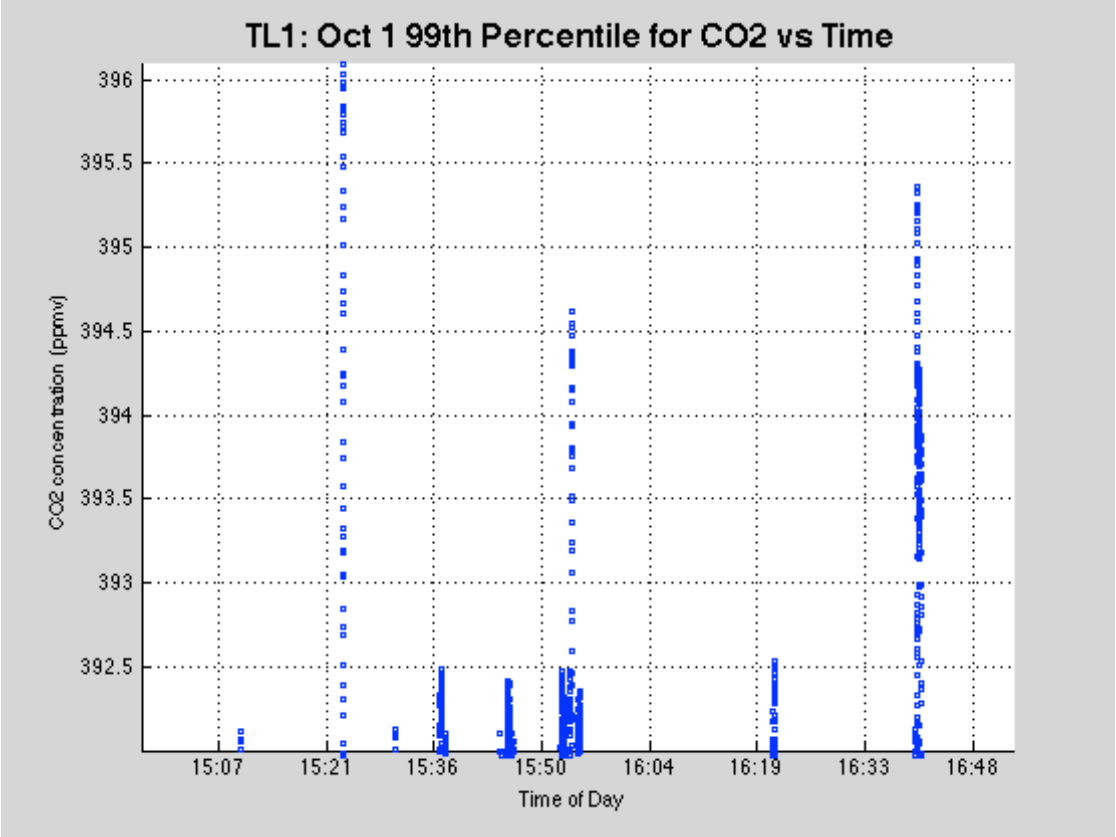
TL1: Oct 1 99th Percentile for CO2 vs Time
CO2 concentration (ppmv)
396
395.5
395
394.5
394
393.5
393
392.5
15:07
15:21
15:36
15:50
16:04
16:19
16:33
16:48
Time of Day

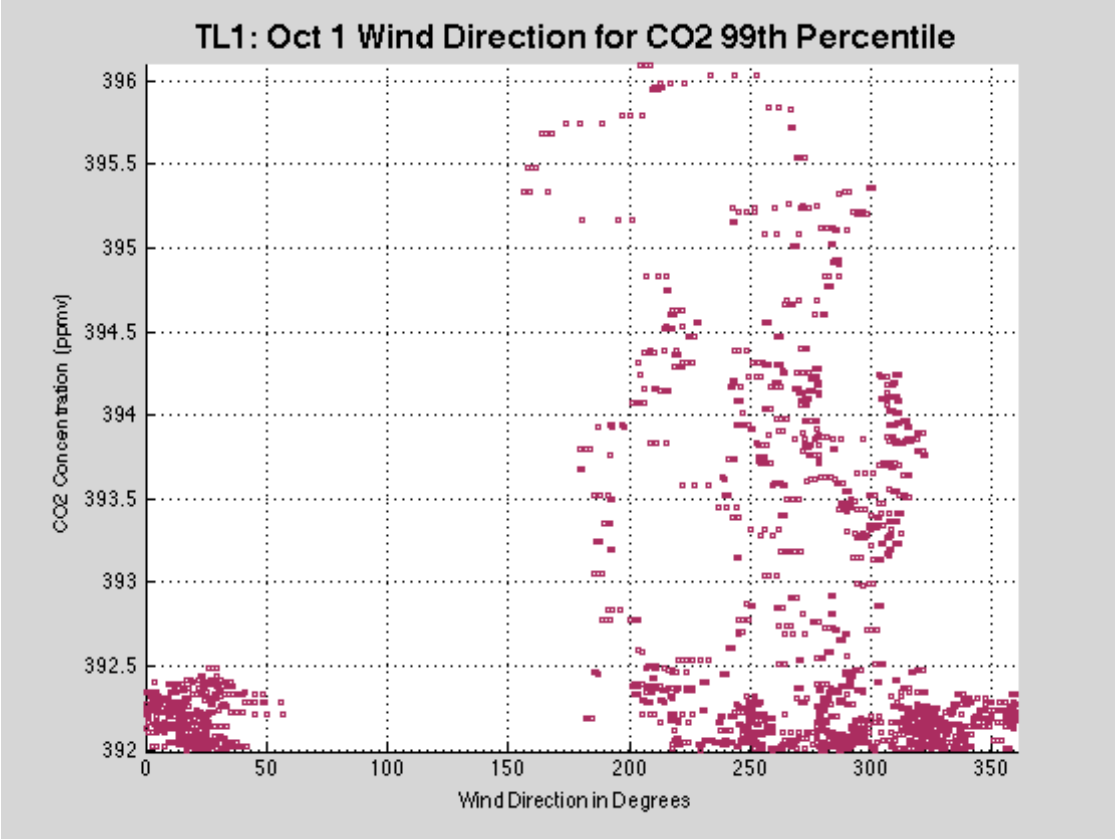
TL1: Oct 1 Wind Direction for CO2 99th Percentile
CO2 Concentration (ppmv)
396
395.5
395
394.5
394
393.5
393
392.5
392
0
50
100
150
200
250
300
350
Wind Direction in Degrees

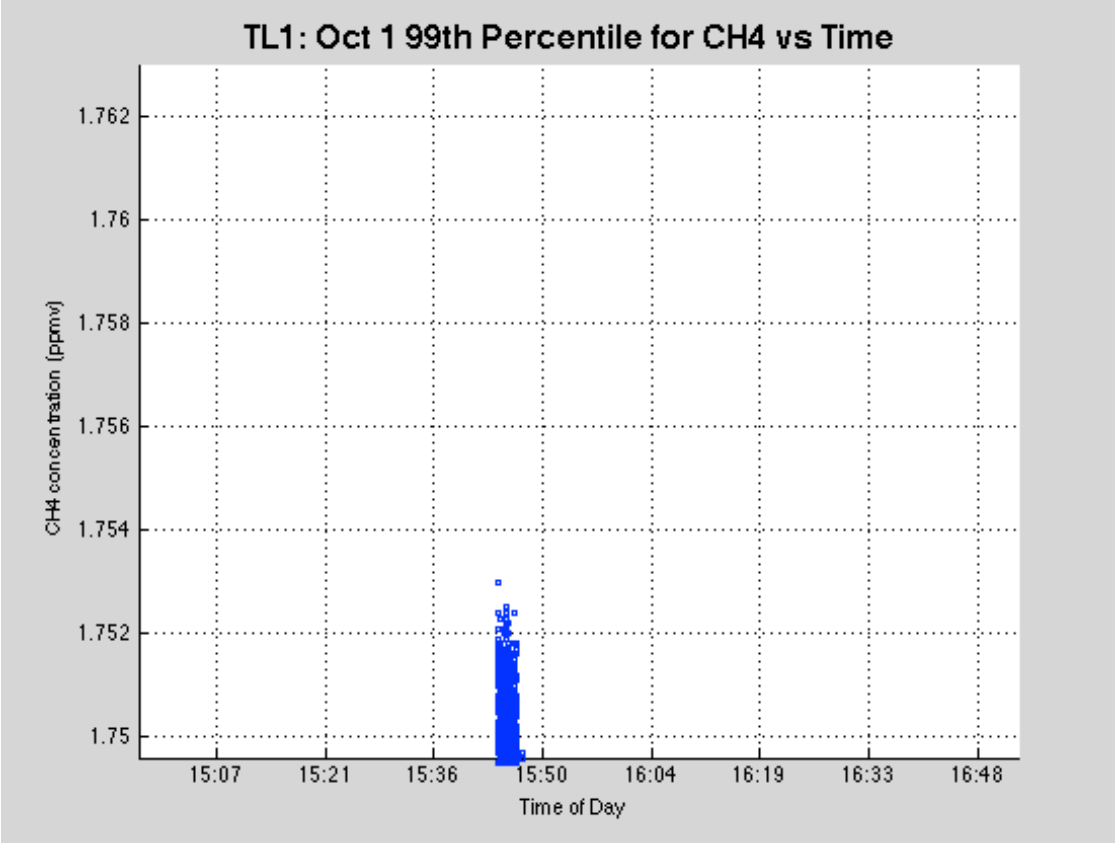
TL1: Oct 1 99th Percentile for CH4 vs Time
CH4 concentration (ppmv)
1.762
1.76
1.758
1.756
1.754
1.752
1.75
15:07
15:21
15:36
15:50
16:04
16:19
16:33
16:48
Time of Day

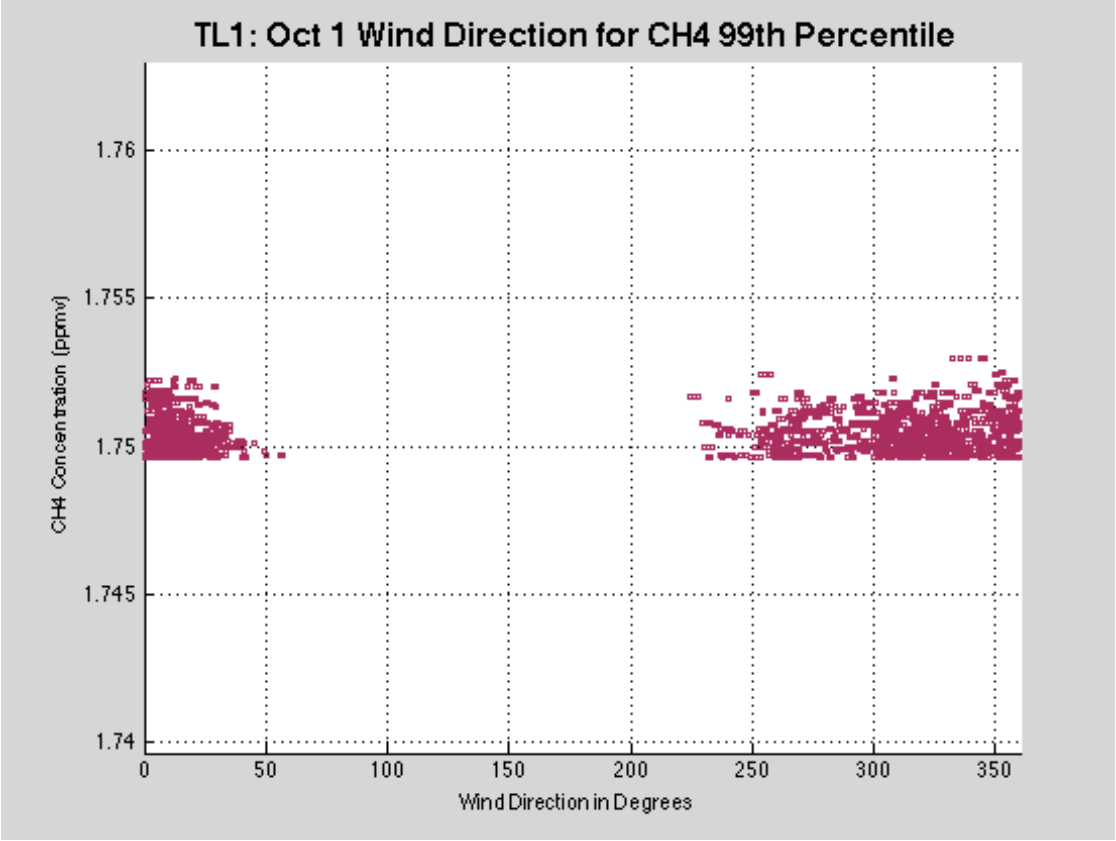
TL1: Oct 1 Wind Direction for CH4 99th Percentile
CH4 Concentration (ppmv)
1.76
1.755
1.75
1.745
1.74
0
50
100
150
200
250
300
350
Wind Direction in Degrees

## D.13 Wednesday, October 2nd, 2013

| | Maximum | Minimum | Average | Standard Deviation | 99th Percentile |
|---|---|---|---|---|---|
| $CO_2$ (ppmv) | 424.2596 | 386.7205 | 397.2707 | 2.7807 | 405.4138 |
| $CH_4$ (ppmv) | 1.818 | 1.7289 | 1.7711 | 0.0155 | 1.8053 |
| UZ (m/s) | 1.4487 | -1.8235 | -0.033 | 0.3495 | N/A |

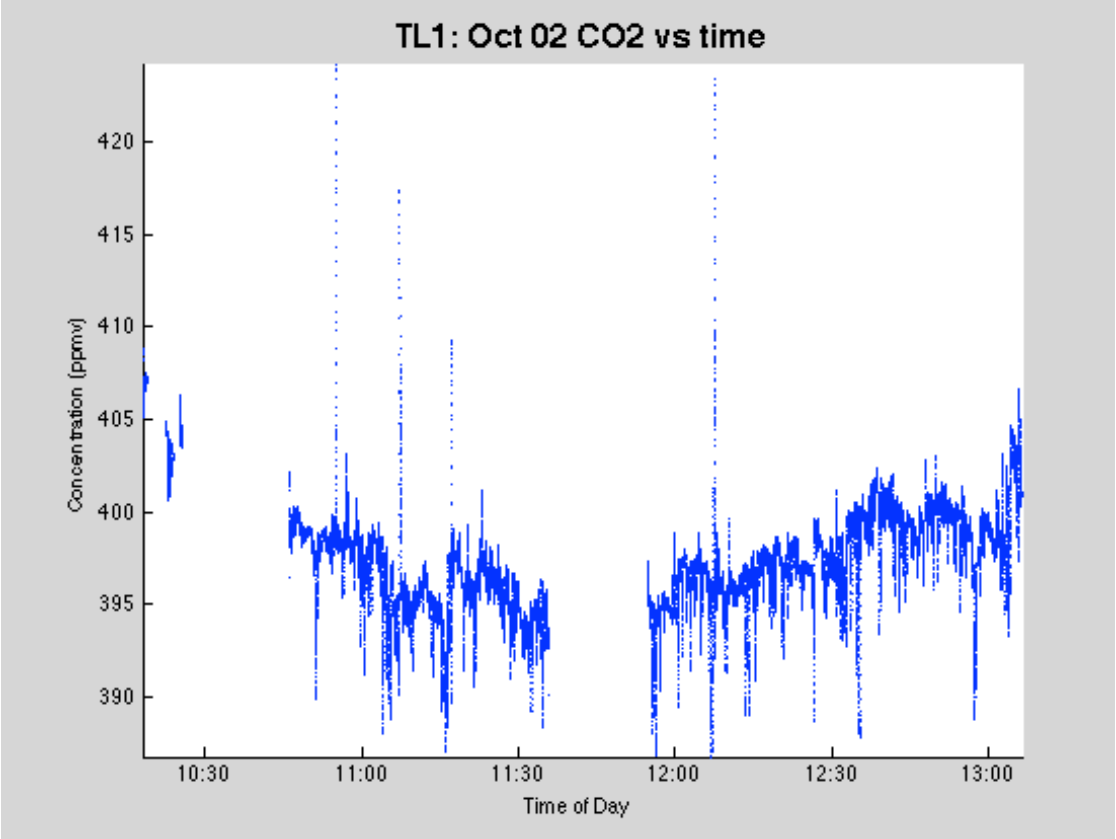

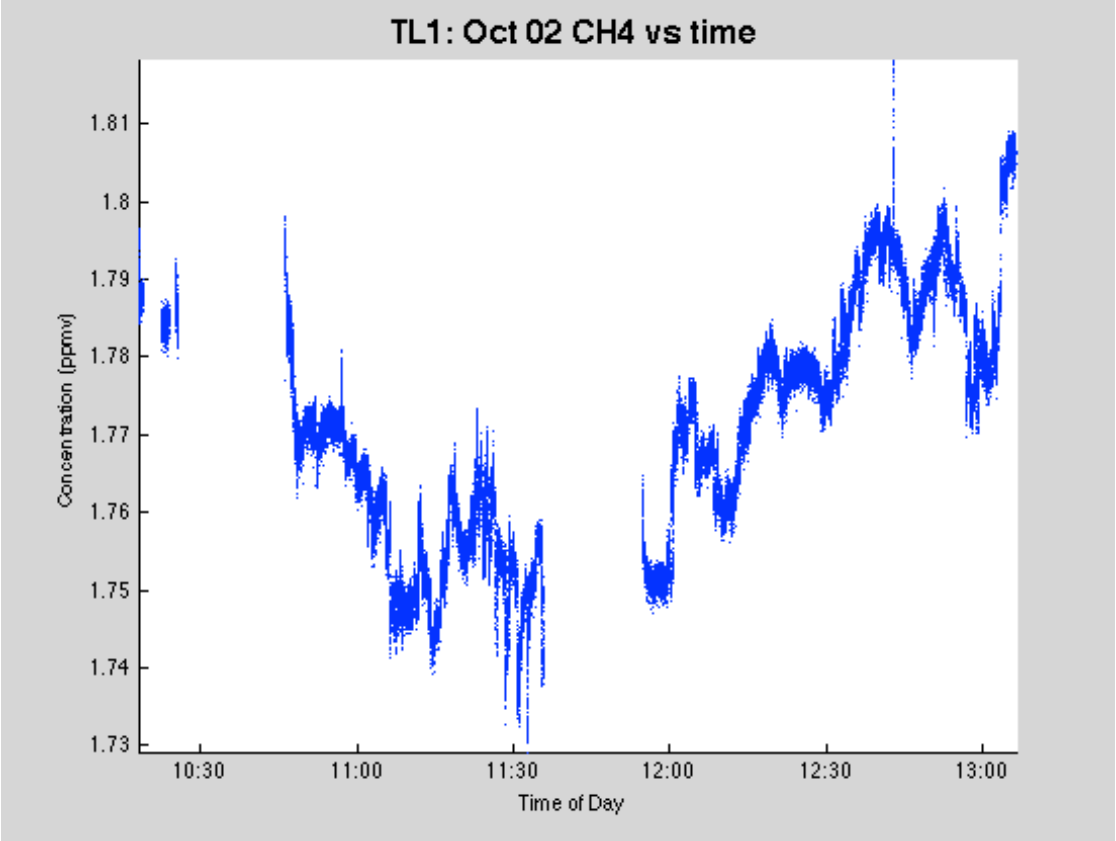
TL1: Oct 02 CH4 vs time
Concentration (ppmv)
1.81
1.8
1.79
1.78
1.77
1.76
1.75
1.74
1.73
10:30
11:00
11:30
12:00
12:30
13:00
Time of Day

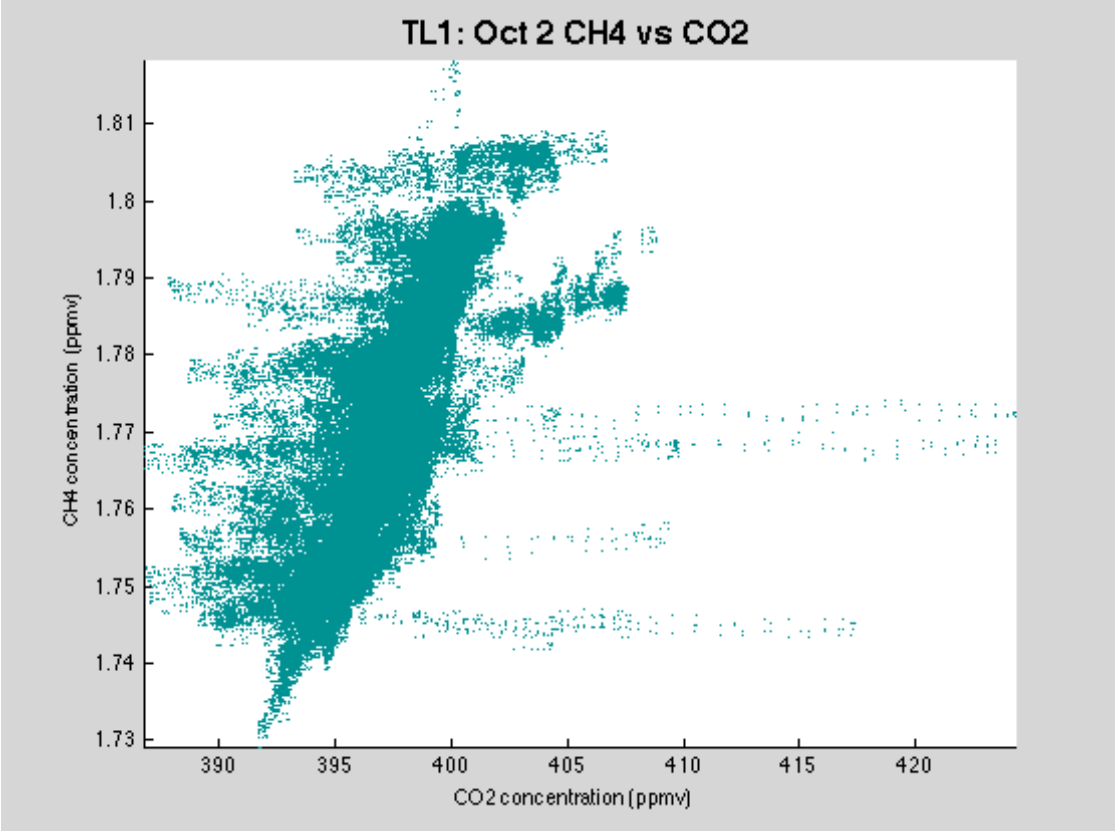
TL1: Oct 2 CH4 vs CO2
CH4 concentration (ppmv)
1.81
1.8
1.79
1.78
1.77
1.76
1.75
1.74
1.73
390
395
400
405
410
415
420
CO2 concentration (ppmv)

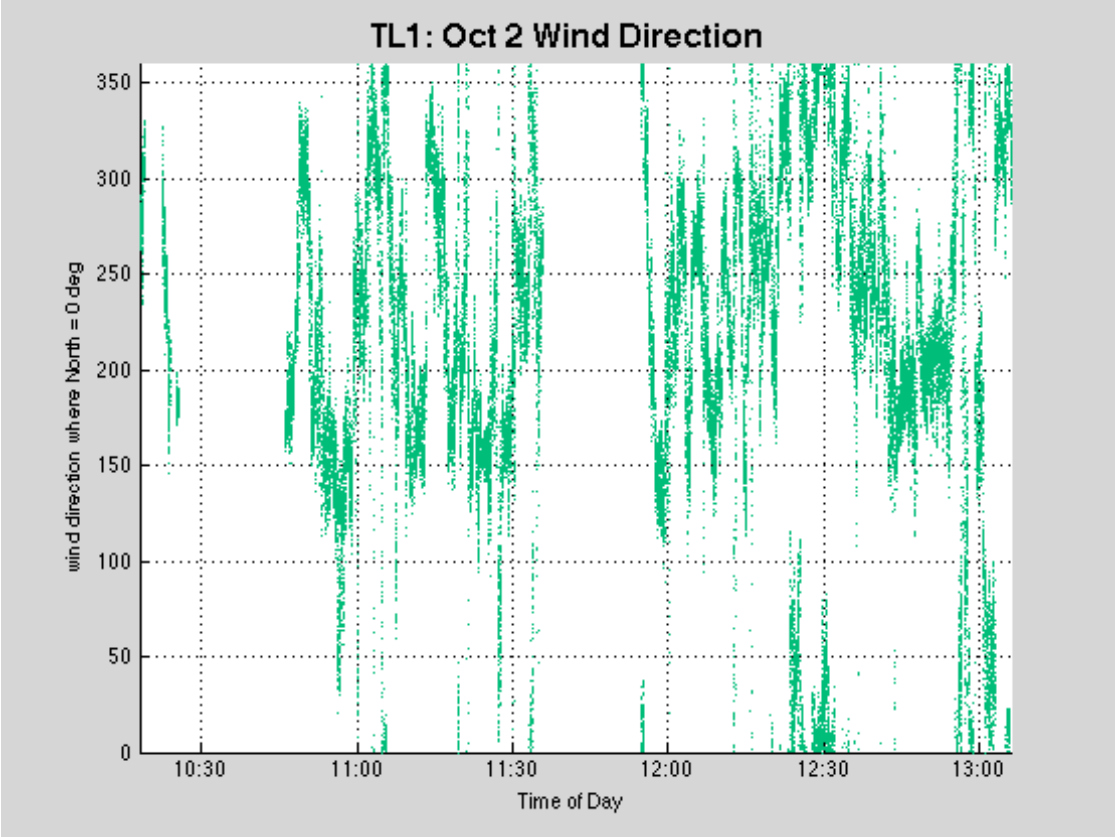
TL1: Oct 2 Wind Direction
wind direction where North = 0 deg
350
300
250
200
150
100
50
0
10:30
11:00
11:30
12:00
12:30
13:00
Time of Day

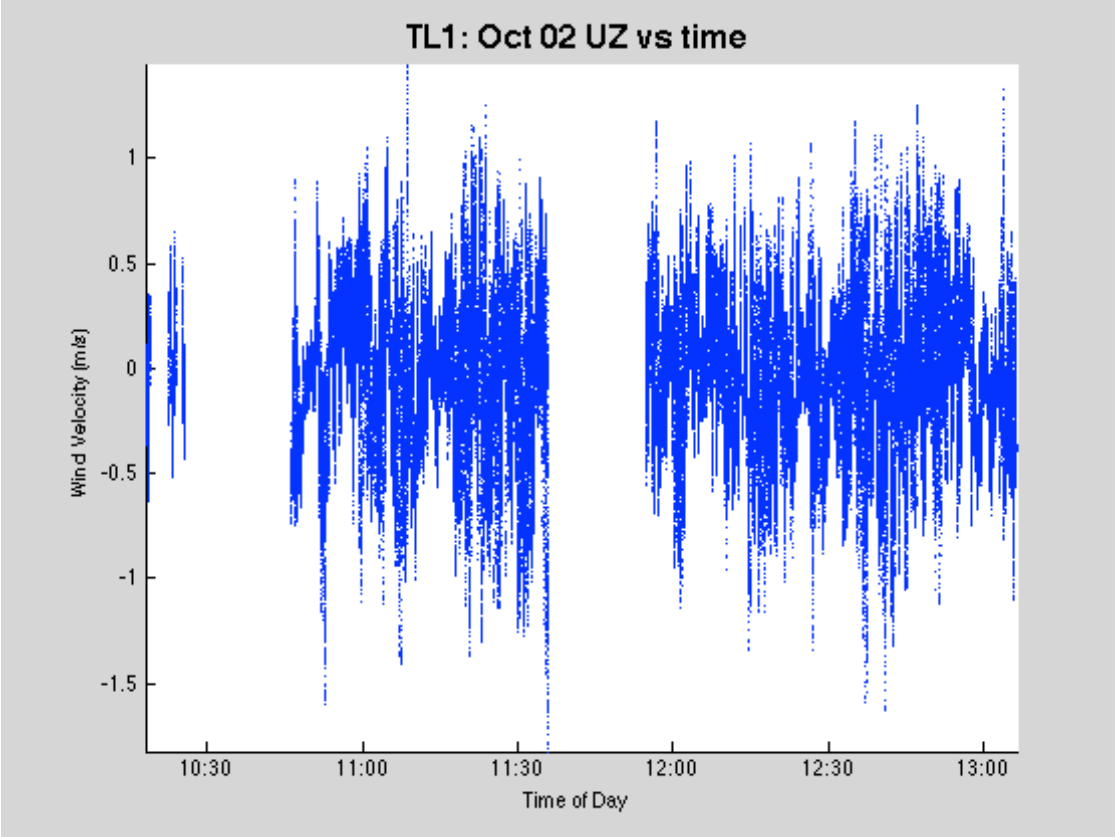
TL1: Oct 02 UZ vs time
Wind Velocity (m/s)
1
0.5
0
-0.5
-1
-1.5
10:30
11:00
11:30
12:00
12:30
13:00
Time of Day

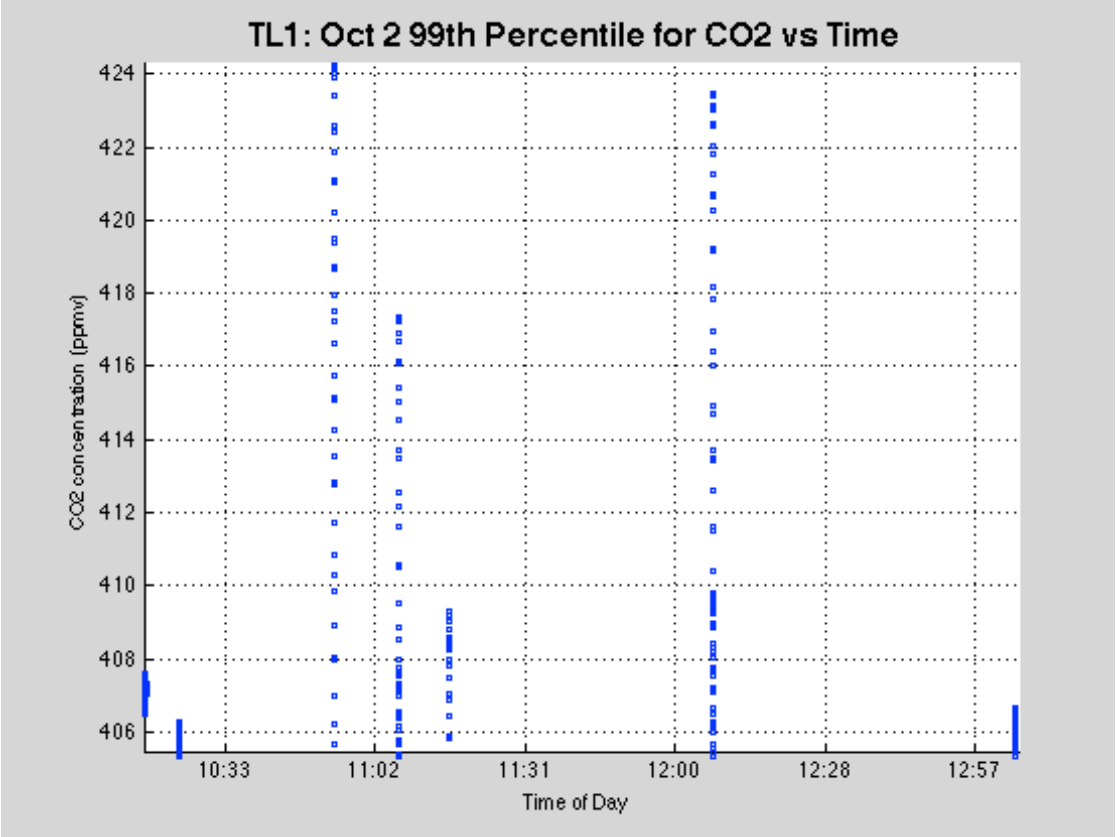
TL1: Oct 2 99th Percentile for CO2 vs Time
CO2 concentration (ppmv)
424
422
420
418
416
414
412
410
408
406
10:33
11:02
11:31
12:00
12:28
12:57
Time of Day

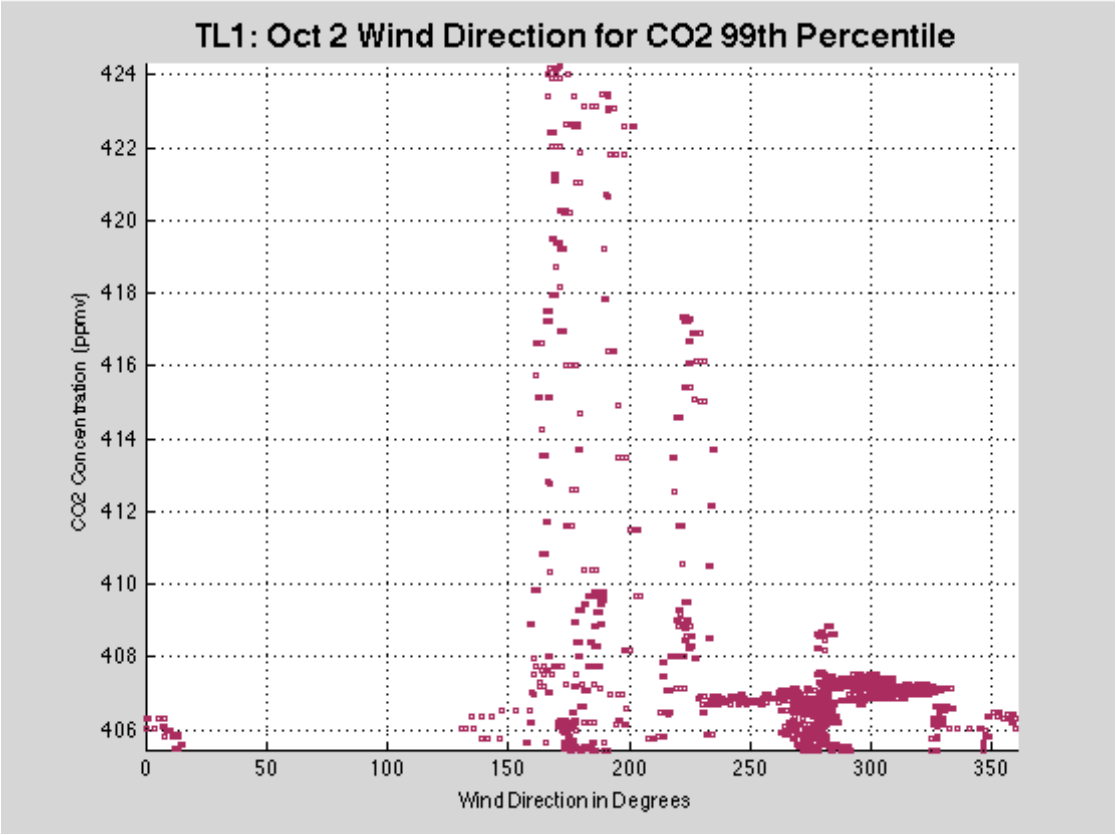
TL1: Oct 2 Wind Direction for CO2 99th Percentile
CO2 Concentration (ppmv)
424
422
420
418
416
414
412
410
408
406
0
50
100
150
200
250
300
350
Wind Direction in Degrees

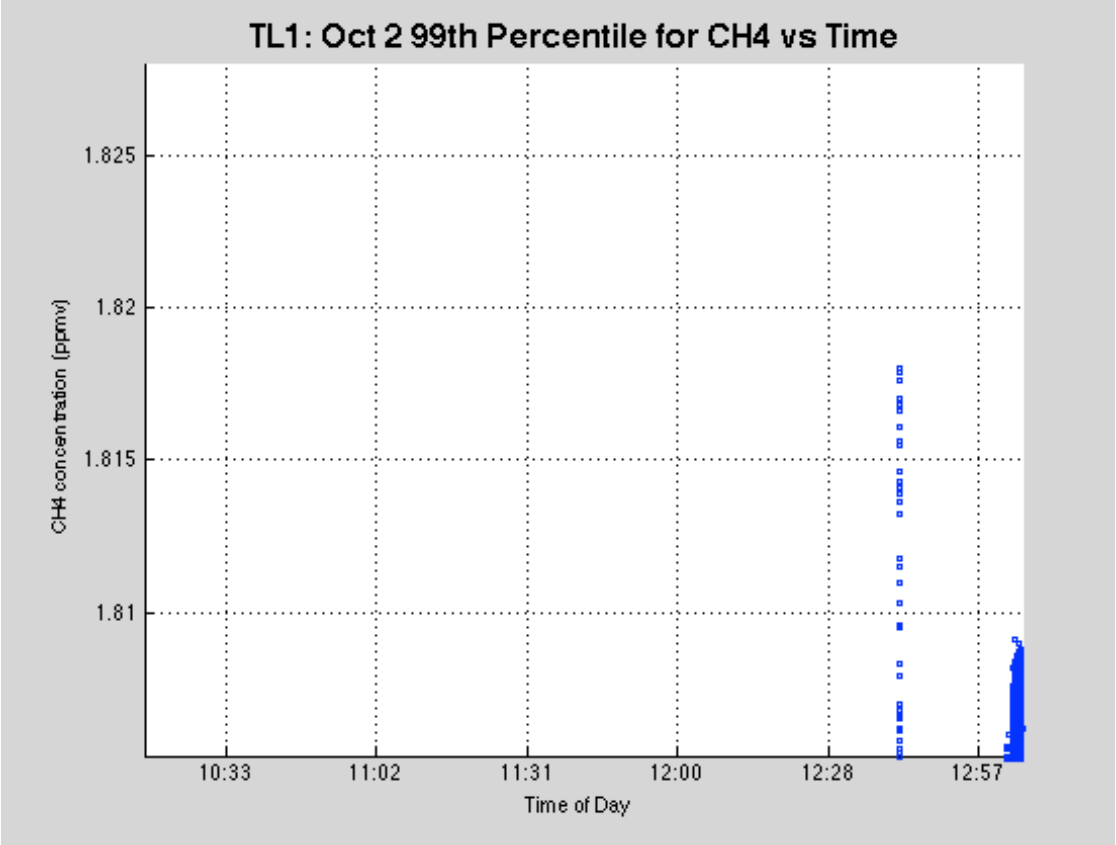
TL1: Oct 2 99th Percentile for CH4 vs Time
CH4 concentration (ppmv)
1.825
1.82
1.815
1.81
10:33
11:02
11:31
12:00
12:28
12:57
Time of Day

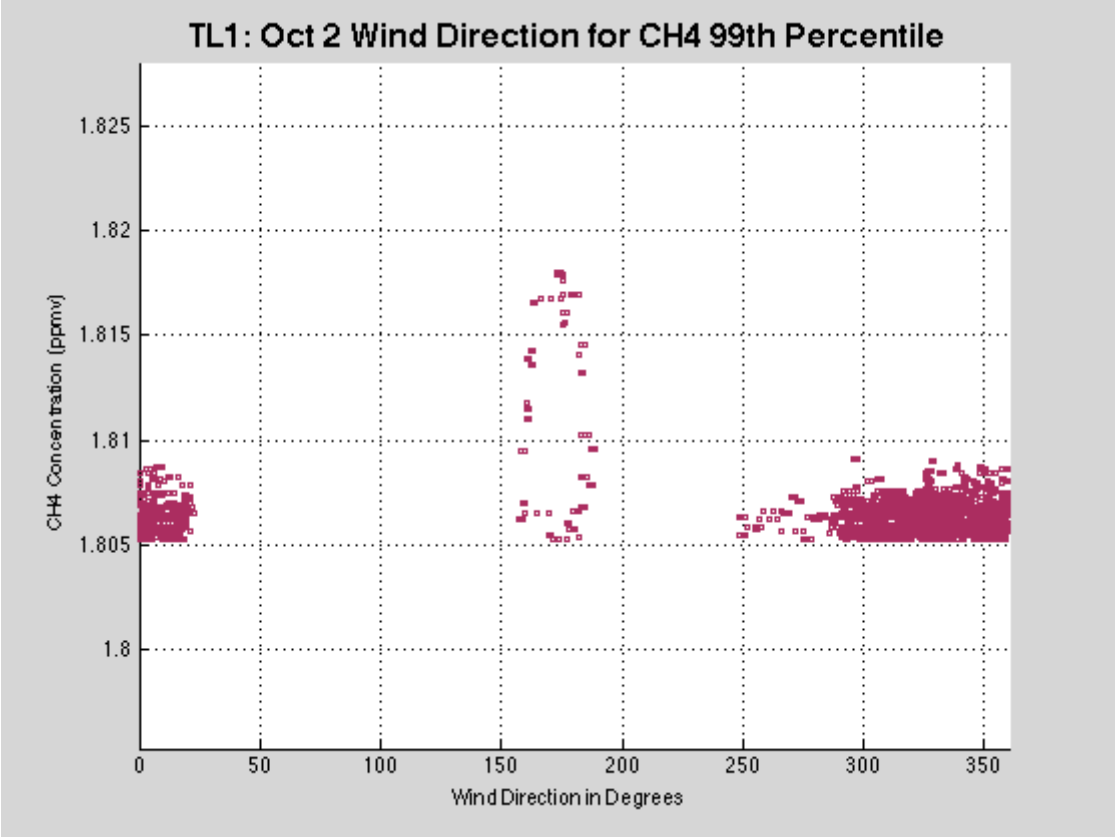
TL1: Oct 2 Wind Direction for CH4 99th Percentile
CH4 Concentration (ppmv)
1.825
1.82
1.815
1.81
1.805
1.8
0
50
100
150
200
250
300
350
Wind Direction in Degrees

D.14 Friday, October 4th, 2013

| | Maximum | Minimum | Average | Standard Deviation | 99th Percentile |
|---|---|---|---|---|---|
| $CO_2$ (ppmv) | 415.2075 | 333.6254 | 388.0341 | 2.7813 | 382.891 |
| $CH_4$ (ppmv) | 1.7766 | 1.7031 | 1.7367 | 0.0049 | 1.7505 |
| UZ (m/s) | 1.7983 | -1.8585 | -0.0211 | 0.3441 | N/A |

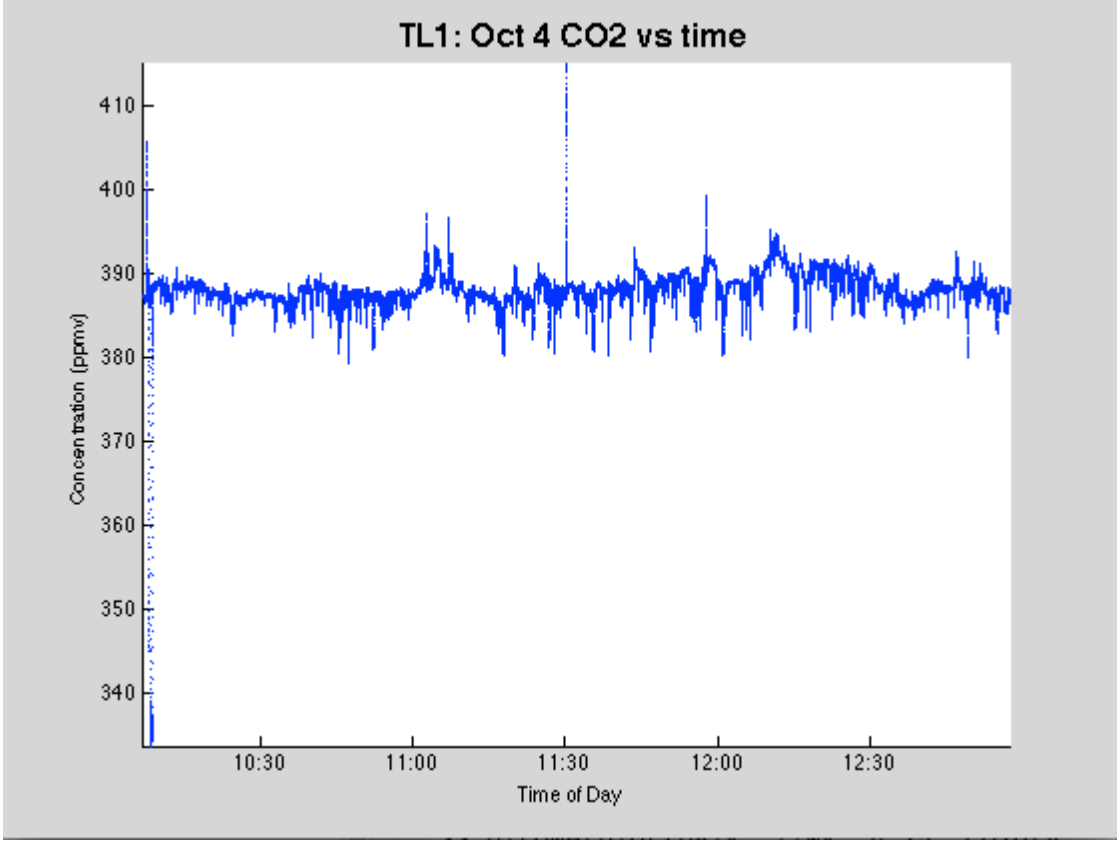

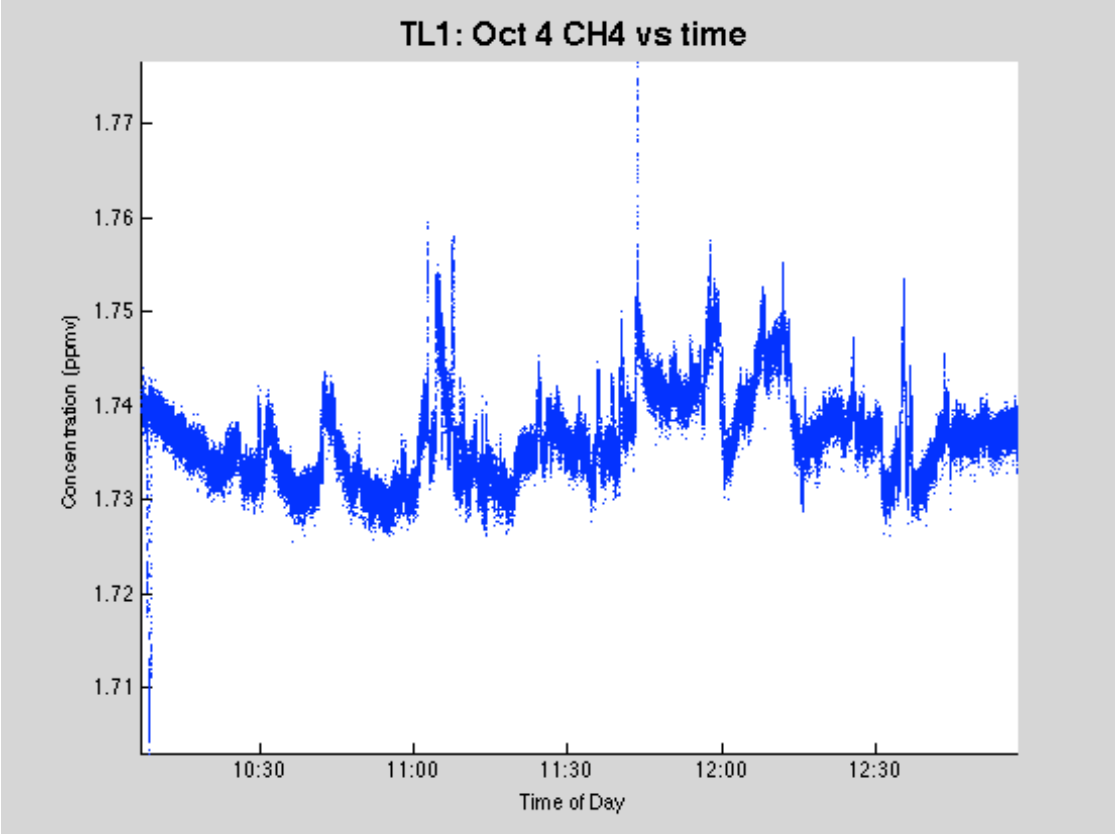
TL1: Oct 4 CH4 vs time
Concentration (ppmv)
1.77
1.76
1.75
1.74
1.73
1.72
1.71
10:30
11:00
11:30
12:00
12:30
Time of Day

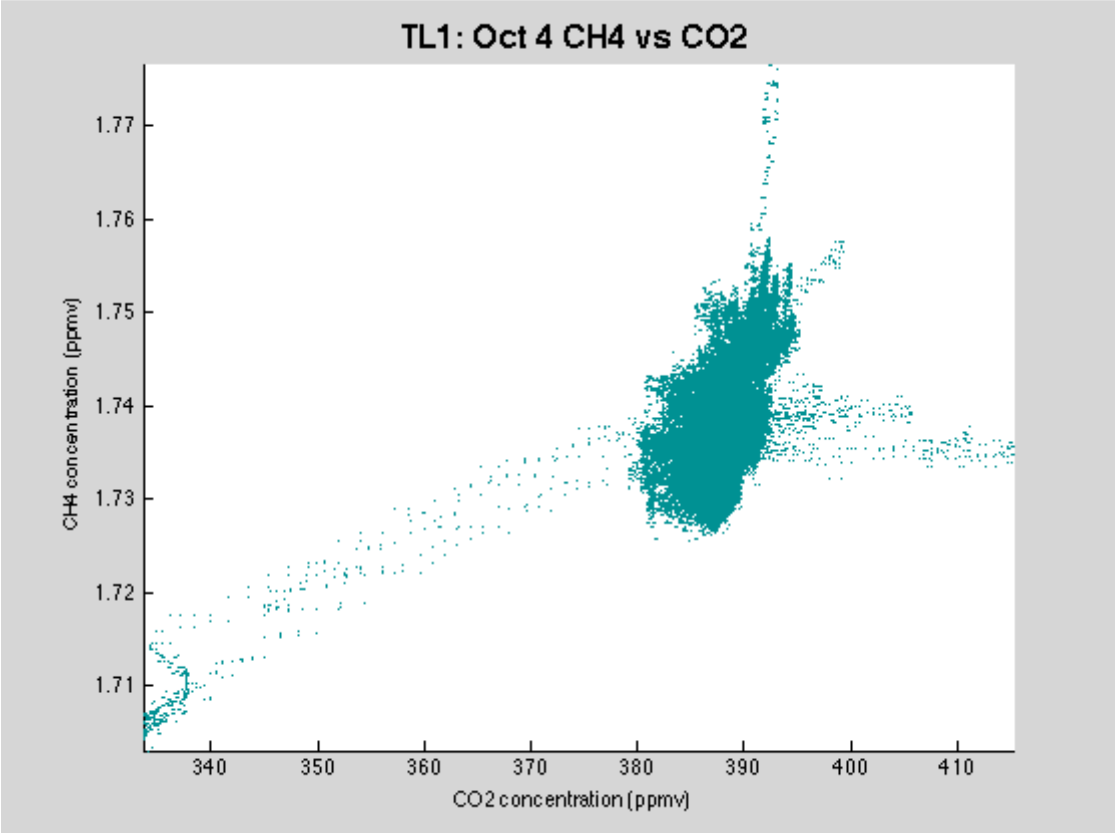
TL1: Oct 4 CH4 vs CO2
CH4 concentration (ppmv)
1.77
1.76
1.75
1.74
1.73
1.72
1.71
340
350
360
370
380
390
400
410
CO2 concentration (ppmv)

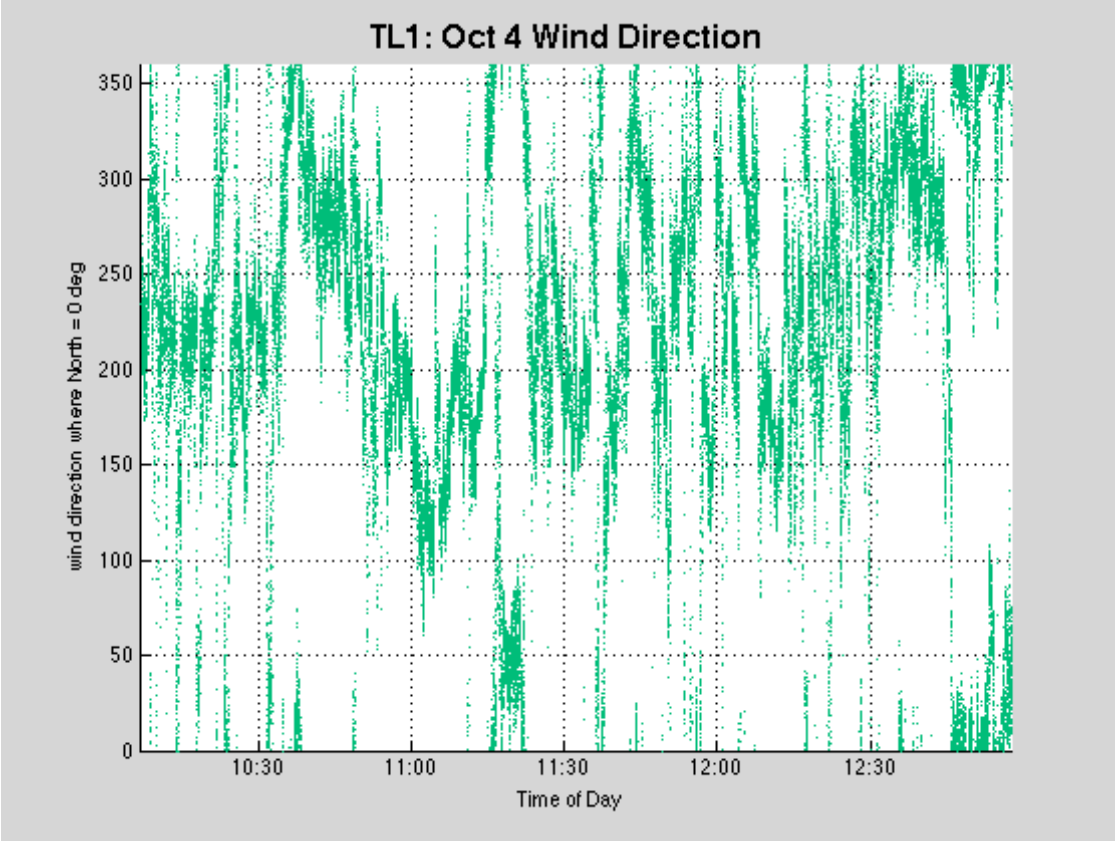
TL1: Oct 4 Wind Direction
wind direction where North = 0 deg
350
300
250
200
150
100
50
0
10:30
11:00
11:30
12:00
12:30
Time of Day

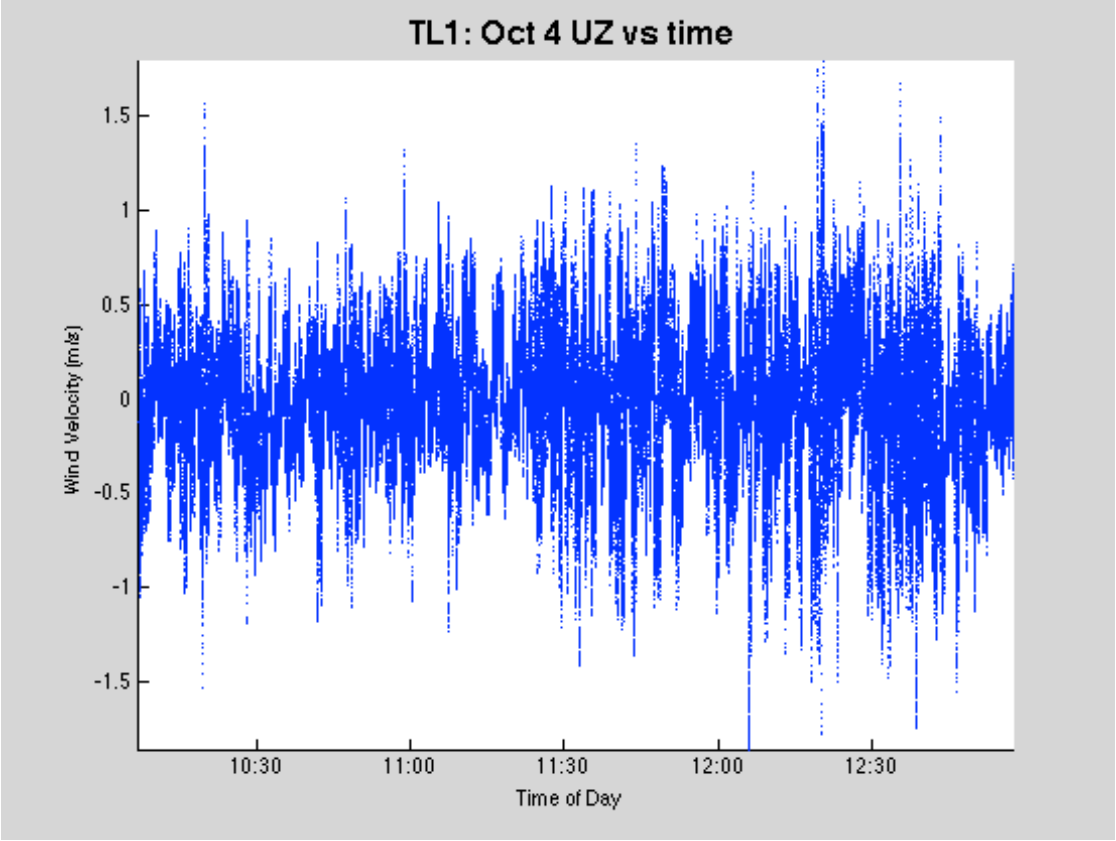
TL1: Oct 4 UZ vs time
Wind Velocity (m/s)
1.5
1
0.5
0
-0.5
-1
-1.5
10:30
11:00
11:30
12:00
12:30
Time of Day

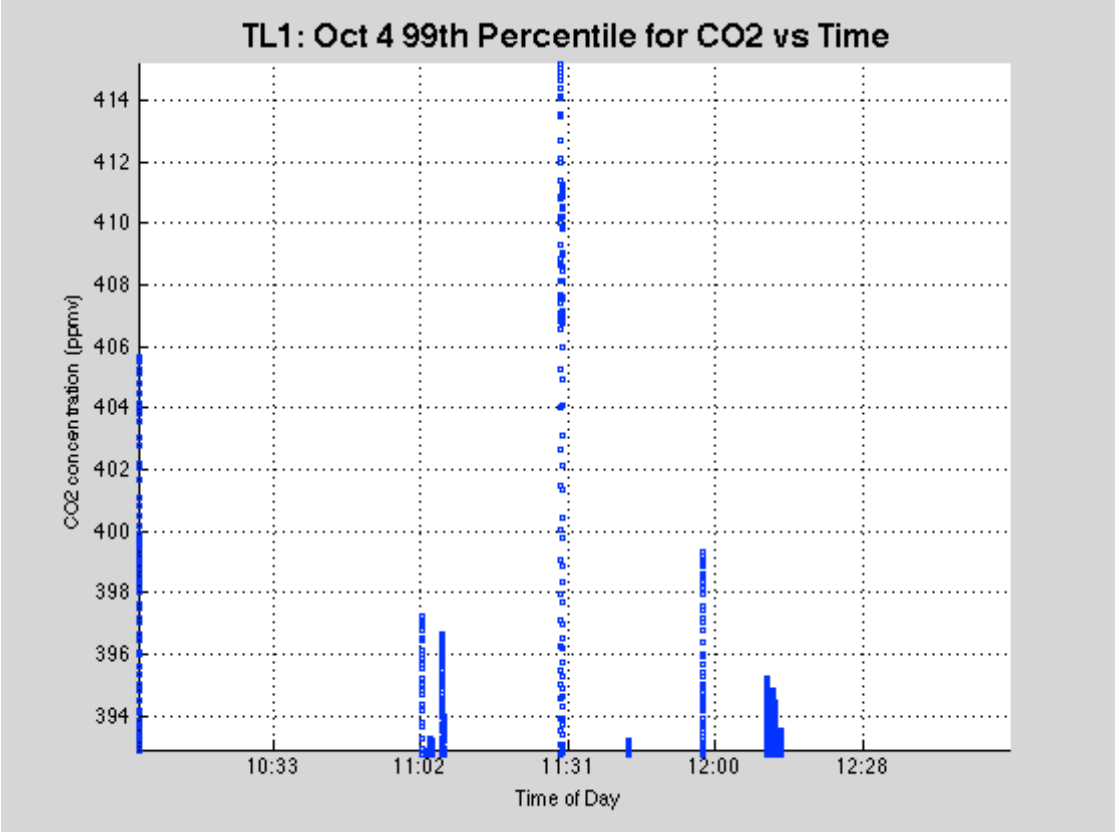
TL1: Oct 4 99th Percentile for CO2 vs Time
CO2 concentration (ppmv)
414
412
410
408
406
404
402
400
398
396
394
10:33
11:02
11:31
12:00
12:28
Time of Day

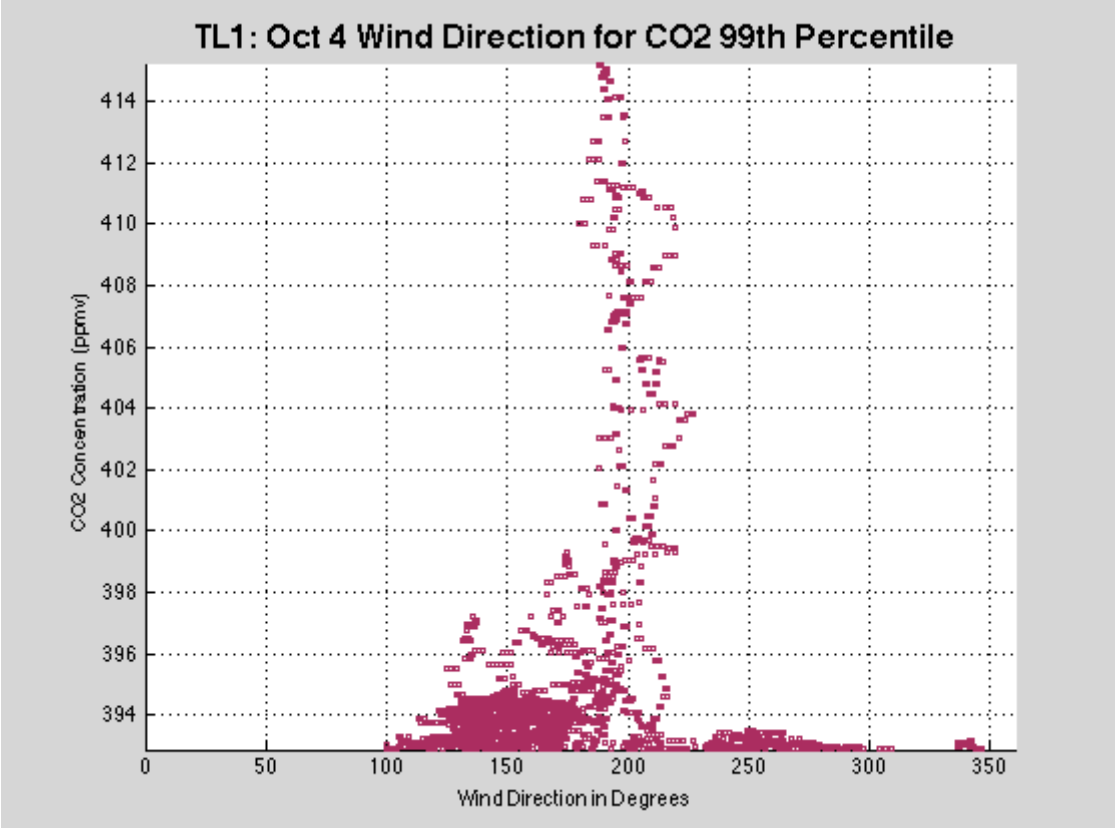
TL1: Oct 4 Wind Direction for CO2 99th Percentile
CO2 Concentration (ppmv)
414
412
410
408
406
404
402
400
398
396
394
0
50
100
150
200
250
300
350
Wind Direction in Degrees

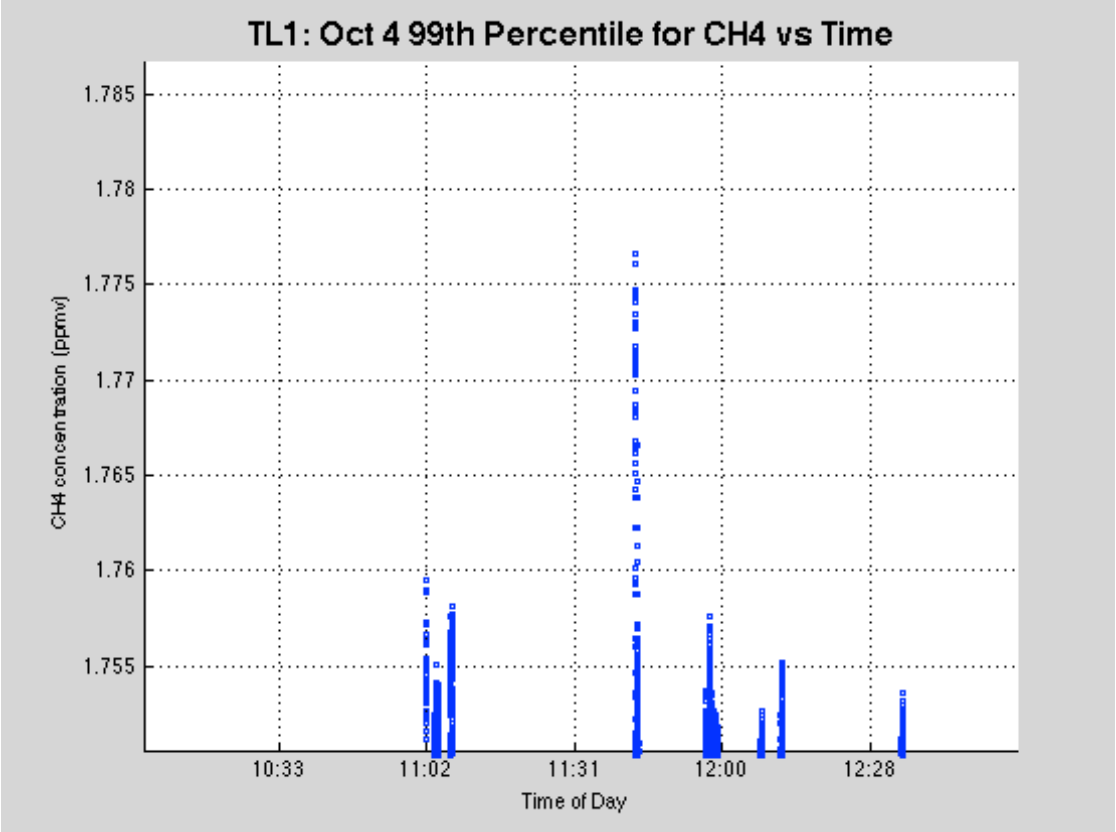
TL1: Oct 4 99th Percentile for CH4 vs Time
CH4 concentration (ppmv)
1.785
1.78
1.775
1.77
1.765
1.76
1.755
10:33
11:02
11:31
12:00
12:28
Time of Day

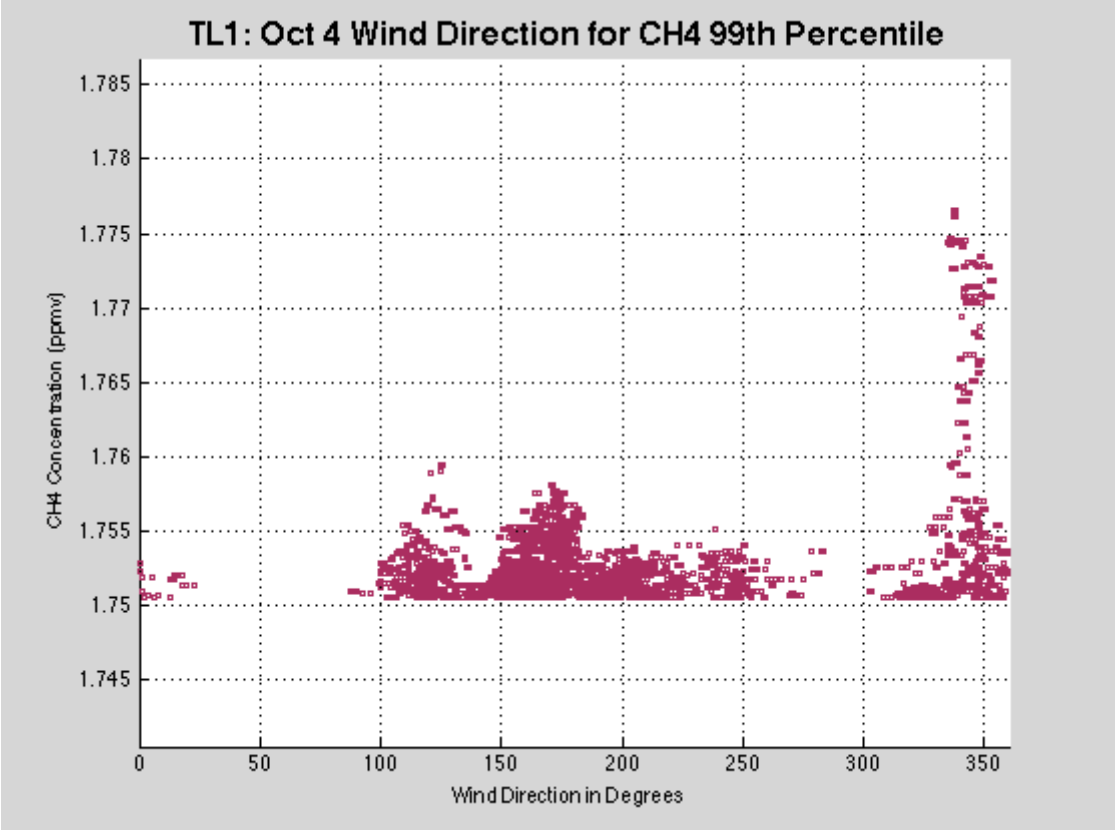
TL1: Oct 4 Wind Direction for CH4 99th Percentile
CH4 Concentration (ppmv)
1.785
1.78
1.775
1.77
1.765
1.76
1.755
1.75
1.745
0
50
100
150
200
250
300
350
Wind Direction in Degrees

D.15 Monday, October 7th, 2013

| | Maximum | Minimum | Average | Standard Deviation | 99th Percentile |
|---|---|---|---|---|---|
| $CO_2$ (ppmv) | 496.2143 | 384.3631 | 395.8359 | 6.5228 | 405.5325 |
| $CH_4$ (ppmv) | 1.8344 | 1.699 | 1.7607 | 0.0475 | 1.829 |
| UZ (m/s) | 1.2952 | -1.42 | -0.0491 | 0.3165 | N/A |

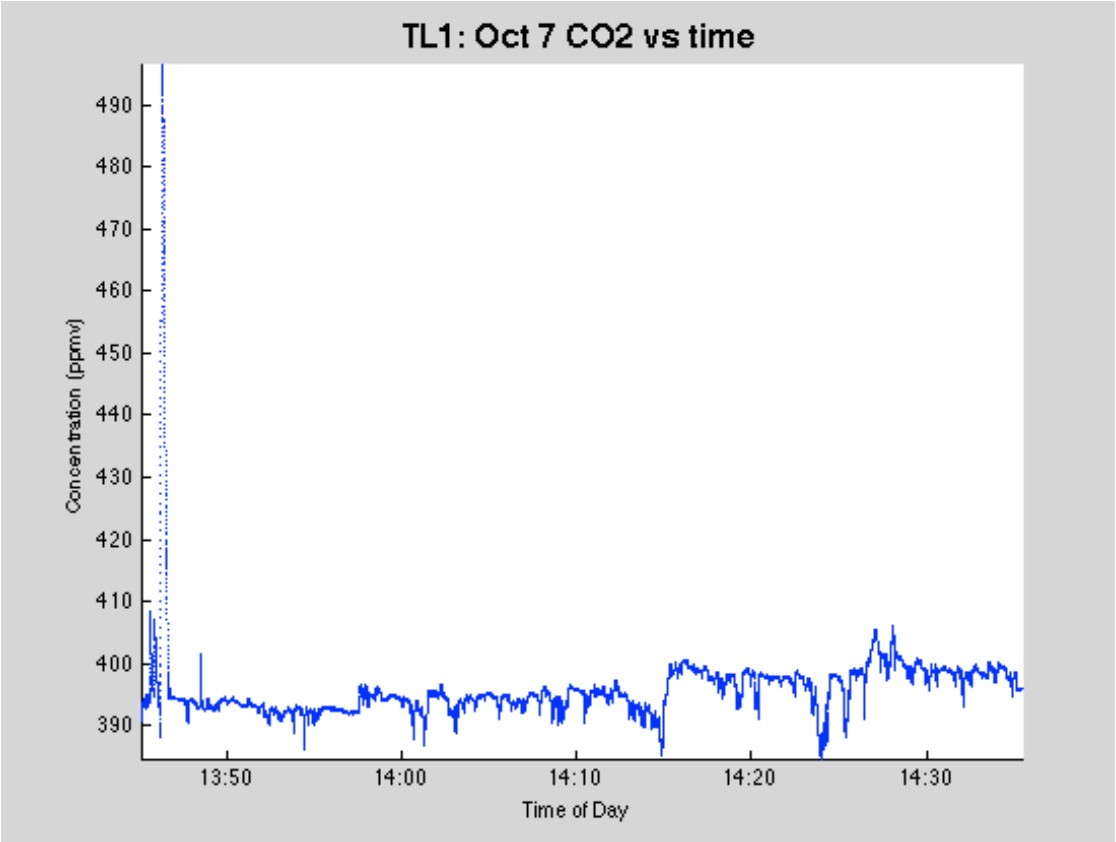

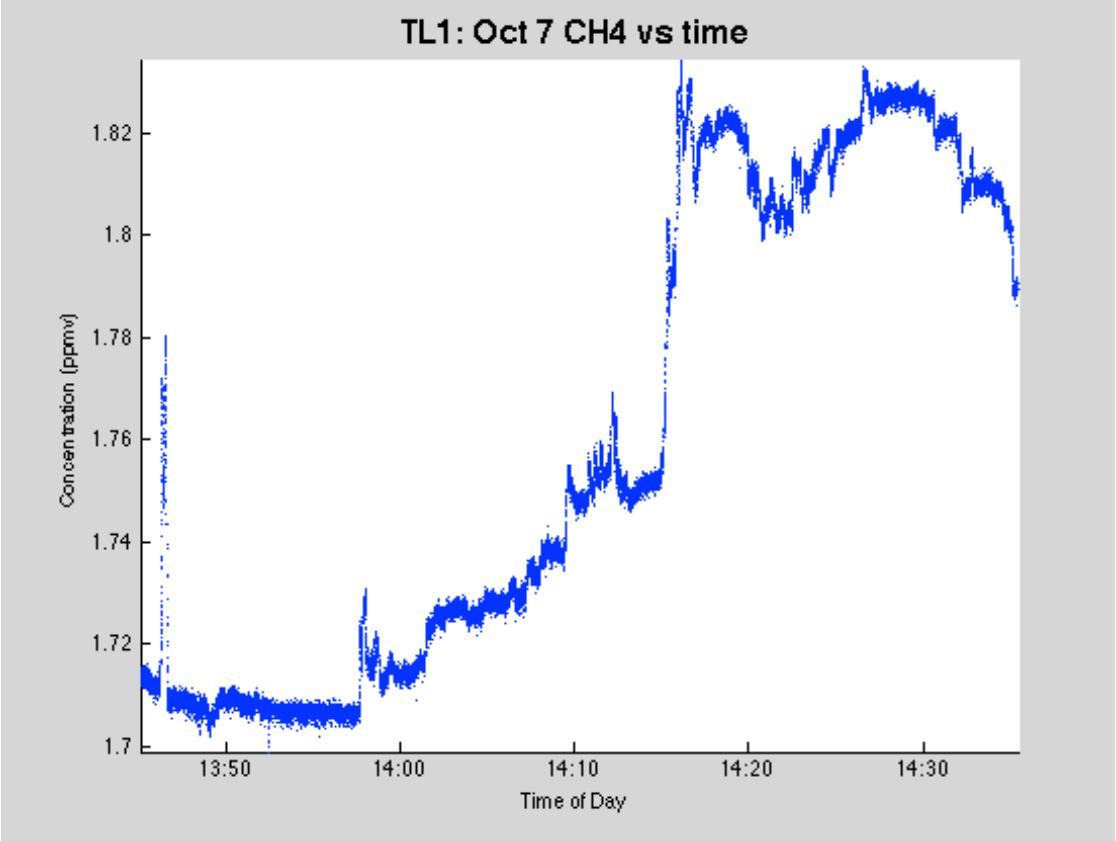
TL1: Oct 7 CH4 vs time
Concentration (ppmv)
1.82
1.8
1.78
1.76
1.74
1.72
1.7
13:50
14:00
14:10
14:20
14:30
Time of Day

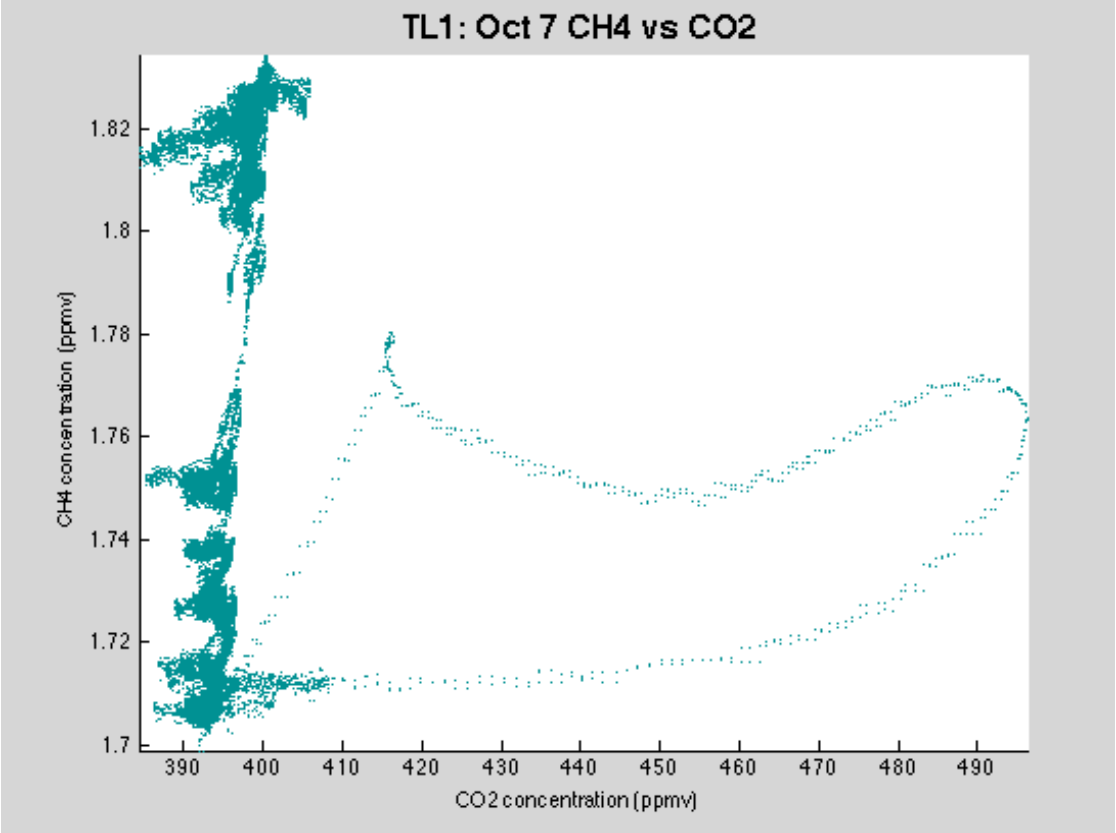
TL1: Oct 7 CH4 vs CO2
CH4 concentration (ppmv)
1.82
1.8
1.78
1.76
1.74
1.72
1.7
390
400
410
420
430
440
450
460
470
480
490
CO2 concentration (ppmv)

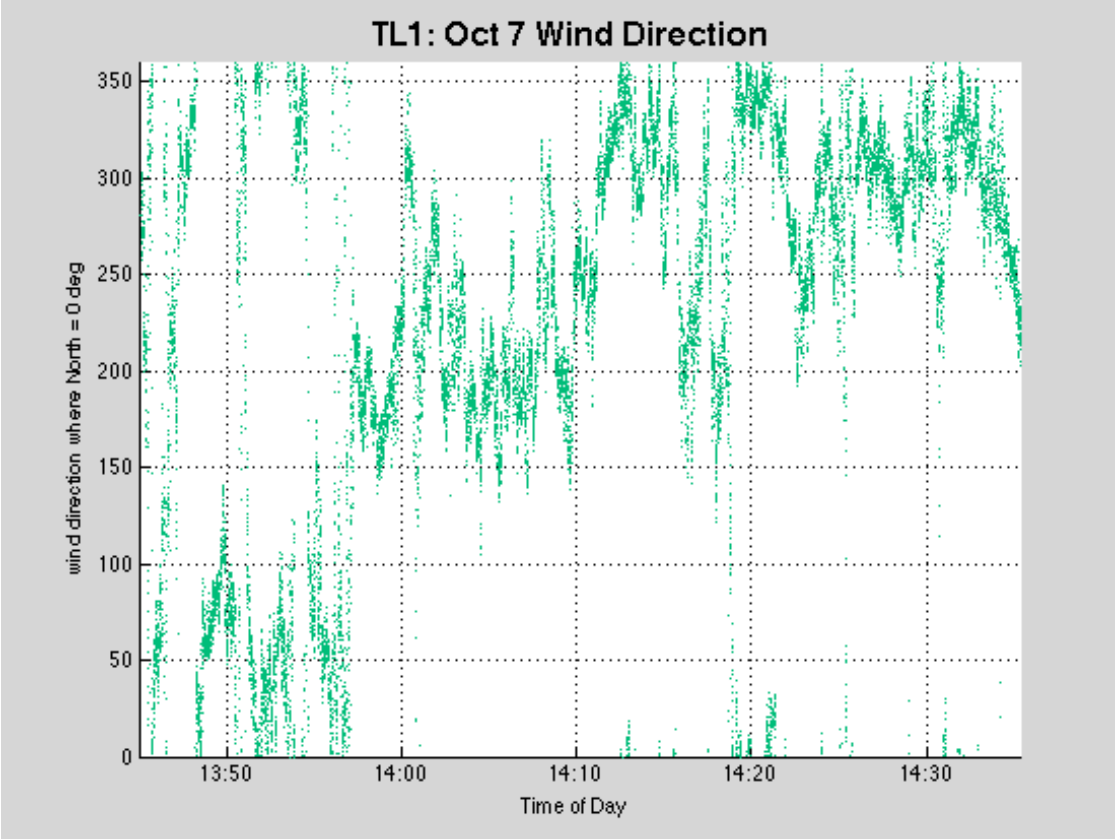
TL1: Oct 7 Wind Direction
wind direction where North = 0 deg
350
300
250
200
150
100
50
0
13:50
14:00
14:10
14:20
14:30
Time of Day

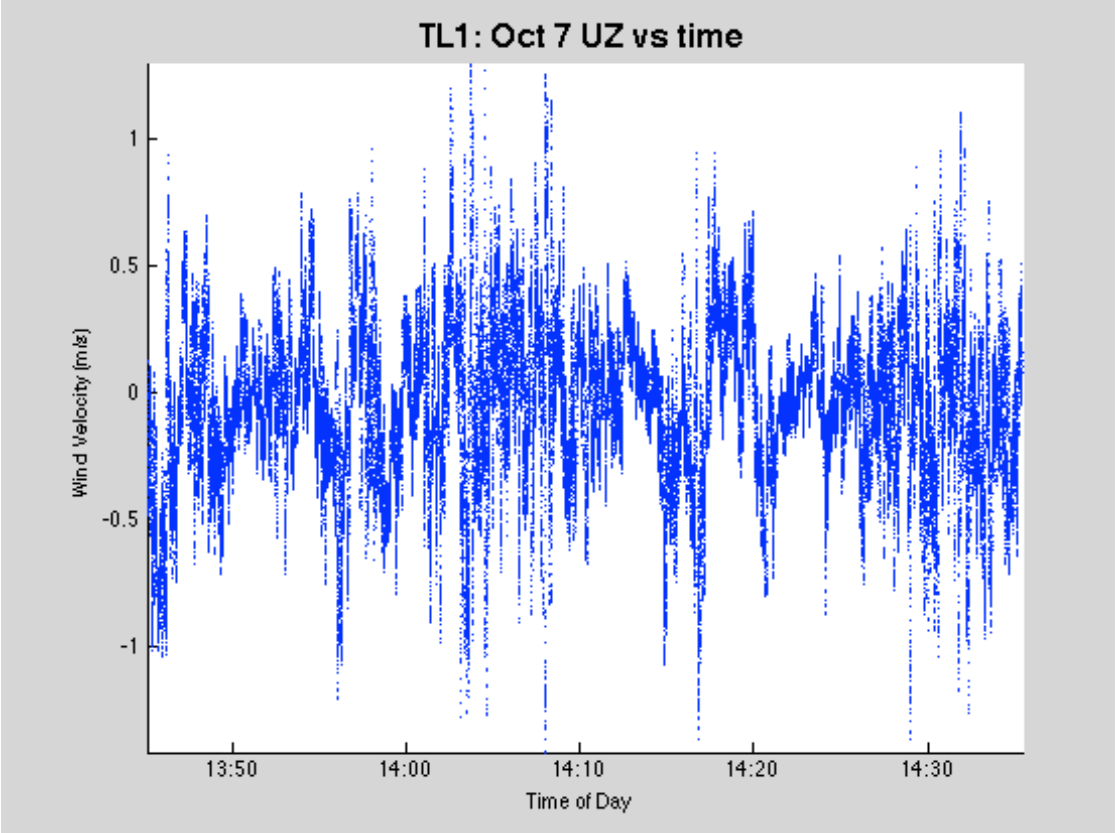
TL1: Oct 7 UZ vs time
Wind Velocity (m/s)
1
0.5
0
-0.5
-1
13:50
14:00
14:10
14:20
14:30
Time of Day

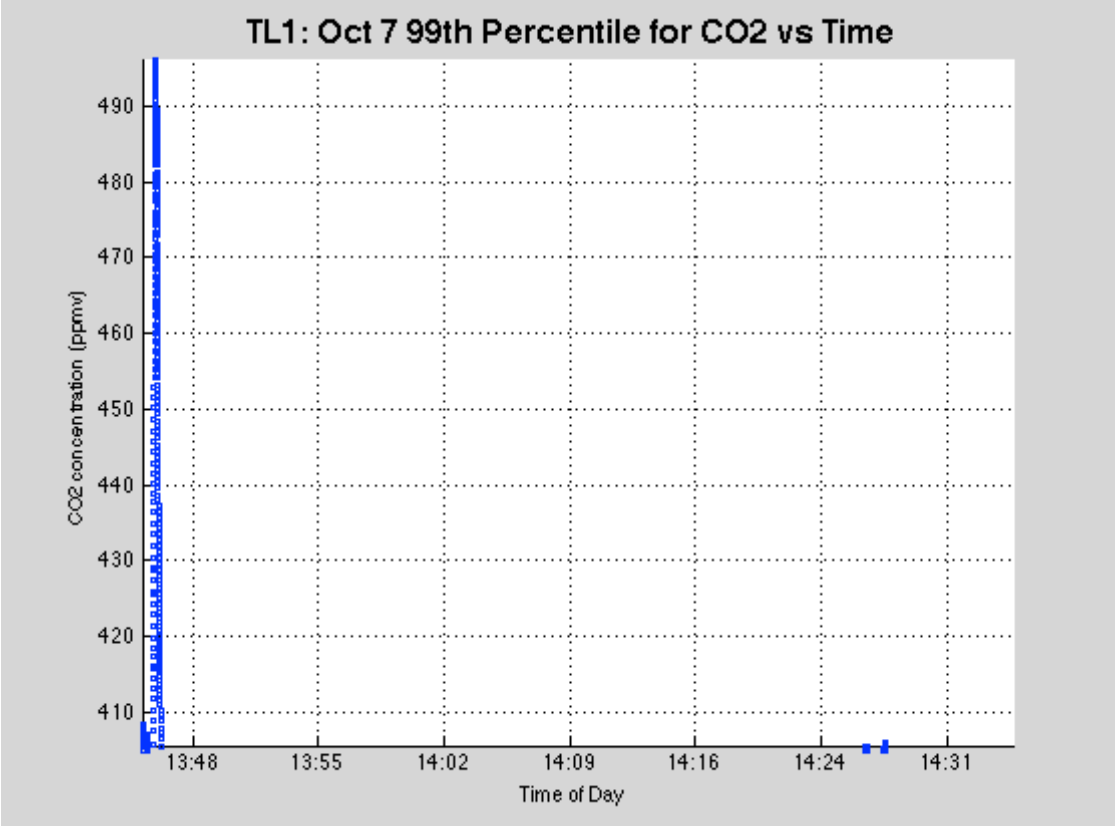
TL1: Oct 7 99th Percentile for CO2 vs Time
CO2 concentration (ppmv)
490
480
470
460
450
440
430
420
410
13:48
13:55
14:02
14:09
14:16
14:24
14:31
Time of Day

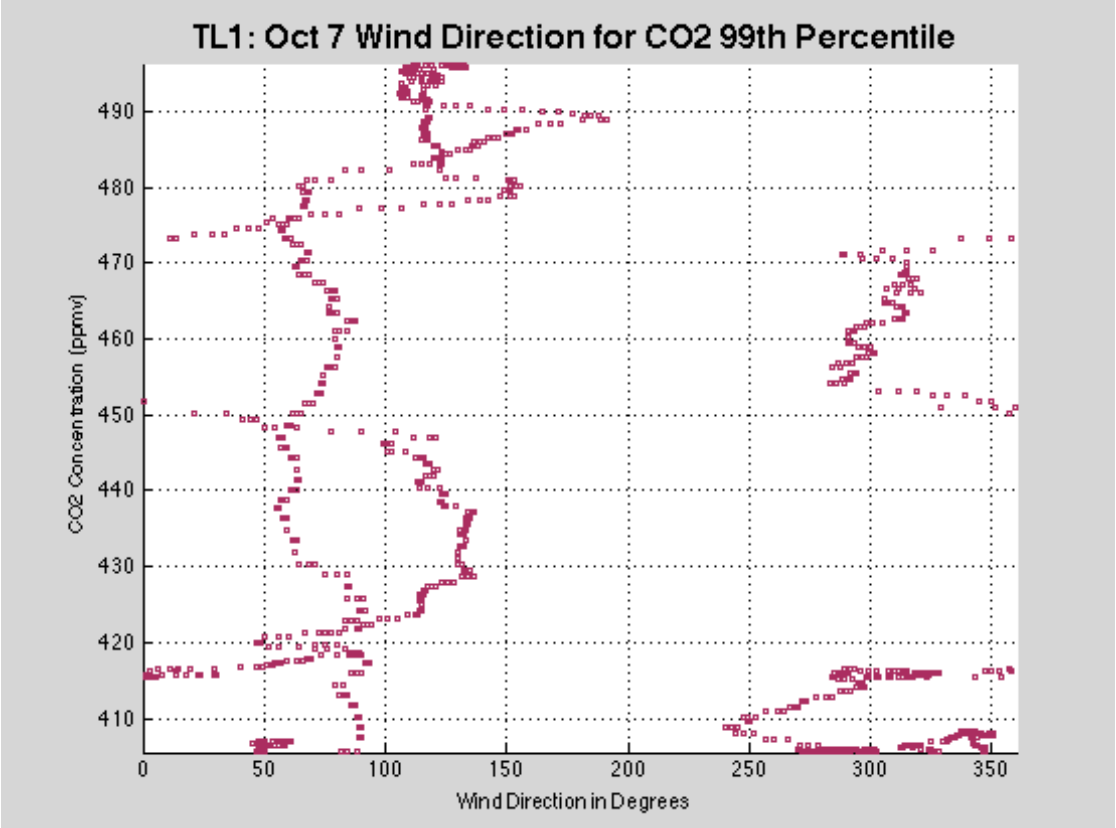
TL1: Oct 7 Wind Direction for CO2 99th Percentile
CO2 Concentration (ppmv)
490
480
470
460
450
440
430
420
410
0
50
100
150
200
250
300
350
Wind Direction in Degrees

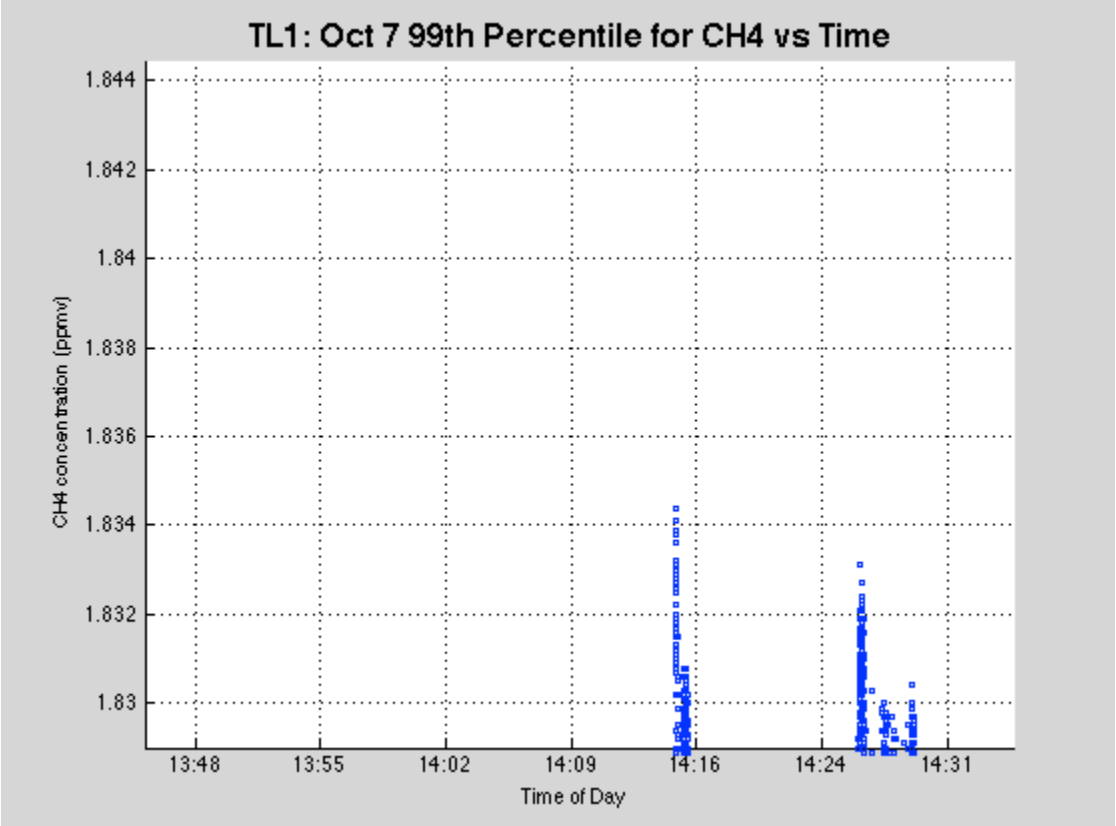
TL1: Oct 7 99th Percentile for CH4 vs Time
CH4 concentration (ppmv)
1.844
1.842
1.84
1.838
1.836
1.834
1.832
1.83
13:48
13:55
14:02
14:09
14:16
14:24
14:31
Time of Day

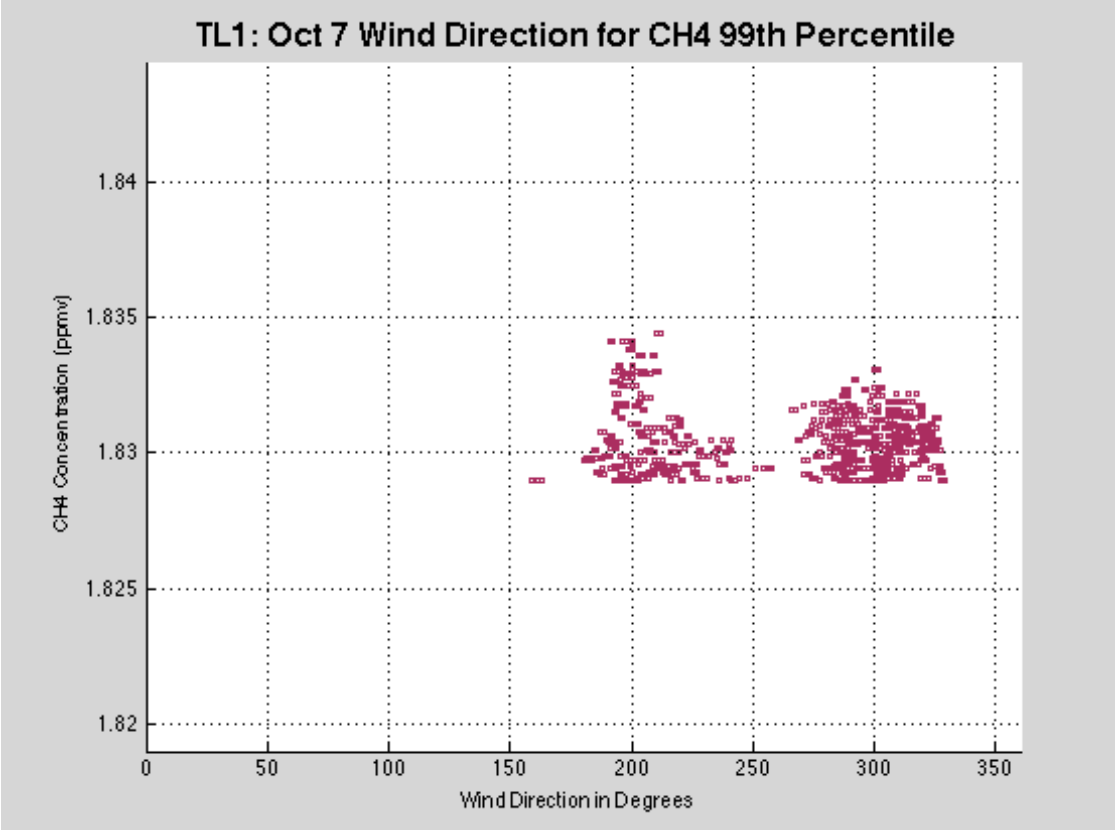
TL1: Oct 7 Wind Direction for CH4 99th Percentile
CH4 Concentration (ppmv)
1.84
1.835
1.83
1.825
1.82
0
50
100
150
200
250
300
350
Wind Direction in Degrees

D.16 Wednesday, October 9th, 2013

| | Maximum | Minimum | Average | Standard Deviation | 99th Percentile |
|---|---|---|---|---|---|
| $CO_2$ (ppmv) | 413.0063 | 379.4651 | 391.656 | 5.2074 | 402.9824 |
| $CH_4$ (ppmv) | 1.7867 | 1.6558 | 1.7083 | 1.7525 | 1.7525 |
| UZ (m/s) | 1.9666 | -2.2089 | -0.0029 | 0.342 | N/A |

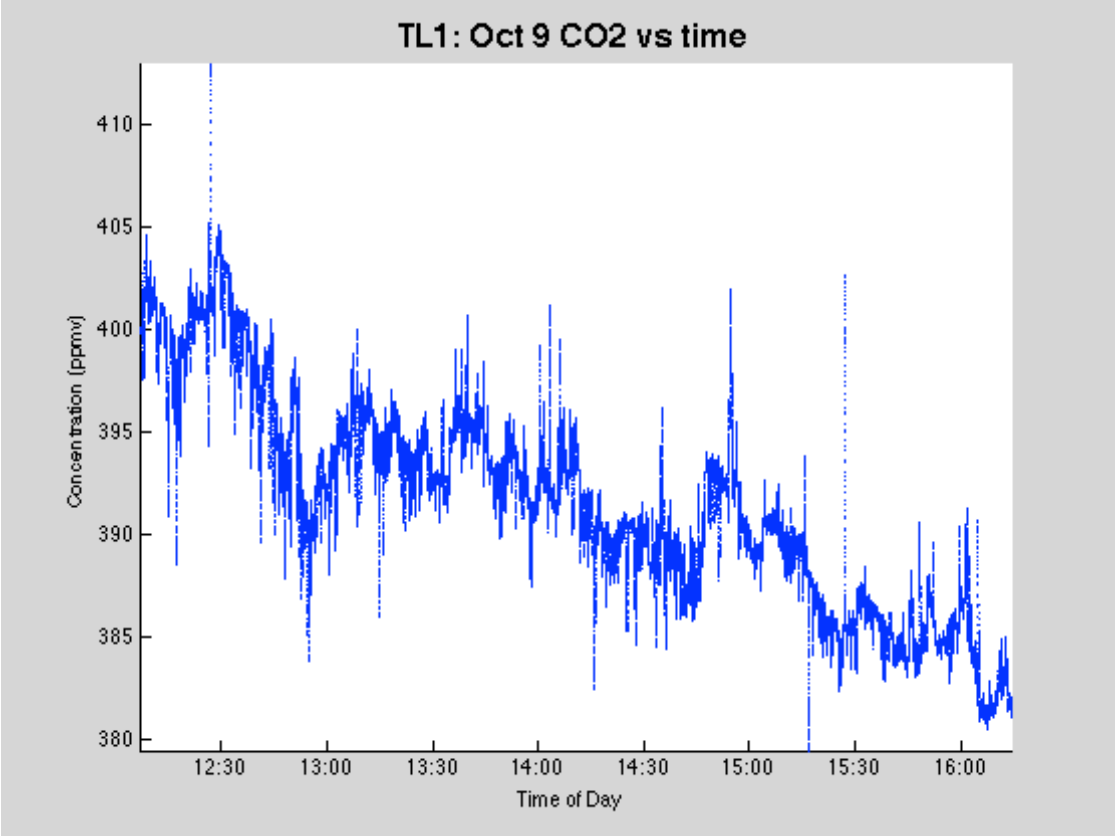

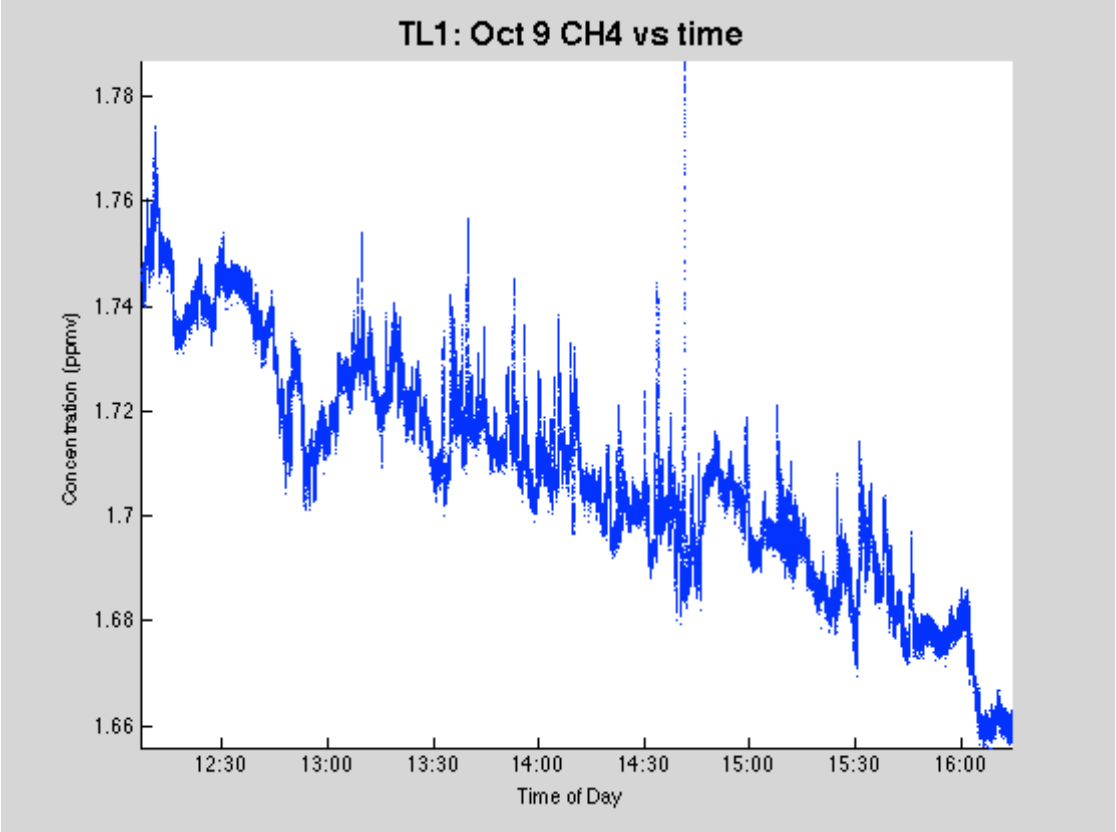
TL1: Oct 9 CH4 vs time
Concentration (ppmv)
1.78
1.76
1.74
1.72
1.7
1.68
1.66
12:30
13:00
13:30
14:00
14:30
15:00
15:30
16:00
Time of Day

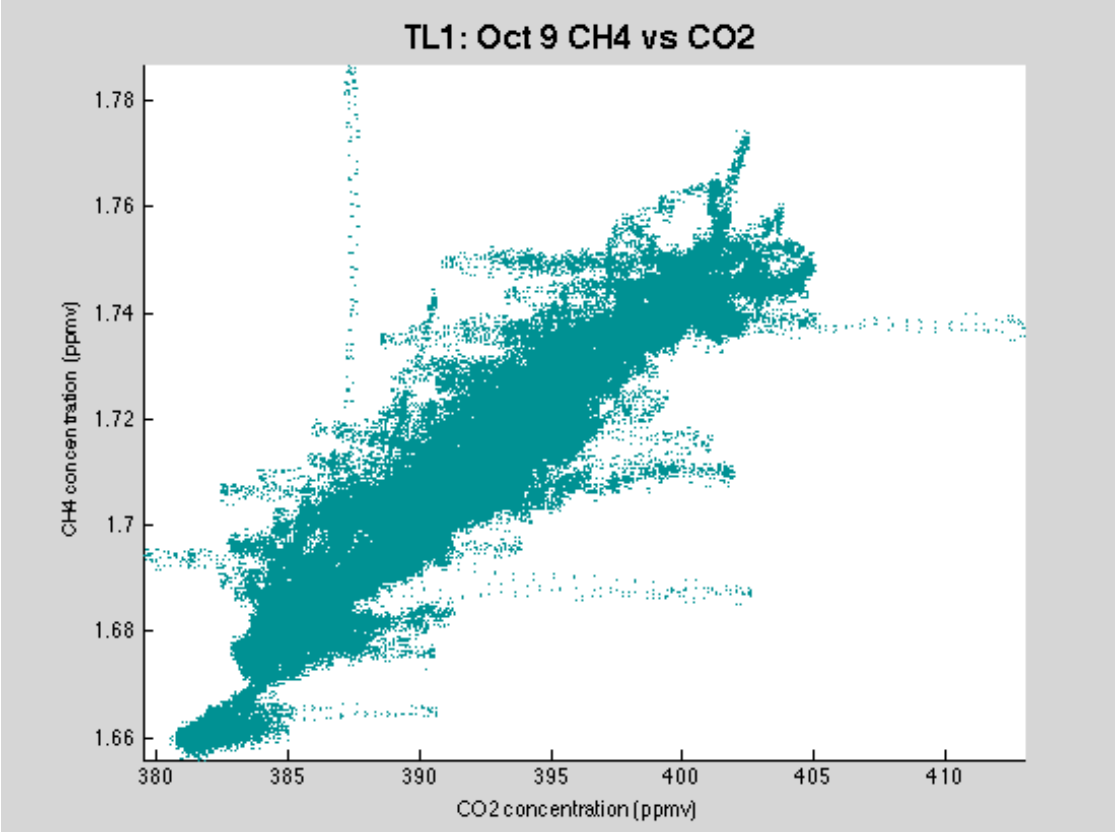
TL1: Oct 9 CH4 vs CO2
CH4 concentration (ppmv)
1.78
1.76
1.74
1.72
1.7
1.68
1.66
380
385
390
395
400
405
410
CO2 concentration (ppmv)

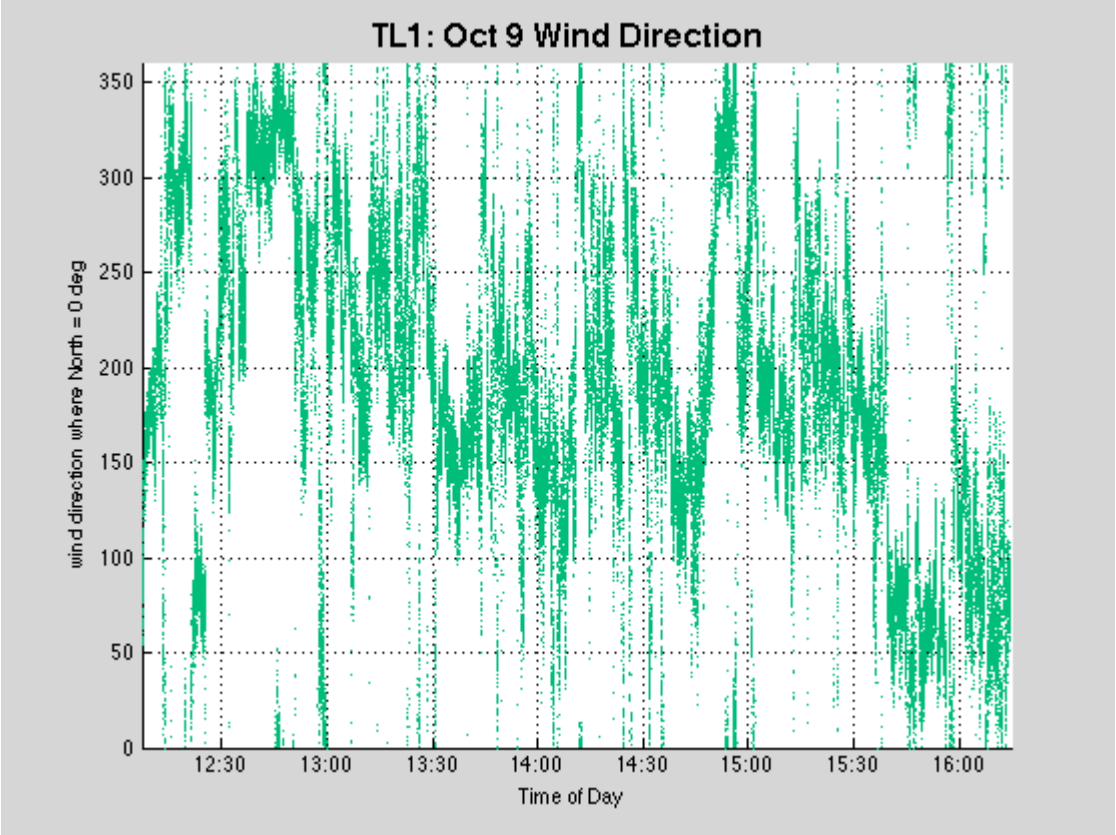
TL1: Oct 9 Wind Direction
wind direction where North = 0 deg
350
300
250
200
150
100
50
0
12:30
13:00
13:30
14:00
14:30
15:00
15:30
16:00
Time of Day

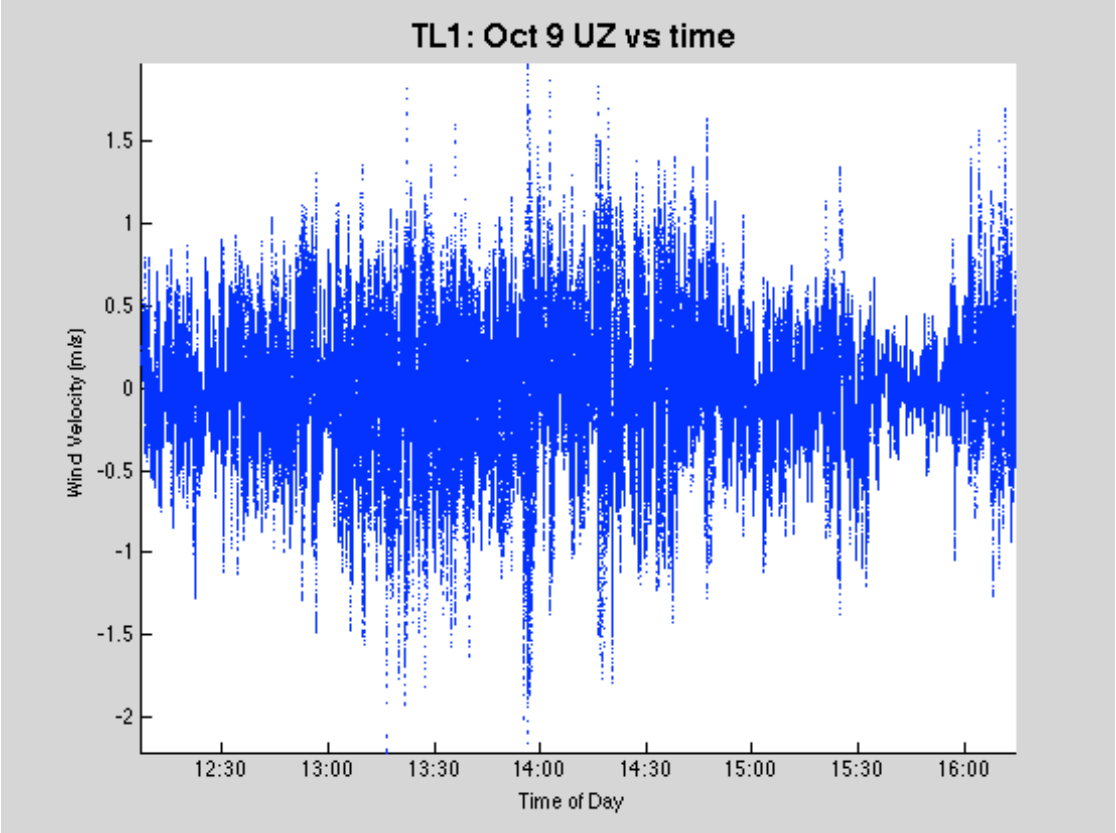
TL1: Oct 9 UZ vs time
Wind Velocity (m/s)
1.5
1
0.5
0
-0.5
-1
-1.5
-2
12:30
13:00
13:30
14:00
14:30
15:00
15:30
16:00
Time of Day

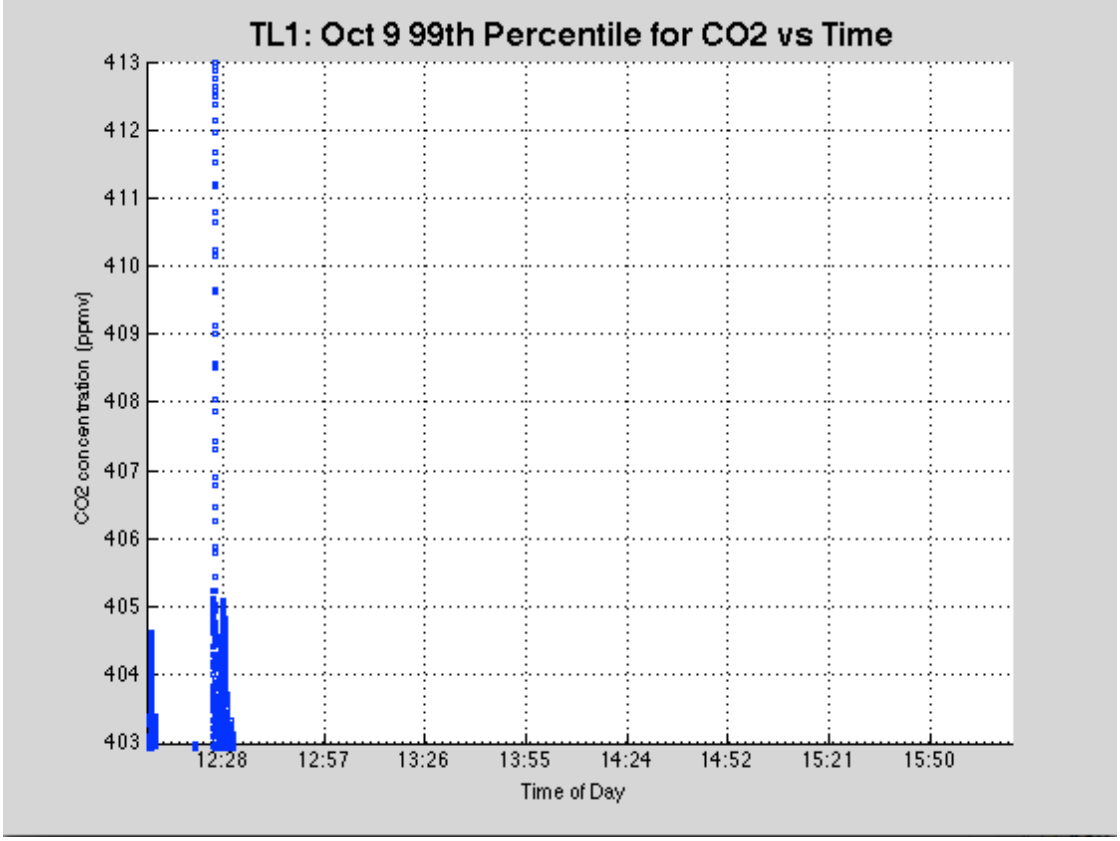
TL1: Oct 9 99th Percentile for CO2 vs Time
CO2 concentration (ppmv)
413
412
411
410
409
408
407
406
405
404
403
12:28
12:57
13:26
13:55
14:24
14:52
15:21
15:50
Time of Day

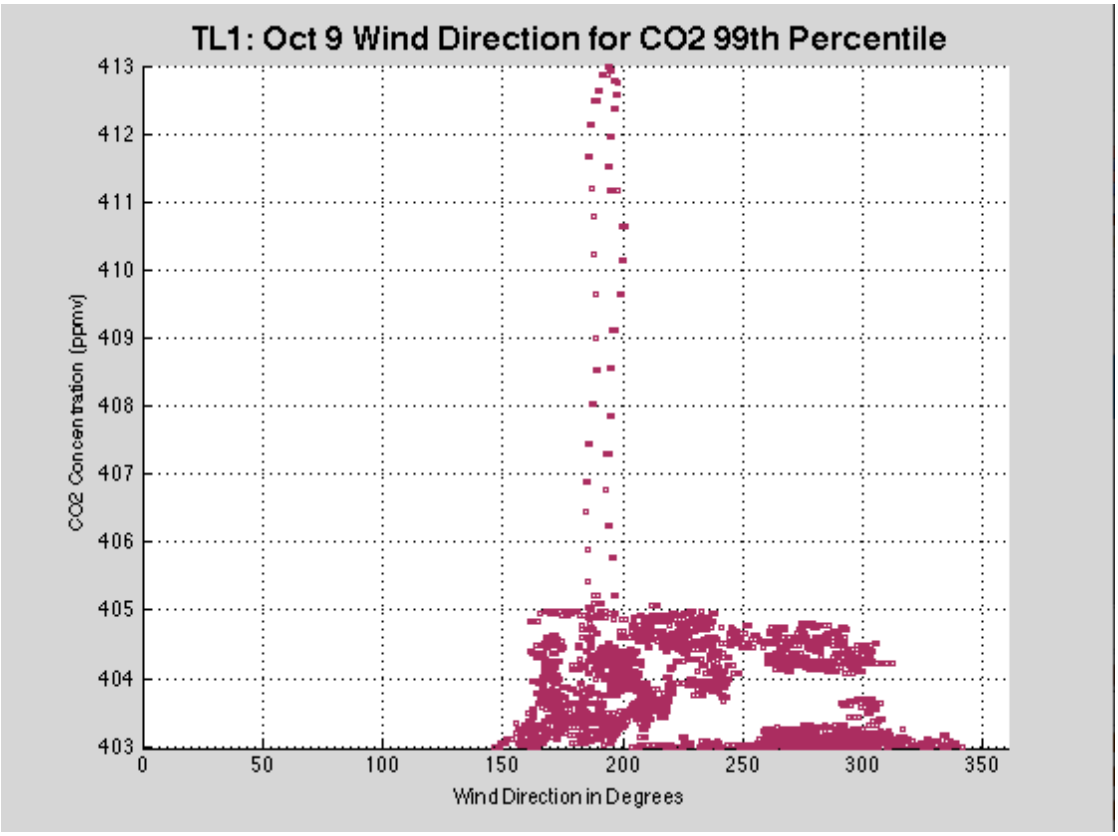
TL1: Oct 9 Wind Direction for CO2 99th Percentile
CO2 Concentration (ppmv)
413
412
411
410
409
408
407
406
405
404
403
0
50
100
150
200
250
300
350
Wind Direction in Degrees

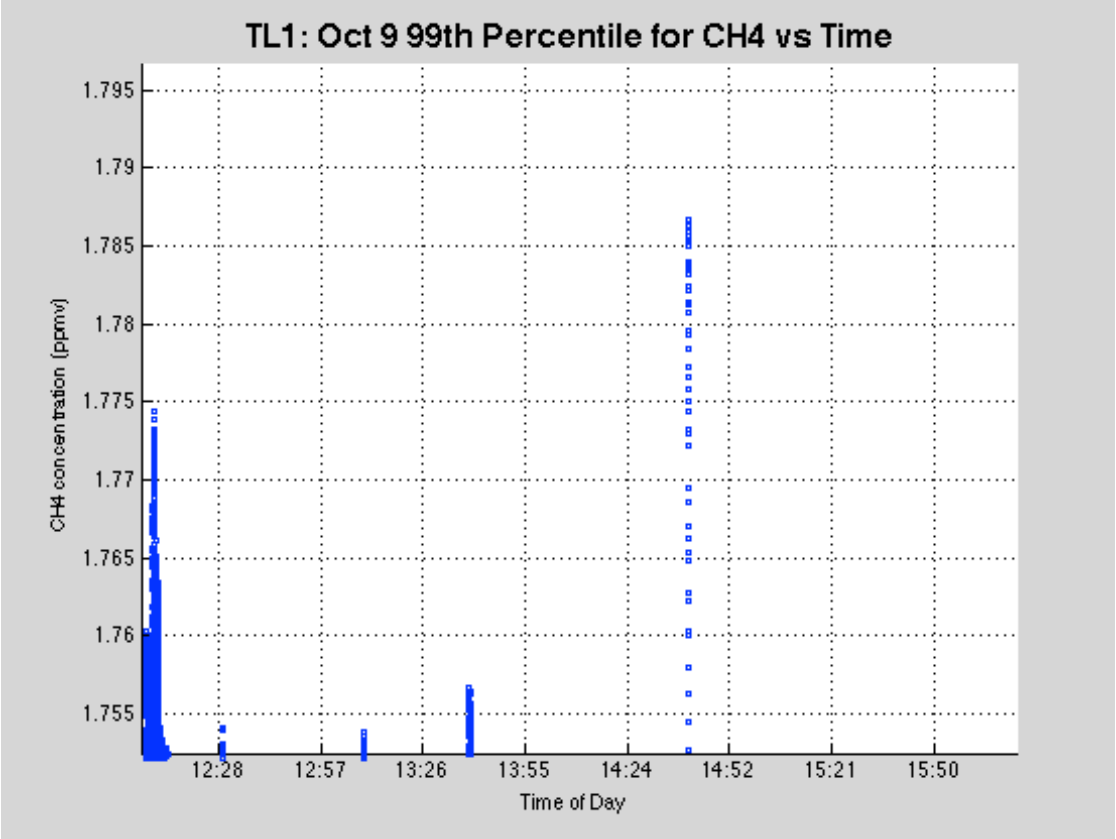
TL1: Oct 9 99th Percentile for CH4 vs Time
CH4 concentration (ppmv)
1.795
1.79
1.785
1.78
1.775
1.77
1.765
1.76
1.755
12:28
12:57
13:26
13:55
14:24
14:52
15:21
15:50
Time of Day

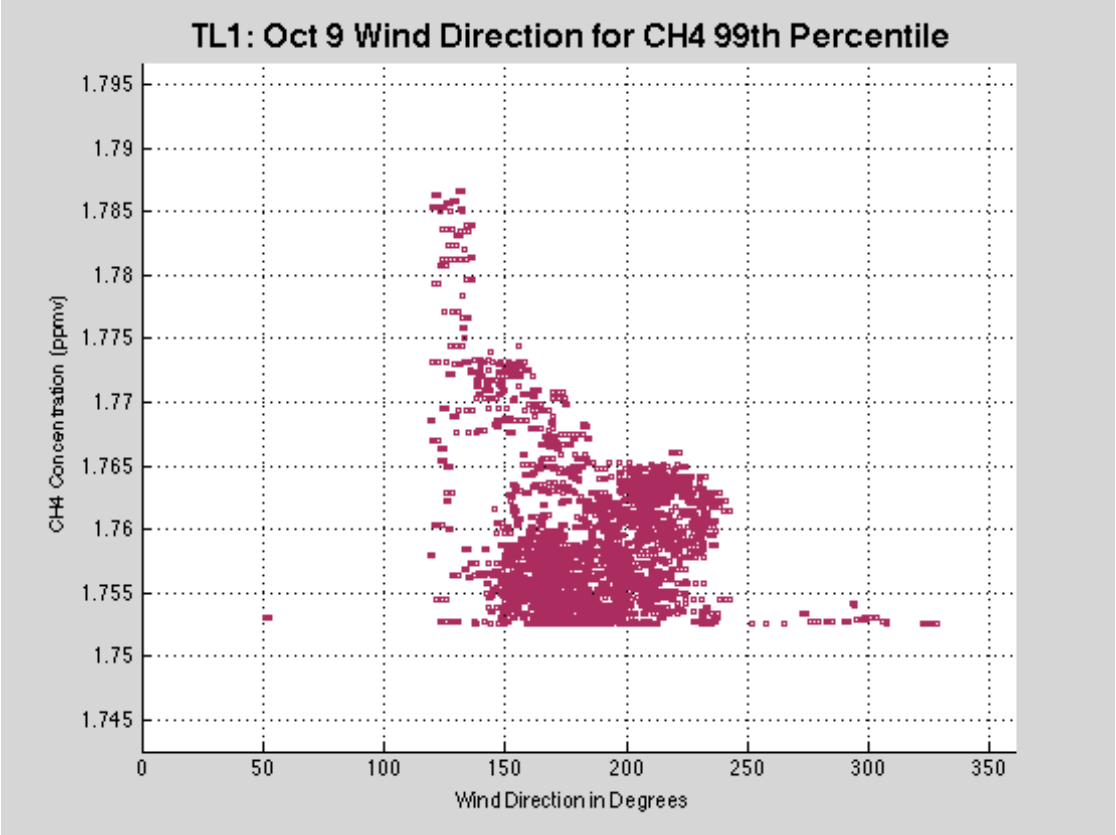
TL1: Oct 9 Wind Direction for CH4 99th Percentile
CH4 Concentration (ppmv)
1.795
1.79
1.785
1.78
1.775
1.77
1.765
1.76
1.755
1.75
1.745
0
50
100
150
200
250
300
350
Wind Direction in Degrees

D.17 Friday, October 11th, 2013

| | Maximum | Minimum | Average | Standard Deviation | 99th Percentile |
|---|---|---|---|---|---|
| $CO_2$ (ppmv) | 388.1539 | 374.893 | 381.6562 | 1.1689 | 384.6042 |
| $CH_4$ (ppmv) | 1.7015 | 1.6787 | 1.6859 | 0.0019 | 1.691 |
| UZ (m/s) | 3.37 | -3.6241 | -0.0799 | 0.5791 | N/A |

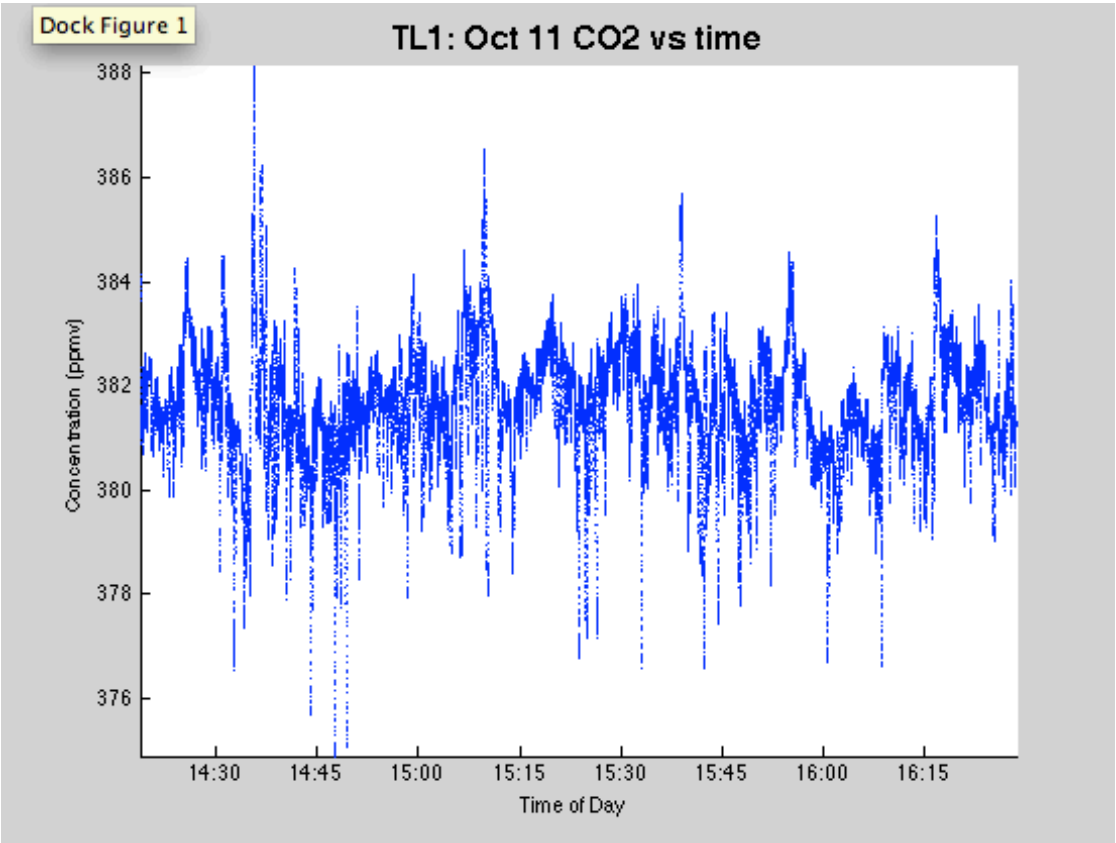

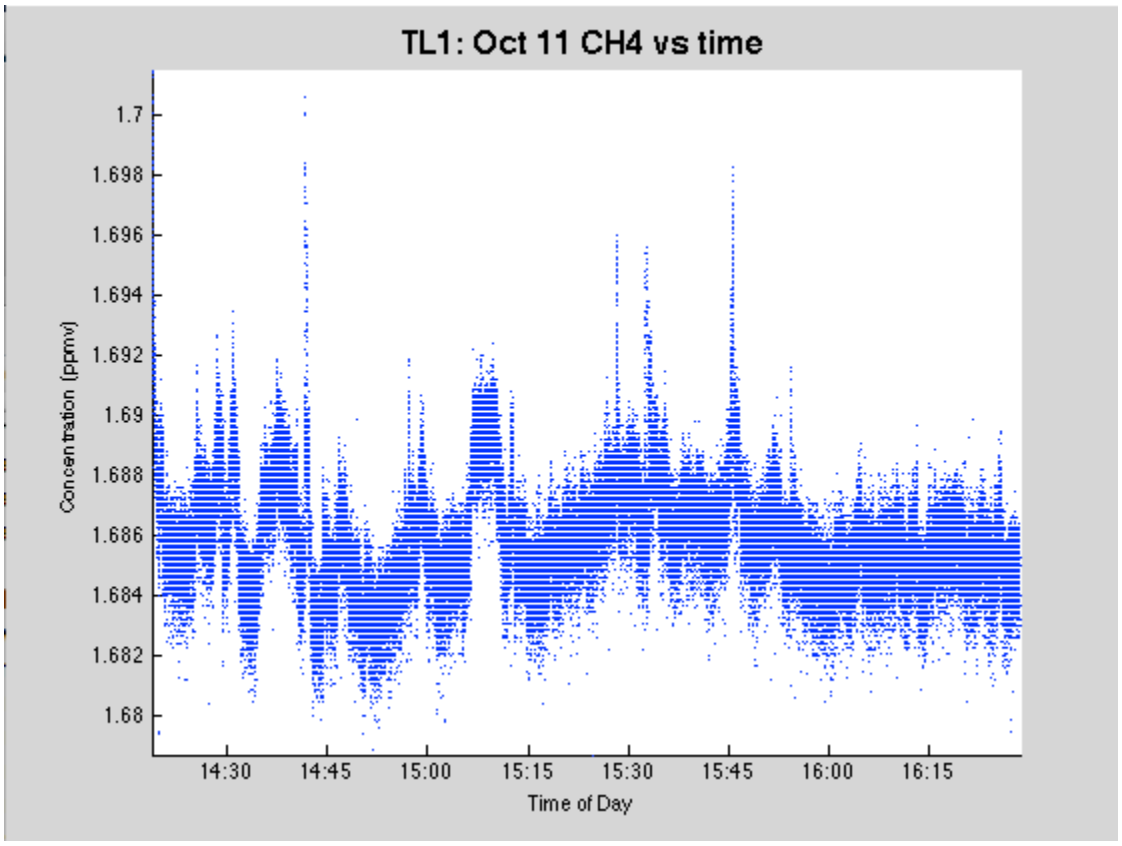
TL1: Oct 11 CH4 vs time
Concentration (ppmv)
1.7
1.698
1.696
1.694
1.692
1.69
1.688
1.686
1.684
1.682
1.68
14:30
14:45
15:00
15:15
15:30
15:45
16:00
16:15
Time of Day

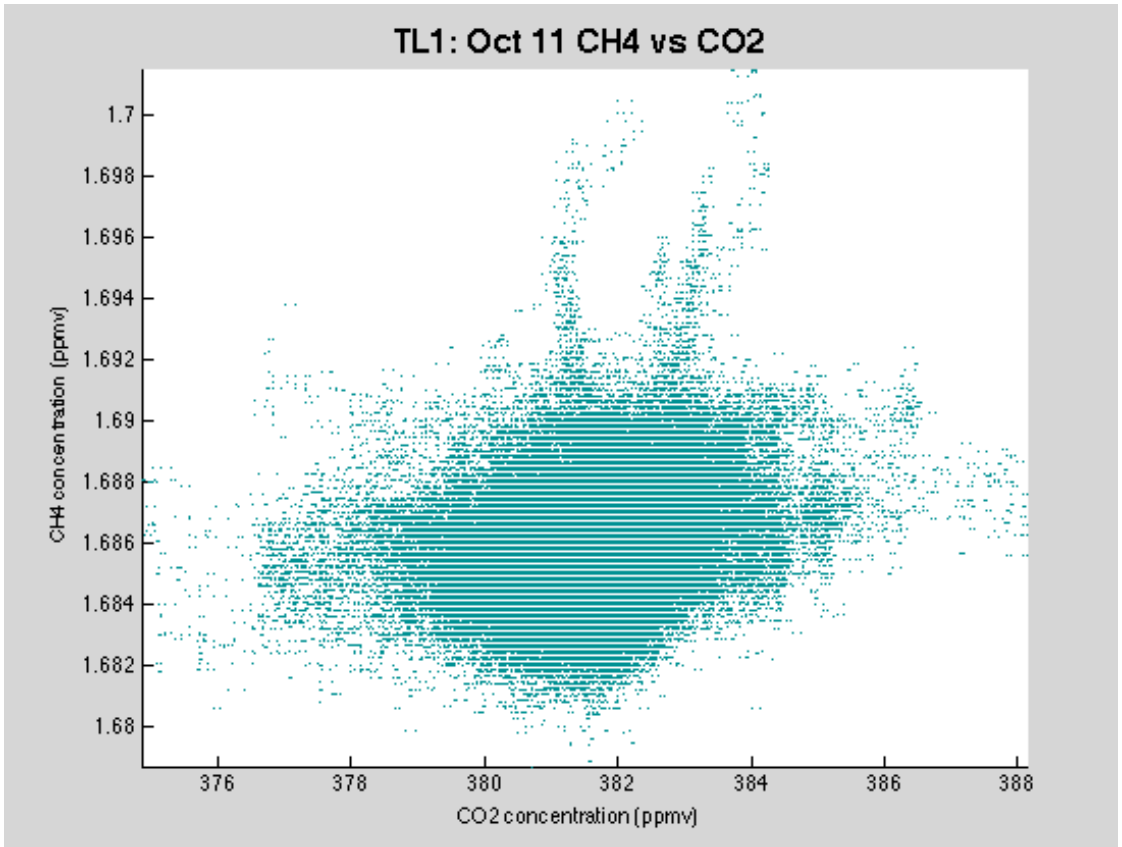
TL1: Oct 11 CH4 vs CO2
CH4 concentration (ppmv)
1.7
1.698
1.696
1.694
1.692
1.69
1.688
1.686
1.684
1.682
1.68
376
378
380
382
384
386
388
CO2 concentration (ppmv)

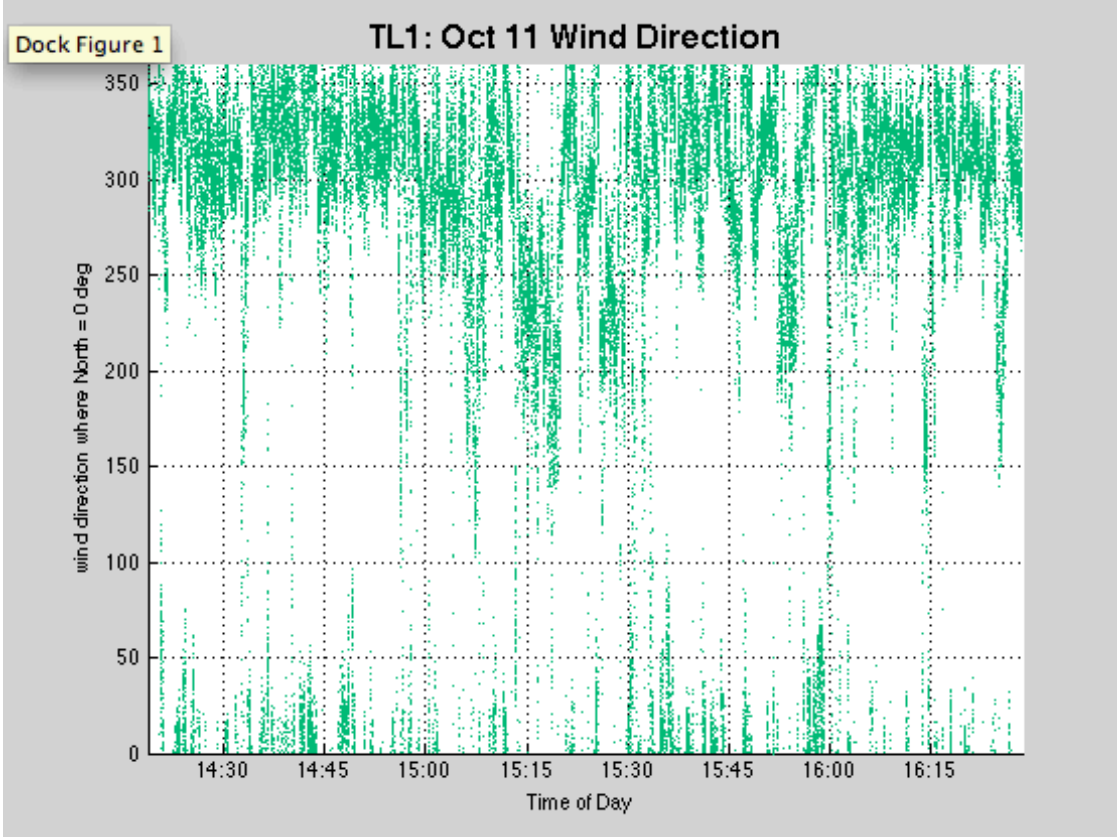
Dock Figure 1
TL1: Oct 11 Wind Direction
wind direction where North = 0 deg
350
300
250
200
150
100
50
0
14:30
14:45
15:00
15:15
15:30
15:45
16:00
16:15
Time of Day

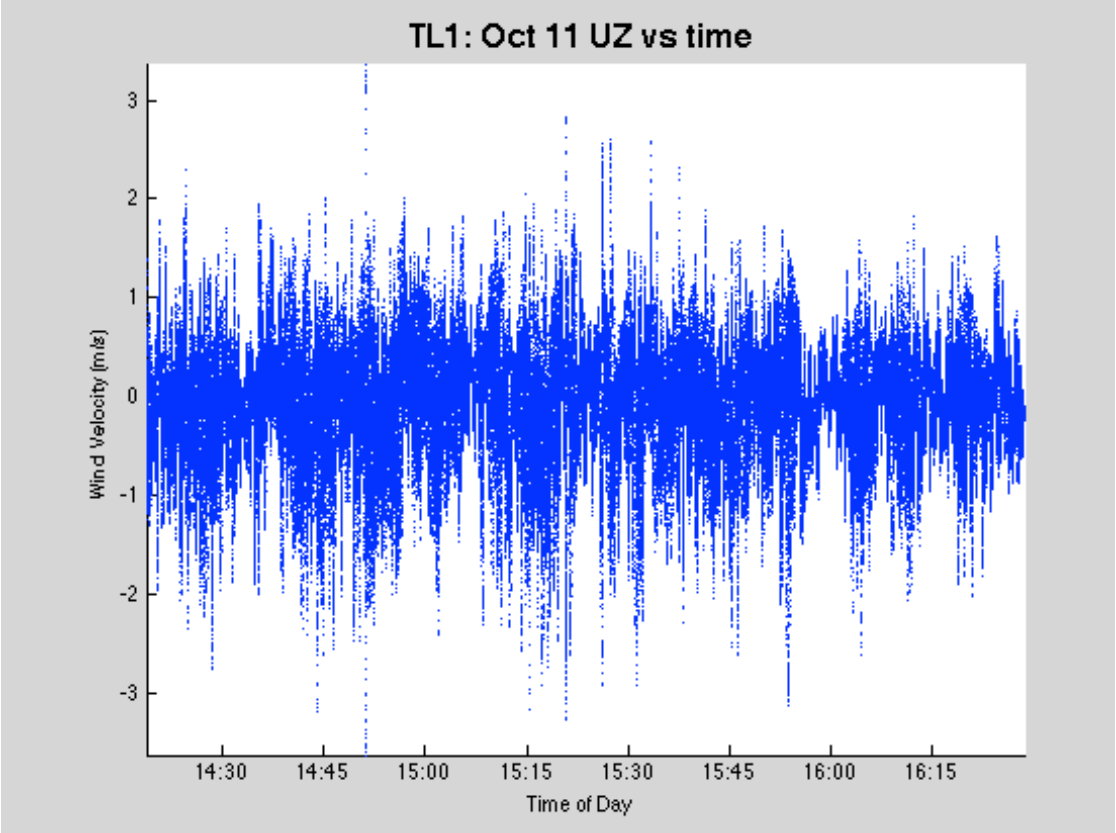
TL1: Oct 11 UZ vs time
Wind Velocity (m/s)
3
2
1
0
-1
-2
-3
14:30
14:45
15:00
15:15
15:30
15:45
16:00
16:15
Time of Day

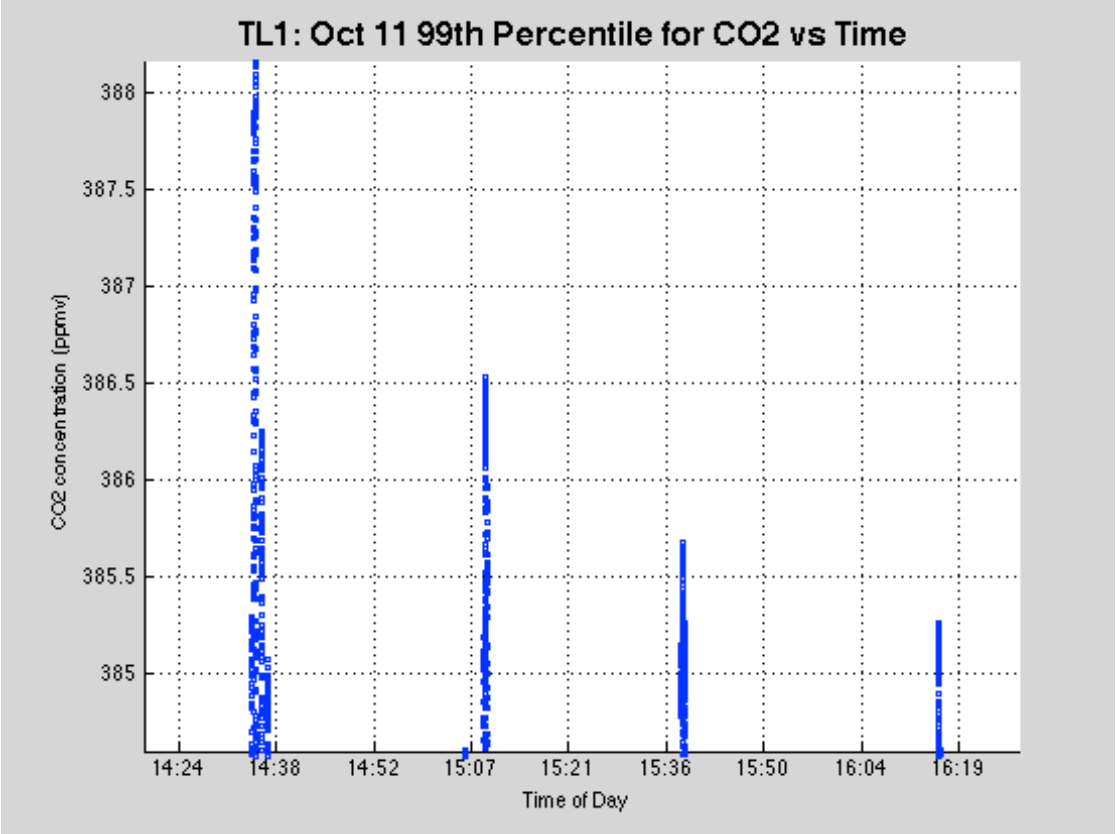
TL1: Oct 11 99th Percentile for CO2 vs Time
CO2 concentration (ppmv)
388
387.5
387
386.5
386
385.5
385
14:24
14:38
14:52
15:07
15:21
15:36
15:50
16:04
16:19
Time of Day

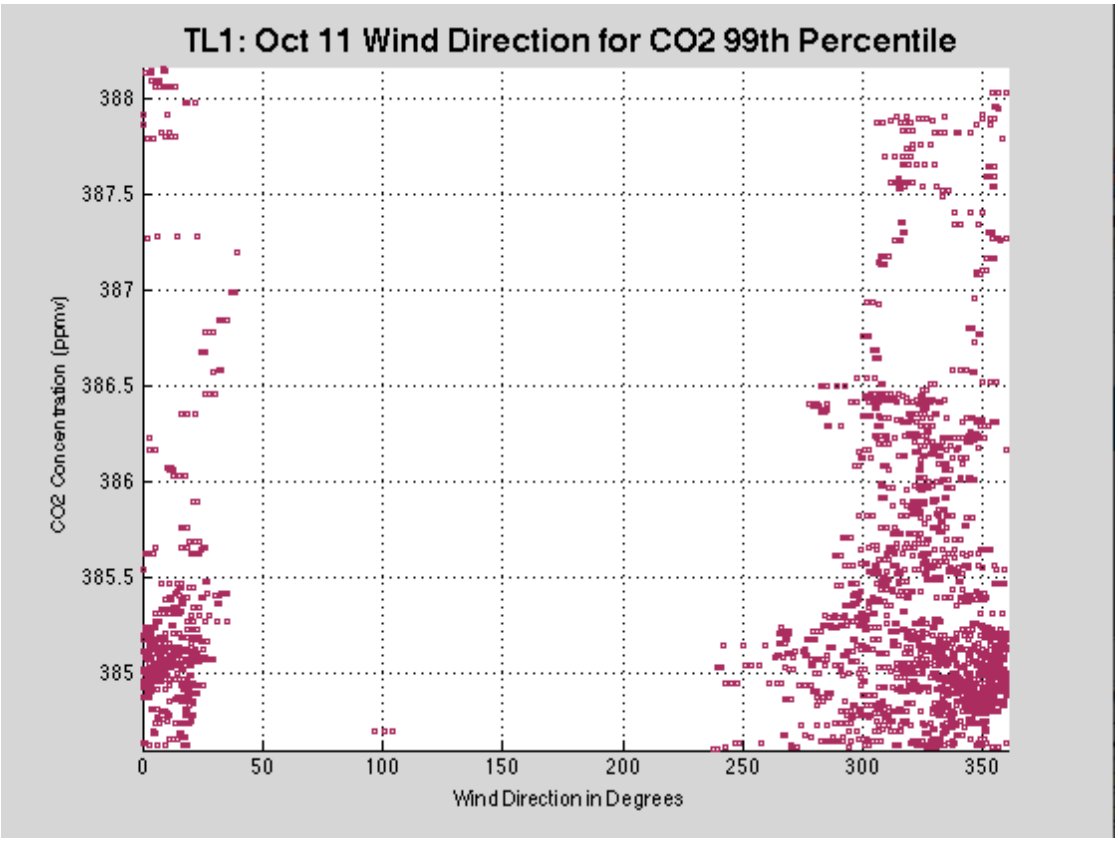
TL1: Oct 11 Wind Direction for CO2 99th Percentile
CO2 Concentration (ppmv)
388
387.5
387
386.5
386
385.5
385
0
50
100
150
200
250
300
350
Wind Direction in Degrees

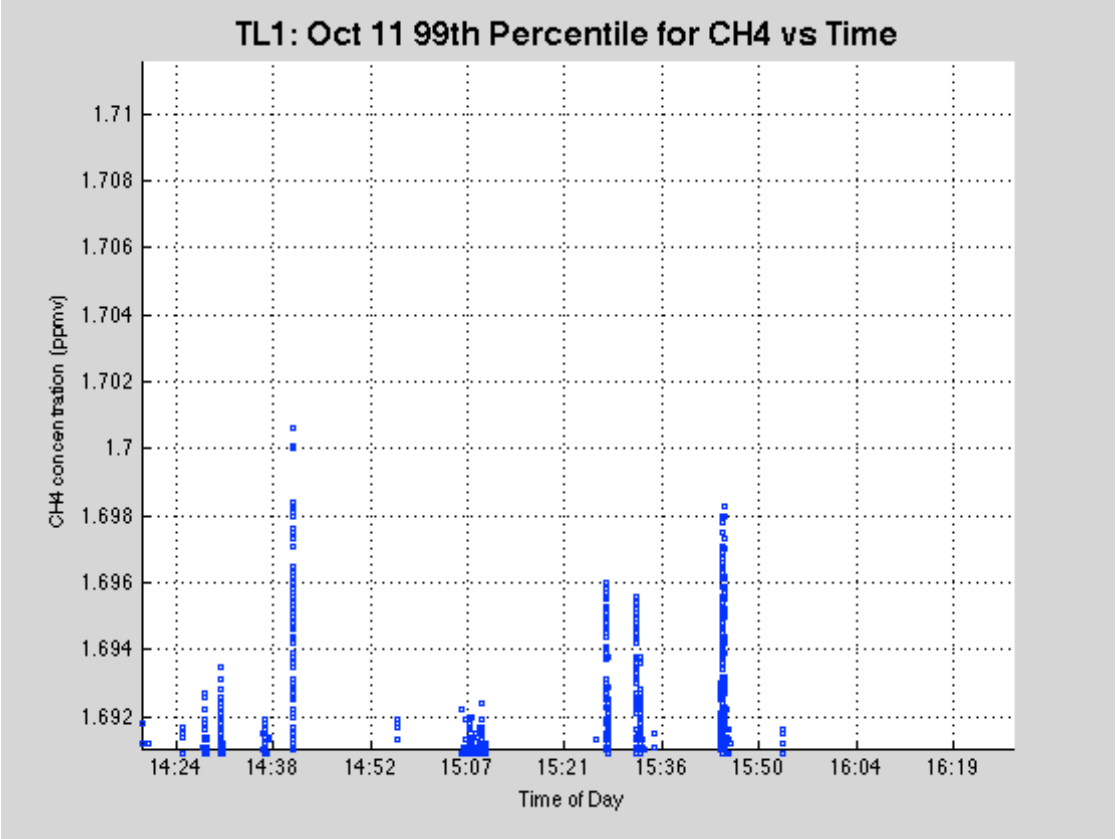
TL1: Oct 11 99th Percentile for CH4 vs Time
CH4 concentration (ppmv)
1.71
1.708
1.706
1.704
1.702
1.7
1.698
1.696
1.694
1.692
14:24
14:38
14:52
15:07
15:21
15:36
15:50
16:04
16:19
Time of Day

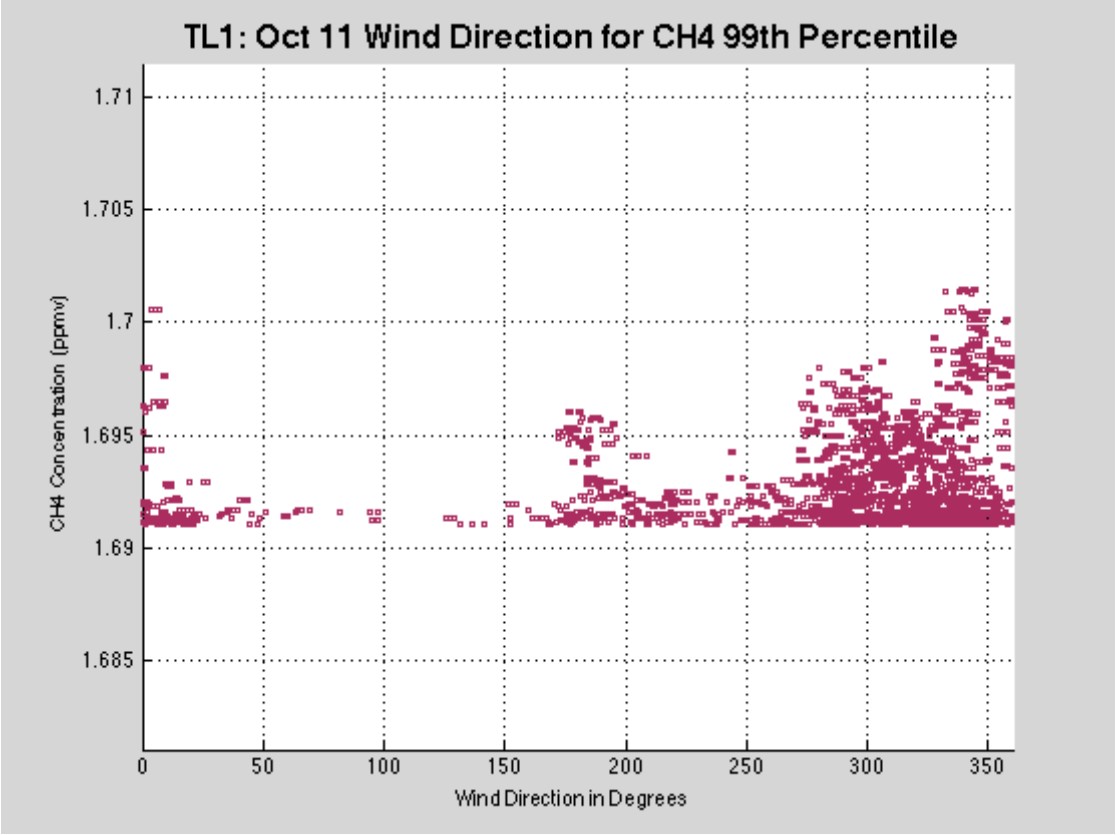
TL1: Oct 11 Wind Direction for CH4 99th Percentile
CH4 Concentration (ppmv)
1.71
1.705
1.7
1.695
1.69
1.685
0
50
100
150
200
250
300
350
Wind Direction in Degrees

# APPENDIX E

## SECOND TOWER LOCATION (FASB1) DATA

The tower was located at the second location (FASB1) beginning October 18th and ending December 2, 2013. Included for each day are the values for the maximum, minimum, average and standard deviation of the two gases ($CO_2$ and $CH_4$) and the vertical velocity (UZ). The 99th percentile is provided for the two gases.
Also included are nine plots of the data for each day.

The plots are;

1. $CO_2$ Concentration vs. Time
2. $CH_4$ Concentration vs. Time
3. $CH_4$ Concentration vs. CO2 Concentration
4. Wind Direction vs. Time
5. Vertical Wind Velocity vs. Time
6. 99th Percentile $CO_2$ Concentration vs. Time
7. 99th Percentile $CO_2$ Concentration vs. Wind Direction
8. 99th Percentile $CH_4$ Concentration vs. Time
9. 99th Percentile $CH_4$ Concentration vs. Wind Direction

The first session at FASB1 was the overnight session and is presented in Appendix G.

E.1 Wednesday, October 23rd, 2013

| | Maximum | Minimum | Average | Standard Deviation | 99th Percentile |
|---|---|---|---|---|---|
| $CO_2$ (ppmv) | 453.8953 | 356.5993 | 415.47 | 10.6003 | 434.8751 |
| $CH_4$ (ppmv) | 1.9249 | 1.7759 | 1.8139 | 0.016 | 1.8582 |
| UZ (m/s) | 1.767 | -2.9445 | -0.0931 | 0.4144 | N/A |

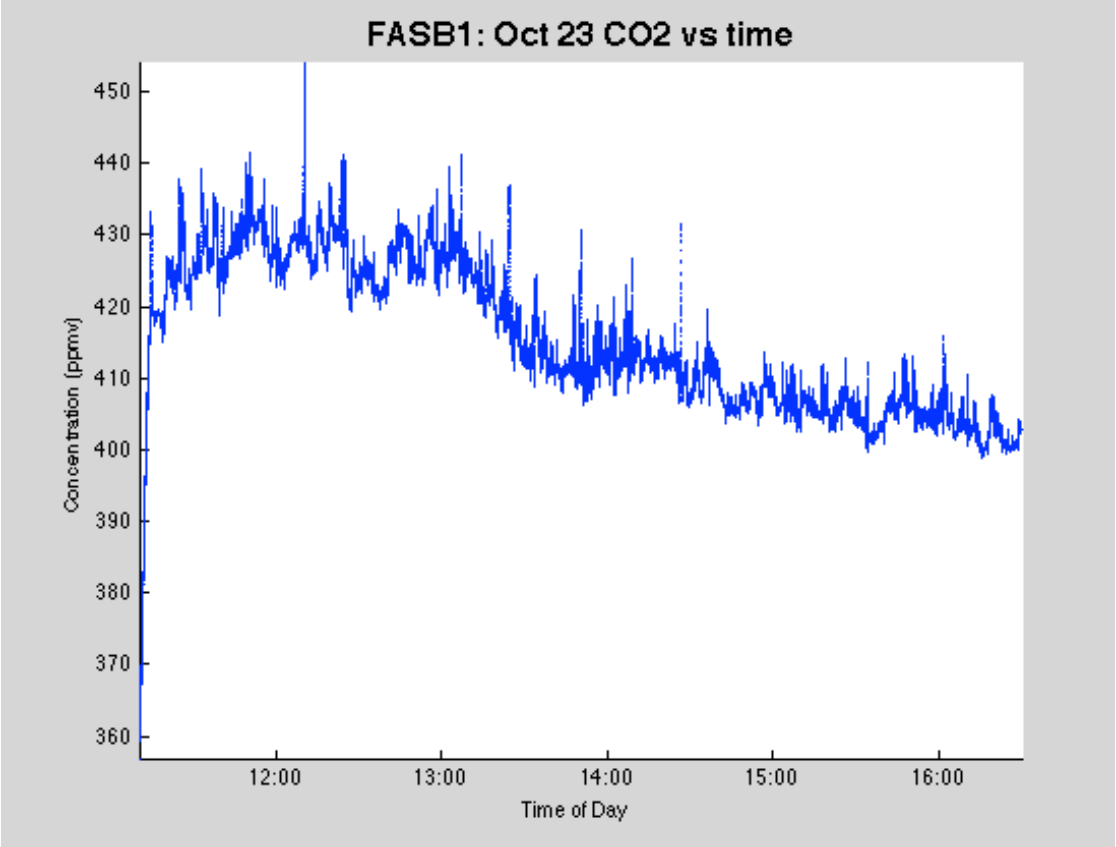

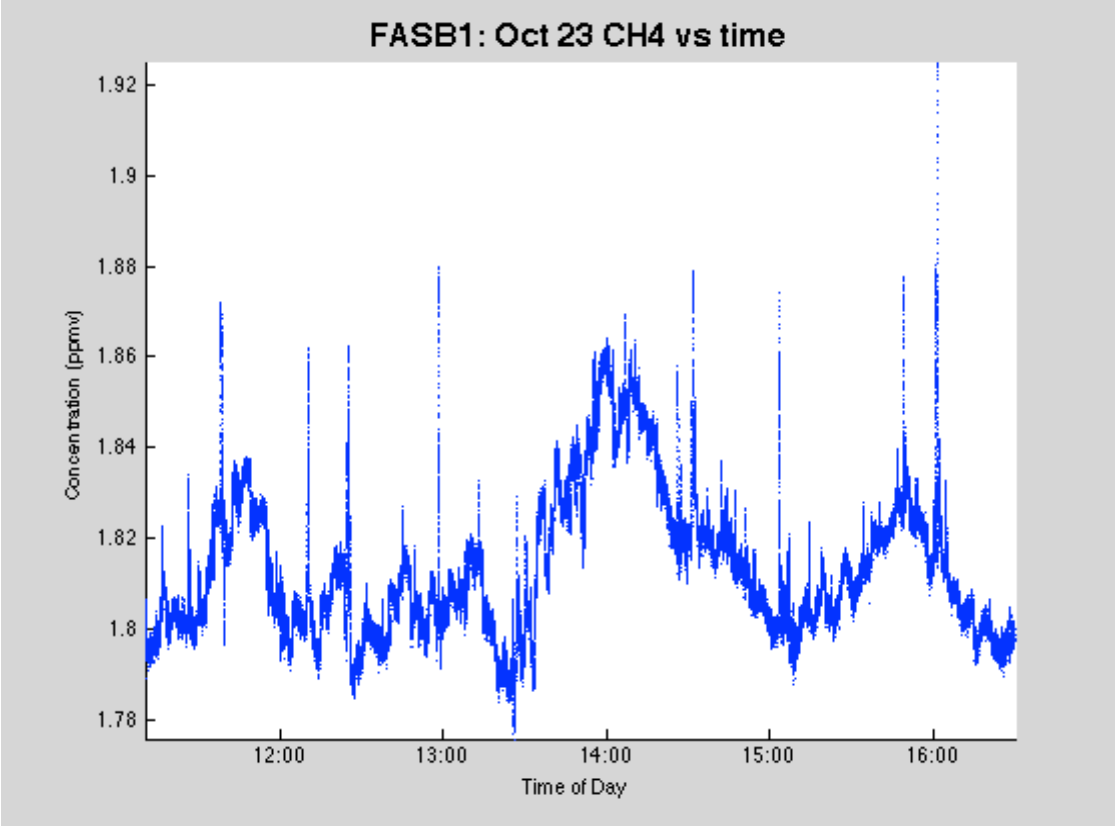
FASB1: Oct 23 CH4 vs time
Concentration (ppmv)
1.92
1.9
1.88
1.86
1.84
1.82
1.8
1.78
12:00
13:00
14:00
15:00
16:00
Time of Day

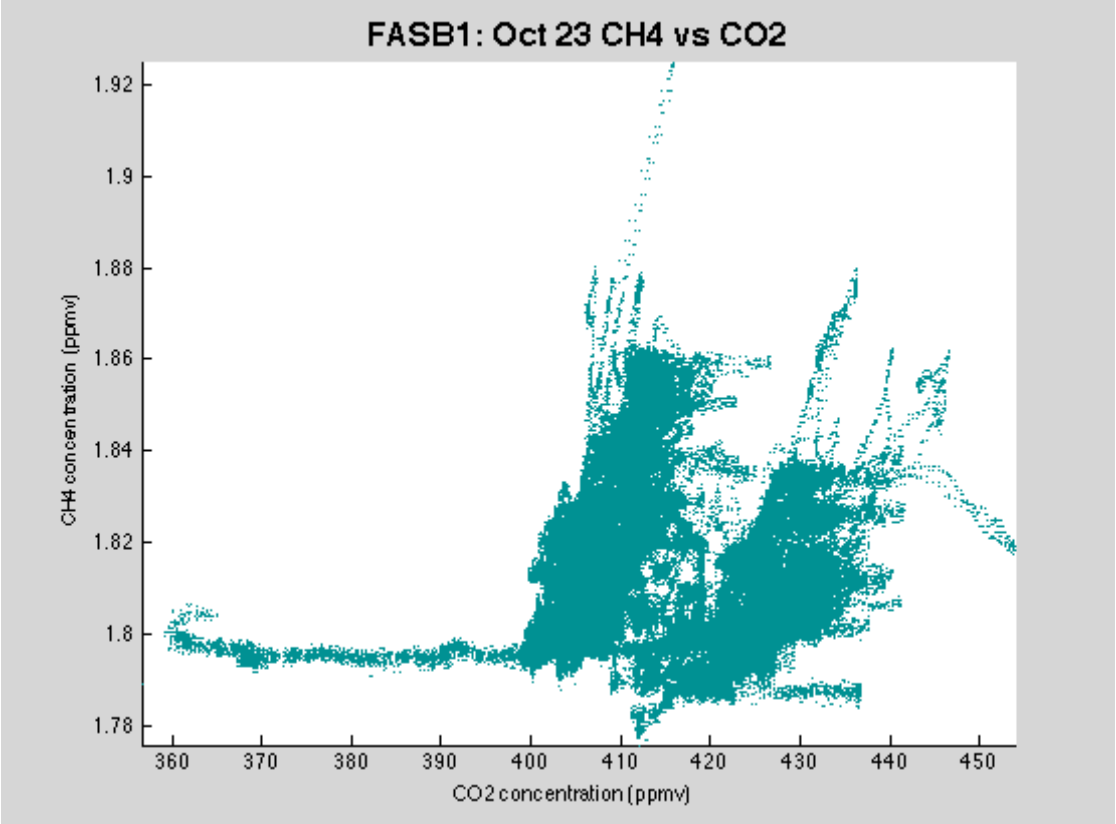
FASB1: Oct 23 CH4 vs CO2
CH4 concentration (ppmv)
1.92
1.9
1.88
1.86
1.84
1.82
1.8
1.78
360
370
380
390
400
410
420
430
440
450
CO2 concentration (ppmv)

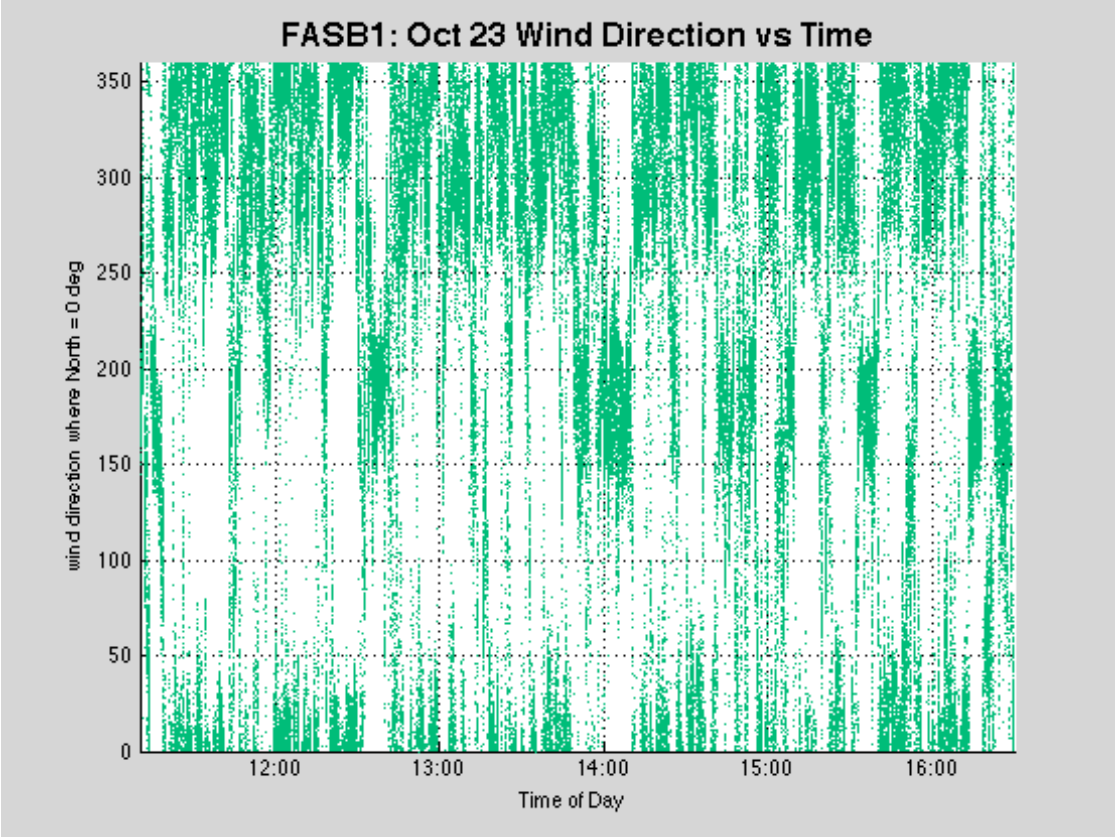
FASB1: Oct 23 Wind Direction vs Time
wind direction where North = 0 deg
350
300
250
200
150
100
50
0
12:00
13:00
14:00
15:00
16:00
Time of Day

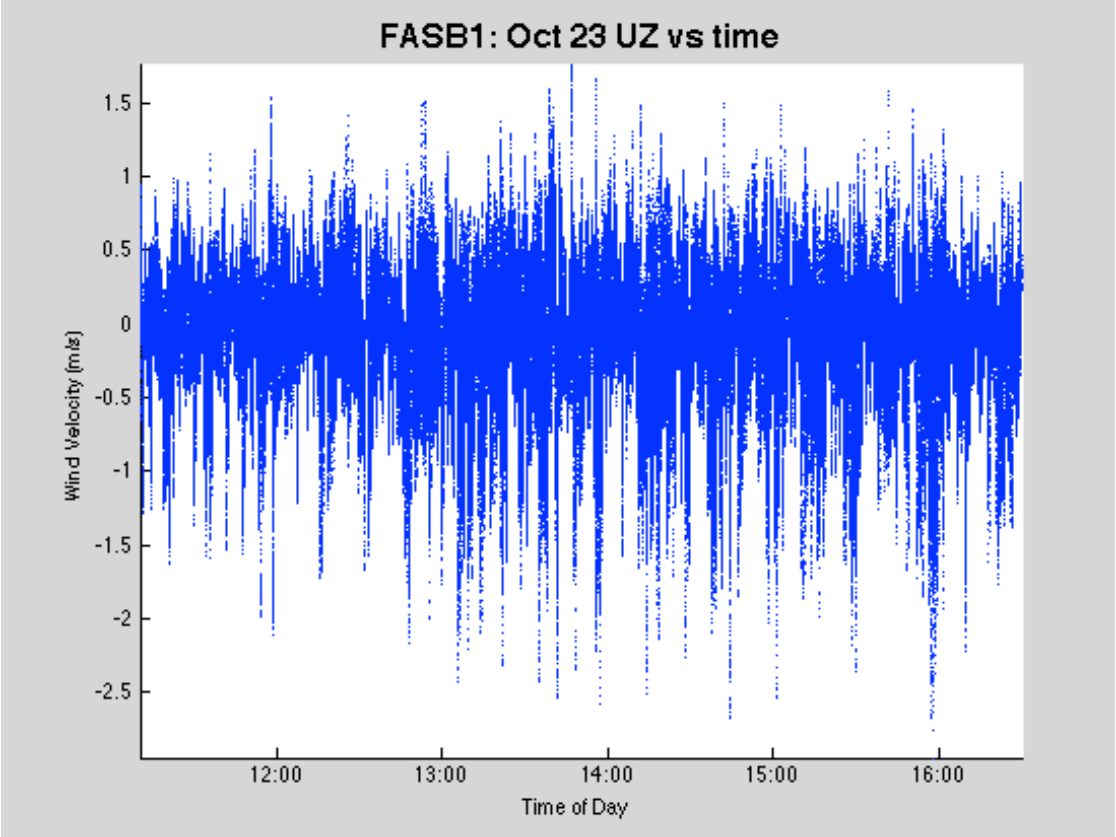
FASB1: Oct 23 UZ vs time
Wind Velocity (m/s)
1.5
1
0.5
0
-0.5
-1
-1.5
-2
-2.5
12:00
13:00
14:00
15:00
16:00
Time of Day

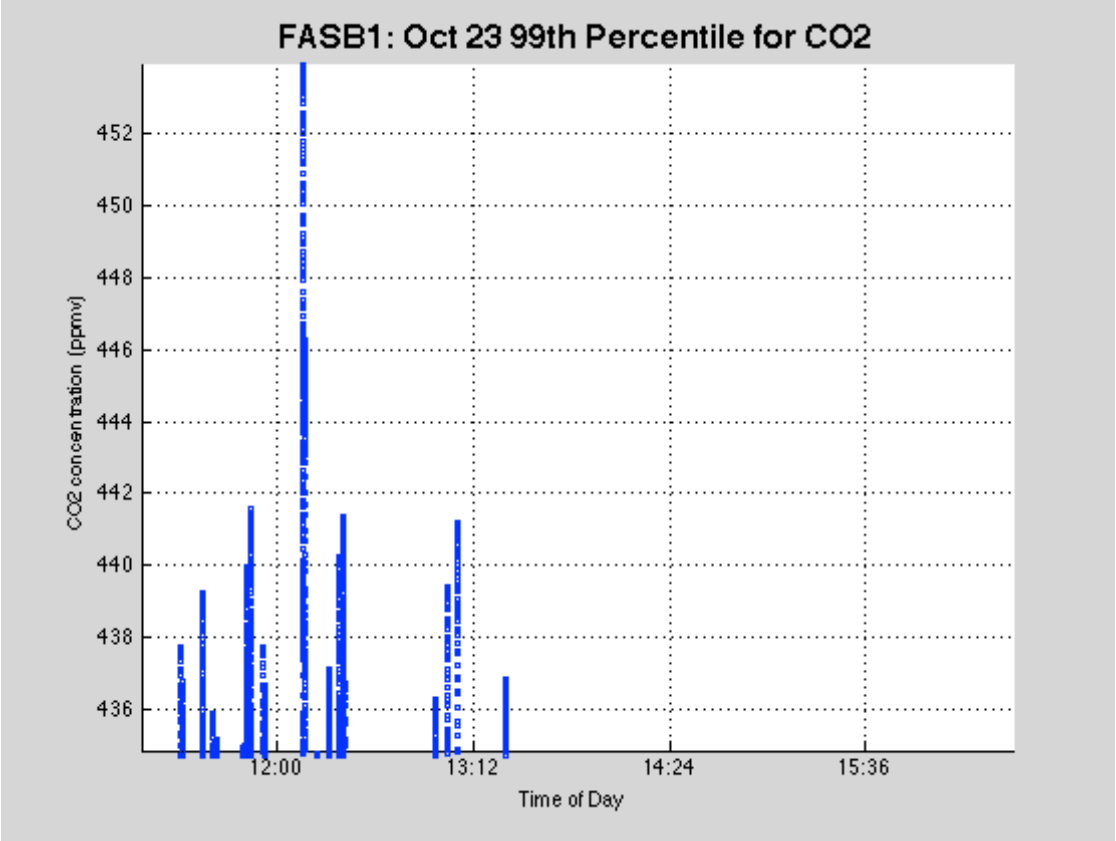
FASB1: Oct 23 99th Percentile for CO2
CO2 concentration (ppmv)
452
450
448
446
444
442
440
438
436
12:00
13:12
14:24
15:36
Time of Day

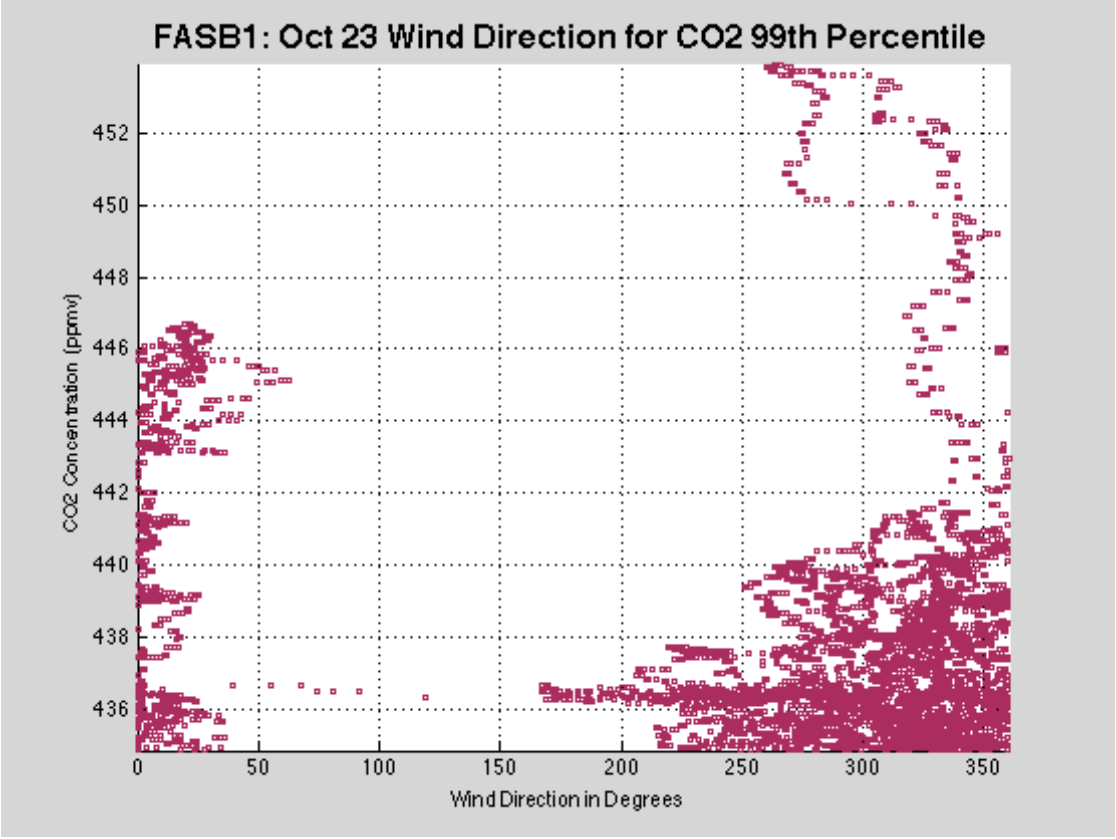
FASB1: Oct 23 Wind Direction for CO2 99th Percentile
CO2 Concentration (ppmv)
452
450
448
446
444
442
440
438
436
0
50
100
150
200
250
300
350
Wind Direction in Degrees

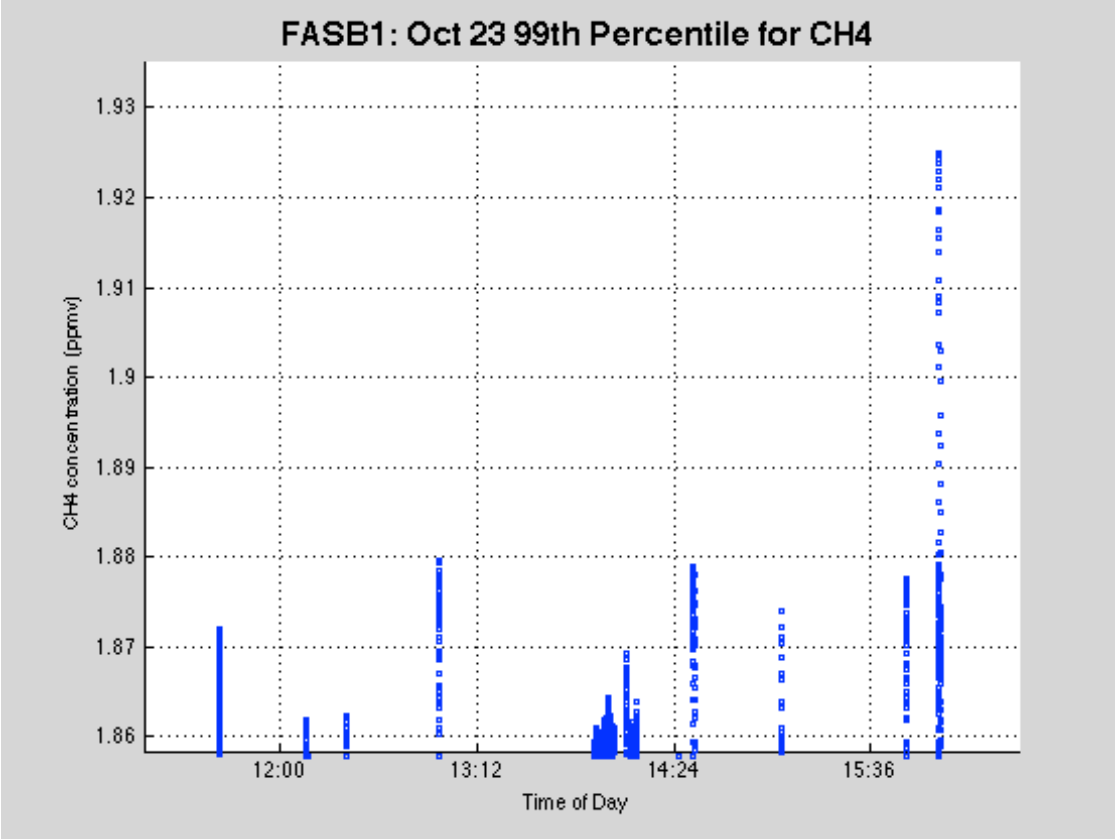
FASB1: Oct 23 99th Percentile for CH4
CH4 concentration (ppmv)
1.93
1.92
1.91
1.9
1.89
1.88
1.87
1.86
12:00
13:12
14:24
15:36
Time of Day

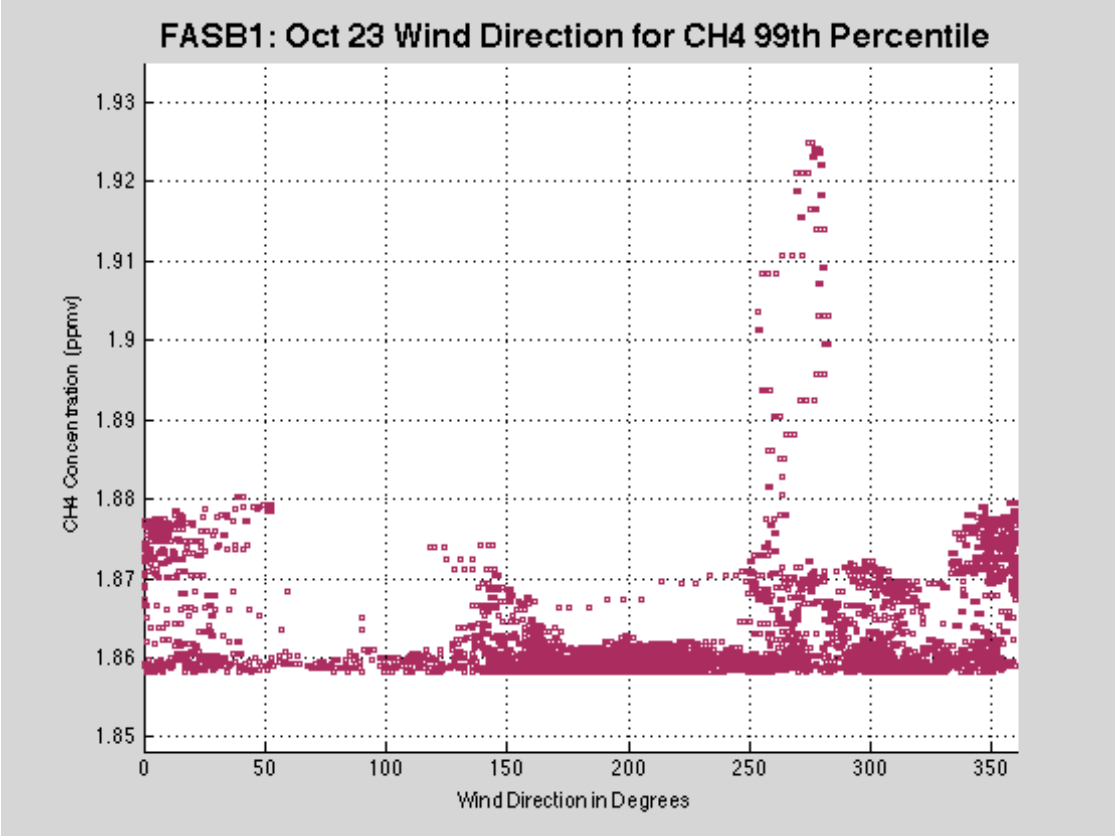
FASB1: Oct 23 Wind Direction for CH4 99th Percentile
CH4 Concentration (ppmv)
1.93
1.92
1.91
1.9
1.89
1.88
1.87
1.86
1.85
0
50
100
150
200
250
300
350
Wind Direction in Degrees

E.2 Friday, November 1st, 2013

| | Maximum | Minimum | Average | Standard Deviation | 99th Percentile |
|---|---|---|---|---|---|
| $CO_2$ (ppmv) | 418.3873 | 380.0346 | 388.1566 | 3.7484 | 399.7971 |
| $CH_4$ (ppmv) | 1.8342 | 1.674 | 1.6951 | 0.0152 | 1.7328 |
| UZ (m/s) | 1.81 | -2.668 | -3.29E-04 | 0.3724 | N/A |

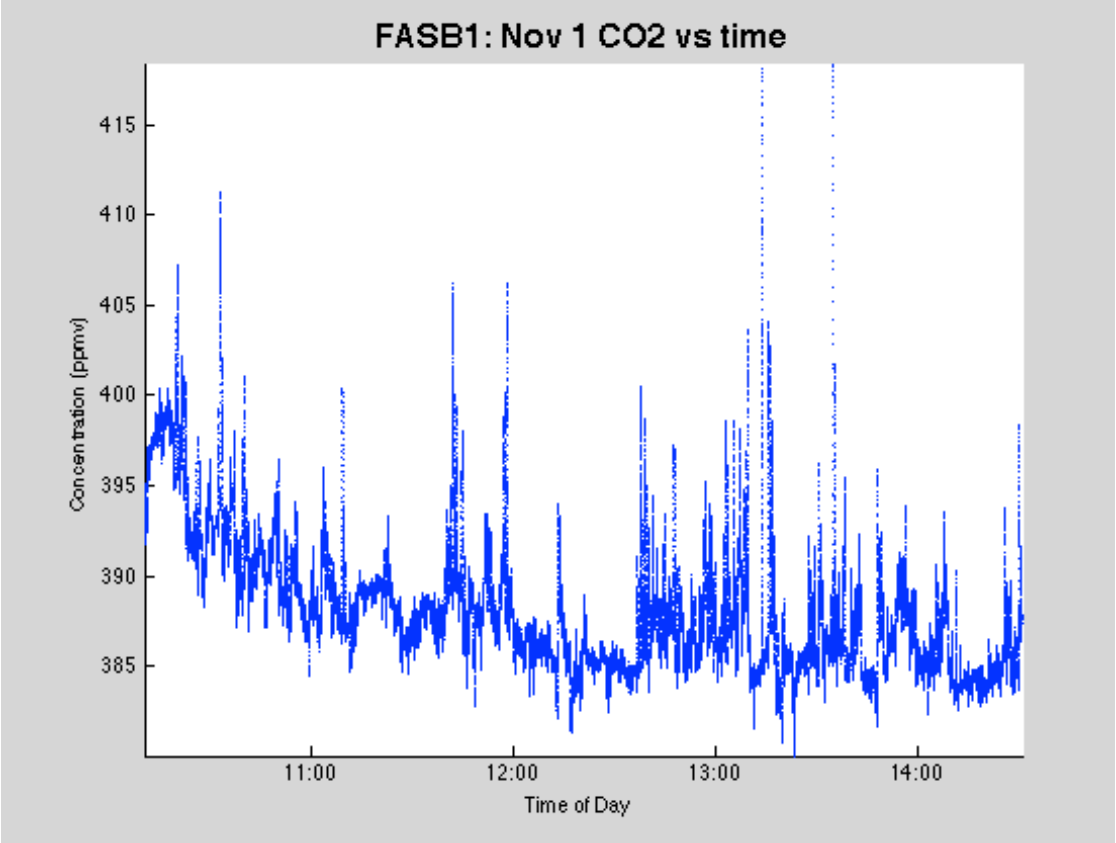

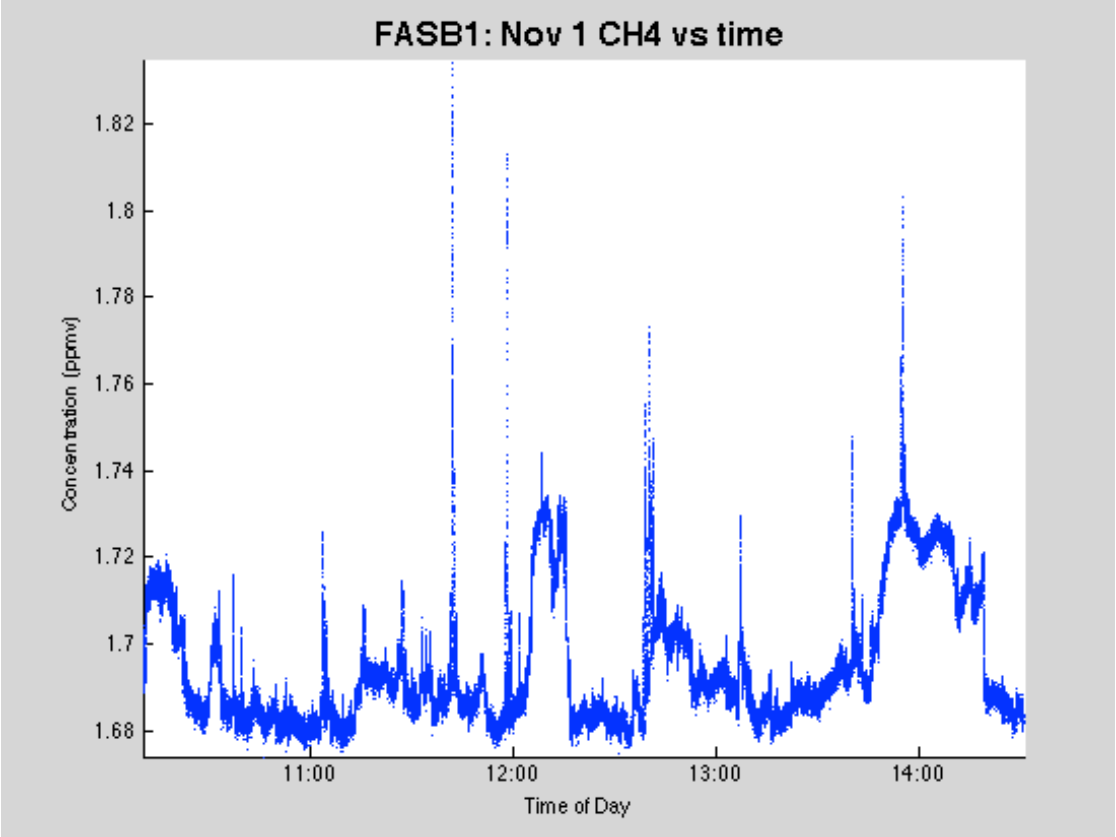
FASB1: Nov 1 CH4 vs time
Concentration (ppmv)
1.82
1.8
1.78
1.76
1.74
1.72
1.7
1.68
11:00
12:00
13:00
14:00
Time of Day

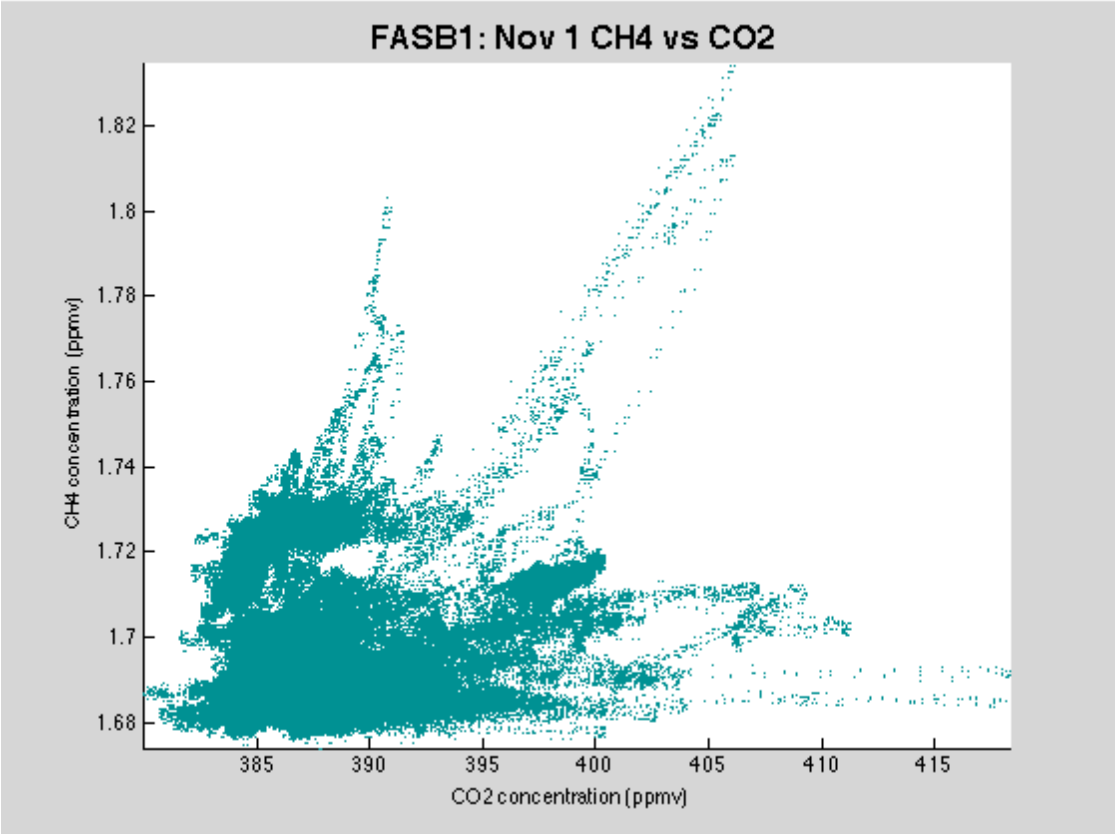
FASB1: Nov 1 CH4 vs CO2
CH4 concentration (ppmv)
1.82
1.8
1.78
1.76
1.74
1.72
1.7
1.68
385
390
395
400
405
410
415
CO2 concentration (ppmv)

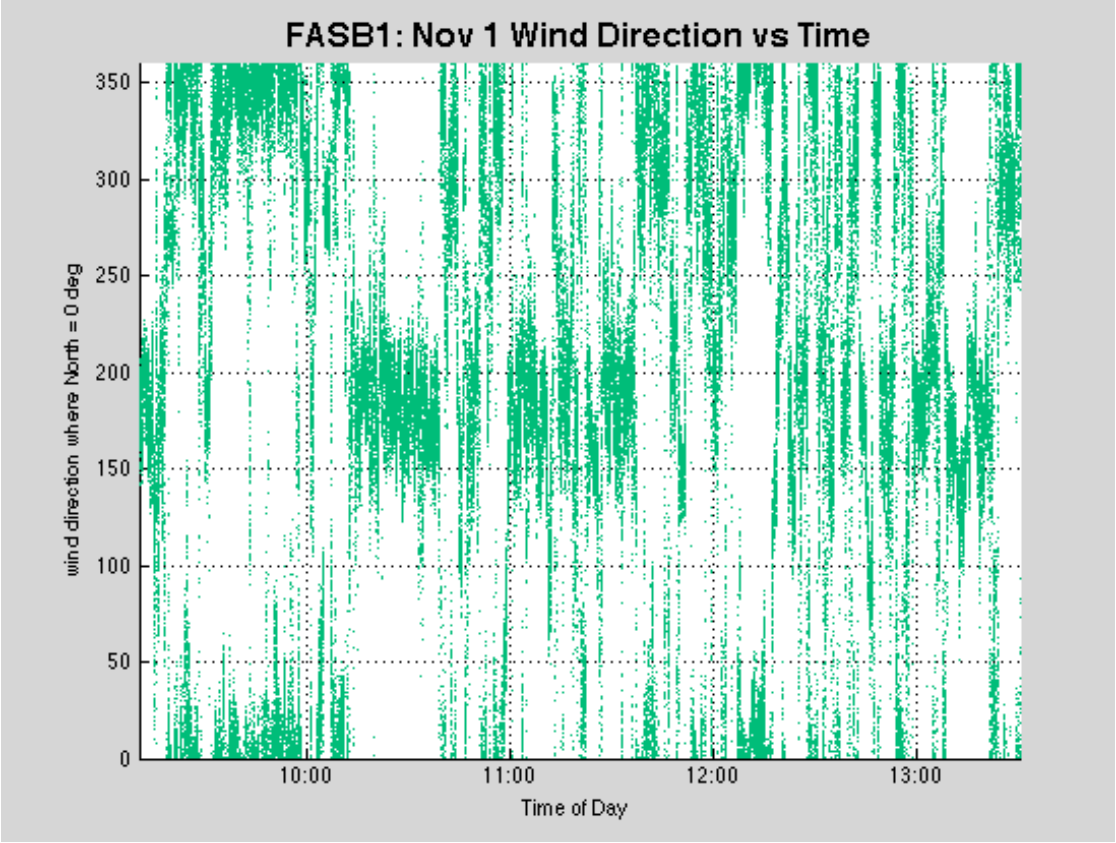
FASB1: Nov 1 Wind Direction vs Time
wind direction where North = 0 deg
350
300
250
200
150
100
50
0
10:00
11:00
12:00
13:00
Time of Day

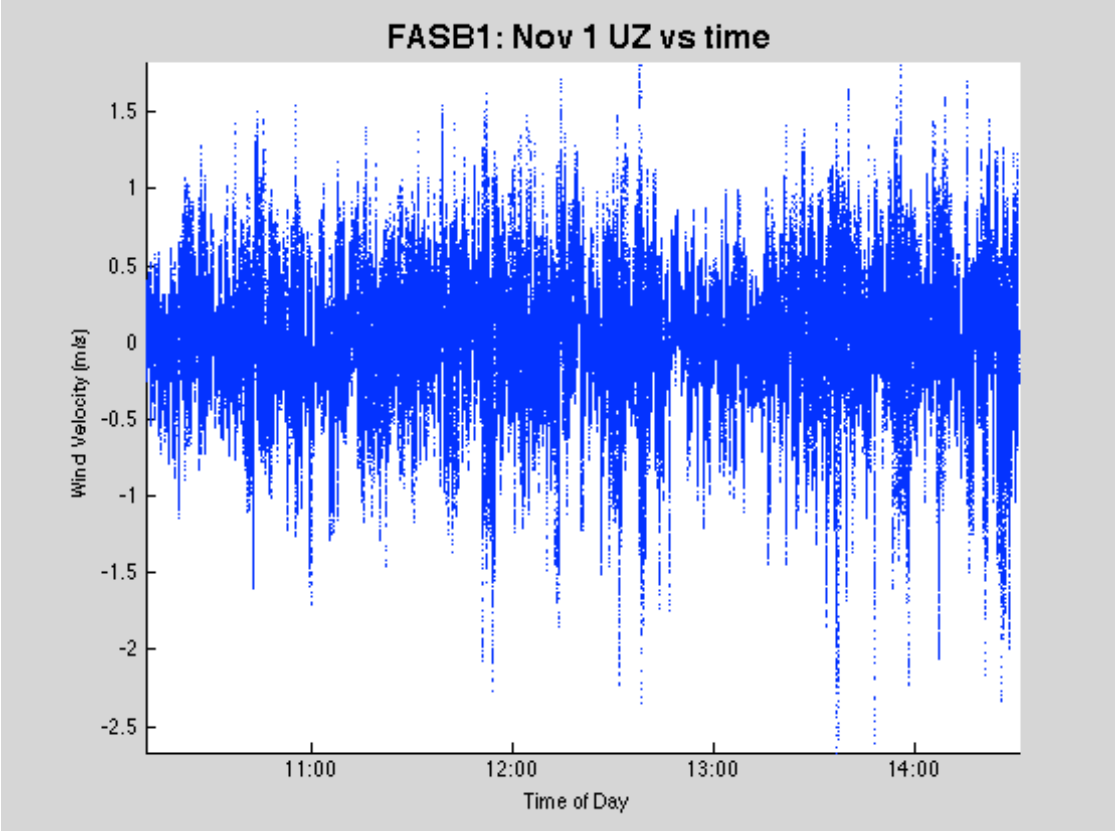
FASB1: Nov 1 UZ vs time
Wind Velocity (m/s)
1.5
1
0.5
0
-0.5
-1
-1.5
-2
-2.5
11:00
12:00
13:00
14:00
Time of Day

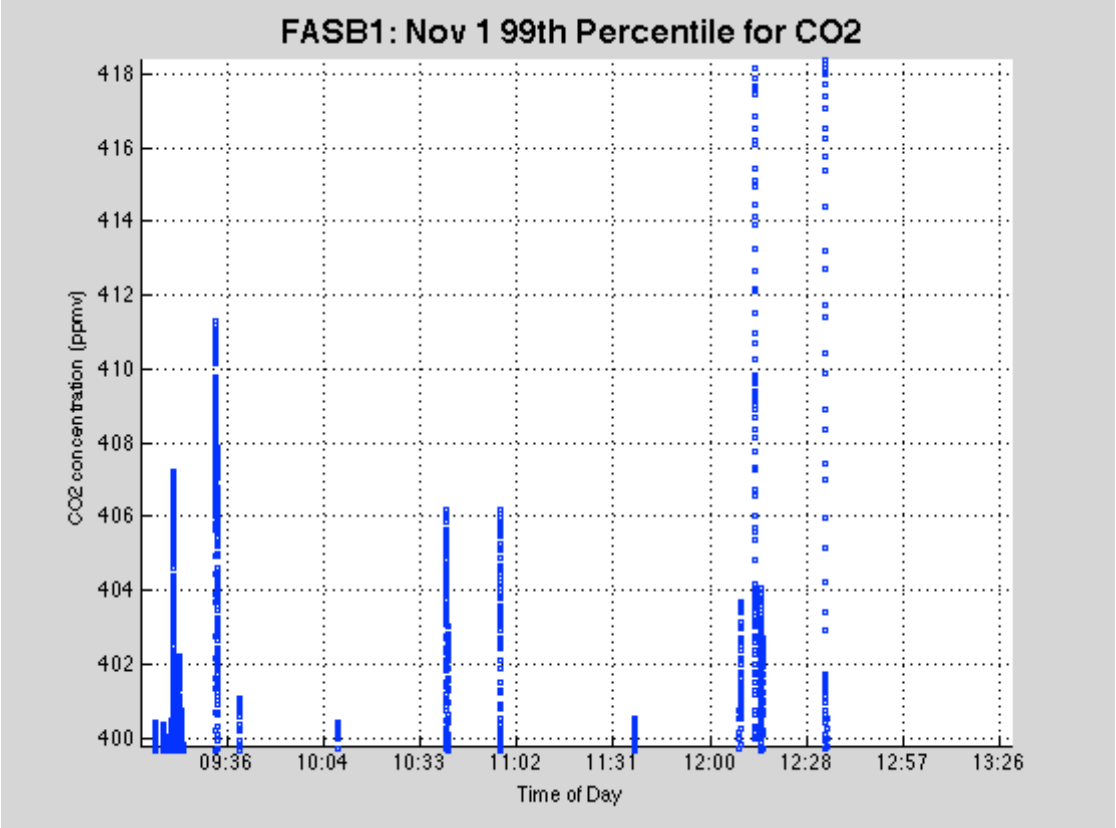
FASB1: Nov 1 99th Percentile for CO2
CO2 concentration (ppmv)
418
416
414
412
410
408
406
404
402
400
09:36
10:04
10:33
11:02
11:31
12:00
12:28
12:57
13:26
Time of Day

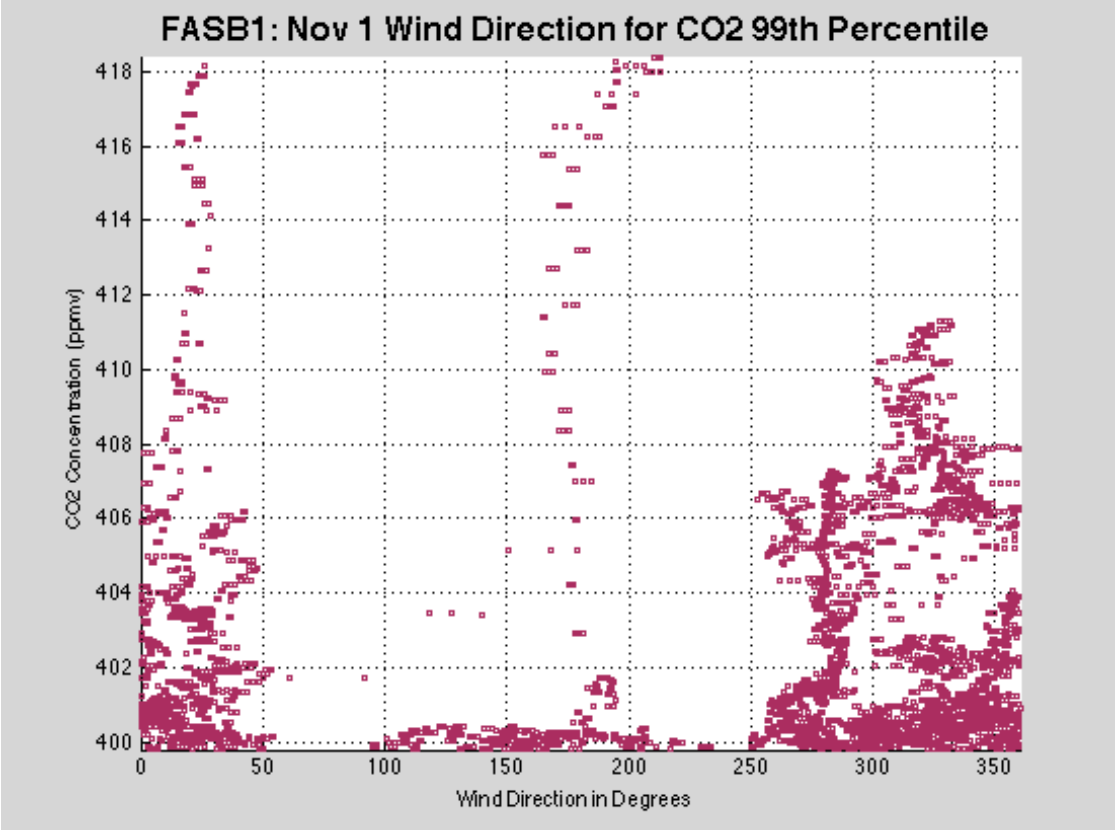
FASB1: Nov 1 Wind Direction for CO2 99th Percentile
CO2 Concentration (ppmv)
418
416
414
412
410
408
406
404
402
400
0
50
100
150
200
250
300
350
Wind Direction in Degrees

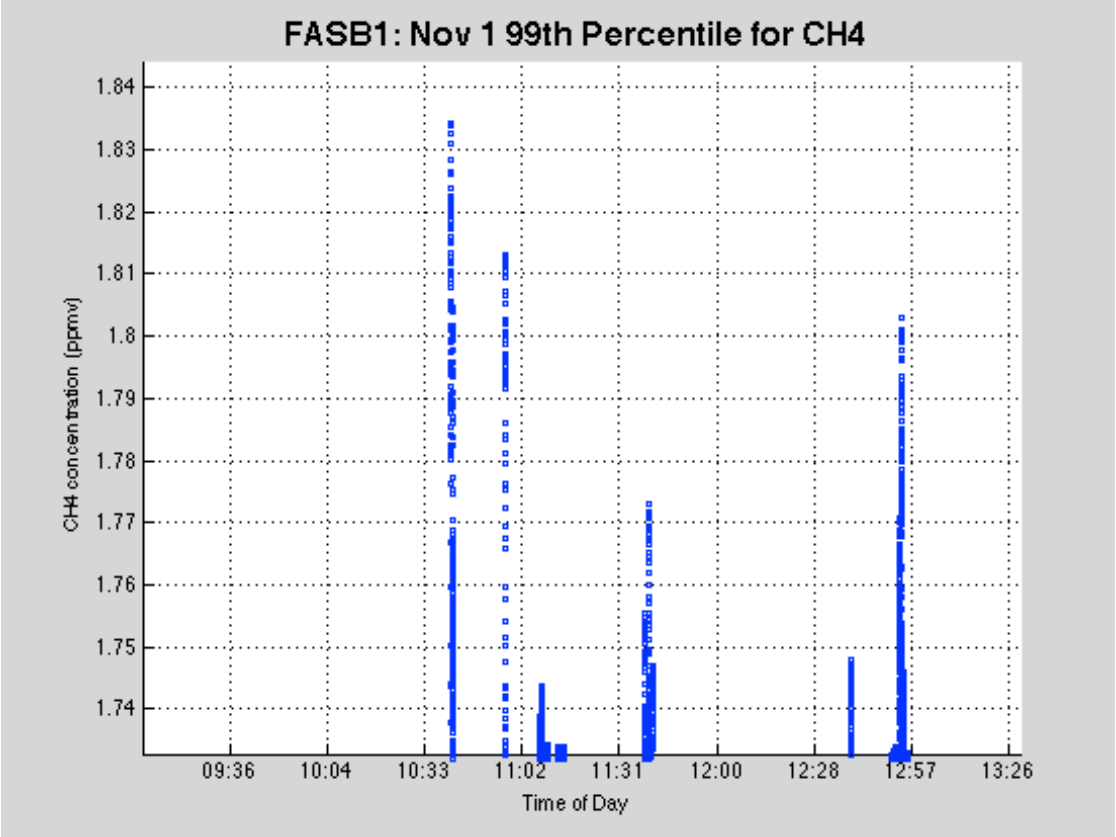
FASB1: Nov 1 99th Percentile for CH4
CH4 concentration (ppmv)
1.84
1.83
1.82
1.81
1.8
1.79
1.78
1.77
1.76
1.75
1.74
09:36
10:04
10:33
11:02
11:31
12:00
12:28
12:57
13:26
Time of Day

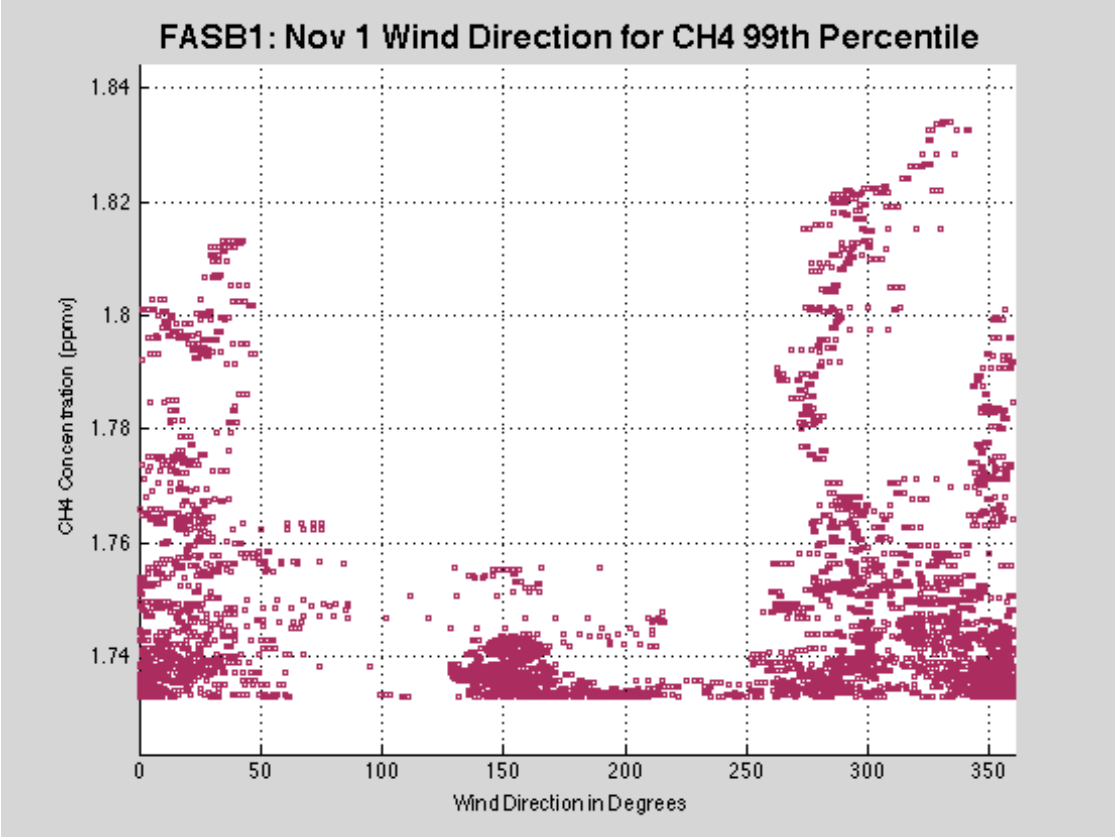
FASB1: Nov 1 Wind Direction for CH4 99th Percentile
CH4 Concentration (ppmv)
1.84
1.82
1.8
1.78
1.76
1.74
0
50
100
150
200
250
300
350
Wind Direction in Degrees

## E.3 Tuesday, November 5th, 2013

| | Maximum | Minimum | Average | Standard Deviation | 99th Percentile |
|---|---|---|---|---|---|
| $CO_2$ (ppmv) | 421.8896 | 363.5842 | 387.3565 | 2.692 | 395.6106 |
| $CH_4$ (ppmv) | 1.7369 | 1.6845 | 1.6959 | 0.0052 | 1.7113 |
| UZ (m/s) | 2.0706 | -2.4719 | -0.042 | 0.3882 | N/A |

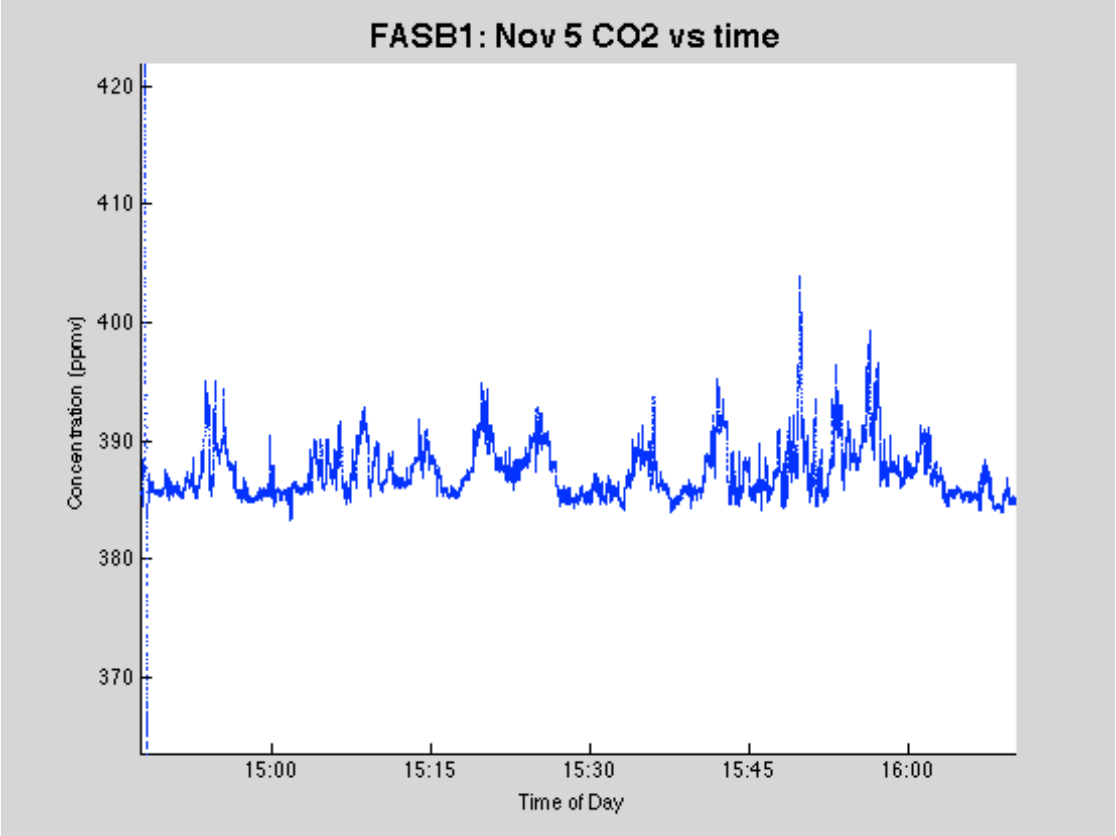

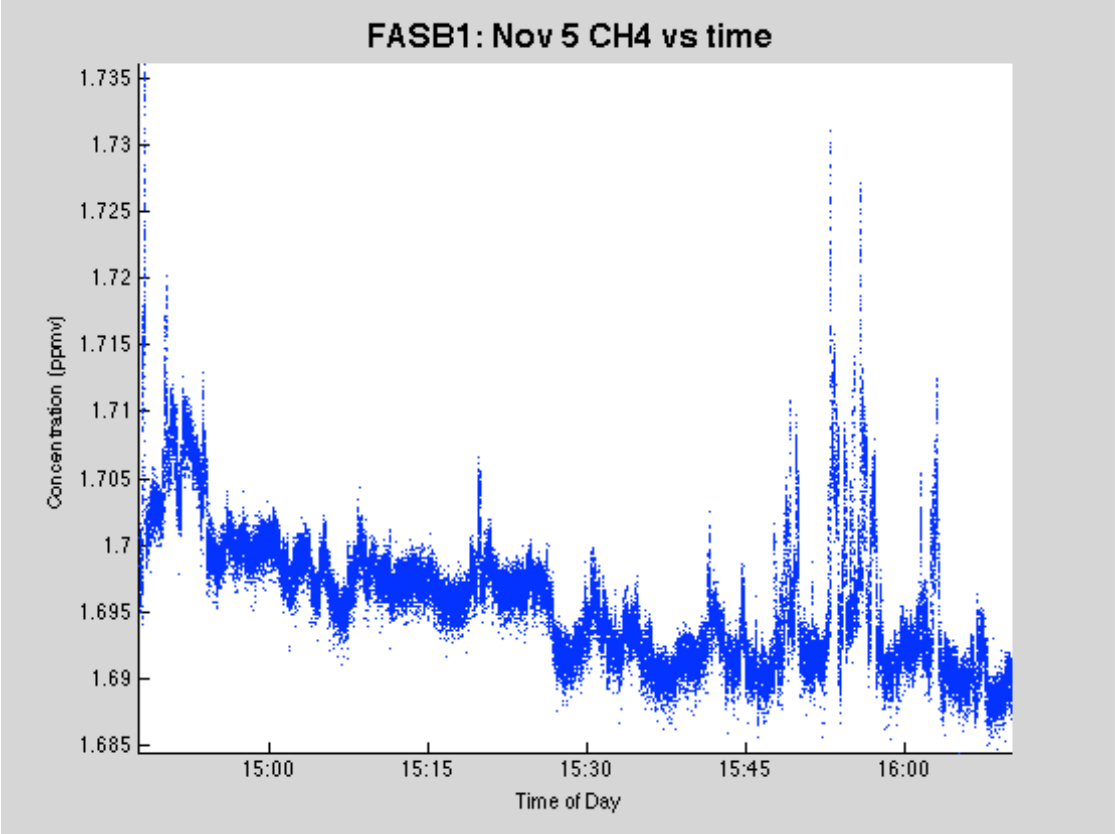
FASB1: Nov 5 CH4 vs time
Concentration (ppmv)
1.735
1.73
1.725
1.72
1.715
1.71
1.705
1.7
1.695
1.69
1.685
15:00
15:15
15:30
15:45
16:00
Time of Day

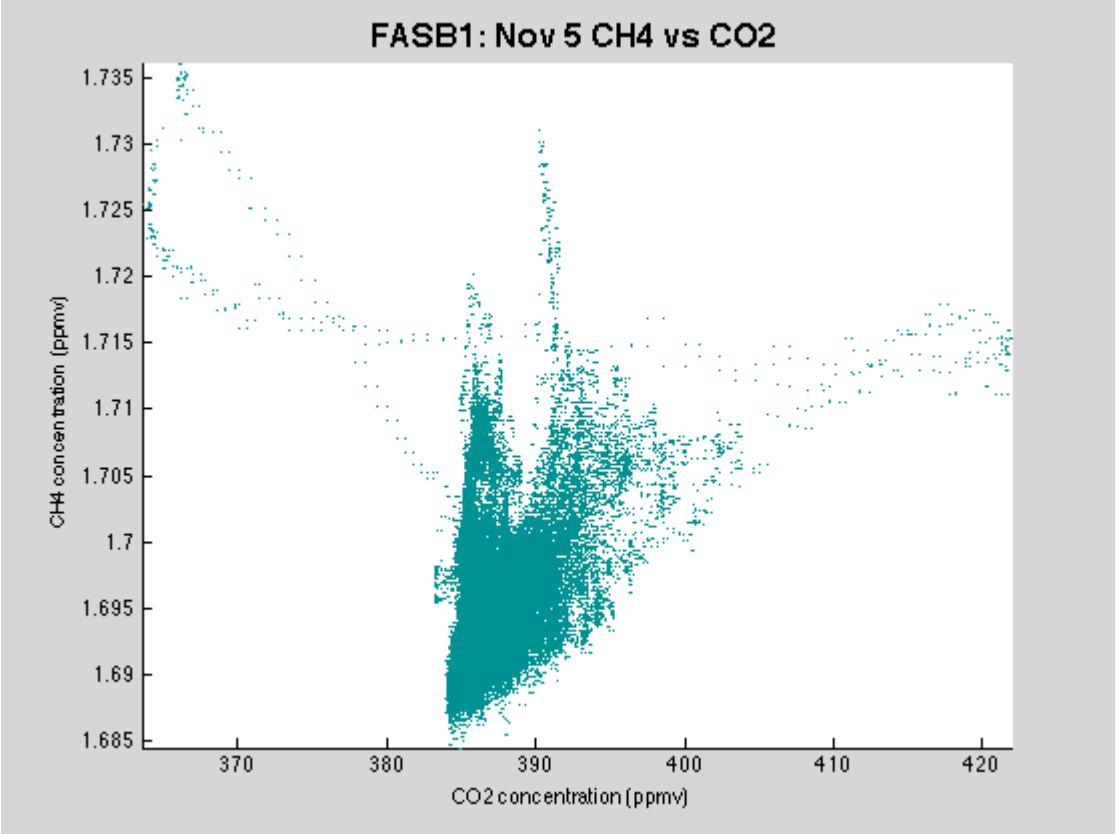
FASB1: Nov 5 CH4 vs CO2
CH4 concentration (ppmv)
1.735
1.73
1.725
1.72
1.715
1.71
1.705
1.7
1.695
1.69
1.685
370
380
390
400
410
420
CO2 concentration (ppmv)

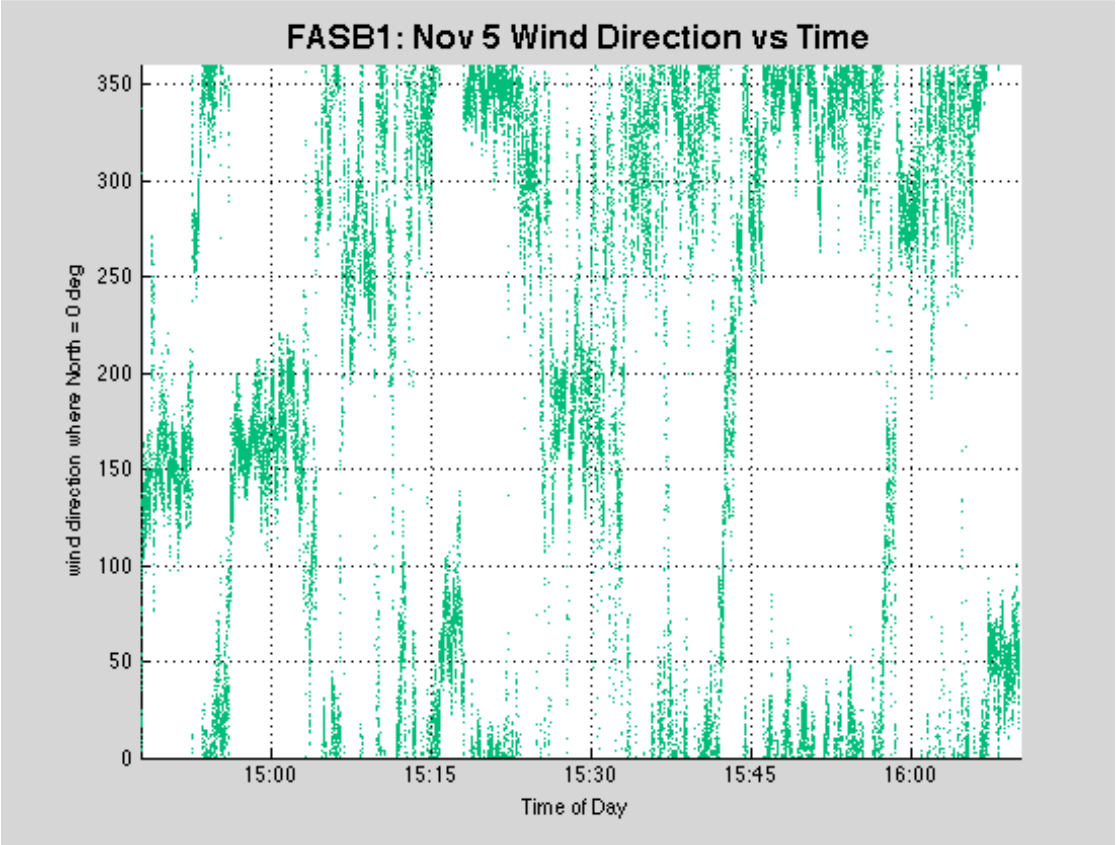
FASB1: Nov 5 Wind Direction vs Time
wind direction where North = 0 deg
350
300
250
200
150
100
50
0
15:00
15:15
15:30
15:45
16:00
Time of Day

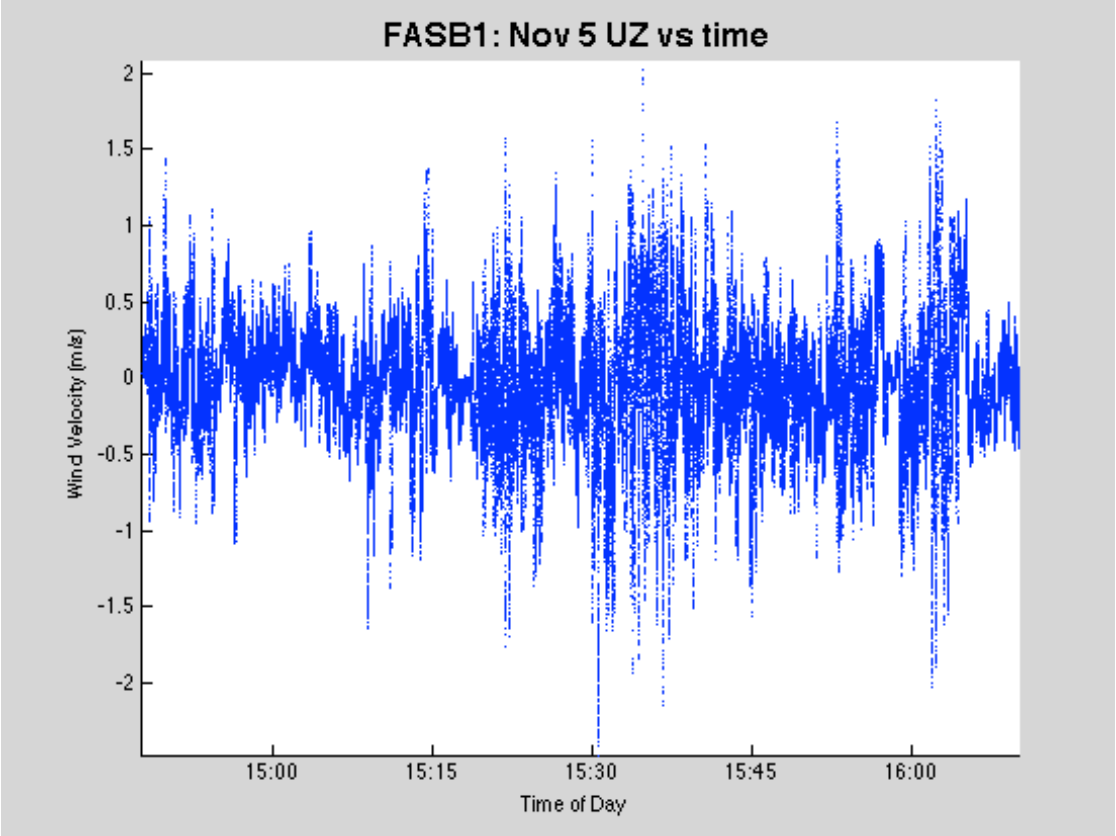
FASB1: Nov 5 UZ vs time
Wind Velocity (m/s)
2
1.5
1
0.5
0
-0.5
-1
-1.5
-2
15:00
15:15
15:30
15:45
16:00
Time of Day

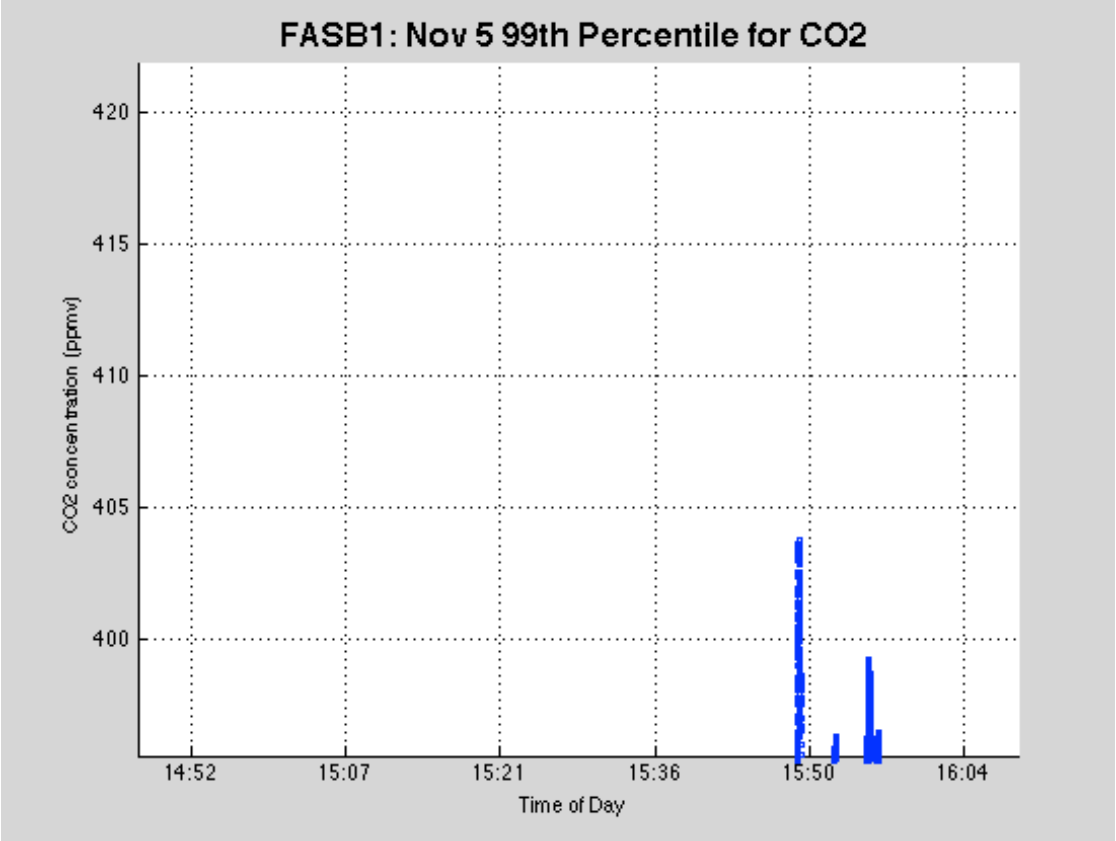
FASB1: Nov 5 99th Percentile for CO2
CO2 concentration (ppmv)
420
415
410
405
400
14:52
15:07
15:21
15:36
15:50
16:04
Time of Day

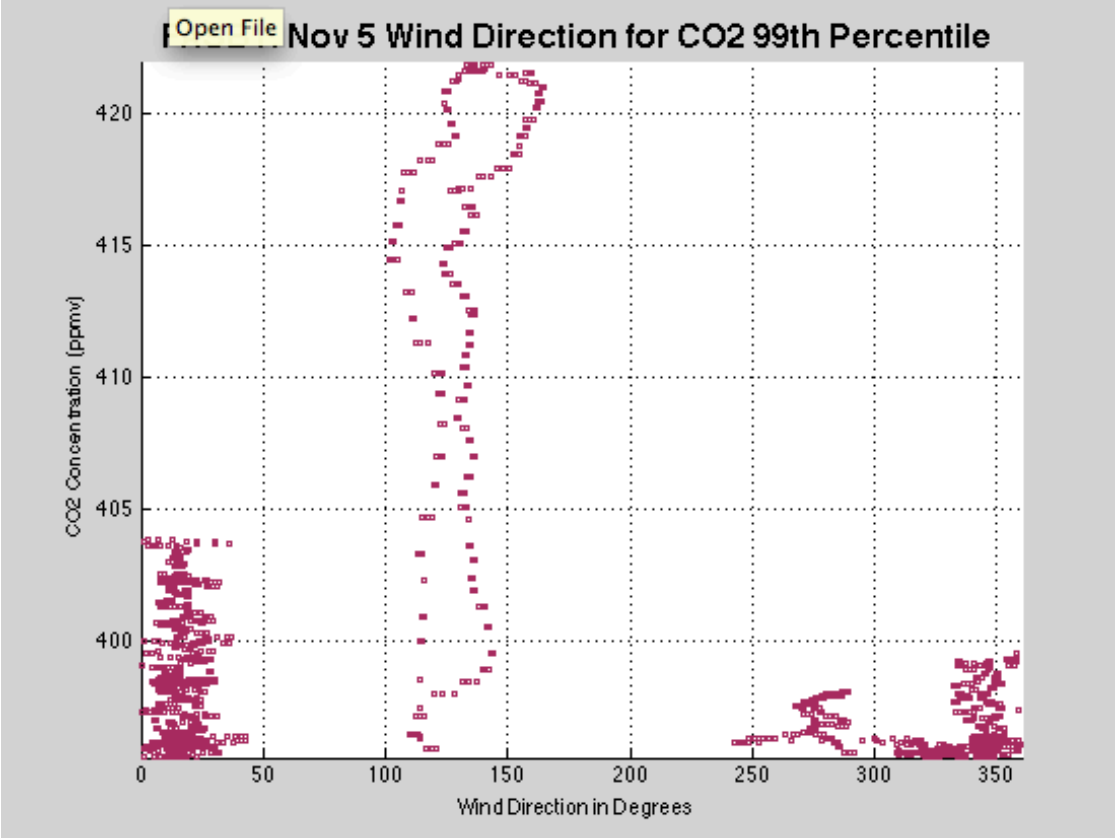
Open File
Nov 5 Wind Direction for CO2 99th Percentile
CO2 Concentration (ppmv)
420
415
410
405
400
0
50
100
150
200
250
300
350
Wind Direction in Degrees

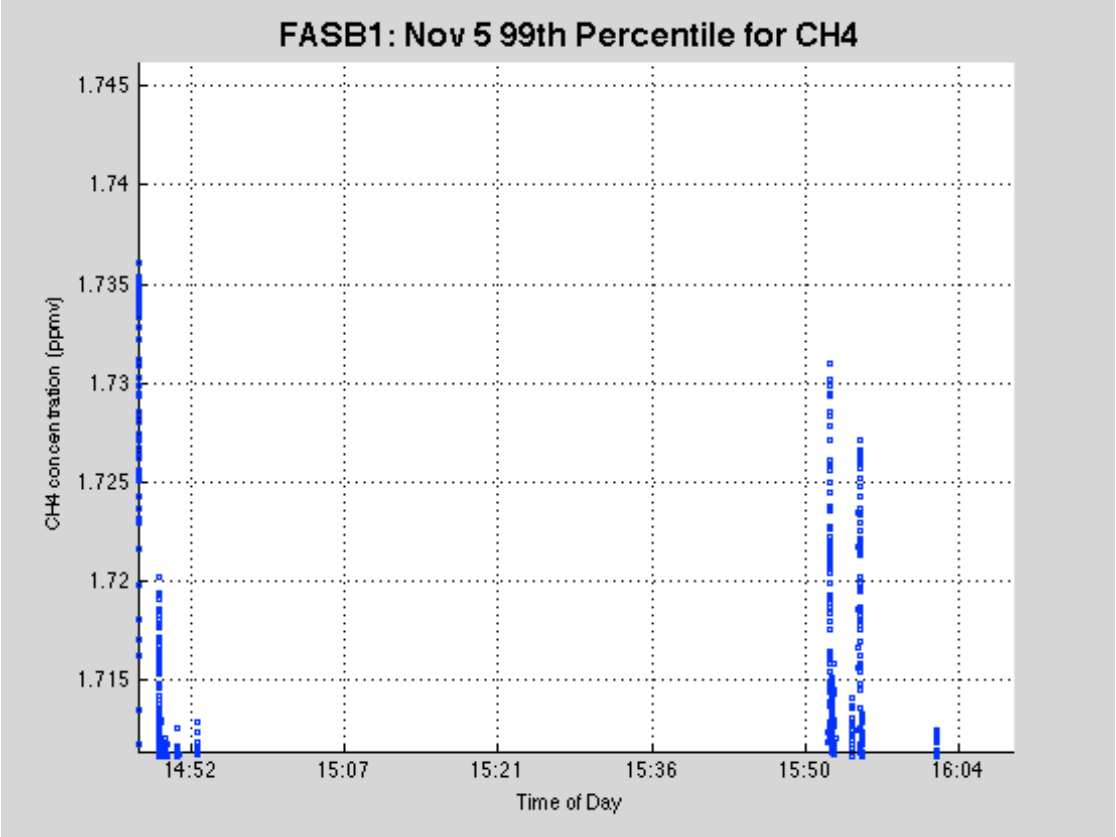
FASB1: Nov 5 99th Percentile for CH4
CH4 concentration (ppmv)
1.745
1.74
1.735
1.73
1.725
1.72
1.715
14:52
15:07
15:21
15:36
15:50
16:04
Time of Day

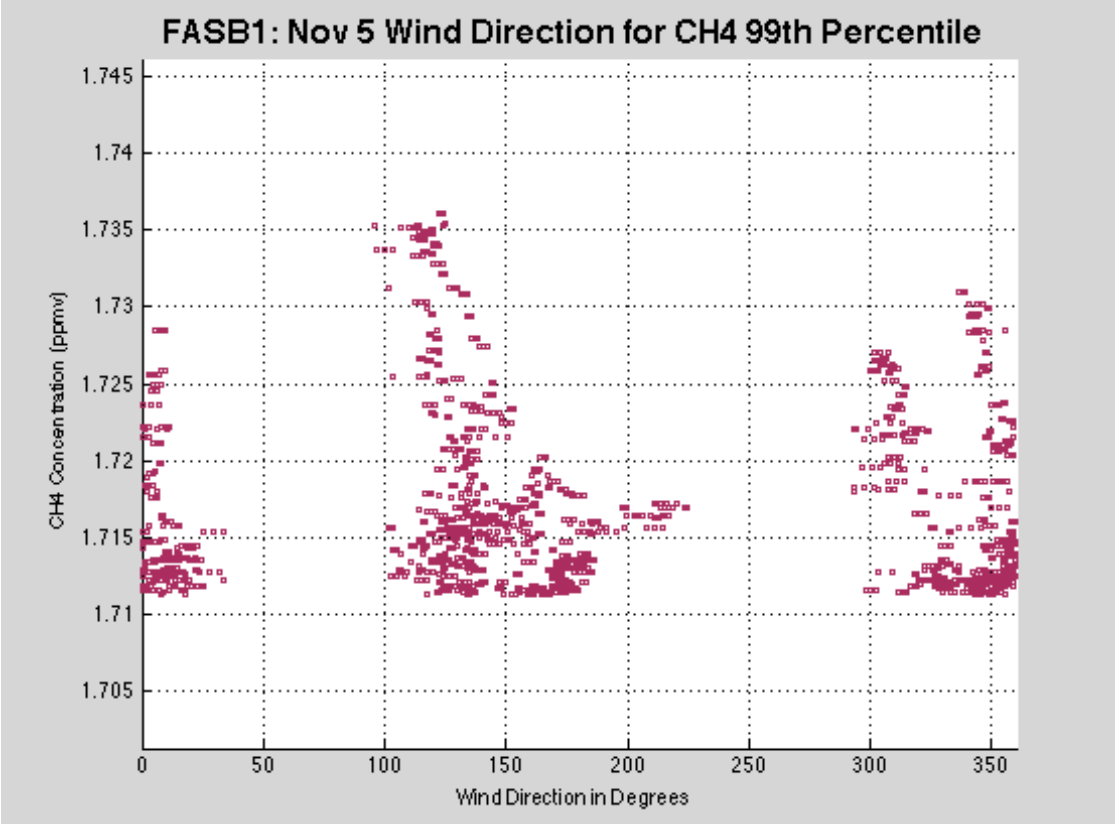
FASB1: Nov 5 Wind Direction for CH4 99th Percentile
CH4 Concentration (ppmv)
1.745
1.74
1.735
1.73
1.725
1.72
1.715
1.71
1.705
0
50
100
150
200
250
300
350
Wind Direction in Degrees

## E.4 Wednesday, November 6th, 2013

| | Maximum | Minimum | Average | Standard Deviation | 99th Percentile |
|---|---|---|---|---|---|
| $CO_2$ (ppmv) | 437.1507 | 402.0288 | 416.9341 | 4.0337 | 429.1065 |
| $CH_4$ (ppmv) | 1.7893 | 1.7224 | 1.7554 | 0.0085 | 1.7893 |
| UZ (m/s) | 1.19 | -1.2189 | 0.0076 | 0.2144 | N/A |

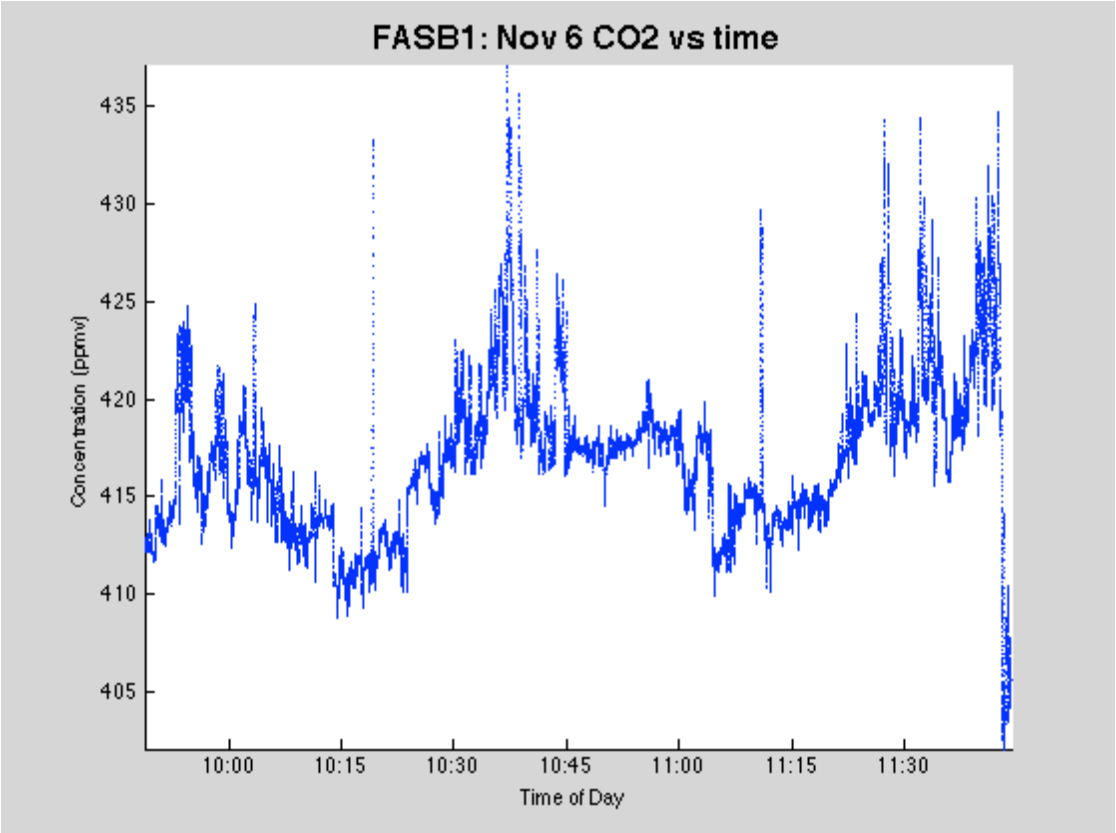

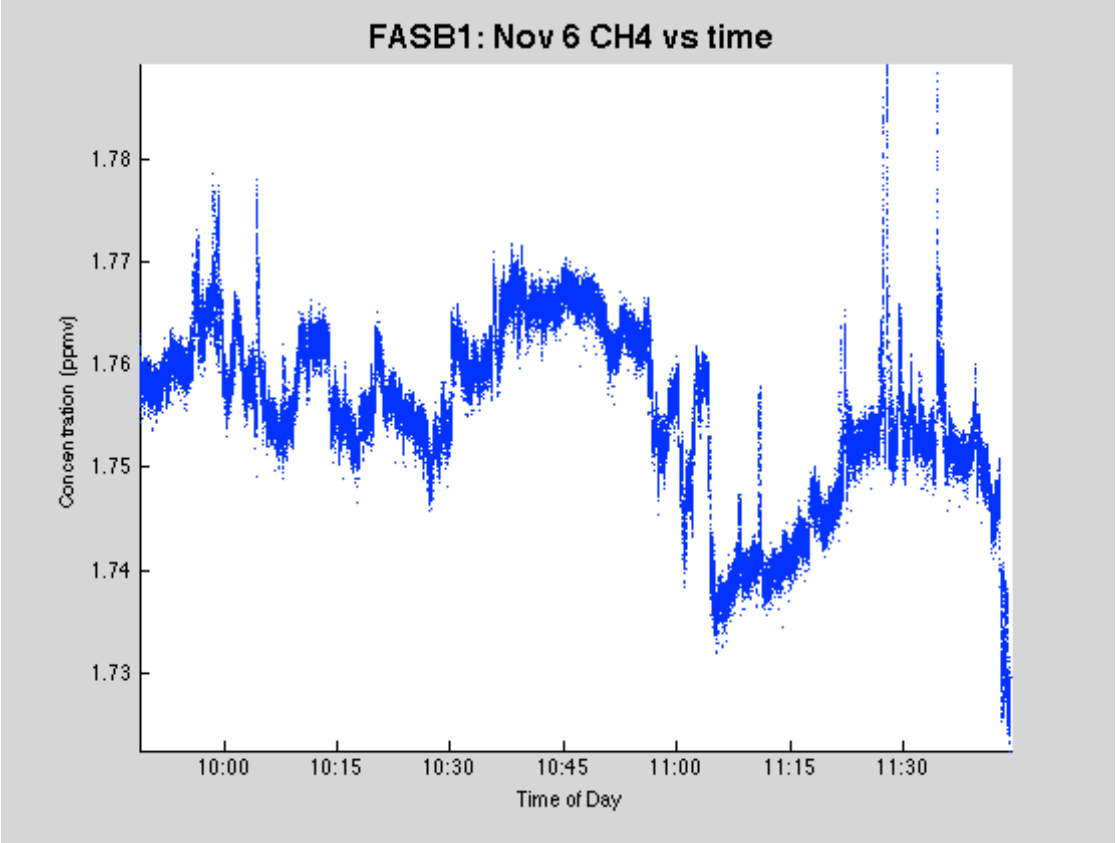
FASB1: Nov 6 CH4 vs time
Concentration (ppmv)
1.78
1.77
1.76
1.75
1.74
1.73
10:00
10:15
10:30
10:45
11:00
11:15
11:30
Time of Day

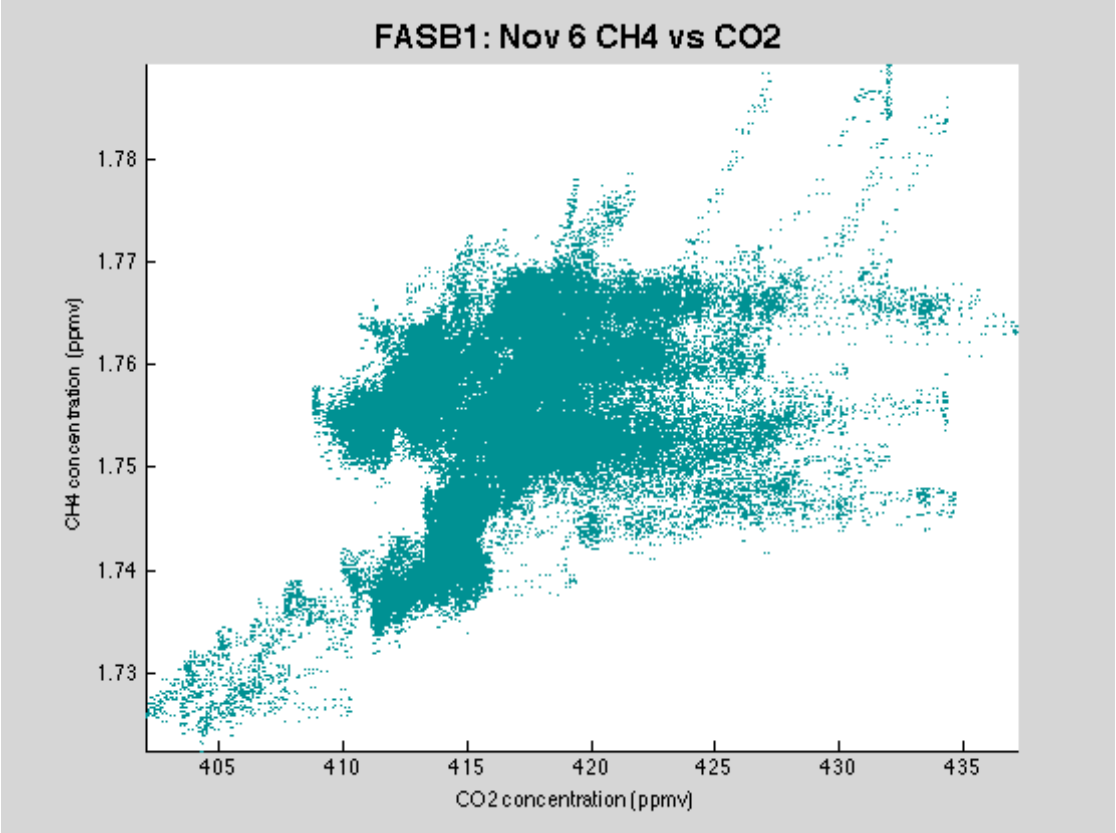
FASB1: Nov 6 CH4 vs CO2
CH4 concentration (ppmv)
1.78
1.77
1.76
1.75
1.74
1.73
405
410
415
420
425
430
435
CO2 concentration (ppmv)

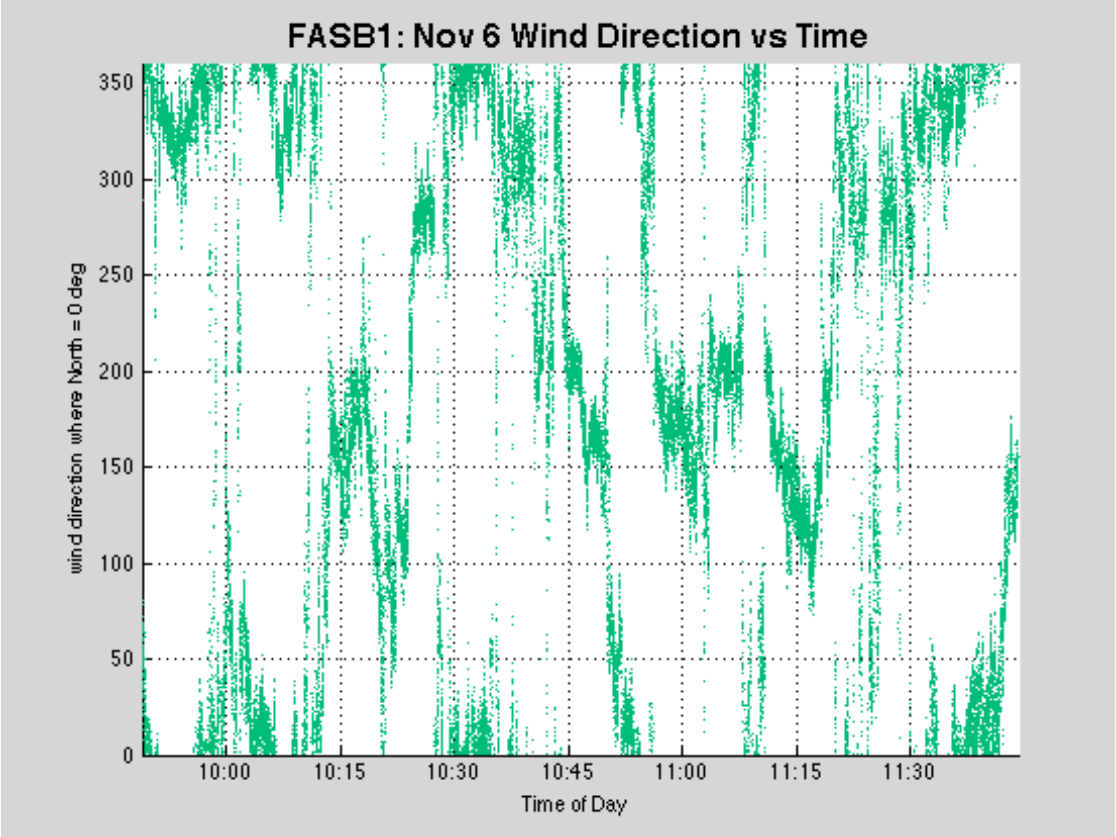
FASB1: Nov 6 Wind Direction vs Time
wind direction where North = 0 deg
350
300
250
200
150
100
50
0
10:00
10:15
10:30
10:45
11:00
11:15
11:30
Time of Day

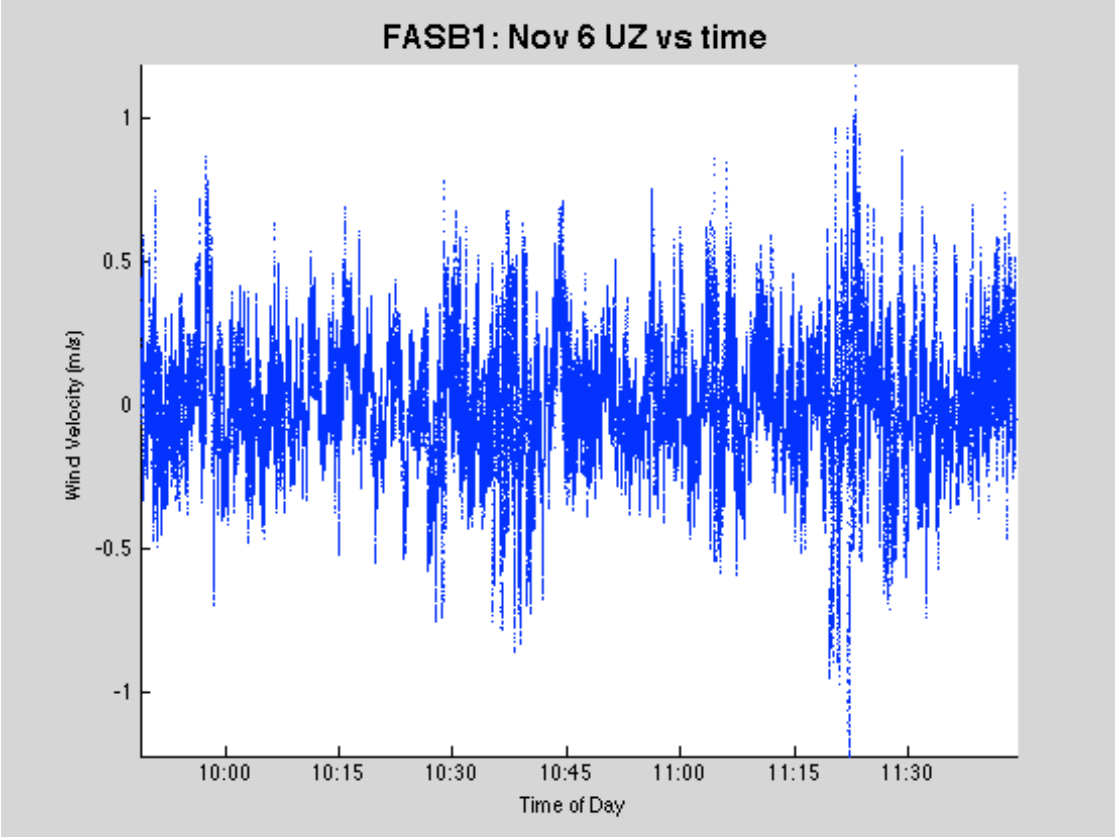
FASB1: Nov 6 UZ vs time
Wind Velocity (m/s)
1
0.5
0
-0.5
-1
10:00
10:15
10:30
10:45
11:00
11:15
11:30
Time of Day

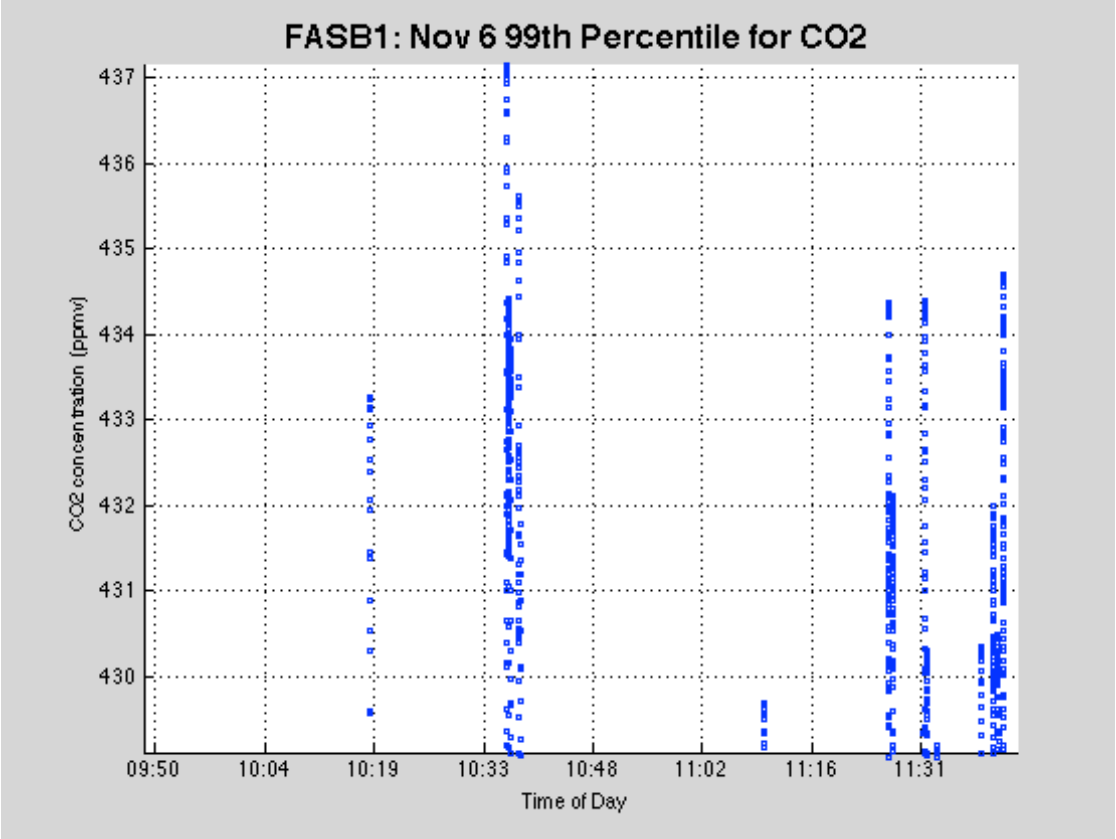
FASB1: Nov 6 99th Percentile for CO2
CO2 concentration (ppmv)
437
436
435
434
433
432
431
430
09:50
10:04
10:19
10:33
10:48
11:02
11:16
11:31
Time of Day

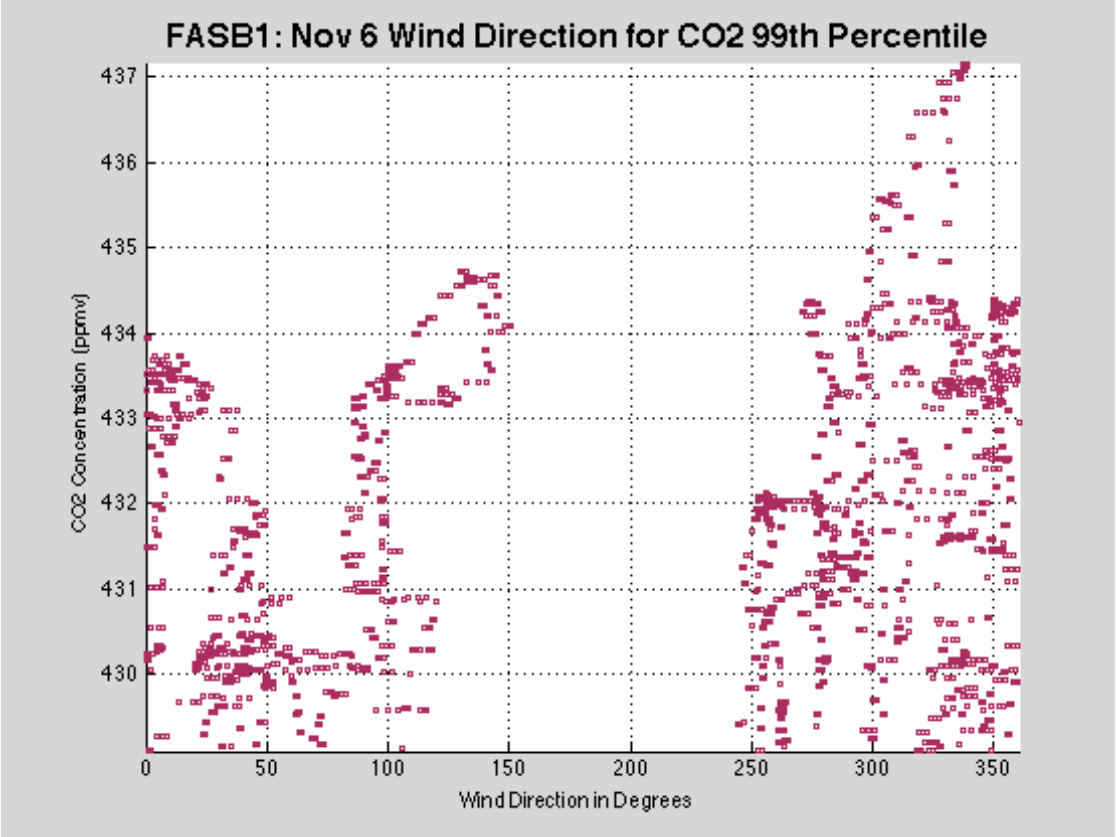
FASB1: Nov 6 Wind Direction for CO2 99th Percentile
CO2 Concentration (ppmv)
437
436
435
434
433
432
431
430
0
50
100
150
200
250
300
350
Wind Direction in Degrees

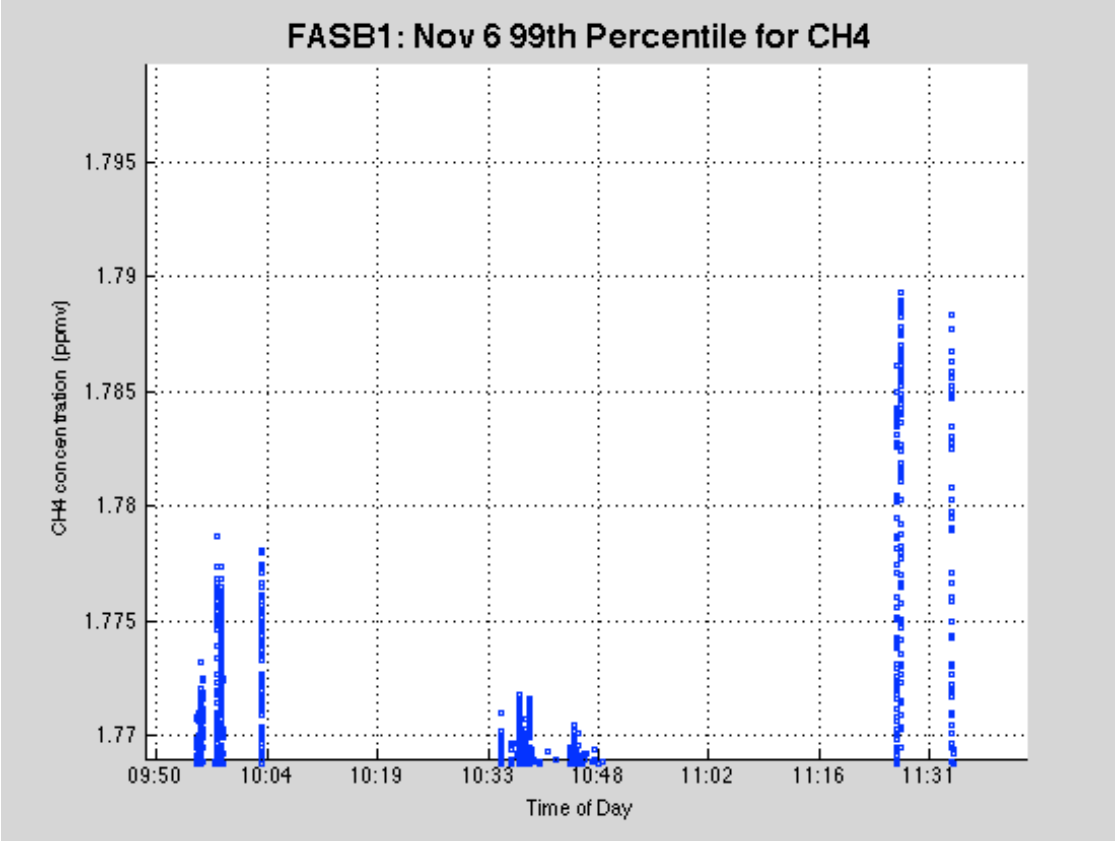
FASB1: Nov 6 99th Percentile for CH4
CH4 concentration (ppmv)
1.795
1.79
1.785
1.78
1.775
1.77
09:50
10:04
10:19
10:33
10:48
11:02
11:16
11:31
Time of Day

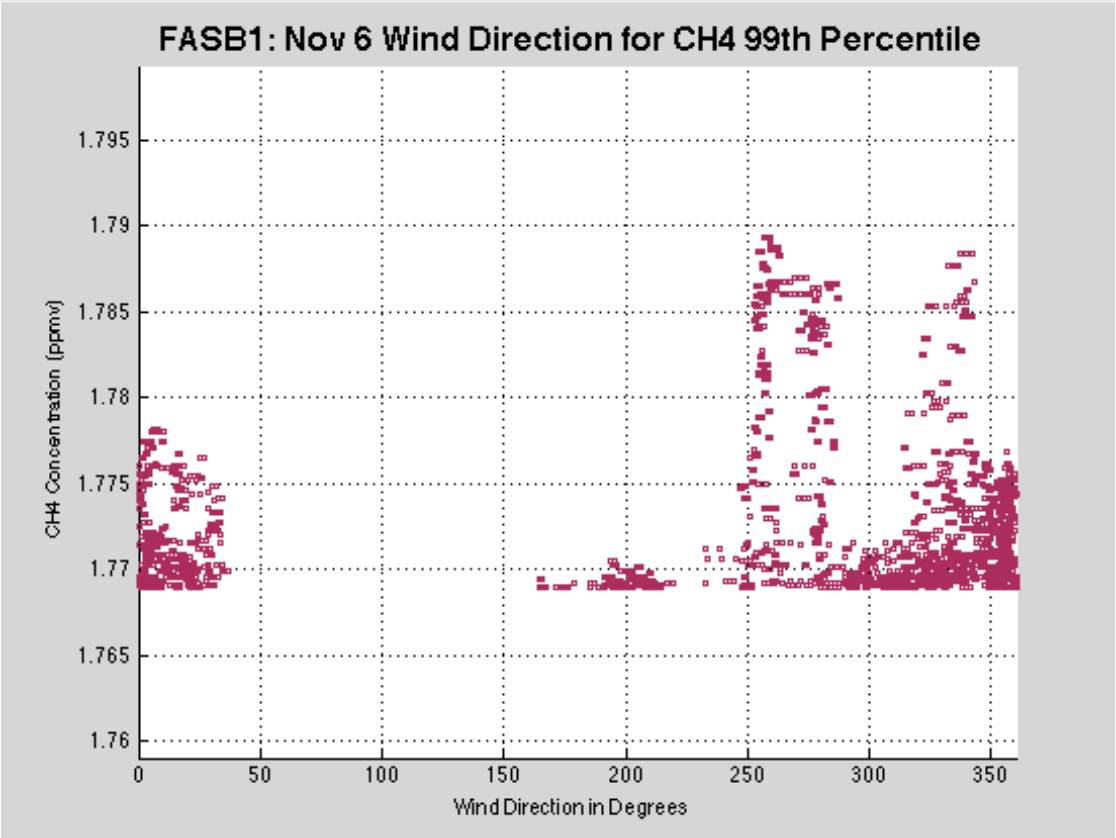
FASB1: Nov 6 Wind Direction for CH4 99th Percentile
CH4 Concentration (ppmv)
1.795
1.79
1.785
1.78
1.775
1.77
1.765
1.76
0
50
100
150
200
250
300
350
Wind Direction in Degrees

E.5 Thursday, November 7th, 2013

| | Maximum | Minimum | Average | Standard Deviation | 99th Percentile |
|---|---|---|---|---|---|
| $CO_2$ (ppmv) | 433.5561 | 391.2656 | 404.3665 | 6.9218 | 423.3795 |
| $CH_4$ (ppmv) | 1.8461 | 1.6967 | 1.7327 | 0.0204 | 1.798 |
| UZ (m/s) | 2.8599 | -2.2757 | -0.0211 | 0.3455 | N/A |

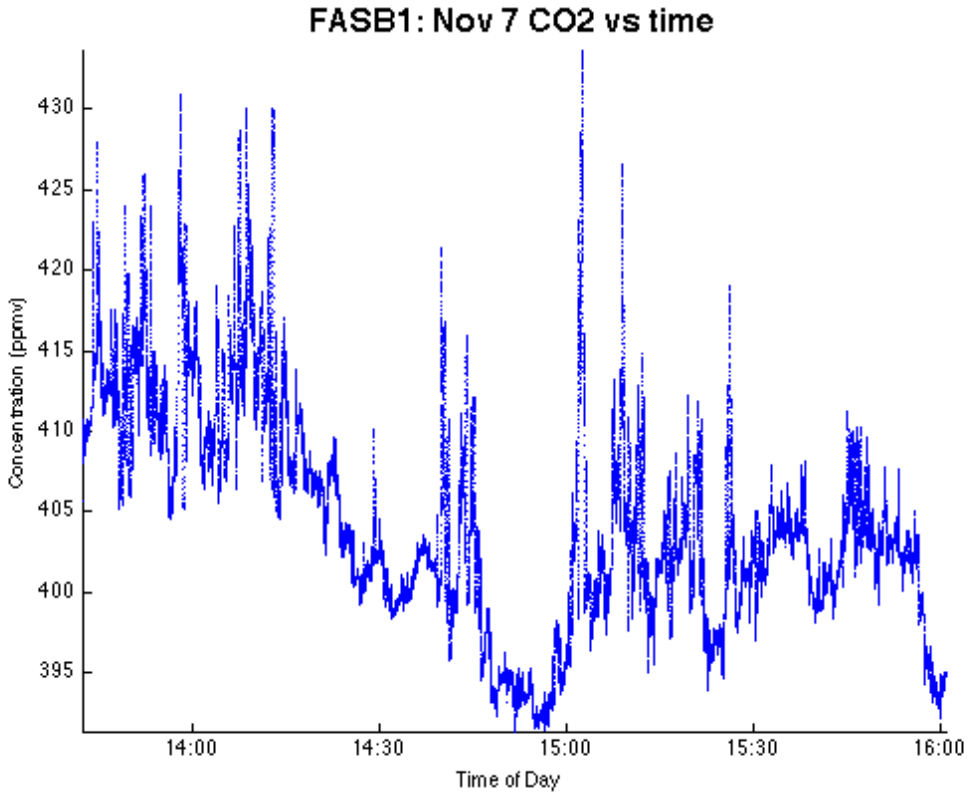

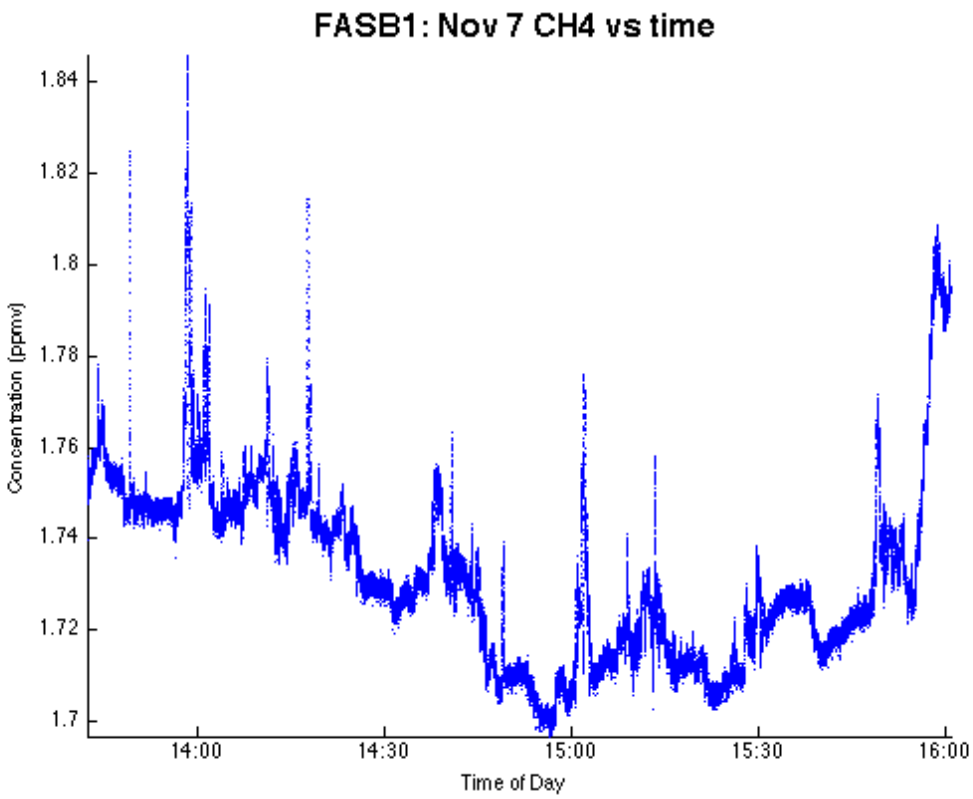
FASB1: Nov 7 CH4 vs time
Concentration (ppmv)
1.84
1.82
1.8
1.78
1.76
1.74
1.72
1.7
14:00
14:30
15:00
15:30
16:00
Time of Day

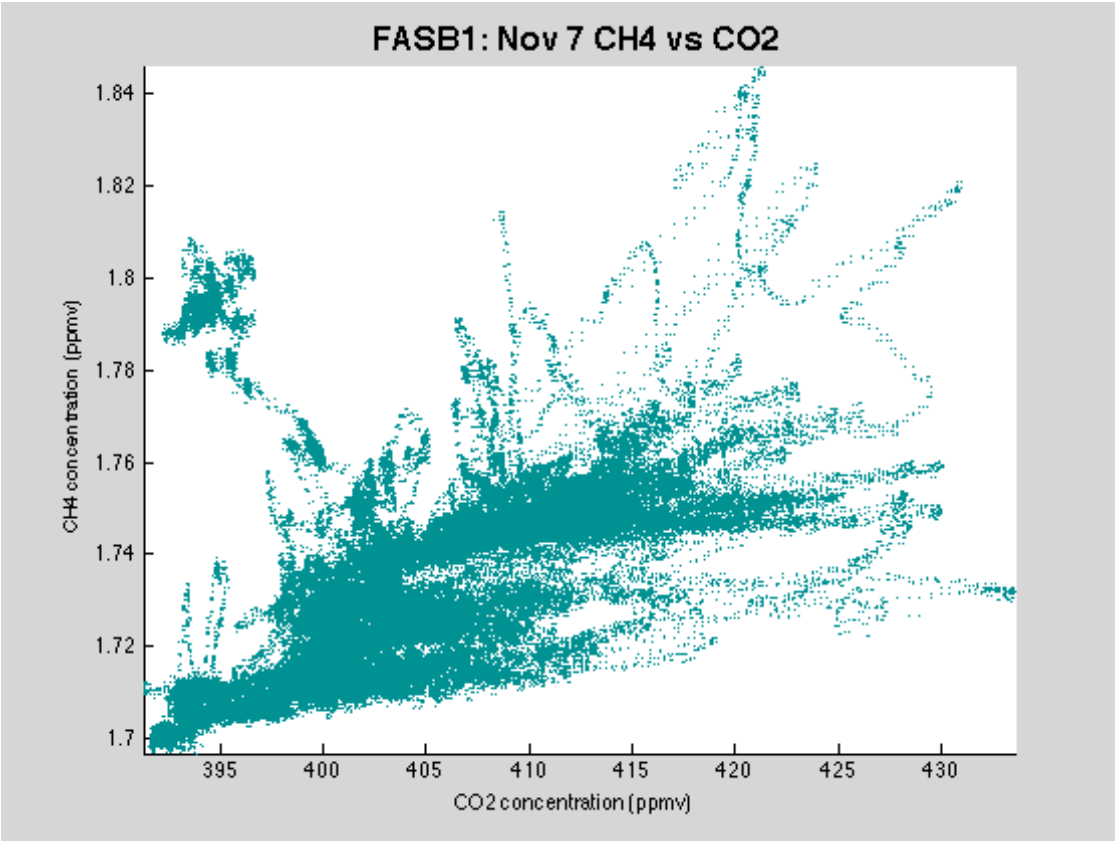
FASB1: Nov 7 CH4 vs CO2
CH4 concentration (ppmv)
1.84
1.82
1.8
1.78
1.76
1.74
1.72
1.7
395
400
405
410
415
420
425
430
CO2 concentration (ppmv)

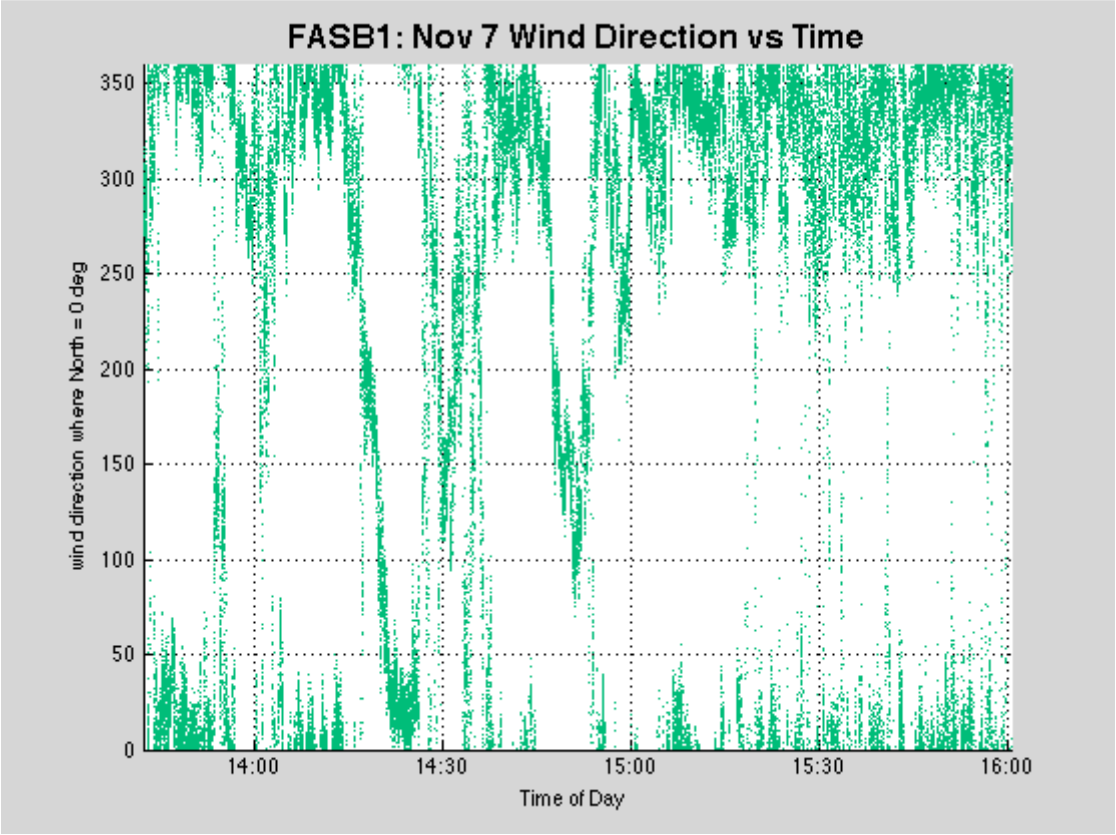
FASB1: Nov 7 Wind Direction vs Time
wind direction where North = 0 deg
350
300
250
200
150
100
50
0
14:00
14:30
15:00
15:30
16:00
Time of Day

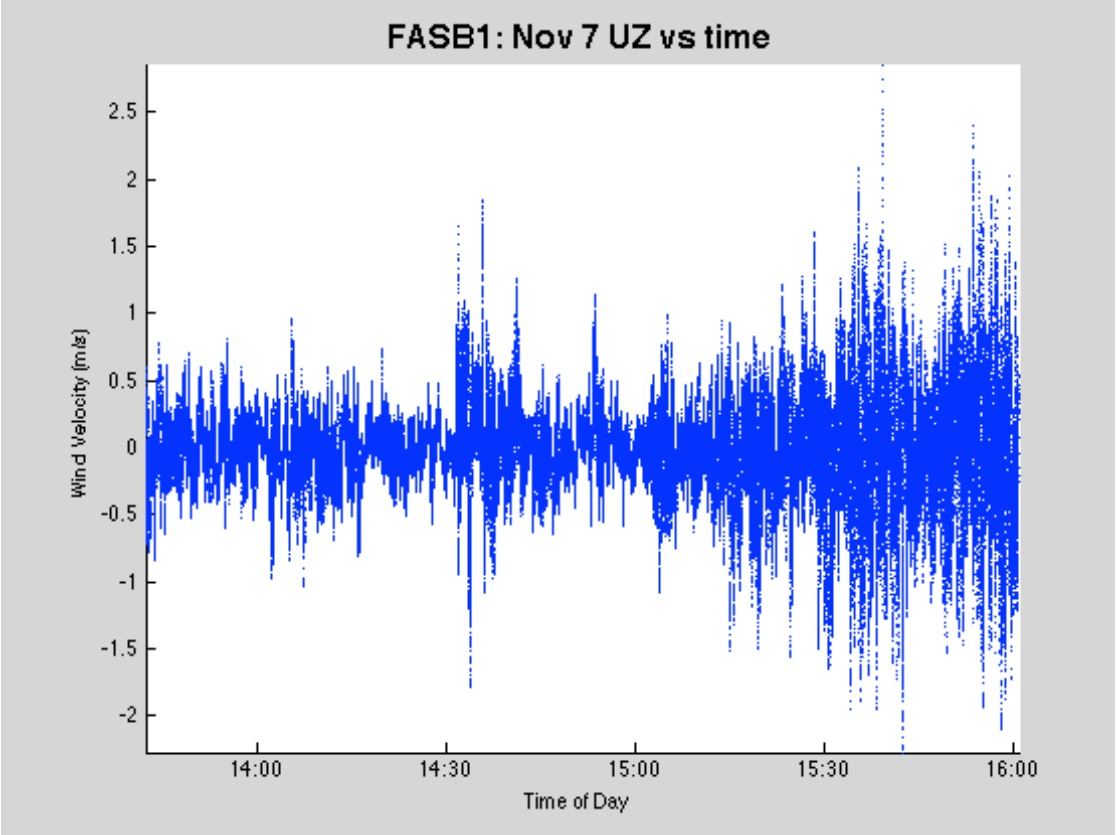
FASB1: Nov 7 UZ vs time
Wind Velocity (m/s)
2.5
2
1.5
1
0.5
0
-0.5
-1
-1.5
-2
14:00
14:30
15:00
15:30
16:00
Time of Day

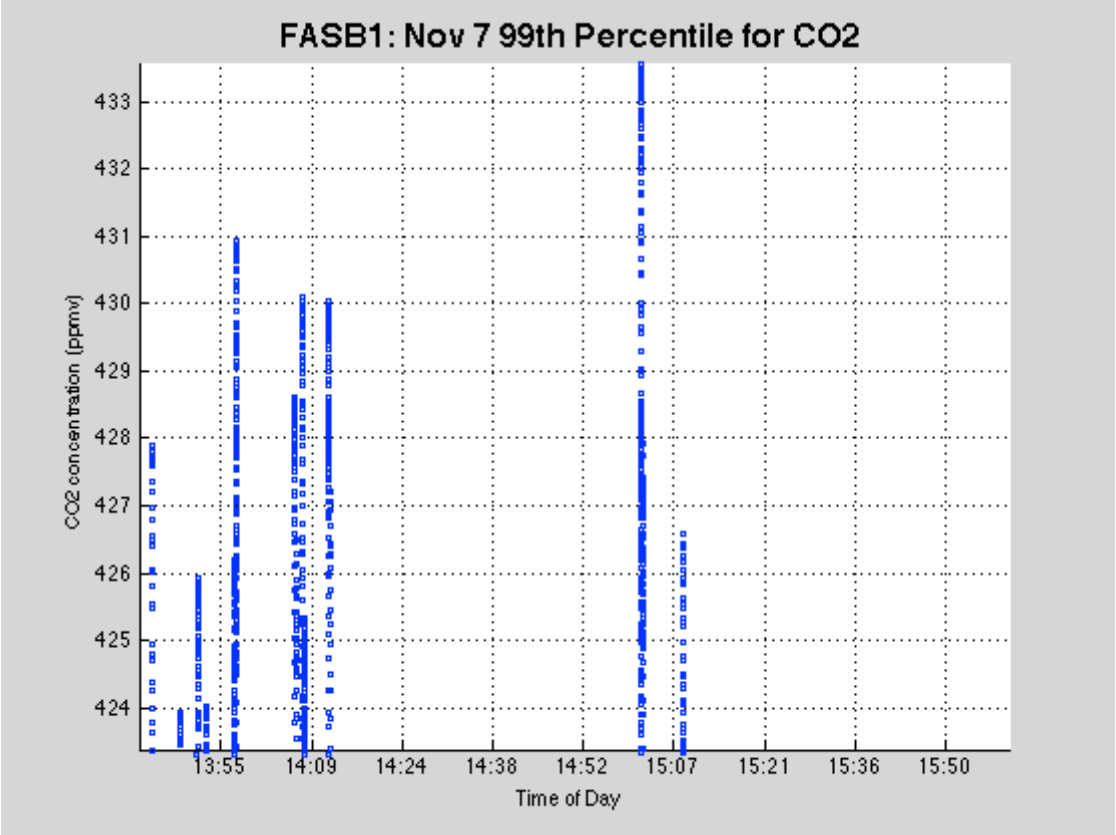
FASB1: Nov 7 99th Percentile for CO2
CO2 concentration (ppmv)
433
432
431
430
429
428
427
426
425
424
13:55
14:09
14:24
14:38
14:52
15:07
15:21
15:36
15:50
Time of Day

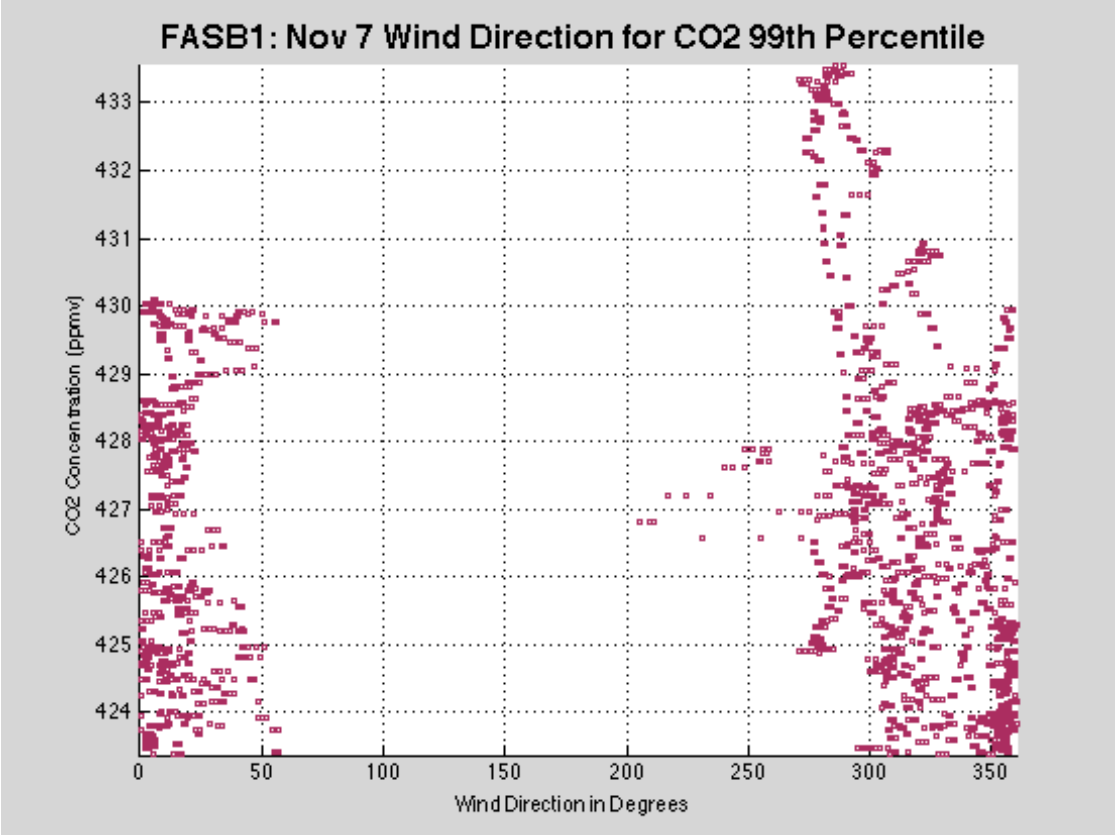
FASB1: Nov 7 Wind Direction for CO2 99th Percentile
CO2 Concentration (ppmv)
433
432
431
430
429
428
427
426
425
424
0
50
100
150
200
250
300
350
Wind Direction in Degrees

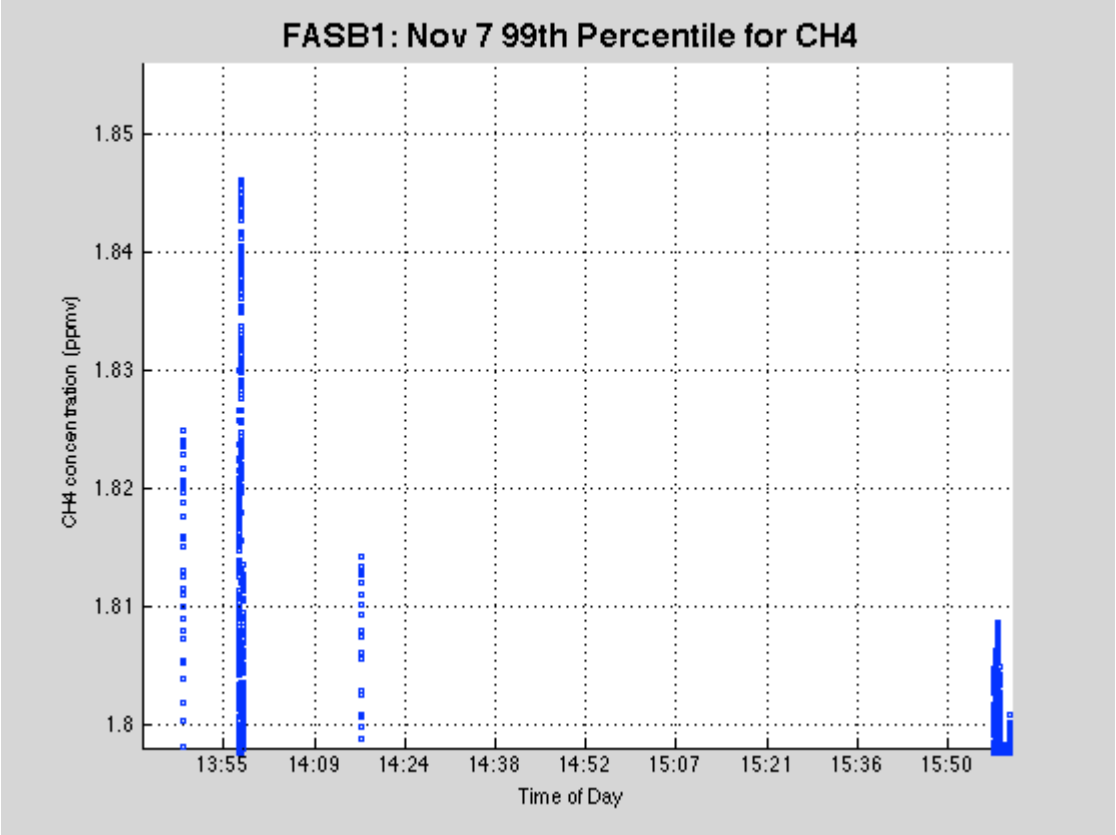
FASB1: Nov 7 99th Percentile for CH4
CH4 concentration (ppmv)
1.85
1.84
1.83
1.82
1.81
1.8
13:55
14:09
14:24
14:38
14:52
15:07
15:21
15:36
15:50
Time of Day

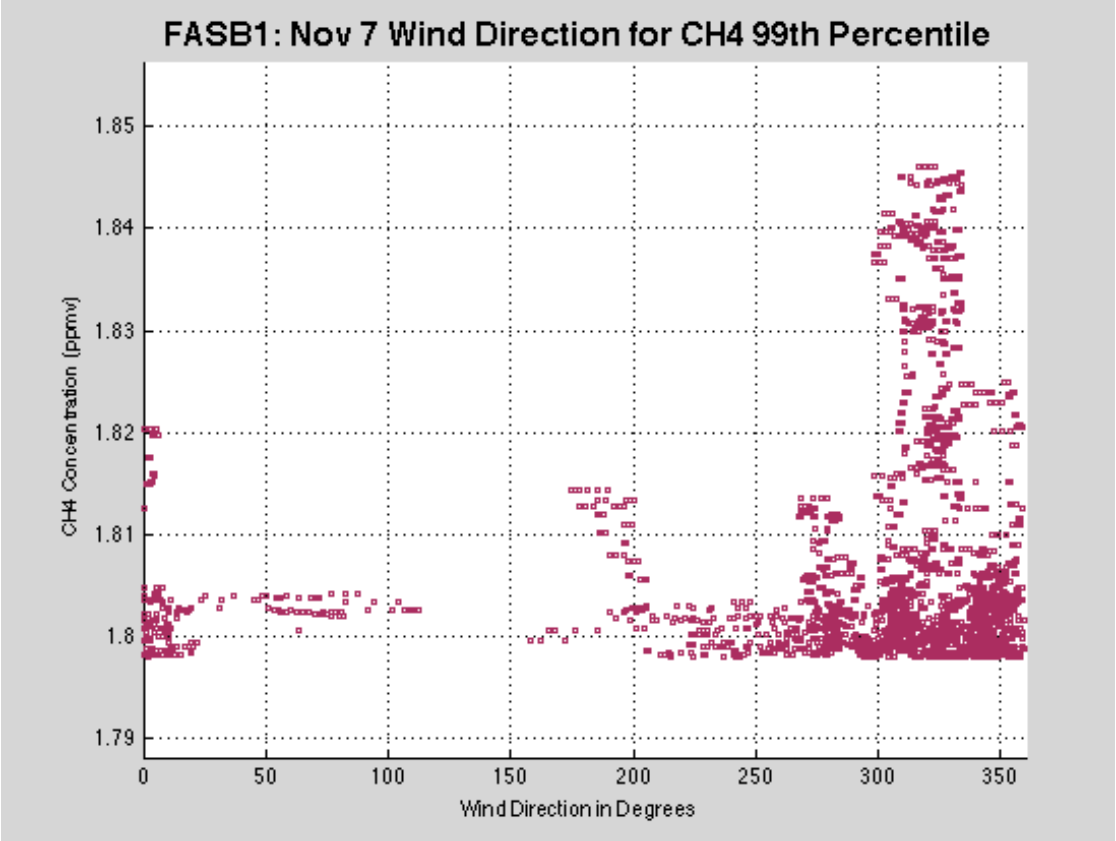
FASB1: Nov 7 Wind Direction for CH4 99th Percentile
CH4 Concentration (ppmv)
1.85
1.84
1.83
1.82
1.81
1.8
1.79
0
50
100
150
200
250
300
350
Wind Direction in Degrees

E.6 Friday, November 8th, 2013

| | Maximum | Minimum | Average | Standard Deviation | 99th Percentile |
|---|---|---|---|---|---|
| $CO_2$ (ppmv) | 432.8675 | 380.8126 | 386.1352 | 3.2273 | 398.2853 |
| $CH_4$ (ppmv) | 1.8283 | 1.6742 | 1.6849 | 0.0065 | 1.7117 |
| UZ (m/s) | 4.7887 | -3.6056 | -0.075 | 0.5974 | N/A |

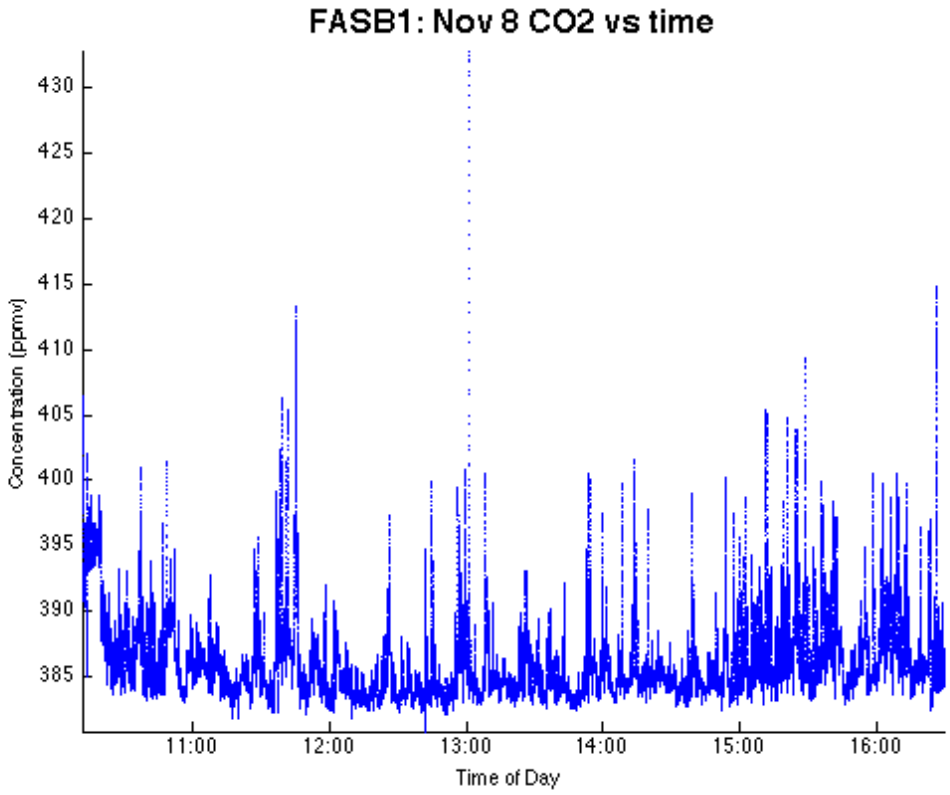

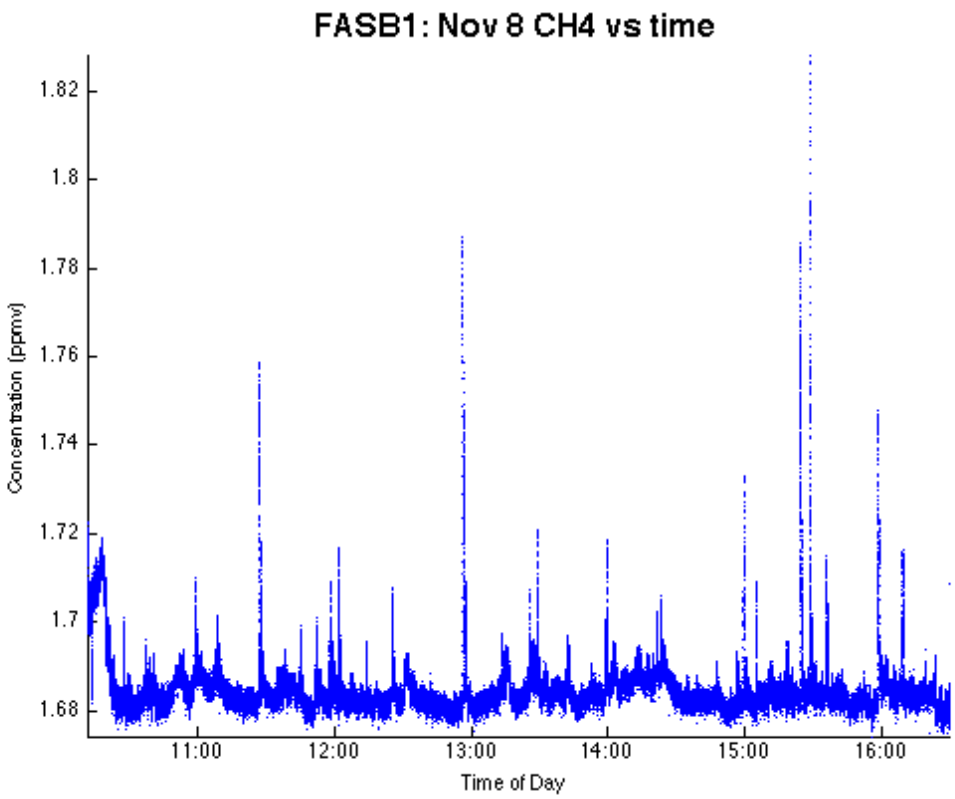
FASB1: Nov 8 CH4 vs time
Concentration (ppmv)
1.82
1.8
1.78
1.76
1.74
1.72
1.7
1.68
11:00
12:00
13:00
14:00
15:00
16:00
Time of Day

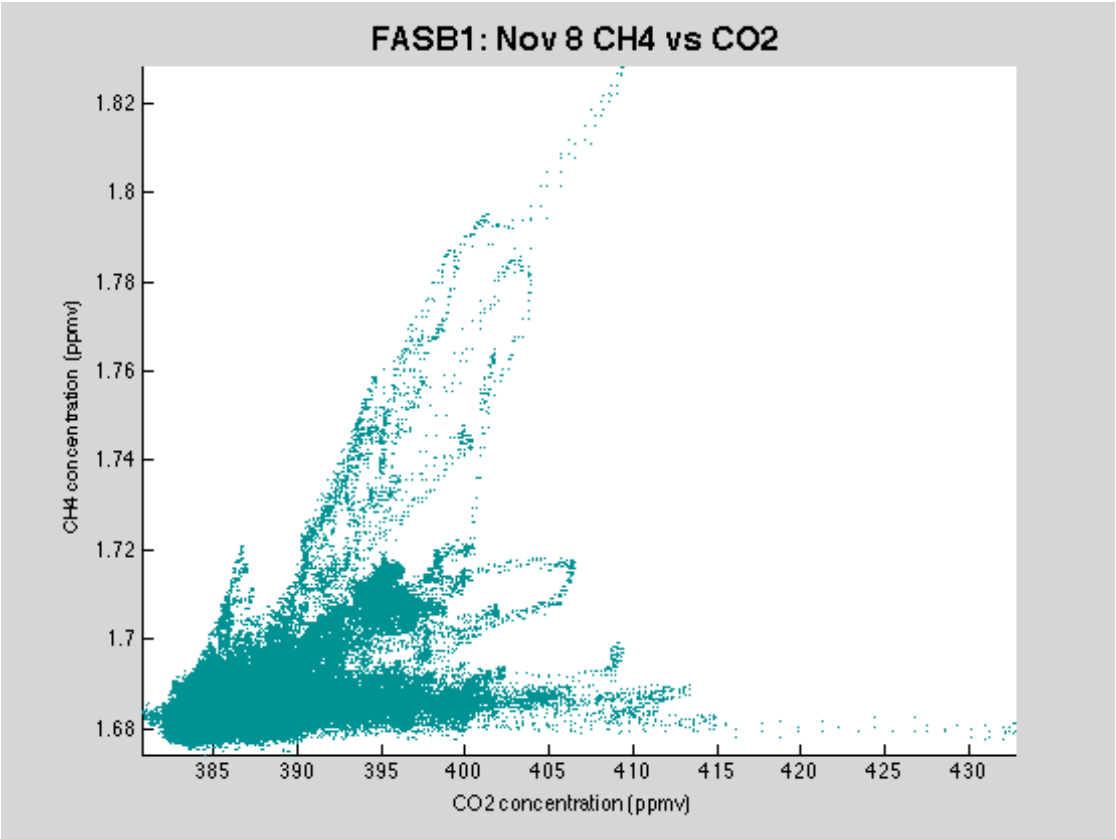
FASB1: Nov 8 CH4 vs CO2
CH4 concentration (ppmv)
1.82
1.8
1.78
1.76
1.74
1.72
1.7
1.68
385
390
395
400
405
410
415
420
425
430
CO2 concentration (ppmv)

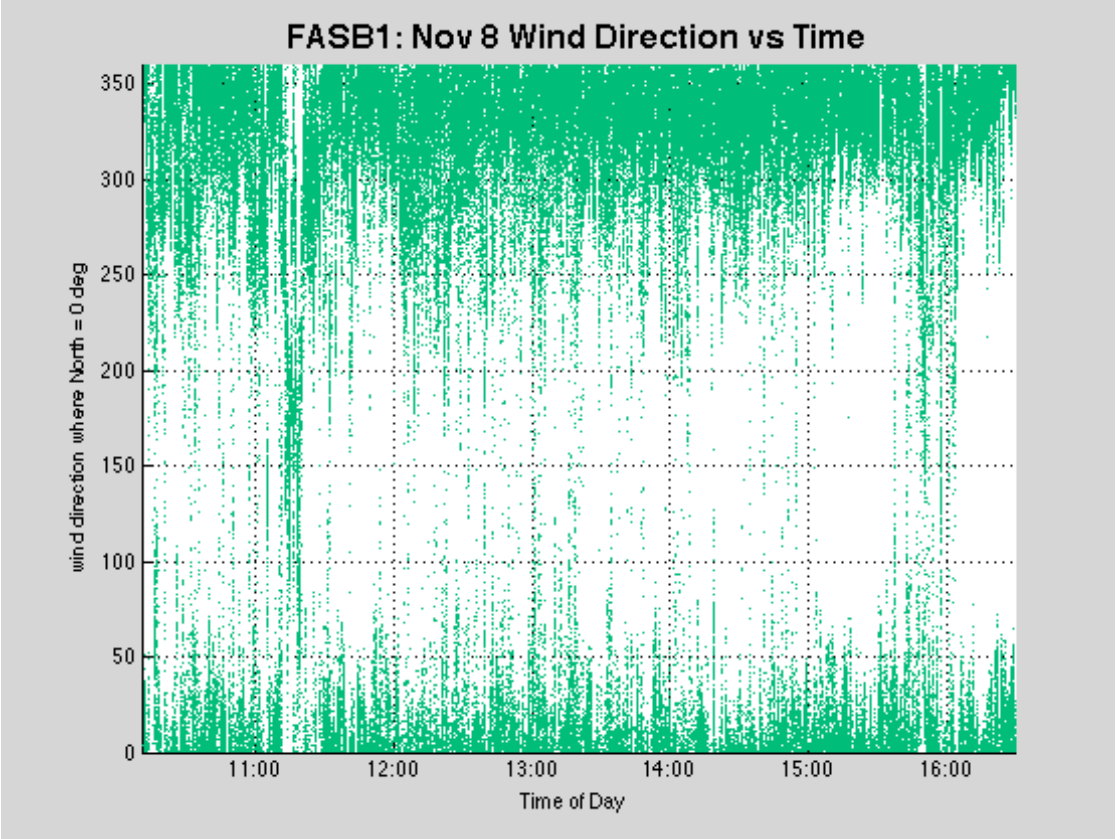
FASB1: Nov 8 Wind Direction vs Time
wind direction where North = 0 deg
350
300
250
200
150
100
50
0
11:00
12:00
13:00
14:00
15:00
16:00
Time of Day

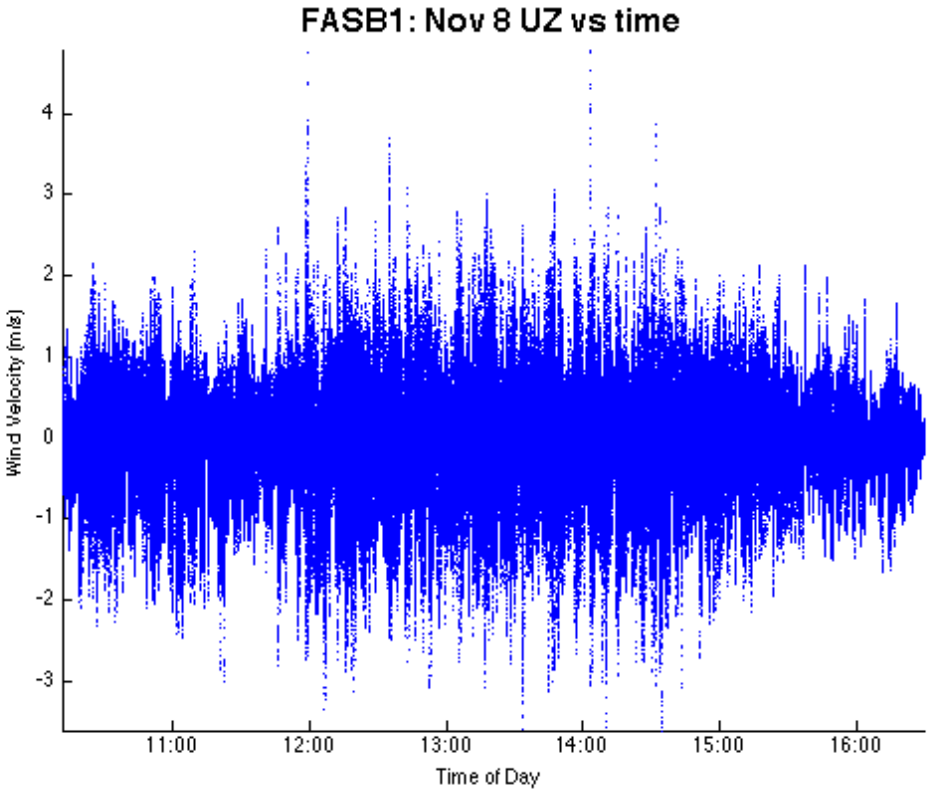
FASB1: Nov 8 UZ vs time
Wind Velocity (m/s)
4
3
2
1
0
-1
-2
-3
11:00
12:00
13:00
14:00
15:00
16:00
Time of Day

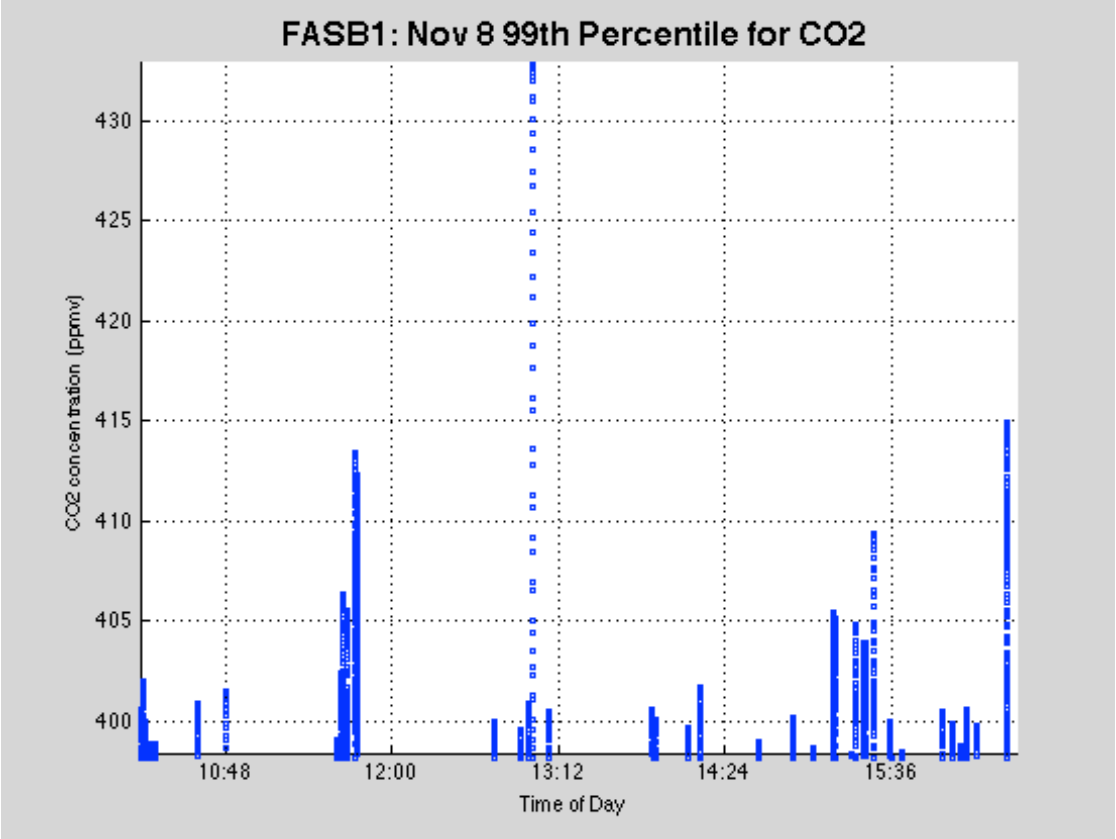
FASB1: Nov 8 99th Percentile for CO2
CO2 concentration (ppmv)
430
425
420
415
410
405
400
10:48
12:00
13:12
14:24
15:36
Time of Day

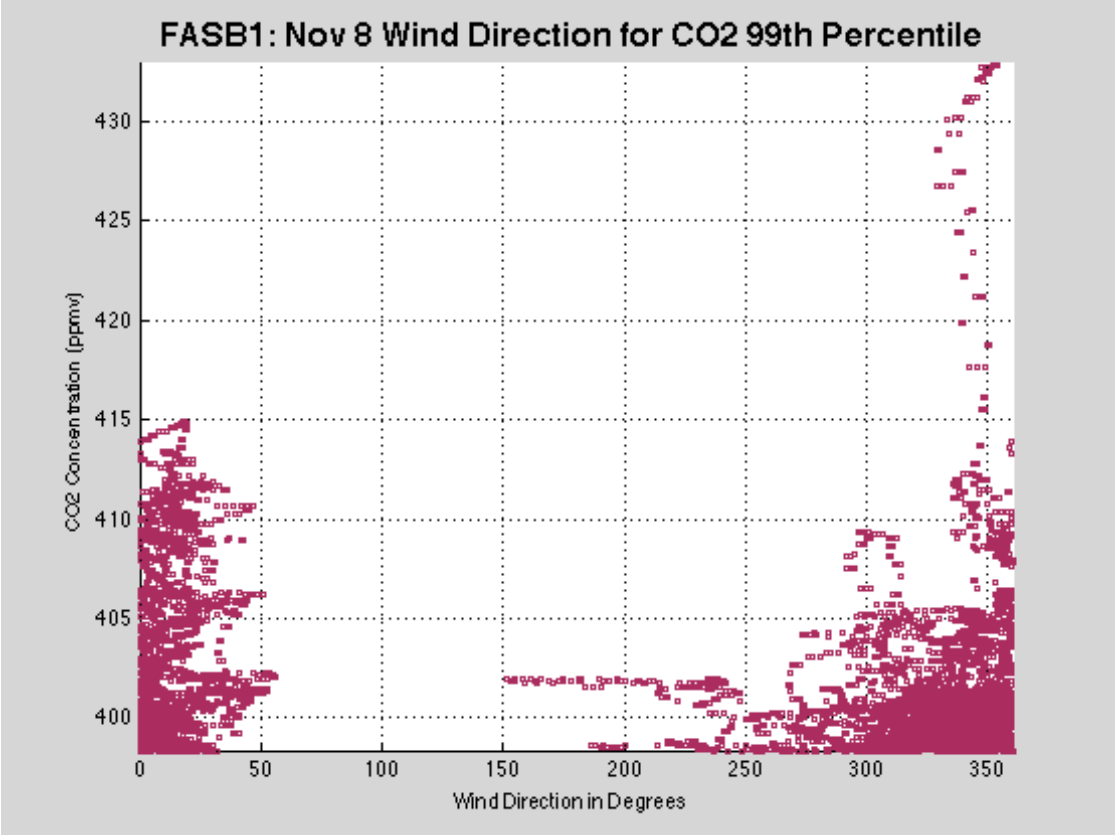
FASB1: Nov 8 Wind Direction for CO2 99th Percentile
CO2 Concentration (ppmv)
430
425
420
415
410
405
400
0
50
100
150
200
250
300
350
Wind Direction in Degrees

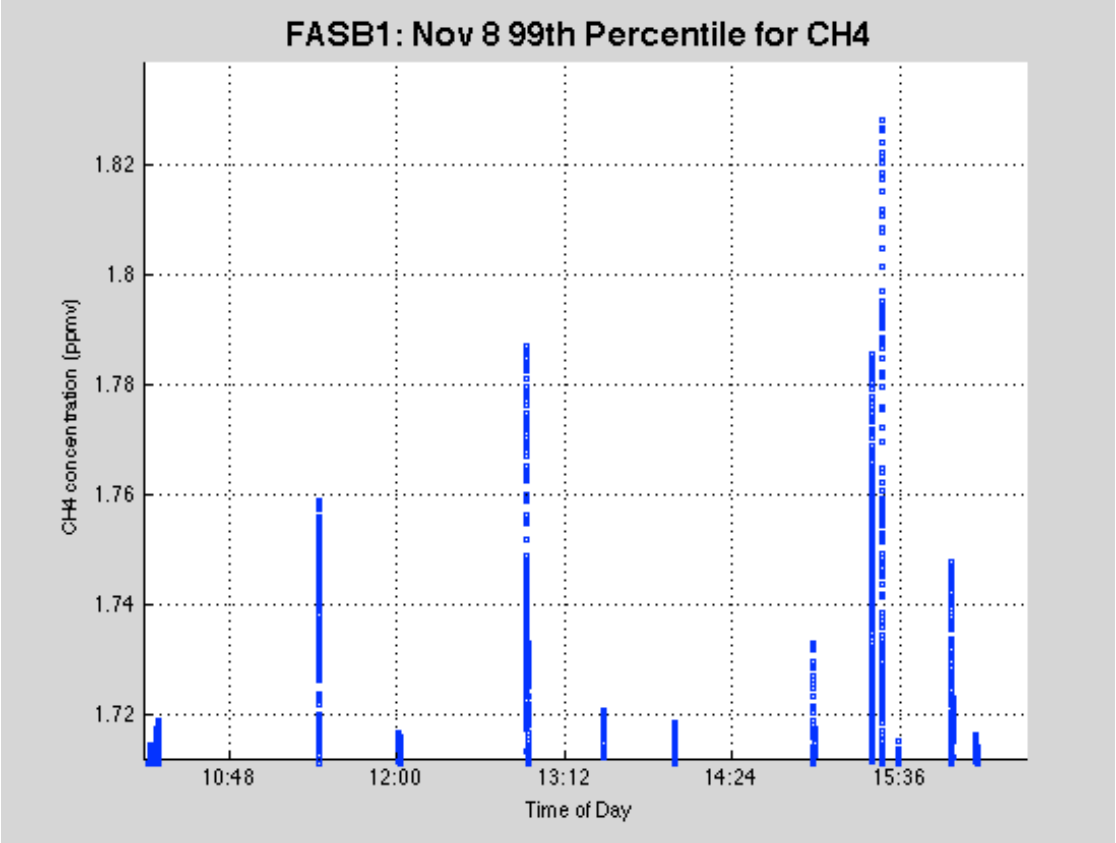
FASB1: Nov 8 99th Percentile for CH4
CH4 concentration (ppmv)
1.82
1.8
1.78
1.76
1.74
1.72
10:48
12:00
13:12
14:24
15:36
Time of Day

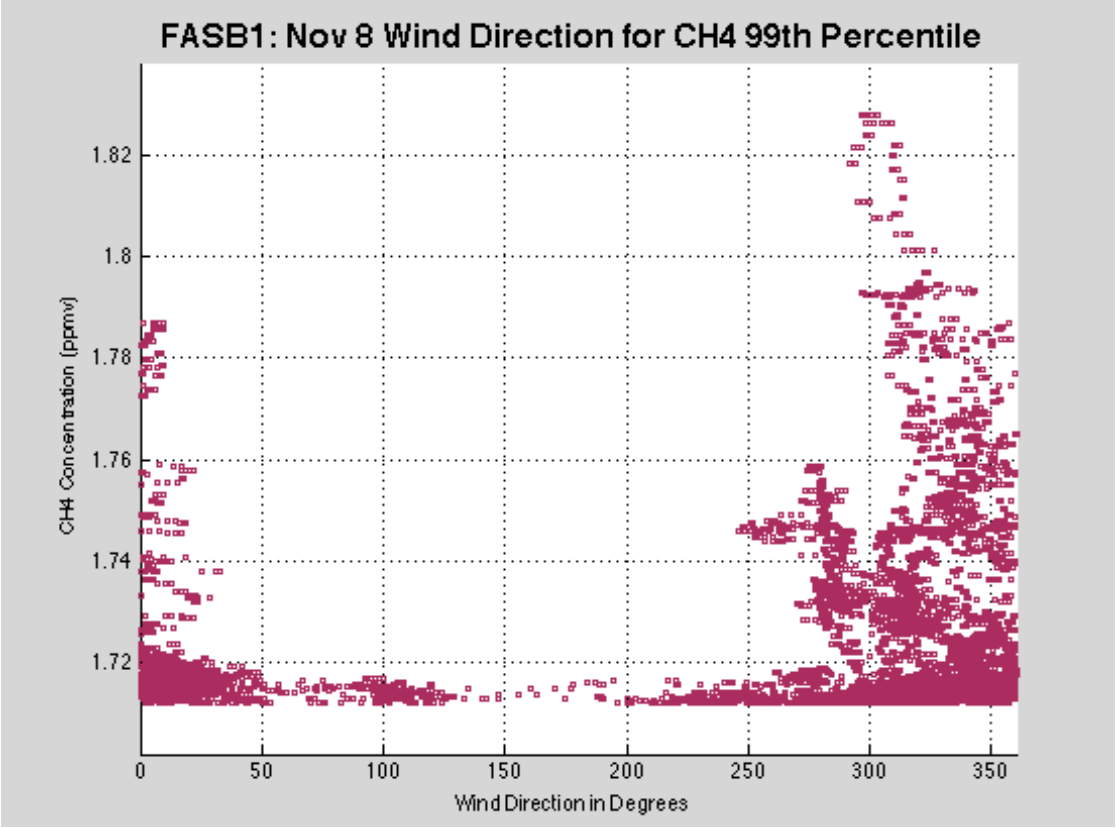
FASB1: Nov 8 Wind Direction for CH4 99th Percentile
CH4 Concentration (ppmv)
1.82
1.8
1.78
1.76
1.74
1.72
0
50
100
150
200
250
300
350
Wind Direction in Degrees

## E.7 Monday, November 11th, 2013

| | Maximum | Minimum | Average | Standard Deviation | 99th Percentile |
|---|---|---|---|---|---|
| $CO_2$ (ppmv) | 449.0827 | 396.2174 | 411.0947 | 6.2118 | 424.5629 |
| $CH_4$ (ppmv) | 1.9016 | 1.7294 | 17931 | 0.031 | 1.8525 |
| UZ (m/s) | 1.7829 | -1.9488 | -0.022 | 0.3434 | N/A |

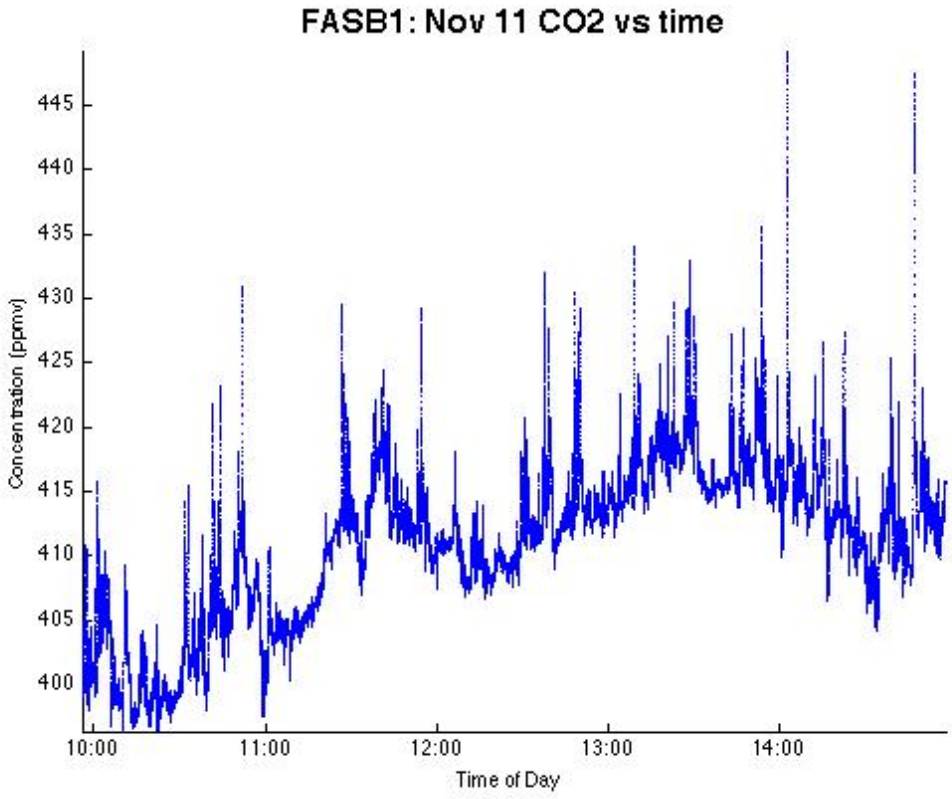

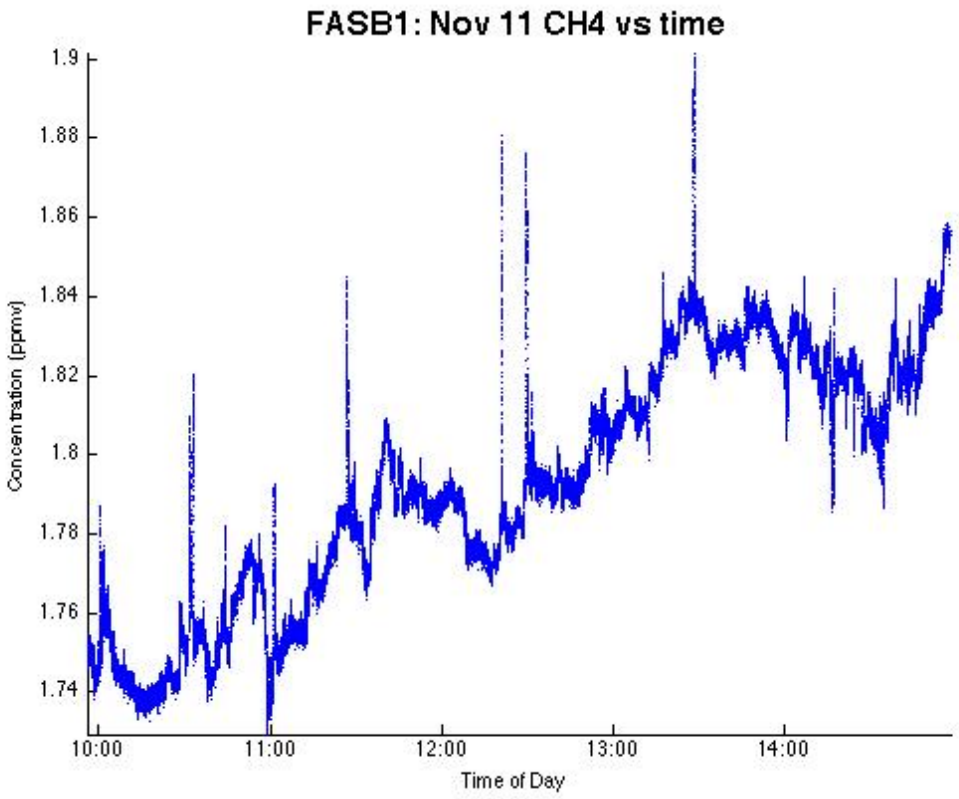
FASB1: Nov 11 CH4 vs time
Concentration (ppmv)
1.9
1.88
1.86
1.84
1.82
1.8
1.78
1.76
1.74
10:00
11:00
12:00
13:00
14:00
Time of Day

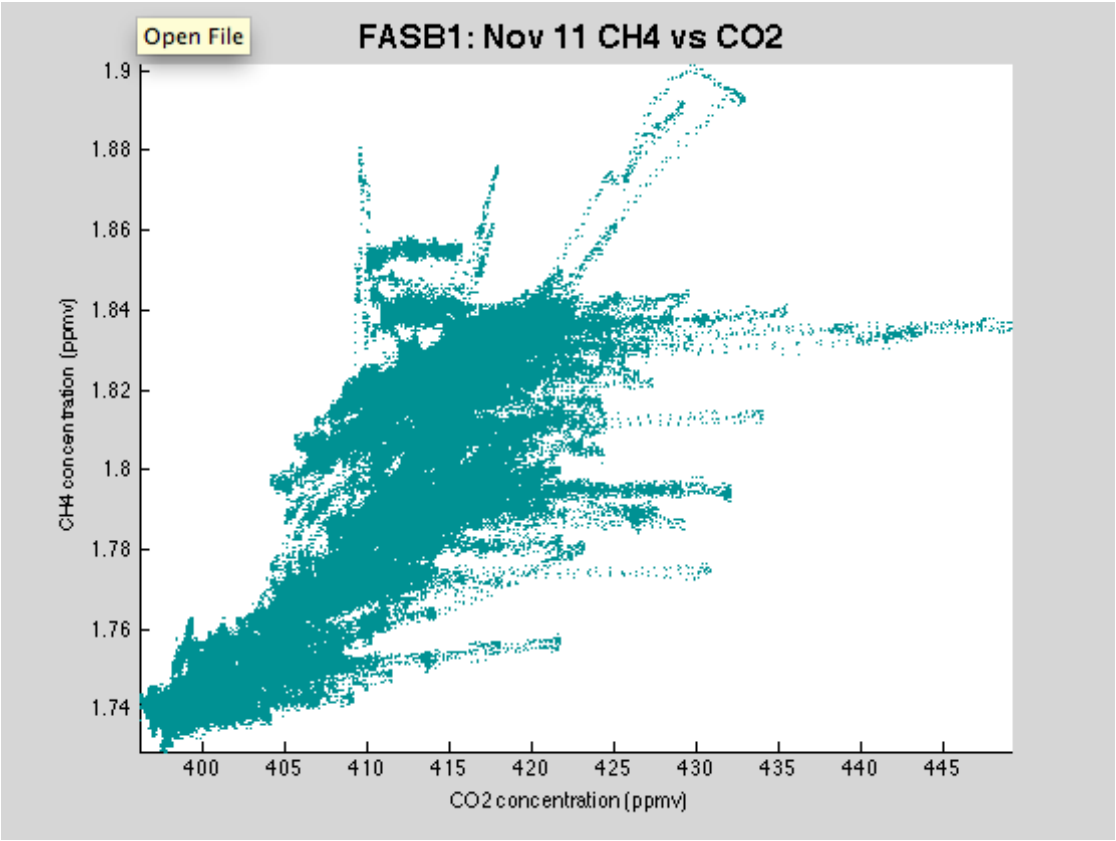
Open File
FASB1: Nov 11 CH4 vs CO2
CH4 concentration (ppmv)
1.9
1.88
1.86
1.84
1.82
1.8
1.78
1.76
1.74
400
405
410
415
420
425
430
435
440
445
CO2 concentration (ppmv)

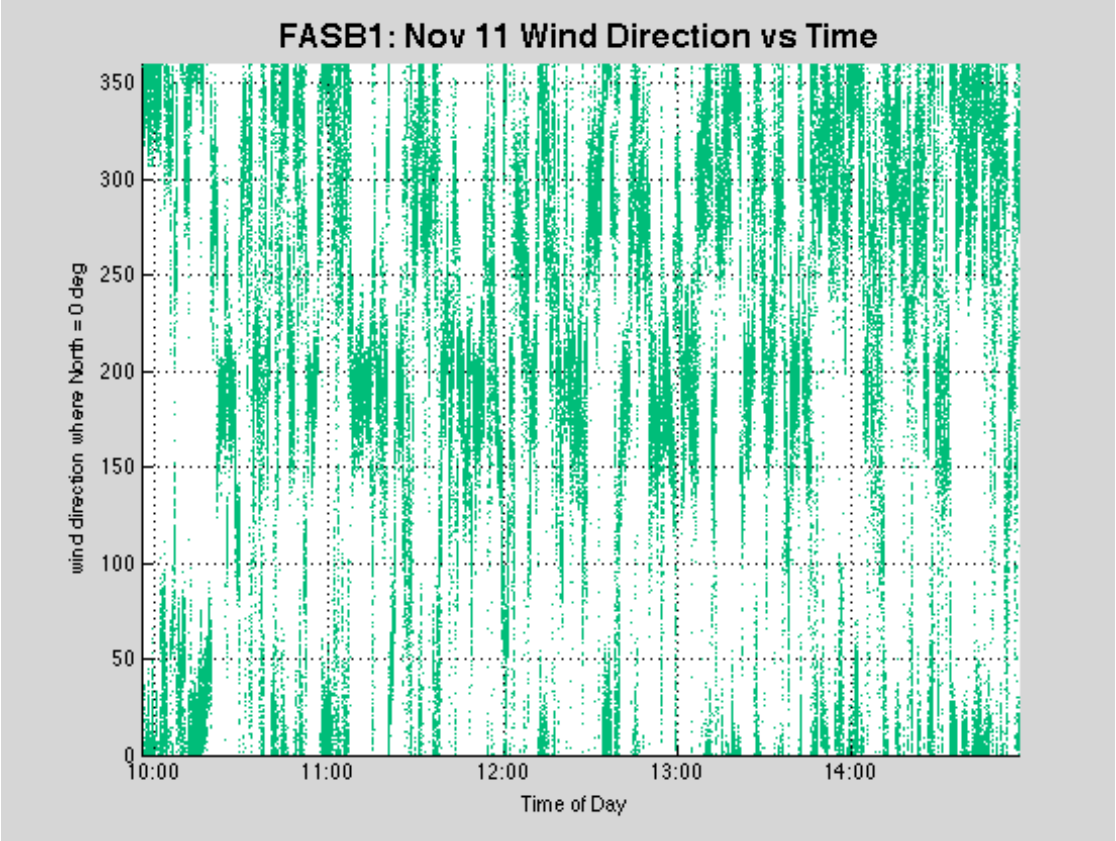
FASB1: Nov 11 Wind Direction vs Time
wind direction where North = 0 deg
350
300
250
200
150
100
50
0
10:00
11:00
12:00
13:00
14:00
Time of Day

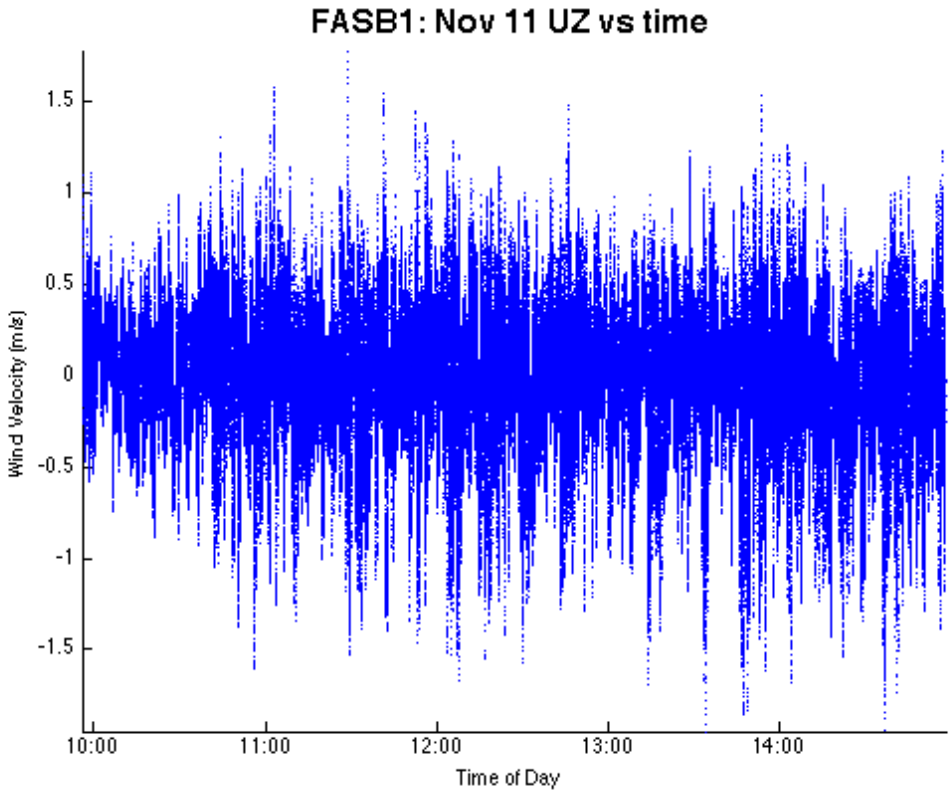
FASB1: Nov 11 UZ vs time
Wind Velocity (m/s)
1.5
1
0.5
0
-0.5
-1
-1.5
10:00
11:00
12:00
13:00
14:00
Time of Day

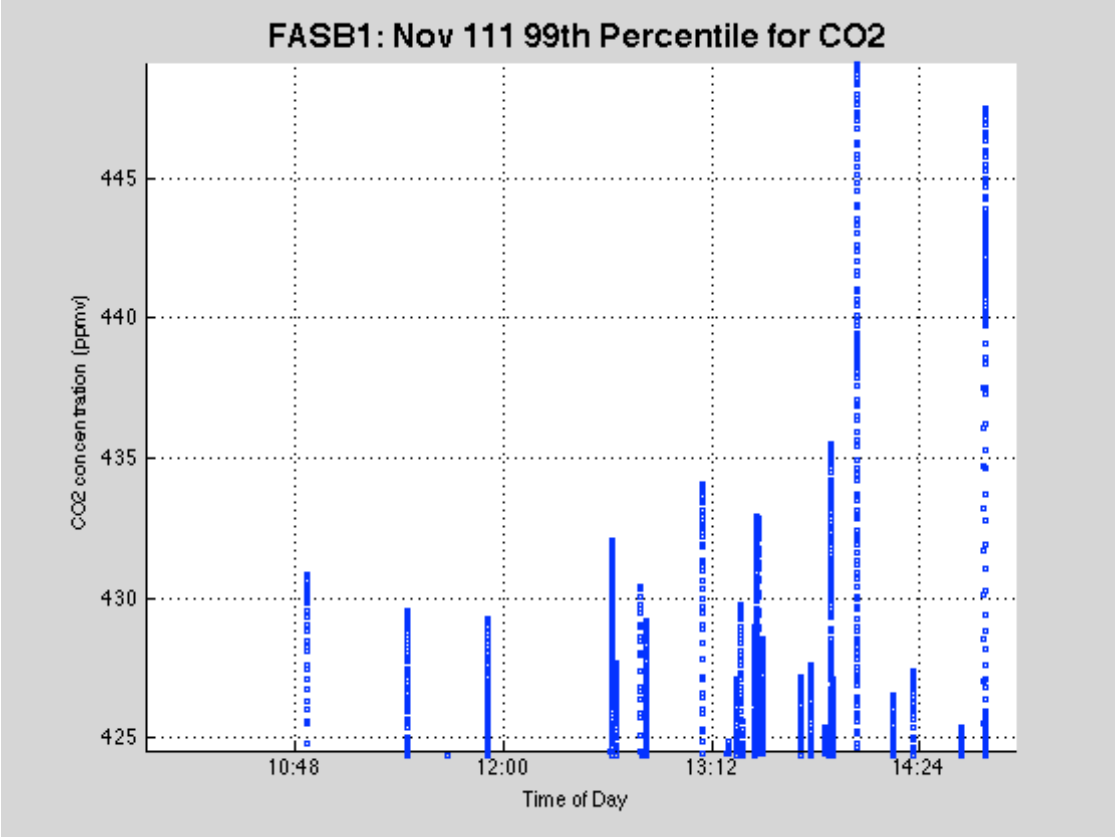
FASB1: Nov 111 99th Percentile for CO2
CO2 concentration (ppmv)
445
440
435
430
425
10:48
12:00
13:12
14:24
Time of Day

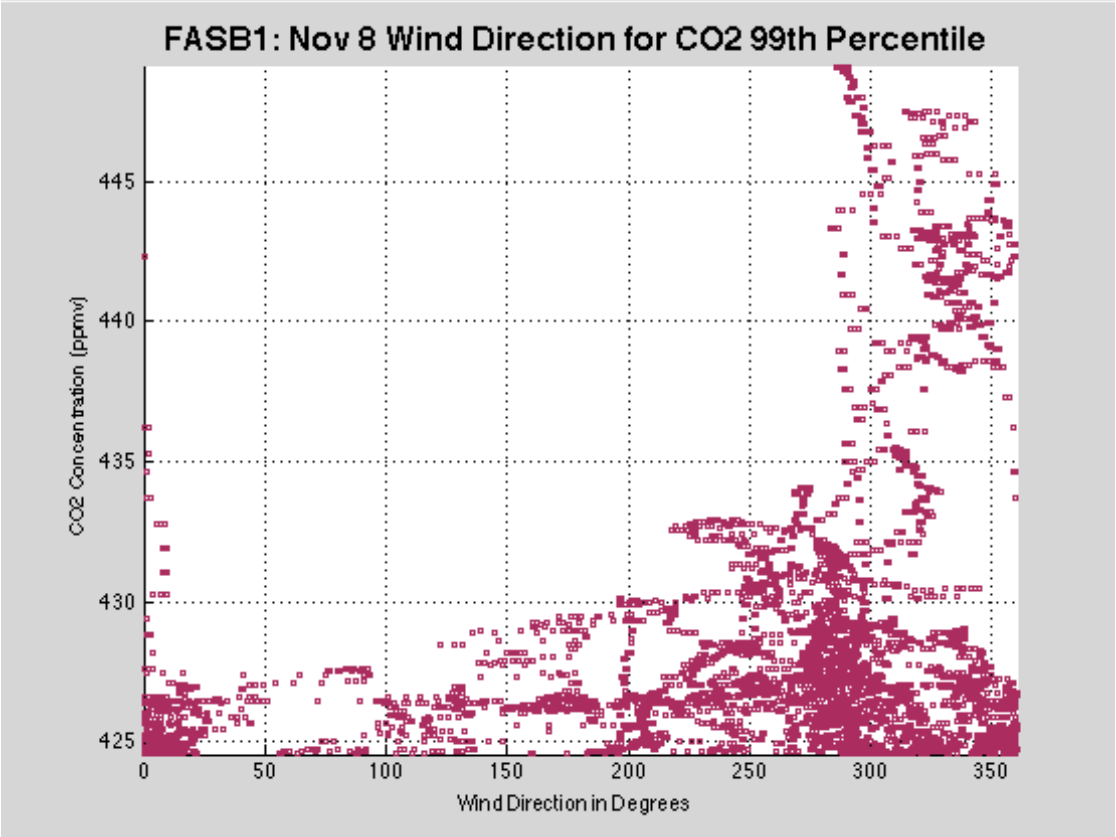
FASB1: Nov 8 Wind Direction for CO2 99th Percentile
CO2 Concentration (ppmv)
445
440
435
430
425
0
50
100
150
200
250
300
350
Wind Direction in Degrees

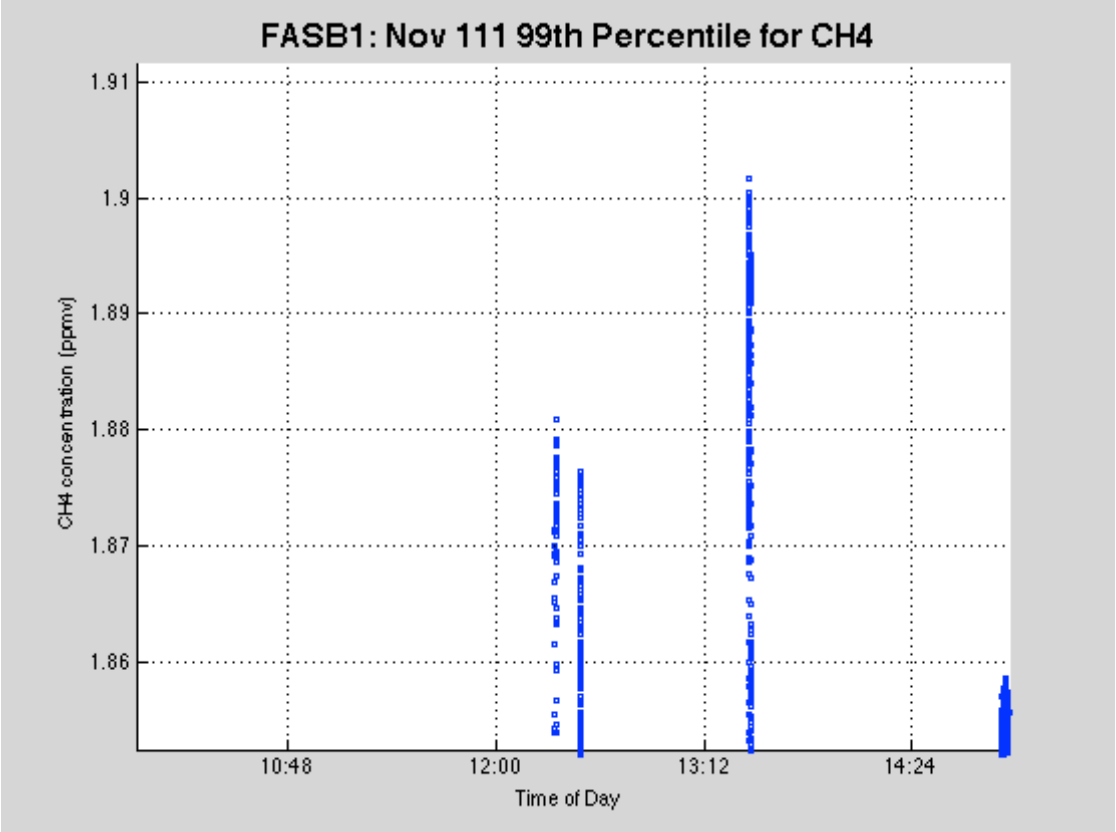
FASB1: Nov 111 99th Percentile for CH4
CH4 concentration (ppmv)
1.91
1.9
1.89
1.88
1.87
1.86
10:48
12:00
13:12
14:24
Time of Day

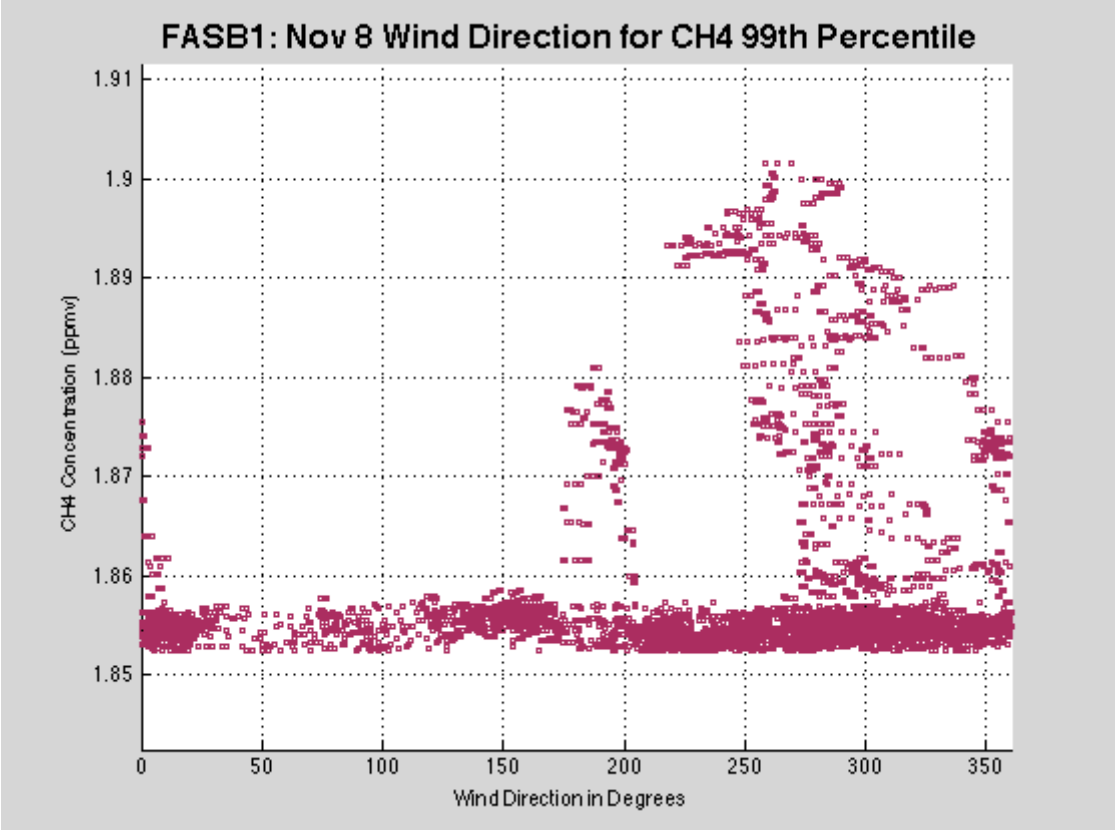
FASB1: Nov 8 Wind Direction for CH4 99th Percentile
CH4 Concentration (ppmv)
1.91
1.9
1.89
1.88
1.87
1.86
1.85
0
50
100
150
200
250
300
350
Wind Direction in Degrees

## E.8 Tuesday, November 12th, 2013

| | Maximum | Minimum | Average | Standard Deviation | 99th Percentile |
|---|---|---|---|---|---|
| $CO_2$ (ppmv) | 436.0412 | 413.6412 | 420.344 | 2.878 | 431.4137 |
| $CH_4$ (ppmv) | 1.9247 | 1.8337 | 1.8503 | 0.0097 | 1.8772 |
| UZ (m/s) | 1.8113 | -2.0924 | -0.0752 | 0.3743 | N/A |

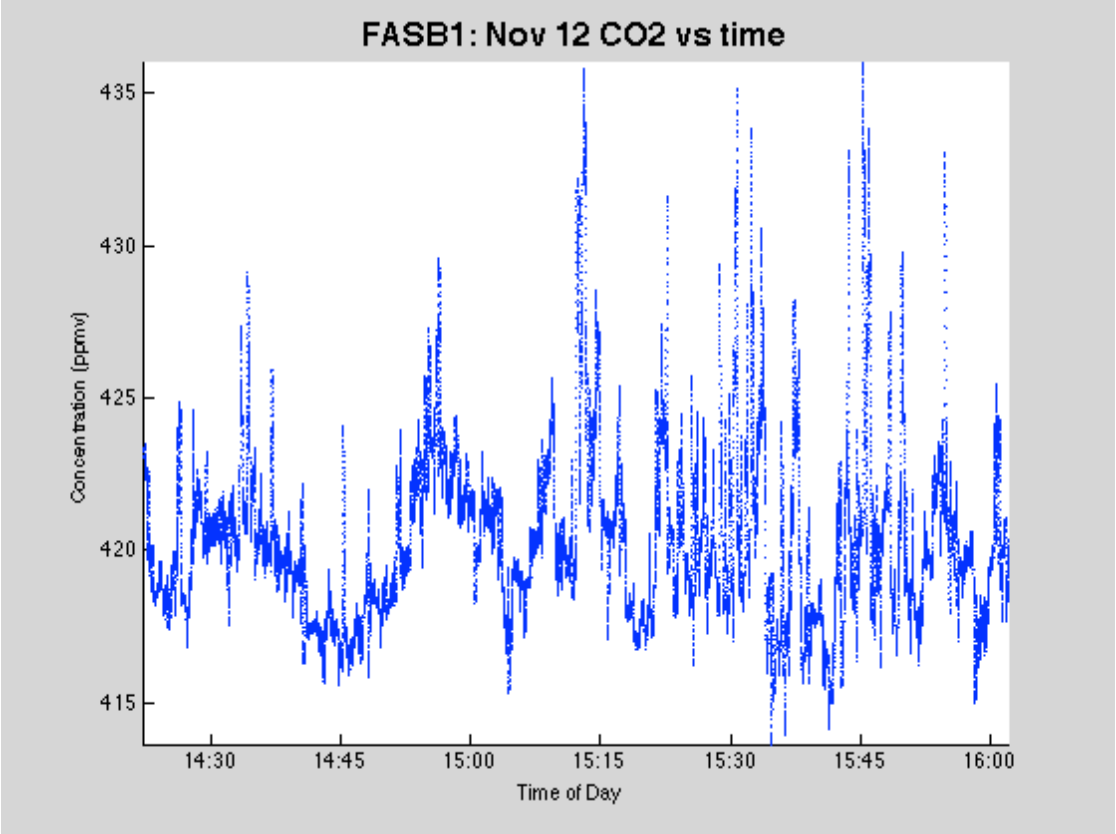

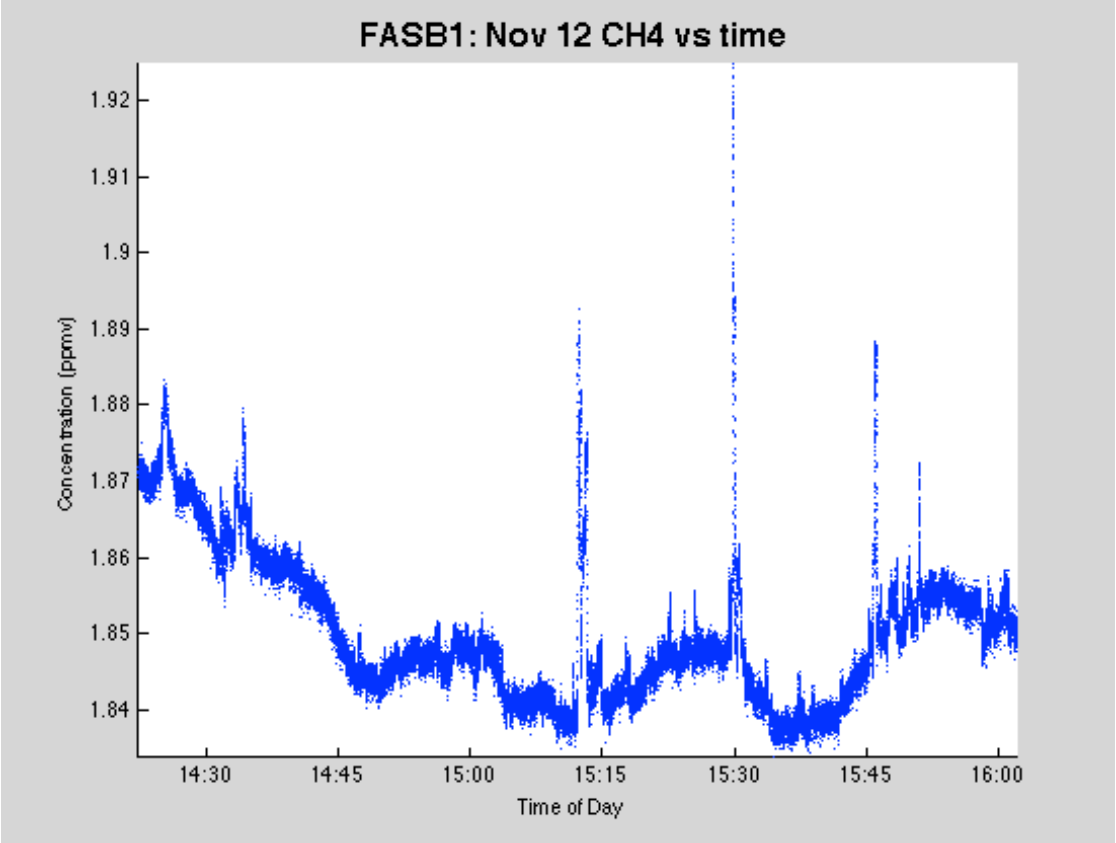
FASB1: Nov 12 CH4 vs time
Concentration (ppmv)
1.92
1.91
1.9
1.89
1.88
1.87
1.86
1.85
1.84
14:30
14:45
15:00
15:15
15:30
15:45
16:00
Time of Day

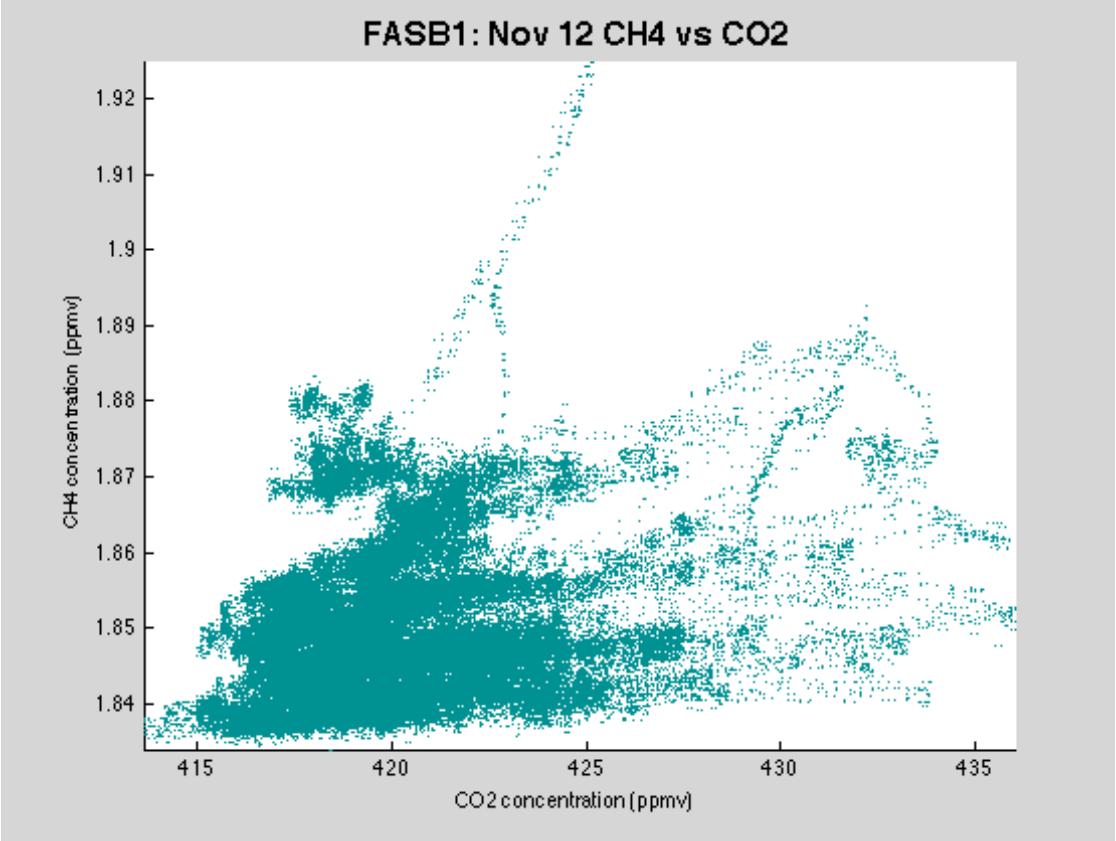
FASB1: Nov 12 CH4 vs CO2
CH4 concentration (ppmv)
1.92
1.91
1.9
1.89
1.88
1.87
1.86
1.85
1.84
415
420
425
430
435
CO2 concentration (ppmv)

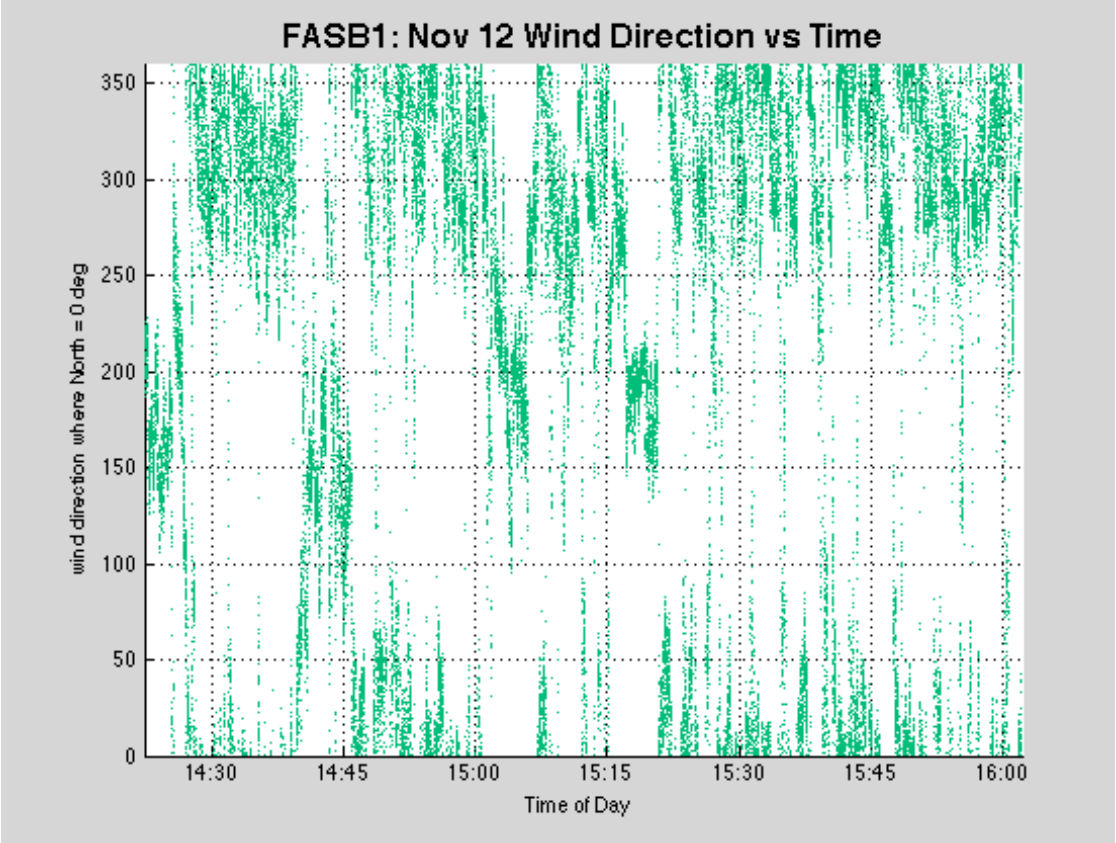
FASB1: Nov 12 Wind Direction vs Time
wind direction where North = 0 deg
350
300
250
200
150
100
50
0
14:30
14:45
15:00
15:15
15:30
15:45
16:00
Time of Day

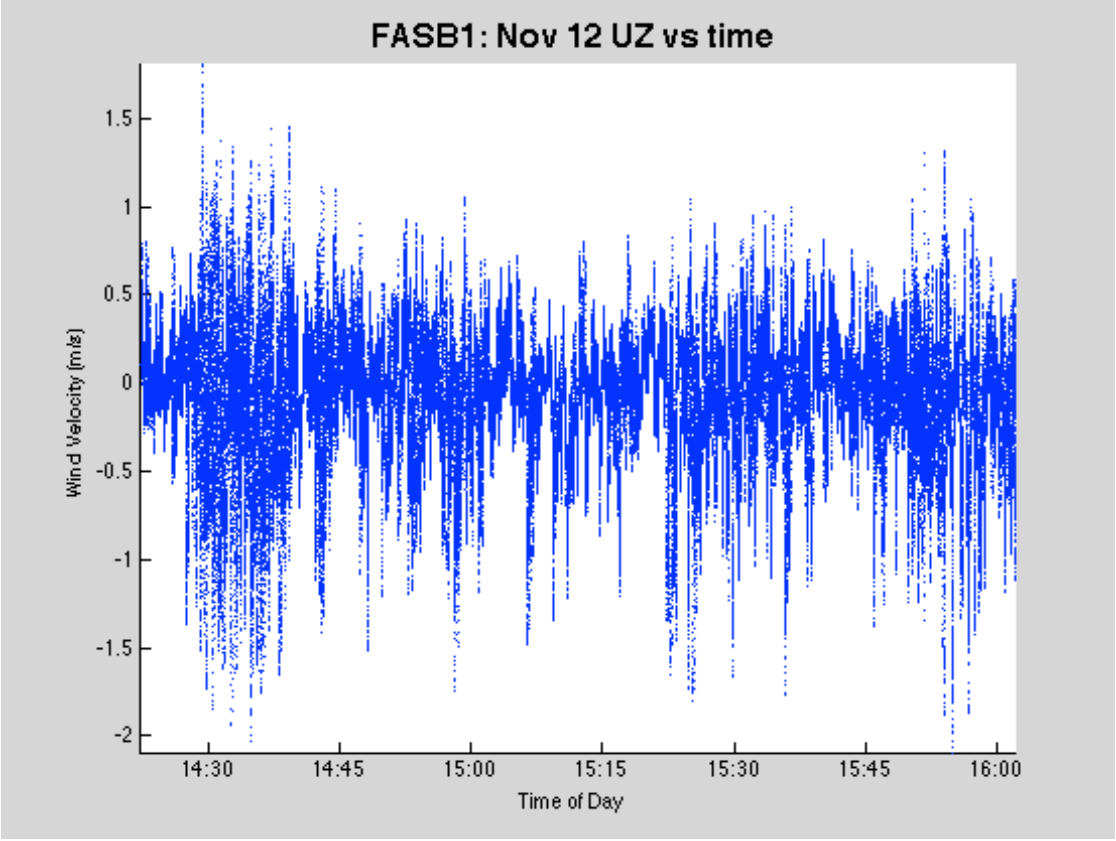
FASB1: Nov 12 UZ vs time
Wind Velocity (m/s)
1.5
1
0.5
0
-0.5
-1
-1.5
-2
14:30
14:45
15:00
15:15
15:30
15:45
16:00
Time of Day

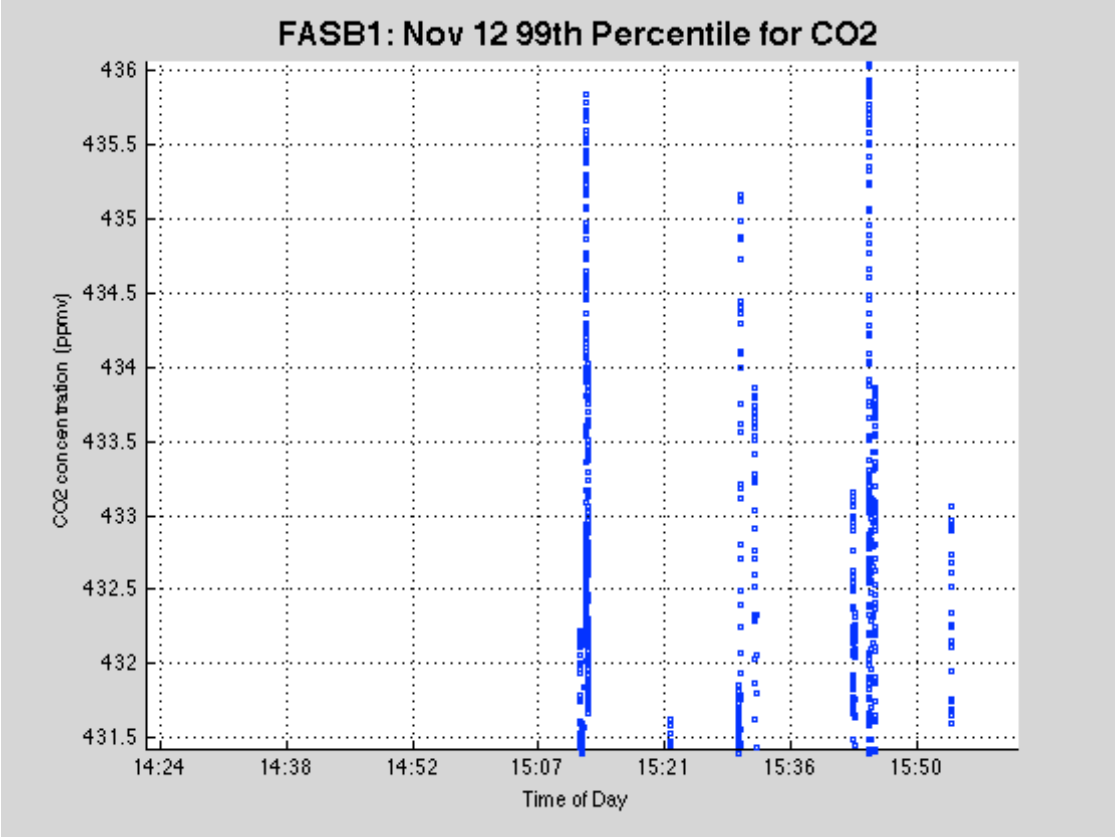
FASB1: Nov 12 99th Percentile for CO2
CO2 concentration (ppmv)
436
435.5
435
434.5
434
433.5
433
432.5
432
431.5
14:24
14:38
14:52
15:07
15:21
15:36
15:50
Time of Day

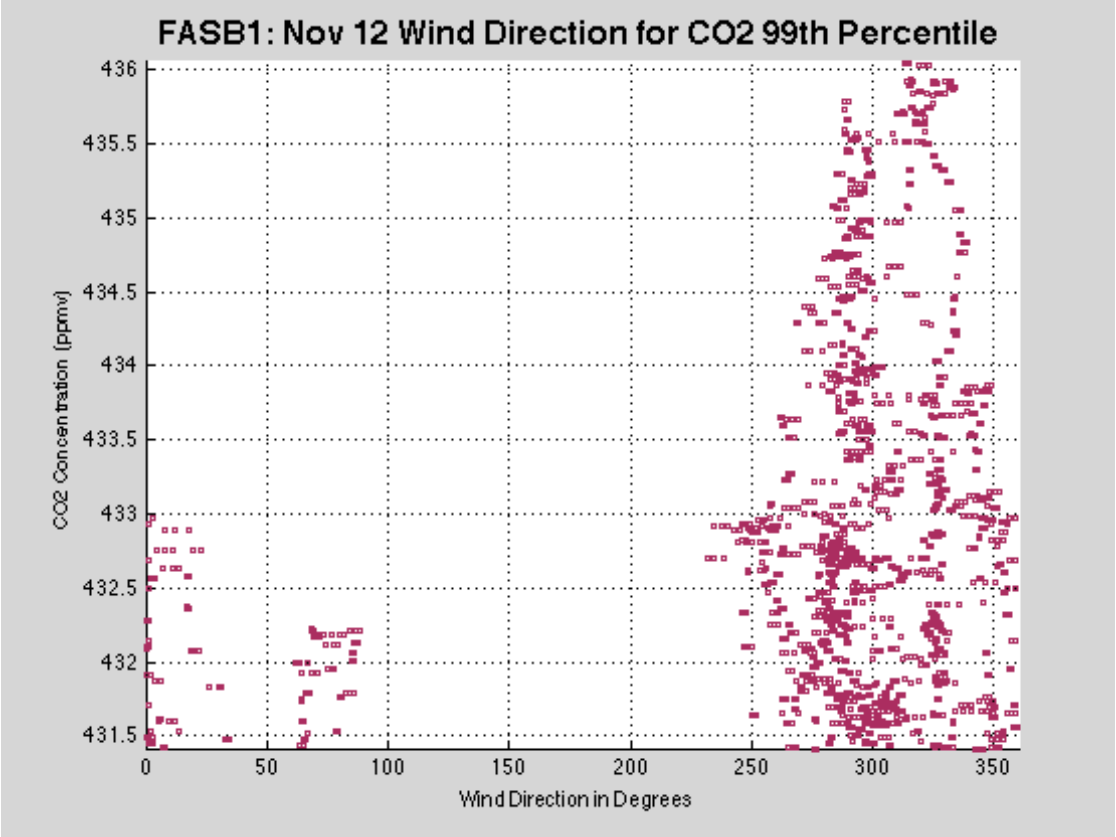
FASB1: Nov 12 Wind Direction for CO2 99th Percentile
CO2 Concentration (ppmv)
436
435.5
435
434.5
434
433.5
433
432.5
432
431.5
0
50
100
150
200
250
300
350
Wind Direction in Degrees

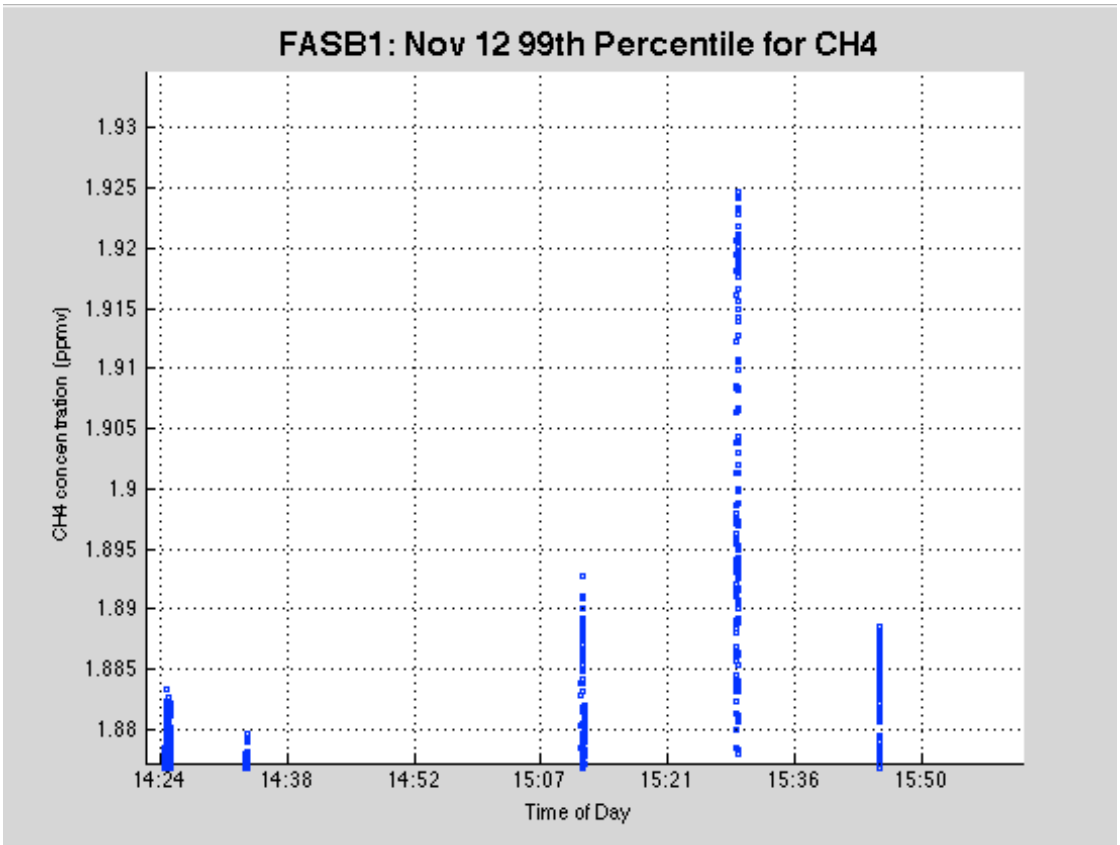
FASB1: Nov 12 99th Percentile for CH4
CH4 concentration (ppmv)
1.93
1.925
1.92
1.915
1.91
1.905
1.9
1.895
1.89
1.885
1.88
14:24
14:38
14:52
15:07
15:21
15:36
15:50
Time of Day

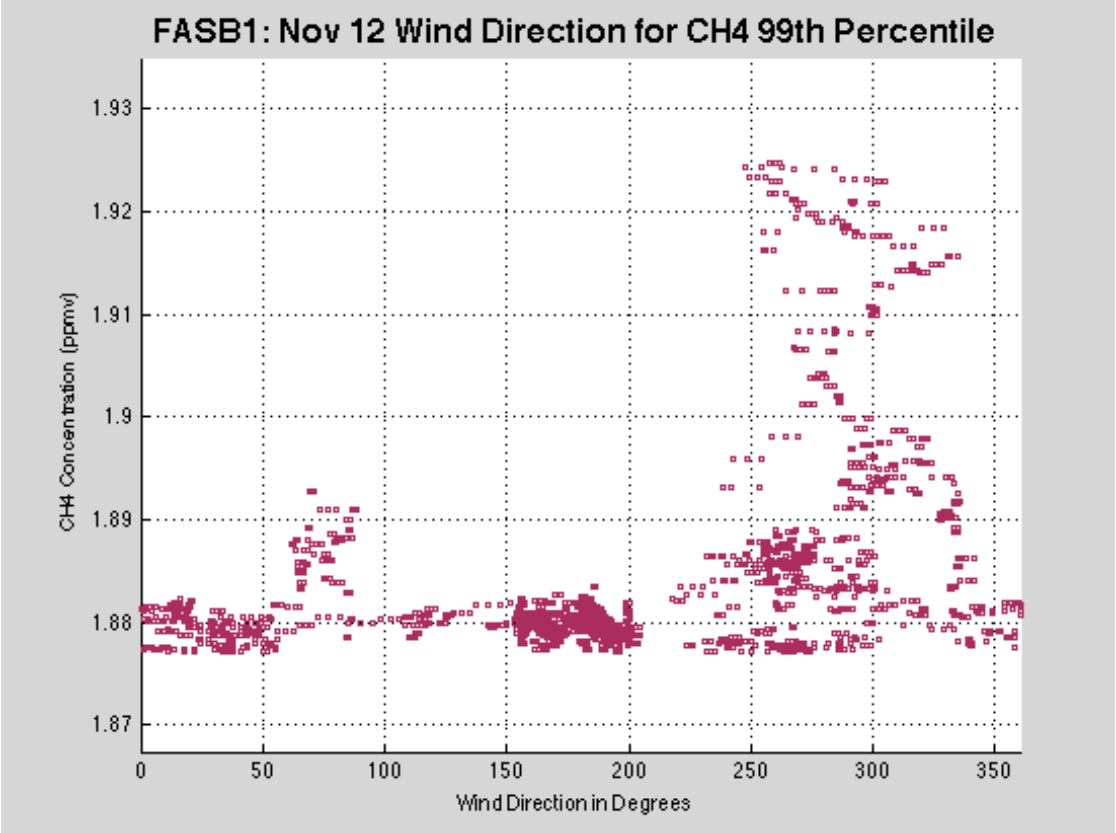
FASB1: Nov 12 Wind Direction for CH4 99th Percentile
CH4 Concentration (ppmv)
1.93
1.92
1.91
1.9
1.89
1.88
1.87
0
50
100
150
200
250
300
350
Wind Direction in Degrees

## E.9 Wednesday, November 13th, 2013

| | Maximum | Minimum | Average | Standard Deviation | 99th Percentile |
|---|---|---|---|---|---|
| $CO_2$ (ppmv) | 500.0065 | 409.5253 | 452.1589 | 18.6956 | 482.6911 |
| $CH_4$ (ppmv) | 2.2591 | 1.8469 | 1.9998 | 0.0971 | 2.2387 |
| UZ (m/s) | 2.2213 | -2.9939 | -0.0139 | 0.3582 | N/A |

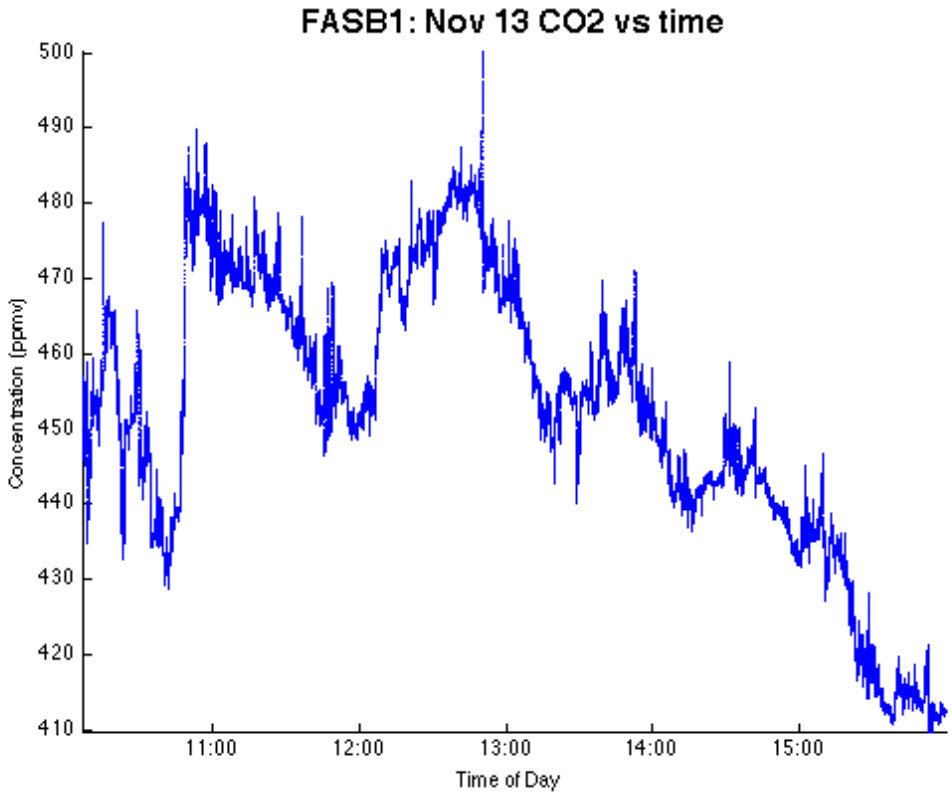

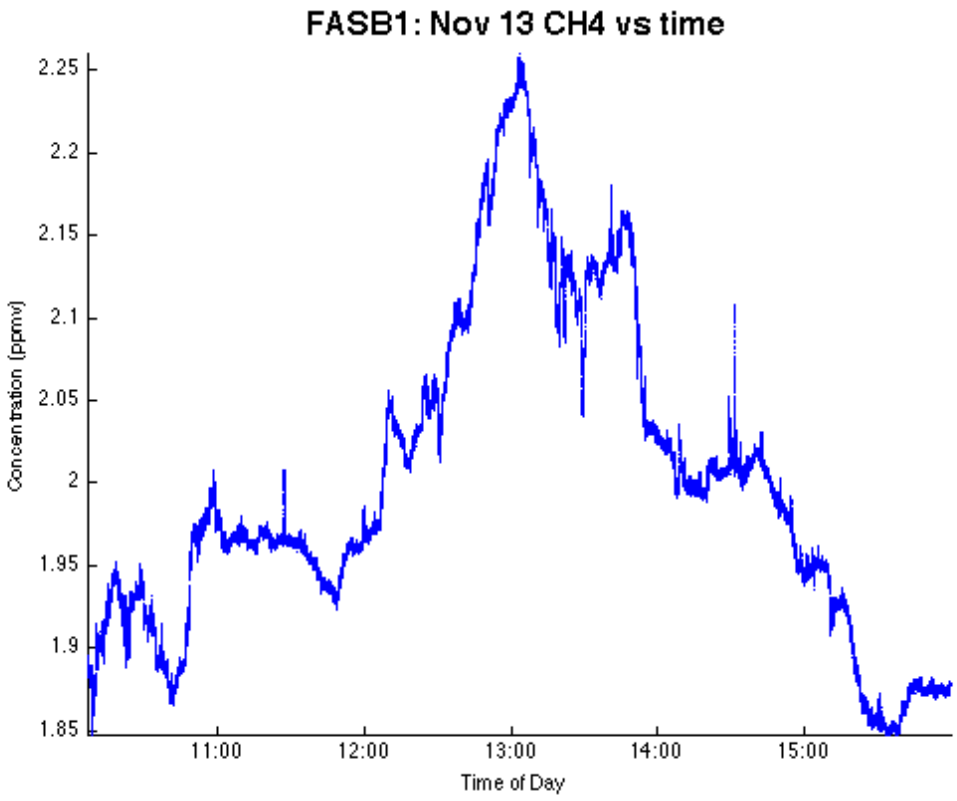
FASB1: Nov 13 CH4 vs time
Concentration (ppmv)
2.25
2.2
2.15
2.1
2.05
2
1.95
1.9
1.85
11:00
12:00
13:00
14:00
15:00
Time of Day

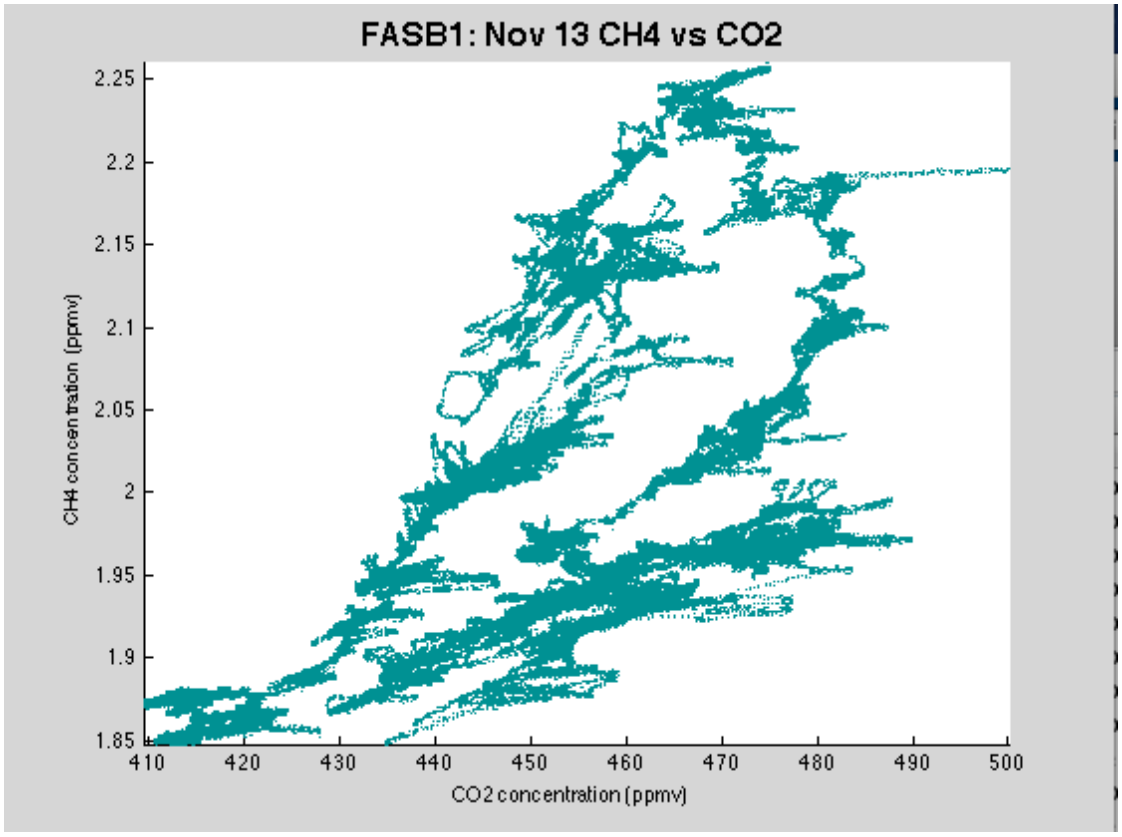
FASB1: Nov 13 CH4 vs CO2
CH4 concentration (ppmv)
2.25
2.2
2.15
2.1
2.05
2
1.95
1.9
1.85
410
420
430
440
450
460
470
480
490
500
CO2 concentration (ppmv)

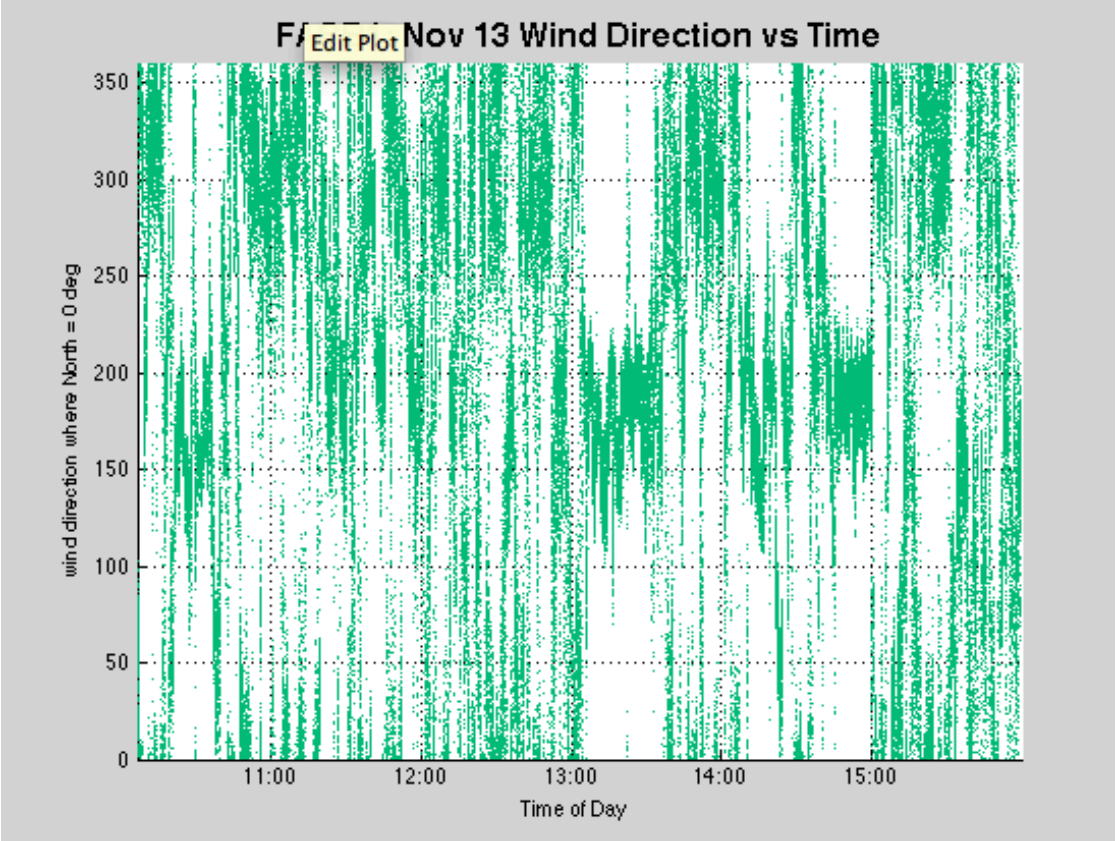
Edit Plot
Nov 13 Wind Direction vs Time
wind direction where North = 0 deg
350
300
250
200
150
100
50
0
11:00
12:00
13:00
14:00
15:00
Time of Day

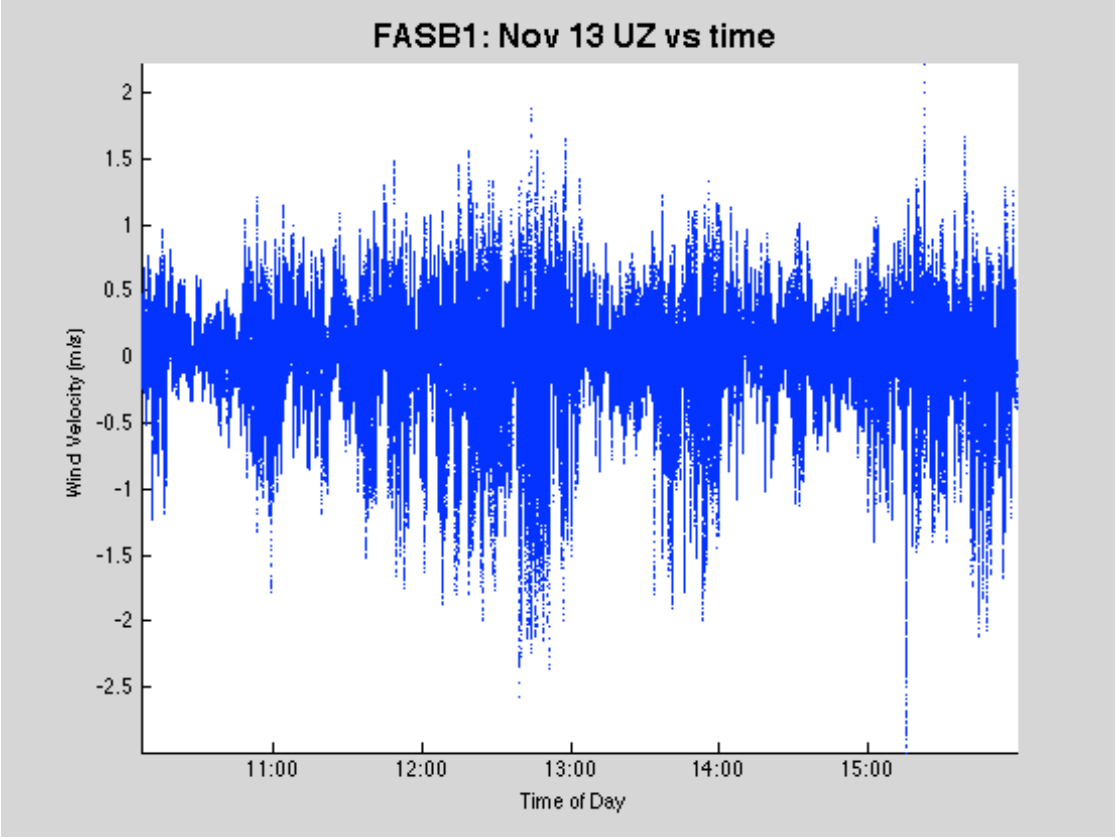
FASB1: Nov 13 UZ vs time
Wind Velocity (m/s)
2
1.5
1
0.5
0
-0.5
-1
-1.5
-2
-2.5
11:00
12:00
13:00
14:00
15:00
Time of Day

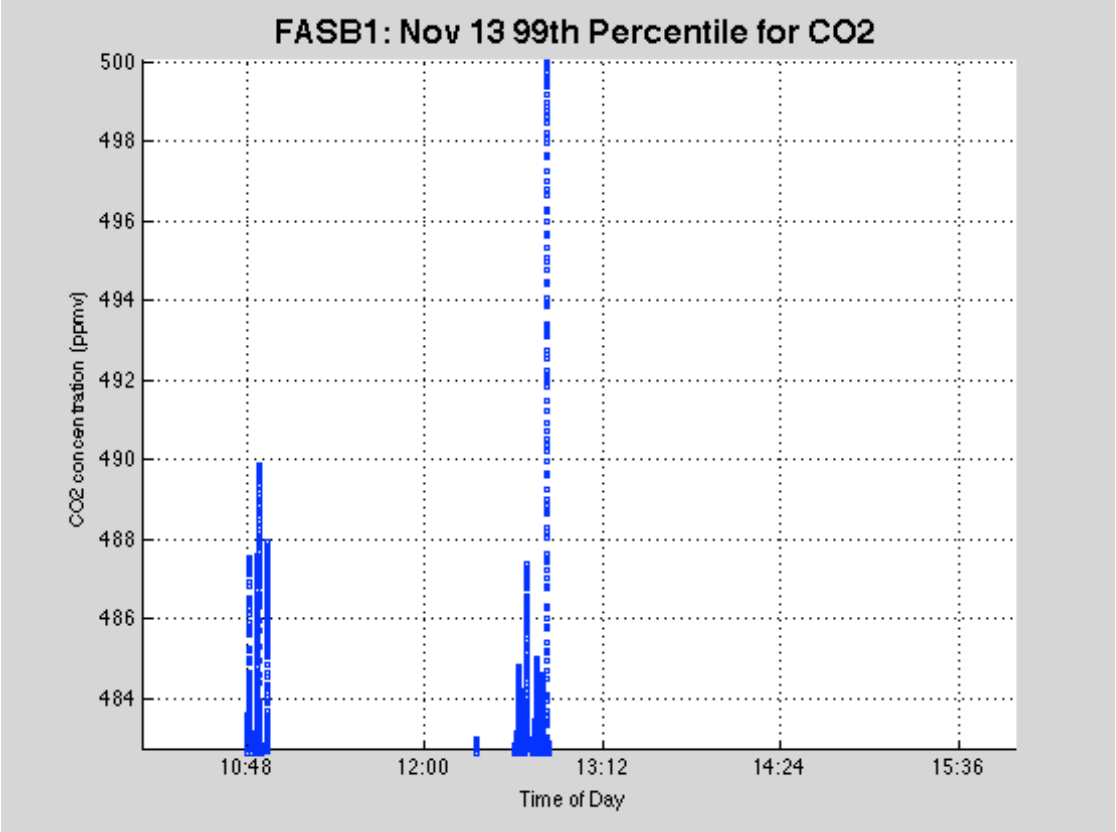
FASB1: Nov 13 99th Percentile for CO2
CO2 concentration (ppmv)
500
498
496
494
492
490
488
486
484
10:48
12:00
13:12
14:24
15:36
Time of Day

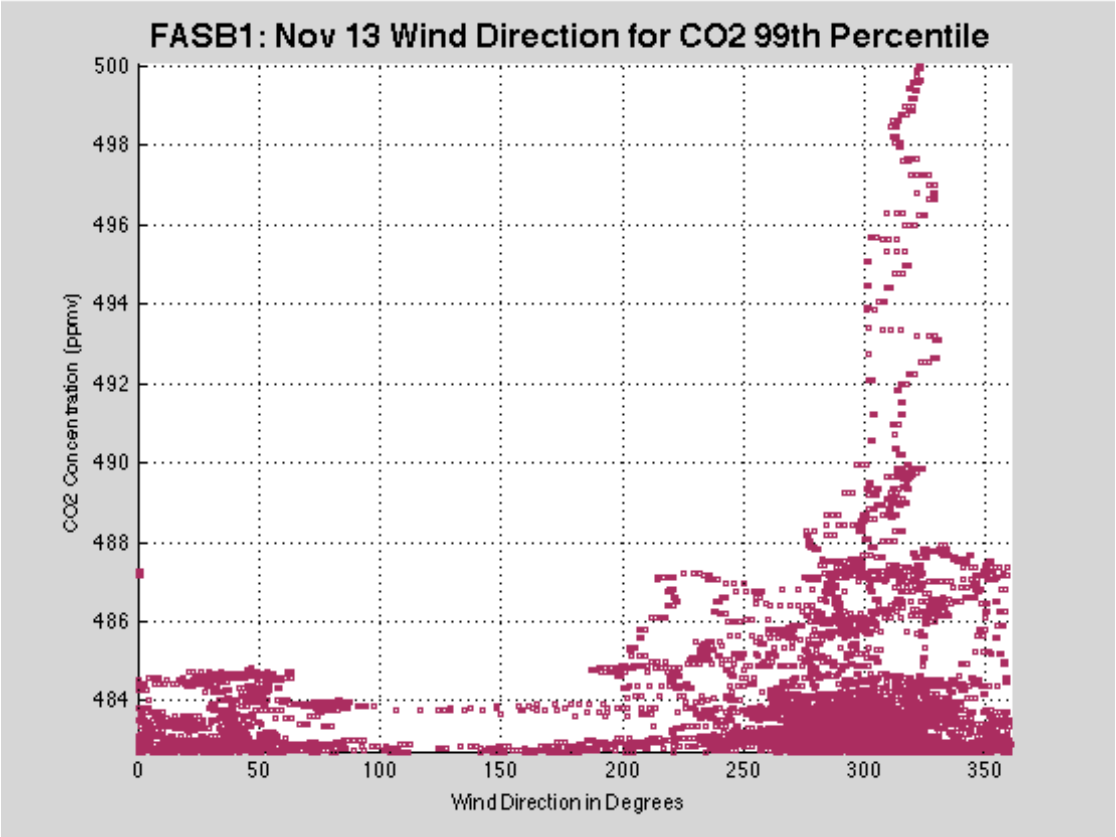
FASB1: Nov 13 Wind Direction for CO2 99th Percentile
CO2 Concentration (ppmv)
500
498
496
494
492
490
488
486
484
0
50
100
150
200
250
300
350
Wind Direction in Degrees

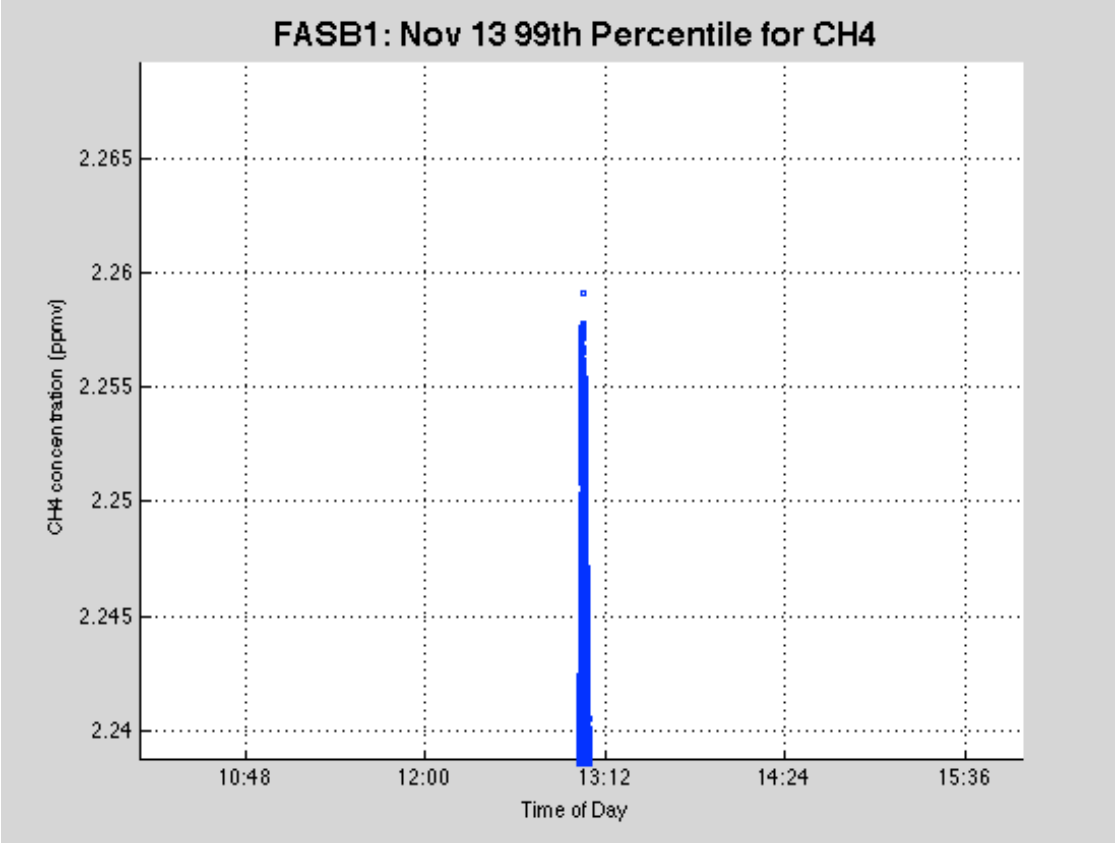
FASB1: Nov 13 99th Percentile for CH4
CH4 concentration (ppmv)
2.265
2.26
2.255
2.25
2.245
2.24
10:48
12:00
13:12
14:24
15:36
Time of Day

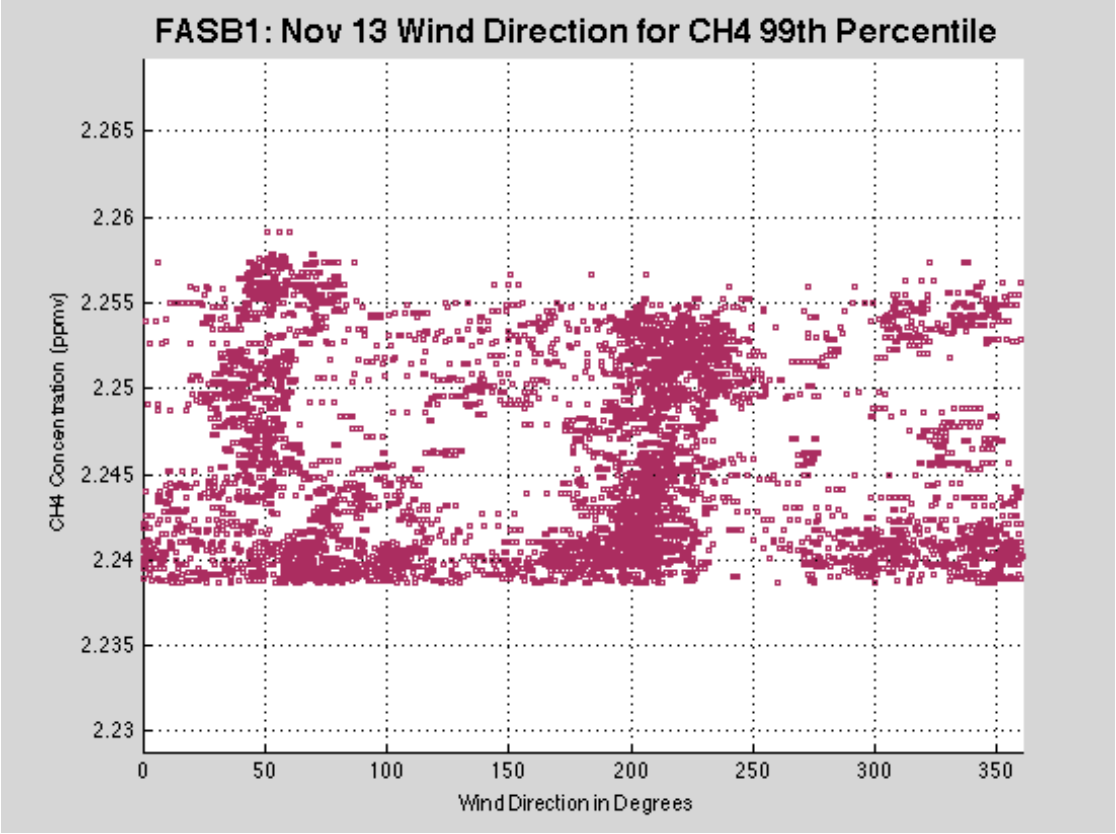
FASB1: Nov 13 Wind Direction for CH4 99th Percentile
CH4 Concentration (ppmv)
2.265
2.26
2.255
2.25
2.245
2.24
2.235
2.23
0
50
100
150
200
250
300
350
Wind Direction in Degrees

E.10 Thursday, November 14th, 2013

| | Maximum | Minimum | Average | Standard Deviation | 99th Percentile |
|---|---|---|---|---|---|
| $CO_2$ (ppmv) | 405.7752 | 385.6474 | 390.1429 | 2.2823 | 398.9857 |
| $CH_4$ (ppmv) | 1.8907 | 1.6849 | 1.7034 | 0.0125 | 1.7538 |
| UZ (m/s) | 2.1227 | -2.4895 | -0.0163 | 0.3544 | N/A |

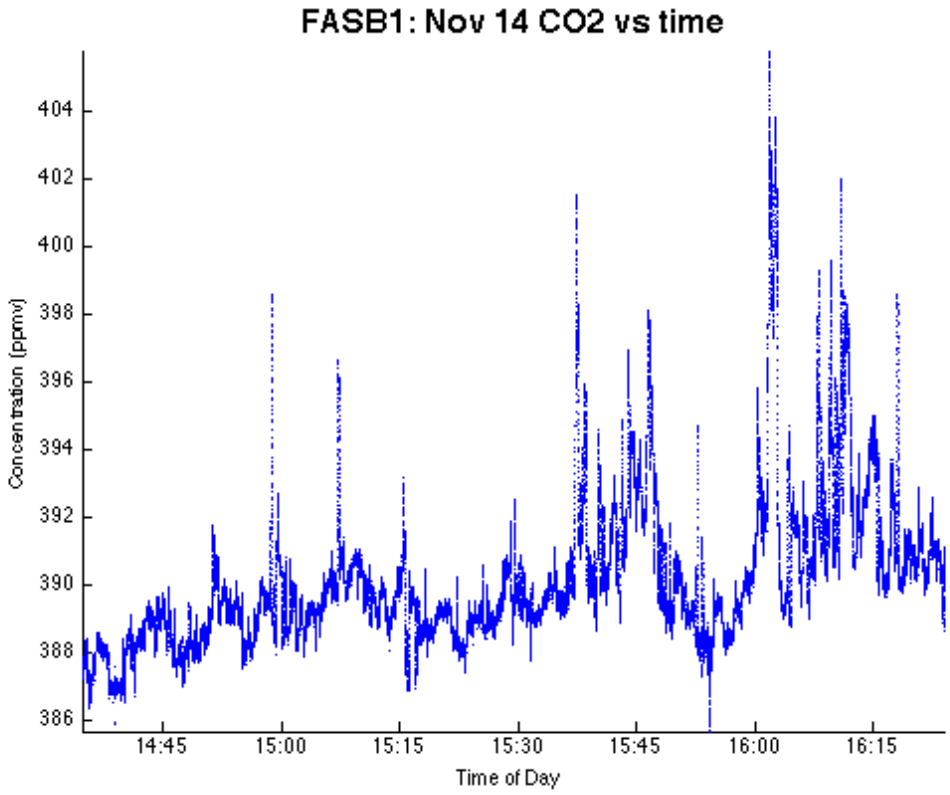

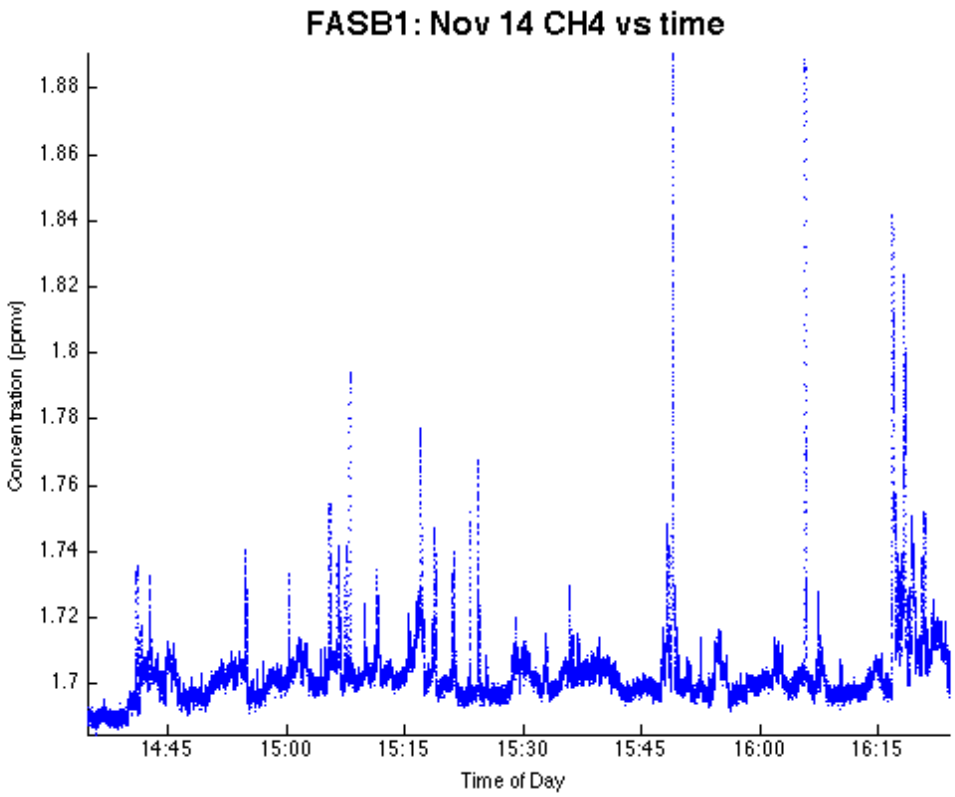
FASB1: Nov 14 CH4 vs time
Concentration (ppmv)
1.88
1.86
1.84
1.82
1.8
1.78
1.76
1.74
1.72
1.7
14:45
15:00
15:15
15:30
15:45
16:00
16:15
Time of Day

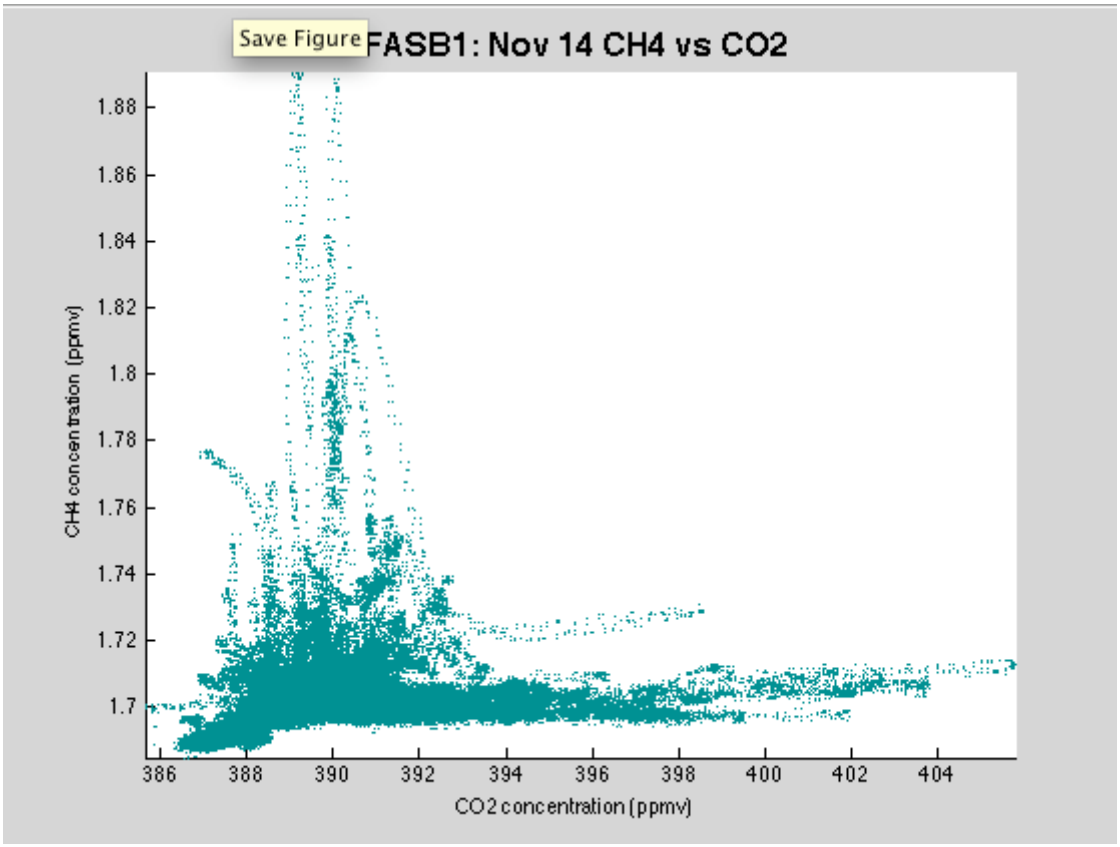
Save Figure
FASB1: Nov 14 CH4 vs CO2
CH4 concentration (ppmv)
1.88
1.86
1.84
1.82
1.8
1.78
1.76
1.74
1.72
1.7
386
388
390
392
394
396
398
400
402
404
CO2 concentration (ppmv)

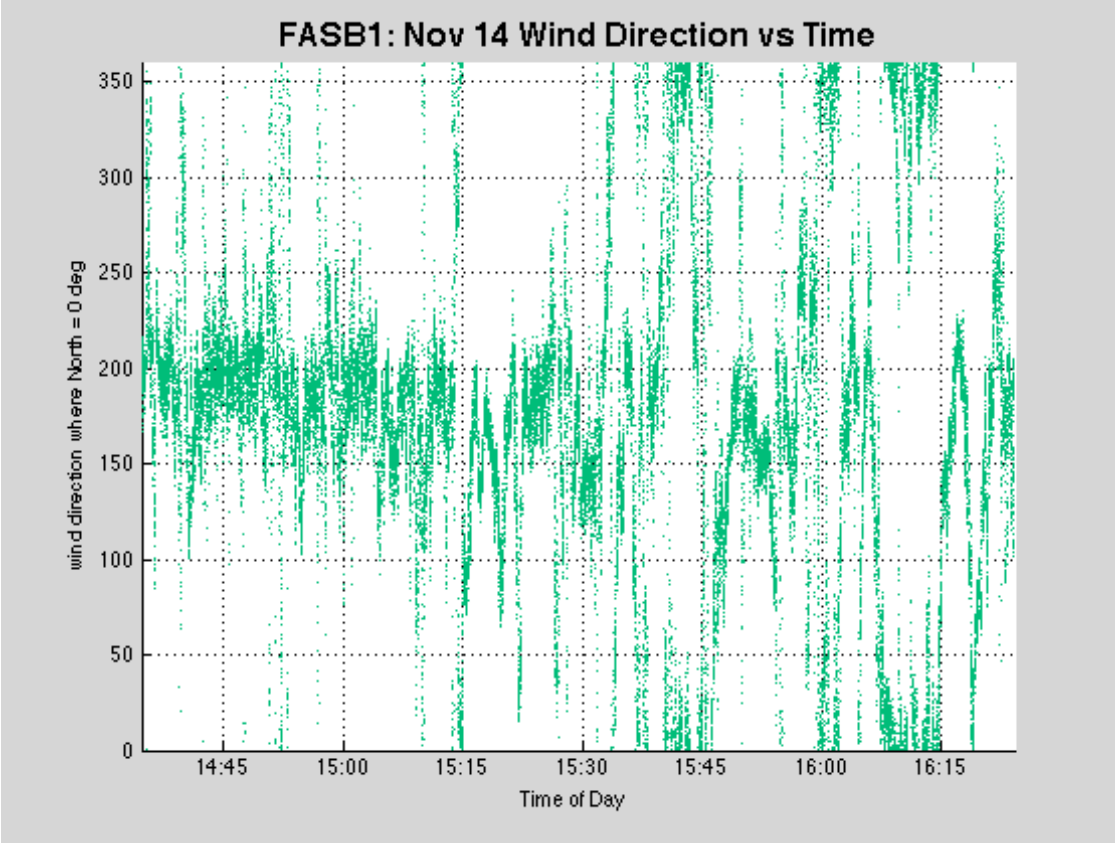
FASB1: Nov 14 Wind Direction vs Time
wind direction where North = 0 deg
350
300
250
200
150
100
50
0
14:45
15:00
15:15
15:30
15:45
16:00
16:15
Time of Day

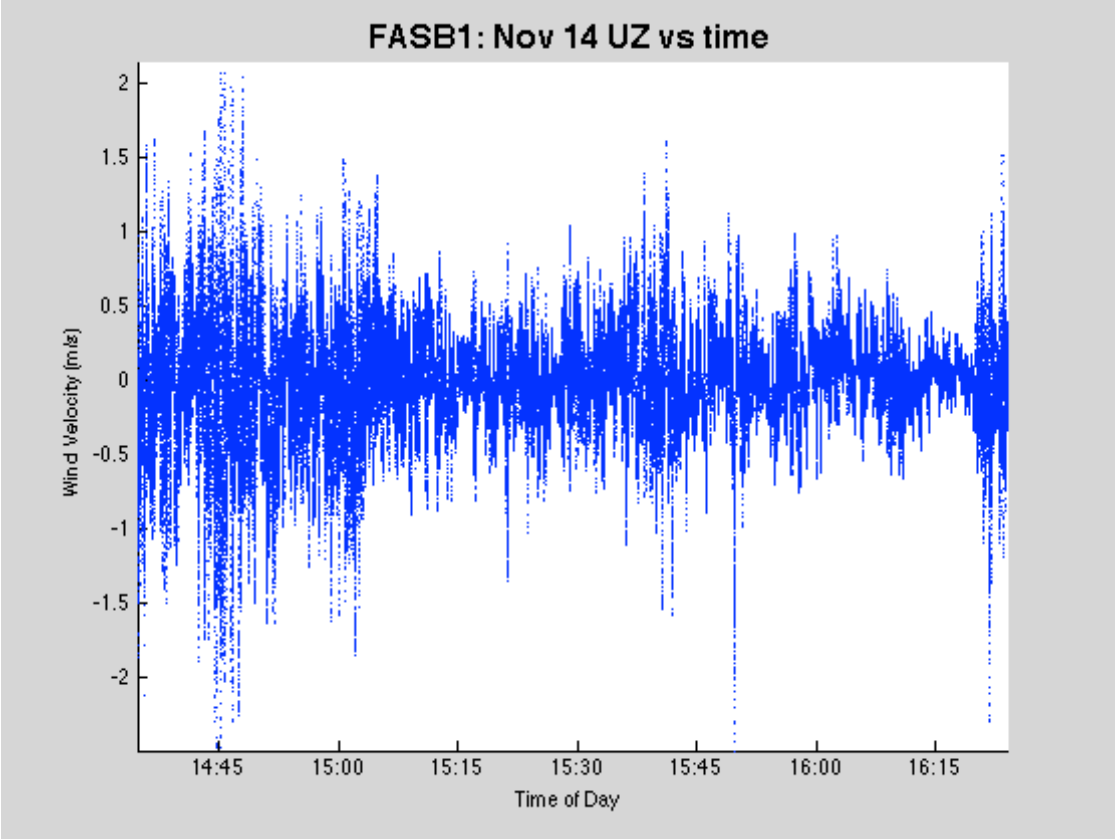
FASB1: Nov 14 UZ vs time
Wind Velocity (m/s)
2
1.5
1
0.5
0
-0.5
-1
-1.5
-2
14:45
15:00
15:15
15:30
15:45
16:00
16:15
Time of Day

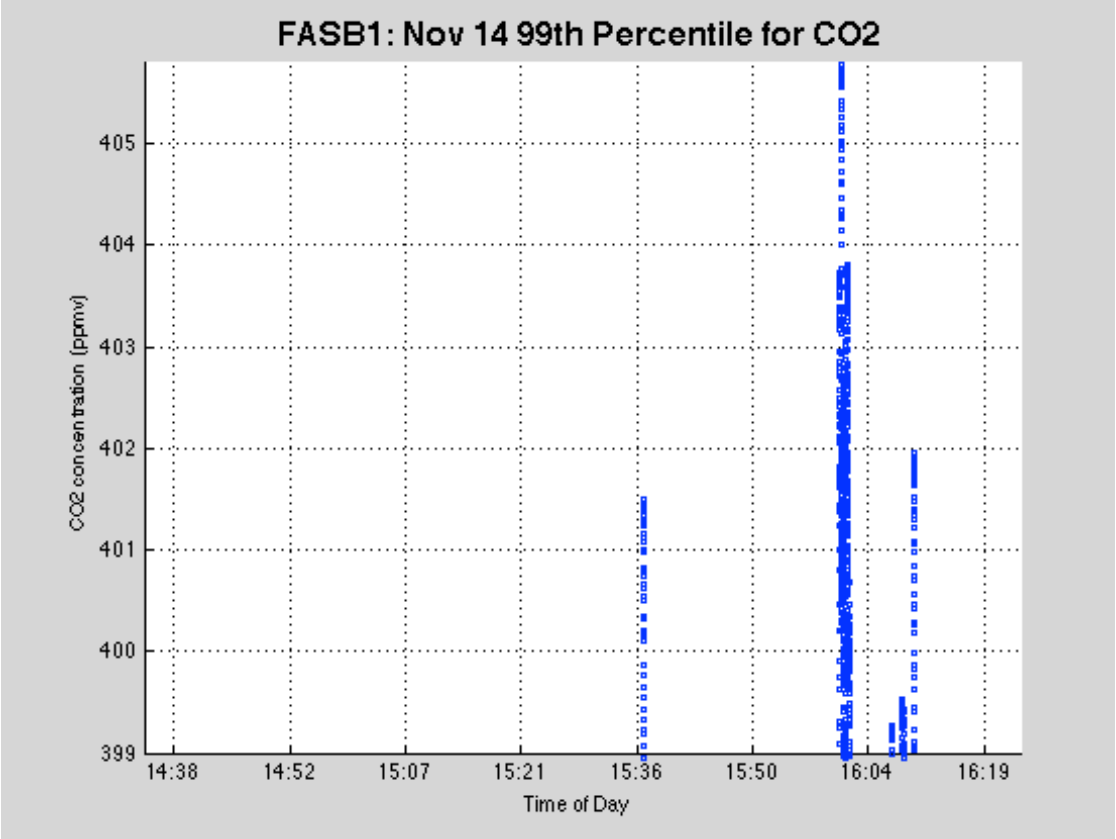
FASB1: Nov 14 99th Percentile for CO2
CO2 concentration (ppmv)
405
404
403
402
401
400
399
14:38
14:52
15:07
15:21
15:36
15:50
16:04
16:19
Time of Day

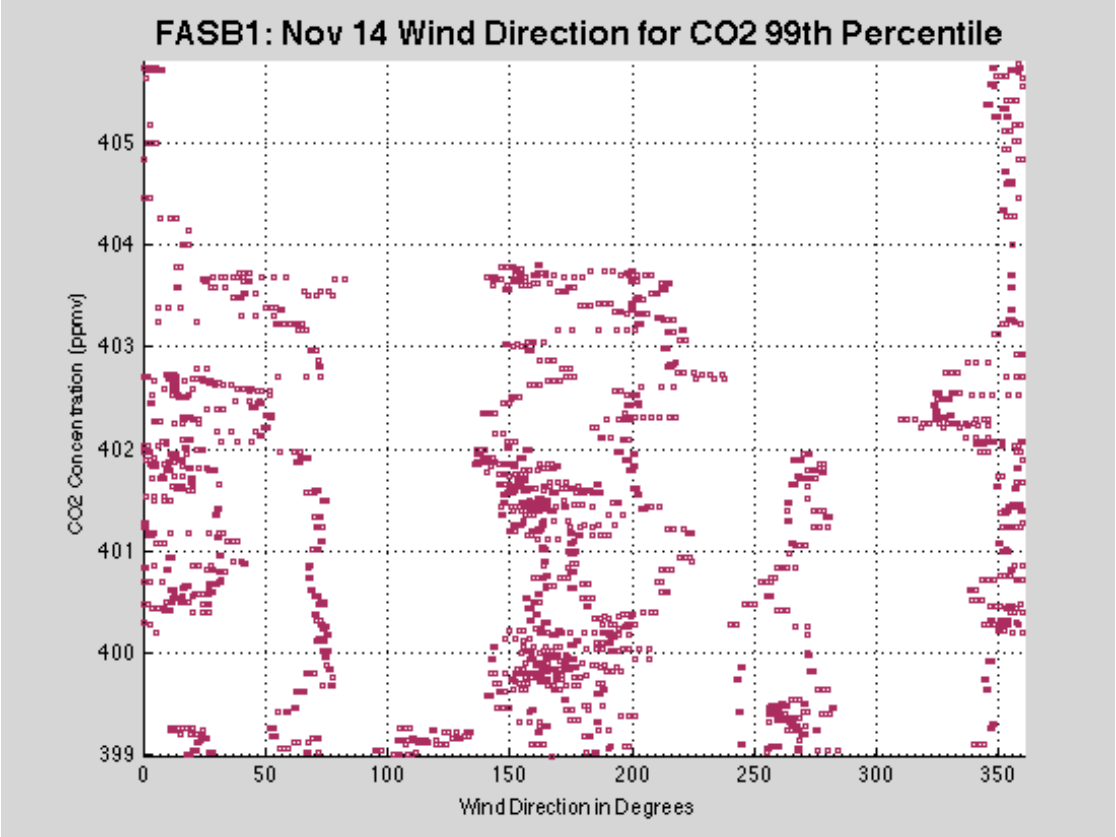
FASB1: Nov 14 Wind Direction for CO2 99th Percentile
CO2 Concentration (ppmv)
405
404
403
402
401
400
399
0
50
100
150
200
250
300
350
Wind Direction in Degrees

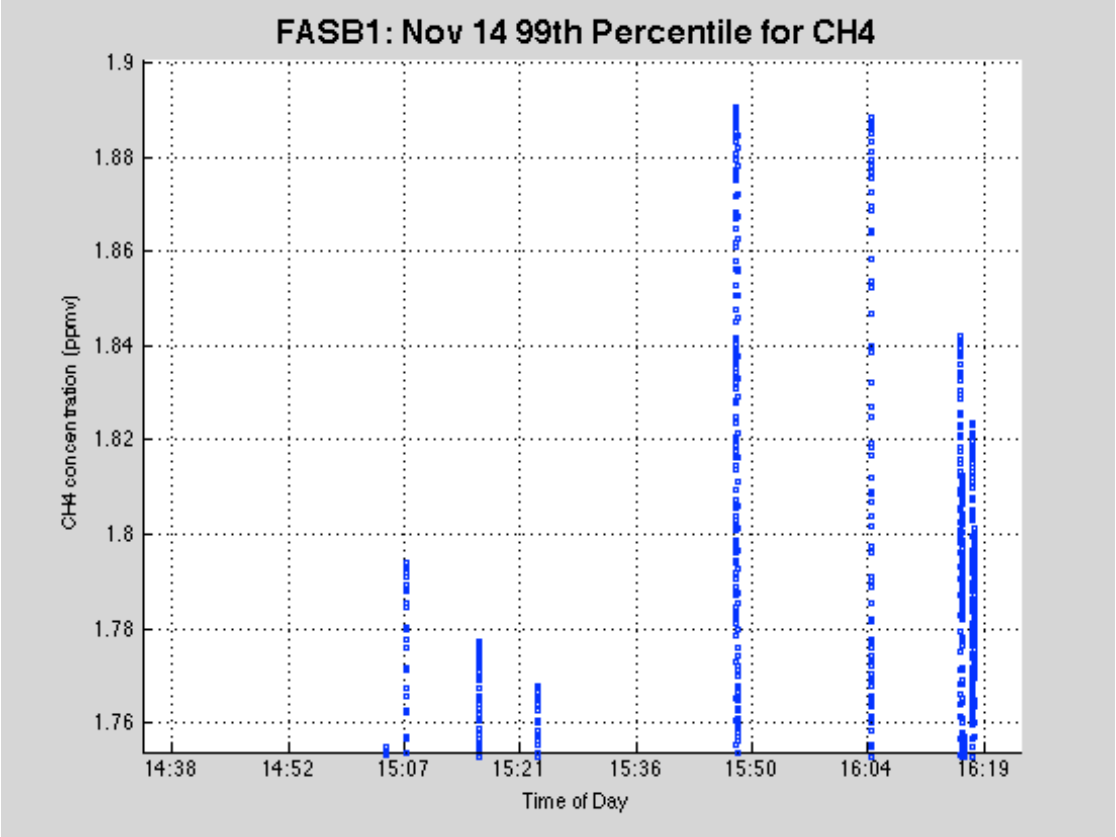
FASB1: Nov 14 99th Percentile for CH4
CH4 concentration (ppmv)
1.9
1.88
1.86
1.84
1.82
1.8
1.78
1.76
14:38
14:52
15:07
15:21
15:36
15:50
16:04
16:19
Time of Day

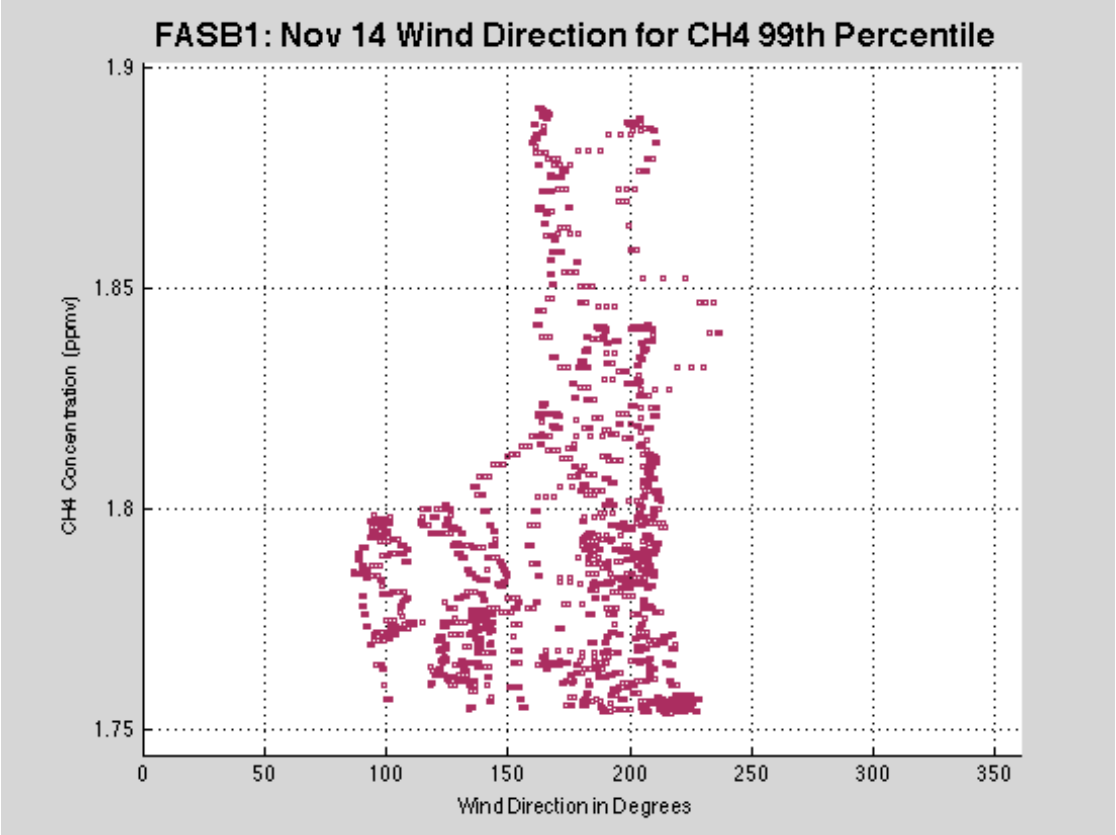
FASB1: Nov 14 Wind Direction for CH4 99th Percentile
CH4 Concentration (ppmv)
1.9
1.85
1.8
1.75
0
50
100
150
200
250
300
350
Wind Direction in Degrees

## E.11 Monday, November 18th, 2013

| | Maximum | Minimum | Average | Standard Deviation | 99th Percentile |
|---|---|---|---|---|---|
| $CO_2$ (ppmv) | 485.0067 | 389.7784 | 411.0335 | 19.3897 | 451.9557 |
| $CH_4$ (ppmv) | 2.0054 | 1.6948 | 1.7374 | 0.0364 | 1.8193 |
| UZ (m/s) | 1.8275 | -2.0157 | -0.0075 | 0.3029 | N/A |

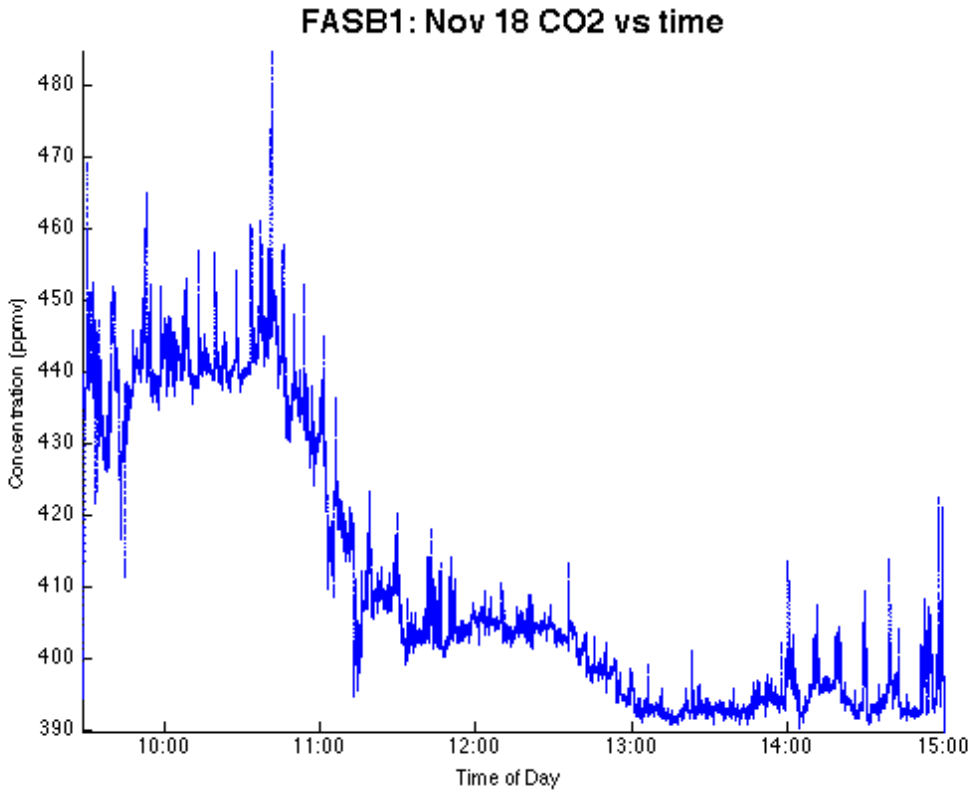

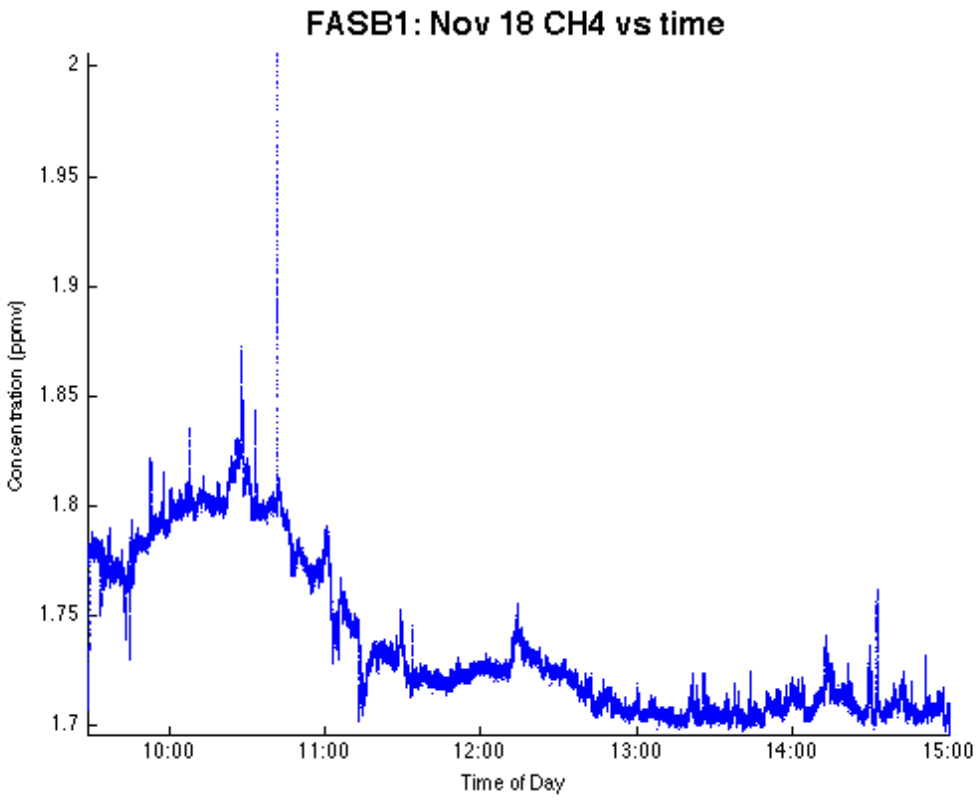
FASB1: Nov 18 CH4 vs time
Concentration (ppmv)
2
1.95
1.9
1.85
1.8
1.75
1.7
10:00
11:00
12:00
13:00
14:00
15:00
Time of Day

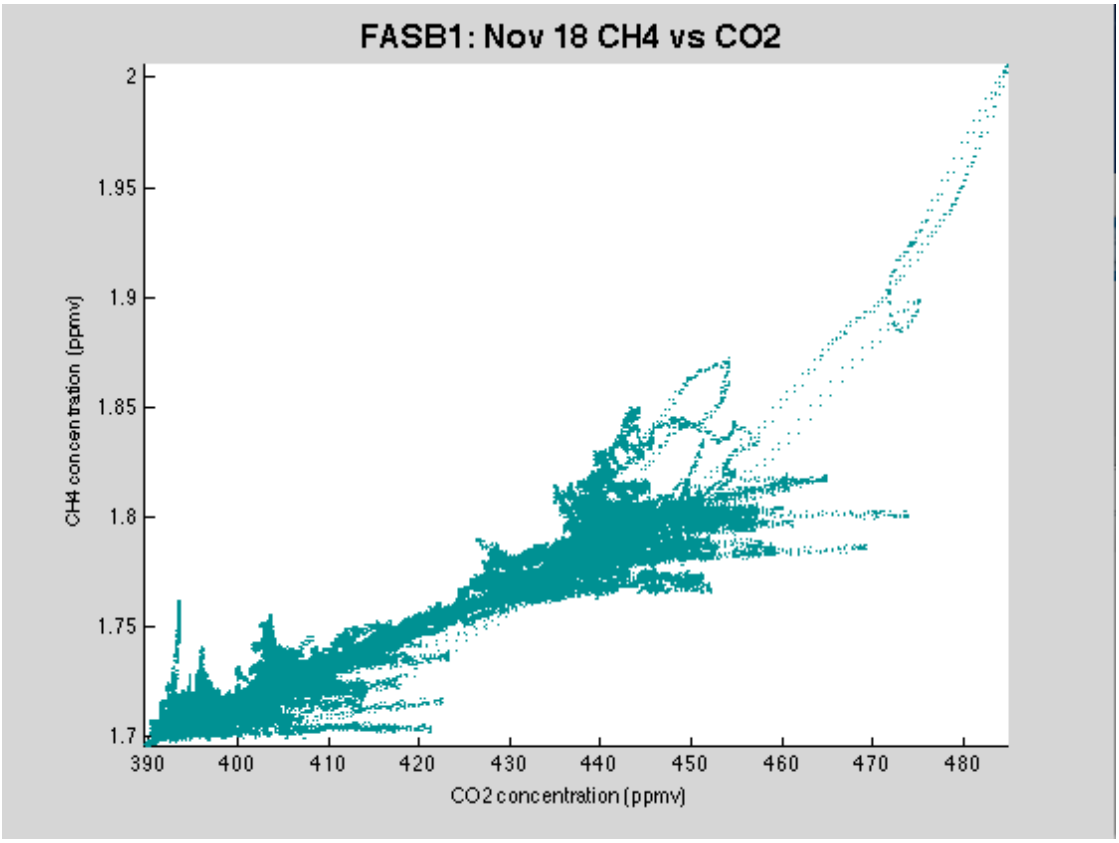
FASB1: Nov 18 CH4 vs CO2
CH4 concentration (ppmv)
2
1.95
1.9
1.85
1.8
1.75
1.7
390
400
410
420
430
440
450
460
470
480
CO2 concentration (ppmv)

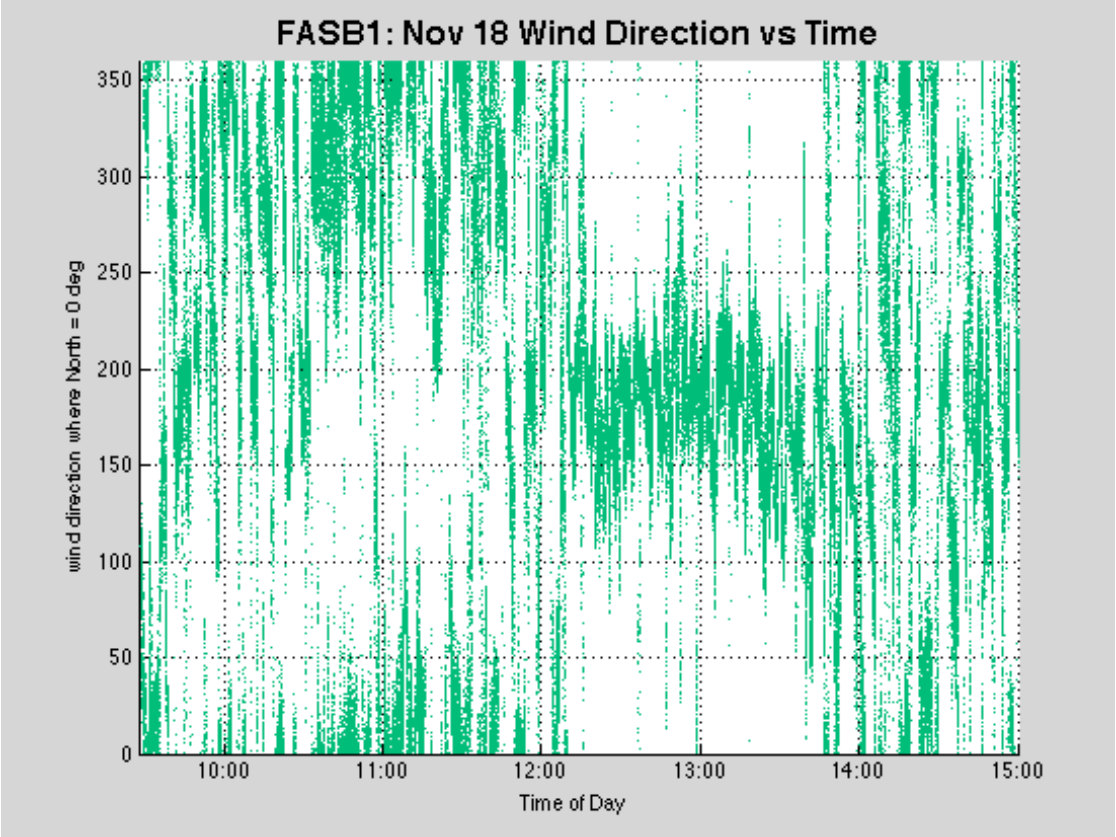
FASB1: Nov 18 Wind Direction vs Time
wind direction where North = 0 deg
350
300
250
200
150
100
50
0
10:00
11:00
12:00
13:00
14:00
15:00
Time of Day

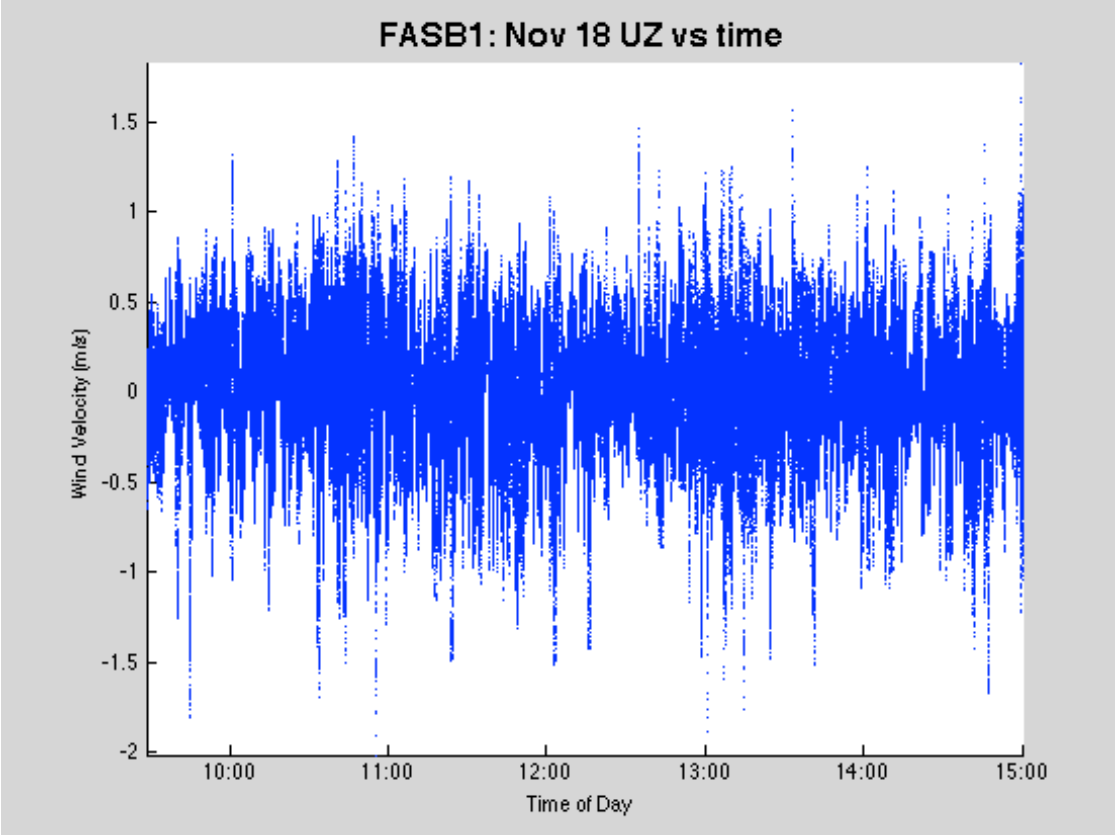
FASB1: Nov 18 UZ vs time
Wind Velocity (m/s)
1.5
1
0.5
0
-0.5
-1
-1.5
-2
10:00
11:00
12:00
13:00
14:00
15:00
Time of Day

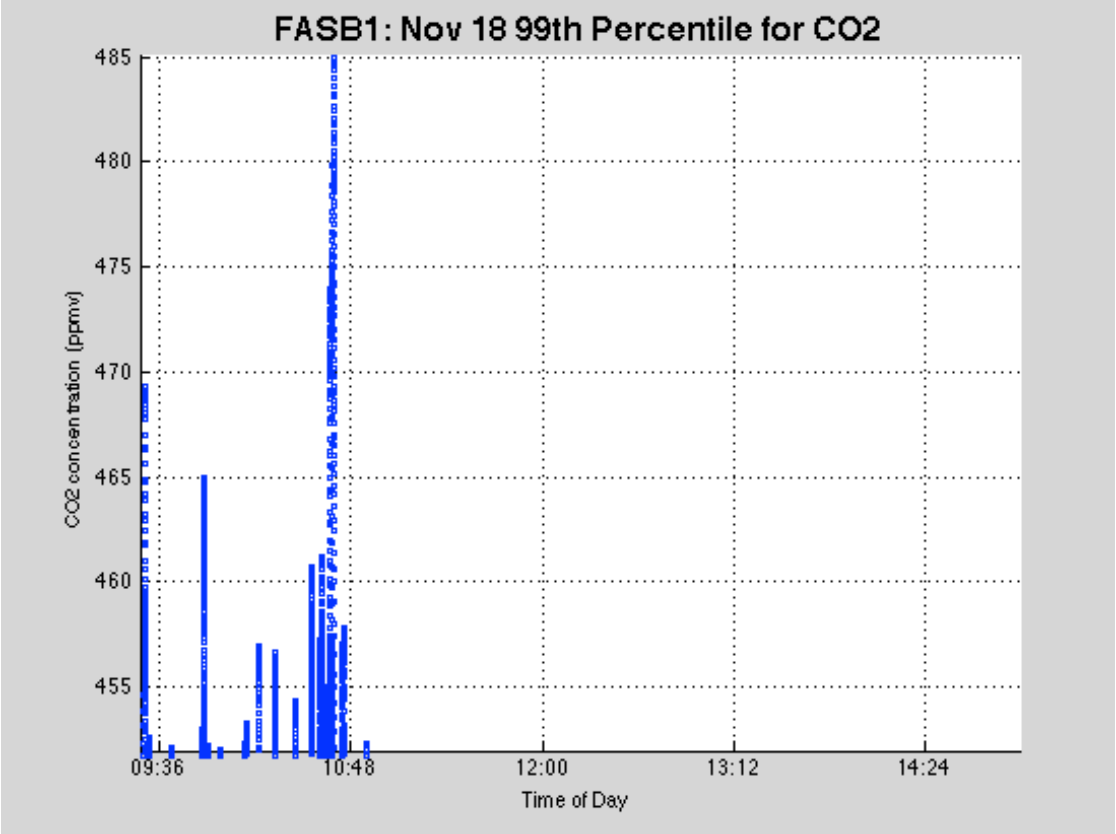
FASB1: Nov 18 99th Percentile for CO2
CO2 concentration (ppmv)
485
480
475
470
465
460
455
09:36
10:48
12:00
13:12
14:24
Time of Day

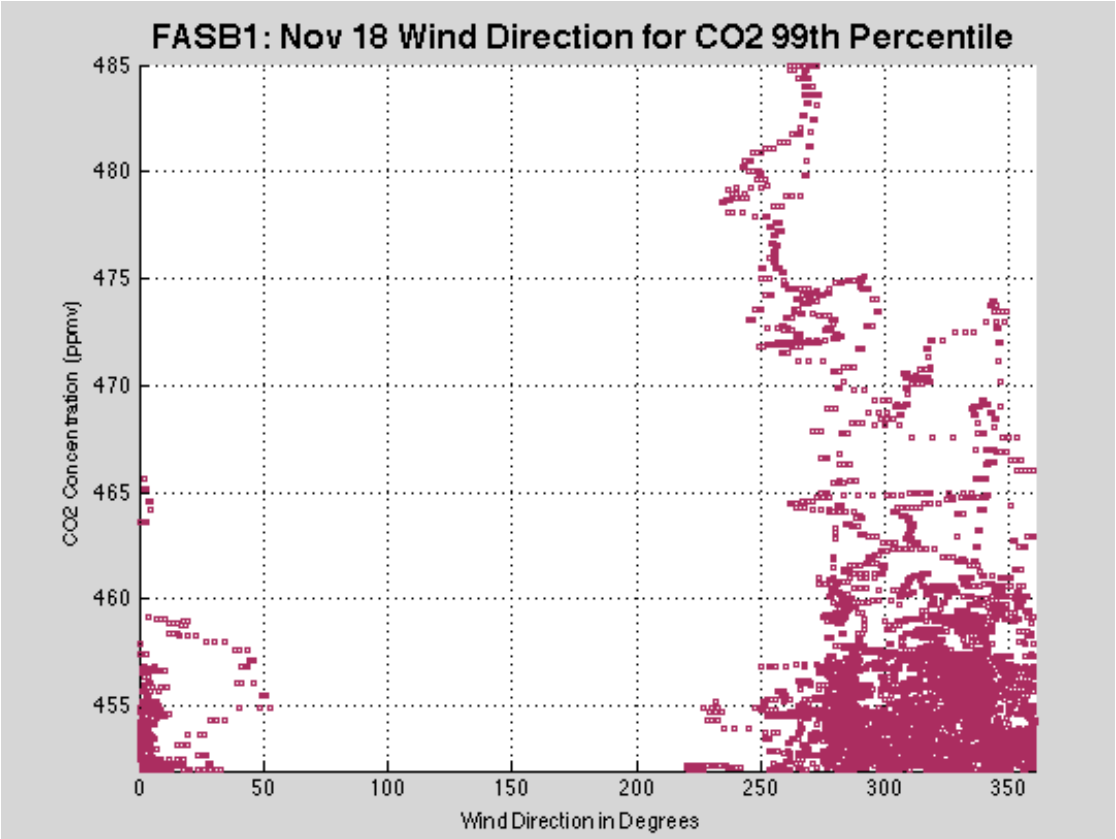
FASB1: Nov 18 Wind Direction for CO2 99th Percentile
CO2 Concentration (ppmv)
485
480
475
470
465
460
455
0
50
100
150
200
250
300
350
Wind Direction in Degrees

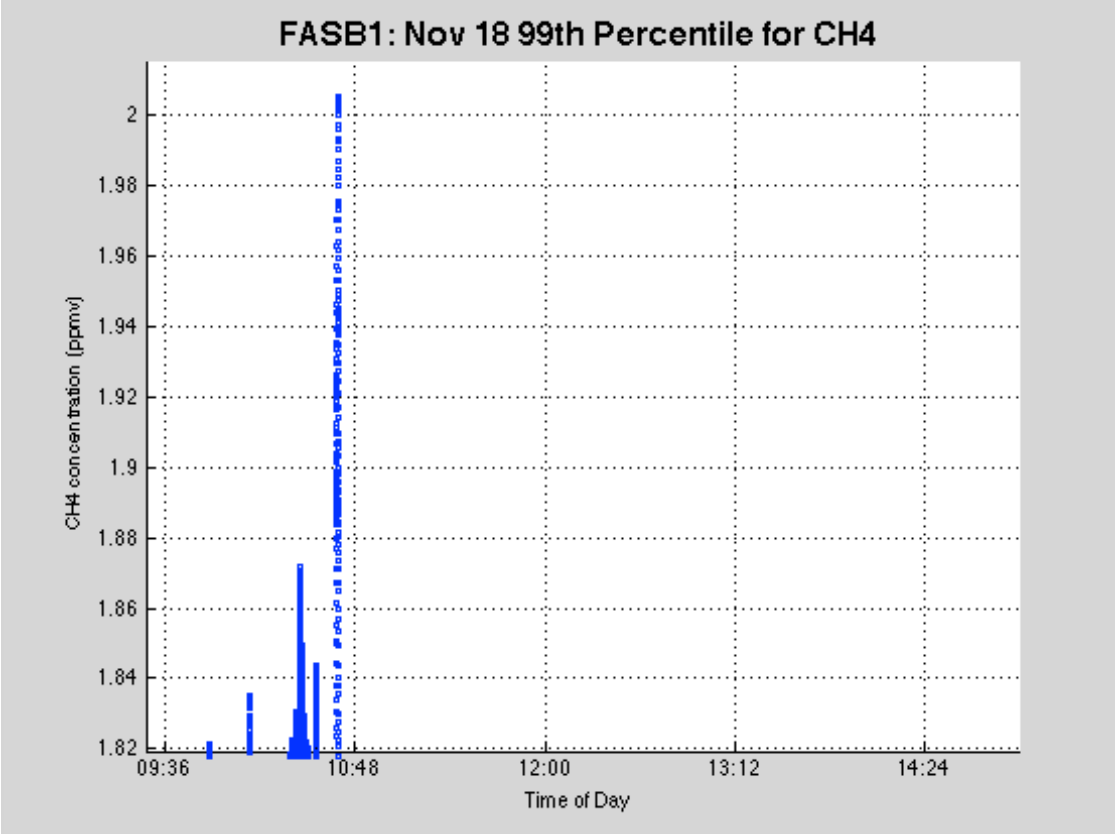
FASB1: Nov 18 99th Percentile for CH4
CH4 concentration (ppmv)
2
1.98
1.96
1.94
1.92
1.9
1.88
1.86
1.84
1.82
09:36
10:48
12:00
13:12
14:24
Time of Day

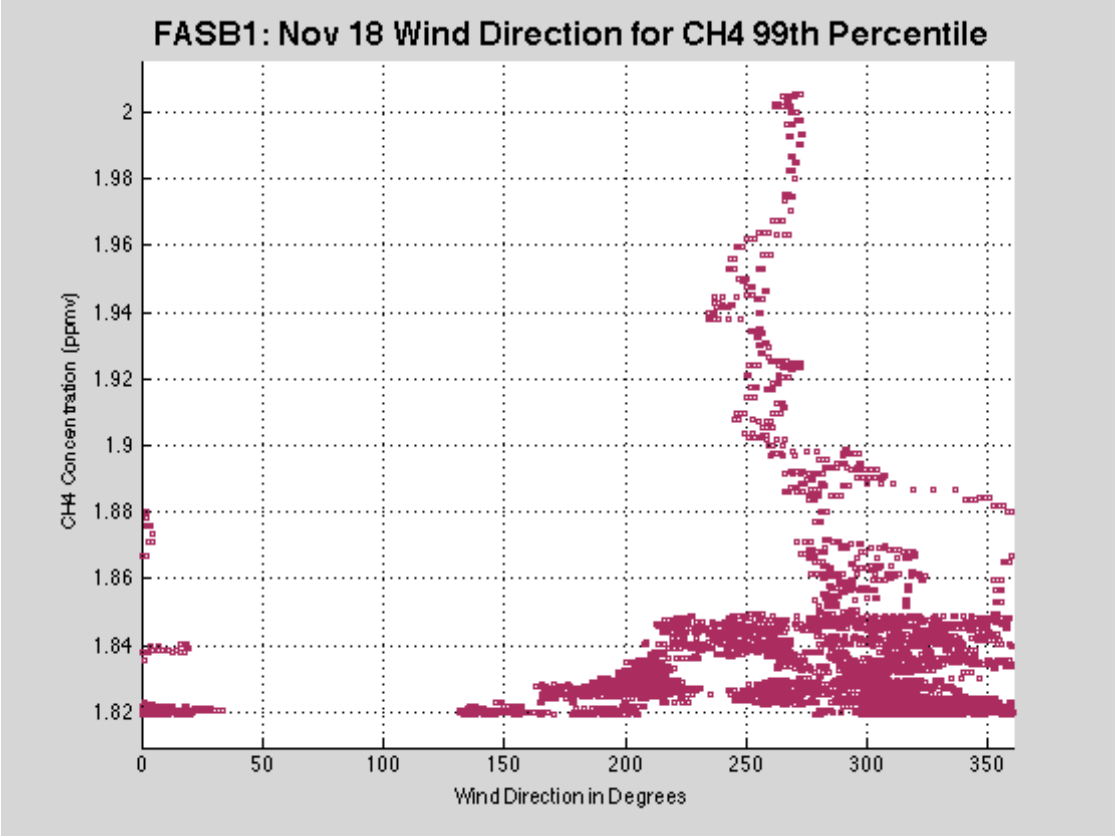
FASB1: Nov 18 Wind Direction for CH4 99th Percentile
CH4 Concentration (ppmv)
2
1.98
1.96
1.94
1.92
1.9
1.88
1.86
1.84
1.82
0
50
100
150
200
250
300
350
Wind Direction in Degrees

E.12 Monday, November 25th, 2013

| | Maximum | Minimum | Average | Standard Deviation | 99th Percentile |
|---|---|---|---|---|---|
| $CO_2$ (ppmv) | 436.8613 | 397.3805 | 409.531 | 4.7388 | 422.5396 |
| $CH_4$ (ppmv) | 2.078 | 1.7498 | 1.7751 | 0.0124 | 1.7989 |
| UZ (m/s) | 2.3236 | -3.8 | -0.0222 | 0.4382 | N/A |

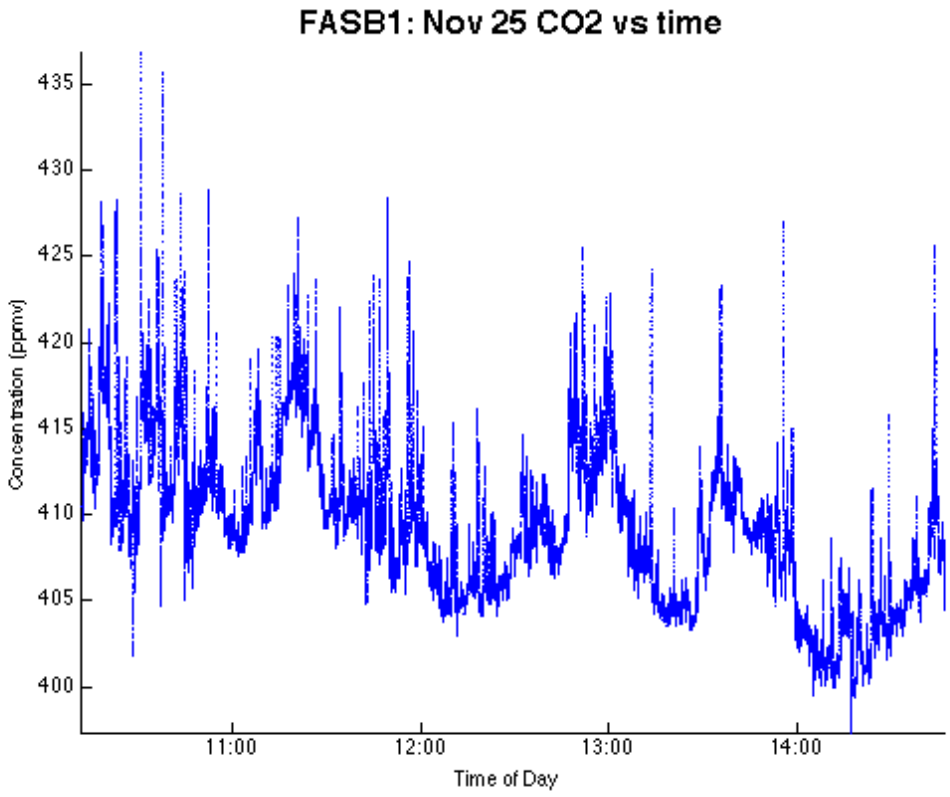

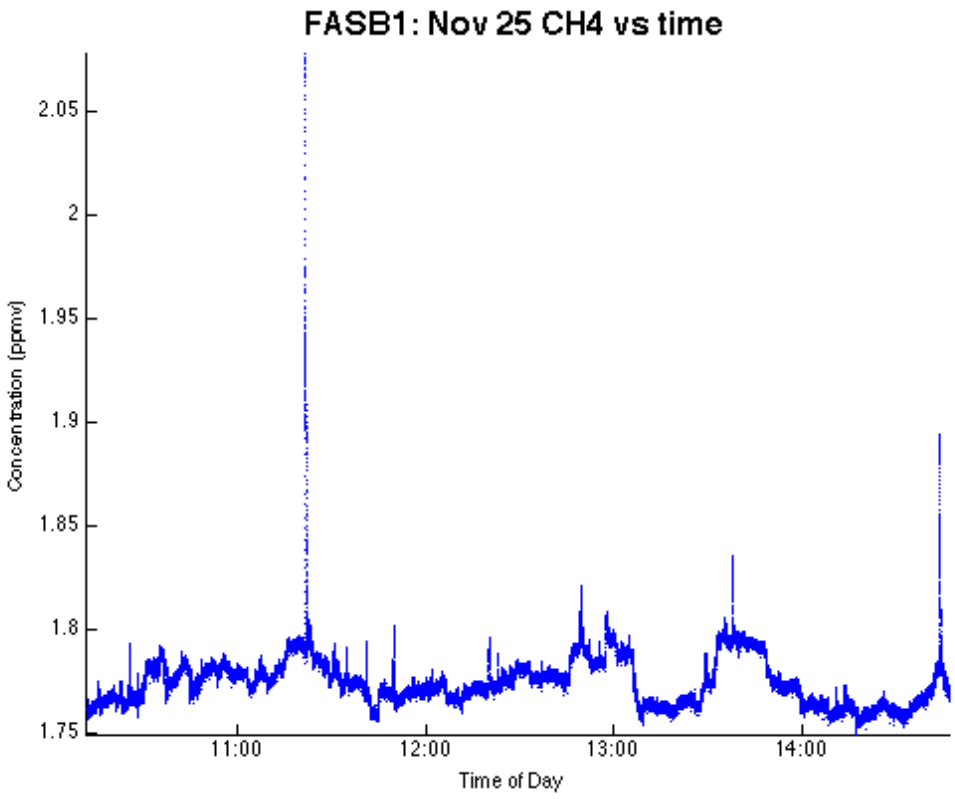
FASB1: Nov 25 CH4 vs time
Concentration (ppmv)
2.05
2
1.95
1.9
1.85
1.8
1.75
11:00
12:00
13:00
14:00
Time of Day

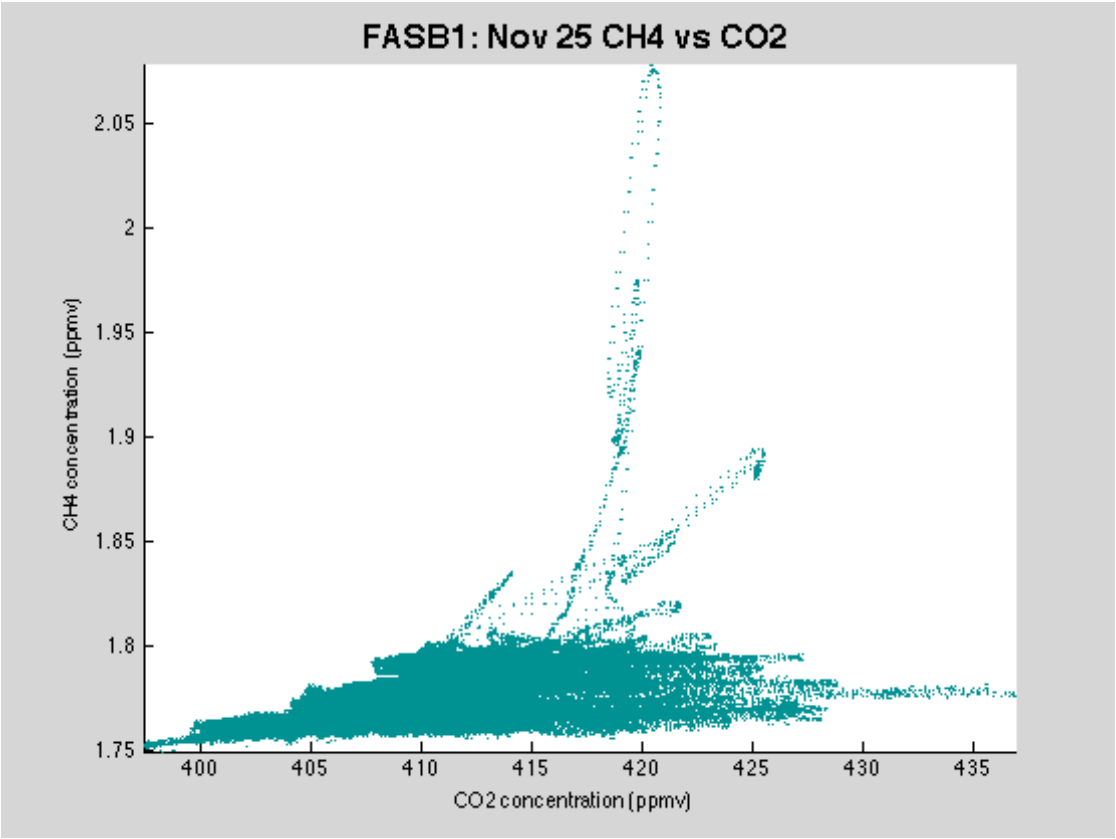
FASB1: Nov 25 CH4 vs CO2
CH4 concentration (ppmv)
2.05
2
1.95
1.9
1.85
1.8
1.75
400
405
410
415
420
425
430
435
CO2 concentration (ppmv)

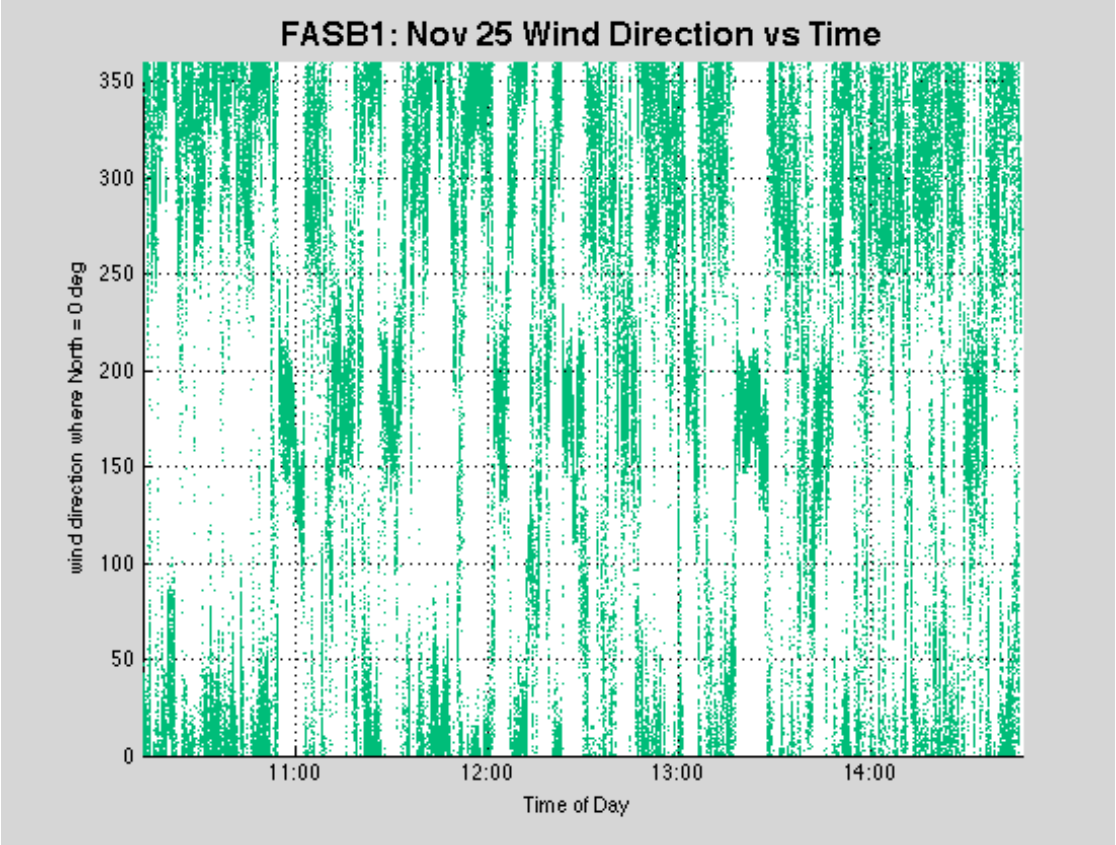
FASB1: Nov 25 Wind Direction vs Time
wind direction where North = 0 deg
350
300
250
200
150
100
50
0
11:00
12:00
13:00
14:00
Time of Day

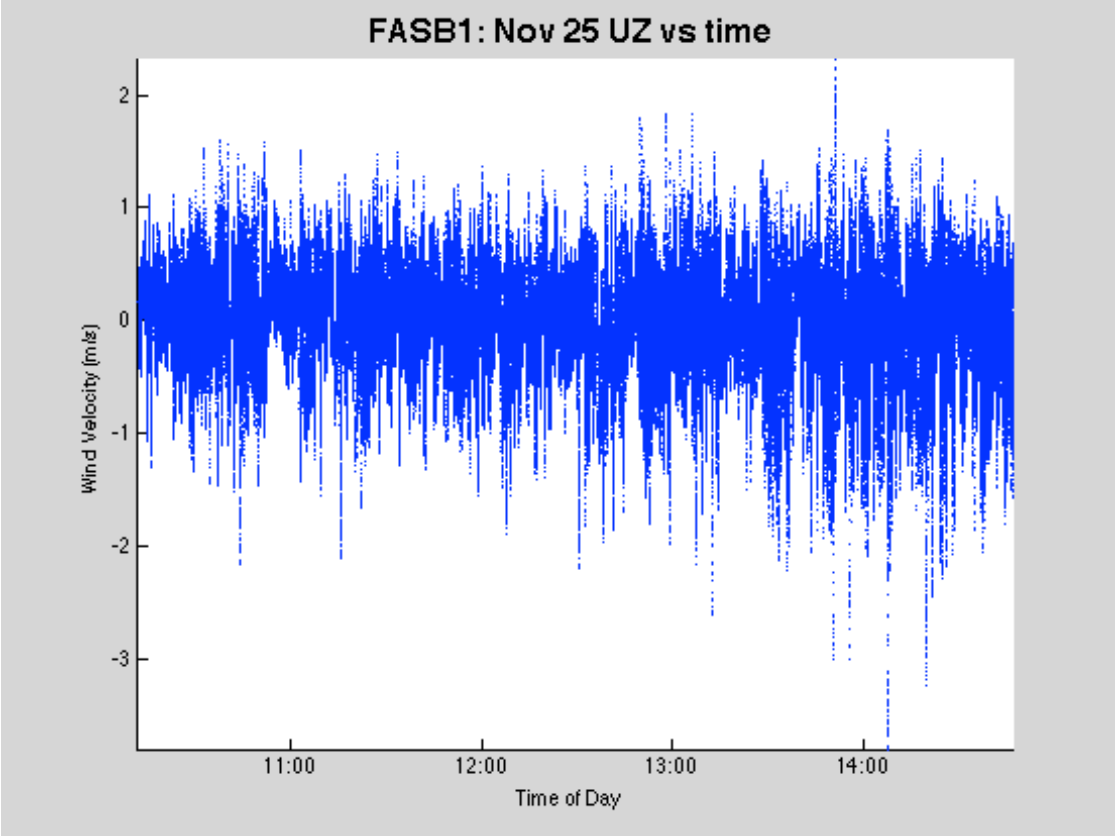
FASB1: Nov 25 UZ vs time
Wind Velocity (m/s)
2
1
0
-1
-2
-3
11:00
12:00
13:00
14:00
Time of Day

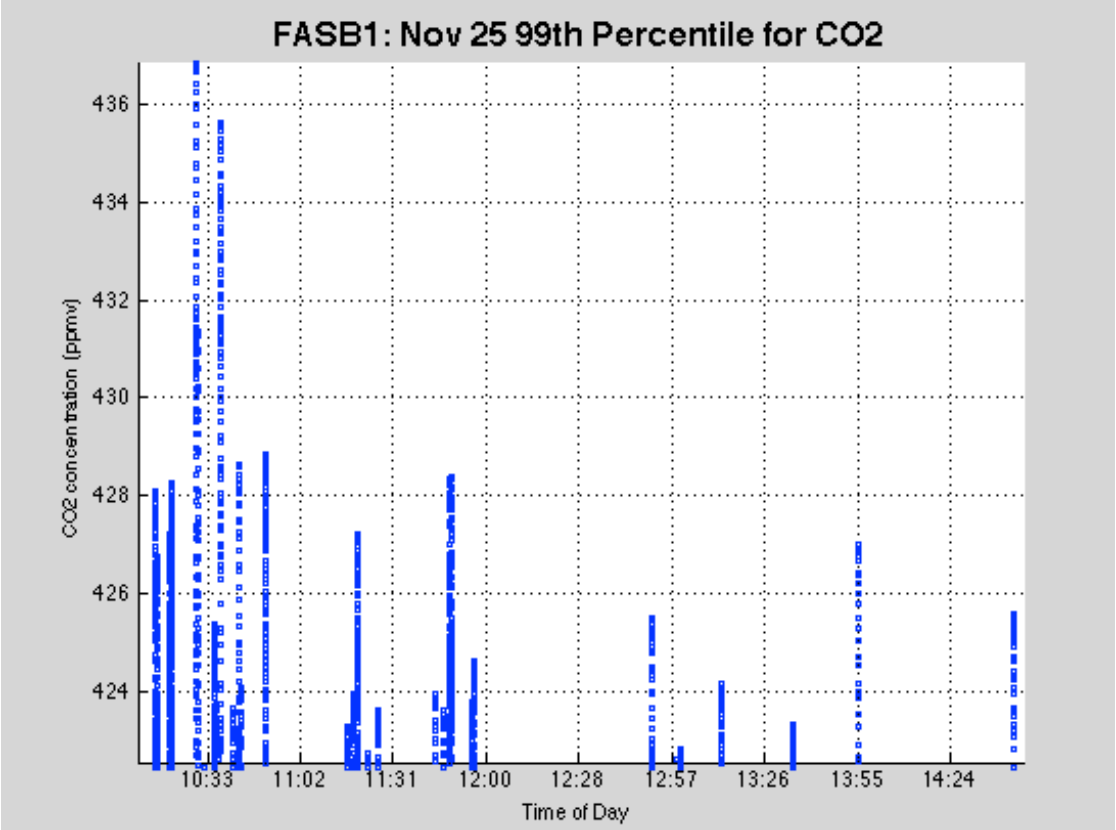
FASB1: Nov 25 99th Percentile for CO2
CO2 concentration (ppmv)
436
434
432
430
428
426
424
10:33
11:02
11:31
12:00
12:28
12:57
13:26
13:55
14:24
Time of Day

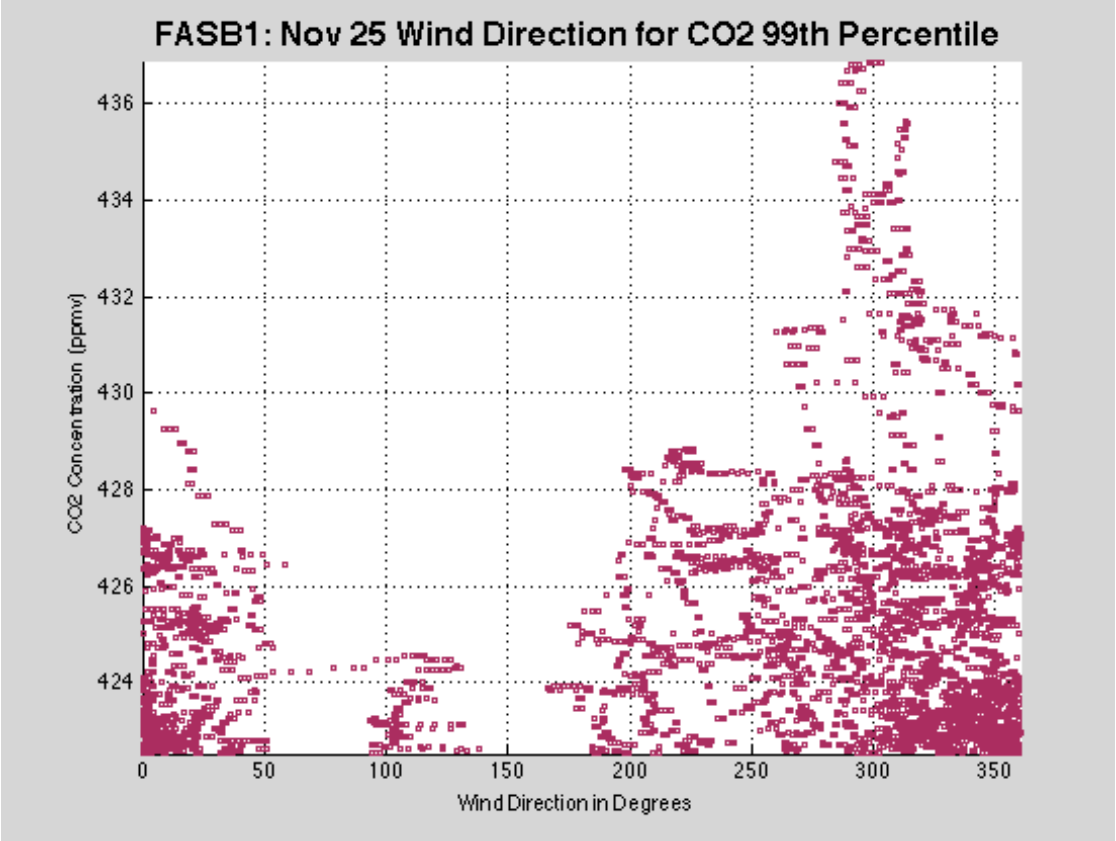
FASB1: Nov 25 Wind Direction for CO2 99th Percentile
CO2 Concentration (ppmv)
436
434
432
430
428
426
424
0
50
100
150
200
250
300
350
Wind Direction in Degrees

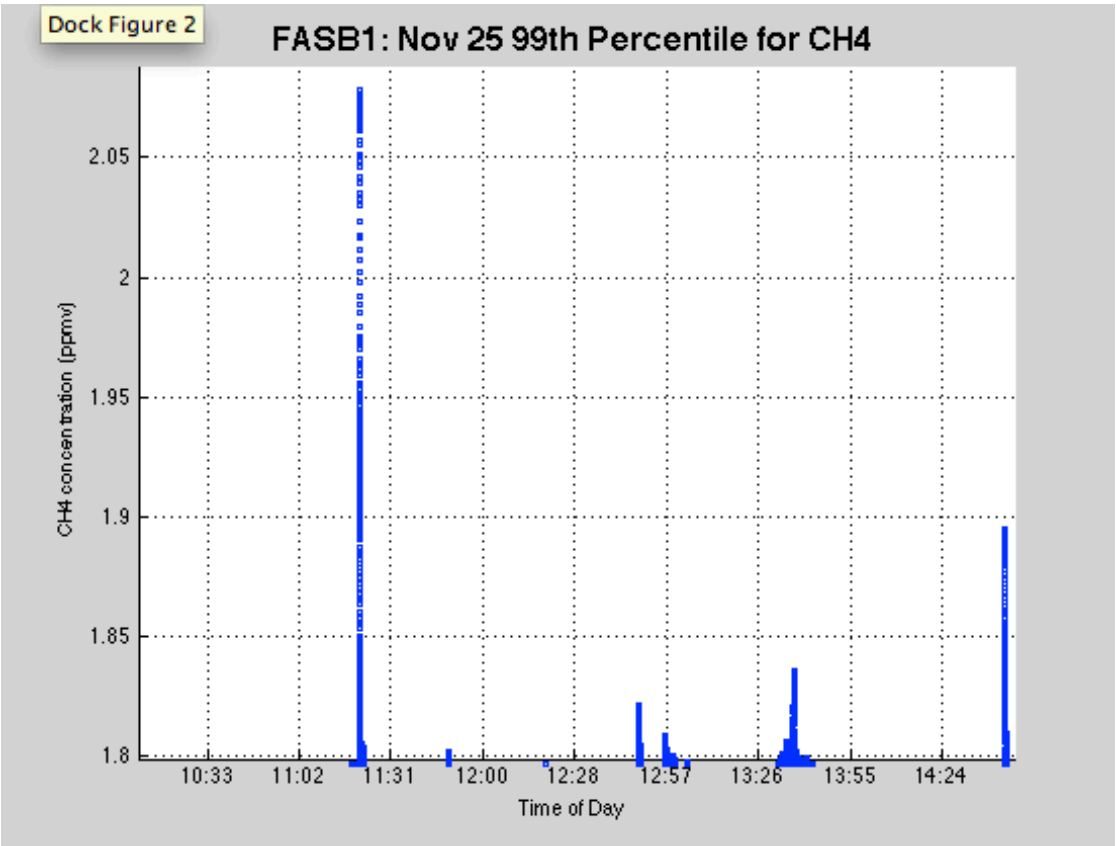
Dock Figure 2
FASB1: Nov 25 99th Percentile for CH4
CH4 concentration (ppmv)
2.05
2
1.95
1.9
1.85
1.8
10:33
11:02
11:31
12:00
12:28
12:57
13:26
13:55
14:24
Time of Day

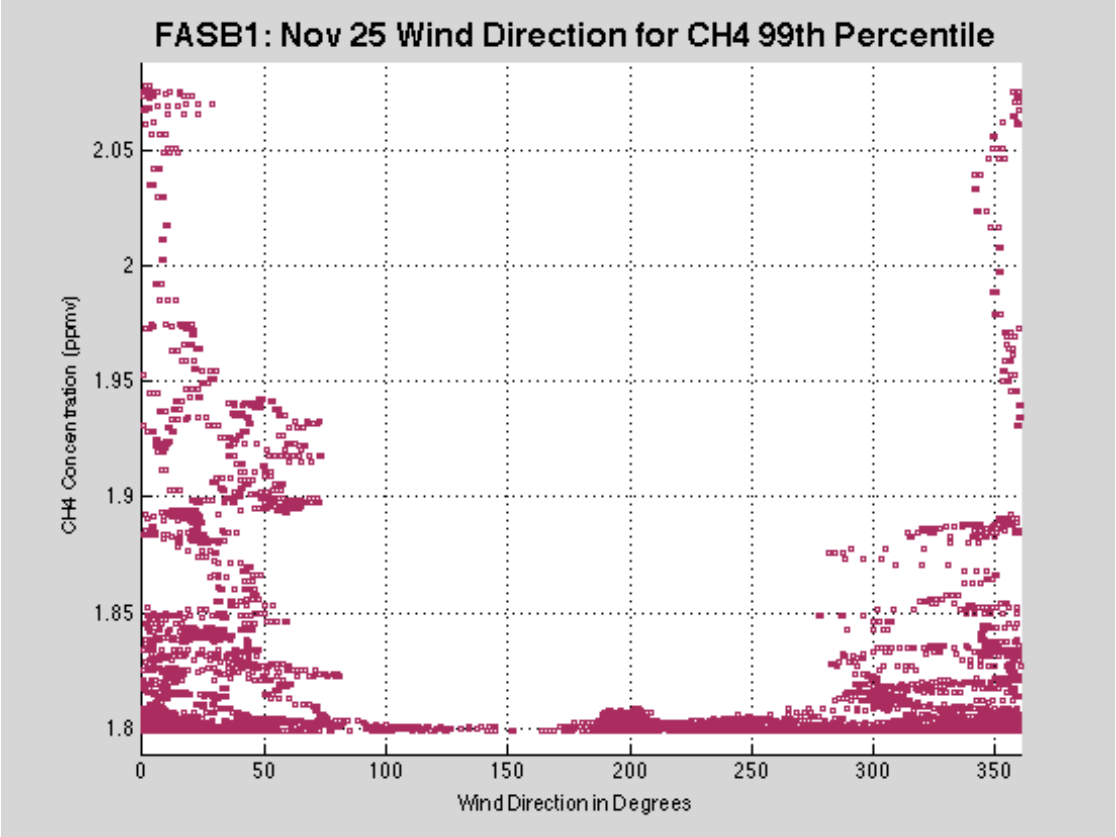
FASB1: Nov 25 Wind Direction for CH4 99th Percentile
CH4 Concentration (ppmv)
2.05
2
1.95
1.9
1.85
1.8
0
50
100
150
200
250
300
350
Wind Direction in Degrees

## E.13 Monday, December 2nd, 2013

| | Maximum | Minimum | Average | Standard Deviation | 99th Percentile |
|---|---|---|---|---|---|
| $CO_2$ (ppmv) | 436.1102 | 383.8838 | 391.8151 | 5.2427 | 413.1845 |
| $CH_4$ (ppmv) | 1.8774 | 1.6654 | 1.684 | 0.0123 | 1.733 |
| UZ (m/s) | 4.556 | -6.5897 | -0.0409 | 0.5032 | N/A |

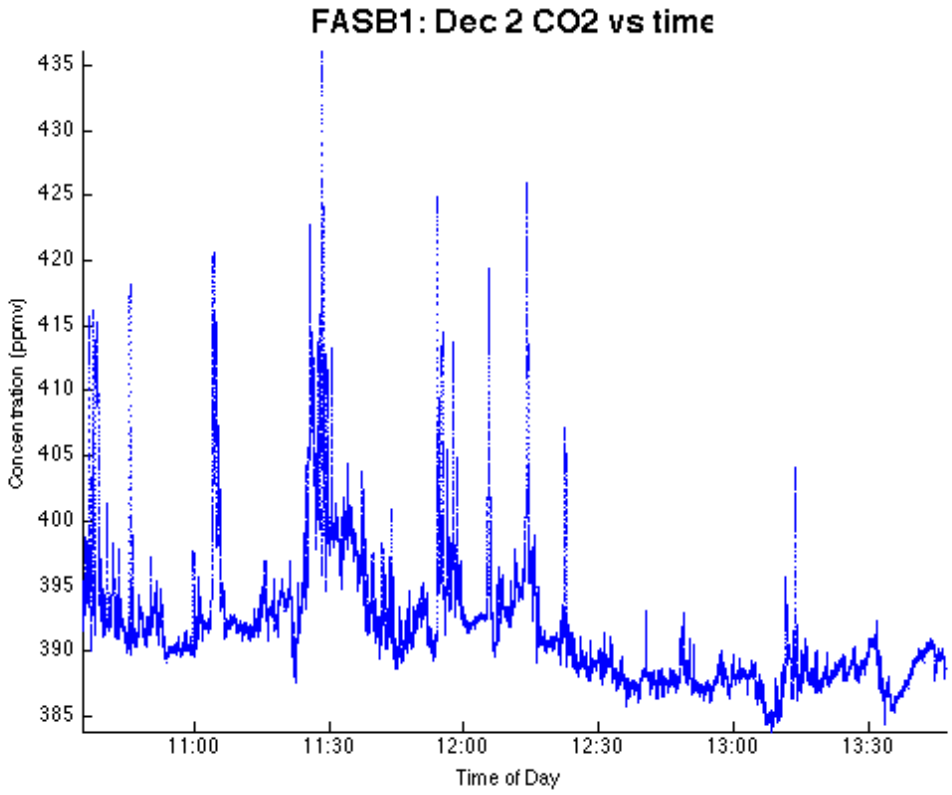

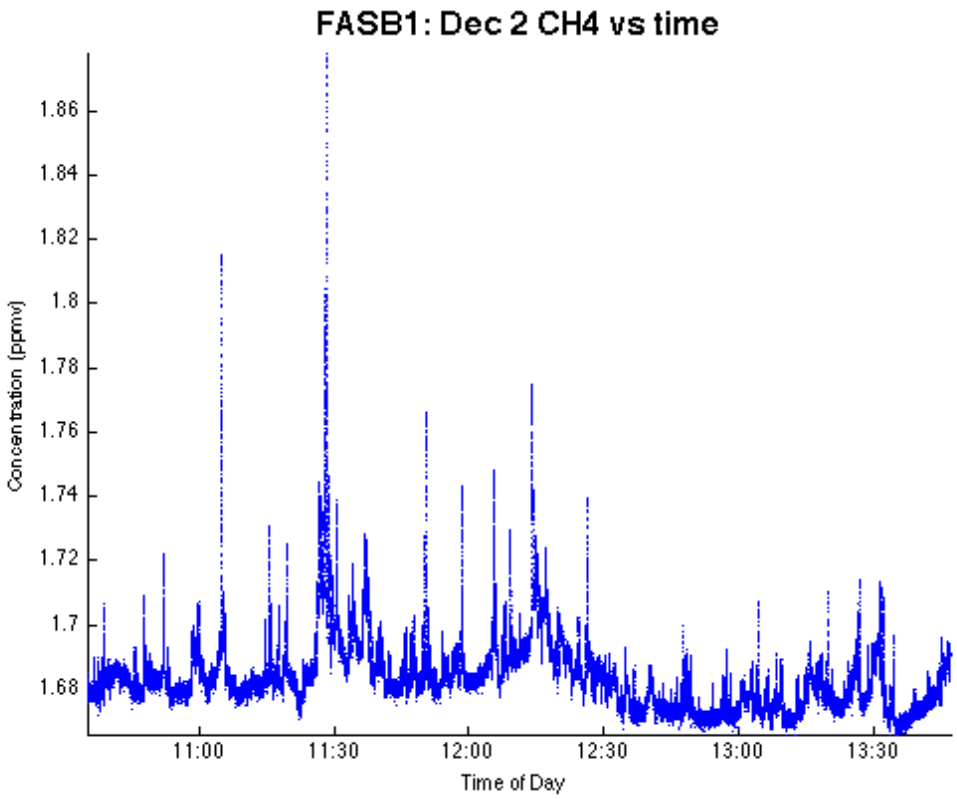
FASB1: Dec 2 CH4 vs time
Concentration (ppmv)
1.86
1.84
1.82
1.8
1.78
1.76
1.74
1.72
1.7
1.68
11:00
11:30
12:00
12:30
13:00
13:30
Time of Day

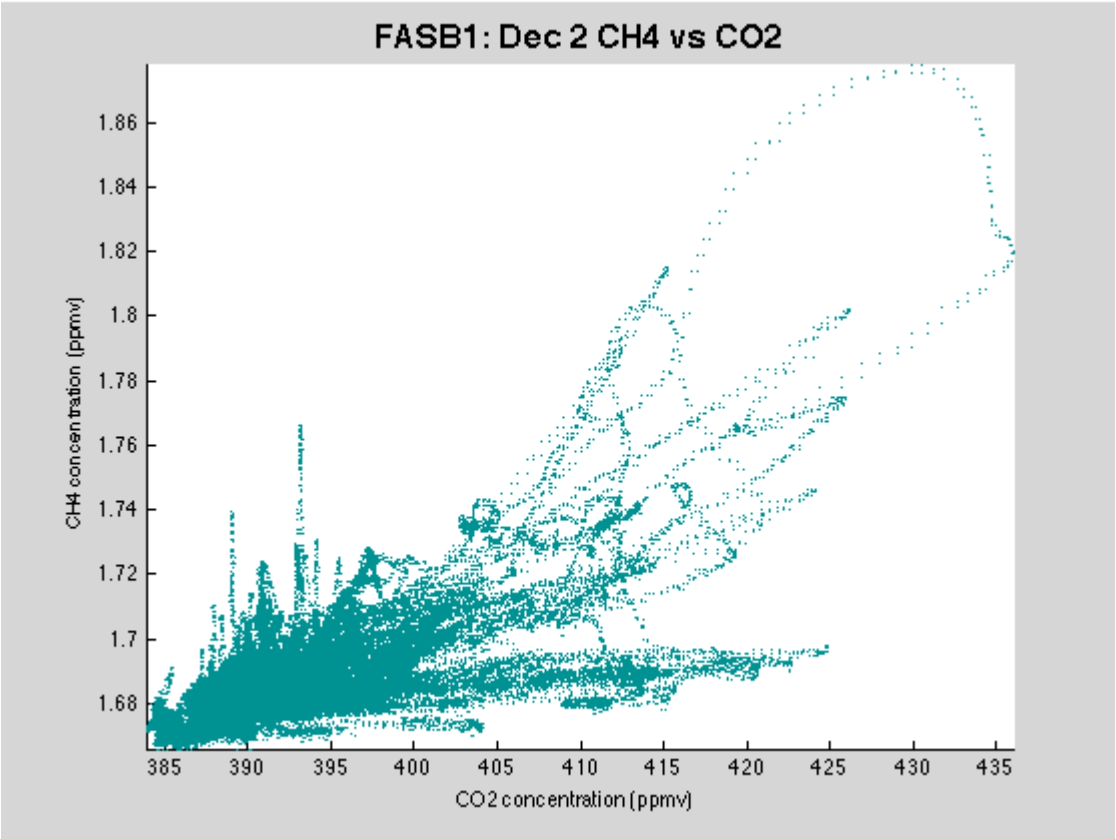
FASB1: Dec 2 CH4 vs CO2
CH4 concentration (ppmv)
1.86
1.84
1.82
1.8
1.78
1.76
1.74
1.72
1.7
1.68
385
390
395
400
405
410
415
420
425
430
435
CO2 concentration (ppmv)

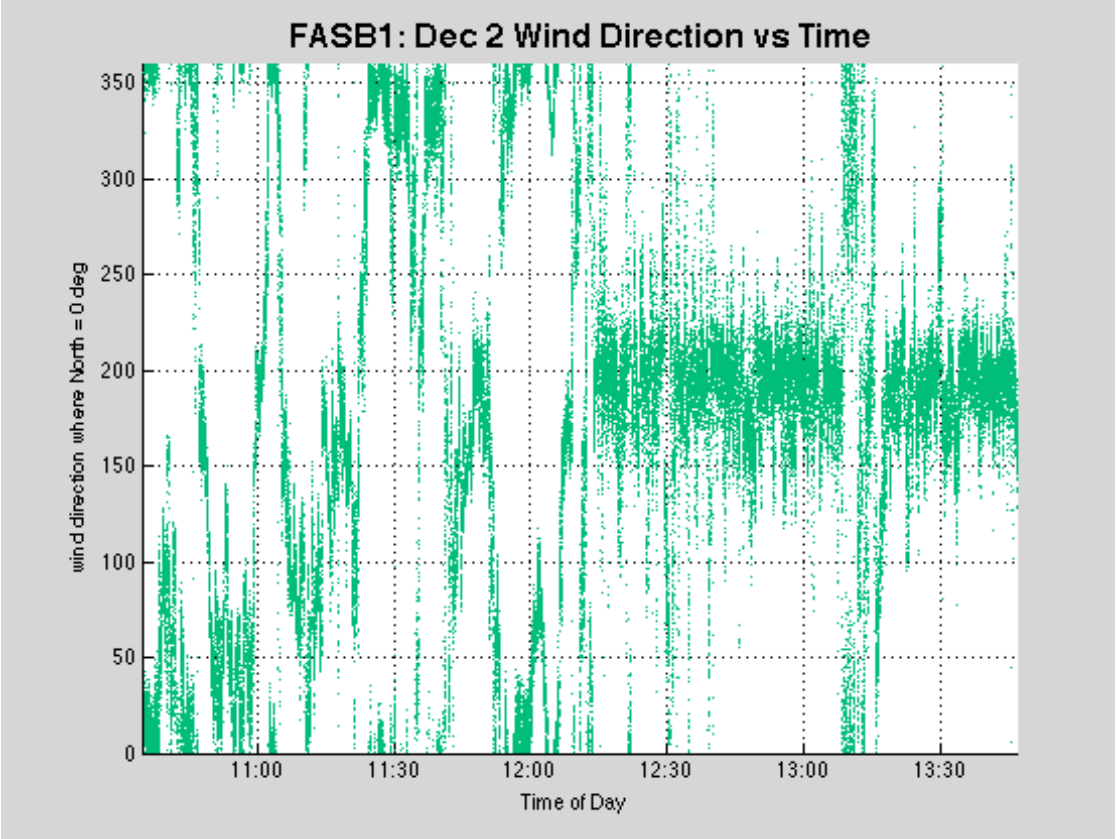
FASB1: Dec 2 Wind Direction vs Time
wind direction where North = 0 deg
0
50
100
150
200
250
300
350
11:00
11:30
12:00
12:30
13:00
13:30
Time of Day

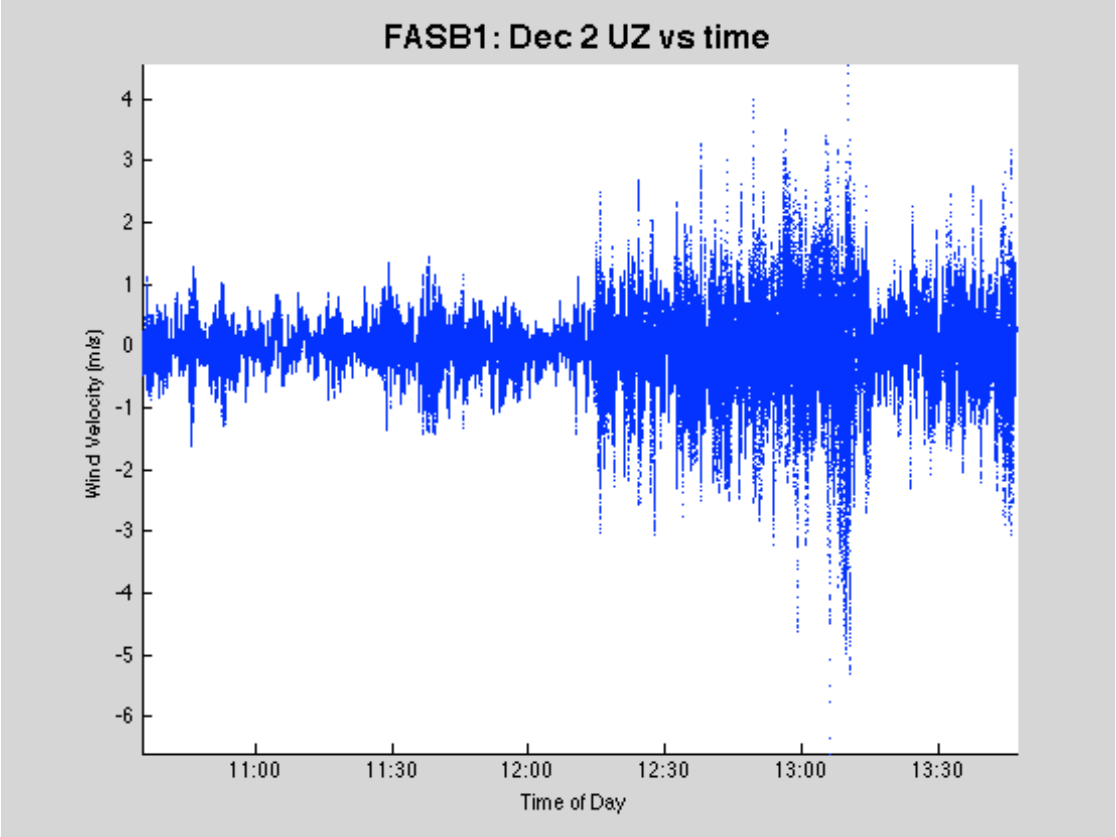
FASB1: Dec 2 UZ vs time
Wind Velocity (m/s)
4
3
2
1
0
-1
-2
-3
-4
-5
-6
11:00
11:30
12:00
12:30
13:00
13:30
Time of Day

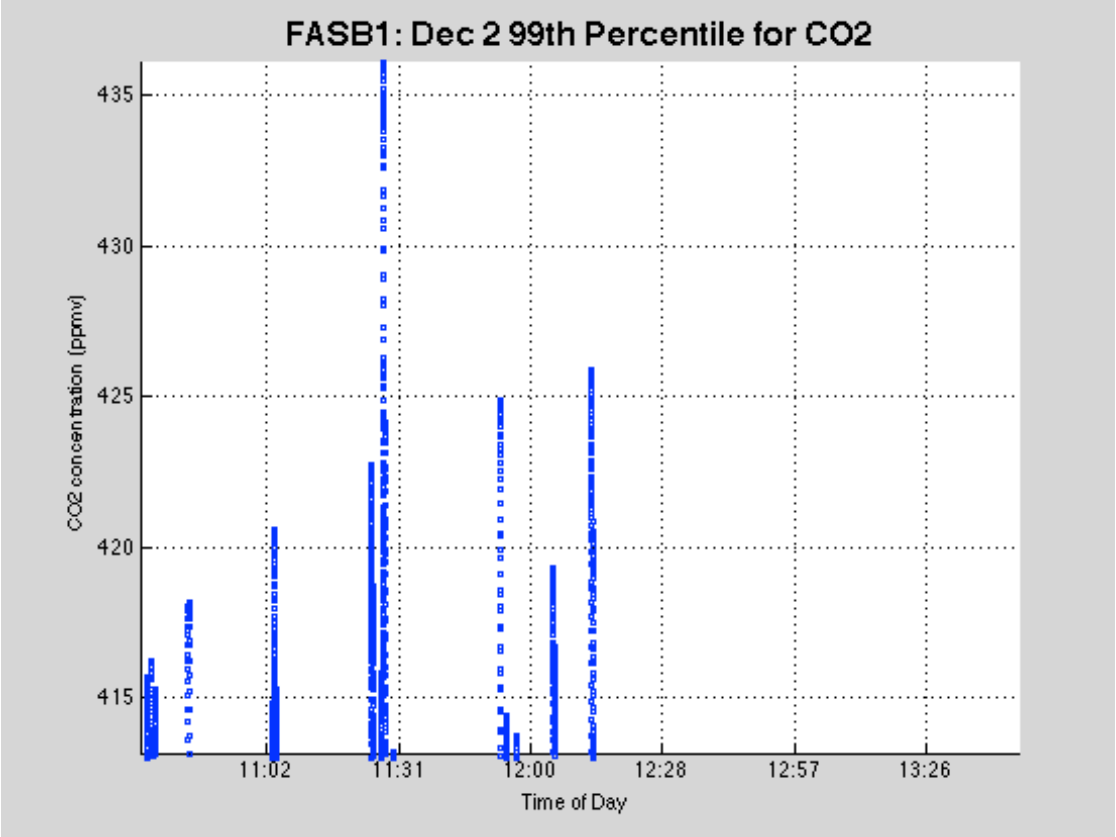
FASB1: Dec 2 99th Percentile for CO2
CO2 concentration (ppmv)
435
430
425
420
415
11:02
11:31
12:00
12:28
12:57
13:26
Time of Day

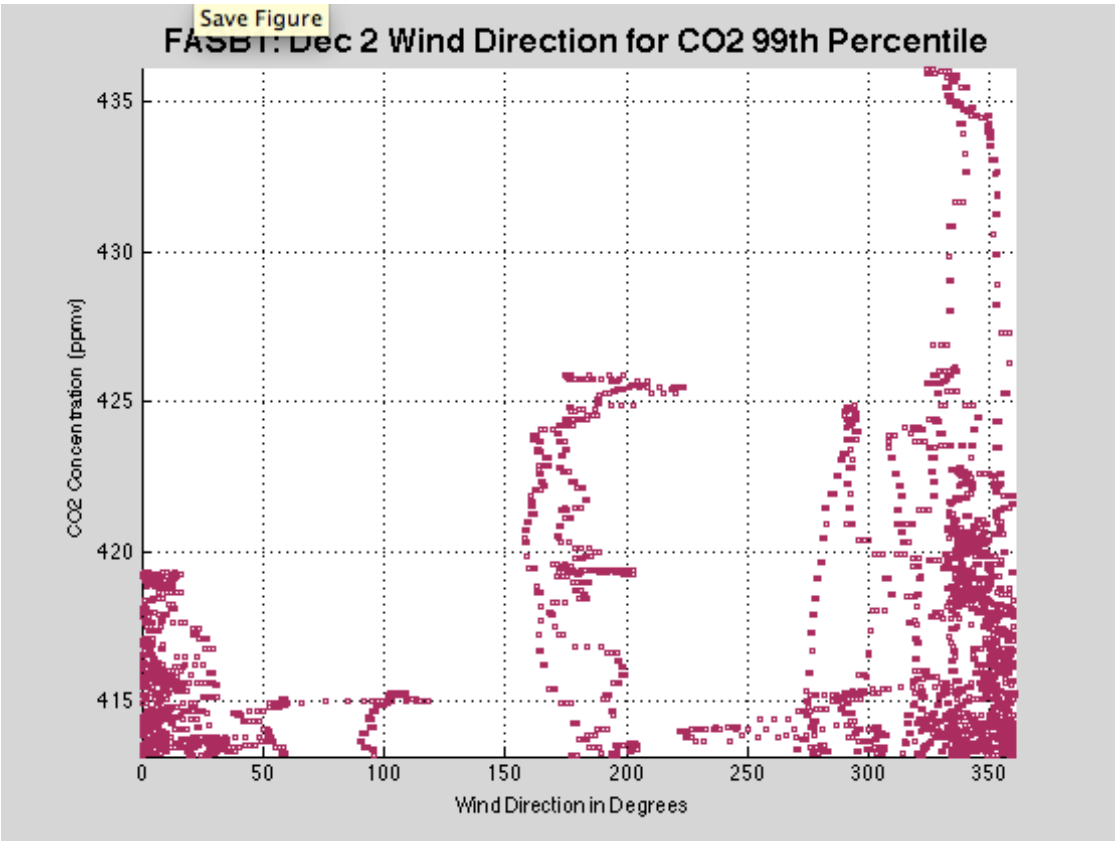
Save Figure
FASB1: Dec 2 Wind Direction for CO2 99th Percentile
CO2 Concentration (ppmv)
435
430
425
420
415
0
50
100
150
200
250
300
350
Wind Direction in Degrees

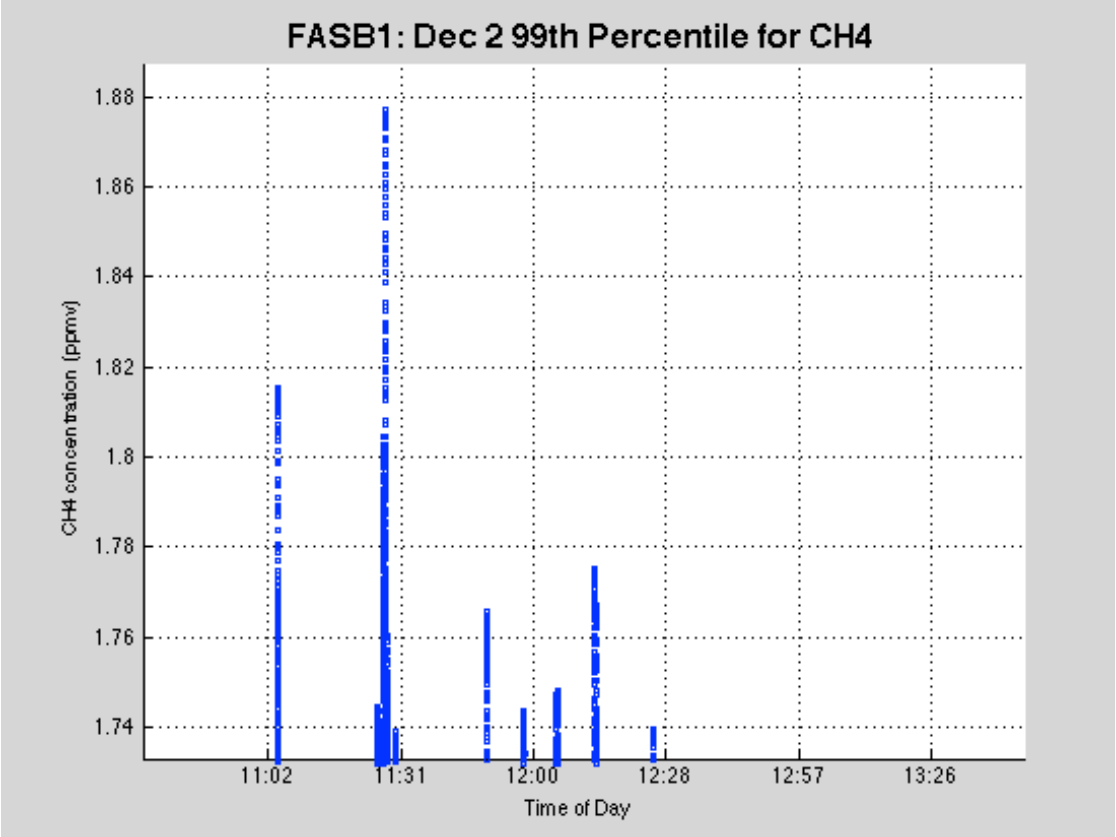
FASB1: Dec 2 99th Percentile for CH4
CH4 concentration (ppmv)
1.88
1.86
1.84
1.82
1.8
1.78
1.76
1.74
11:02
11:31
12:00
12:28
12:57
13:26
Time of Day

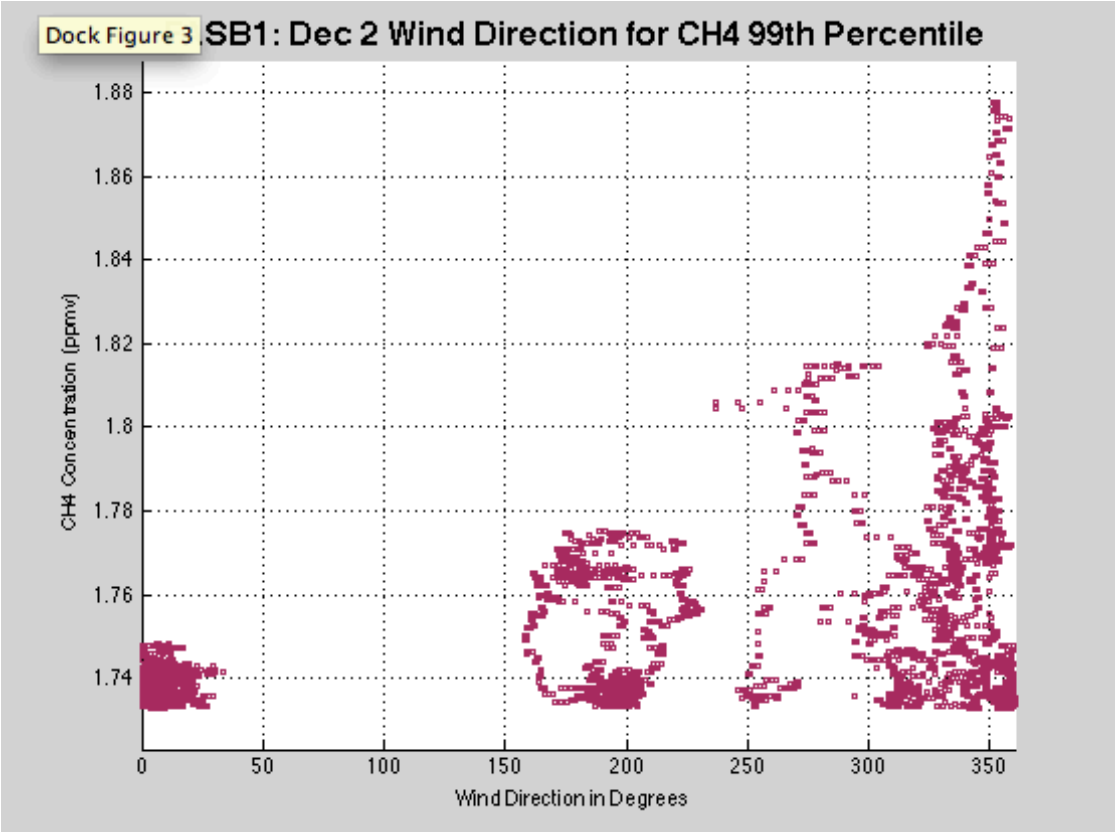
Dock Figure 3
SB1: Dec 2 Wind Direction for CH4 99th Percentile
CH4 Concentration (ppmv)
1.88
1.86
1.84
1.82
1.8
1.78
1.76
1.74
0
50
100
150
200
250
300
350
Wind Direction in Degrees

# APPENDIX F

## THIRD TOWER LOCATION (FASB2) DATA

The tower was located at the third location (FASB2) March 6th, 7th and 8th, 2013. Included for each day are the values for the maximum, minimum, average and standard deviation of the two gases ($CO_2$ and $CH_4$) and the vertical velocity (UZ). The 99th percentile is provided for the two gases.
Also included are nine plots of the data for each day.

The plots are;

1. $CO_2$ Concentration vs. Time
2. $CH_4$ Concentration vs. Time
3. $CH_4$ Concentration vs. CO2 Concentration
4. Wind Direction vs. Time
5. Vertical Wind Velocity vs. Time
6. 99th Percentile $CO_2$ Concentration vs. Time
7. 99th Percentile $CO_2$ Concentration vs. Wind Direction
8. 99th Percentile $CH_4$ Concentration vs. Time
9. 99th Percentile $CH_4$ Concentration vs. Wind Direction

## F.1 Thursday, March 6th, 2014

| | Maximum | Minimum | Average | Standard Deviation | 99th Percentile |
|---|---|---|---|---|---|
| $CO_2$ (ppmv) | 456.7776 | 388.0941 | 399.9705 | 6.932 | 424.9641 |
| $CH_4$ (ppmv) | 2.1657 | 1.685 | 1.7164 | 0.0164 | 1.7816 |
| UZ (m/s) | 5.3016 | -4.3133 | 0.0091 | 0.3974 | N/A |

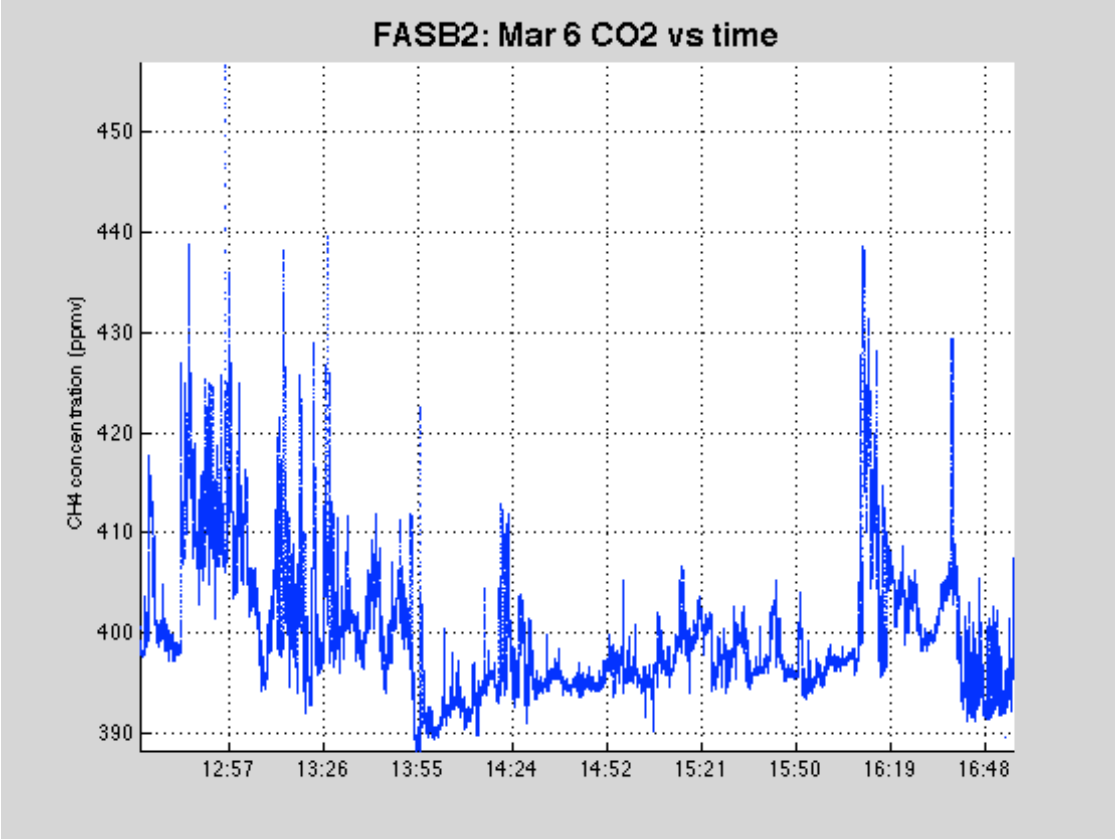

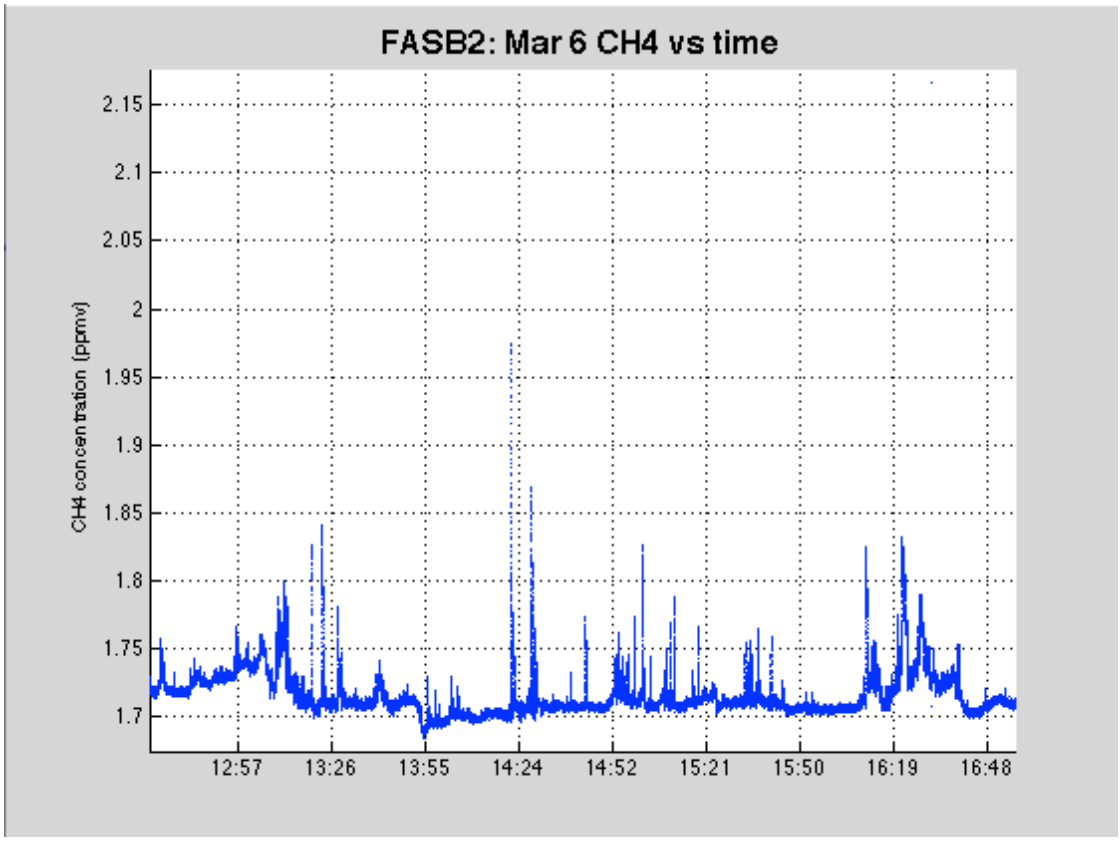
FASB2: Mar 6 CH4 vs time
CH4 concentration (ppmv)
2.15
2.1
2.05
2
1.95
1.9
1.85
1.8
1.75
1.7
12:57
13:26
13:55
14:24
14:52
15:21
15:50
16:19
16:48

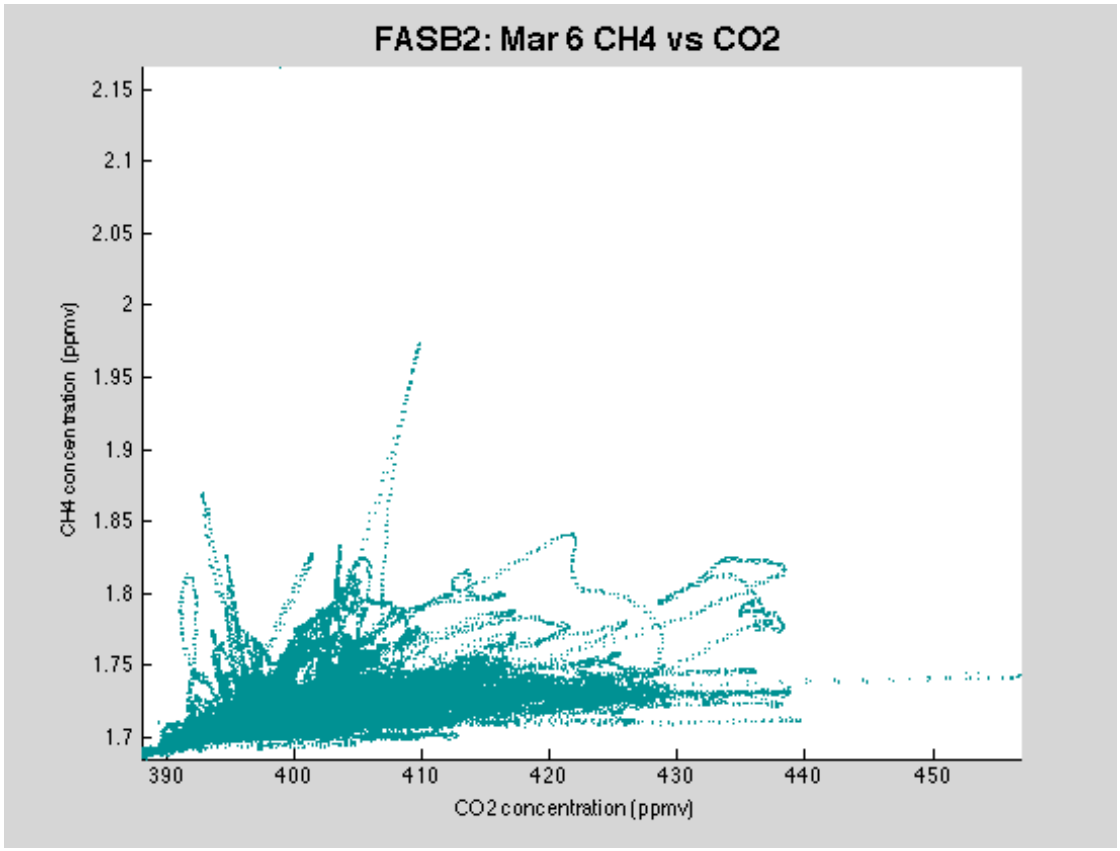
FASB2: Mar 6 CH4 vs CO2
CH4 concentration (ppmv)
2.15
2.1
2.05
2
1.95
1.9
1.85
1.8
1.75
1.7
390
400
410
420
430
440
450
CO2 concentration (ppmv)

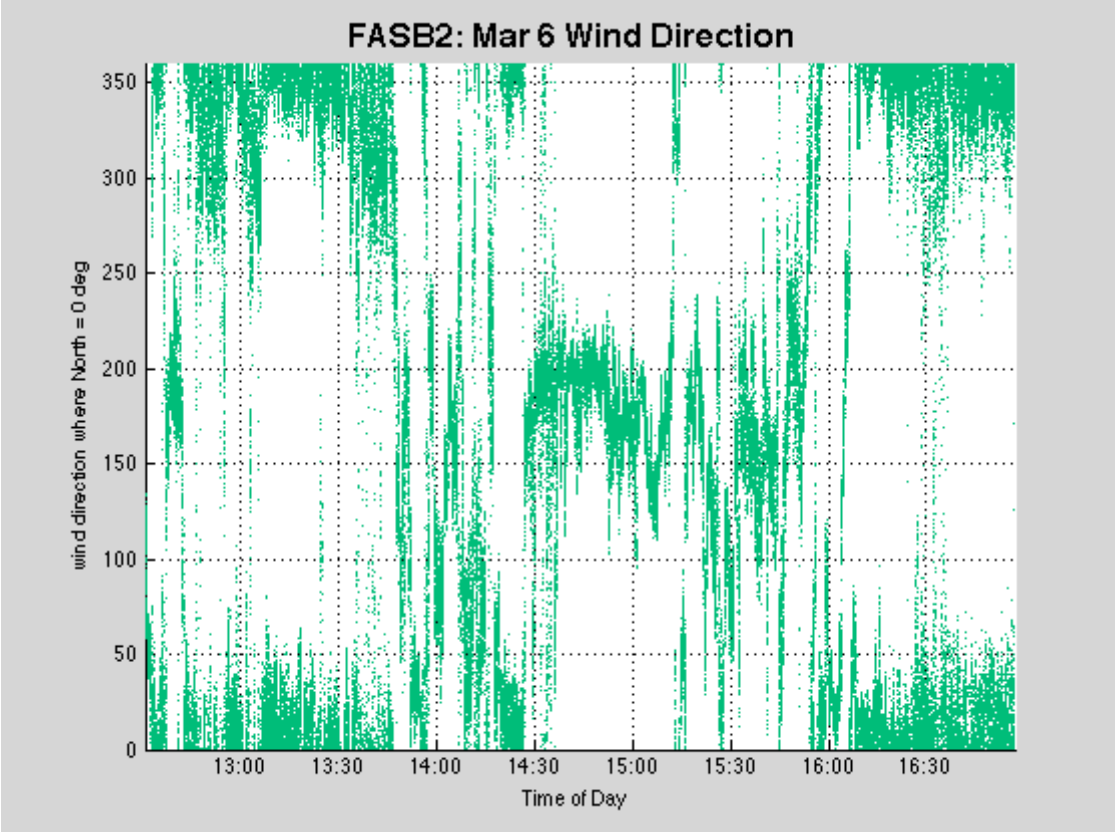
FASB2: Mar 6 Wind Direction
wind direction where North = 0 deg
0
50
100
150
200
250
300
350
13:00
13:30
14:00
14:30
15:00
15:30
16:00
16:30
Time of Day

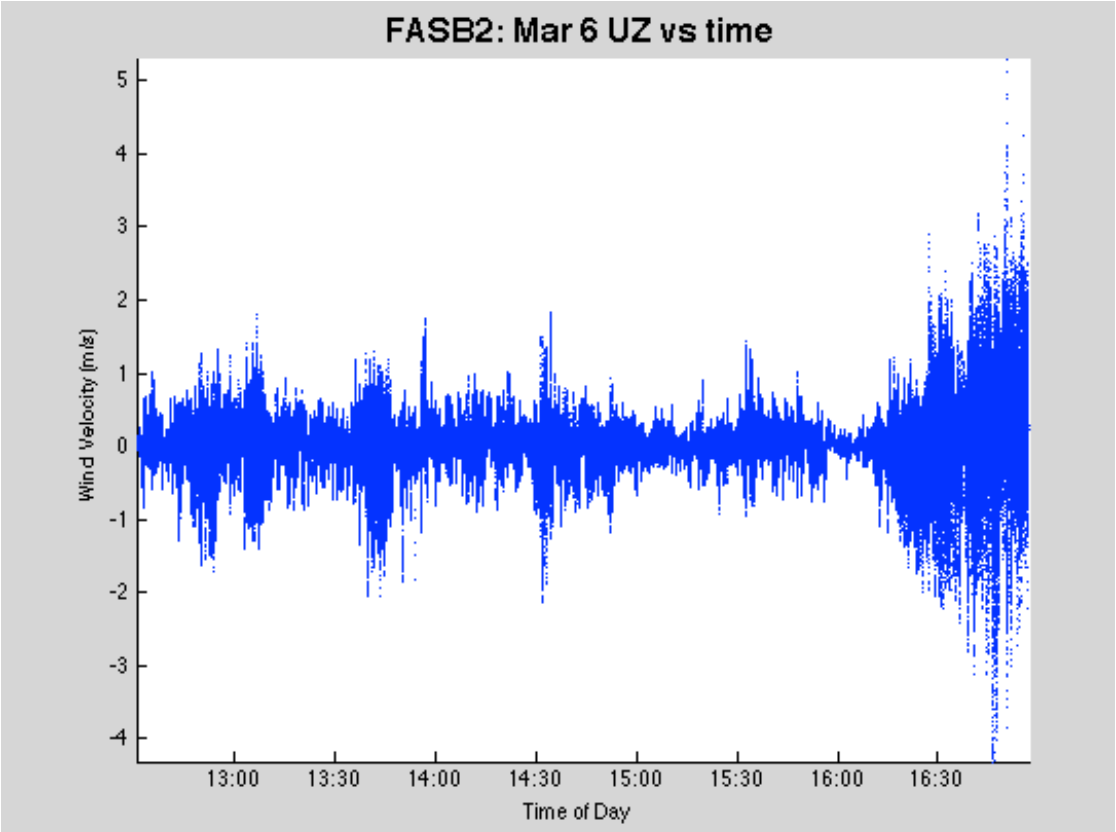
FASB2: Mar 6 UZ vs time
Wind Velocity (m/s)
5
4
3
2
1
0
-1
-2
-3
-4
13:00
13:30
14:00
14:30
15:00
15:30
16:00
16:30
Time of Day

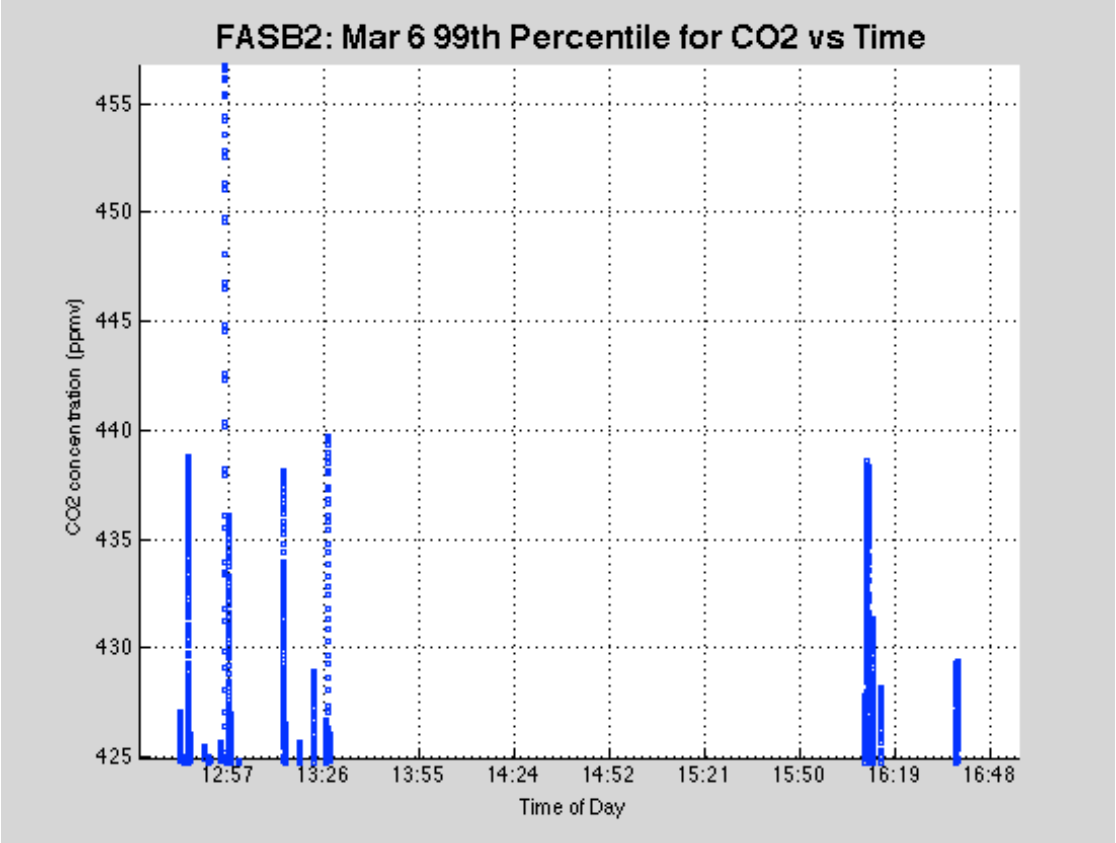
FASB2: Mar 6 99th Percentile for CO2 vs Time
CO2 concentration (ppmv)
455
450
445
440
435
430
425
12:57
13:26
13:55
14:24
14:52
15:21
15:50
16:19
16:48
Time of Day

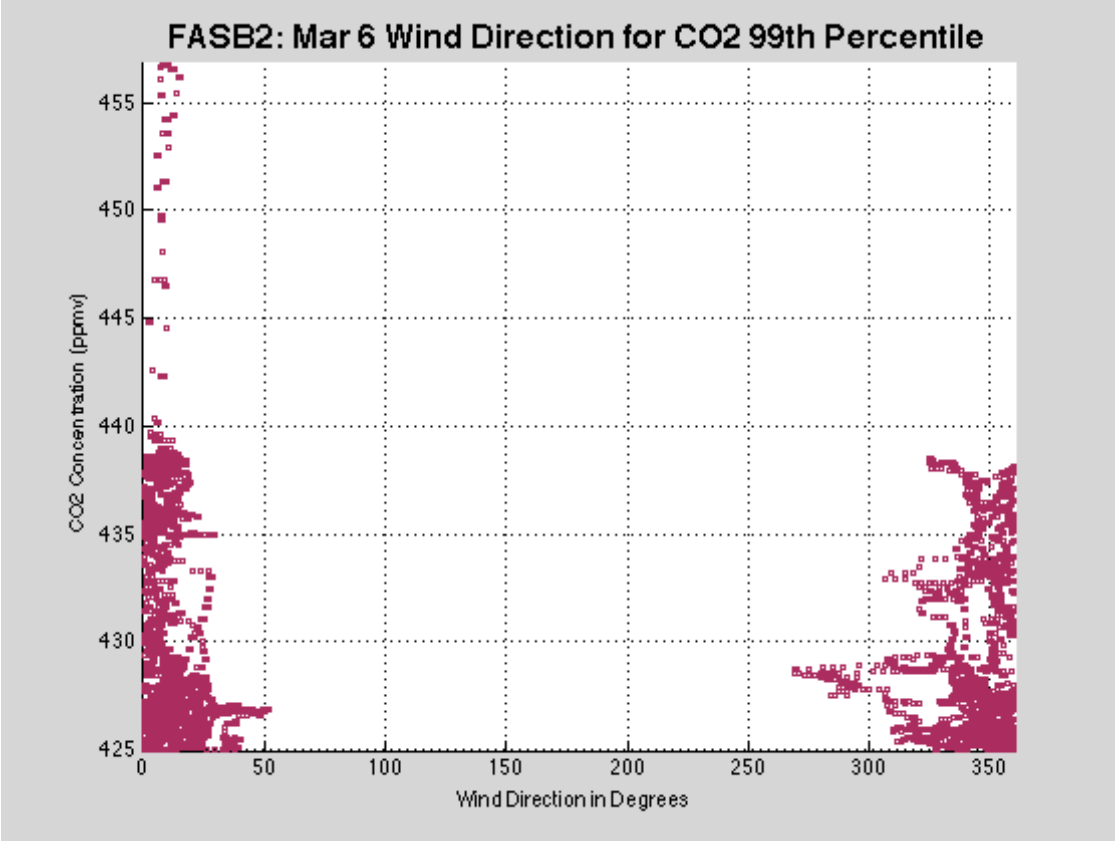
FASB2: Mar 6 Wind Direction for CO2 99th Percentile
CO2 Concentration (ppmv)
455
450
445
440
435
430
425
0
50
100
150
200
250
300
350
Wind Direction in Degrees

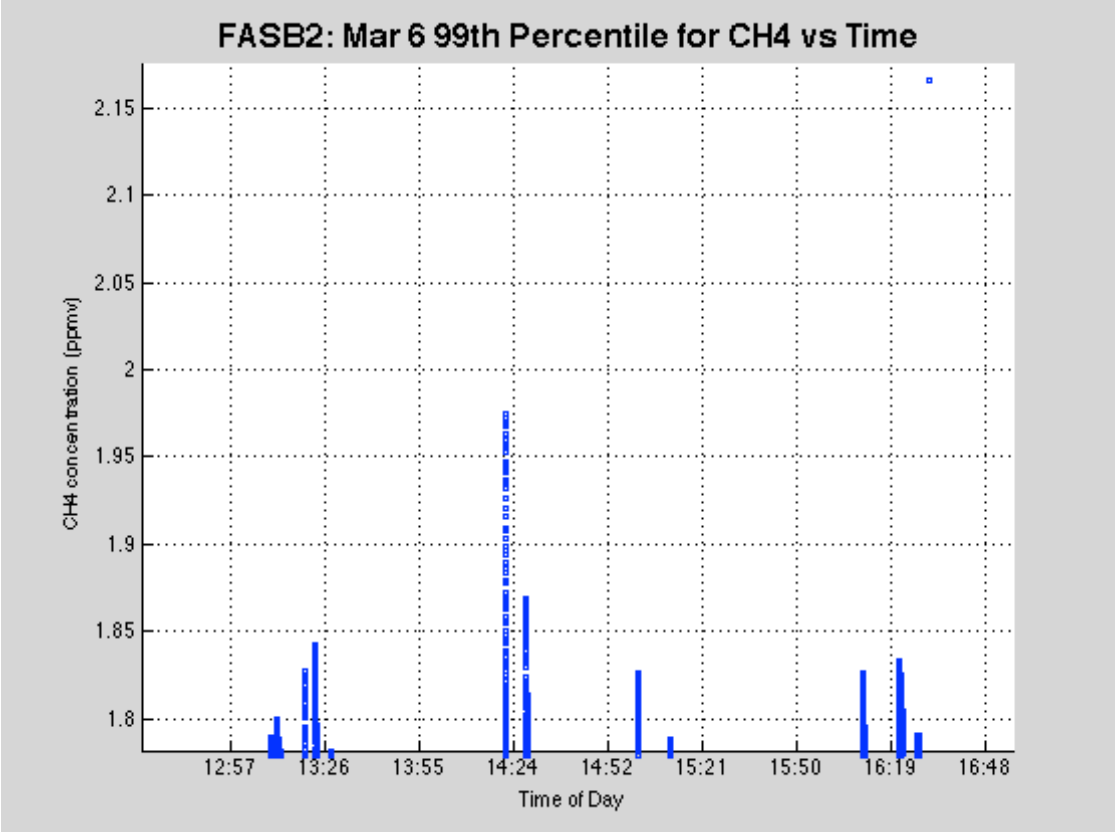
FASB2: Mar 6 99th Percentile for CH4 vs Time
CH4 concentration (ppmv)
2.15
2.1
2.05
2
1.95
1.9
1.85
1.8
12:57
13:26
13:55
14:24
14:52
15:21
15:50
16:19
16:48
Time of Day

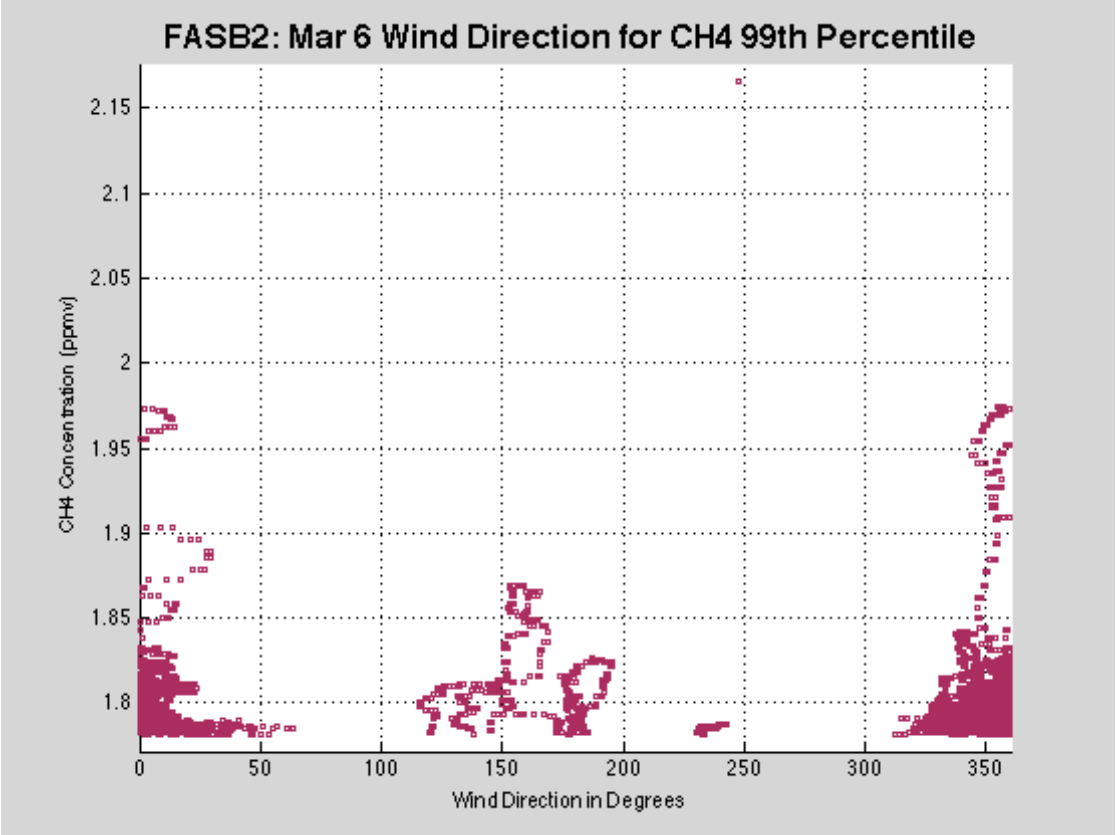
FASB2: Mar 6 Wind Direction for CH4 99th Percentile
CH4 Concentration (ppmv)
2.15
2.1
2.05
2
1.95
1.9
1.85
1.8
0
50
100
150
200
250
300
350
Wind Direction in Degrees

F.2 Friday, March 7th, 2014

| | Maximum | Minimum | Average | Standard Deviation | 99th Percentile |
|---|---|---|---|---|---|
| $CO_2$ (ppmv) | 410.9216 | 386.4944 | 390.6684 | 1.8488 | 397.5731 |
| $CH_4$ (ppmv) | 1.7932 | 1.6898 | 1.699 | 0.0043 | 1.7139 |
| UZ (m/s) | 4.6245 | -5.6785 | -0.1307 | 0.8936 | N/A |

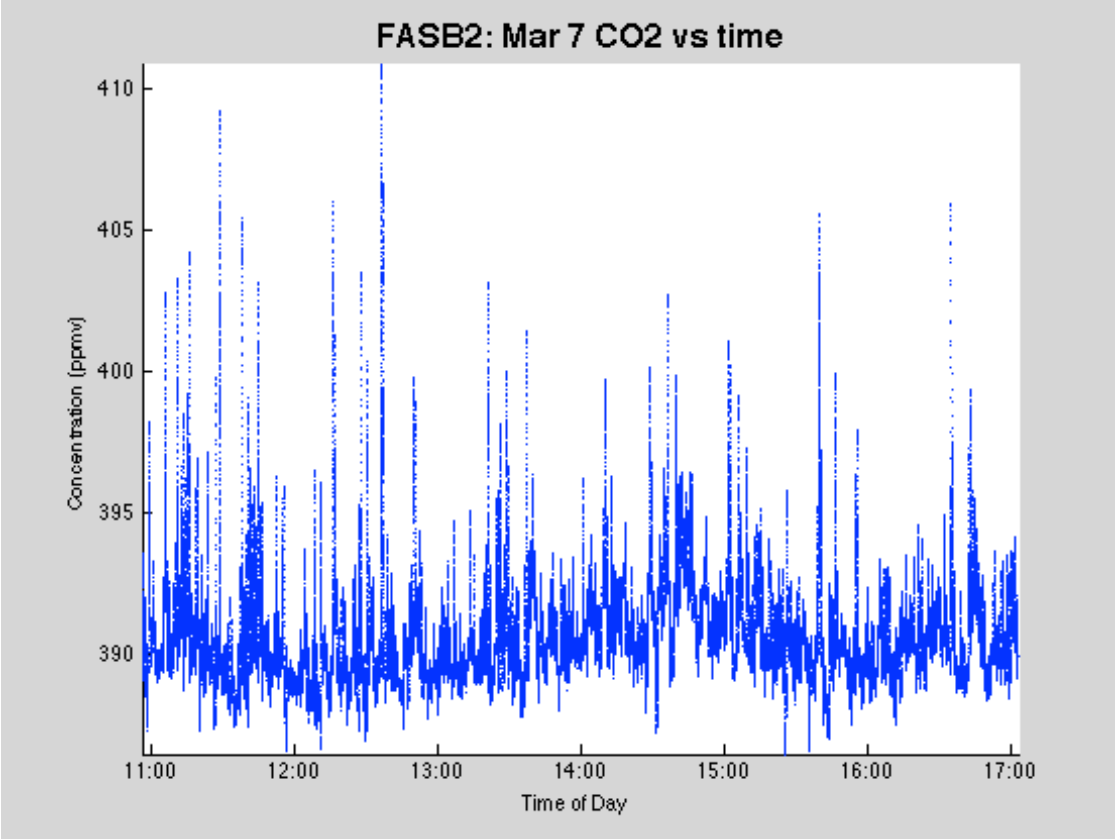

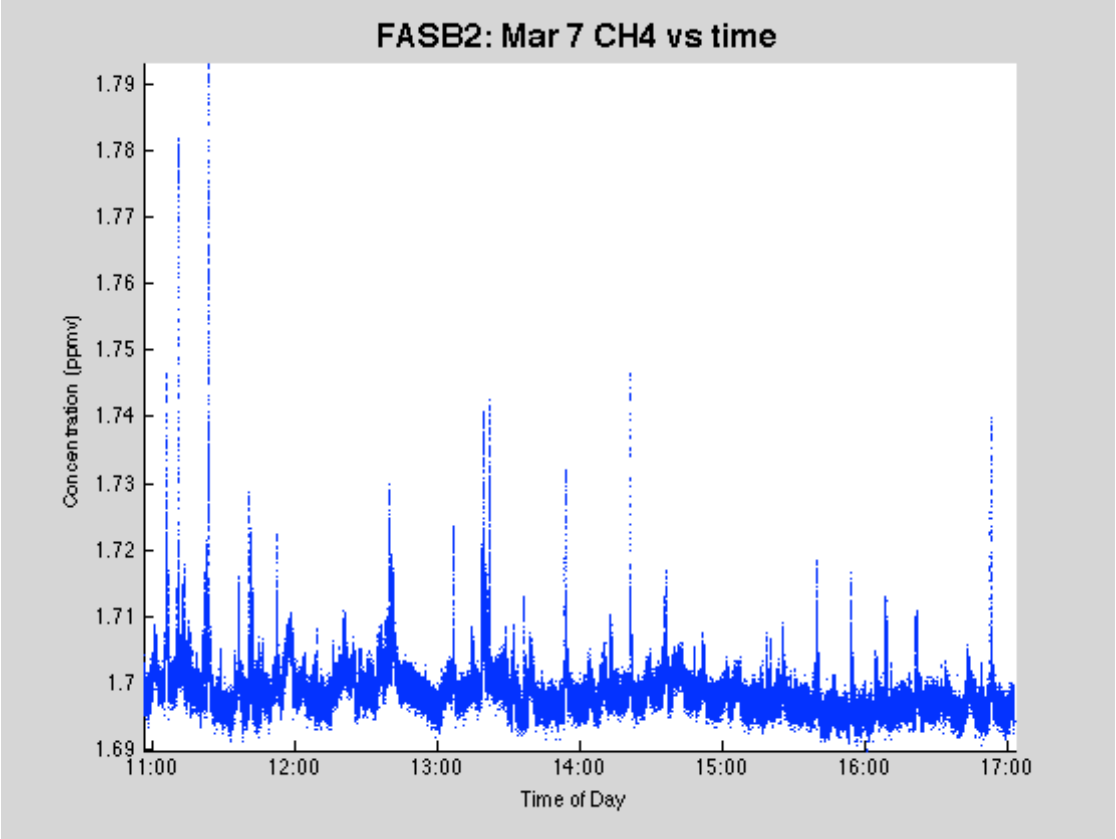
FASB2: Mar 7 CH4 vs time
Concentration (ppmv)
1.79
1.78
1.77
1.76
1.75
1.74
1.73
1.72
1.71
1.7
1.69
11:00
12:00
13:00
14:00
15:00
16:00
17:00
Time of Day

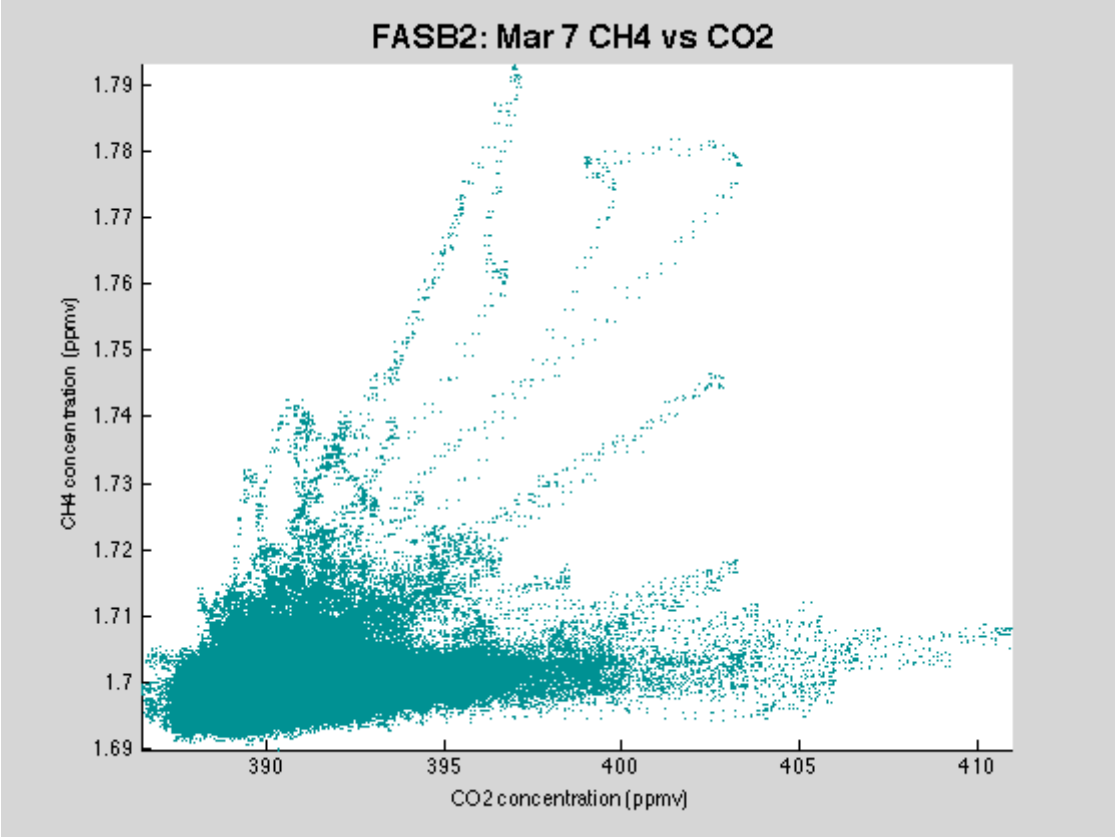
FASB2: Mar 7 CH4 vs CO2
CH4 concentration (ppmv)
1.79
1.78
1.77
1.76
1.75
1.74
1.73
1.72
1.71
1.7
1.69
390
395
400
405
410
CO2 concentration (ppmv)

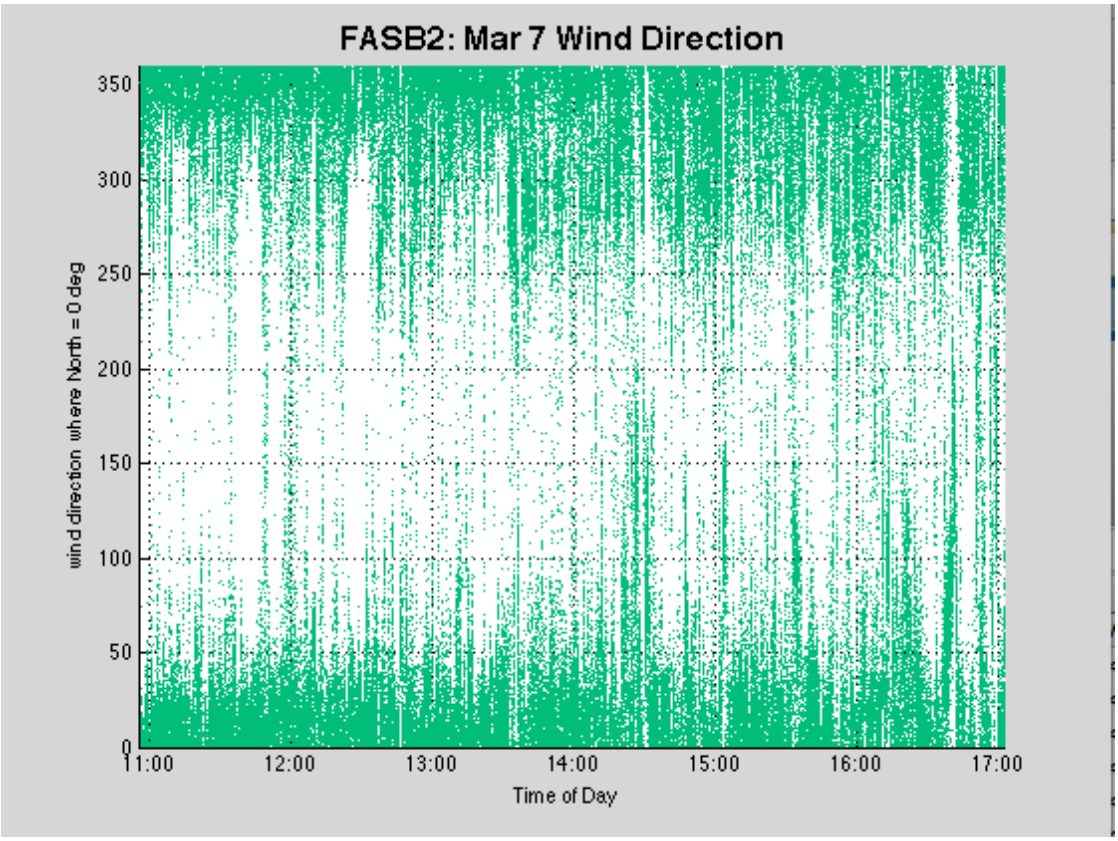
FASB2: Mar 7 Wind Direction
wind direction where North = 0 deg
350
300
250
200
150
100
50
0
11:00
12:00
13:00
14:00
15:00
16:00
17:00
Time of Day

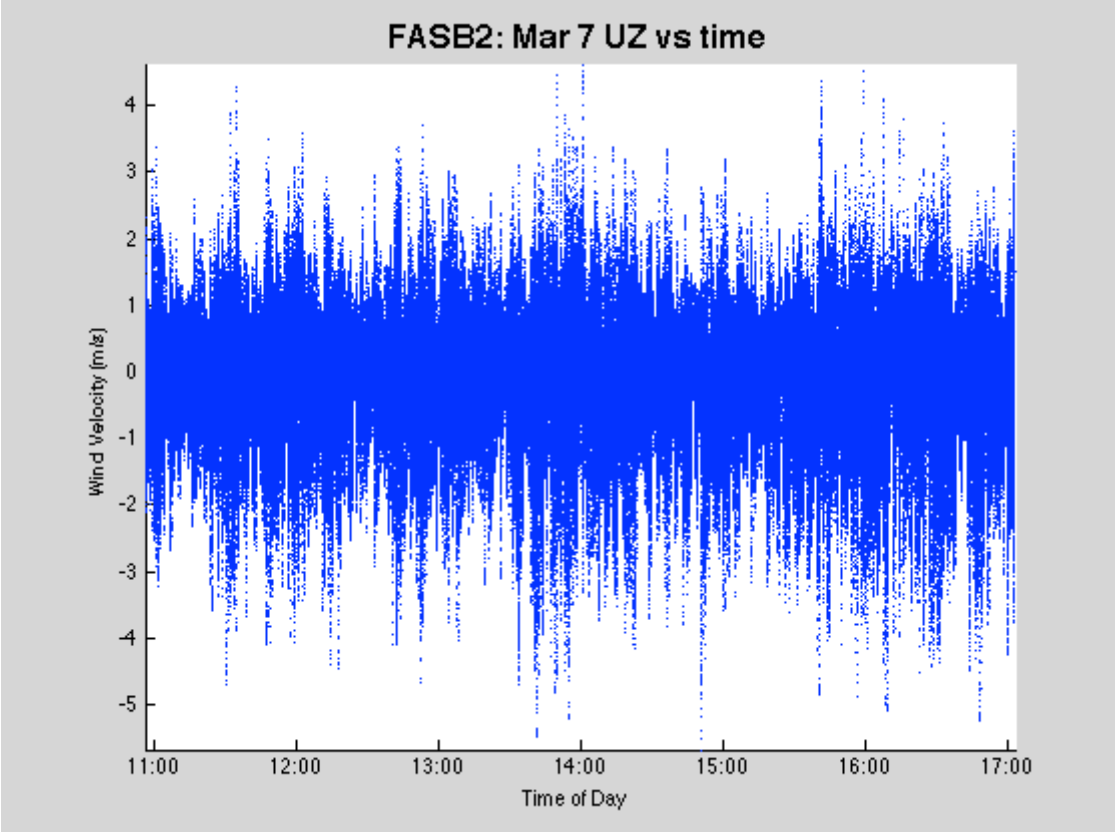
FASB2: Mar 7 UZ vs time
Wind Velocity (m/s)
4
3
2
1
0
-1
-2
-3
-4
-5
11:00
12:00
13:00
14:00
15:00
16:00
17:00
Time of Day

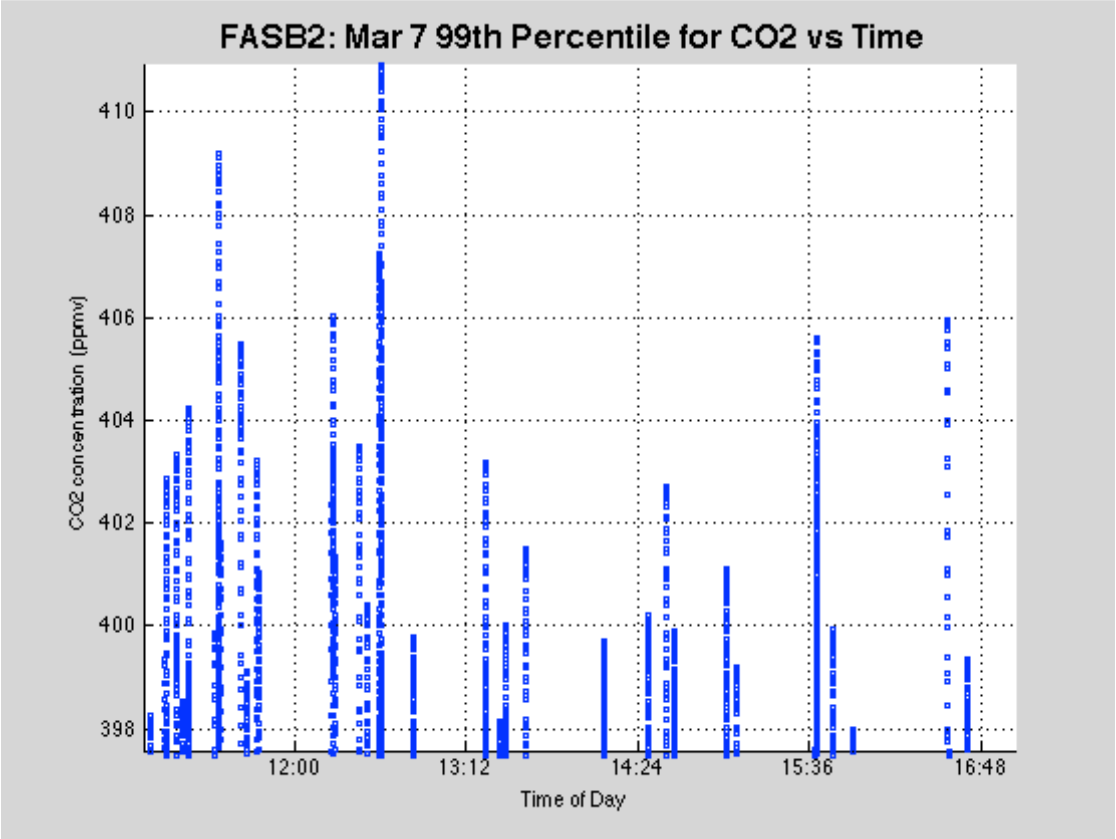
FASB2: Mar 7 99th Percentile for CO2 vs Time
CO2 concentration (ppmv)
410
408
406
404
402
400
398
12:00
13:12
14:24
15:36
16:48
Time of Day

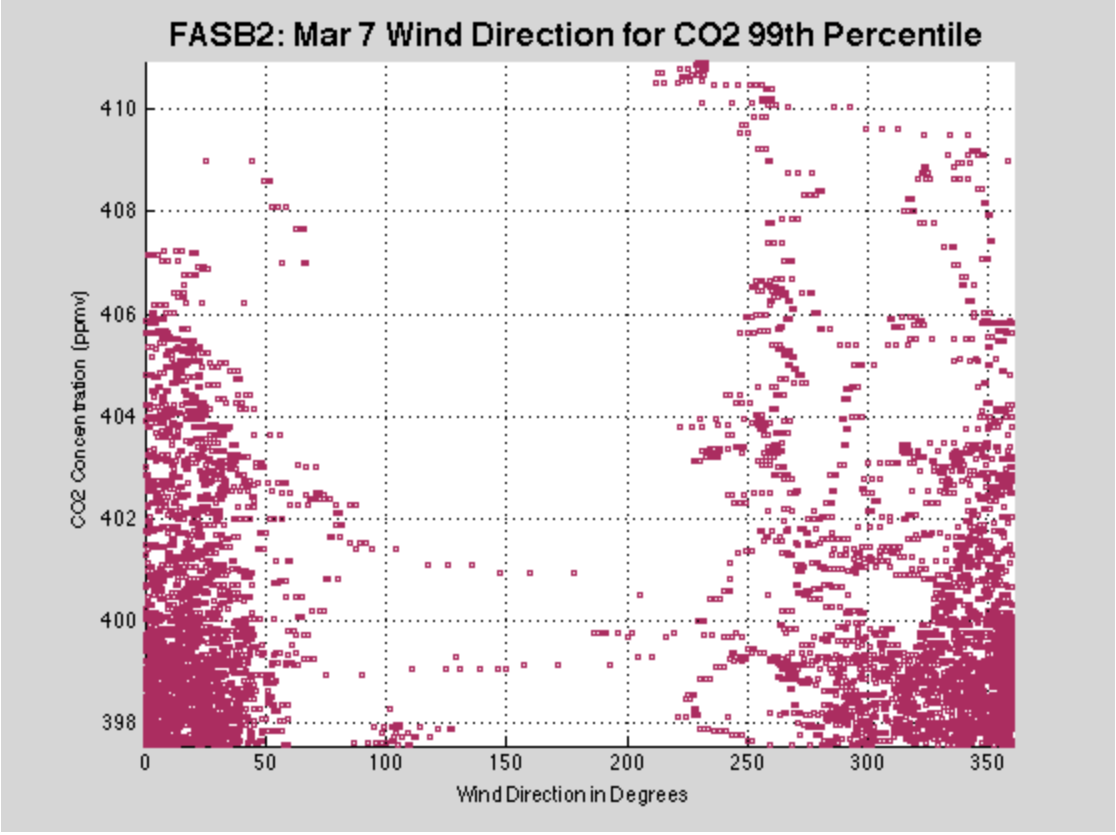
FASB2: Mar 7 Wind Direction for CO2 99th Percentile
CO2 Concentration (ppmv)
410
408
406
404
402
400
398
0
50
100
150
200
250
300
350
Wind Direction in Degrees

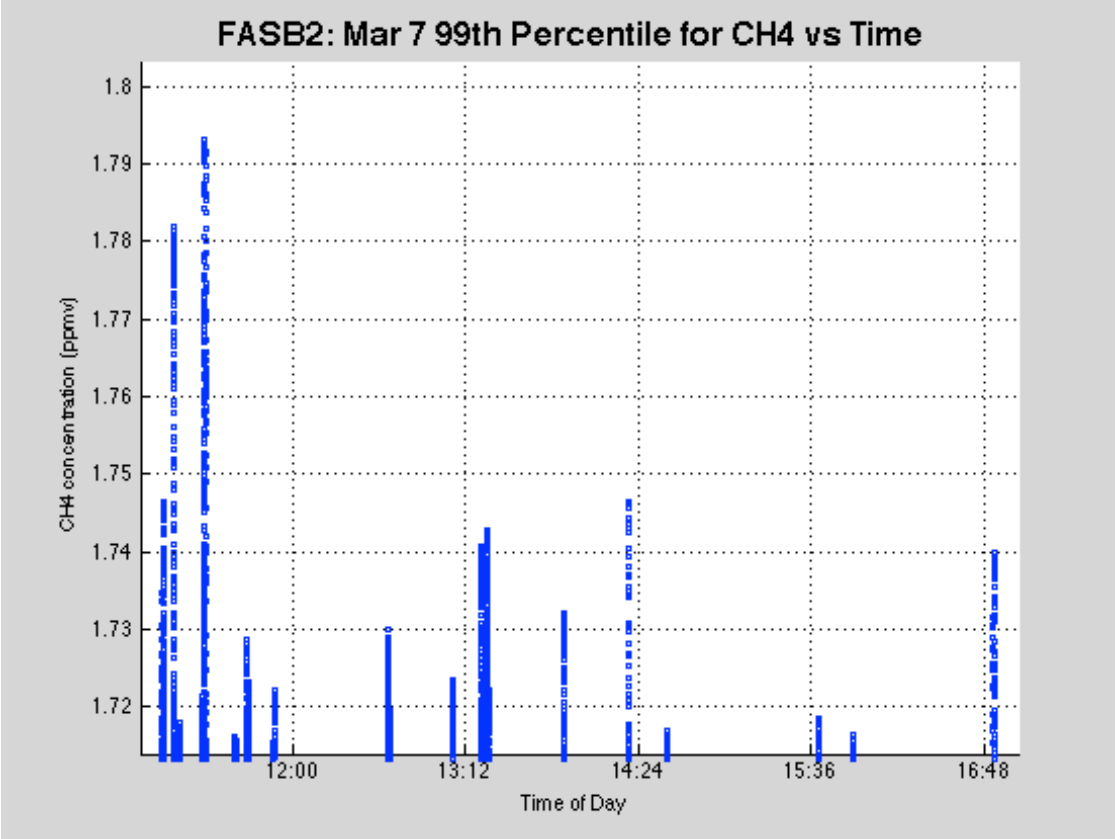
FASB2: Mar 7 99th Percentile for CH4 vs Time
CH4 concentration (ppmv)
1.8
1.79
1.78
1.77
1.76
1.75
1.74
1.73
1.72
12:00
13:12
14:24
15:36
16:48
Time of Day

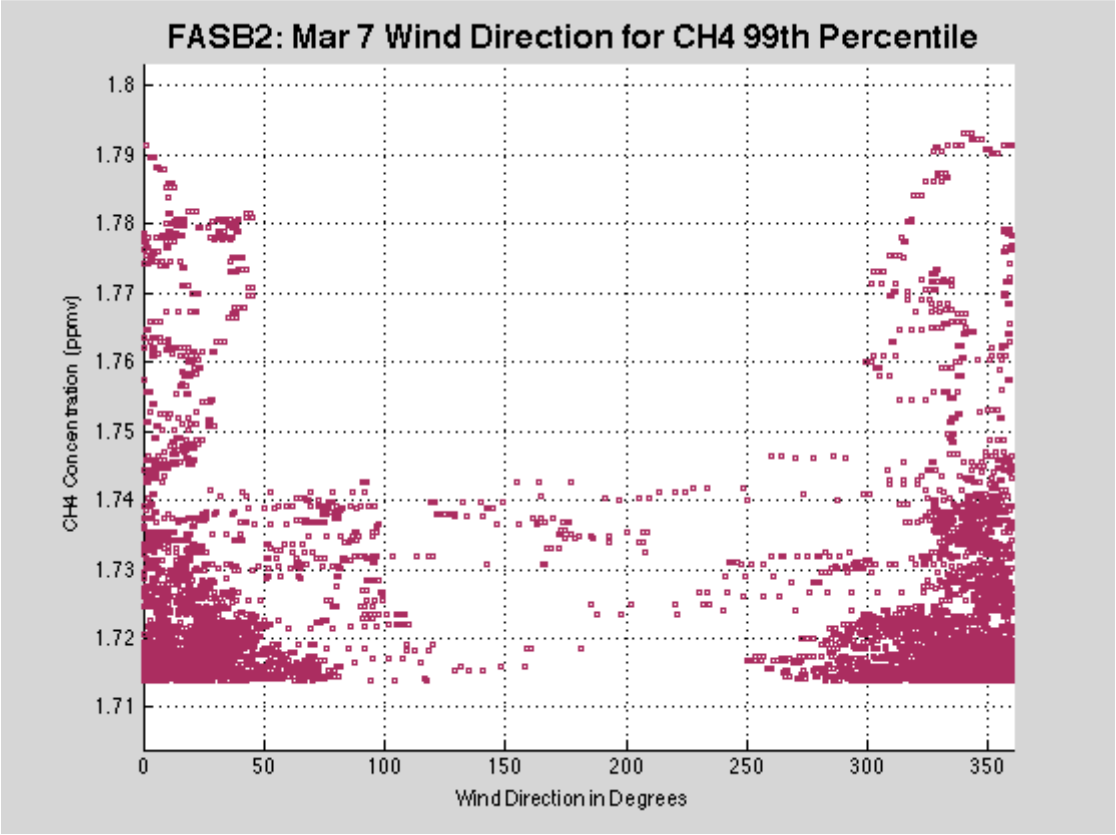
FASB2: Mar 7 Wind Direction for CH4 99th Percentile
CH4 Concentration (ppmv)
1.8
1.79
1.78
1.77
1.76
1.75
1.74
1.73
1.72
1.71
0
50
100
150
200
250
300
350
Wind Direction in Degrees

F.3 Saturday, March 8th, 2014

| | Maximum | Minimum | Average | Standard Deviation | 99th Percentile |
|---|---|---|---|---|---|
| $CO_2$ (ppmv) | 407.9189 | 389.22.57 | 395.5716 | 2.3448 | 403.727 |
| $CH_4$ (ppmv) | 1.7663 | 1.7083 | 1.7308 | 0.0097 | 1.7567 |
| UZ (m/s) | 3.2206 | -4.3447 | -0.0346 | 0.5304 | N/A |

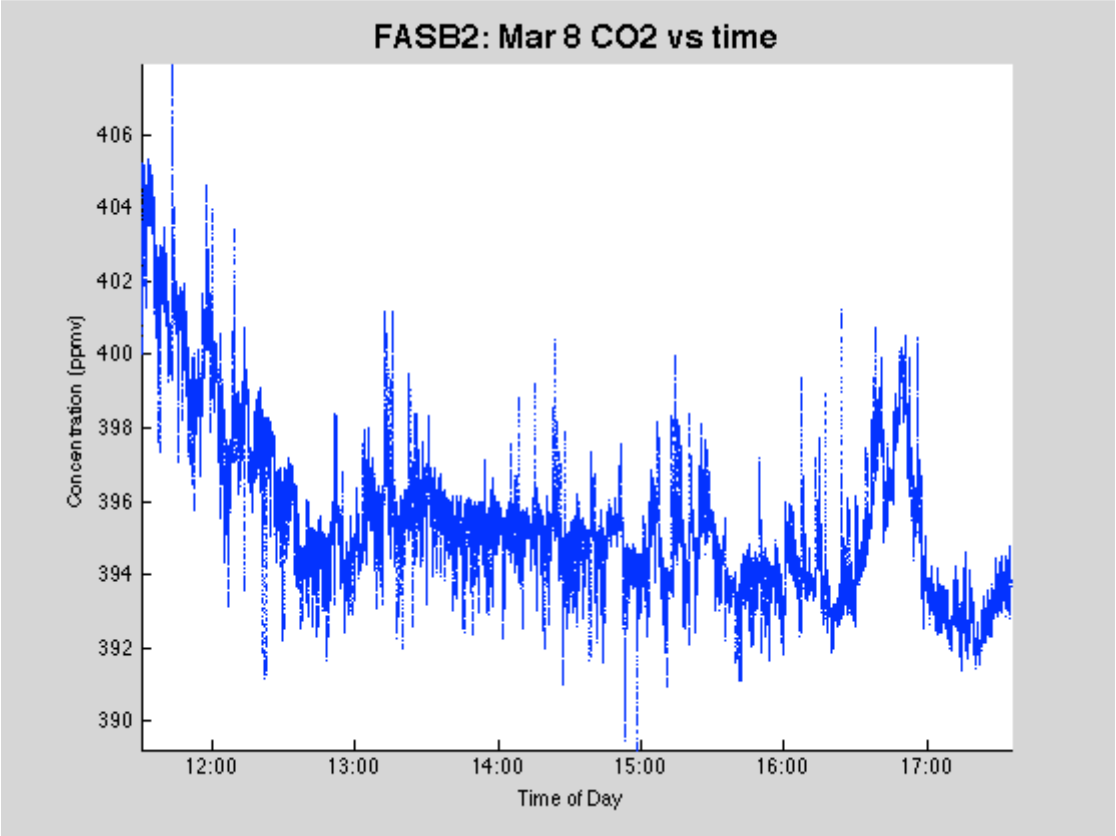

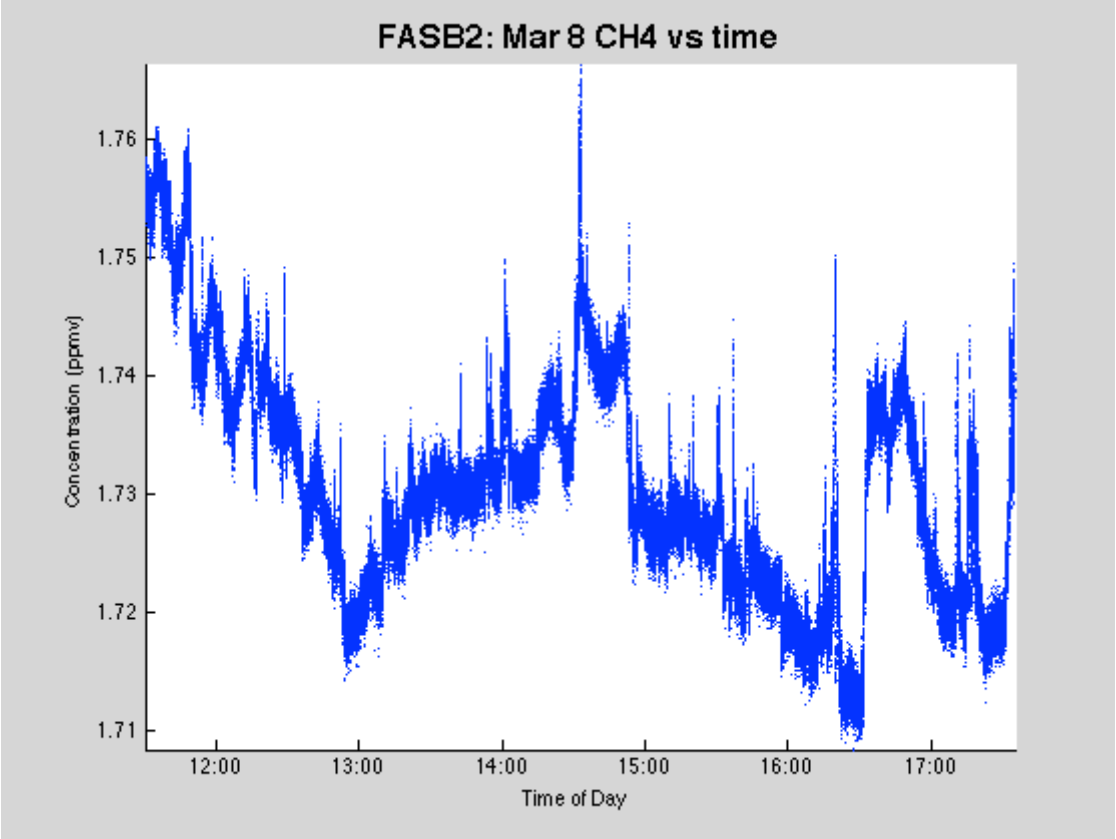
FASB2: Mar 8 CH4 vs time
Concentration (ppmv)
1.76
1.75
1.74
1.73
1.72
1.71
12:00
13:00
14:00
15:00
16:00
17:00
Time of Day

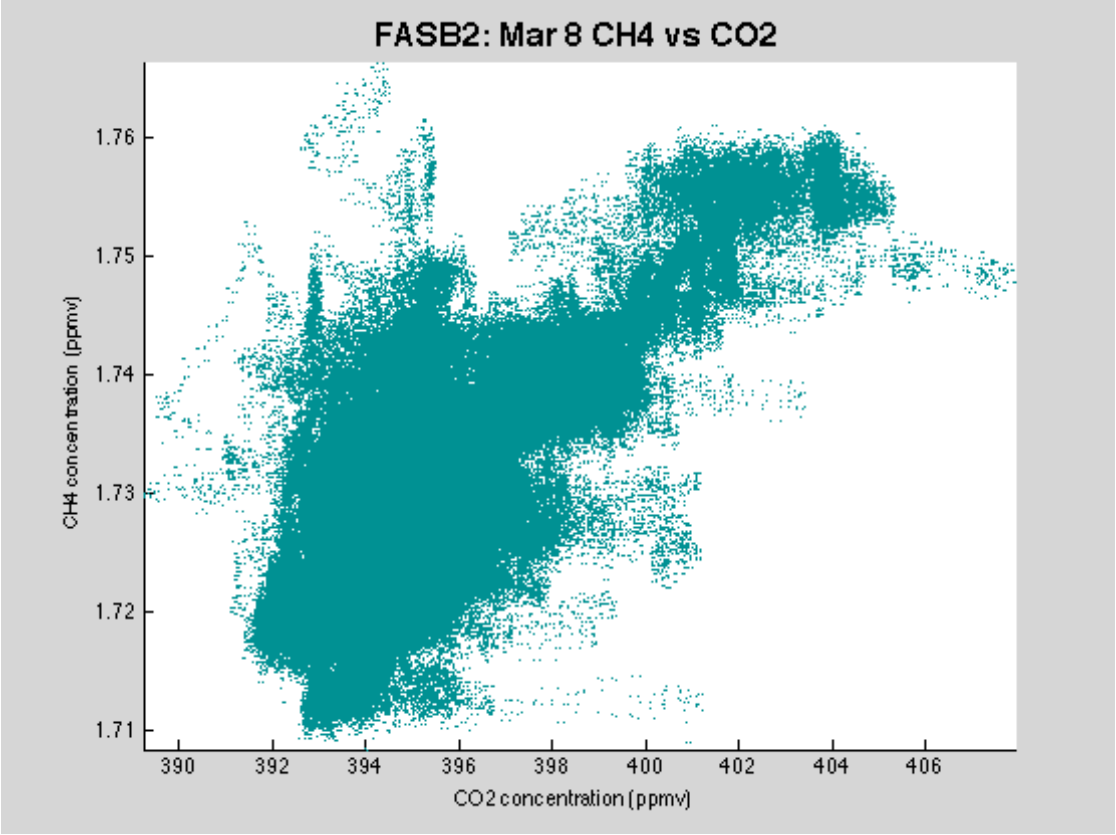
FASB2: Mar 8 CH4 vs CO2
CH4 concentration (ppmv)
1.76
1.75
1.74
1.73
1.72
1.71
390
392
394
396
398
400
402
404
406
CO2 concentration (ppmv)

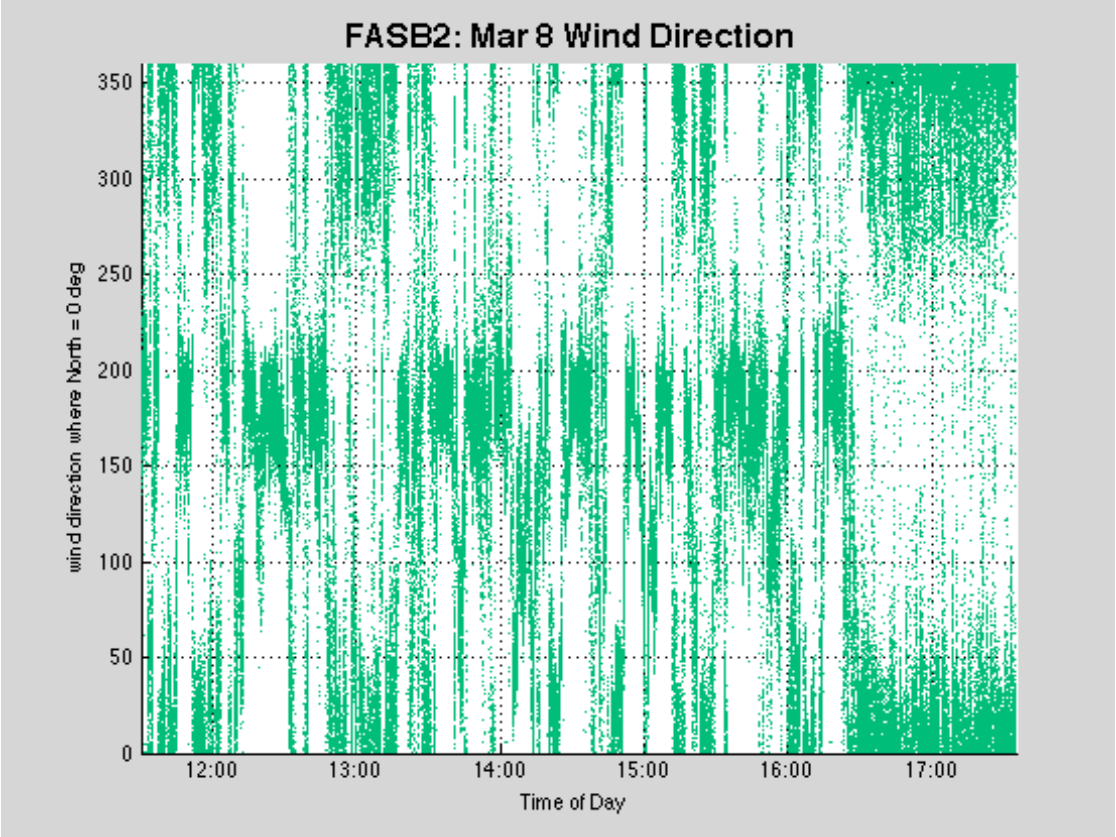
FASB2: Mar 8 Wind Direction
wind direction where North = 0 deg
0
50
100
150
200
250
300
350
12:00
13:00
14:00
15:00
16:00
17:00
Time of Day

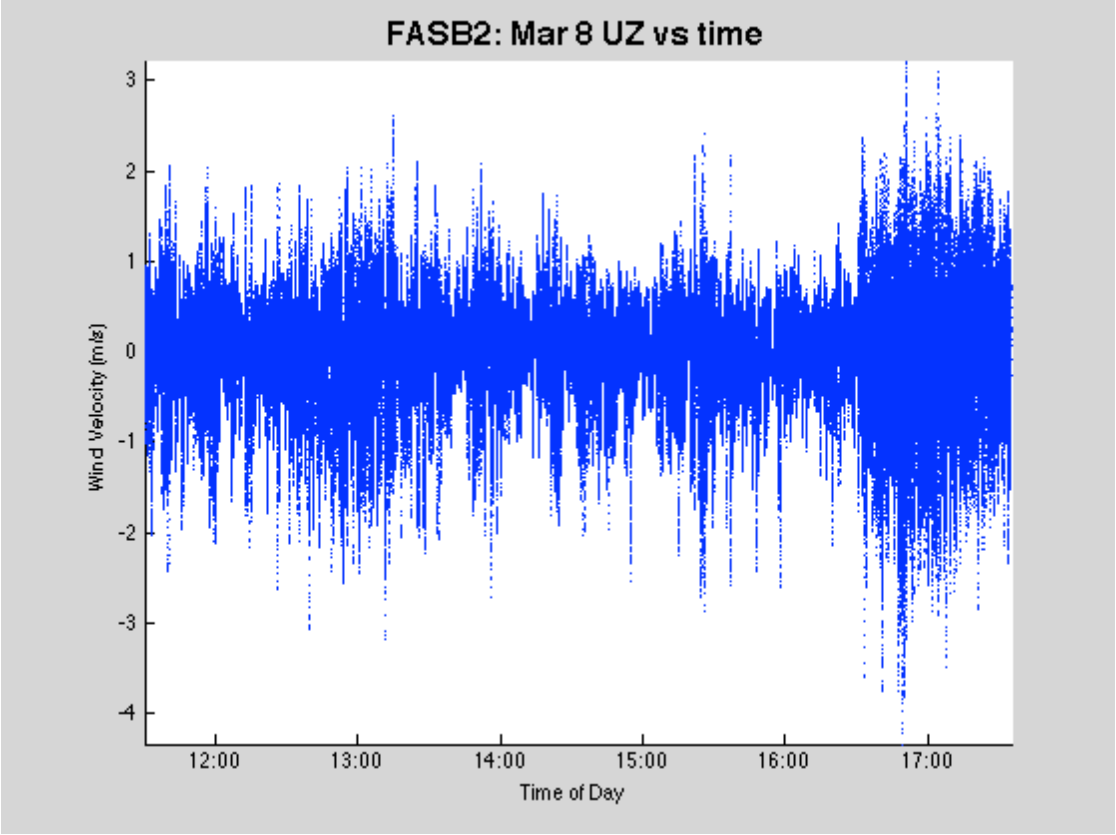
FASB2: Mar 8 UZ vs time
Wind Velocity (m/s)
-4
-3
-2
-1
0
1
2
3
12:00
13:00
14:00
15:00
16:00
17:00
Time of Day

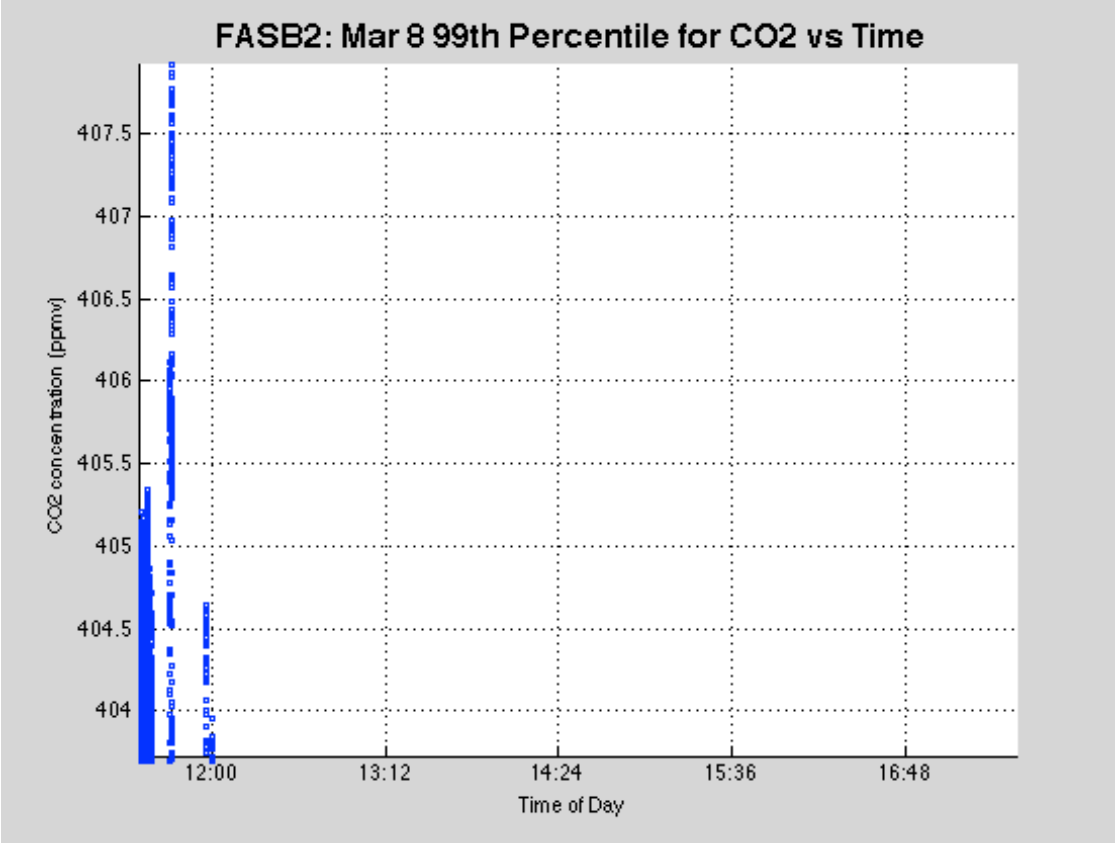
FASB2: Mar 8 99th Percentile for CO2 vs Time
CO2 concentration (ppmv)
407.5
407
406.5
406
405.5
405
404.5
404
12:00
13:12
14:24
15:36
16:48
Time of Day

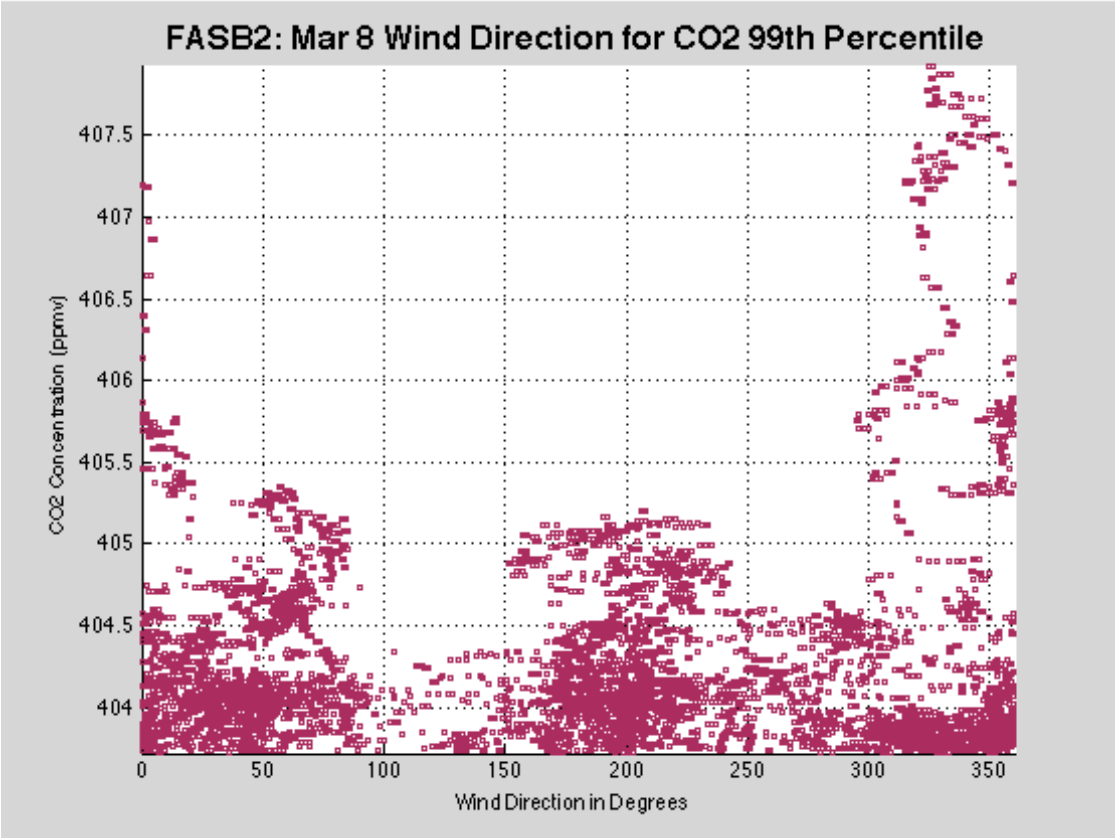
FASB2: Mar 8 Wind Direction for CO2 99th Percentile
CO2 Concentration (ppmv)
407.5
407
406.5
406
405.5
405
404.5
404
0
50
100
150
200
250
300
350
Wind Direction in Degrees

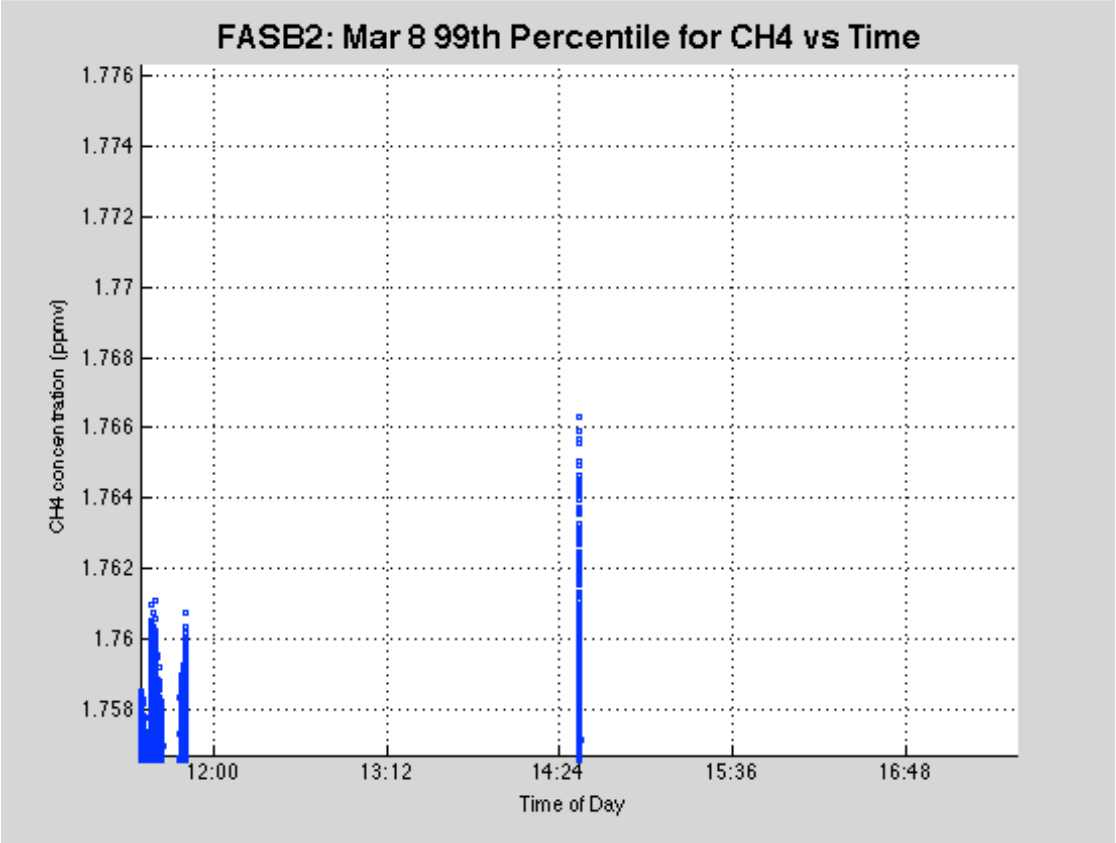
FASB2: Mar 8 99th Percentile for CH4 vs Time
CH4 concentration (ppmv)
1.776
1.774
1.772
1.77
1.768
1.766
1.764
1.762
1.76
1.758
12:00
13:12
14:24
15:36
16:48
Time of Day

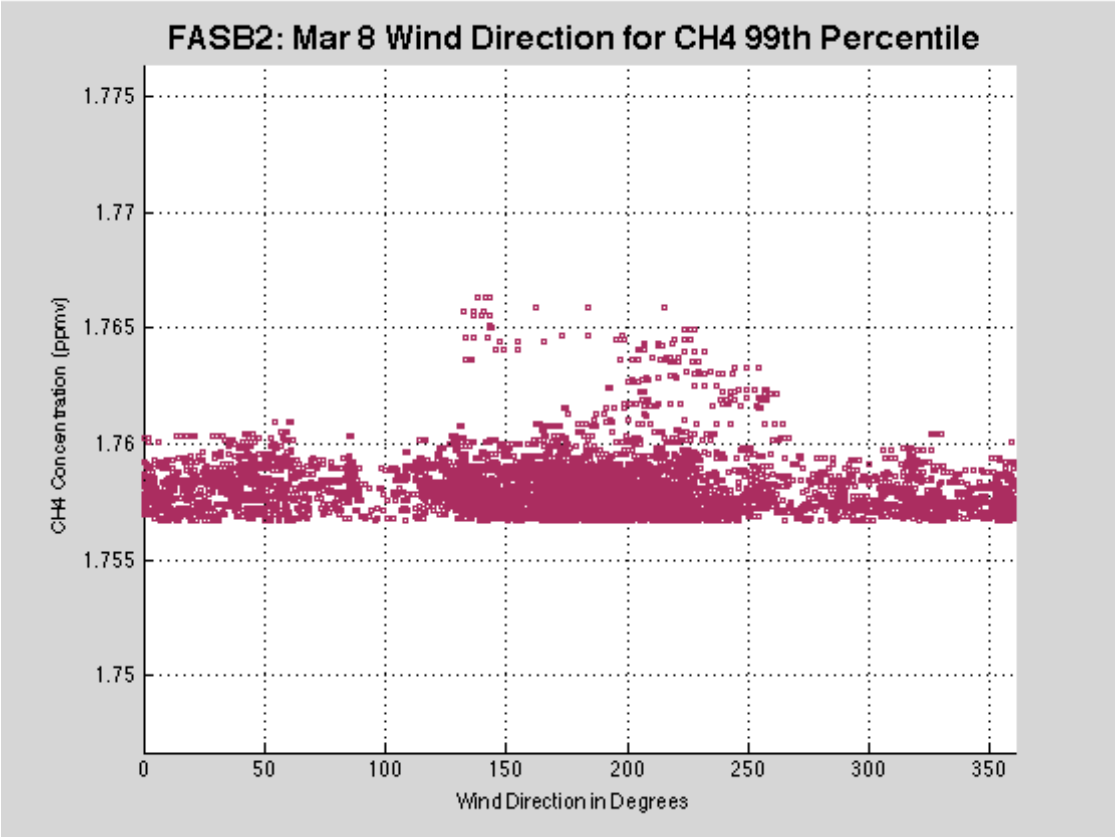
FASB2: Mar 8 Wind Direction for CH4 99th Percentile
CH4 Concentration (ppmv)
1.775
1.77
1.765
1.76
1.755
1.75
0
50
100
150
200
250
300
350
Wind Direction in Degrees

# APPENDIX G

## TOWER OVERNIGHT SESSIONS DATA

Two overnight continuous data collections occurred during the project duration. The first was at Tower Location 1 (TL1) from October 17$^{th}$ thru October 18$^{th}$. The second was at the FASB1 tower location from October 18$^{th}$ thru October 19$^{th}$. Included for each data set are the maximum, minimum, average and 99$^{th}$ percentile values for each gas. Also included are nine plots of the data for each day.

The plots are;

1. $CO_2$ Concentration vs. Time
2. $CH_4$ Concentration vs. Time
3. Wind Direction vs. Time
4. 99$^{th}$ Percentile $CO_2$ Concentration vs. Time
5. 99$^{th}$ Percentile $CO_2$ Concentration vs. Wind Direction
6. 99$^{th}$ Percentile $CO_2$ Concentration vs. *Reduced Degree Wind Direction
7. 99$^{th}$ Percentile $CH_4$ Concentration vs. Time
8. 99$^{th}$ Percentile $CH_4$ Concentration vs. Wind Direction
9. 99$^{th}$ Percentile $CH_4$ Concentration vs. *Reduced Degree Wind Direction

* the reduced degree wind direction is 150-175 for TL1 and 0-45 for FASB1

Also included for the overnight sessions are wind probability diagrams. These are broken down by gas and then in wind speed increments. The diagrams represent the probability of 99$^{th}$ percentile concentration for wind directions associated with the desired wind speed percentage.

The plots are;

1. Low Wind Speed (0-33%) for $CO_2$ Concentration Probability
2. Low Wind Speed (0-33%) for $CH_4$ Concentration Probability
3. Middle Wind Speed (33-67%) for $CO_2$ Concentration Probability
4. Middle Wind Speed (33-67%) for $CH_4$ Concentration Probability
5. High Wind Speed (67-100%) for $CO_2$ Concentration Probability
6. High Wind Speed (67-100%) for $CH_4$ Concentration Probability
7. All Wind Speed (0-100%) for $CO_2$ Concentration Probability
8. All Wind Speed (0-100%) for $CH_4$ Concentration Probability

## G.1 TL1: Thursday, October 17th thru Friday, October 18th Overnight Session

| | Maximum | Minimum | Average | 99th Percentile |
|---|---|---|---|---|
| $CO_2$ (ppmv) | 485.39 | 317.55 | 398.45 | 450.03 |
| $CH_4$ (ppmv) | 2.11 | 1.68 | 1.75 | 2.03 |

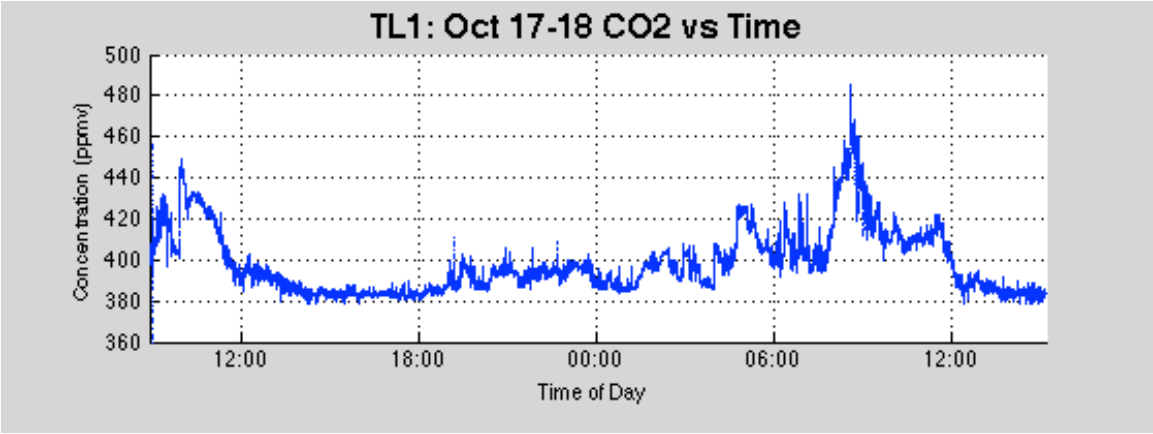


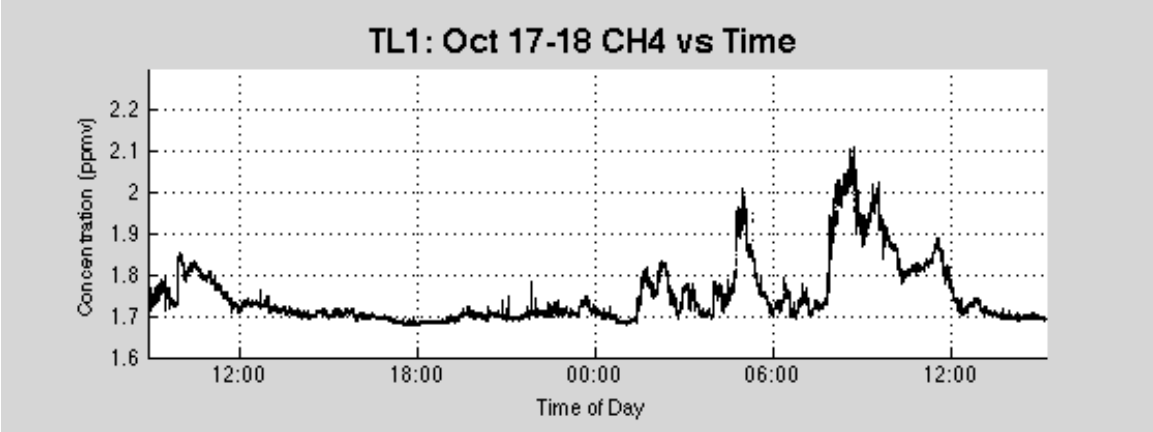

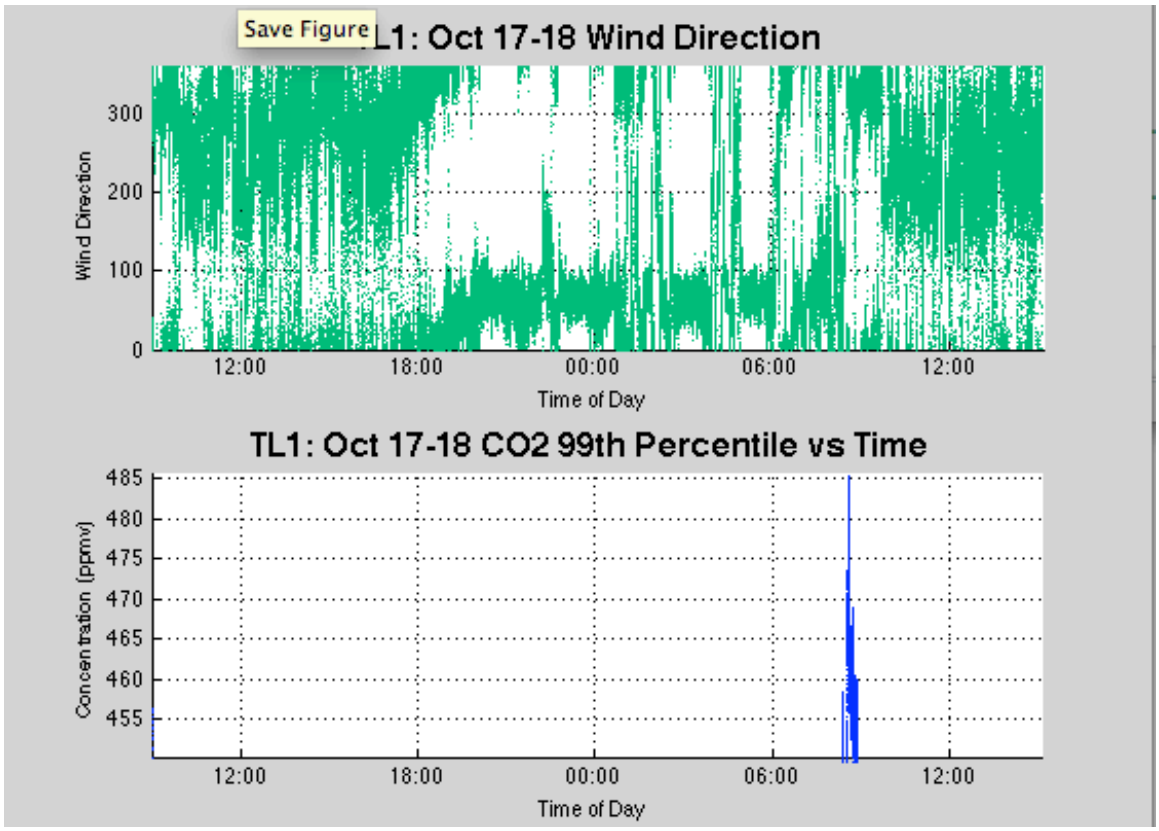
Save Figure
L1: Oct 17-18 Wind Direction
Wind Direction
300
200
100
0
12:00
18:00
00:00
06:00
12:00
Time of Day
TL1: Oct 17-18 CO2 99th Percentile vs Time
Concentration (ppmv)
485
480
475
470
465
460
455
12:00
18:00
00:00
06:00
12:00
Time of Day

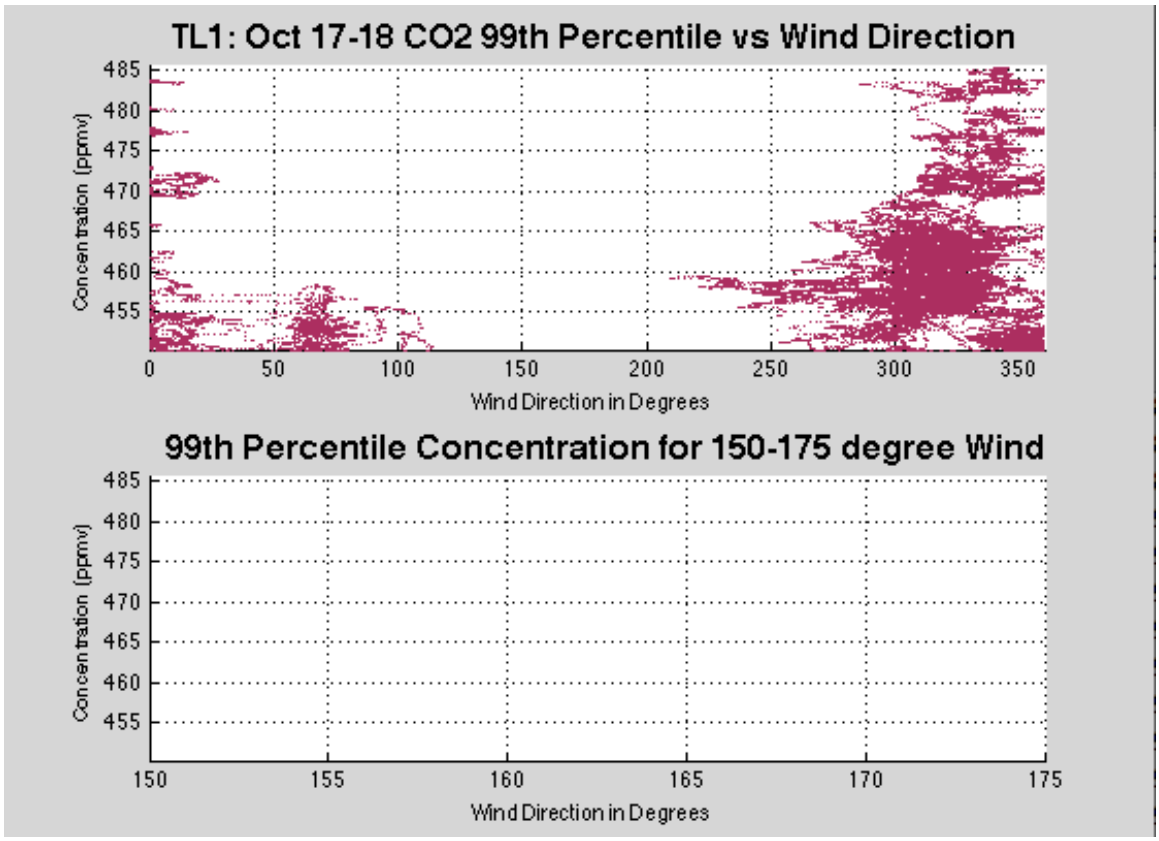
TL1: Oct 17-18 CO2 99th Percentile vs Wind Direction
Concentration (ppmv)
485
480
475
470
465
460
455
0
50
100
150
200
250
300
350
Wind Direction in Degrees
99th Percentile Concentration for 150-175 degree Wind
Concentration (ppmv)
485
480
475
470
465
460
455
150
155
160
165
170
175
Wind Direction in Degrees

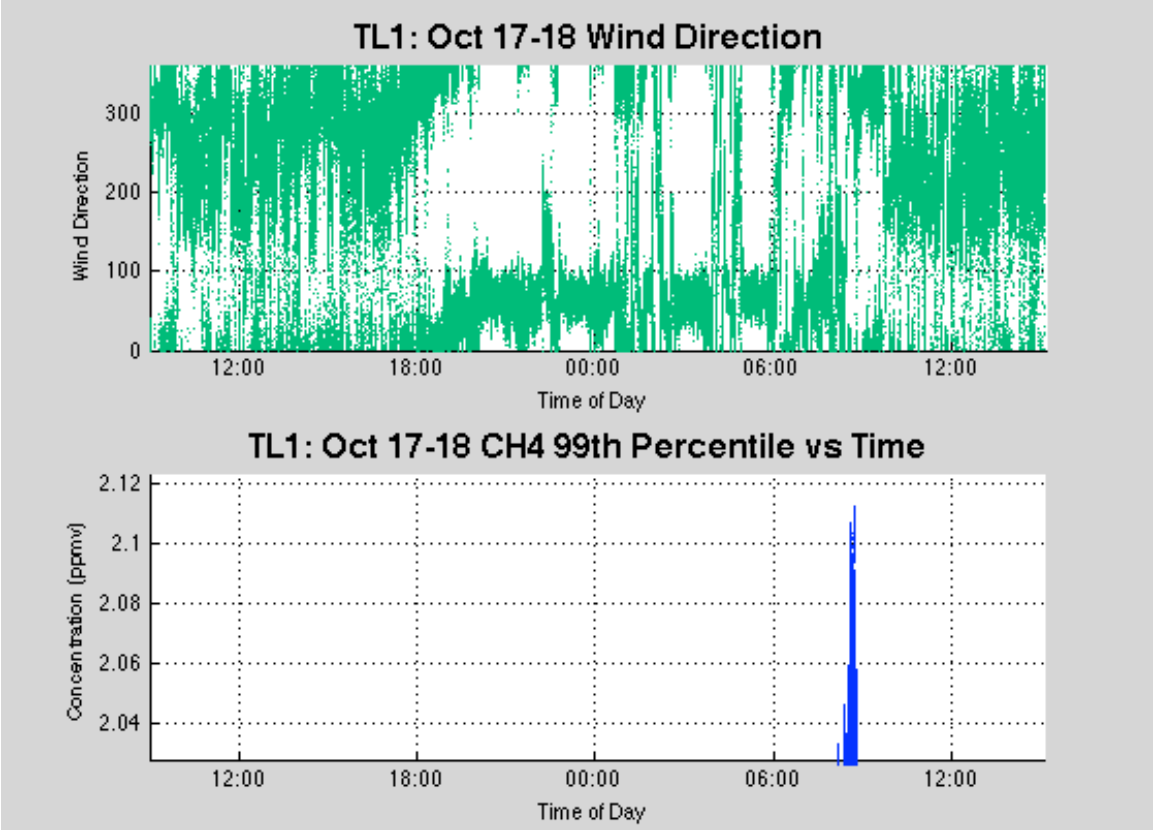
TL1: Oct 17-18 Wind Direction
Wind Direction
300
200
100
0
12:00
18:00
00:00
06:00
12:00
Time of Day
TL1: Oct 17-18 CH4 99th Percentile vs Time
Concentration (ppmv)
2.12
2.1
2.08
2.06
2.04
12:00
18:00
00:00
06:00
12:00
Time of Day

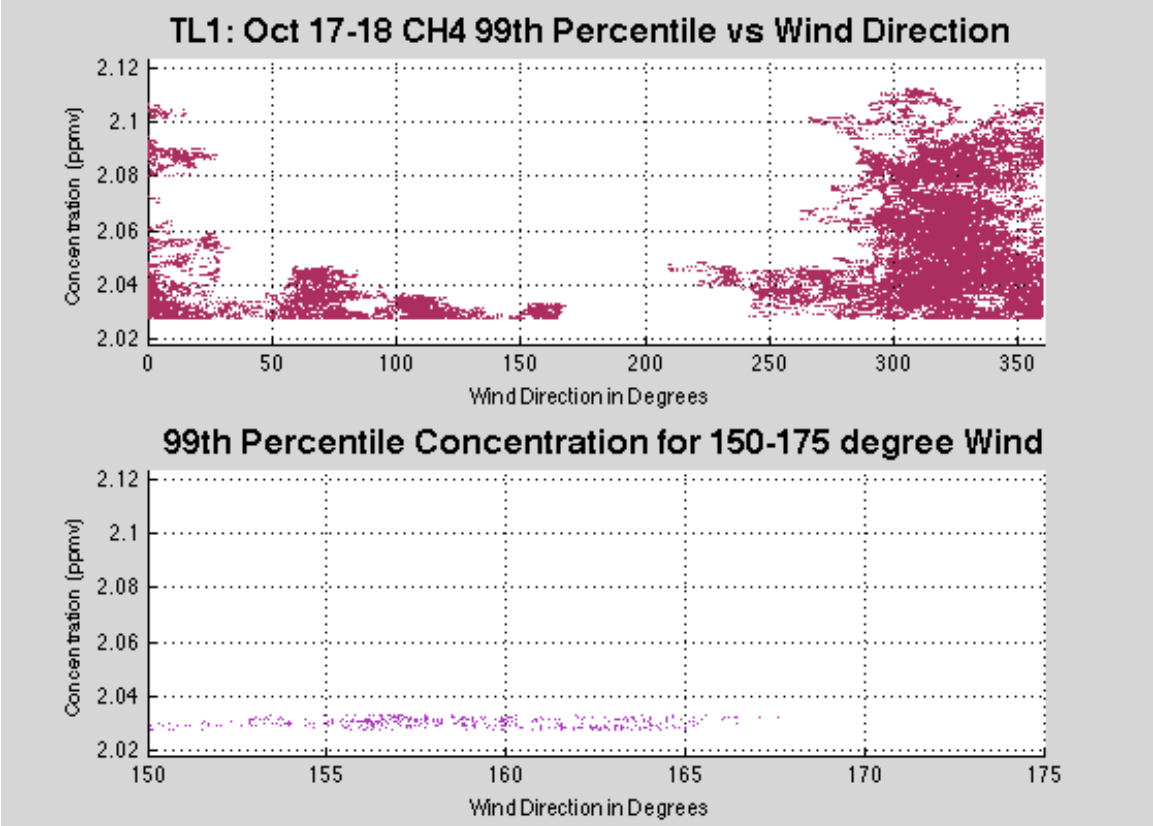
TL1: Oct 17-18 CH4 99th Percentile vs Wind Direction
Concentration (ppmv)
2.12
2.1
2.08
2.06
2.04
2.02
0
50
100
150
200
250
300
350
Wind Direction in Degrees
99th Percentile Concentration for 150-175 degree Wind
Concentration (ppmv)
2.12
2.1
2.08
2.06
2.04
2.02
150
155
160
165
170
175
Wind Direction in Degrees

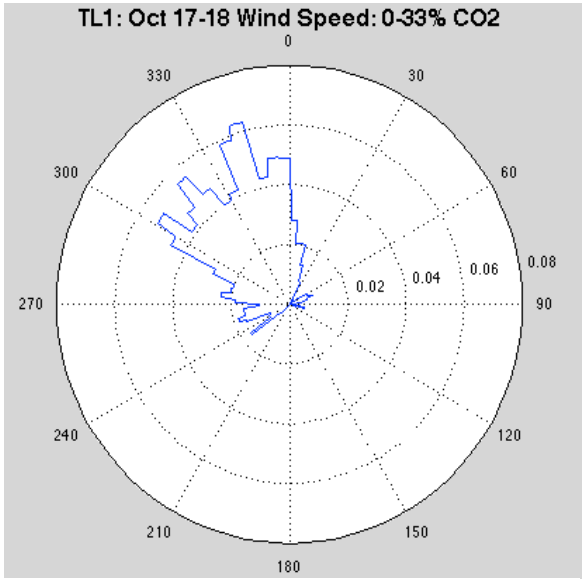
TL1: Oct 17-18 Wind Speed: 0-33% CO2
0
30
60
90
120
150
180
210
240
270
300
330
0.02
0.04
0.06
0.08

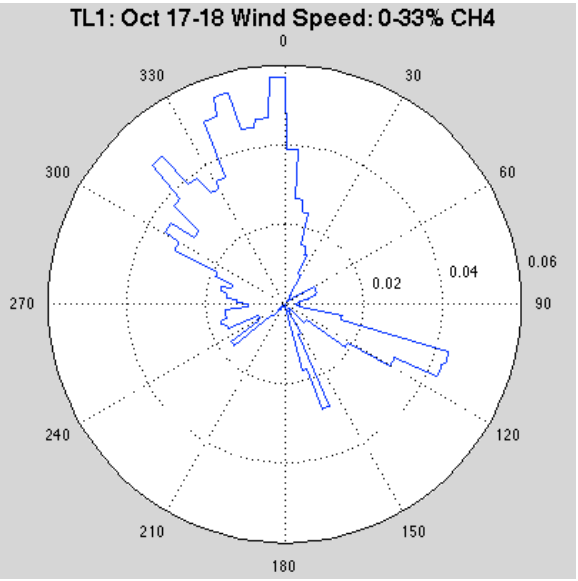
TL1: Oct 17-18 Wind Speed: 0-33% CH4
0
30
60
90
120
150
180
210
240
270
300
330
0.02
0.04
0.06

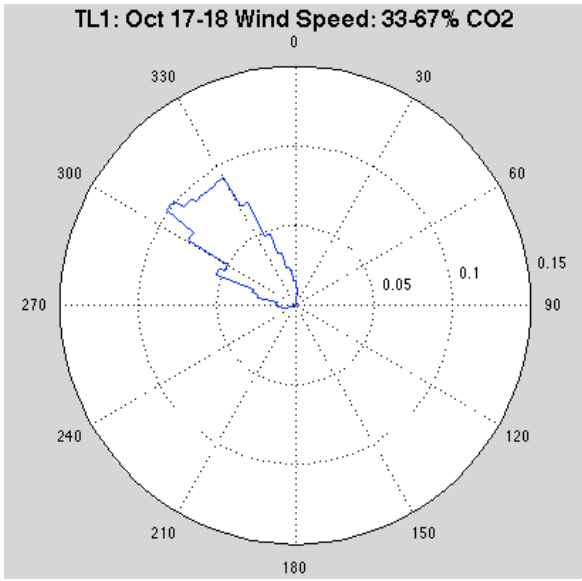
TL1: Oct 17-18 Wind Speed: 33-67% CO2
0
30
60
90
120
150
180
210
240
270
300
330
0.05
0.1
0.15

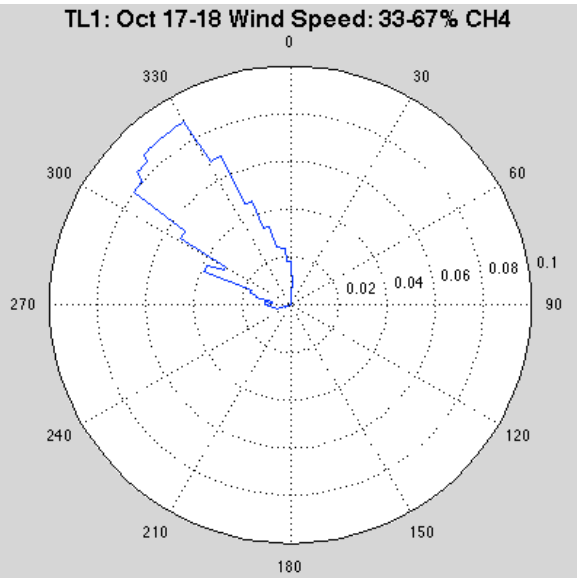
TL1: Oct 17-18 Wind Speed: 33-67% CH4
0
30
60
90
120
150
180
210
240
270
300
330
0.02
0.04
0.06
0.08
0.1

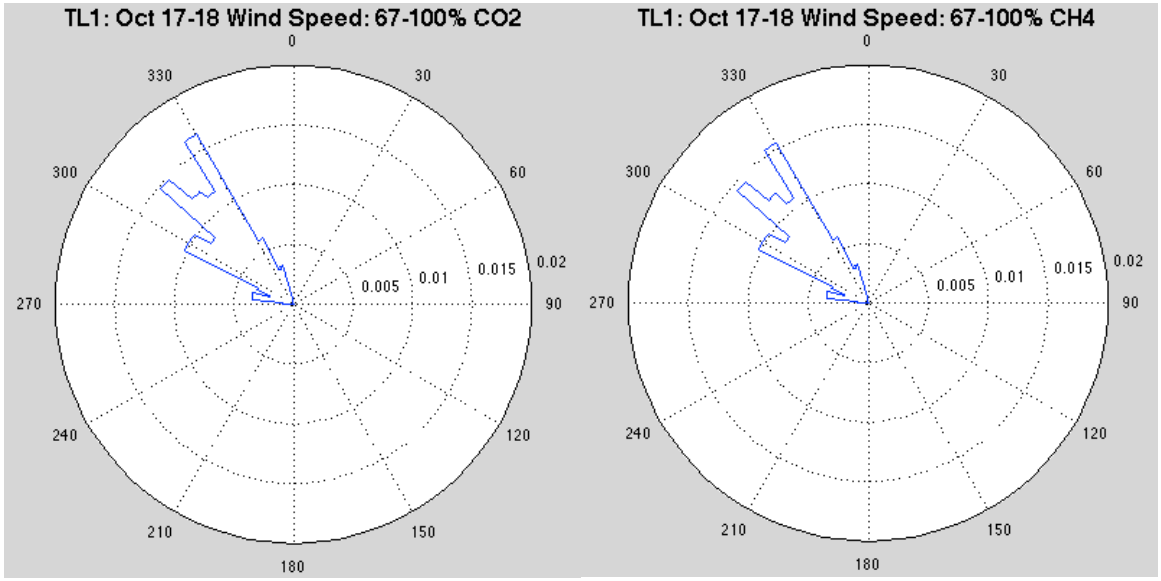
TL1: Oct 17-18 Wind Speed: 67-100% CO2
TL1: Oct 17-18 Wind Speed: 67-100% CH4
0
30
60
90
120
150
180
210
240
270
300
330
0.005
0.01
0.015
0.02

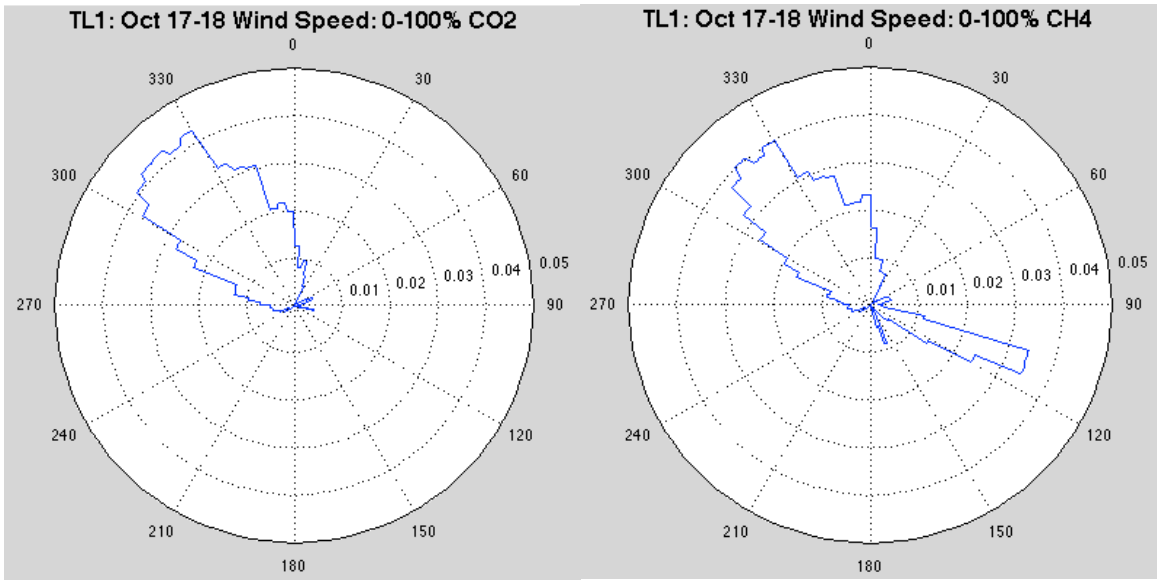
TL1: Oct 17-18 Wind Speed: 0-100% CO2
TL1: Oct 17-18 Wind Speed: 0-100% CH4
0
30
60
90
120
150
180
210
240
270
300
330
0.01
0.02
0.03
0.04
0.05

## G.2 FASB1: Friday, October 18th thru Saturday, October 19th Overnight Session

| | Maximum | Minimum | Average | 99th Percentile |
|---|---|---|---|---|
| $CO_2$ (ppmv) | 424.81 | 381.19 | 391.74 | 416.17 |
| $CH_4$ (ppmv) | 1.83 | 1.68 | 1.71 | 1.79 |

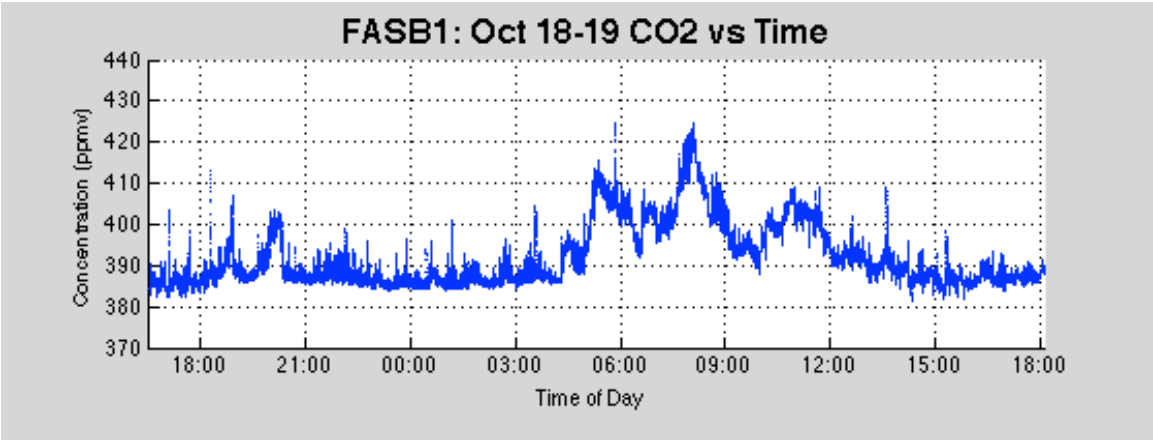


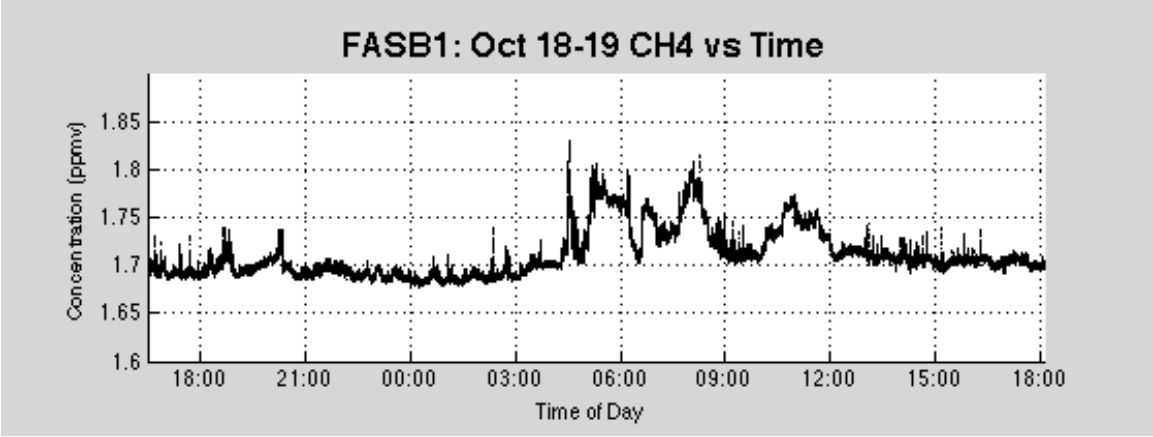

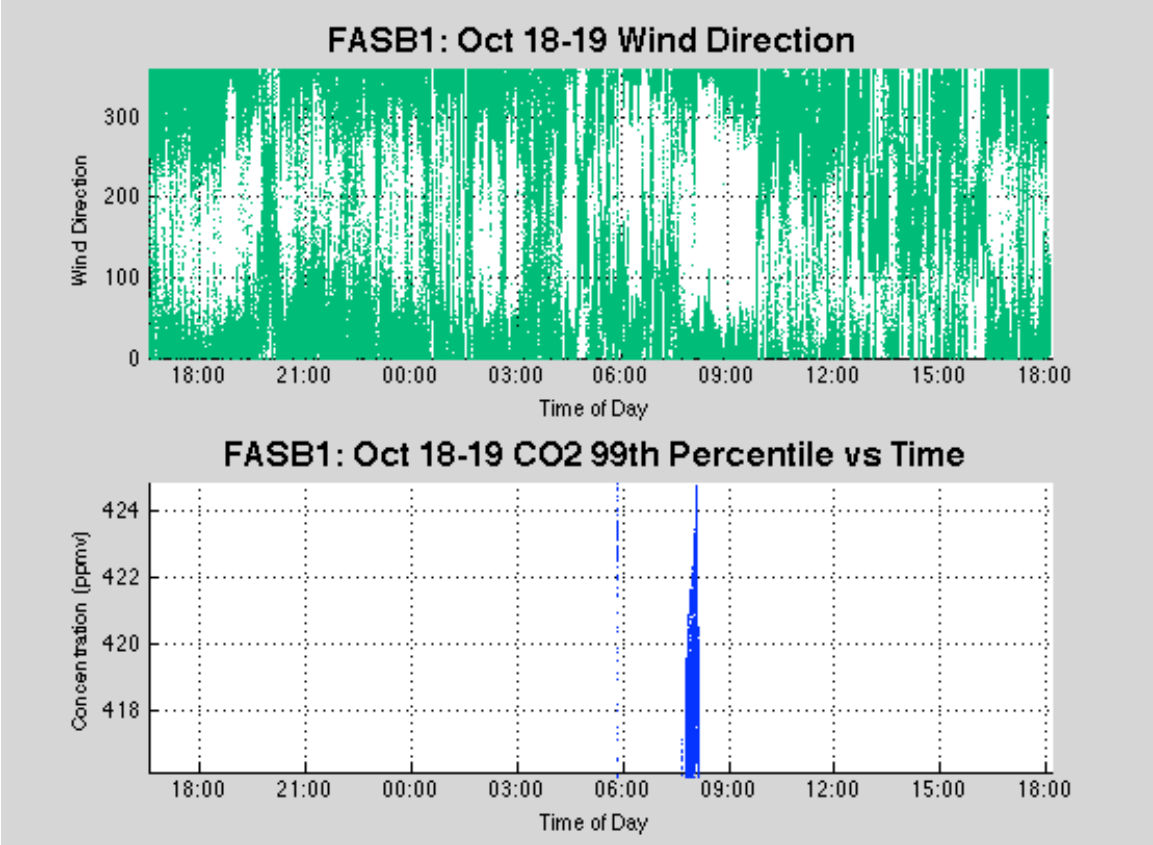
FASB1: Oct 18-19 Wind Direction
Wind Direction
300
200
100
0
18:00
21:00
00:00
03:00
06:00
09:00
12:00
15:00
18:00
Time of Day
FASB1: Oct 18-19 CO2 99th Percentile vs Time
Concentration (ppmv)
424
422
420
418
18:00
21:00
00:00
03:00
06:00
09:00
12:00
15:00
18:00
Time of Day

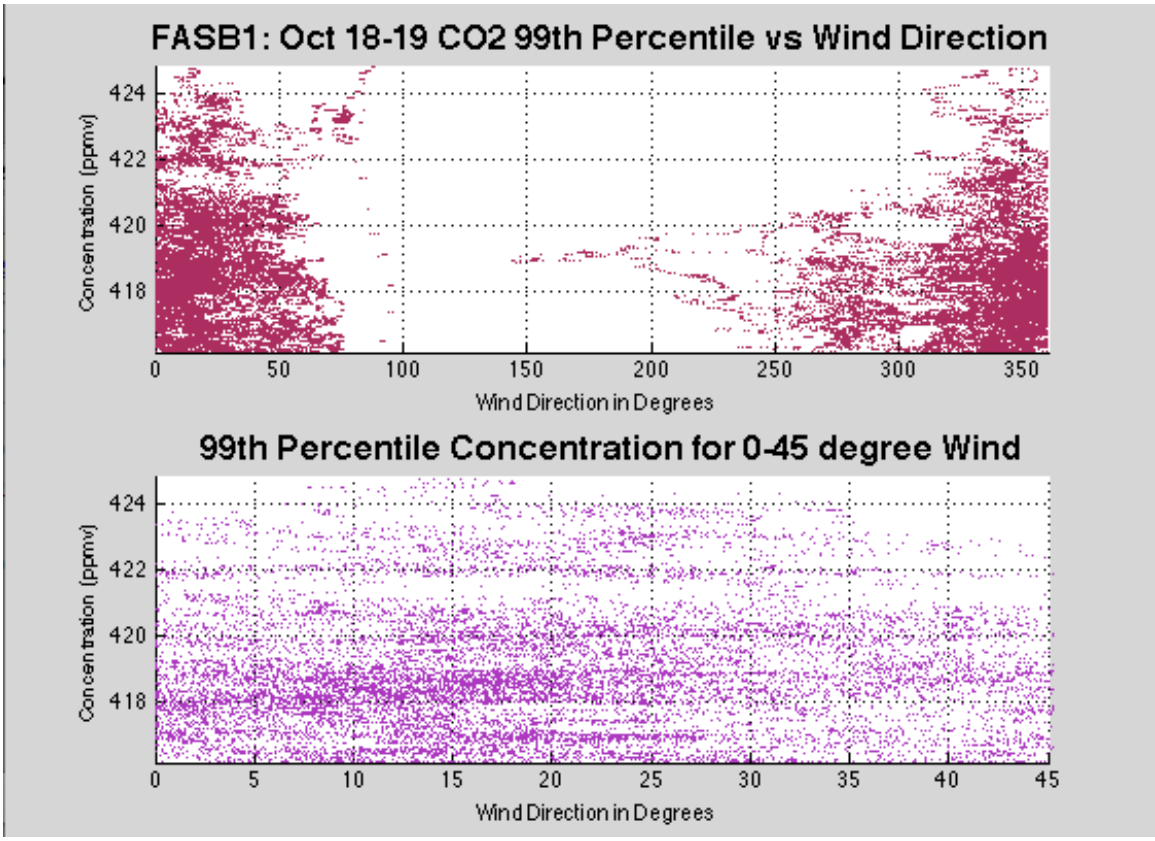
FASB1: Oct 18-19 CO2 99th Percentile vs Wind Direction
Concentration (ppmv)
424
422
420
418
0
50
100
150
200
250
300
350
Wind Direction in Degrees
99th Percentile Concentration for 0-45 degree Wind
Concentration (ppmv)
424
422
420
418
0
5
10
15
20
25
30
35
40
45
Wind Direction in Degrees

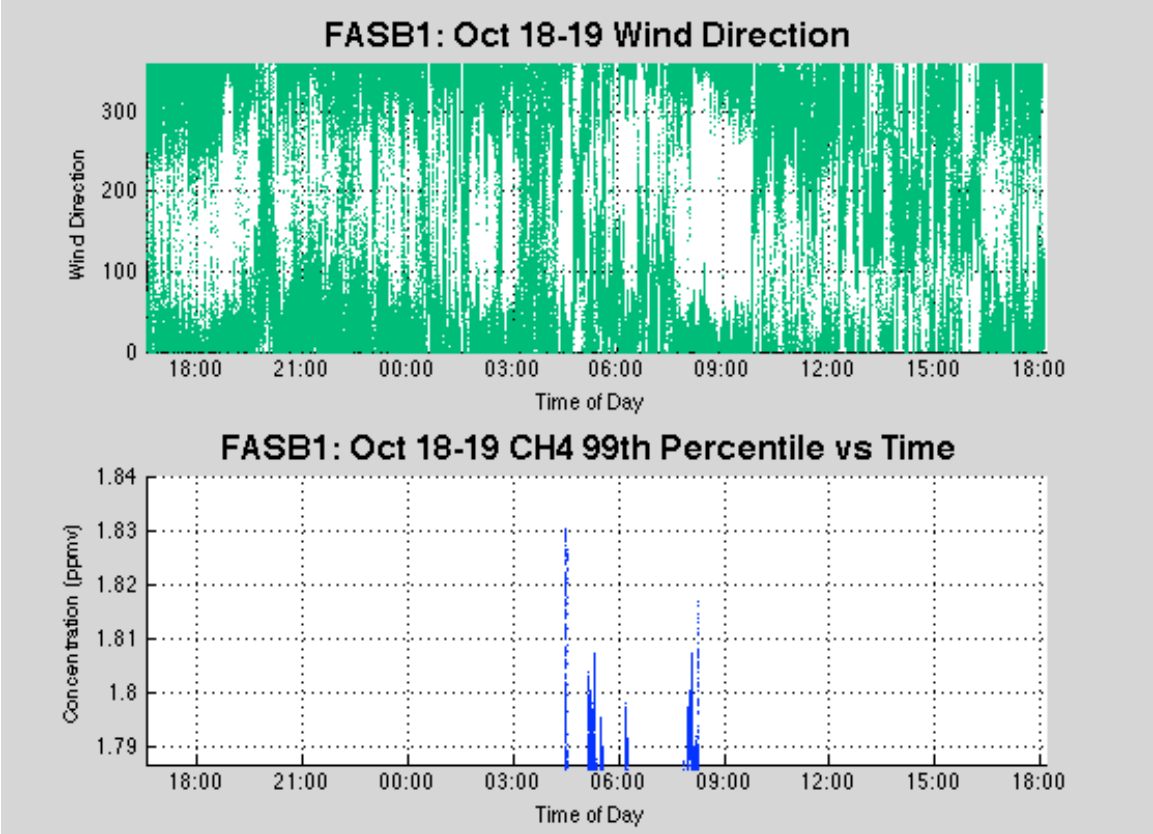
FASB1: Oct 18-19 Wind Direction
Wind Direction
300
200
100
0
18:00
21:00
00:00
03:00
06:00
09:00
12:00
15:00
18:00
Time of Day
FASB1: Oct 18-19 CH4 99th Percentile vs Time
Concentration (ppmv)
1.84
1.83
1.82
1.81
1.8
1.79
18:00
21:00
00:00
03:00
06:00
09:00
12:00
15:00
18:00
Time of Day

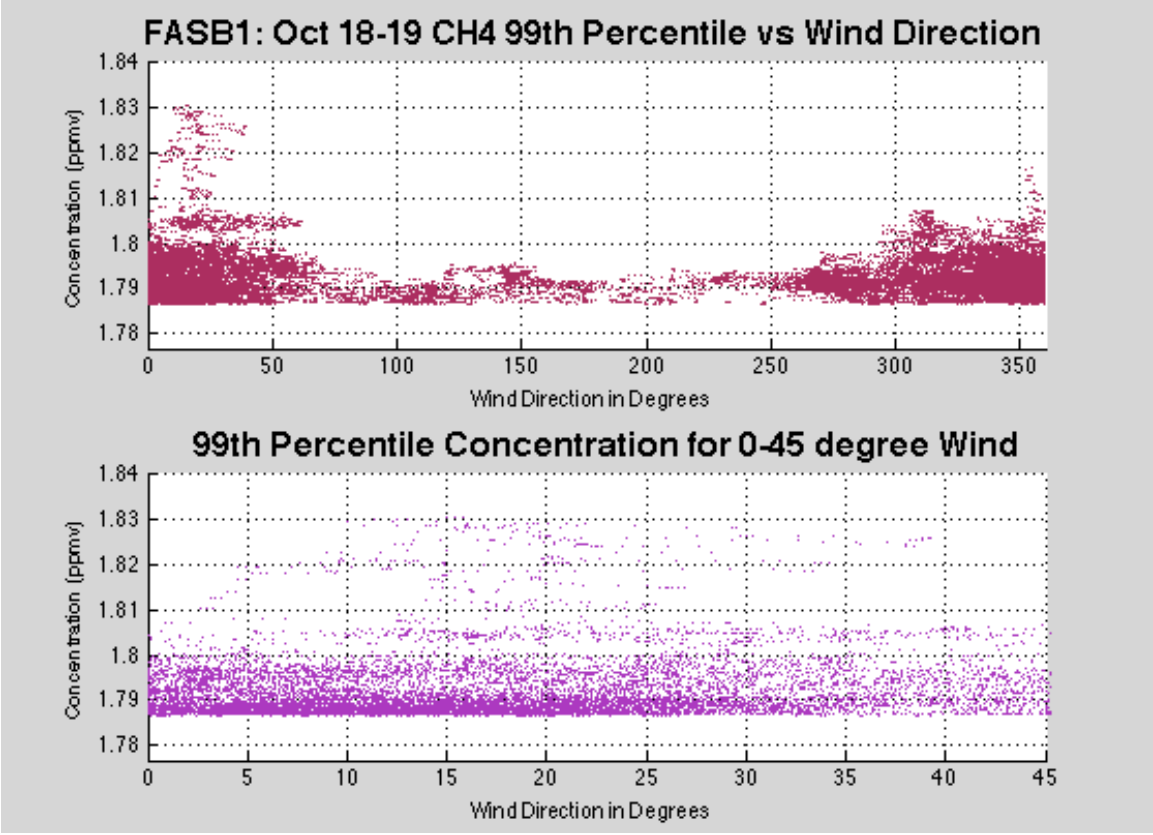
FASB1: Oct 18-19 CH4 99th Percentile vs Wind Direction
Concentration (ppmv)
1.84
1.83
1.82
1.81
1.8
1.79
1.78
0
50
100
150
200
250
300
350
Wind Direction in Degrees
99th Percentile Concentration for 0-45 degree Wind
Concentration (ppmv)
1.84
1.83
1.82
1.81
1.8
1.79
1.78
0
5
10
15
20
25
30
35
40
45
Wind Direction in Degrees

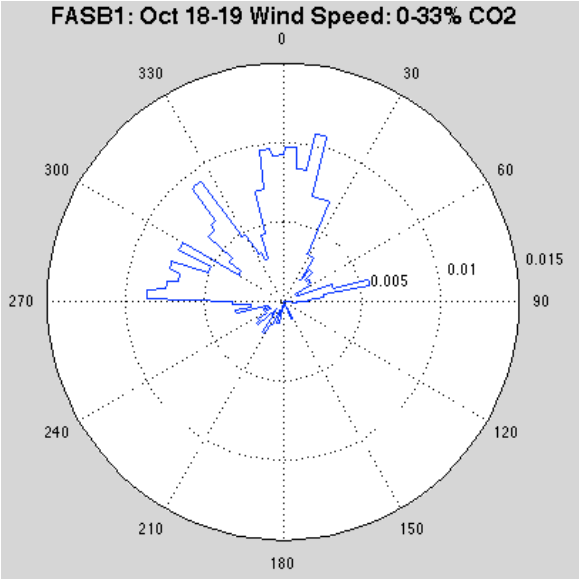
FASB1: Oct 18-19 Wind Speed: 0-33% CO2
0
30
60
90
120
150
180
210
240
270
300
330
0.005
0.01
0.015

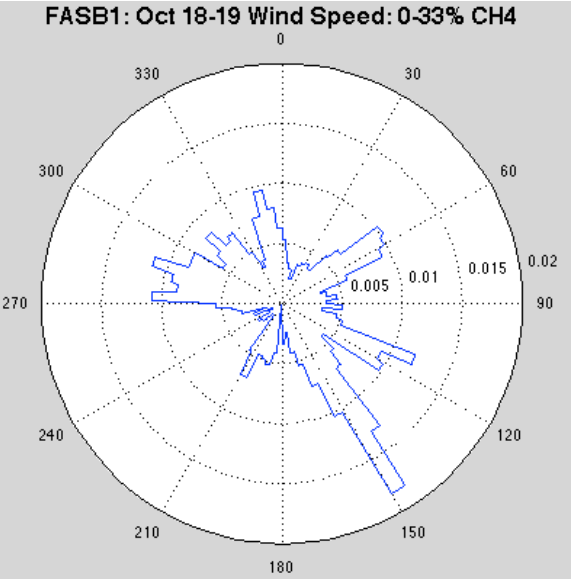
FASB1: Oct 18-19 Wind Speed: 0-33% CH4
0
30
60
90
120
150
180
210
240
270
300
330
0.005
0.01
0.015
0.02

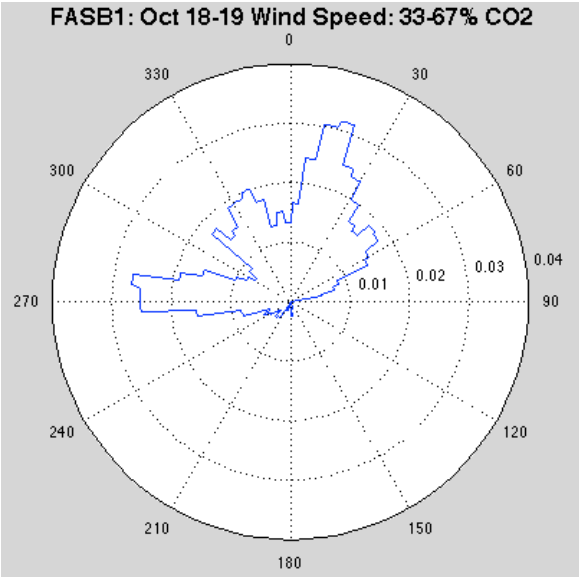
FASB1: Oct 18-19 Wind Speed: 33-67% CO2
0
30
60
90
120
150
180
210
240
270
300
330
0.01
0.02
0.03
0.04

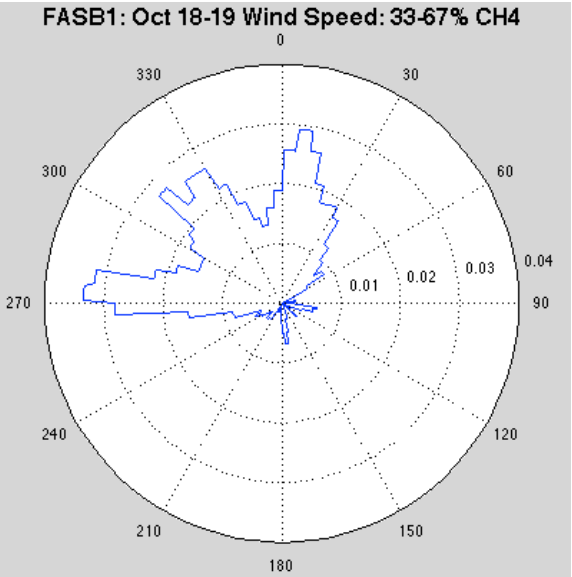
FASB1: Oct 18-19 Wind Speed: 33-67% CH4
0
30
60
90
120
150
180
210
240
270
300
330
0.01
0.02
0.03
0.04

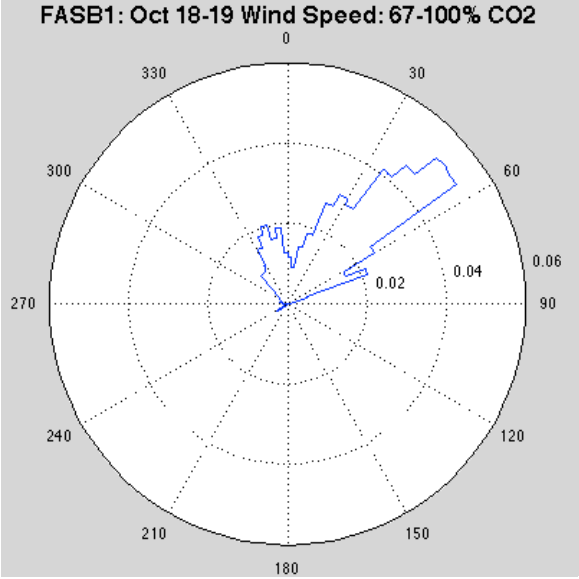
FASB1: Oct 18-19 Wind Speed: 67-100% CO2
0
30
60
90
120
150
180
210
240
270
300
330
0.02
0.04
0.06

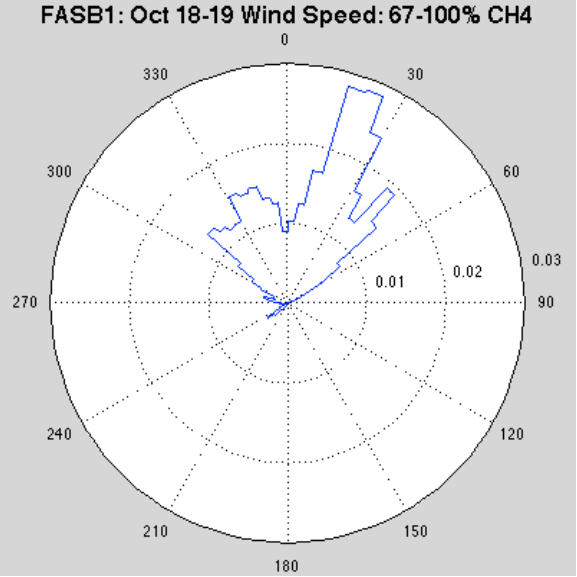
FASB1: Oct 18-19 Wind Speed: 67-100% CH4
0
30
60
90
120
150
180
210
240
270
300
330
0.01
0.02
0.03

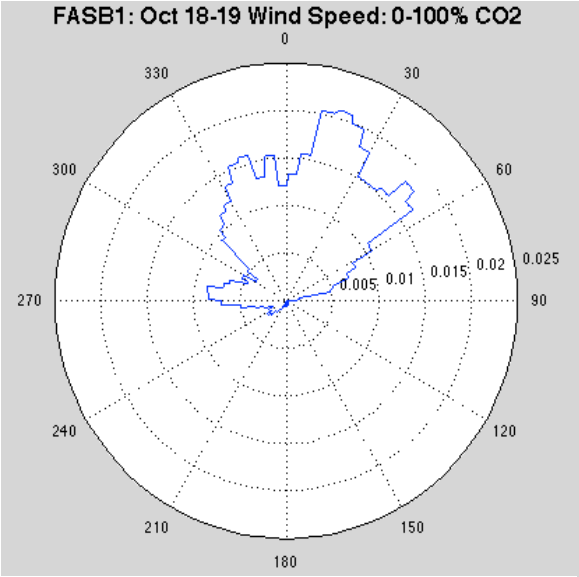
FASB1: Oct 18-19 Wind Speed: 0-100% CO2
0
30
60
90
120
150
180
210
240
270
300
330
0.005
0.01
0.015
0.02
0.025

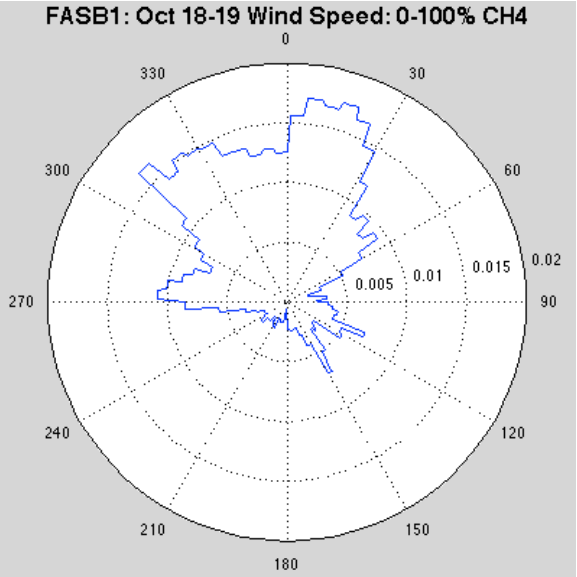
FASB1: Oct 18-19 Wind Speed: 0-100% CH4
0
30
60
90
120
150
180
210
240
270
300
330
0.005
0.01
0.015
0.02

# REFERENCES


Applied Technologies, Inc. (2013). *Operator's manual for a three axis sonic anemometer/thermometer revision J2:45*. Longmont, CO: Applied Technologies, Inc.

Baldocchi, D. (2012, October). *Lecture 17, wind and turbulence, part 2, surface boundary layer: Theory and principles*. Lecture conducted from University of California, Berkeley, CA.

Baldocchi, D., & Falge, E. (2001). FLUXNET: A new tool to study the temporal and spatial variability of ecosystem–scale carbon dioxide, water vapor, and energy flux densities. *Bulletin of the American Meteorological Society, 82*(11), 2415-2434.

Businger, J. (1986). Evaluation of the accuracy with which dry deposition can be measured with current micrometeorological techniques. *Journal of Climate and Applied Meteorology, 25*(8), 1100-1124.

Cheng, H., & Castro, I. (2002). Near wall flow over urban-like roughness. *Boundary-Layer Meteorology, 104*(2), 229-259.

Cubasch, U., Wuebbles, D., Chen, D., Facchini, M. C., Frame, D., Mahowald, N., … Winther, J.-G. (2013). Introduction. In T. F. Stocker, D. Qin, G.-K. Plattner, M. Tignor, S. K. Allen, J. Boschung, A. Nauels, Y. Xia, V. Bex, & P. M. Midgley (Eds.), *Climate change 2013: The physical science basis. Contribution of working group I to the fifth assessment report of the intergovernmental panel on climate change* (pp. 119-158). Cambridge, UK and New York, NY: Cambridge University Press.

Finnigan, J. (2004). The footprint concept in complex terrain. *Agricultural and Forest Meteorology, 127*(3–4), 117-129.

Grimmond, C. S. B., & King, T. S. (2002). Local-scale fluxes of carbon dioxide in urban environments: Methodological challenges and results from Chicago. *Environmental Pollution 116, Supplement 1*(0), S243-S254.

Horst, T. W., & Weil, J. C. (1992). Footprint estimation for scalar flux measurements in the atmospheric surface layer. *Boundary-Layer Meteorology, 59*(3), 279-296.

Horst, T. W., & Weil, J. C. (1994). How far is far enough?: The fetch requirements for micrometeorological measurement of surface fluxes. *Journal of Atmospheric and Oceanic Technology, 11*(4), 1018-1025.

Kljun, N., & Calanca, P. (2004). A simple parameterisation for flux footprint predictions. *Boundary-Layer Meteorology, 112*(3), 503-523.

Kljun, N., & Kormann, R. (2003). Comparison of the langrangian footprint. *Boundary-Layer Meteorology, 106*(2), 349-355.

Kljun, N., & Rotach, M. W. (2002). A three-dimensional backward lagrangian footprint model for a wide range of boundary-layer stratifications. *Boundary-Layer Meteorology, 103*(2), 205-226.

Kormann, R., & Meixner, F. (2001). An analytical footprint model for non-neutral stratification. *Boundary-Layer Meteorology, 99*(2), 207-224.

Lane, D. (2010, September 20). Percentiles. Retrieved from the OpenStax-CNX Web site: http://cnx.org/content/m10805/2.11/

Leclerc, M. Y., & Thurtell, G. W. (1990). Footprint prediction of scalar fluxes using a markovian analysis. *Boundary-Layer Meteorology, 52*(3), 247-258.

Lewicki, J. L., & Hilley, G. E. (2009). Detection of $CO_2$ leakage by eddy covariance during the ZERT project's $CO_2$ release experiments. *Energy Procedia, 1*(1), 2301-2306.

LI-COR (2007). *LI-8100 automated soil CO2 flux system & LI-850 multiplexer instruction manual*. Lincoln, NE: LI-COR, Inc.

Omega (2001). *FMA 5400/FMA 5500 mass flow controllers user's guide*. Stamford, CT: Omega Engineering, Inc.

Otte, T. L., & Lacser, A. (2004). Implementation of an urban canopy parameterization in a mesoscale meteorological model. *Journal of Applied Meteorology, 43*(11).

Picarro (2012). *Picarro G2311-f 10Hz CO2, CH4 and H2O analyzer for eddy covariance flux user's guide, Picarro analyzer user's guide.* Santa Clara, CA: Picarro, Inc.

Rella, C. (2010). *Accurate greenhouse gas measurements in humid gas streams using the Picarro G1301 carbon dioxide/methane/water vapor gas analyzer (white paper).* Sunnyvale, CA: Picarro, Inc.

Savitzky, A., & Golay, M. (1964). Smoothing and differentiation of data by simplified least squares procedures. *Analytical Chemistry, 36*(8), 1627-1639.

Schmid, H. P. (2002). Footprint modeling for vegetation atmosphere exchange studies: A review and perspective. *Agricultural and Forest Meteorology, 113*(1–4), 159-183.

Schuepp, P. H., & Leclerc, M. Y. (1990). Footprint prediction of scalar fluxes from analytical solutions of the diffusion equation. *Boundary-Layer Meteorology, 50*(1-4), 355-373.

Steinfeld, G., & Raasch, S. (2008). Footprints in homogeneously and heterogeneously driven boundary layers derived from a lagrangian stochastic particle model embedded into large-eddy simulation. *Boundary-Layer Meteorology, 129*(2), 225-248.

Stull, R. (2000). *Meteorology for scientists and engineers: A technical companion book with Ahrens' meteorology today*. Pacific Grove, CA: Brooks/Cole.

United States Environmental Protection Agency. (2011). *Greenhouse gas emissions from a typical passenger vehicle.* (Office of Transportation and Air Quality Publication No. EPA 420-F-14-040). Washington, DC: U.S. Government Printing Office.

United States Environmental Protection Agency. (2014). *Inventory of US greenhouse gas emissions and sinks: 1990-2012* (USEPA Publication No. EPA 430-R-14-003). Washington, DC: U.S. Government Printing Office.

Varland, A. (2014). *Engineering design and assembly of a surface methane and carbon dioxide gas flux measurement chamber with a case study on the university of Utah campus* (Unpublished master's thesis). University of Utah, Salt Lake City, UT.

Vesala, T., & Kljun, N. (2008). Flux and concentration footprint modeling: State of the art. *Environmental Pollution, 152*(3), 653-666.

Wiernga, J. (1993). Representative roughness parameters for homogeneous terrain. *Boundary-Layer Meteorology, 63*(4), 323-363.

Wilczak, J., & Oncley, S. (2001). Sonic anemometer tilt correction algorithms. *Boundary-Layer Meteorology, 99*(1), 127-150.